Bioaccumulation of trace elements in Seychelles marine food webs

Magali Sabino

Manuscrit de thèse de doctorat

BIOACCUMULATION OF TRACE ELEMENTS IN SEYCHELLES MARINE FOOD WEBS

MAGALI SABINO

2021

La Rochelle Université

LA ROCHELLE UNIVERSITÉ

ÉCOLE DOCTORALE
EUCLIDE

Laboratoire LIttoral ENvironnement et Sociétés (LIENSs)

THÈSE

présentée par :

Magali SABINO

soutenue le 11 octobre 2021
pour l'obtention du grade de Docteur de l'Université de La Rochelle

Discipline : Biologie de l'environnement, des populations, écologie

Bioaccumulation of trace elements in Seychelles marine food webs

---

Composition du jury :

Catherine MUNSCHY	Cadre de recherche (HDR), Ifremer, Rapportrice
Marc METIAN	Chercheur ONU (HDR), International Atomic Energy Agency (IAEA), Rapporteur
Anne LORRAIN	Directrice de recherche, IRD, Examinatrice
Christel LEFRANÇOIS	Professeure, La Rochelle Université, Examinatrice
Paco BUSTAMANTE	Professeur, La Rochelle Université, Directeur de thèse
Nathalie BODIN	Chargée de recherche, IRD, Co-directrice de thèse
Heidi PETHYBRIDGE	Research Scientist, CSIRO Oceans and atmosphere, Co-encadrante de thèse

“Knowing is the key to caring, and with caring there is hope that people will be motivated to take positive actions. They might not care even if they know, but they can’t care if they are unaware.”

Sylvia Earle

REMERCIEMENTS

Ça y est, il est désormais temps pour moi de conclure ces trois années de thèse, et cela ne peut se faire sans remercier toutes les personnes qui ont participé de près ou de loin à ce projet. Une thèse a beau être un projet de recherche personnel, dans lequel nous nous plongeons corps et âme pendant trois années entières, elle ne pourrait pas exister sans les soutiens financiers, matériels, scientifiques et personnels de nombreuses personnes.

Tout d'abord, je voudrais remercier Nathalie pour m'avoir fait confiance et m'avoir permis de travailler sur ce sujet. Merci à Nathalie, mais aussi Paco, pour m'avoir accompagnée durant cette thèse, et pour votre encadrement tout au long de ces trois années. Un grand merci pour vos suggestions et vos commentaires, qui ont contribué à améliorer ce manuscrit.

Je remercie également les membres de mon comité de thèse, Heidi Pethybride, David Point, Marie Vagner et François Le Loch, pour leurs suggestions et leurs idées. Vous m'avez éclairée et m'avez aidée à y voir plus clair sur de nombreux points.

Je remercie vivement tous les membres de mon jury, qui ont accepté d'évaluer mes travaux de thèse. Un grand merci notamment à mes rapporteurs, Catherine Munschy et Marc Métian, qui ont accepté de commenter ce manuscrit.

Mes remerciements vont bien sûr à la *Seychelles Fishing Auhority* (SFA) pour avoir financé ce projet de thèse. Un grand (très grand) merci également à toute l'équipe de techniciens de la SFA sans qui l'échantillonnage n'aurait pas été possible ! Je ne compte pas le nombre d'heures que vous avez passées à empaqueter/identifier/broyer/lyophiliser tous ces tubes.

Je tiens également à remercier mes soutiens techniques à La Rochelle. Gaël, merci pour ta gentillesse et ton aide à l'analyse isotopique. Merci aussi à Benoit Simon-Bouhet pour son aide sur R, *tidyverse* n'a (presque) plus de secret pour moi grâce à toi ! Un grand GRAND merci également à Maud et Carine pour leur accueil chaleureux au sein de la plateforme *Analyse élémentaire*. Merci pour votre bonne humeur, vos blagues et vos sourires, j'ai énormément appris auprès de vous. Merci d'avoir été présentes pour me montrer le fonctionnement de toutes les manips, et pour avoir partagé vos astuces de labo avec moi. Merci également pour les (très très) nombreuses heures que vous avez passées à acidifier et passer mes échantillons

à l'ICP. Et merci Carine pour ta patience face à mes nombreuses questions, tu mérites très largement ton diplôme de la patience !!

Les remerciements à mes soutiens techniques ne seraient bien sûr pas complets sans Fabienne Le Grand et Antoine Bideau, de la plateforme LIPIDOCEAN à Brest (LEMAR). Je n'ai passé que peu de temps avec vous durant ces trois années de thèse, mais vous avez été présents à chaque fois que j'avais besoin de vous. Merci Fabienne pour ta patience à vérifier mes chromatogrammes, et pour avoir pris le temps de répondre à mes questions farfelues. Merci Antoine pour ta bonne humeur au labo, les manips « acides gras » n'auraient pas été les mêmes sans tes blagues et sans AC/DC.

Un grand merci au département de biologie pour m'avoir fait confiance et m'avoir confié des heures de TP et TD. Vous m'avez permis de découvrir les plaisirs de l'enseignement, même si cela a duré trop peu de temps à mon goût. Je n'oublierai jamais le plaisir du contact avec les étudiants, et de leur transmettre des savoirs. Merci pour cette expérience enrichissante.

Des remerciements s'imposent également pour toi, Lydie. Je n'aurais pas pu rêver meilleur encadrante pour mon stage de master 2. Merci d'avoir partagé ta passion de la recherche et des sciences fondamentales avec moi, merci pour ta présence et tes encouragements. Tu m'as donné envie de me lancer dans l'aventure de la recherche et de faire une thèse, et je ne serai probablement pas là où j'en suis sans toi.

Merci à tous ceux avec qui j'ai partagé des bons moments, vous qui avez réussi à me sortir le nez de ma thèse lorsque j'en avais le plus besoin, vous qui avez été là dans les meilleurs moments comme dans les pires. La thèse peut être une expérience difficile, entre remise en question et doutes, mais vous avez toujours su me remonter le moral quand j'en avais besoin.

Merci à mes co-occupants de bureau. Léa, même si tu étais souvent à Chizé, tu as eu le temps de partager ta passion des amphibiens et de la génétique. Je te souhaite le meilleur pour la fin de ta thèse, et pour la suite ! Gauthier, nos discussions sur les ornithologues vont me manquer. J'aurais vraiment aimé participer à un de tes terrains oiseaux (surtout celui des calanques, on ne va pas se mentir ! =P), mais malheureusement mon calendrier de thèse en a décidé autrement. A quand une soirée frites pour que vous me racontiez vos aventures, tous les deux ? Merci aussi à tous ceux que j'ai pu croiser au LIENSs ILE, Martine, Elizabeth, Mélanie, Clémence, ceux que j'ai côtoyés au CCA, et tous les autres.

Merci à toute l'équipe organisatrice du 18ème festival du film [pas trop] scientifique (ADocs ou non d'ailleurs), vous nous avez préparé un festival digne des 20 ans ! Merci également à l'équipe des réalisateurs, Caroline, Romain, Etienne, Yann, Fanny, et les autres, les réunions d'avancement devant une petite bière nous ont tous aidé à avancer et c'était vraiment top. Sortir le nez de mes échantillons pour passer du temps avec vous a été un vrai plaisir. Merci à Caroline pour ta bonne humeur et tous tes encouragements.

Un grand merci à tout le groupe PélaBEER, Etienne, Jasmin, Mathieu, Rose, Manon, Camille, et tous les stagiaires, pour m'avoir aussi fait sortir le nez de ma grotte. Merci pour ces pauses entre deux analyses de mercure, et merci pour ses soirées de détente au coin d'une bière.

Merci également à toute la bande de nouveaux nantais (Chloé, Guillaume, Alice, Loïc), aux Pays-Bahés (oui je sais, on dit néerlandais, Anouk et Romain) et à Cyril. On se souviendra longtemps des apéros-Skype-Covid, avec nos supers connexions internet qui figent tout le monde dans des positions stupides. Merci à vous pour votre présence, votre soutien et vos encouragements pendant ces trois années, la thèse n'aurait pas été la même sans vous. Alice, Loïc, promis un jour on arrivera à se coordonner un week-end pour venir casser des murs et mettre de la peinture partout chez vous !

Un énorme merci à mes copains de master, qui sont là pour moi depuis si longtemps. Thibaud, avec tes jeux de mots et tes questions qui fâchent ; Emeline, avec nos délires à distance (c'est loin Maurice…) ; Joséphine, avec tes idées cathartiques. A quand des retrouvailles en Breizhanie ? Joe, promis je passerai bientôt à Lyon pour t'emmener des pousses de mini jungle !

Un grand merci à mes parents et à ma grand-mère, qui ont toujours cru en moi, qui m'ont toujours soutenue et encouragée, même dans les moments difficiles. Merci à vous de m'avoir écouté parler (parfois trop) de mon sujet de thèse, même si c'était probablement incompréhensible pour vous la moitié du temps.

Et enfin, un immense merci à mon plus grand soutien pendant ces trois ans. Toi qui as été la plus inattendue mais aussi la plus belle des rencontres. Toi qui me supporte au quotidien, qui sais comment me faire rire même dans les pires moments, et qui trouves toujours les mots pour me réconforter. J'espère être un aussi grand soutien pour toi que tu ne l'es pour moi.

Bientôt la fin de thèse pour toi aussi, et de nouveaux projets pour nous deux. Vers l'infini et au-delà !

Merci à tous !!

FOREWORD

STRUCTURE OF THE MANUSCRIPT

This PhD thesis is organised on the model of a monograph, that is with a general "introduction" presenting the context of the thesis, a general "material and method" presenting laboratory techniques and methods of data analysis used in the thesis, chapters presenting the results of the thesis and the related specific discussions, and a general "discussion" in which all results and conclusions are compared and discussed together. In each chapter, a specific context is given to bring additional important elements, or to remind the reader of what elements will be important to understand the chapter.

I preferred this structure over the "collection of papers" structure in order to avoid potential repetitions among subsections, particularly among chapters using similar methods, whether it is for laboratory techniques or for data analysis. In addition, the "monograph" model allowed me to add more results and to sometimes go futher in data analysis, which is more representative of the work I achieved during the three years of my PhD. As papers are also a big part of PhD work, they are presented as "supplementary documents" at the end of the thesis, and are mentioned in each related chapter when appropriate.

CONTEXT OF THE PHD PROJECT: THE SEYFISH PROJECT

This PhD project is included in the SEYFISH project (Nutrients and Contaminants in Seychelles fisheries resources) led by the Seychelles Fishing Authority (SFA) and co-funded by the French National Research Institute for Sustainable Development (IRD) and the SFA.

The Seychelles are considered as a hotspot of marine biodiversity, with emblematic ecosystems including coral reefs, mangroves and seagrass beds. Do to their remoteness and insularity, the Seychelles are particularly reliant on their marine resources for local economy and subsistence through commercial fisheries. However, global changes and their consequences on the marine environment, such as habitat degradation and biodiversity loss, raised questions regarding the resilience of Seychelles marine ecosystems facing human

pressure. This may alter the quantity and quality of fisheries resources, and thus have negative impacts on nutrient supply and contaminant exposure in Seychelles population's diet.

The main questions of the SEYFISH project are thus related to two main topics, that is the nutritional aspect of capture fisheries resources (i.e. "What do capture fisheries provide in terms of valuable nutrients for the Seychelles populations?", "How important are they for ensuring food and nutrition security in Seychelles?", "How and to which extend may global change affect the health benefits and risks associated with wild fish consumption?") and the ecological aspect (i.e. "How are the Seychelles marine ecosystems structured?", "How are they able to cope with increasing global changes?", What could be recommended in terms of ecosystems' and fisheries' monitoring and conservation measures?").

In this context, the current PhD thesis studies essential, potentially essential and non-essential trace elements in Seychelles capture fisheries resources that is their micronutrient and contaminant content. Two questions in particular are addressed: (1) what are the factors controlling trace element bioaccumulation and subsequent concentrations in Seychelles capture fisheries species and (2) what are the risk and benefit of capture fisheries resource consumption in Seychellois capture fisheries resources-based diets in terms of contaminant exposure micronutrient supply?

PEER-REVIEWED PUBLICATIONS

First author publications

Sabino, M.A., Bodin, N., Govinden, R., Albert, R., Churlaud, C., Pethybridge, H., Butamante, P. (in review) The role of tropical capture fisheries in trace element delivery for a Small Island Developing State community, the Seychelles. Submitted in *Marine Pollution Bulletin*.

Sabino, M.A., Bustamante, P., Govinden, R., Albert, R., Churlaud, C., Pethybridge, H., Bodin, N. (in prep) Ontogeny and seasonal variation of environmental parameters influence trace element bioaccumulation in emperor red snapper (*Lutjanus sebae*). To be submitted in *Environmental Research*.

Sabino, M.A., Bodin, N., Hollanda, S., Albert, R., Pillay, N., Churlaud, C., Romanov, E., West, W., Bustamante, P. (in prep) Regional patterns in mercury (Hg) and selenium (Se) concentration in swordfish from the Indian Ocean. To be submitted in *Chemosphere*.

Sabino, M.A., Govinden, R., Pethybridge, H., Blamey, L., Le Grand, F., Sardenne, F., Rose, M., Bustamante, P., Bodin, N. (2021) Habitat degradation increases interspecific trophic competition between three spiny lobsters in Seychelles. *Estuarine, Coastal and Shelf Science* **256**, 107368. doi: 10.1016/j.ecss.2021.107368

Co-author publications

Sardenne, F., Bodin, N., Barret, L., Blamey, L., Govinden, R., Gabriel, K., Mangroo, R., Munaron, J-M., Le Loc'h, F., Bideau, A., Le Grand, F., **Sabino, M.A.**, Bustamante, P., Rowat, D. (2021) Diet of spiny lobsters from Mahé Island reefs, Seychelles inferred by trophic tracers. *Regional Studies in Marine Science* **42**, 101640. doi: 10.1016/j.rsma.2021.101640

CONFERENCES

Oral presentations

Sabino, M.A., Bodin, N., Hollanda, S., Albert, R., Pillay, N., Churlaud, C., Romanov, E., West, W., Bustamante, P. (2019) Regional patterns in mercury and selenium concentrations of swordfish in the Indian Ocean. In Future Oceans$_2$ IMBeR Open Science conference, Brest, France.

Munschy, C., **Sabino, M.A.**, Bely, N., Héas-Moisan, K., Olivier, N., Pollono, C., Bustamante, P., Churlaud, C., Arrisol, R., Pillay, N., Pascal, A., Hollanda, S., Govinden, R., Bodin., N. (2019) Are Seychelles wild fish exposed to chemical contaminants? An overview. In From Ocean to Health conference, Mahé Island, Seychelles. (presented with C. Munschy)

Bodin, N., **Sabino, M.A.**, Elvevoll, E., Jensen, I-J., Pethybridge, H., Govinden, R., Belmont, C., Pascal, A., Souffre, A., Bustamante, P. (2019) Nutritional value of Seychelles wild fish and their contribution to food security. In From Ocean to Health conference, Mahé Island, Seychelles. (presented with N. Bodin, I-J. Jensen and H. Pethybridge)

Sabino, M.A., Bodin, N., Bustamante, P. (2021) Bioaccumulation des éléments traces dans les chaînes trophiques marines des Seychelles. In Colloque des doctorants de La Rochelle Université, La Rochelle, France.

Poster presentations

Sabino, M.A., Bodin, N., Hollanda, S., Albert, R., Pillay, N., Churlaud, C., Romanov, E., West, W., Bustamante, P. (2019) Regional patterns in mercury and selenium concentrations of swordfish in the Indian Ocean. In WIOMSA scientific symposium, Mauritius. (presented by N. Bodin)

Sabino, M.A., Govinden, R., Pethybridge, H., Blamey, L., Bustamante, P., Le Grand, F., Bodin, N. (2019) Resource partitioning between three sympatric species of spiny lobsters in the Seychelles coastal waters. In From Ocean to Health conference, Mahé Island, Seychelles. Available at: https://www.researchgate.net/publication/354023516_Resource_partitioning_between_three_sympatric_species_of_spiny_lobsters_in_the_Seychelles_coastal_waters

Sabino, M.A., Bodin, N., Arrisol, R., Pillay, N., Pascal, A., Hollanda, S., Churlaud, C., Govinden, R., Bustamante, P. (2019) Are Seychelles wild fish exposed to chemical contaminants? Non-essential trace elements. In From Ocean to Health conference, Mahé Island, Seychelles.

Bodin, N., **Sabino, M.A.**, Elvevoll, E., Jensen, I-J., Pethybridge, H., Govinden, R., Belmont, C., Pascal, A., Souffre, A., Bustamante, P. (2019) Nutritional value of Seychelles wild fish and their contribution to food security. In From Ocean to Health conference, Mahé Island, Seychelles. (poster shared with N. Bodin, I-J. Jensen and H. Pethybridge)

Sabino, M.A., Bodin, N., Bustamante, P. (2021) Bioaccumulation des nutriments et contaminants dans les chaînes trophiques marines des Seychelles [in FRENCH]. In Colloque des doctorants de La Rochelle Université, La Rochelle, France. Available at: https://www.researchgate.net/publication/354059373_Bioaccumulation_des_nutriments_et_contaminants_dans_les_chaines_trophiques_marines_des_Seychelles.

SCIENTIFIC REPORTS

Sabino, M.A., Bodin, N., Butamante, P. (2019) Nutrients and contaminants in Seychelles fisheries resources (SEYFISH), Research Agreement Collaboration between SFA and LIENSs, Progress report of the study period May 2018 – May 2019. La Rochelle University – CNRS UMR 7266, 44p.

Sabino, M.A., Bodin, N., Butamante, P. (2020) Nutrients and contaminants in Seychelles fisheries resources (SEYFISH), Research Agreement Collaboration between SFA and LIENSs, Progress report of the study period May 2019 – May 2020. La Rochelle University – CNRS UMR 7266, 137p.

R SCRIPTS

All statistical analyses performed in this thesis are freely available on GithHub repositories.

Repositoty created for all thesis analyses (one script by chapter)

Sabino, M.A. (2022) Analyses of trace element bioaccumulation performed in the thesis Sabino (2021). R script available at: https://github.com/magalisabino/Analyses_of_trace_element_bioaccumulation

Repositories created as part of peer-reviewed publications

Sabino, M.A. (2021) Fatty acid and isotopic niche computing with the nicheROVER package. Created as part of Sabino *et al*. (2021), entitled "*Habitat degradation increases interspecific trophic competition between three spiny lobsters in Seychelles*" (doi: 10.1016/j.ecss.2021.107368). R script available at: https://github.com/magalisabino/FattyAcid_Isotopic_niche_computing

Sabino, M.A. (2022) Clustering analysis from trace element profiles. Created as part of Sabino *et al*. (in review), entitled "*Regional patterns in mercury (Hg) and selenium (Se) concentration in swordfish from the Indian Ocean*". R script available at: https://github.com/magalisabino/TraceElement_Cluster_Analysis

SCIENCE POPULARISATION

Sabino, M.A. (2019) L'écologie dans ton assiette. Video presented as part of the 18th Festival du film [pas trop] scientifique, La Rochelle Université, La Rochelle, France. URL: https://www.dailymotion.com/video/x7n00lp

ABBREVIATIONS

%TFA	Percentage of Total Fatty Acid
Ag	Silver
AIC	Akaike Information Criterion
As	Arsenic
Cd	Cadmium
CI95%	Confidence Interval at 95%
Co	Cobalt
Cr	Chromium
CRM	Certified Reference Material
Cu	Copper
DL	Detection Limit
dw	Dry Weight
EEZ	Economic Exclusive Zone
FAME	Fatty Acid Methyl Ester
Fe	Iron
GAM	Generalised Additive Model
GLM	General Linear Model
Hg	Mercury
iAs	Inorganic Arsenic
ICP	Induced Coupled Plasma
JECFA	Joint FAO/WHO Expert Committee on Food Additives
LOQ	Limit of Quantification
MeHg	Methylmercury
Mn	Manganese
MS	Mass Spectrometry
Ni	Nickel
nMDS	Non-Metric Multidimensional Scaling
NWM	Northwest Monsoon
OES	Optical Emission Absorption
Pb	Lead
PCA	Principal Component Analysis
pH	Potential Hydrogen
PTI	Provisional Tolerable Intake
RDI	Recommended Daily Intake
rpm	Rotation Per Minute
Se	Selenium
SEM	Southeast Monsoon
SFA	Seychelles Fishing Authority
SIDS	Small Island Developing State
UN	United Nations
US-EPA and US-FDA	United States Environmental Protection Agency and United States Food and Drug Administration
V	Vanadium
ww	Wet Weight
Zn	Zinc

TABLE OF CONTENTS

LIST OF APPENDICES

1. GENERAL INTRODUCTION

Content

1.1. WHY STUDYING TRACE ELEMENT CONCENTRATIONS IN SEAFOOD?

One of the biggest challenges of the 21st century is the insurance of food security in a context of rapid growth of the global population. While the world population was estimated at 7.7 billion individuals in 2019, it is predicted to be around 9.7 by 2050, and almost 11 billion by 2100 (United Nations 2019). In this respect, the United Nations (UN) established 17 major goals to promote sustainable development, including goals related to food security: zero hunger (goal n°2; "end hunger, achieve food security and improved nutrition and promote sustainable agriculture") and good health and well-being (goal n°3; ensure healthy lives and promote well-being for all at all ages") (United Nations 2015) (Fig. 1.1). The UN also included goals related to resource management: responsible consumption and production (goal n°12; "ensure sustainable consumption and production patterns"), life below water (goal n°14; "conserve and sustainably use the oceans, seas and marine resources for sustainable development") and life on land (goal n°15; "protect, restore and promote sustainable use of terrestrial ecosystems, sustainably manage forests, combat desertification, and halt and reverse land degradation and halt biodiversity loss") (United Nations 2015) (Fig. 1.1).

Fig. 1.1. Sustainable development goals set by the United Nations (2015), with particular focus on those related to food security and resource management.

Ensuring food security is thus linked to three key aspects, (1) guarantee food supply while (2) sustainably manage resources so that it ensures food stocks for future generations,

and (3) guarantee a healthy diet for the global population. This implies that, in sustainable development, food nutritional quality, that is the fight against unbalanced diets, is as important as food quantity, i.e. the fight against malnutrition. In 2016, over 650 million people were obese (WHO 2020), thus being more exposed to developing diseases such as diabetes and cardiovascular diseases (Scherer and Hill 2016). In 2017, nearly 2 billion people suffered from nutrient deficiency across the world (Hawkes *et al.* 2017). It is thus critical to increase knowledge on the nutritional quality of food items, in order to better understand nutritional intakes and to improve diets.

Defining a healthy diet is a tricky process, as there is no consensus on the topic, although some trends can be highlighted (Skerrett and Willett 2010). A well-balanced and healthy diet includes consumption of macronutrients (i.e. carbohydrates, proteins and fats) and micronutrients (i.e. vitamins and minerals) (Koolman and Röhm 2011). Some of these nutrients, like carbohydrates, provide energy for human metabolism but are not essential to human health, as they can be synthesized from many molecules through human metabolism (Horn *et al.* 2005). Others, however, are not biosynthesized, or in insufficient quantities to meet physiological needs, and thus must be provided through the diet (Trustwell and Mann 2017). This is the case for amino acids, fatty acids, minerals and vitamins.

Minerals have many roles in animals, including structural, physiological, catalytic and regulatory ones (Alais *et al.* 2008; Koolman and Röhm 2011). For example, they can be a structural component of hard tissues like bones (i.e. calcium), participate to osmotic balance (i.e. potassium), serve as co-factors of proteins, enzymes or vitamins (e.g. cobalt – Co, manganese – Mn, selenium – Se, and zinc – Zn), or participate to respiratory pigment formation (e.g. copper – Cu for hemocyanin and iron – Fe) (Fox and Zimba 2018). Only some minerals are essentials, and they can be sorted in two categories: macroelements, of which the daily needed intake is superior to 100 mg (calcium, chlorine, magnesium, phosphorus, potassium and sodium) and microelements or trace elements, of which the daily needed intake is inferior to 100 mg (bore, Co, Cu, Fe, fluorine, iodine, Mn, molybdenum, Se, silicon and Zn) (Alais *et al.* 2008; Zoroddu *et al.* 2019). The essentiality of some other elements, like arsenic (As), chromium (Cr), nickel (Ni) and vanadium (V) is still under debate (Zoroddu *et al.* 2019). Both As and Cr deficiencies were shown to have negative effects on some animal metabolisms, such as perturbation of the amino acid methionine metabolism in rats (Uthus 2003) or diabetes

symptoms in goats (Frank *et al.* 2000), respectively. However, As role in human metabolism is still unclear, and recent works on Cr suggest that it would not be an essential element in mammals (Di Bona *et al*. 2011; Vincent 2017). These elements can therefore be classified as "potentially essential" trace elements.

Although the most common essential trace elements-related nutritional problems are associated with low intakes and thus nutrient deficiency, problems can also arise from too high intakes resulting in trace element toxicity (Goldhaber 2003). For example, at critical level, Cu and Fe can cause liver damage, or have negative effects on cardiovascular and central nervous systems in the case of Fe (Goldhaber 2003). Thus, the essentiality of a trace element for human metabolism depends on the dose (Fig. 1.2), with some essential trace elements having narrow ranges for which they are neither in deficiency or in excess (e.g. Fe) (American Food and Nutrition Board of the Institute of Medicine National Academy of Sciences 2019a, b).

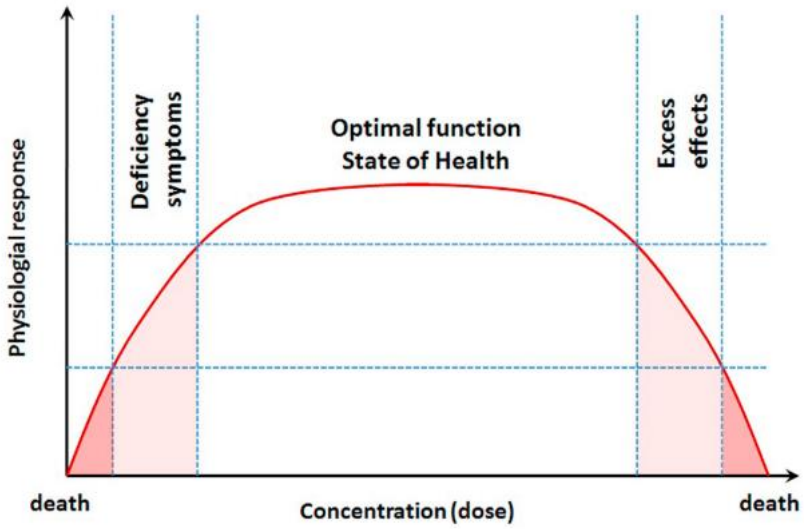

Fig. 1.2. Dose-response diagram for an essential trace element (from Zoroddu *et al*. 2019).

Some problems can also arise from the presence of non-essential trace elements in the food, such as cadmium (Cd), mercury (Hg), or lead (Pb), which are toxic even at low concentrations (Mudgal *et al.* 2010). Exposure to non-essential elements can cause both acute and chronic effects (Bosch *et al*. 2016). Although non-essential elements are naturally present in the environment at trace levels, anthropogenic activities contributed to increase those levels, especially in the aquatic environments (Mudgal *et al*. 2010; Zand *et al*. 2015). Hg in particular, has become a worldwide public health concern due to its high presence in the marine

environment (Jaishankar *et al*. 2014). Its most toxic form is its methylated form, methylmercury (MeHg), as it is the most bioavailable, and thus is readily bioaccumulated (i.e. increase in concentration through time) in animal tissues and biomagnified (i.e. increase in concentration from one trophic level to another; Bienfang *et al.* 2013) through food chains (Bosch *et al*. 2016).

Due to similar chemical properties between some trace elements (Hill and Matrone 1970), essential trace elements may modify health risks from exposure to non-essential trace elements, but deficiency in those essential trace elements may enhance non-essential trace elements accumulation, thus may increase potential toxicity. As an example, a diet rich in Zn has been shown to reduce Cd toxicity (Webb 1979), while Fe and Zn deficiency enhances Cd and Pb absorption (Goyer 1997). Such increase in toxicity for non-essential trace elements would thus add to essential trace element deficiency negative effects on human metabolism.

In regards to these nutritional needs, seafood has long been known to play an important role in a healthy and balanced diet, as it provides numerous essential macro- and micronutrients (Larsen *et al.* 2011; Weichselbaum *et al.* 2013). The most recognized nutrients are two omega-3 long-chain polyunsaturated fatty acids (the eicosapantaenoic acid and the docosahexaenoic acid) that are most known to help reduce cardiovascular disease risks (Lu *et al*. 2011) and to have anti-inflammatory properties (Figueras *et al*. 2011). Moreover, seafood is also known to contain significant levels of essential trace elements, such as Cu, Fe and Zn (Gupta and Gupta 2014). It has been reported that fish and lobsters can provide up to 50% of the needed dietary intake in a balanced diet (Copper Development Association 2019). Fish is also a good source of heme Fe, which is more readily absorbed than other forms of Fe (Ohio State University 2015). However, seafood is especially known to be a good source of Se, whose main function is as a component of important antioxidant enzymes, and therefore participates to protect the body against oxidative damage (Weichselbaum *et al*. 2013). It also has a protection role against MeHg toxicity. Indeed, MeHg is a highly neurotoxic organic form of Hg and Se has a high binding affinity to it, reducing its deleterious effects (Bernhoft 2012; Syversen and Kaur 2012). It has been recognized that seafood is the main pathway of exposure to MeHg in the human body (Mergler *et al*. 2007). Besides Hg, seafood also contains other non-essential elements like Cd and Pb that can harm human consumers (Bosch *et al.* 2016). As a consequence of its high micronutrient contents, seafood consumption is thought to be critical in promoting

food security and healthy diets (Béné *et al.* 2015), and it could have the largest impact of all foods in the fight against micronutrient deficiency (Hicks *et al*. 2019).

1.2. FACTORS INFLUENCING TRACE ELEMENT CONCENTRATIONS IN CAPTURE FISHERIES SPECIES: IMPORTANCE OF TROPHIC ECOLOGY AND PHYSIOLOGICAL PROCESSES

Essential and non-essential trace element concentrations in marine organisms depend directly on the bioaccumulation capacity of the considered species, that is its ability to accumulate trace elements through time, which itself varies according to many intrinsic and extrinsic factors (Fig. 1.3). In addition, the presence of trace elements in the environment, and especially in the ocean, is also function of many biotic and abiotic factors, either natural or human-induced.

The accumulation of trace elements in marine consumers first depends on the equilibrium between absorption and excretion rates, meaning that bioaccumulation occurs when absorption rate is higher than excretion rate (Hodson 1988). This equilibrium is first linked to the physiological role of the considered element, and essential trace elements that have important roles in biological processes (e.g. Co, Cu, Fe, Mn, and Zn) are supposed to be preferentially retained. Indeed, metabolic requirements will favour the retention of the elements that are needed by organisms. In this respect, the chemical properties of non-essential trace elements are important factors to consider, as some of them have similar properties than essential trace elements (Hill and Matrone 1970). For example, because they have properties than are similar to metallothionein-associated trace elements (i.e. Cu and Zn), some non-essential elements (i.e. Ag, Cd, and Hg) bind to metallothioneins, which are proteins involved in the cellular regulation of Cu and Zn, both being essential trace elements (Rainbow 2007). As a consequence, these non-essential trace elements may be more readily bioaccumulated through co-accumulation on metallothioneins (Rainbow 2007). Finally, the equilibrium between absorption and excretion is highly influenced by excretion capacity (i.e. the efficiency, presence or absence of a detoxifying process) and excretion rate (Kojadinovic *et al*. 2007; Raimundo *et al*. 2013).

In a more general aspect, the accumulation of trace elements, either essentials or non-essentials, is dependent on many physiological processes in marine organisms that can be species (Bustamante *et al*. 1998; Nair *et al*. 2006; Metian *et al.* 2008; Hédouin *et al*. 2009; Rejomon *et al.* 2010; Le Croizier *et al*. 2016), age- (Raimundo *et al*. 2013; Goutte *et al*. 2015) or

size-dependent (Anan *et al.* 2005; Kojadinovic *et al*. 2007; Barone *et al*. 2013). Although some studies found no differences of trace element accumulation between males and females (e.g. Chouvelon *et al.* 2017), physiological needs can also be sex-dependant, which may influence trace element bioaccumulation in marine consumers.

In addition to physiological considerations, the absorption of trace elements by a marine consumer will also depend on the bioavailability of the considered element, that is the proportion which is able to be absorbed through the intestinal epithelium and which will therefore interact with the consumers' metabolism (Hodson 1988). In the ocean, trace elements are present under many physicochemical forms, and only bioavailable trace element forms will be assimilated and retained by marine organisms while non-bioavailable forms will be egested (Neff 2002a).

First, trace element in the environment will depend on trace element inputs, either naturally or from anthropogenic activities, through runoffs, rivers and estuaries and even sewage pipes (Herut and Kress 1997). For example, both Cd and Hg are naturally present in very low concentrations in seawater, originating from volcanic activity for example, while anthropogenic activities, including industrial processes, mining activities and even burning of fossil fuels, contributed to increase their concentrations in seawater (Boening 2000; Bernhoft 2013). As a consequence, trace element exposure and bioaccumulation in marine consumers is expected to vary regionally according to local hydrodynamics and/or importance of local human activities.

Trace element availability will also differ according to the considered compartment (i.e. benthic *vs* demersal *vs* pelagic; coastal *vs* offshore) as a result of chemical and/or biochemical reactions in the water column. For example, sediments are known to be a reservoir for trace elements (Abdallah 2008; Velusamy *et al*. 2014), as several trace elements forms in the water tend to adsorb and/or precipitate, and will thus deposit and accumulate on the seafloor (Neff 2002a). As a consequence, benthic and benthic feeding organisms will be more exposed to some trace elements (Ratte 1999; Lee *et al.* 2000; Abdallah 2008). Among them, burrowing species are also more exposed to trace element intake and accumulation by being in constant contact with the sediment (Rainbow 1998; Copaja *et al.* 2017). Demersal species are also expected to have higher trace element concentrations than pelagic ones as a result of their

interaction with benthic species and the regular contact with metal-enriched bottom sediments (Rejomon *et al*. 2010).

Although trace element bioavailability in the water column is essential to understand bioaccumulation in capture fisheries species, it is generally admitted that the trophic pathway is the main route for trace element bioaccumulation in marine consumers (Raimundo *et al.* 2013). In this respect, primary producers constitute a key trophic level as they form the first link between waterborne elements and primary consumers, and as they have a capacity for high trace element intake (Milinki *et al.* 2011; Bonanno and Orlando-Bonaca 2018). Moreover, taxonomic differences in trace element concentrations exist among macroalgae and microalgae (Twining and Baines 2013; Twining *et al*. 2015; Cabrita *et al*. 2016), which may induce differences in trace element trophic transfer between coastal and offshore food webs for example. Linked with dietary exposure, trophic interactions (i.e. length and complexity of the food web) play an important role in the variation of trace element concentrations in capture fisheries species, as it may enhance (i.e. biomagnification) or diminish (i.e. biodilution) trace element bioaccumulation in marine consumers (e.g. Wang 2002; Chouvelon *et al*. 2012; Metian *et al.* 2013; Penicaud *et al*. 2017).

In light of these elements, it is expected that trace element concentrations in marine consumers will be the result of the interaction between physiological processes and trophic ecology of the consumer. Given the important role of trace element availability and thus of the trophic pathway, it is thus crucial to study their flow in marine food webs. This is especially true in a changing climate, as anthropogenic modifications of ecosystems due to biodiversity loss and thus changes in trophic chain structure could directly affect capture fisheries resources-based human diets.

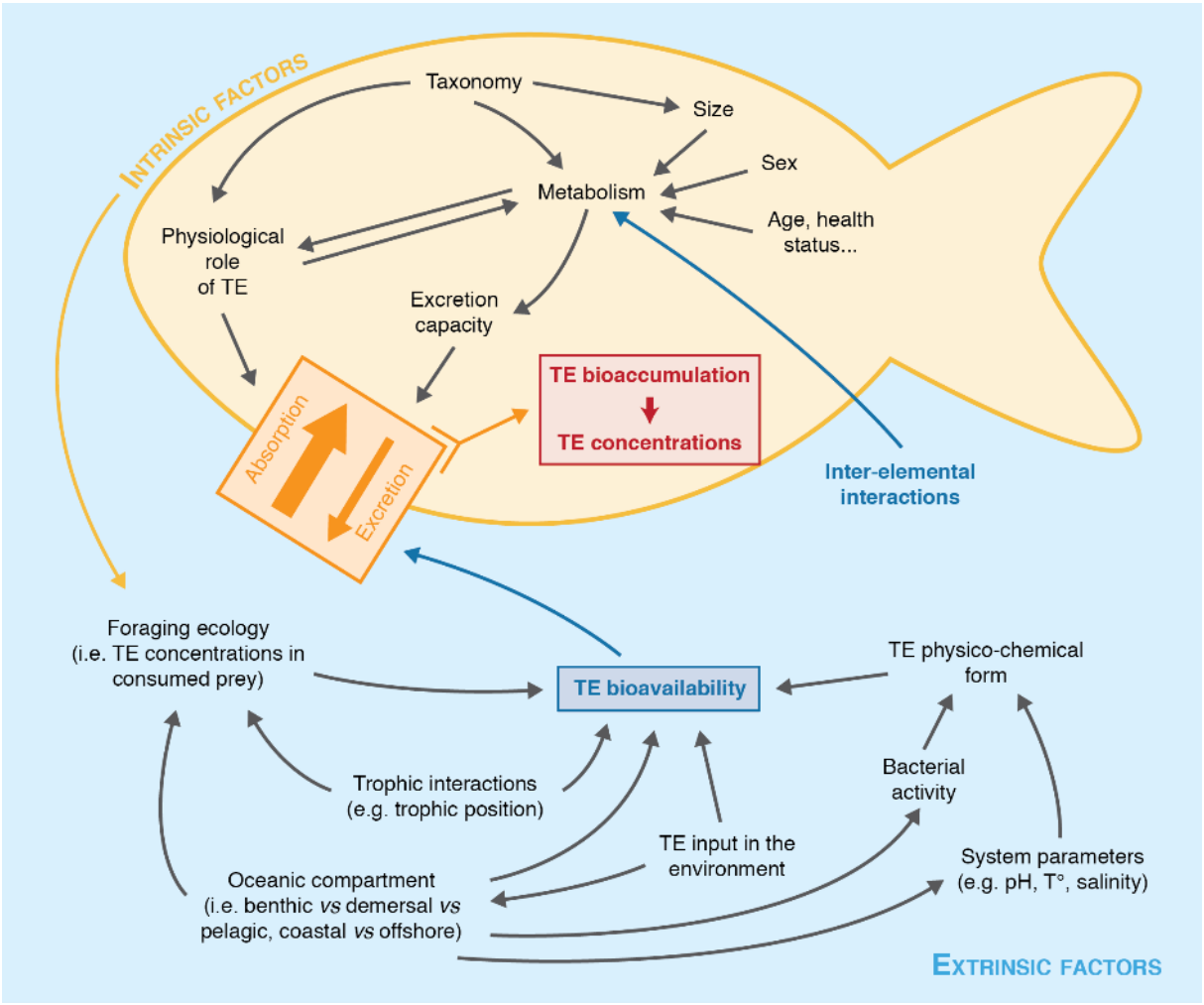

Fig. 1.3. Factors potentially influencing trace element (TE) bioaccumulation in marine consumers. Summarised from section 1.2.

1.3. TOOLS FOR THE STUDY OF TROPHIC ECOLOGY IN MARINE ORGANISMS

To investigate trophic ecology, several tracers have proven to be useful, based on the idea of "you are what you eat", that is the biochemical composition of a consumer reflects that of the prey. In this respect, stable isotopes of carbon ($\delta^{13}C$) and nitrogen ($\delta^{15}N$) are the most commonly used (Layman *et al.* 2011). The $\delta^{13}C$ is considered a reliable indicator of primary production sources in aquatic environments, as they differ in carbon isotope composition and the trophic fractionation of this isotope is low, i.e. comprised between 0-1 ‰ from one level to another (Post 2002). The $\delta^{15}N$ reflects the metabolism of protein from the diet, and follows an enrichment of 3-4 ‰, from one trophic level to another (Post 2002; Ramos and González-Solís 2012). It thus can be used to assess the trophic level (i.e. absolute trophic position) of an organism by conversion of the $\delta^{15}N$ values to trophic factor using an isotopic baseline, or to

compare relative trophic position (i.e. $\delta^{15}N$ ratios) when the baseline is not available (Post 2002; Perkins *et al*. 2014).

The use of the fatty acid composition of organisms is another powerful trophic tracer (reviewed in Dalsgaard *et al*. 2003; Budge *et al*. 2006; Iverson 2009). Fatty acids are rather ubiquitous in the marine environment, but the specific fatty acid composition of an organism can be seen as its "signature". As ingested fatty acids are incorporated into animal tissues largely unmodified, it is possible to distinguish fatty acids biosynthesized by the consumers from fatty acids that come only from the diet (Iverson 2009). Thus, studying the fatty acid composition of consumers can bring insight into their foraging ecology.

By studying spatial and temporal changes in the biochemical composition of consumers, it is possible to examine intra- and intergroup variations in trophic ecology. For this, trophic niches inferred from stable isotope or fatty acid data are particularly useful, as their metrics (i.e. niche size and probability of niche overlap) give both intra- and intergroup information. Typically, a group of individuals' niche size can be used as a proxy for the diversity of biochemically distinct prey eaten by this group (i.e. intragroup variability), while the probability of overlap between two groups of individuals gives indications on the degree of similarity of the biochemical composition of their prey (i.e. intergroup variability) (Costa-Pereira *et al*. 2019) (Fig. 1.4).

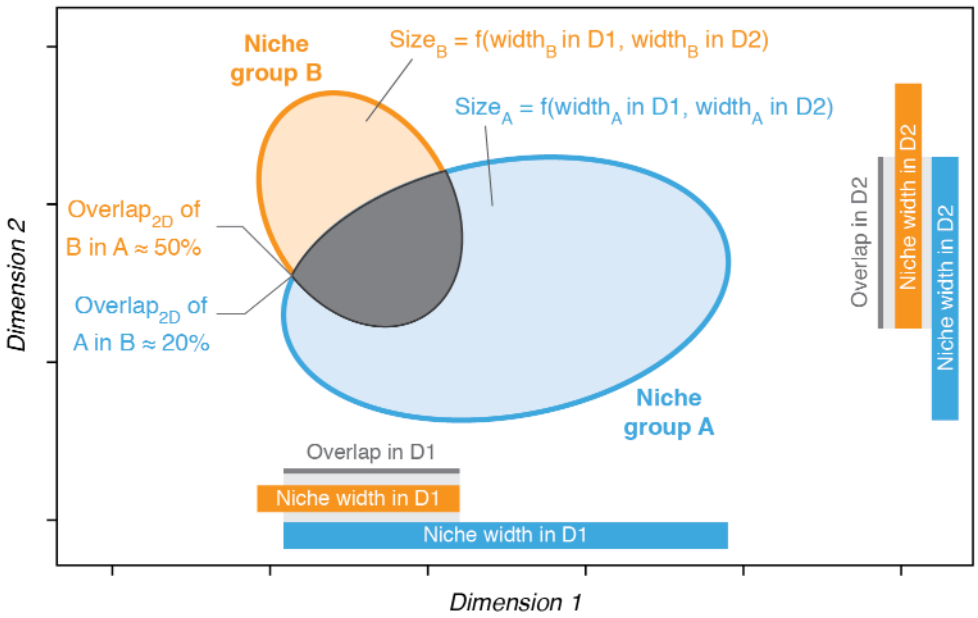

Fig. 1.4. Niche metrics and their interpretation in terms of trophic ecology. Niche overlap (%) represents the probability of an individual from group A to be found in the niche of group B. D = dimension.

As trophic tracers are influenced by both environmental and biological processes, the use of one tracer only can lead to misinterpretations of trophic structure (Ramos and González-Solís 2012). However, combining several tracers, like stable isotopes and fatty acids, can help reduce misinterpretations and even strengthen interpretations when tracers are correlated (Sardenne *et al*. 2017). In addition, both types of trophic tracers can give complementary information on a consumers' diet, due to different times of integration (i.e. turnover rates) in consumers' tissues. In the muscle tissues of large consumers, the turnover rate of stable isotopes ranges from a few months to several years (Hesslein *et al*. 1993) while, in fatty tissues (e.g. digestive tissues or muscle in some fatty consumer species), the turnover rate of fatty acids ranges from days to weeks (Budge *et al*. 2006; Arts *et al.* 2009). Thus, combining the analysis of these tissues, stable isotopes can be considered as long-term trophic tracers while fatty acids reflect short-term trophic ecology. Many studies combined both stable isotopes and fatty acids to investigate trophic ecology of marine consumers (e.g. Alfaro *et al*. 2006; Jaschinski *et al*. 2011; Connan *et al*. 2014; Brewster *et al*. 2017; Wang *et al*. 2019), showing the complementarity of both trophic tracer types.

1.4. STUDYING TRACE ELEMENT BIOACCUMULATION IN CAPTURE FISHERIES RESOURCES AS A MAJOR CONCERN FOR SMALL ISLAND DEVELOPING STATES (SIDS): CASE OF THE SEYCHELLES ISLANDS

Small Island Developing States (SIDS) have the particular feature to highly rely on marine resources for local subsistence of their populations and for their economy, due to their small land size (i.e. limited terrestrial resources), insularity and remoteness (Briguglio 1995). Among them, the Seychelles Islands are a typical example, as fisheries, together with marine resource-related tourism, are the two pillars of its economy (Heath-Brown 2016). In this country, the fisheries sector accounts for 15-20% of total gross domestic products and around 27% of global value added (Robinson *et al.* 2006; Bistoquet *et al.* 2018). There are three major types of fisheries in the Seychelles. The industrial fishery, mainly composed of foreign licensed vessels, targets tunas and tuna-like species in the Seychelles economic exclusive zone. The semi-industrial fishery, consisting of local longliners, also targets large pelagic fish (i.e. tunas and billfishes) in the Seychelles Exclusive Economic Zone (EEZ). Finally, the artisanal small-scale fisheries consist of a diverse range of boats and gears, and target various species in nearshore waters of the Mahé Plateau, notably reef fishes, spiny lobsters and sea cucumbers (Robinson

et al. 2006; WorldBank 2017). The industrial fishery, especially through the tuna canning industry, is a key source of revenue for the Seychelles, as it represents around 17% of the country's employment and 68% of the entire export trade (WorldBank 2017; Seychelles Fishing Authority 2018). However, the artisanal fisheries are of key importance for local food security and local livelihoods (Zeller and Pauly 2019). Capture fisheries products generated by those fisheries is the main source of proteins and micronutrients for the local population, resulting in Seychelles Islands having one the highest rate of marine fish consumption in the world (57 $kg.person^{-1}.year^{-1}$) (WorldBank 2017; Hicks *et al*. 2019).

The reliance of the Seychelles on fisheries and, more generally, on marine resources, make them particularly vulnerable to climate change and its related consequences on biodiversity and ecosystems health and production (Government of Seychelles 2013; Khan and Amelie 2015). This has led the Seychelles to be a leading stakeholder in integrating the 'Blue Economy' concept by adopting its principles as national priorities (Khan and Amelie 2015; Moustahfid *et al*. 2018). As capture fisheries resources are the main Hg exposure pathway, its toxicological risk, for example, has been extensively investigated through an international research project, the Seychelles Child Development Study (Shamlaye *et al.* 2004). This project aimed to study the link between Hg exposure during pregnancy and child development in the Seychelles population and led to numerous publications on the topic, from the mid-1980s until today. Recent studies have also been conducted on trace elements in pelagic systems on tuna and billfish species (e.g. Bodin *et al*. 2017; Hollanda *et al*. 2017). However, other systems like demersal or benthic ecosystems remain largely poorly documented in many aspects whereas they provide an important fraction of the capture fisheries resources consumed by the local population. There is thus great need of specific studies on this matter, in order to better understand the current and future availability of nutrients for the Seychelles population, and their potential exposure to marine non-essential elements (i.e. Cd, Hg and Pb) and related toxicological risk.

1.5. OBJECTIVES OF THE PROJECT

The importance of essential and non-essential elements in capture fisheries species for food security in SIDS such as the Seychelles Islands is now well established. But those concentrations depending on many intrinsic and extrinsic factors, such as physiology or trophic ecology, it is evident that studying trace element concentrations only is not sufficient in a context of

changing climate. To better understand their variation in capture fisheries species and to foresee future essential trace element supply and non-essential trace element exposure for SIDS populations, it is essential to also investigate their bioaccumulation in capture fisheries species, and thus the factors influencing those concentrations.

The **main objectives** of the project were (1) to **characterise the levels of the concentrations of** essential, potentially essential and non-essential **trace elements in a wide range of Seychelles capture fisheries species** and (2) to **better understand the factor influencing their bioaccumulation which led to these levels**. As trace element concentrations in a given species are influenced by many intrinsic and extrinsic factors, the latter were explored first in this manuscript, before investigating nutrient availability and trace element exposure for Seychellois' capture fisheries resources-based diet.

In this respect, in the first part of the results (**Chapter 1**), I searched for **patterns in Seychelles capture fisheries species trace element concentrations**. In addition to providing a broader approach on trace element concentrations than when considering the species level, it also allowed the first assessment on the ecological factors influencing trace elements concentrations in Seychelles marine systems.

Habitat is a major factor influencing interspecific variations in trace element concentrations in capture fisheries species, but also influences trophic tracers like nitrogen stable isotope (i.e. $\delta^{15}N$ baseline and thus the determination of the trophic position). When baselines are not available, like in the Seychelles marine systems, this makes difficult or even impossible the investigation and comparison of the effects of trophic ecology on trace element bioaccumulation for all species at the same time. In addition, physiological processes are highly taxonomic- and thus species-dependant. Thus, in order to bring insight into trace element bioaccumulation processes in emblematic marine systems of the Seychelles, it seemed appropriate to select one model species per marine compartment.

The **second part** of the manuscript thus **investigates the factors influencing trace element bioaccumulation in the three marine compartments** (i.e. benthic, demersal and pelagic) **through the study of model species** (i.e. spiny lobsters in chapter 2, emperor red snapper in chapter 3 and swordfish in chapters 4 and 5). This allowed the exploration of both intrinsic factors, such as individual sizes (i.e. proxy of age and physiological needs) and sex, and extrinsic factors, such as habitat, diet and/or trophic position. Specific factors linked to the habitat of model species

(e.g. effect of coral bleaching on reef-associated model species) were also considered. As swordfish is a highly migratory species and as trace element bioaccumulation vary regionally as a result of different input dynamics, the regional variation of Hg and Se bioaccumulation at the scale of the Indian Ocean was also investigated (Chapter 4).

Finally, in **Chapter 6**, trace element concentrations in capture fisheries species were compared to exposure safety limits and nutritional recommended daily intakes, in order to **establish a baseline on the essential trace element supply and non-essential trace element exposure in Seychellois' diet**.

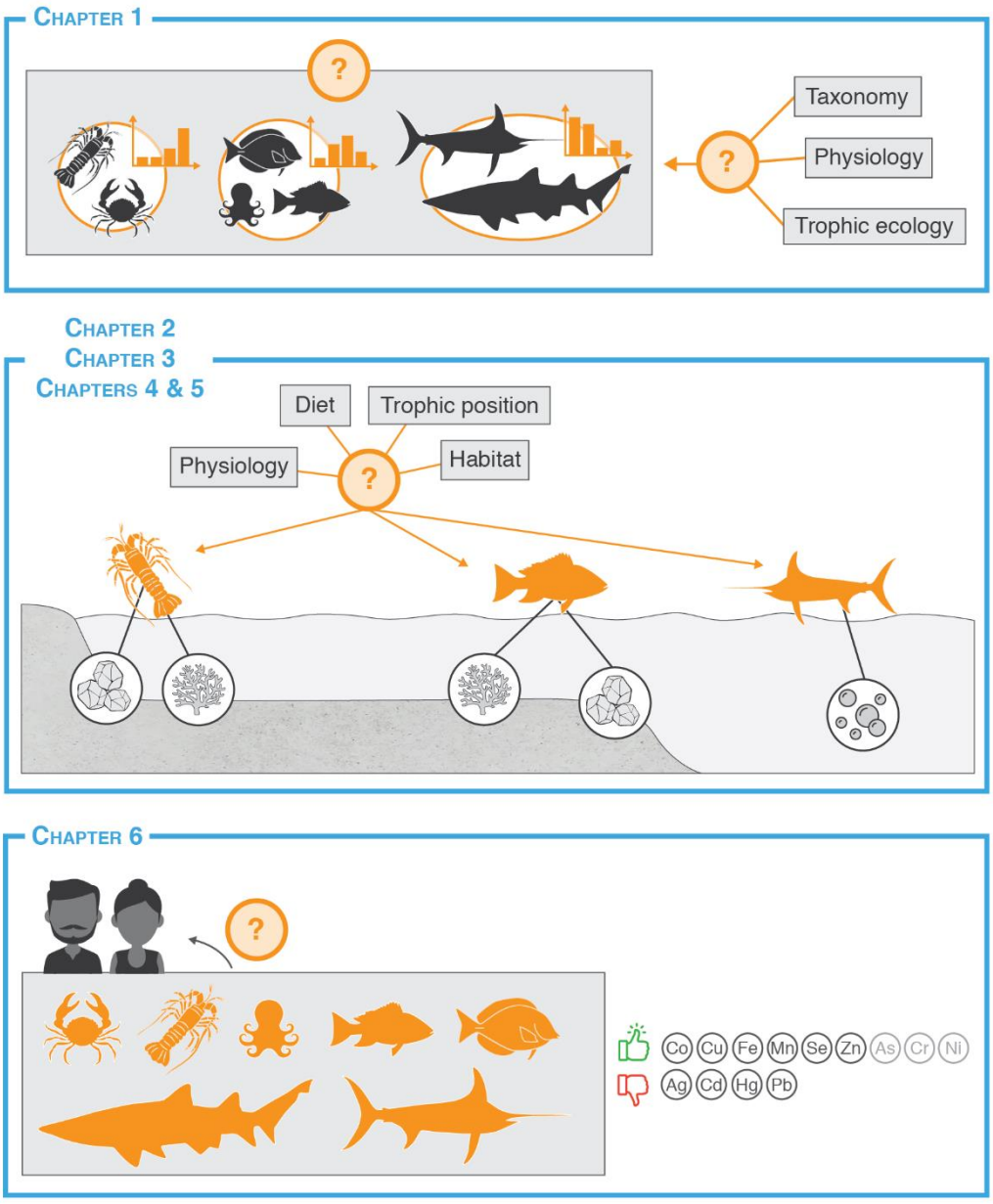

Fig. 1.5. Graphical summary of the questions investigated in the different chapters.

2. General material & methods

Content

2.1. STUDY AREA: THE SEYCHELLES ISLANDS

The Seychelles is an African small island developing state in the Western Indian Ocean, composed of an archipelago comprising 115 islands which are distributed over an EEZ of about 1.3 million km^2 (Robinson et al. 2006) (Fig. 2.1). The islands are classified into two main groups, the Inner Islands, comprising the granitic islands of the Mahé Plateau, and the Outer Islands, comprising the coralline islands of the Amirantes group, the Farquhar group and the Aldabra group (Jennings *et al*. 2000) (Fig. 2.1). Most of the Seychelles population reside on the three main islands (i.e. Mahé, Praslin and La Digue), which caused most of the fisheries and fishing grounds to be centralized around the Mahé Plateau.

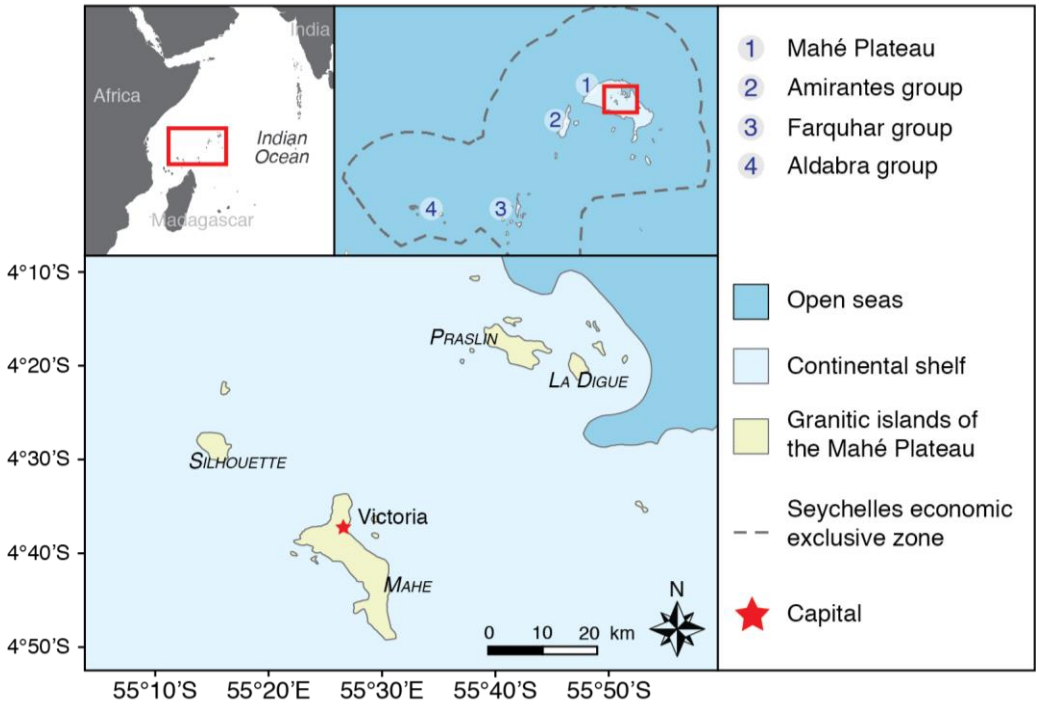

Fig. 2.1. Location of the Seychelles Islands in the Western Indian Ocean and Inner Islands on the Mahé Plateau.

The climate of the Seychelles is humid tropical, with high temperatures (mean 26.9°C) and high humidity (mean 80%) (Jennings *et al.* 2000), and is characterised by two main monsoon seasons separated by two short pre-monsoon periods (Chang-Seng 2007) (Fig. 2.2). The northwest monsoon (NWM, i.e. December to March) is considered as the summer season and the principal rainy season, and thus it is characterised by warm temperatures and abundant rains. Winds are predominantly from the west/north-west but are generally light. It is also the

cyclone season in the Southern Indian Ocean, which has an indirect effect on the climate of the Seychelles Islands by bringing high rates of rain, especially over the southern islands. The pre-southeast monsoon (pre-SEM, i.e. April) is the calmest and warmest period. It marks the end of the rainy season and, during this month, winds weaken and reverse to the south-east direction. The southeast monsoon (SEM, i.e. May to October) is a drier and cooler season. Rains during this period are usually sparse, light and short-lived. Winds are predominantly from the south-east. Finally, the pre-northwest monsoon (pre-NWM, i.e. November) is a warm season, with very light winds. It is characterised by a shift in wind regime from south-east to north-west and it marks the onset of the rainy season (Chang-Seng 2007).

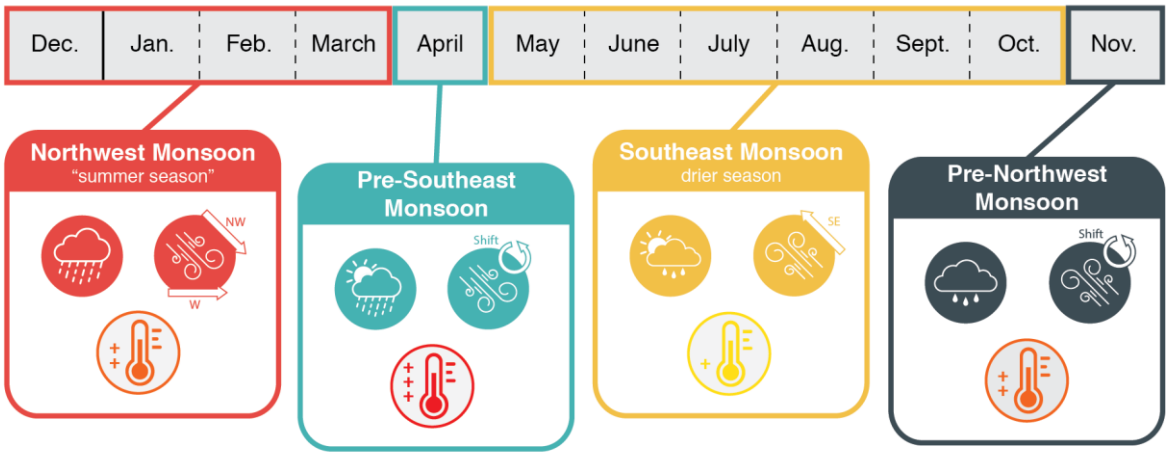

Fig. 2.2. Climate of the Seychelles Islands and characteristics of each season. Summarised from Chang-Seng (2007). For temperature, colour intensity is function of mean temperature during each season (i.e. yellow for cooler temperature and red for warmer temperatures).

Data on the primary production occurring in the oceanic waters surrounding the Seychelles are scarce, and thus little is known about the effect of climate on the primary production. However, waters are known to be characterised by low rates of production that vary according to the monsoon seasons. In general, primary production is relatively higher during the southeast monsoon season than during the northeast monsoon season (ASCLME 2012). Moreover, some regions may be more productive than others. For example, atolls may induce upwelling, which would help to increase production locally. Also, the nutrient regime is different between granitic and coralline islands. While nutrient inputs around coralline islands are from oceanic waters, localized upwelling and nitrogen fixation, the granitic islands of the

inner Seychelles receive more rainfall and are often forested, so high nutrient concentrations are expected to be present in runoffs (Jennings *et al*. 2000).

2.2. SAMPLE COLLECTION AND PREPARATION

A total of 54 marine species (1 cephalopod species, 4 crustacean, 7 elasmobranch and 42 teleost fish species) were caught by semi-industrial and artisanal fishing boats with various fishing gears between 2013 and 2019 (Table 2.1). Tissue samples were collected either directly onboard fishing or research vessels by trained fishers or scientists and stored frozen until landing (maximum 12 days at -20°C), or after fish unloading by scientists at the Seychelles Fishing Authority Research Laboratory. All samples were then stored as soon as possible in a deep-freezer (-80°C) until further specific pre-treatment and analysis.

As one of the main objectives of the project was to characterise essential trace element supply and non-essential trace element exposure through capture fisheries resources consumption, only edible parts (i.e. mantle for octopus, tail muscle for spiny lobster, body muscle for spanner crab and dorsal muscle for teleosts and elasmobranchs) were used for trace element analysis. Samples were analysed for 14 trace elements, i.e. silver (Ag), arsenic (As), cadmium (Cd), cobalt (Co), chromium (Cr), copper (Cu), iron (Fe), mercury (Hg), manganese (Mn), nickel (Ni), lead (Pb), selenium (Se), vanadium (V) and zinc (Zn). Stable isotopes of carbon ($\delta^{13}C$) and of nitrogen ($\delta^{15}N$) were also analysed in those tissues for use as long-term trophic tracers. Subsamples for the analysis of trace elements and stable isotopes were freeze-dried over 72 hr and stored in a dry environment prior to any analysis.

Fatty acids were analysed in hepatopancreas tissues from spiny lobsters and in muscle tissues from swordfish, for use as short-term trophic tracers. These subsamples remained fresh-frozen at -80°C until fatty acid analysis.

Table 2.1. Details on the studied species.

Classification	Order	Family	Scientific name	English name	French name	Seychelles creole name	FAO code	Fishery type	Fishing gear	Habitat
Cephalopod	Cephalopoda	Octopodidae	*Octopus cyaneus*	Big blue octopus	Gros poulpe bleu	Zourit	OQC	Artisanal	Hand gathering	Nearshore Reef
Crustacean	Brachyura	Raninidae	*Ranina ranina*	Spanner crab	Ranine dentée	Krab ziraf	RAQ	Artisanal	Gillnets and entangling nets	Nearshore Plateau
	Reptantia	Palinuridae	*Panulirus longipes*	Longlegged spiny lobster	Langouste diablotin	Oumar rouz	LOJ	Artisanal	Hand gathering	Nearshore Reef
			Panulirus penicillatus	Pronghorn spiny lobster	Langouste fourchette	Oumar gro latet	NUP	Artisanal	Hand gathering	Nearshore Reef
			Panulirus versicolor	Painted spiny lobster	Langouste barriolée	Oumar ver	NUV	Artisanal	Hand gathering	Nearshore Reef
Elasmobranch	Carcharhiniformes	Carcharhinidae	*Carcharhinus amblyrhynchos*	Grey reef shark	Requin à queue noire	Reken bar	AML	Artisanal	Hooks and lines	Nearshore Plateau
			Carcharhinus brevipinna	Spinner shark	Requin gracile	Reken nennen pwent	CCB	Artisanal	Hooks and lines	Nearshore Plateau
			Carcharhinus limbatus	Blacktip shark	Requin pointes noires	Reken nennen pwent	CCL	Artisanal	Hooks and lines	Nearshore Plateau
			Carcharhinus sorrah	Spot-tail shark	Requin à queue tachetée	Reken nennen pwent	CCQ	Artisanal	Hooks and lines	Nearshore Plateau
			Galeocerdo cuvier	Tiger shark	Requin tigre commun	Reken demwazel	TIG	Artisanal	Hooks and lines	Offshore
		Sphyrnidae	*Sphyrna mokarran*	Great hammerhead	Grand requin marteau	Reken marto blan	SPK	Artisanal	Hooks and lines	Offshore
			Sphyrna lewini	Scalloped hammerhead	Requin-marteau halicorne	Reken marto rouz	SPL	Artisanal	Hooks and lines	Nearshore Plateau
Teleost fish	Acanthuroidei	Acanthuridae	*Acanthurus mata*	Elongate surgeonfish	Chirurgien élégant	Sirizyen navi / Makwer	DGW	Artisanal	Traps	Nearshore Reef
Teleost fish	Acanthuroidei	Siganidae	*Siganus sutor*	Shoemaker spinefoot	Sigan pintade	Kordonnyen blan	IUU	Artisanal	Traps	Nearshore Reef

Table 2.1. Details on the studied species. (continued)

Classification	Order	Family	Scientific name	English name	French name	Seychelles creole name	FAO code	Fishery type	Fishing gear	Habitat
Teleost fish	Acanthuroidei	Siganidae	*Siganus argenteus*	Streamlined spinefoot	Sigan vermiculé / Cordonnier soule femme	Kordonnyen soulfanm / Kannalo	IGA	Artisanal	Traps	Nearshore Reef
	Perciformes	Sphyraenidae	*Sphyraena jello*	Pickhandle barracuda	Bécune jello	Bekin karo	BAC	Artisanal	Hooks and lines	Nearshore Plateau
	Percoidei	Carangidae	*Caranx sexfasciatus*	Bigeye trevally	Carangue vorace	Karang nwar / Karang grolizye	CXS	Artisanal	Hooks and lines	Nearshore Plateau
			Gnathanodon speciosus	Golden trevally	Carangue royale	Karang saser	GLT	Artisanal	Hooks and lines	Nearshore Plateau
			Carangoides malabaricus	Malabar trevally	Carangue monique	Manik	NGS	Artisanal	Hooks and lines	Nearshore Plateau
			Carangoides fulvoguttatus	Yellowspotted trevally	Carangue pailletée	Karang plat	NGU	Artisanal	Hooks and lines	Nearshore Plateau
			Carangoides gymnostethus	Bludger	Carangue blanc	Karang balo	NGY	Artisanal	Hooks and lines	Nearshore Plateau
			Caranx melampygus	Bluefin trevally	Carangue aîle bleue	Karang ver	NXM	Artisanal	Hooks and lines	Nearshore Plateau
		Lethrinidae	*Gymnocranius grandoculis*	Blue-lined large-eye bream	Empereur tatoué	Kaptenn blan	GMW	Artisanal	Hooks and lines	Nearshore Plateau
			Lethrinus crocineus	Yellowtail emperor	Empereur à queue jaune	Laskar	ICZ	Artisanal	Hooks and lines	Nearshore Plateau
			Lethrinus microdon	Smalltooth emperor	Empereur tidents	Bek bek	LEN	Artisanal	Hooks and lines	Nearshore Plateau
			Lethrinus nebulosus	Spangled emperor	Empereur Saint Pierre	Kaptenn rouz	LHN	Artisanal	Hooks and lines	Nearshore Plateau
			Lethrinus variegatus	Slender emperor	Empereur bas cou	Baksou	LHV	Artisanal	Hooks and lines	Nearshore Plateau
			Lethrinus enigmaticus	Blackeye emperor	Lascar	Laskar	LTE	Artisanal	Hooks and lines	Nearshore Plateau

Table 2.1. Details on the studied species. (continued)

Classification	Order	Family	Scientific name	English name	French name	Seychelles creole name	FAO code	Fishery type	Fishing gear	Habitat
Teleost fish	Percoidei	Lethrinidae	*Lethrinus mahsena*	Sky emperor	Empereur mahsena	Madanm beri	LTQ	Artisanal	Hooks and lines	Nearshore Plateau
			Lethrinus lentjan	Pink ear emperor	Empereur lentille	Zekler	LTS	Artisanal	Hooks and lines	Nearshore Plateau
		Lutjanidae	*Aprion virescens*	Green jobfish	Vivaneau job	Zob gri	AVR	Artisanal	Hooks and lines	Nearshore Plateau
			Etelis coruscans	Deepwater longtail red snapper	Vivaneau flamme	Zob laflanm	ETC	Artisanal	Hooks and lines	Nearshore Plateau
			Lutjanus bohar	Two-spot red snapper	Vivaneau chien rouge	Varavara	LJB	Artisanal	Hooks and lines	Nearshore Plateau
			Lutjanus gibbus	Humpback red snapper	Vivaneau pagaie	Terez	LJG	Artisanal	Hooks and lines	Nearshore Plateau
			Lutjanus lutjanus	Bigeye snapper	Vivaneau gros yeux	Madras rouz / Madras pate	LJL	Artisanal	Hooks and lines	Nearshore Plateau
			Lutjanus sebae	Emperor red snapper	Vivaneau bourgeois	Bourzwa	LUB	Artisanal	Hooks and lines	Nearshore Plateau
			Lutjanus sanguineus	Humphead snapper	Vivaneau têtu	Bordmar	LZJ	Artisanal	Hooks and lines	Nearshore Plateau
		Mullidae	*Parupeneus barberinus*	Dash-and-dot goatfish	Rouget-barbet barberin	Rouze tas / Rouze pwent	RFP	Artisanal	Traps	Nearshore Reef
			Parupeneus rubescens	Rosy goatfish	Rouget-barbet sellé	Rouze	QZH	Artisanal	Traps	Nearshore Reef
		Scaridae	*Scarus ghobban*	Blue-barred parrotfish	Perroquet barbe bleue	Kakatwa blan	USY	Artisanal	Traps	Nearshore Reef
		Serranidae	*Cephalopholis argus*	Peacock hind	Vieille la prude	Vyey kwizinyen	CFF	Artisanal	Hooks and lines	Nearshore Plateau
			Epinephelus fasciatus	Blacktip grouper	Mérou oriflamme	Madanm dilo	EEA	Artisanal	Hooks and lines	Nearshore Plateau

Table 2.1. Details on the studied species. (continued)

Classification	Order	Family	Scientific name	English name	French name	Seychelles creole name	FAO code	Fishery type	Fishing gear	Habitat
Teleost fish	Percoidei	Serranidae	*Epinephelus merra*	Honeycomb grouper	Mérou gâteau de cire	Vyey sat	EER	Artisanal	Hooks and lines	Nearshore Plateau
			Epinephelus chlorostigma	Brownspotted grouper	Mérou pintade	Makonde bordaz	EFH	Artisanal	Hooks and lines	Nearshore Plateau
			Cephalopholis sonnerati	Tomato hind	Vieille ananas	Msye angar	EFT	Artisanal	Hooks and lines	Nearshore Plateau
			Epinephelus fuscoguttatus	Brown-marbled grouper	Mérou marron	Vyey goni	EWF	Artisanal	Hooks and lines	Nearshore Plateau
			Epinephelus octofasciatus	Eightbar grouper	Mérou huit raies	NA	EWO	Artisanal	Hooks and lines	Nearshore Plateau
			Epinephelus multinotatus	White-blotched grouper	Mérou plate grise	Vyey plat	EWU	Artisanal	Hooks and lines	Nearshore Plateau
			Epinephelus longispinis	Longspine grouper	Mérou longues épines	Vyey prine	EWW	Artisanal	Hooks and lines	Nearshore Plateau
			Variola louti	Yellow-edged lyretail	Croissant queue jaune	Krwasan / Gran Ke	VRL	Artisanal	Hooks and lines	Nearshore Plateau
	Scombroidei	Scombridae	*Gymnosarda unicolor*	Dogtooth tuna	Bonite à gros yeux	Ton ledan	DOT	Artisanal	Hooks and lines	Nearshore Plateau
			Euthynnus alletteratus	Little tunny (=Atl.black skipj)	Thonine commune	Bonit fol	LTA	Artisanal	Hooks and lines	Nearshore Plateau
			Rastrelliger kanagurta	Indian mackerel	Maquereau des Indes	Makro dou	RAG	Artisanal	Gillnets and entangling nets	Nearshore Plateau
		Xiphiidae	*Xiphias gladius*	Swordfish	Espadon	Espadron	SWO	Semi industrial	Hooks and lines	Offshore

2.3. SELECTION OF MODEL SPECIES

In order to study trace element bioaccumulation dynamics in the three marine compartments of the Seychelles waters (i.e. coastal benthic, nearshore demersal and pelagic offshore), it was necessary to use model species. Selected species were spiny lobsters (longlegged spiny lobster *Panulirus longipes*, painted spiny lobster *P. versicolor* and pronghorn spiny lobster *P. penicillatus*), that are benthic feeders living in coastal coral and rocky reefs (Box 2.1), the emperor red snapper (*Lutjanus sebae*), a demersal feeder living in nearshore reefs (Box 2.2), and the swordfish (*Xiphias gladius*), a pelagic offshore species that is able to dive to great depths to feed (Box 2.3). These species are considered good indicators of environmental contamination by bioaccumulating and/or biomagnifying trace elements because of their long life (Nakamura 1985; Rainbow 1998; Grandcourt *et al*. 2008). As migratory top predators, swordfish are also known to record spatial variation in environmental contamination and to accumulate high levels of bioaccumulating/biomagnifying trace elements like Hg, with reported concentrations higher than in other top predators like tunas and tuna-like species (Nakamura 1985; Bodin *et al*. 2017).

In addition, spiny lobsters, emperor red snapper and swordfish are emblematic species for the Seychelles fisheries. The lobster fishery is a historically well-established, licensed and seasonally managed fishery, while emperor red snapper and swordfish are among the main species caught by the artisanal demersal and semi-industrial fisheries, respectively (Seychelles Fishing Authority 2019).

Box 2.1. Focus on spiny lobsters

Studied species. Pronghorn spiny lobster (*Panulirus penicillatus*), longlegged spiny lobster (*Panulirus longipes*) and painted spiny lobster (*Panulirus versicolor*) (Illustration 1).

Habitat. Benthic and coastal; found in rocky and coral reefs where there is strong wave action, in shallow waters (0-15 m) (Intès *et al*. 1979).

General behaviour. Nocturnal species. They usually hide in the crevices of reefs during the day, while they come out at night to feed and mate (Holthuis 1991).

Foraging ecology. Generalist feeders and scavengers; they feed on benthic prey, like molluscs (bivalves and gastropods), crustaceans (barnacles and crabs), polychaetes and echinoderms (Butler and Kintzing 2016). Feeding on coralline algae, sponges, fish and macroalgae has also been reported (e.g. Mayfield *et al*. 2000; Blamey *et al.* 2019; Sardenne *et al.* 2021).

Reproduction. Mature size is reached after 3 years; females are known to be reproductive all year (Intès *et al*. 1979).

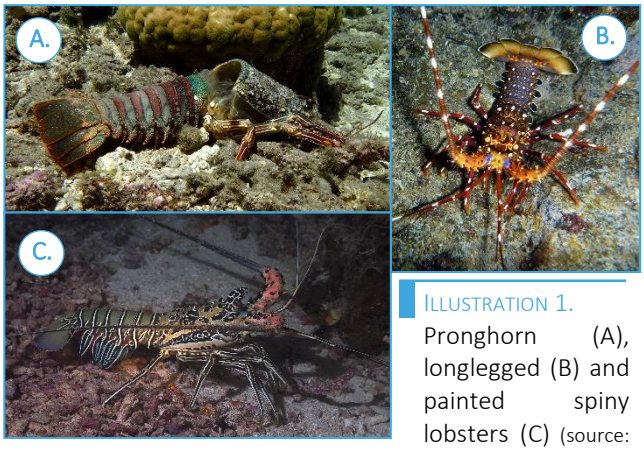

ILLUSTRATION 1. Pronghorn (A), longlegged (B) and painted spiny lobsters (C) (source: Wikimedia Commons).

Seychelles fishery. Spiny lobsters are one of the main resources for the artisanal fishery. The pronghorn and longlegged spiny lobsters comprise most of the catches, although the painted spiny lobster is also caught (Seychelles Fishing Authority 2016).

Fishing stocks are unstable in the Seychelles, with unpredictable catch variability from one fishing season to another (e.g. 30.1 kg by fishing trip during the 1994/1995 fishing season *vs* 10.1 kg by fishing trip during the 2012/2013 fishing season) (Seychelles Fishing Authority 2016). In addition to policies already in place (e.g. fishing license, minimum size of capture and no capture of berried females), seasonal closures are implemented to allow stocks to recover (Seychelles Fishing Authority 2018).

Blamey, L.K., de Lecea, A.M., Jones, L.D.S., Branch, G.M., 2019. Diet of the spiny lobster *Jasus paulensis* from the Tristan da Cunha archipelago: Comparisons between islands, depths and lobster sizes. *Estuar. Coast. Shelf Sci.* **219**, 262-272.
Butler, M.J., Kintzing, M.D., 2016. An exception to the rule: Top-down control of a coral reef macroinvertebrate community by a tropical spiny lobster. *Bull. Mar. Sci.* **92**, 137-152.
Holthuis, L.B., 1991. FAO species catalogue Vol. 13. Marine lobsters of the world. An annotated and illustrated catalogue of species of interest to fisheries known to date. *FAO Fisheries Synopsis* **13**, 1-4.
Intès, A., Laboute, P., Menou, J.L., 1979. Les langoustes coralliennes aux Seychelles : prospection. 21p.
Mayfield, S., Atkinson, L.J., Branch, G.M., Cockcroft, A.C., 2000. Diet of the west coast rock lobster *Jasus lalandii*: Influence of lobster size, sex, capture depth, latitude and moult stage. *Afr. J. Mar. Sci*. **22**, 57-69.
Sardenne, F., Bodin, N., Barret, L., Blamey, L., Govinden, R., Gabriel, K., *et al*., 2021. Diets of spiny lobsters from Mahé Island reefs, Seychelles reefs inferred by trophic tracers. *Reg. Stud. Mar. Sci.* **42**, 101640.
Seychelles Fishing Authority, 2016. Report on the spiny lobster fishery - Summary of fishing activity for the 2015-2016 season. 13p.
Seychelles Fishing Authority, 2018. Lobster survey report 2018. 8p.

Box 2.2. Focus on emperor red snapper (*Lutjanus sebae*)

Demographic information. Long lifepan (28 years) and slow growth rate, with late sexual maturity (age = 9 years for males and females) (Grandcourt *et al*. 2008).

Habitat. Demersal species. Generally occurs near coral or rocky reefs, but can also be found over adjacent sand flats and gravel patches. Found in depths between 5 and 180 m deep (Allen 1985).

General behaviour. Resident species (Froese and Pauly 2020). Although large individuals are generally found deeper than their smaller counterparts, they are known to move to shallower waters in winter (Williams and Russ 1992).

Foraging ecology. Feed on fish, benthic crustaceans like crabs, and on cephalopods (Froese and Pauly 2020).

Reproduction. Aggregate to spawn, usually between October and May (i.e. during the Northwest Monsoon and both inter-monsoon seasons), but with peaks of activity in March to May and in October to November (Robinson *et al.* 2004).

ILLUSTRATION 1.
Emperor red snapper (source: Wikimedia Commons).

Seychelles fishery. In the Seychelles, among all demersal species, the emperor red snapper is the most commercially exploited by the artisanal fishery. Caught mainly on the Mahé Plateau. Stock status shows signs of overexploitation (Grandcourt *et al*. 2008).

Allen, G., 1985. FAO species catalogue. Vol. 6. Snappers of the world. An annotated and illustrated catalogue of Lutjanid species known to date. *FAO Fisheries Synopsis* **125**, 208p.

Froese, R., Pauly, D., 2020. FishBase. World Wide Web electronic publication. URL: www.fishbase.org.

Grandcourt, E.M., Hecht, T., Booth, A.J., Robinson, J., 2008. Retrospective stock assessment of the Emperor red snapper (*Lutjanus sebae*) on the Seychelles Bank between 1977 and 2006. *ICES J. Mar. Sci.* **65**, 889-898.

Robinson, J., Isidore, M., Marguerite, M.A., Öhman, M.C., Payet, R.J., 2004. Spatial and temporal distribution of reef fish spawning aggregations in the Seychelles – An interview-based survey of artisanal fishers. *Western Indian Ocean J. Mar. Sci.* **3**, 63-69.

Williams, D., Russ, G.R., 1992. Review of the data on fishes of commercial and recreational fishing interest on the Great Barrier Reef. Great Barrier Reef Marine Park Authority, Townsville, Volume 1. 106p.

BOX 2.3. Focus on swordfish (*Xiphias gladius*)

Habitat. Pelagic and offshore; generally occurs between 0-650 m (Nakamura 1985), but can dive to depth up to 1000 m (Abascal *et al.* 2010). Its presence is often correlated to great variations of bathymetry, like continental slope or seamounts (Sabarros *et al.* 2013).

General behaviour. Stay in the mixed layer during the night, but dive to deep waters during the day to feed, following the movements of the deep scattering layer (Ward and Elscot 2000; Abascal *et al.* 2010). Highly migratory species.

Foraging ecology. Pelagivore opportunist; they feed mainly on pelagic fish, cephalopods and crustaceans (Potier *et al.* 2007). Usually forage in deep waters (Abascal *et al.* 2010).

Reproduction. Spawning is highly influenced by environmental factors, especially surface temperature. Generally spawn at temperatures from 23 to 26°C (Abid and Idrissi 2006).

ILLUSTRATION 1.
Swordfish (source: Wikimedia Commons).

Seychelles fishery. In the Seychelles, swordfish is one of the main target of the semi-industrial fishery, along with bigeye and yellowfin tuna (Seychelles Fishing Authority 2020).

Abascal, F.J., Mejuto, J., Quintans, M., Ramos-Cartelle, A., 2010. Horizontal and vertical movements of swordfish in the Southeast Pacific. *ICES J. Mar. Sci.* **67**, 466-474.

Abid, N., Idrissi, M., 2006. Swordfish. In: ICCAT Manual (Ed. International commission for the conservation of Atlantic tunas). Accessible at: https://www.iccat.int/en/iccatmanual.html

Nakamura, 1985. FAO Species catalogue - Vol. 5 Billfishes of the world. An Annotated and Illustrated Catalogue of Marlins, Sailfishes, Spearfishes and Swordfishes known to date. Available at: http://www.fao.org/3/ac480e/ac480e00.htm

Potier, M., Marsac, F., Cherel, Y., Lucas, V., Sabatié, R., Maury, O., Ménard, F., 2007. Forage fauna in the diet of three large pelagic fishes (lancetfish, swordfish and yellowfin tuna) in the western equatorial Indian Ocean. *Fish. Res.* **83**, 60-72.

Sabarros, P.S., Romanoov, E., Le Foulgoc, L., Richard, E., Dargorne, D., Bach, P., 2013. Exploratory analysis of relationships between swordfish captures and environmental features in the southwest Indian Ocean. IOTC–2013–WPB11–30 Rev_1.

Seychelles Fishing Authority, 2020. The semi-industrial longline fishery. URL: http://www.sfa.sc/index.php/fisheries/semi-industrial/general-information-semi-industrial. Last accessed: 10/03/2021.

Ward, P., Elscot, S., 2000. Broadbill swordfish: Status of world fisheries. *IOTC Proceeding no. 3*, 208-213.

2.4. TRACE ELEMENTS

2.4.1. Trace element analysis

Analysis of Ag, As, Cd, Co, Cr, Cu, Fe, Mn, Ni, Pb, Se, V and Zn were carried out at the UMR LIENSs (Joint research unit – Littoral, Environment and Societies) in La Rochelle (France). Samples were analysed by Induced Coupled Plasma (ICP), using a Varian Vista-Pro ICP coupled with optical emission spectrometry (OES) and a Thermo Fisher Scientific XSeries 2 ICP coupled with mass spectrometry (MS). Aliquots of the biological samples (90-200 mg) were digested

with 6ml 67-70% of nitric acid (HNO_3) and 2 ml 34-37% of hydrochloric acid (HCl) (Fisher Scientific, trace element grade quality). Acidic digestion of the samples was carried out overnight at room temperature, then using a Milestone microwave (30 min with constantly increasing temperature up to 120°C, then 15 min at this maximal temperature). Each digested sample was completed to 50 ml with milli-Q water. Seven control samples (five Certified Reference Materials, CRMs, and two blanks) treated and analysed in the same way as the samples were included in each analytical batch. CRMs fish homogenate IAEA 407, tuna fish flesh homogenate IAEA 436, scallop (*Pecten maximus*) IAEA 452, marine tropical clam (*Gafrarium tumidum*) IAEA-461, dogfish liver DOLT-5 (National Research Council Canada) and lobster hepatopancreas TORT-3 (National Research Council Canada). Mean recovery rates for all trace elements ranged from 74 to 128% (Appendix 2.1A).

Total Hg analyses were carried out at the Seychelles Fishing Authority in Victoria (Seychelles) and UMR LIENSs (Joint research unit – Littoral, Environment and Societies) in La Rochelle (France). Samples were analysed with a Direct Mercury Analyser (Milestone DMA 80) and an Advanced Mercury Analyser atomic absorption spectrophotometer (Altec AMA 254), respectively. Both devices are based on the same method, which does not require preliminary acidic digestion of the samples. Dry grounded subsamples from 2 to 10 mg were thus directly analysed. Hg determination involved progressive heating until 750 °C was reached, that allowed complete burning of the matrix and evaporation of the element. The evaporated element is then fixed on a golden net by amalgamation. Collected Hg on the amalgamator was then liberated by its heating at 950 °C, and measured by atomic absorption spectrophotometry. Each sample was analysed at least twice until the relative standard deviation (RSD) was below 10%.

Hg concentrations were validated by the analysis of a CRM, DOLT-5 (dogfish liver; National Research Council, Canada), every 10 samples. CRM aliquots were treated and analysed according to the same conditions as the samples. Masses of the CRM were adjusted to correspond to the same Hg amounts as in the samples. Blanks were also analysed at the beginning of each set of samples, and the quantification limit was 0.1 ng (5*DL, with DL the detection limit = 3*standard deviation of 8 blanks).

2.4.2. Data preparation

For nutritional interpretation and in order to compare trace element concentrations with nutritional requirements and maximum limit of contaminants for human consumption, all trace

element data were converted from dry weight to wet weight (ww). As the moisture content was not available for every individual and every species of the database, a conversation ratio was calculated whenever possible (Eq. 2.1). For species for which the percentage of moisture was available, the conversion factor was calculated for each individual and the mean conversion factor for each species was used to convert concentration to ww (Appendix 2.2). For species for which the percentage of moisture was not available, the percentage of moisture used to calculate the conversion factor was 75%.

$$\text{Conversion factor} = 100 / (100 - \%\text{moisture}) \qquad \textbf{(Eq. 2.1)}$$

For ecological interpretations, observations below the limit of quantification (LOQ) were substituted with values drawn randomly from the range]0;LOQ[and only trace elements with detection frequencies > 70% (i.e. at least 70% of the measured values are above the LOQ) were used (Appendix 2.1B) (Carravieri *et al*. 2020). As all measures of V were below LOQ, this element was definitely removed from the database for all analyses.

2.5. STABLE ISOTOPES

2.5.1. Sample preparation for $\delta^{13}C$ determination

Because lipids are usually more depleted in ^{13}C than other tissue components and could thus introduce a bias in the results, reserve lipids must be removed before $\delta^{13}C$ determination or mathematical correction must be applied on measured $\delta^{13}C$ values (De Niro and Epstein 1978). However, lipid extraction or mathematical correction must not be applied when the carbon-to-nitrogen ratio (C:N) < 3.5 (or total lipid content TLC < 5% dw) as it corresponds to minor lipid bias and correction may lead to higher $\delta^{13}C$ incertitude (Post *et al*. 2007; Logan *et al*. 2008; Bodin *et al*. 2009). Lipids were thus removed or corrected only when necessary (i.e. on samples with high C:N ratios).

Although lipid removal gives precise $\delta^{13}C$ lipid-free values, some methods can affect $\delta^{15}N$ values by also removing some protein compounds linked to lipids (e.g. lipoproteins) (Sotiropoulos *et al*. 2004; Murry *et al*. 2006). Although separate analysis of $\delta^{13}C$ (i.e. on lipid-free samples) and $\delta^{15}N$ (i.e. on bulk samples) is possible, it is expensive and time-consuming, and thus mathematical correction is a good alternative in such cases. Swordfish muscle tissues are particularly high in lipid storage content (total lipid content of 26.2 ± 18.9% dw, Bodin *et al*. 2017), thus mathematical correction was chosen to correct $\delta^{13}C$ values in those samples. Lipids

were removed in the other muscle tissue samples, except in spiny lobster muscle tissues, which were poor in lipid content (0.74 ± 0.14% ww, Sabino *et al*. 2021) and for which the C:N ratio was < 3.5.

2.5.1.1. Lipid removal

For each sample, between 10 and 12 mg of powdered sample was placed in a glass tube with 4 ml of cyclohexane. Tubes were then agitated during 10 minutes at room temperature and centrifuged during 5 minutes at 4500 rotation per minute (rpm) before removal of extraction solvent. Agitation, centrifugation and solvent-removal steps were repeated three times before putting tubes for drying in an oven at 45 °C for a night.

2.5.1.2. Mathematical correction

The mathematical correction method consists of mathematical models that predict lipid-corrected isotope values using stable isotope analysis of bulk tissue and different covariates, including a proxy of lipid content. By first characterising the relationship between the difference in $\delta^{13}C$ between lipid-free and bulk values in a sample and the sample's lipid content or its proxy (generally the C:N ratio in the bulk sample), it is then possible to establish the correction equation to obtain a corrected value of $\delta^{13}C$ (Logan *et al*. 2008).

To allow for $\delta^{13}C$ correction in swordfish muscle tissues, 32 swordfish muscle tissue samples were analysed for stable isotopes of carbon and nitrogen before (i.e. measure of $\delta^{13}C_{bulk}$ and $C:N_{bulk}$) and after lipid removal (i.e. measure of $\delta^{13}C_{lipid\text{-}free}$). The equation used to correct $\delta^{13}C^{bulk}$ values was the one proposed in Logan *et al.* (2008):

$$\delta^{13}C_{corrected} = \frac{7.05 * C{:}N_{bulk} - 22.4}{C{:}N_{bulk} - 0.44} + \delta^{13}C_{bulk} \quad \textbf{(Eq. 2.2.)}$$

As other correction models were also available in the literature (i.e. McConnaughey and McRoy 1979; Fry 2002), the process of model choice and constant determination is described in Appendix 2.2.

2.5.2. Sample preparation for $\delta^{15}N$ determination in elasmobranchs: urea extraction

Elasmobranch species are known to retain urea ($(NH_2)_2CO$) and trimethylamine oxide (C_3H_9CO) in their muscle tissues to osmoregulate (Ballantyne 1997; Hazon *et al*. 2003). Urea and trimethylamine oxide are rich in ^{14}N, and thus have low $\delta^{15}N$ values (Kim and Koch 2012), which was shown to bias $\delta^{15}N$ values measured in elasmobranch muscle tissues (e.g. Logan and

Lutcavage 2010; Kim and Koch 2012; Li *et al*. 2016). In addition, urea and trimethylamine oxide concentrations within organisms vary according to tissue type (Ballantyne 1997), ambient salinity (Hazon *et al*. 2003; Pillans *et al*. 2005) and diet (Wood *et al*. 2010). It is thus necessary to remove urea when analysing stable isotopes in muscle tissues of elasmobranch species. For this, rinsing with deionised water was proven to be effective (e.g. Kim and Koch 2012; Li *et al*. 2016).

Here, muscle tissue samples from all analysed elasmobranch species were thus rinsed with deionised water after lipid-removal in order to avoid any bias linked to the presence of urea and trimethylamine oxide in these tissues. For this, 1 ml of milli-Q water was added in each tube containing the samples, and tubes were then vortexed during 30 sec to homogenise. Samples were left in milli-Q water for 24 h before centrifugation (5 min at 5000 rpm) and removal of rinsing water with a pipette. These steps were repeated 3 times before freeze-drying the samples during 24 h to insure they were properly dry for stable isotope analysis.

2.5.3. Stable isotope analysis

For $\delta^{13}C$ and $\delta^{15}N$ determination, between 250 and 500 µg of sample was weighed in tin capsules. The samples were analysed by continuous flow on a Thermo Scientific Flash 2000 elemental analyser coupled to a Delta V Plus interface mass spectrometer. International isotopic standards of known $\delta^{13}C$ and $\delta^{15}N$ were used: USGS-61 and USGS-62. Results are expressed in the δ unit notation as deviations from standards (Vienna Pee Dee Belemnite for $\delta^{13}C$ and atmospheric nitrogen for $\delta^{15}N$) following the formula: $\delta^{13}C$ or $\delta^{15}N$ = [(Rsample/Rstandard) - 1] x 1000, where R is $^{13}C/^{12}C$ or $^{15}N/^{14}N$, respectively. Measurement errors (SD) of SI, calculated on all measured values of $\delta^{13}C$ and $\delta^{15}N$ in isotopic reference materials, were < 0.10 ‰ for both the nitrogen and carbon isotope measurements. This was in accordance with the analytical precision given by the manufacturer (i.e. < 0.10 ‰ for $\delta^{13}C$ and < 0.15 ‰ for $\delta^{15}N$; Thermo Scientific). For each sample, the C:N ratio was calculated, and never exceeded 3.5 proving that reserve lipids were adequately removed, or that there was no need of lipid removal or normalisation (Post *et al*. 2007).

2.6. FATTY ACIDS

2.6.1. Fatty acid analysis

Lipids were extracted using a modified Folch method (Folch *et al.* 1957). Briefly, for each sample, around 200 mg of wet tissue was placed in a 7 mL glass vial before adding 6 mL of the extraction solvent, a Folch solution (i.e. chloroform:methanol 2:1 v/v). Samples were then vortexed and sonicated in an ultrasonic bath for 15 min. Extracts were stored during 12h-24h at -20 °C prior to fatty acid methyl ester (FAME) preparation.

FAME were prepared using 1 mL of lipid extract. For each sample, 20 µL of an internal standard (tricosanoic acid, C23:0, 0.115 µg/µL) was added to allow fatty acid quantification. Samples were then evaporated under a stream of nitrogen and trans-esterified with 800 µL of methanolic sulphuric acid (MeOH-H_2SO_4 3.4% v/v), before being placed in a heating block at 100 °C during 10 min. After cooling, formed FAME were retrieved by adding 800 µL of hexane. Three washing were carried out using hexane-saturated distilled water, and the upper phase was transferred to a 2 mL vial before being stored at -20 °C for further gas chromatography analysis.

FAME were then analysed using a gas chromatograph (Varian CP3800) with auto-sampler equipped with both polar and apolar capillary columns (ZB-WAX, 30 m length x 0.25 mm i.d. x 0.25 µm film thickness and ZB-5 30 m length x 0.25 mm i.d. x 0.25 µm film thickness), a splitless injector and a flame ionization detector. Oven temperature was raised to 150 °C at 50 °C/min, then to 170 °C at 3.5 °C/min, to 185 °C at 1.5 °C/min, to 225 °C at 2.4 °C/min, and finally to 250 °C at 5.5 °C/min. The identification of FAME was carried out by comparison of retention times with a commercially available standard 37-component FAME mix. The concentration for each fatty acid was converted from the area of chromatogram peaks by using the C23:0 peak as reference.

2.6.2. Data preparation

Fatty acids were coded as C:Xn-Y where C is the number of carbons, X is the number of double bonds, and Y is the position the first double bond from the terminal methyl end of the molecule (Fig. 2.3). In non-methyl interrupted (NMI) fatty acids, double bonds are not separated by only one methyl group, thus they are labelled as C:X NMI (n), where C is the number of carbons, X the number of double bonds and n the position(s) of the double bonds from the terminal

methyl end of the molecule. Fatty acids were expressed as percentage of total fatty acid (%TFA) for trophic ecology analysis.

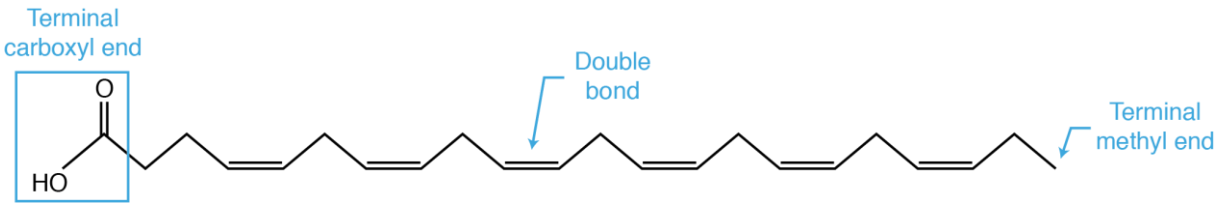

Fig. 2.3. Structure of a fatty acid with terminal carboxyl and terminal methyl ends. Fatty acid represented here is the docosahexaenoic acid, formula 22:6n-3.

Only fatty acids detected above trace levels (> 0.8 %TFA) were used for any statistical comparison and are presented here. For fatty acids measured in spiny lobsters hepatopancreas, those under trace levels included the saturated fatty acids 19:0, 21:0, 22:0, 24:0, the monounsaturated fatty acids 16:1n-5, 16:1n-9, 17:1n-7, 18:1n-5, 18:1n-11, 22:1n-7, 22:1n-9, 22:1n-11, 24:1n-9, the polyunsaturated fatty acids 16:2n-4, 16:3n-4, 16:3n-6, 16:4n-3, 18:3n-3, 18:3n-4, 18:3n-6, 18:4n-3, 20:3n-3, 20:3n-6, 20:4n-3, 22:6n-3, the branched fatty acids iso15:0, ante15:0, iso16:0, the NMI fatty acids 20:2 NMI (5,11), 20:2 NMI (5,13), 22:3 NMI (7,13,16) and the DMA 16:1n-7DMA, 16:0DMA. For fatty acids measured in swordfish white muscle, they included the saturated fatty acids 15:0, 19:0, 20:0, 21:0, 22:0 and 24:0, the monounsaturated fatty acids 16:1n-5, 16:1n-9, 18:1n-5, 20:1n-7, 20:1n-11, 21:5n-3, 22:1n-7, 22:1n-9 and 22:1n-11, the polyunsaturated fatty acids 16:2n-4, 18:2n-4, 18:2n-6, 18:3n-3, 18:3n-4, 18:3n-6, 18:4n-3, 18:4n-6, 20:2n-6, 20:3n-3, 20:3n-6, 20:4n-3 and 22:4n-6, the branched fatty acids iso15:0, iso16:0, iso17:0 and anteiso17:0, the NMI fatty acids 20:2 NMI (5,11), 20:2 NMI (5,13), and the DMA 16:0DMA and 18:0DMA.

2.7. DATA TREATMENT

2.7.1. Software

All statistical tests were performed under R 3.5.2 software (R Core Team 2018); all R scripts used in this thesis are available at: https://github.com/magalisabino/Analyses_of_trace_element_bioaccumulation. Correlation plots were computed using the *corrplot* package (Wei and Simko 2017), and all other figures were computed using the *ggplot2* package (Wickham 2016). For maps, the *rgdal* (Bivand *et al.*

2019), *sp* (Pebesma and Bivand 2005) and *sf* (Pebesma 2018) packages were used to plot points with the right projection (i.e. UTM 40S), and the *ggspatial* package (Dunnington 2018) was used to plot them in combination with the *ggplot* package.

2.7.2. Univariate statistics and correlations

Prior to any statistical analysis, data were tested for normality and homoscedasticity, using Fligner and Shapiro tests respectively. T-tests (for parametric data) or Wilcoxon tests (for non-parametric data) were used to test for significant difference between two groups. ANOVA (for parametric data) or Kruskal-Wallis (for non-parametric data) were used to test for significant difference between more than two groups. When difference was significant ($p < 0.05$), a post-hoc test was performed: Tukey's HSD after ANOVA and Dunn test with Benjamini-Hochberg adjustment after Kruskal-Wallis. To test for a relationship between two numeric variables, Pearson (for parametric data) or Kendall (for non-parametric data) correlation tests were computed.

T-tests, Wilcoxon tests, ANOVA, Kruskal-Wallis and Tukey's HSD were computed using the included *stats* package, while Dunn post-hoc test was computed using the *FSA* package (Ogle *et al*. 2018). Correlation tests were computed by using the *cor.test* function from the included *stats* R package, in which the wanted method (i.e. Pearson for parametric and Kendall for non-parametric test) was specified.

2.7.3. Multivariate statistics

Unconstrained multivariate ordination methods are useful tools that allow to visualise the dispersion of objects (e.g. sample points) in complex multidimensional datasets without *a priori* grouping, as well as to identify groups of co-varying variables. They include methods like principal component analysis (PCA) and non-metric multidimensional scaling (nMDS) (Borcard *et al*. 2018).

The principle of a PCA is to decompose a complex data frame with possibly correlated measurements into a new set of uncorrelated (i.e. orthogonal) variables called principal components of eigenvectors (Abdi 2004). Thus, when computing a PCA using a data frame with n dimensions, one can expect a PCA with n principal components. All computed dimensions are orthogonal to each other and correspond to the successive dimensions of maximum variance of the scatter points. When using a PCA, the point is not to represent all variability explained

by all dimensions of the data frame, but rather the maximum possible. As a consequence, PCA results are usually presented as PCA biplots (using principal components 1 and 2) or 3D plots (using principal components 1, 2 and 3) (Borcard *et al*. 2018).

The principle of an nMDS is similar to that of the PCA method, but allows the decomposition of a complex data frame into a predetermined small number of axes (Borcard *et al.* 2018). This method is thus interesting when the first three axes of a PCA are not sufficient to explain most of the in-between objects variation, and when there is a need to constraint the number of axes.

Here, PCA were first used in order to visualise grouping of samples according to several dimensions (i.e. either trace element concentrations, size of sampled individuals and $\delta^{13}C$ and $\delta^{15}N$ values, only trace element concentrations or fatty acid proportions) and to identify potential groups of co-varying variables. Except for fatty acid proportions, all data were first normalised, that is centred and divided by the standard deviation (*scale* function in the included *base* R package), to avoid any interference of the different dimensions' scales in calculating the distance between two points (Juszczak *et al*. 2002). PCA were then computed using the *PCA* function in the *FactoMineR* R package (Sébastien *et al*. 2008). However, for all computed PCA, the first three axes explained less than 60% of the explained variance, thus nMDS were preferred. nMDS ordinations were generated using the *metaMDS* function from the R *vegan* package (Oksanen *et al*. 2019).

2.7.4. Clustering method: grouping samples according to their similarities

In order to group samples according to their biochemical profiles (i.e. trace element or fatty acid profiles), Ward's hierarchical agglomerative clustering method was used (Ward 1963; Murthagh and Legendre 2014). This method is based on a sum-of-squares criterion, and thus has the advantage of producing groups that minimize within-group error sum of squares (i.e. within-group dispersion). Another advantage is that Ward's method uses a multivariate Euclidean space to look for groups, which is also the reference space for multivariate ordination methods like PCA. These methods can thus be used in complement of Ward's hierarchical agglomerative clustering method to visually represent the variance among observations in a 2 dimensions ordination diagram (Murthagh and Legendre 2014).

Here, data (i.e. trace element concentrations or fatty acid proportions) were first normalised (described in section 1.7.3) then translated to avoid any negative numbers, and a

Euclidean matrix was computed. Clustering was performed using the *hclust* function from the included *stats* R package, with the method Ward D2 (Murthagh and Legendre 2014). The most suitable number of groups was determined using the function *NbClust* from the *NbClust* R package (Charrad *et al.* 2014).

2.7.5. Trophic niche computing and trace element profile representation

To compare trophic niches between groups of samples, fatty acid and isotopic trophic niches were computed and their sizes and overlaps were calculated using the *nicheROVER* R package (see Swanson *et al.* (2015) for details on the method). This package uses a model developed in a Bayesian framework to calculate probabilistic niche metrics (i.e. niche size and probabilities of overlap) as opposed to the more traditional geometric-based computations. This method is insensitive to sample size and can account for statistical uncertainty. Fatty acid and isotopic trophic niches were computed separately, and niche metrics were calculated using 1000 iterations of ellipses. More specifically, niche overlaps were expressed in percentage of the niche of each group and represent the probability of individuals from group A being found in the niche of group B. As fatty acid profiles contained a high number of dimensions (i.e. 23 fatty acids above trace levels for spiny lobsters and 14 fatty acids above trace levels for swordfish), nMDS ordinations using a Bray-Curtis dissimilarity matrix were first generated and nMDS coordinates of dimensions 1 and 2 were used to compute fatty acid trophic niches. For stable isotopes, $\delta^{15}N$ and $\delta^{13}C$ values were used to calculate isotopic trophic niches. R scripts used to compute fatty acid and isotopic niches are available at: https://github.com/magalisabino/FattyAcid_Isotopic_niche_co mputing (Sabino *et al.* 2021).

The *nicheROVER* package was also used to represent trace element profile ellipses by taking into account uncertainty due to small sample size. First, trace element concentrations were normalised with the R included *scale* function and translated to avoid any negative data. Then, the same method as for fatty acids (i.e. nMDS ordination and use of nMDS dimensions 1 and 2) was used to compute ellipses. The ellipse probabilities of overlap were also calculated for trace element profile ellipses as a proxy of resemblance of computed trace element profiles between species or among levels of the same factor for a single species.

For visual representation of fatty acid and isotopic trophic niches and of trace element profile ellipses, mean ellipses coordinates were calculated using the mean coordinates of the 1000 ellipses from the Bayesian model. For representation of statistical uncertainty,

coordinates of the uncertainty ellipses were calculated using the mean coordinates of the 10% smallest ellipses, and the 10% largest ellipses.

Finally, the associated probability was used to compare niche metrics between species or among levels of the same factor. For each iteration of the model, a value of 1 was given if one niche metric value was greater than the other, 0 if not. The mean value calculated for the 1000 iterations represented the probability that one metric value was greater than the other. A probability > 0.95 would be associated with a high certainty.

2.7.6. Modelling the relationship between trace element concentrations and factors affecting their concentrations

In order to model the relationship between trace element concentrations (i.e. the response variable) and several factors potentially controlling their bioaccumulation (i.e. explaining variables), generalised linear models (GLM) and/or generalised additive models (GAM) were used.

Classical linear models make the assumption that data have normally distributed errors that is, for a given x value, the residuals of the model are normally distributed around the model-estimated y value. When it is not the case, it is preferable to use GLMs. Indeed, GLMs include data transformation methods (i.e. transformation of y for each x) inside the model, through a link function, in order to allow for non-normally-distributed errors, even if the magnitude of the variance of each measurement is a function of its predicted value (Zhao 2012). In the case of non-linear relationship, GAMs are a good alternative to GLMs. They use smoothing curves to model the relationship between the response variable and the explaining variables, and thus allow modelling of both linear and non-linear relationships (Zuur *et al*. 2007).

Although it is usually not recommended to pre-transform the response variable prior to fit a GLM or a GAM, as both include the possibility of within-model transformation through a link function, previous work on trace elements showed that applying a log-transformation prior to fitting models improved the models (e.g. Méndez-Fernandez *et al*. 2013; Chouvelon *et al.* 2014, 2017). Thus, here, all GLMs and GAMs were fitted on log-transformed trace element concentrations with a Gaussian distribution and an identity link function, using the *glm* function of the included stats R package and the *gam* function from the *mgcv* R package (Wood 2011) respectively.

For each model performed, the complete model was first compared to a null model (i.e. containing only the intercept terms) using the Akaike Information Criterion (AIC) (Akaike 1981). This allowed to the capacity of the complete model to explain the variability of the response variable. If the null model was better than the complete model (i.e. had a lower AIC), analyses did not go further. If the complete model was better than the null model, a stepwise procedure was used to select the most parsimonious model, again using the AIC. For this, explanatory variables were successively removed from the complete model until all remaining variables significantly improved the model (i.e. no significant lowering of the AIC). When the AIC was not significantly different between two compared models, the simplest model was preferred (Zuur *et al.* 2007). Finally, all selected models were validated by checking the normality and homoscedasticity of residuals, and the potential presence of outliers (Zuur *et al.* 2007).

3. Chapter 1 – Trace element concentration patterns in capture fisheries resources from the Seychelles nearshore and offshore waters

Content

The first part of this chapter is included in a paper submitted in Marine Pollution Bulletin *and presented in Supp. Doc. 1.*

3.1. CONTEXT AND OBJECTIVES

As mentioned in the general introduction, seafood is a key food item in healthy and balanced human diets, especially in SIDS like the Seychelles where capture fisheries resources are the main source of proteins and micronutrients (Weichselbaum *et al*. 2013; Hicks *et al*. 2019). Nutrient intake and contaminant exposure both depend on the trace element content, and thus bioaccumulation, in the edible parts of capture fisheries species. However, in marine organisms, trace element bioaccumulation is controlled by many intrinsic (e.g. size, physiology and/or metabolic rate) and extrinsic factors (e.g. feeding habitat, diet) (Bustamante *et al*. 1998; Kojadinovic *et al*. 2007; Metian *et al*. 2008; Rejomon *et al.* 2010) that can be influenced by climate change-induced environmental changes, like the increase in sea surface temperature or in seawater pH. At the individual level, water temperature can affect the metabolic rate (i.e. the higher the temperature the higher the metabolic rate) and growth (i.e. the higher the temperature the lower the growth rate) of marine organisms (Bruno *et al*. 2015; Barneche and Allen 2018). As body size is also known to affect trophic structure in ecosystems, by influencing the growth and size of the higher trophic levels, water temperature can also affect food web dynamics by trophic cascade (Jochum *et al*. 2012; Bruno *et al*. 2015). High temperatures also have a critical role in water column stratification, which can influence primary production by limiting nutrient fluxes to the surface (Winder and Sommer 2012). In addition to indirect effects on trace element bioaccumulation in marine organisms through modifications of their physiology and trophic ecology, ocean warming and acidification were shown to have a direct effect on trace element bioaccumulation in various species such as squids (Lacoue-Labarthe *et al.* 2011), mussels (Baines and Fisher 2008; Sezer *et al*. 2020) or fish (Pouil *et al.* 2018). As a consequence, climate change is expected to alter trace element flow in food webs, and thus their bioaccumulation in marine organisms, including in capture fishery species.

To better understand and anticipate climate change-induced variation in trace element availability in capture fishery species, it is thus crucial to have base knowledge on the processes influencing trace element bioaccumulation in these species. However, data are still lacking for many species in tropical and subtropical environments, on which SIDS depend for their subsistence. As an example, in the Seychelles, trace element concentrations were documented in pelagic species, showing low concentrations of Cd and Pb and relatively high concentrations of Fe, Hg, Se and Zn (Bodin *et al*. 2017; Hollanda *et al*. 2017). Hg bioaccumulation in some

pelagic and demersal fishes and in some benthic crustaceans were also documented, demonstrating Hg biomagnification potential (Sardenne *et al*. 2017). However, there is a lack of data on the vast majority of species that are exploited, particularly demersal and reef species.

In this chapter, I investigate the factors influencing the bioaccumulation of 9 trace elements (i.e. As, Cd, Cu, Fe, Hg, Mn, Ni, Se and Zn) in capture fishery species from various taxa, functional groups and habitats and with various diets and trophic positions. This allowed me to identify patterns of bioaccumulation according to the taxon (linked to presence/absence of detoxifying mechanisms) and to the feeding vertical habitat. By exploring trace element concentrations within patterns, I could also select intrinsic (i.e. size) and extrinsic (i.e. habitat through $\delta^{13}C$ values and trophic position through $\delta^{15}N$ values) factors to include in the following chapters. Finally, results confirm that the trophic pathway is the dominant route for trace element exposure for the cephalopod, crustacean, elasmobranch and teleost species analysed here, as hypothesised in previous work on these taxa (Wang 2002; Mathews and Fisher 2009).

3.2. METHODOLOGY

3.2.1. Dataset

In this chapter, all 54 sampled species were used for data treatment, in order to have the largest dataset possible. This way, the dataset included both nearshore and offshore species, from different functional groups and habitat types, and with different diet types (Table 3.1).

Table 3.1. Analysed species and associated details. Length refers to dorsal mantle length for cephalopods, cephalothorax length for crustaceans, lower jaw-fork length for swordfish, and fork length for other teleost fish and for elasmobranchs. Lengths and stable isotope values are presented as mean ± SD. Functional groups, trophic groups, habitat and diet types are derived from SeaLifeBase (Palomares and Pauly 2020) and FishBase (Froese and Pauly 2020). N = number of samples.

Functional group	English name	N	Length (cm)	$\delta^{13}C$ (‰)	$\delta^{15}N$ (‰)	Fishing location	Habitat type	Trophic group	Diet type
Benthic crustacean	Longlegged spiny lobster	44	7.8 ± 1.0	-14.0 ± 0.7	11.3 ± 0.4	Nearshore	Rocky reefs	Carnivore	Benthivore/scavenger
	Pronghorn spiny lobster	47	9.8 ± 1.8	-13.6 ± 0.7	11.6 ± 0.4	Nearshore	Rocky reefs	Carnivore	Benthivore/scavenger
	Painted spiny lobster	15	8.2 ± 1.8	-13.7 ± 0.8	10.4 ± 0.3	Nearshore	Coral reefs	Carnivore	Benthivore/scavenger
	Spanner crab	5	9.7 ± 1.1	-14.5 ± 0.4	12.0 ± 0.5	Nearshore	Sandy areas	Carnivore	Benthivore/scavenger
Benthic cephalopod	Big blue octopus	17	13.5 ± 2.8	-15.4 ± 1.0	11.5 ± 0.6	Nearshore	Coral reefs	Carnivore	Benthivore/scavenger
Benthic teleost fish	Blue-barred parrotfish	10	28.4 ± 2.9	-15.6 ± 1.4	10.2 ± 1.3	Nearshore	Coral reefs	Herbivore	Scraper
	Streamlined spinefoot	10	26.0 ± 1.5	-18.9 ± 2.2	9.9 ± 0.6	Nearshore	Coral reefs	Herbivore	Grazer
	Shoemaker spinefoot	9	25.5 ± 2.0	-16.8 ± 2.2	9.7 ± 0.8	Nearshore	Coral reefs	Herbivore	Grazer
	Rosy goatfish	3	25.5 ± 5.2	-15.0 ± 0.5	14.8 ± 0.6	Nearshore	Sandy areas	Carnivore	Benthivore
	Dash-and-dot goatfish	5	26.9 ± 3.3	-13.6 ± 2.1	11.9 ± 1.6	Nearshore	Sandy areas	Carnivore	Benthivore
	Slender emperor	18	29.3 ± 1.8	-16.3 ± 0.6	13.2 ± 0.4	Nearshore	Sandy areas	Carnivore	Benthivore
Demersal teleost fish	Elongate surgeonfish	6	38.0 ± 13.6	-16.9 ± 1.5	11.3 ± 1.0	Nearshore	Rocky and coral reefs	Carnivore	Planktivore
	Yellowtail emperor	13	33.1 ± 4.5	-15.1 ± 0.9	13.3 ± 0.3	Nearshore	Coral reefs	Carnivore	Benthopelagivore
	Spangled emperor	14	42.4 ± 6.4	-16.2 ± 1.7	12.7 ± 0.5	Nearshore	Rocky and coral reefs	Carnivore	Benthopelagivore
	Smalltooth emperor	10	44.6 ± 3.4	-16.3 ± 0.4	14.1 ± 0.7	Nearshore	Coral reefs	Carnivore	Benthopelagivore
	Blackeye emperor	2	33.5 ± 0.7	-14.9 ± 0.1	13.6 ± 0.1	Nearshore	Coral reefs	Carnivore	Benthopelagivore
	Sky emperor	21	34.5 ± 5.3	-15.6 ± 1.0	13.4 ± 0.5	Nearshore	Coral reefs	Carnivore	Benthopelagivore
	Pink ear emperor	3	41.8 ± 5.8	-14.9 ± 0.8	13.9 ± 0.7	Nearshore	Sandy areas	Carnivore	Benthopelagivore
	Blue-lined large-eye bream	5	51.9 ± 6.2	-15.9 ± 0.5	14.2 ± 0.2	Nearshore	Rocky and coral reefs	Carnivore	Benthopelagivore
	Two-spot red snapper	56	52.6 ± 14.9	-16.3 ± 0.5	13.7 ± 0.5	Nearshore	Coral reefs	Carnivore	Pelagobenthivore
	Deepwater longtail red snapper	10	57.3 ± 11.3	-18.0 ± 0.2	13.6 ± 0.3	Nearshore	Rocky reefs	Carnivore	Pelagobenthivore
	Humpback red snapper	16	35.8 ± 3.9	-16.7 ± 0.3	13.2 ± 0.2	Nearshore	Coral reefs	Carnivore	Pelagobenthivore
	Bigeye snapper	1	39.5	-16.0	14.9	Nearshore	Coral reefs	Carnivore	Pelagobenthivore
	Emperor red snapper	78	58.9 ± 13.3	-16.2 ± 0.4	14.3 ± 0.4	Nearshore	Rocky and coral reefs	Carnivore	Pelagobenthivore
	Humphead snapper	5	62.2 ± 5.3	-16.5 ± 0.4	13.1 ± 0.6	Nearshore	Rocky and coral reefs	Carnivore	Pelagobenthivore
	Green jobfish	113	56.0 ± 9.6	-16.8 ± 0.4	13.4 ± 0.5	Nearshore	Coral reefs	Carnivore	Pelagobenthivore
	Blacktip grouper	3	ND	-17.0 ± 0.1	13.0 ± 0.2	Nearshore	Coral reefs	Carnivore	Pelagobenthivore
	Honeycomb grouper	4	33.8 ± 1.6	-15.2 ± 0.2	13.2 ± 0.1	Nearshore	Coral reefs	Carnivore	Benthopelagivore

Table 3.1. Analysed species and associated details. Length refers to dorsal mantle length for cephalopods, cephalothorax length for crustaceans, lower jaw-fork length for swordfish, and fork length for other teleost fish and for elasmobranchs. Lengths and stable isotope values are presented as mean ± SD. Functional groups, trophic groups, habitat and diet types are derived from SeaLifeBase (Palomares and Pauly 2020) and FishBase (Froese and Pauly 2020). N = number of samples. (continued)

Functional group	English name	N	Length (cm)	$\delta^{13}C$ (‰)	$\delta^{15}N$ (‰)	Fishing location	Habitat type	Trophic group	Diet type
Demersal teleost fish	Brownspotted grouper	76	35.1 ± 3.9	-16.8 ± 0.3	13.8 ± 0.3	Nearshore	Reefs and associated habitats	Carnivore	Pelagobenthivore
	Brown-marbled grouper	2	70.8 ± 3.2	-15.7 ± 0.4	14.1 ± 0.2	Nearshore	Coral reefs	Carnivore	Benthopelagivore
	Eightbar grouper	4	68.0 ± 3.9	-16.5 ± 0.4	14.4 ± 0.3	Nearshore	Rocky reefs	Carnivore	Pelagobenthivore
	White-blotched grouper	22	64.7 ± 11.7	-16.5 ± 0.4	13.4 ± 0.5	Nearshore	Reefs and associated habitats	Carnivore	Pelagobenthivore
	Longspine grouper	2	42.5 ± 3.5	-16.3 ± 0.1	13.9 ± 0.1	Nearshore	Rocky and coral reefs	Carnivore	Benthopelagivore
	Tomato hind	14	41.4 ± 4.1	-16.9 ± 0.2	14.2 ± 0.4	Nearshore	Rocky and coral reefs	Carnivore	Pelagobenthivore
	Peacock hind	42	21.0 ± 6.2	-13.7 ± 1.1	13.1 ± 0.6	Nearshore	Coral reefs	Carnivore	Pelagobenthivore
	Yellow-edged lyretail	38	46.0 ± 6.6	-16.7 ± 0.4	13.4 ± 0.5	Nearshore	Rocky and coral reefs	Carnivore	Pelagobenthivore
	Bludger	25	56.3 ± 15.9	-17.2 ± 0.3	13.6 ± 0.4	Nearshore	Rocky and coral reefs	Carnivore	Pelagobenthivore
	Bluefin trevally	9	49.3 ± 11.6	-16.5 ± 0.4	13.8 ± 0.5	Nearshore	Coral reefs	Carnivore	Pelagobenthivore
	Bigeye trevally	8	58.5 ± 8.3	-16.6 ± 0.4	13.9 ± 0.3	Nearshore	Coral reefs	Carnivore	Pelagobenthivore
	Golden trevally	7	52.3 ± 14.0	-17.4 ± 0.4	12.8 ± 0.1	Nearshore	Coral reefs	Carnivore	Pelagobenthivore
	Malabar trevally	2	67.5 ± 6.4	-15.9 ± 0.3	14.3 ± 0.1	Nearshore	Rocky and coral reefs	Carnivore	Benthopelagivore
	Yellowspotted trevally	36	59.1 ± 16.2	-16.7 ± 0.3	14.1 ± 0.4	Nearshore	Rocky and coral reefs	Carnivore	Pelagobenthivore
	Pickhandle barracuda	26	61.0 ± 10.3	-16.4 ± 0.3	14.5 ± 0.4	Nearshore	Coral reefs	Carnivore	Pelagobenthivore
Pelagic-neritic teleost fish	Little tunny	5	49.0 ± 3.3	-17.3 ± 0.2	13.4 ± 0.4	Nearshore	Pelagic-neritic	Carnivore	Pelagivore opportunist
	Indian mackerel	17	25.6 ± 0.6	-17.4 ± 0.2	12.1 ± 0.3	Nearshore	Pelagic-neritic	Carnivore	Planktivore
	Dogtooth tuna	7	87.1 ± 13.5	-16.5 ± 0.2	13.9 ± 0.4	Nearshore	Coral reefs	Carnivore	Pelagobenthivore
Pelagic-neritic elasmobranch	Grey reef shark	1	74.0	-16.2	15.6	Nearshore	Pelagic-neritic	Carnivore	Benthopelagivore
	Spinner shark	1	78.0	-16.5	15.2	Nearshore	Rocky and coral reefs	Carnivore	Pelagivore opportunist
	Blacktip shark	1	139.0	-15.3	16.6	Nearshore	Rocky and coral reefs	Carnivore	Pelagivore opportunist
	Spot-tail shark	1	66.0	-15.8	15.1	Nearshore	Rocky and coral reefs	Carnivore	Benthopelagivore
	Scalloped hammerhead	16	45.4 ± 25.0	-15.9 ± 0.1	16.5 ± 0.3	Offshore	Pelagic-neritic	Carnivore	Pelagobenthivore
Pelagic-oceanic elasmobranch	Tiger shark	1	169.0	-15.8	15.6	Offshore	Benthopelagic	Carnivore	Benthopelagivore
	Great hammerhead	1	77.0	-15.8	15.5	Offshore	Epipelagic	Carnivore	Benthopelagivore
Pelagic-oceanic teleost fish	Swordfish	132	152.9 ± 29.4	-16.6 ± 0.5	14.1 ± 0.6	Offshore	Bathypelagic	Carnivore	Pelagivore opportunist

3.2.2. Identification of trace element bioaccumulation patterns

All analysed species were grouped according to their trace element profiles. For this, only trace elements for which the detection frequency was > 70% were selected (i.e. As, Cd, Cu, Fe, Hg, Mn, Ni, Se and Zn; Appendix 2.1) (Carravieri *et al*. 2020) and data below the LOQ were replaced as described in section 2.3.2. For each species, the mean concentration of each trace element was calculated and data were scaled (i.e. centred and divided by the standard deviation). Species were then grouped using hierarchical cluster analysis (Ward's clustering method), as described in section 2.6.2. Trace element concentrations were compared between inferred groups using Kruskal-Wallis followed by Dunn post-hoc test, in order to identify group(s) with the highest concentrations, group(s) with intermediate concentrations and group(s) with the lowest concentrations.

3.2.3. Investigating the effects of intrinsic and extrinsic factors on trace element bioaccumulation patterns

The composition of each group inferred from mean trace element concentrations, in terms of functional group, habitat and diet type, was investigated by calculating the presence of each factor in each group. $\delta^{13}C$ and $\delta^{15}N$ values were also compared between inferred groups using Kruskal-Wallis followed by Dunn post-hoc test.

To assess the influence of length, $\delta^{13}C$ (i.e. proxy of origin of energy) and $\delta^{15}N$ (i.e. proxy of trophic position) on trace element concentrations among individuals of the same group, non-metric multidimensional scaling (nMDS) ordinations of Bray-Curtis similarity matrices of capture fisheries species length, $\delta^{13}C$ and $\delta^{15}N$ values and trace element concentrations were computed for each group. Arrows were represented on the plots to show the influence of each factor. Briefly, the longer the arrow, the higher the influence. In addition, two arrows pointing in the same direction are possibly positively correlated, while they are possibly negatively correlated if they point in opposite directions. $\delta^{13}C$ and $\delta^{15}N$ values measured in all analysed species are presented in Table 3.1.

3.3. RESULTS

3.3.1. Groups inferred from trace element concentrations

Four groups were inferred from mean trace element concentrations in Seychelles capture fisheries species (Fig. 3.1A). Among all groups, group 1 and group 3 had the highest mean concentrations of Cd (Dunn test, $p < 0.001$) and group 1 and group 4 had the highest mean Ni concentrations (Dunn test, $p = 0.001$ between groups 1 and 2, $p < 0.001$ for all other comparisons) (Fig. 3.1B, C). Group 2 and group 3 had the lowest mean Cu concentrations (Dunn test, $p < 0.001$). Group 1 also had the highest mean As, Cu, Mn and Zn concentrations (Dunn test, all $p < 0.001$), and the lowest mean Hg, Fe and Se concentrations (Dunn test, all $p < 0.001$). Group 3 also had the highest mean Hg and Se concentrations (Dunn test, both $p < 0.001$) while having the lowest mean Ni and Mn concentrations (Dunn test, both $p < 0.001$). Group 4 also had the highest mean Fe concentration (Dunn test, $p < 0.001$). Finally, group 2 also had the lowest mean Cd (Dunn test, $p < 0.001$) and mean Zn (Dunn test, $p = 0.001$ with group 2, $p < 0.001$ with all other groups) concentrations.

Group 1 was composed only of benthic crustaceans (Fig. 3.2). Groups 2 and 4 were mainly composed of demersal teleost fish (but group 2 includes the octopus), and group 3 was composed only of pelagic species, including pelagic-neritic and pelagic-oceanic elasmobranch, and teleost fish species. There was no clear clustering among species' habitat or diet types. Indeed, for most of habitats and diets, a given type could be found in at least two groups.

Group 1 had a higher mean $\delta^{13}C$ value than the three other groups (Dunn test, $p < 0.001$) (Fig. 3.3). Group 3 had the highest mean $\delta^{15}N$ value (Dunn test, $p < 0.001$), while group 1 had the lowest mean $\delta^{15}N$ value (Dunn test, $p < 0.001$) (Fig. 3.3).

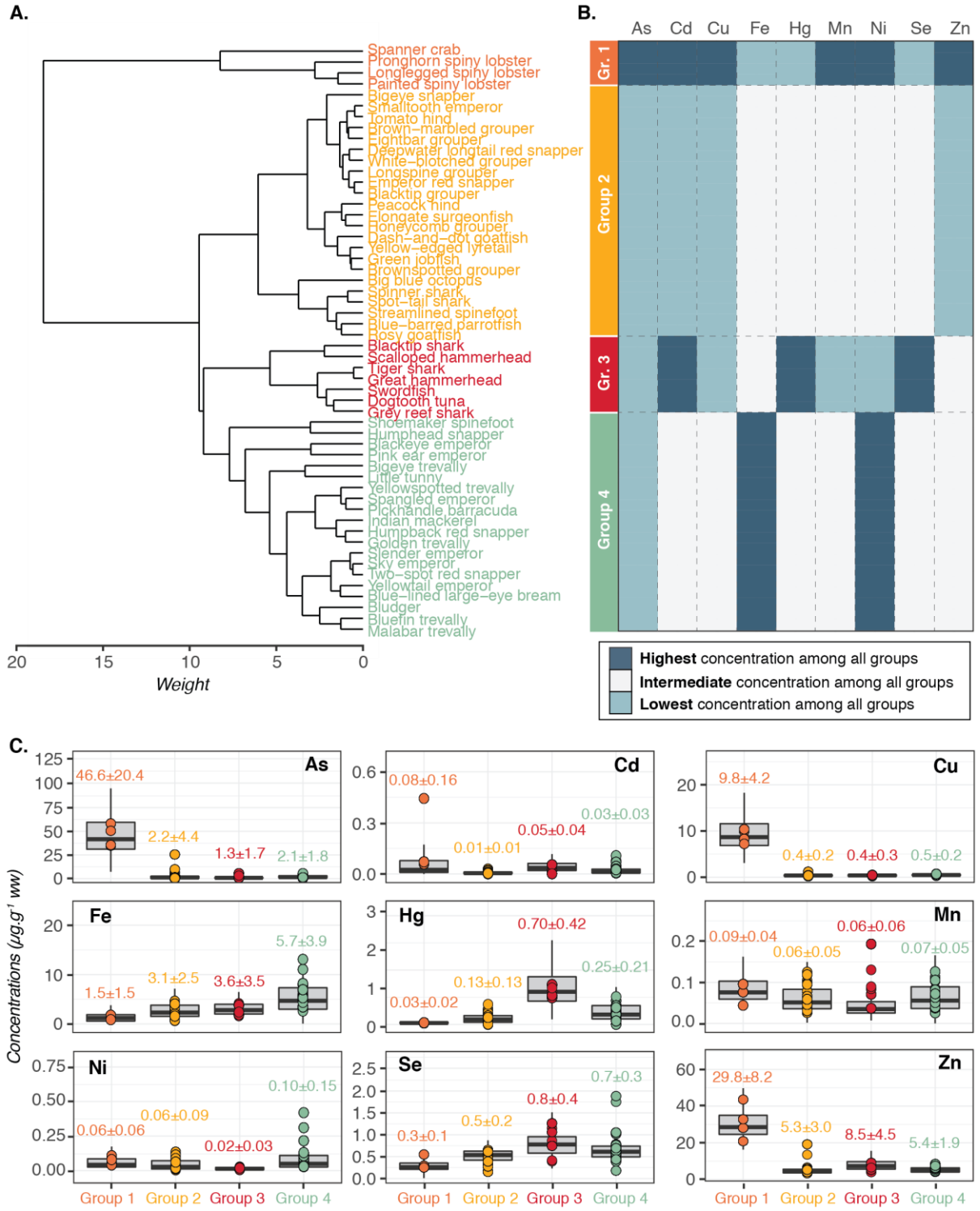

Fig. 3.1. Groups inferred from mean trace element concentrations in capture fisheries species from the Seychelles (A) and their trace element profiles (B).

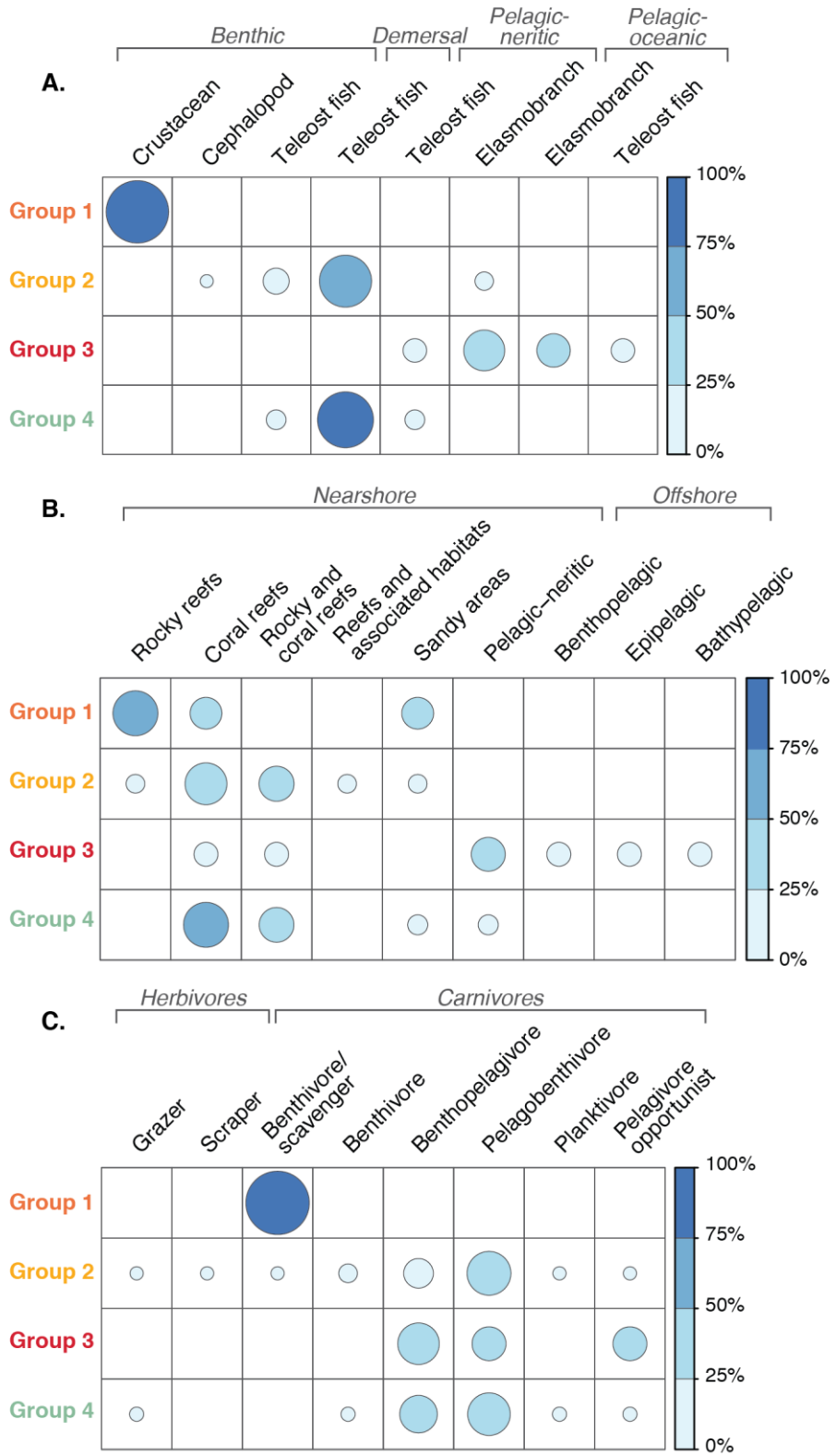

Fig. 3.2. Compositions of groups inferred from mean trace element concentrations in Seychelles capture fisheries species in terms of functional group (A), habitat type (B) and diet type (C). Circles' colour intensity and size are proportional to the percentage of each functional group, habitat or diet type in each trace element profile group.

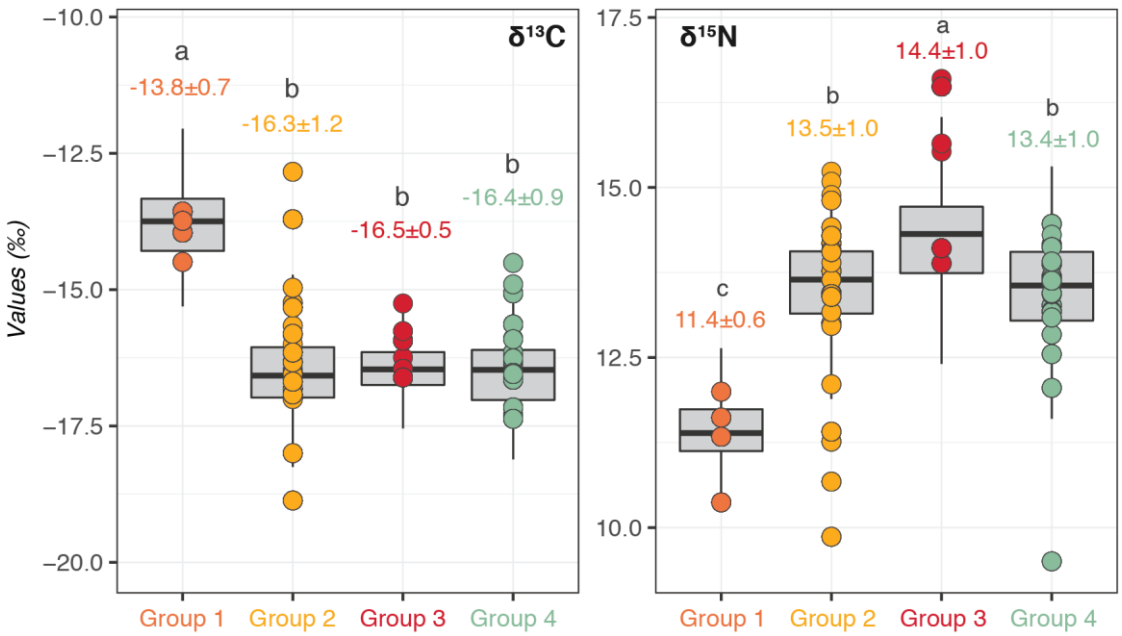

Fig. 3.3. $\delta^{13}C$ and $\delta^{15}N$ values (‰) measured in muscle tissues of capture fisheries species in each group determined from trace element profiles. Points represent the mean value for each species present in the group, and the mean value in each group (mean ± SD) is indicated above each boxplot in the corresponding colour. A different letter indicates a significant difference between groups.

3.3.2. Intragroup variation in trace element bioaccumulation

In group 1, Hg seemed to be highly positively correlated with length while trace elements such as Cd, Cu, Mn and Se seemed to be negatively correlated with length (Fig. 3.4). As seemed to be positively correlated with $\delta^{15}N$, and Zn seemed to be positively correlated with both $\delta^{15}N$ and length. Fe seemed to be negatively correlated with $\delta^{15}N$.

In group 2, Se seemed to be positively correlated with length and negatively correlated with $\delta^{13}C$. Hg seemed to be influenced (i.e. positive correlation) by both length and $\delta^{15}N$. In addition, As, Cu, Mn and Zn seemed to be negatively correlated with $\delta^{15}N$.

In group 3, length seemed to influence Cd and Hg (i.e. positive correlation), as well as As, Mn and Se (i.e. negative correlation). Cu, Fe, Ni and Zn seemed to be negatively correlated with both $\delta^{13}C$ and $\delta^{15}N$.

Finally, in group 4, Hg was mainly influenced by $\delta^{15}N$ (i.e. positive correlation), although length seemed to also have an influence. Both As and Se seemed to be highly positively correlated with $\delta^{13}C$.

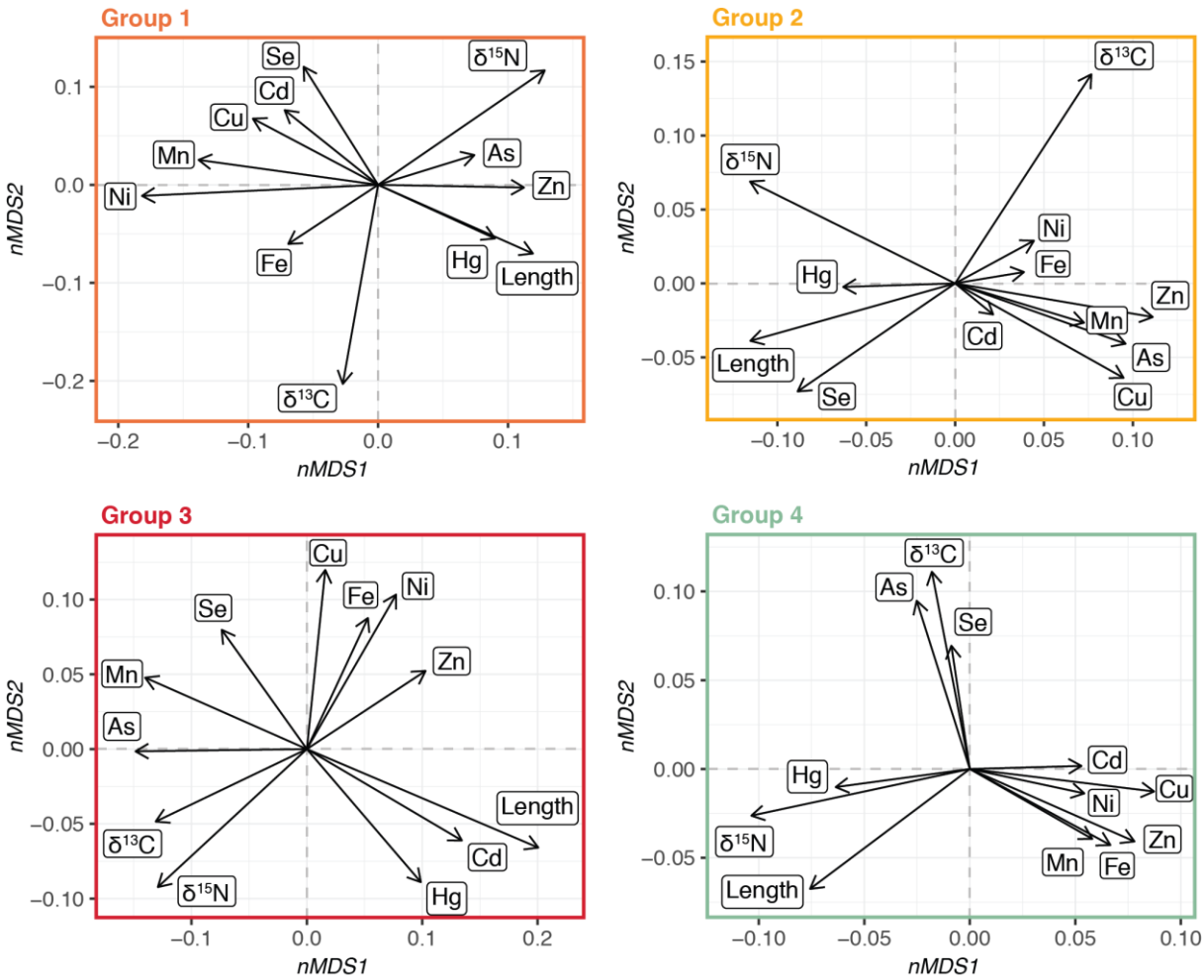

Fig. 3.4. Non-metric multidimensional scaling (nMDS) ordination of Bray-Curtis similarity matrix of capture fisheries species length, $\delta^{13}C$ and $\delta^{15}N$ values and trace element concentrations in each group inferred from mean trace element concentrations.

3.4. DISCUSSION

3.4.1. Trace element bioaccumulation patterns: influence of taxa, vertical feeding habitat, diet and trophic position

In marine organisms, trace element bioaccumulation is influenced by the combination of intrinsic (e.g. physiology) (Kojadinovic *et al*. 2007; Rainbow 2007) and extrinsic factors (e.g. trophic ecology) (Metian *et al*. 2013; Chouvelon *et al.* 2017), and by the availability of trace elements in the consumers' environment and/or diet (Bustamante *et al.* 1998; Raimundo *et al.* 2013). In our study, these factors were also key to explain the results which evidenced that the trophic pathway is the dominant route for trace element exposure for marine organisms (Wang 2002; Mathews and Fisher 2009).

Here, crustacean species were grouped together in the clustering, being the species with the highest As, Cu and Zn concentrations, and the lowest Fe, Hg and Se concentrations. Such pattern can be explained largely by the physiology of these species. Decapod crustaceans are known to have high Cu and Zn uptake rates from food due to high physiological needs for these elements (Rainbow 2002). Zn is well-known to be a cofactor in numerous enzymes (Rainbow 2002) while Cu constitutes an essential compound of hemocyanin, a protein involved in the transport of oxygen in the blood of crustaceans (Taylor and Anstiss 1999). In addition, decapod crustaceans are known to detoxify trace elements by storing them into trace element-rich granules (Rainbow 1998) and previous work reported that the most common granules were those containing Cu and Zn (Nassiri *et al.* 2000). The low concentrations of other trace elements in the muscle of the three crustacean species analysed in our study could also be explained by the morphology of these species: as their body is covered by an impermeable cuticle, trace element uptake from water is highly limited for decapod crustaceans (Rainbow 1998). The trophic pathway would thus be the main pathway for these crustaceans' exposure to trace elements, as shown for cephalopods, elasmobranchs and teleost fishes (e.g. Bustamante et al. 2002, 2004, Mathews and Fisher 2009). This suggests that their food items contain low levels of Fe, Hg and Se and/or these elements are poorly assimilated and retained. In the case of Hg, usually known to biomagnify through food webs (Wang 2002), this would be consistent with the trophic positions of the crustacean species analysed in this study, which seemed to be lower than all other species (i.e. they had the lowest $\delta^{15}N$ values). Although we could not calculate their absolute trophic positions due to a lack of isotopic baseline in the Seychelles, this was supported by previously estimated trophic positions of these species compared to pelagic and demersal species (Sardenne *et al.* 2017). In addition, all species analysed here were scavengers and thus fed partially on large pieces of animal tissue (Palomares and Pauly 2020). Although digestive tissues like liver or digestive gland are known to be trace elements-rich, being detoxifying organs, muscle generally has a limited role both in terms of detoxification and storage (Afandi *et al.* 2018). For scavenging decapod crustaceans, low trace element intake is thus expected from their food, which would partly explain their low concentrations in some trace elements (Rainbow 1998).

In crustacean species analysed in this study, As concentrations were also remarkably high compared to elasmobranchs and teleost fishes (21 to 36 times higher). Decapod crustaceans, like the spiny lobster and crab species analysed here, are known to preferentially

retain As in the form of arsenobetaine (Khokiattiwong *et al*. 2009), which could explain high As concentrations in these species. However, concentrations exceeding the maximum values reported in crustaceans (i.e. 95.3 $\mu g.g^{-1}$ ww) suggest a link with the bioavailability of As in their food items. Indeed, the four crustacean species analysed here are known to feed partly on invertebrates like bivalves (Baylon and Tito 2012; Sardenne *et al.* 2021), while the pronghorn, longlegged and painted spiny lobsters have been reported to also feed on macrolagae (Sardenne *et al*. 2021). Although bivalves generally display low As uptake from seawater (Gómez-Batista *et al*. 2007; Hédouin *et al.* 2010), As accumulation can be very high when there is a disequilibrium between phosphorous (P) and nitrogen (N). As can replace P in phytoplankton growing in enriched-N waters, leading to As bioaccumulation to high levels as shown in some filter-feeder bivalves from New Caledonia (Metian *et al*. 2008; Hédouin *et al*. 2009). Such processes could also occur in waters surrounding the granitic islands of the Mahé Plateau, especially around Mahé Island, where crustaceans were caught. Indeed, due to local rainfall dynamics and to sewage discharge, waters in this area tend to be enriched in N, further destabilising the N:P ratio (Littler *et al*. 1991). The subsequent enhanced As bioaccumulation in both primary producers and bivalves could thus travel up the food chain to crustaceans feeding on them, thus enhancing As bioaccumulation in their tissues. This deserves further investigation to determine if As highly bioaccumulates in bivalves from the Seychelles coastal waters and effectively transfers from bivalves to crustaceans, or if dietary As could originate from another prey in decapod crustaceans' diet. Analyses of the physicochemical forms under which As is present in crustacean species' prey (i.e. proportions of arsenobetaine and iAs) are also needed.

Although taxonomy significantly played a role in trace element bioaccumulation for crustaceans, there was no clear clustering between elasmobranch and teleost fishes. Previous work on trace elements bioaccumulation in these species showed differences in trace elements uptake from seawater (Jeffree *et al*. 2006, 2010), while assimilation efficiency from food was generally similar between elasmobranchs and teleosts (Mathews *et al*. 2008). Our results thus support the hypothesis that the main pathway for trace element uptake in these species is from food and not from the dissolved phase (Mathews and Fisher 2009).

Habitat and diet types poorly explained trace element patterns in the clustering, but species were mainly grouped according to their vertical feeding habitats (i.e. benthic, demersal and pelagic), suggesting that trace element exposure varies according to the considered marine

compartment. This is supported by trace element dynamics in the marine environment, as sediments are known to be reservoir of trace elements (Neff 2002a). Benthic species, feeding on prey living on the seafloor, are thus more exposed to trace element intake through the trophic pathway (Wang 2002). In addition, by feeding close to the seafloor, demersal species are more prone to feed on benthic feeders and thus are expected to be more exposed to trace element uptake than pelagic species (Rejomon *et al.* 2010). It is also possible that trophic position played a role in trace element bioaccumulation in each marine compartment. Pelagic species, in group 3, had the highest Hg and Se concentrations among all groups and were among the species with the highest $\delta^{15}N$ values. As Hg is known to biomagnify through food webs (Lavoie *et al*. 2013), and as Se was suggested to co-accumulate with Hg especially in case of high Hg concentrations (Azad *et al*. 2019), it was thus expected that pelagic species in this study had the highest Hg and Se concentrations.

3.4.2. Trace element bioaccumulation within identified patterns: influence of size, feeding habitat and trophic position

Contrary to the other trace elements, the effects of length on Hg bioaccumulation seemed to be the same for all identified groups. In all groups, Hg concentrations seemed to be positively correlated with individual length, suggesting that Hg bioaccumulates with age, regardless of any other factor. For trophic position, however, the effects on Hg bioaccumulation were less evident. Hg seemed to be correlated with $\delta^{15}N$ only in group 2 and 4, suggesting that the level of carnivory does not always significantly affect Hg bioaccumulation, or that other factors could be more significant and would mask the effects of trophic position. For example, among species of group 1, species feed on varied prey items in terms of trophic position and/or Hg exposure through habitat. Indeed, crustaceans of group 1 feed on many benthic prey such as other crustaceans, fish and molluscs, but also on polychaetes, echinoderms and macroalgae for spiny lobsters (Baylon and Tito 2012; Sardenne *et al.* 2021). In this case, given the difference of foraging habitats and habits among consumed prey, it is evident that Hg exposure through the trophic pathway will vary from one prey to another, which could have masked Hg biomagnification in crustacean species.

For the other trace elements in this study, the effects of length, origin of energy and trophic position on their bioaccumulation were variable from one group to another. As and Zn seemed to biomagnify in benthic crustacean species, while they seemed to biodilute in the

demersal teleost species of group 2. However, the effect of trophic position on the bioaccumulation of Cu and Fe was the same (i.e. biodilution) regardless of the group. Similarly, Zn concentrations seemed positively correlated with length in benthic crustaceans, while they seemed negatively correlated with length in demersal teleost species (groups 2 and 3). Finally, regardless or the species group, $\delta^{13}C$ values were correlated, either positively or negatively, with the concentrations of one or more trace elements. These results suggest that, regardless of the functional group or vertical feeding habitat, length (and thus age), trophic position and origin of energy all have systematically an effect on the bioaccumulation of one or more trace elements. However, this also suggest that the significance and nature (i.e. positive or negative relationship) of this effect on the bioaccumulation of one given trace element will vary according to functional group and/or vertical feeding habitat.

3.5. CHAPTER HIGHLIGHTS

Chap. 1 – Main findings

- Trace element bioaccumulation was highly influenced by the **type and/or level of activity of regulation mechanisms**.
- The **trophic pathway** (i.e. intake through the diet) was the **main route of exposure to trace elements** for the species analysed in this chapter.
- In addition to metabolism processes, **size and trophic ecology** (i.e. trophic position, feeding vertical habitat, trophic position and diet) also **had key roles in trace element bioaccumulation**.
- As a consequence: **crustacean species** had particularly **high As, Cu and Zn concentrations** while **top predators** had **high Hg and Se concentrations**.

3.6. IMPLICATIONS FOR THE FOLLOWING CHAPTERS

In this chapter, we demonstrated the importance of intrinsic factors, such as the presence of regulation mechanisms or the length of the considered organism, but also the importance of extrinsic factors linked to trophic ecology, such as the habitat, the trophic position or the diet

of the considered organism, in understanding trace element bioaccumulation in marine organisms. Vertical habitat, especially, appeared to be a key parameter in determining trace element exposure and thus uptake in marine consumers. Within groups of species with similar trace element profiles, length, origin of energy and trophic position seemed to have significant effects on trace element bioconcentration, with different relationships (i.e. non-significant effect, positive or negative correlation) from one group to another.

As a consequence, in the following chapters, we will examine trace element bioaccumulation in the three main vertical habitats using model species (i.e. spiny lobsters in benthic habitats, emperor red snapper in demersal habitat and swordfish in pelagic habitat; species presented in section 2.3). For this, in addition to specific ecological factors that can influence trace element bioaccumulationin these species, we will consider the effects of length, origin of energy (through $\delta^{13}C$) and trophic position (through $\delta^{15}N$).

4. CHAPTER 2 – TRACE ELEMENT BIOACCUMULATION IN TROPICAL BENTHIC SYSTEMS: CASE OF THE SPINY LOBSTERS

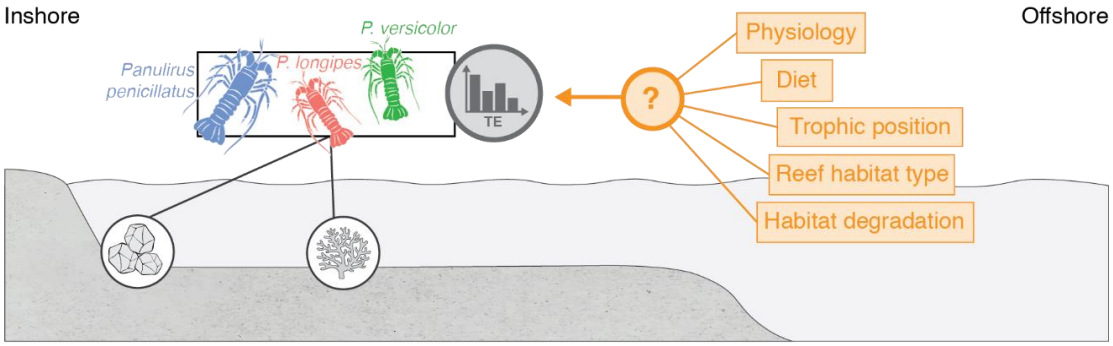

Content

4.1. CONTEXT AND OBJECTIVES

On a general aspect, decapod crustaceans are known to be particularly rich in trace elements like Cu and Zn (Miao *et al.* 2001; Baki *et al*. 2018; Chapter 1), due to high physiological needs for these elements (Rainbow 2002; Chapter 1). Some decapod crustaceans, including spiny lobster species, are also able to bioaccumulate elevated concentrations of As, most probably due to the high concentrations of arsenobetaine in some of their food items (Metian *et al*. 2008; Hédouin *et al.* 2009; Palomares and Pauly 2020) and to their preferential retention of As under the arsenobetaine form (Khokiattiwong *et al.* 2009; Chapter 1). Although mechanisms of trace element bioaccumulation through physiological processes in decapod crustaceans has been extensively reviewed (Rainbow 1998, 2002, 2007), there is a lack of data on the other intrinsic and extrinsic factors that might influence trace element bioaccumulation in these species, like size, sex and trophic ecology. Sardenne *et al*. (2017) made a link between trophic position and Hg bioaccumulation in Seychelles spiny lobsters compared to other marine species, but could not investigate the factors explaining intraspecific variability.

As commented in the introduction, in addition to physiological processes, intrinsic factors influencing trace element bioaccumulation in marine organisms can also include the size of individuals, as shown in many fish species (Anan *et al.* 2005; Kojadinovic *et al*. 2007; Barone *et al*. 2013). Although previous works showed no difference of trace element bioaccumulation between sexes in fish species (e.g. Chouvelon *et al.* 2017), physiological needs and individual size (i.e. sexual dimorphism) in these species can be sex-dependent (Qiao *et al*. 2016). Sex may thus have an effect on trace element retention (e.g. due to different composition of the gonads) and elimination (e.g. trough spawning) in some marine species, including crustaceans. In addition, the trophic pathway seems to be the main way of exposure to trace element for many marine organisms like teleosts, elasmobranchs and bivalve molluscs (Wang 2002; Mathews and Fisher 2009; Chapter 1). As a consequence, extrinsic factors influencing trace element bioaccumulation in these species mainly include trophic ecology (i.e. habitat, diet composition and trophic position) (e.g. Wang 2002; Le Croizier *et al*. 2016; Chouvelon *et al*. 2018, 2019; Chapter 1). Similarly to teleosts, elasmobranchs and bivalve molluscs, trophic ecology-related exposure may thus lead to variation in trace element bioaccumulation in decapod crustaceans (i.e. here, spiny lobster species), as already suggested in Chapter 1.

Spiny lobsters are coastal species, found in rocky and coral reefs, where they use the crevices to hide from predators during the day, while they leave their den at dusk to feed and mate during the night (Intès *et al.* 1979; Holthuis 1991). They are considered generalist feeders, which opportunistically forage on a large diversity of benthic prey like crustaceans, echinoderms, algae and molluscs (Williams 2007; Sabino *et al.* 2021; Sardenne *et al*. 2021). Their diet composition is thus thought to be highly dependent on prey availability, depending on their habitat characteristics (Blamey *et al.* 2019; Sabino *et al*. 2021). Habitat quality, including the type and complexity of coverage, is thus fundamentally important for spiny lobsters in respect of their foraging and antipredation strategies (Holthuis 1991; MacArthur *et al*. 2011). However, coastal reefs are under high human pressure in the Seychelles due to increasing coastal development and global climate change (Khan and Amelie 2015). In the last 25 years, coral reefs and granitic reefs supporting encrusting corals have been degraded through multiple bleaching events, with the 2016 bleaching event affecting around 50% of hard corals in the Seychelles (Obura *et al*. 2017). The subsequent modification of prey availability through coral degradation and its associated loss of species diversity (Robinson *et al.* 2019) partially altered local spiny lobsters' diet (Sabino *et al.* 2021). This may have consequences on their trace element intake and their subsequent bioaccumulation.

In respect of these elements, here I investigated the effects of several intrinsic (i.e. species, size and sex) and extrinsic (i.e. diet composition, trophic position, habitat reef type and coral reef degradation) factors on trace element bioaccumulation in Seychelles spiny lobster species (i.e. pronghorn spiny lobster – *Panulirus penicillatus*; longlegged spiny lobster – *P. longipes*; painted spiny lobster – *P. versicolor*). In the Chapter 1, some of the effects of physiology, diet, size, $\delta^{13}C$ and $\delta^{15}N$ on trace element bioaccumulation have been identified in decapod crustaceans. The present chapter thus aims to further explore these effects through the use of model species, i.e. spiny lobsters, as well as to assess the importance of habitat type and quality in influencing trace element bioaccumulation in these benthic reef species.

4.2. METHODOLOGY

4.2.1. Dataset

Pronghorn, longlegged and painted spiny lobsters were sampled as part of the annual Participatory Lobster Monitoring Program led by the Seychelles Fishing Authority (SFA) in

collaboration with local fishermen (Seychelles Fishing Authority 2014). A total of 106 spiny lobsters (47 pronghorn spiny lobsters, 44 longlegged spiny lobsters and 15 painted spiny lobsters), were caught in several fishing areas on the west coast of the island of Mahé, Seychelles, during five sampling campaigns in October/November from 2014 to 2018 (Fig. 4.1). The date, GPS location and reef type (i.e. carbonate or granite reef) were recorded for each collected lobster. They were also sexed and measured for carapace length (to the nearest 0.1 mm).

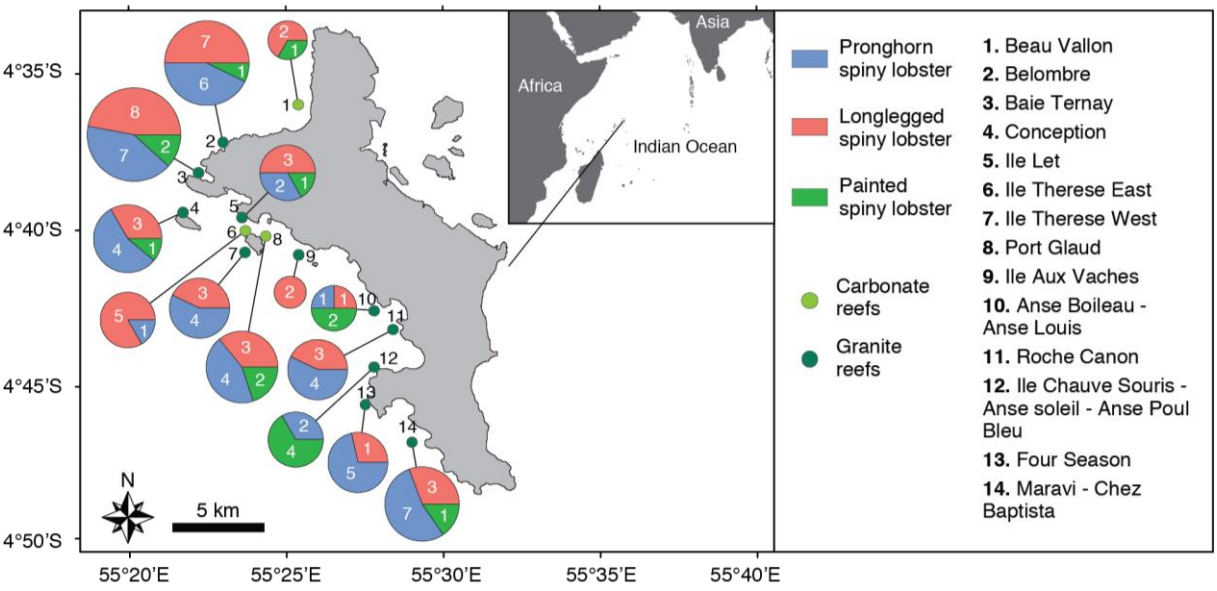

Fig. 4.1. Fishing locations for the three species of spiny lobster caught from the west coast of Mahé (Seychelles, Western Indian Ocean). The number of individuals caught per species is indicated in the corresponding chart; size of charts is proportional to the total number of spiny lobsters per site.

In this chapter, only As, Cd, Cr, Cu, Hg, Mn, Ni, Pb, Se and Zn (i.e. DF > 70%, Appendix 2.1) were used to characterise trace element profiles. Trophic tracers (i.e. FA analysed in hepatopancreas of 64 individuals and stable isotopes analysed in tail muscle tissues of all 106 individuals) were also used to link trace element bioaccumulation to feeding on certain types of prey. Detailed numbers of the spiny lobsters sampled and analysed for trace elements across sexes, habitat types (i.e. carbonate and granite reefs) and time periods of coral degradation (i.e. pre- (2014-2015) and post-bleaching (2016-2018) periods) are given in Appendix 4.1.

4.2.2. Trophic ecology as a key information to understand trace element bioaccumulation

Although the annual Participatory Lobster Monitoring Program allowed for the acquisition of the tail muscle samples analysed in this thesis, its purpose is mainly to monitor spiny lobsters' stocks to improve stock management for the artisanal lobster fishery. Thus, until recently, Seychelles spiny lobsters' trophic ecology, and especially their foraging behaviour and adapting capacity to habitat change (i.e. coral reef degradation), were poorly known. It thus appeared to us that improving knowledge on these points was the first step before investigating trace element bioaccumulation in these species. Results were published in the journal *Estuary, Coastal and Shelf Science* and a copy of the paper (Sabino *et al.* 2021) is presented in supplementary documents (Supp. Doc. 2). I chose not to present these results in the main text of the thesis as they were not directly related to trace element bioaccumulation. However, they are important to understand some aspects of trace element bioaccumulation in spiny lobsters' muscle tissues and the paper is thus briefly described in this subsection.

One of our paper main aim was to examine interspecific variations in habitat use and dietary overlap. For this, we computed fatty acid and isotopic trophic niches for the three species, as described in section 2.7.5. We then used niche metrics, i.e. niche size and especially probability of overlap between species, to assess dietary similarities and divergences among the three spiny lobster species. The **pronghorn spiny lobster**, as the **largest species**, had the **higher trophic position** and seemed to have a **higher level of carnivory** than the longlegged and painted spiny lobsters, due to higher consumption of prey items like carnivore gastropods and fish. The **longlegged and painted spiny lobster** had very **similar diets**, as demonstrated by their high fatty acid trophic niche overlap. However, the **painted spiny lobster had a lower trophic position**, seemingly feeding on smaller/earlier life stage prey **than longlegged spiny lobster** individuals.

In addition, our paper showed that **spiny lobsters were sensitive to habitat degradation** like coral bleaching, and that **it altered their trophic ecology by increasing their dietary overlap**. Indeed, trophic niches were also computed and niche sizes and overlaps calculated, whenever possible, for each reef habitat type (i.e. carbonate and granite reefs) and for each period of reef habitat degradation (i.e. the pre- and post-2016 coral bleaching event). This revealed that the **dietary overlap** between the three species was **higher in granite reefs than in carbonate reefs**,

and that the **bleaching event caused an increase of dietary overlap** between the pronghorn and longlegged spiny lobsters. As carbonate reefs are more sensitive to degradation than granite reefs, and bleaching events are predicted to increase in frequency due to climate change, we hypothesised that **dietary overlap between the three spiny lobster species would probably increase in the future**.

4.2.3. Fatty acid trophic marker selection and identification

Well-known fatty acid trophic markers were used to provide insight into the foraging ecology of lobsters. This included trophic markers of bacteria (i.e. 16:1n-7, iso and anteiso-branched fatty acids), phytoplankton (i.e. 16:1n-7, 20:5n-3, 22:-6n-3), seagrass and/or macroalgae (i.e. 18:1n-9, 18:2n-6, 20:4n-6, 20:5n-3, 22:6n-3), bivalves molluscs and carnivorous gastropods (NMI fatty acids and DMA) and animal prey in general (i.e. 18:1n-9, 20:1n-9, 22:6n-3) (Budge *et al*. 2006; Iverson 2009; Kelly and Scheibling 2012; Meyer *et al*. 2019). Although it is not a particularly known trophic marker, the fatty acid 20:1n-7 was also selected as it was one of the fatty acids responsible for the difference between the pronghorn spiny lobster and both other species (Sabino *et al.* 2021). As some fatty acids can be trophic markers of several types of prey, correlations were tested among trophic tracers (i.e. fatty acid proportions and stable isotope values) to discriminate between possible prey of origin for each fatty acid trophic marker. Correlation results are presented in Sabino *et al.* (2021) and in the associated supplementary materials.

4.2.4. Investigation of factors involved in trace element bioaccumulation

Correlation tests were used to assess the relationship between spiny lobsters' trace element concentrations in tail muscle tissues and their size (i.e. cephalothorax length). Correlations were also tested between trace element concentrations and trophic markers (i.e. $\delta^{13}C$ and $\delta^{15}N$ and selected fatty acid trophic markers) in order to link intake of a specific trace element to consumption of specific prey or group of prey whenever possible.

To investigate the interspecific variations in trace element profiles and to compare them to fatty acid and isotopic trophic niches in Sabino *et al*. (2021), trace element profile ellipses were computed for each species, and ellipse sizes and probabilities of overlap were calculated. For each species, probabilities of overlap were also calculated for trace element profile ellipses of each sex, habitat reef type and time period of habitat degradation to serve as proxy of

similarity between levels of the same factor. Computed corresponding ellipses are only presented in appendices (Appendix 4.2 for factor sex, Appendix 4.3 for factor reef habitat type and Appendix 4.4 for factor time period of coral degradation). To complete these analyses, ANOVA/Kruskal-Wallis followed by their associated post-hoc tests (Tukey's HSD and Dunn test respectively) were used to individually compare trace element concentrations between species and, for each species, t-tests/Wilcoxon tests were used to compare trace element concentrations between sexes, reef habitat types and time periods of reef degradation.

No intraspecific comparison of trophic ecology (i.e. for a given species, between sexes, between habitat reef types and between time periods of habitat degradation) was made in Sabino *et al.* (2021). There were thus done here in order to be able to discriminate between size, physiology and trophic ecology to explain potential variations in trace element bioaccumulation. For this, fatty acid and isotopic trophic niches were computed for each sex of each species, and the probabilities of trophic niche overlap between sexes were calculated (Appendix 4.5 and Appendix 4.6). Isotopic trophic niches were also computed for each habitat reef type for each species and each time period of habitat degradation for pronghorn and longlegged spiny lobsters; associated probabilities of overlap were also calculated (Appendix 4.7 and Appendix 4.8, respectively). Finally, $\delta^{13}C$ and $\delta^{15}N$ values were compared between levels of the same factor using t-tests/Wilcoxon tests. Mean (± SD) values for each species and each level of each factor, with their associated statistical results, are presented in Appendix 4.9.

4.3. RESULTS

4.3.1. Size of sampled spiny lobsters

Over the sampling period, the pronghorn spiny lobster was significantly larger than the two other species, but there was no significant difference in cephalothorax length among individuals of the same species between reef habitat types, between sampling years and between the pre- and post-bleaching periods (Sabino *et al*. 2021).

Among pronghorn and among longlegged spiny lobster individuals, males were larger than females (Wilcoxon test, $p < 0.001$ for pronghorn spiny lobster; t-test, $p = 0.008$ for longlegged spiny lobster) (Fig. 4.2). There was no significant difference in cephalothorax length between sexes among painted spiny lobster individuals ($p > 0.05$).

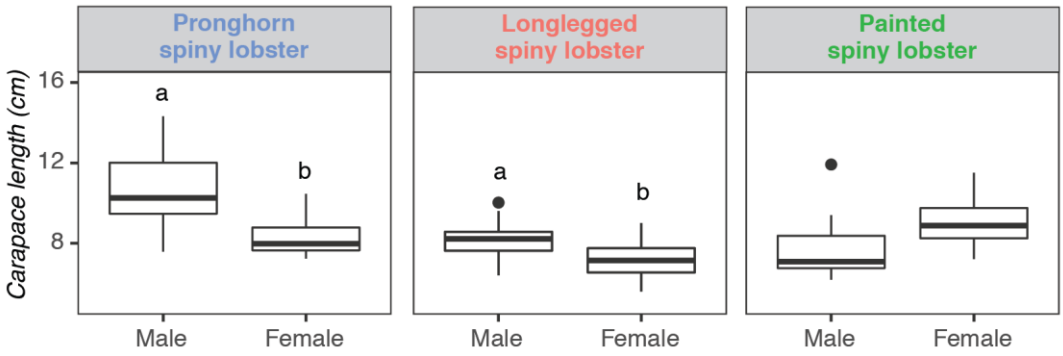

Fig. 4.2. Cephalothorax length (cm) of sampled spiny lobsters according to sex (B). A different letter indicates a significant difference ($p < 0.05$).

4.3.2. Interspecific variation in trace element profiles

Among the three lobster species, the painted spiny lobster had the largest trace element profile ellipse (0.41 [0.25 – 0.65] *vs* 0.14 [0.10 – 0.18] for the pronghorn spiny lobster and 0.22 [0.16 – 0.29] for the longlegged spiny lobster; associated probability of 1 for painted larger than pronghorn spiny lobster and of 0.99 for painted larger than longlegged spiny lobster) (Fig. 4.3A). The longlegged spiny lobster also had a larger trace element profile ellipse than the pronghorn spiny lobster (associated probability of 0.99). Both the profile ellipse of the pronghorn and of the longlegged spiny lobsters were included in the profile ellipse of the painted spiny lobster (overlaps of 93.6% [72.1 – 99.9%] for pronghorn in painted spiny lobster and of 91.6% [75.5 – 99.3%] for longlegged in painted spiny lobster) (Fig. 4.3B).

The pronghorn and painted spiny lobsters were separated from the longlegged spiny lobster by As while the painted spiny lobster was separated from the pronghorn spiny lobster by Cr, Mn and Ni and the longlegged spiny lobster was separated from the pronghorn spiny lobster by Cr, Ni, Hg and Pb (Fig. 4.3A).

Among the three lobster species, the pronghorn spiny lobster had higher Mn concentrations than the longlegged spiny lobster and lower Mn concentrations than the painted spiny lobster (0.09 ± 0.04 $\mu g.g^{-1}$ ww *vs* 0.08 ± 0.04 $\mu g.g^{-1}$ ww for longlegged spiny lobster and 0.11 ± 0.04 $\mu g.g^{-1}$ ww for painted spiny lobster; Dunn test, $p = 0.003$ with longlegged spiny lobster and $p = 0.001$ with painted spiny lobster) (Fig. 4.3D). This species also had higher Pb concentrations than the painted spiny lobster (0.013 ± 0.016 $\mu g.g^{-1}$ ww *vs* 0.008 ± 0.010 $\mu g.g^{-1}$ ww; Dunn test, $p = 0.029$). The pronghorn spiny lobster had the lowest Ni concentrations (0.04 ± 0.04 $\mu g.g^{-1}$ ww *vs* 0.07 ± 0.06 $\mu g.g^{-1}$ ww for longlegged spiny lobster and 0.12 ± 0.08

µg.g^{-1} ww for painted spiny lobster; Dunn test, p = 0.003 with longlegged spiny lobster and p = 0.024 with painted spiny lobster) and the highest Zn concentrations (32 ± 7 µg.g^{-1} ww *vs* 28 ± 6 µg.g^{-1} ww for longlegged spiny lobster and 23 ± 6 µg.g^{-1} ww for painted spiny lobster; Dunn test, p = 0.017 with longlegged spiny lobster and p = 0.013 with painted spiny lobster), while the painted spiny lobster had the highest Ni concentrations (Dunn test, p = 0.024 with pronghorn spiny lobster and p < 0.001 with longlegged spiny lobster) and the lowest Zn concentrations (Dunn test, p = 0.013 with pronghorn spiny lobster and p < 0.001 with longlegged spiny lobster). The painted spiny lobster also had the lowest Hg concentrations (0.028 ± 0.041 µg.g^{-1} ww *vs* 0.032 ± 0.012 µg.g^{-1} ww for pronghorn spiny lobster and 0.033 ± 0.020 µg.g^{-1} ww for longlegged spiny lobster; Dunn test, p = 0.002 with pronghorn spiny lobster and p < 0.001 with longlegged spiny lobster). The longlegged spiny lobster had the lowest As concentrations (35 ± 14 µg.g^{-1} ww vs 56 ± 17 µg.g^{-1} ww for pronghorn and 40 ± 25 µg.g^{-1} ww in painted spiny lobsters; Dunn test, p < 0.001 with pronghorn spiny lobster, p = 0.001 with painted spiny lobster).

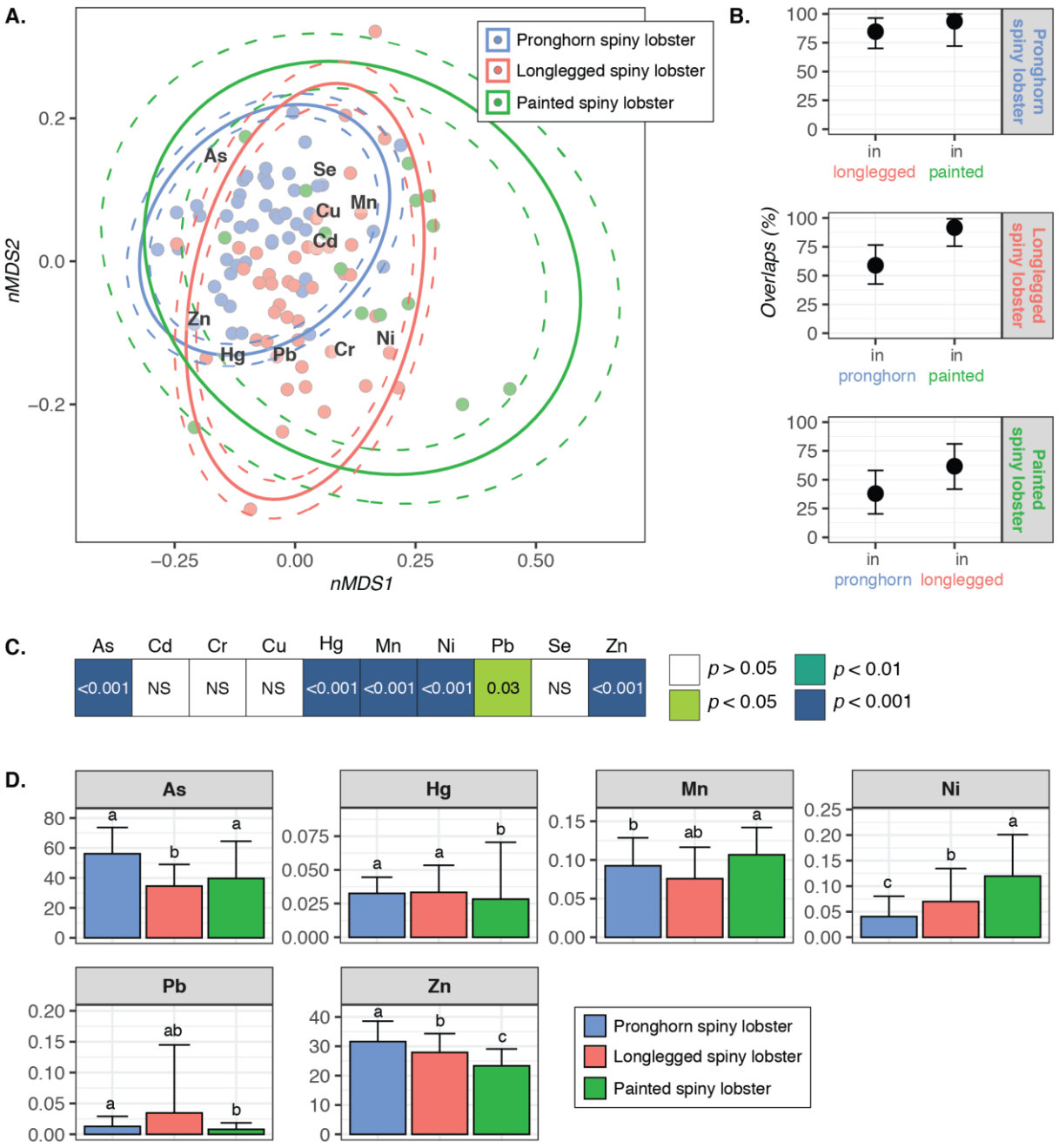

Fig. 4.3. Non-metric multidimensional scaling (nMDS) ordination of Bray-Curtis similarity matrix of tail muscle tissue trace element composition in the three spiny lobster species (A), probabilities of trace element ellipse overlap (%) between species (B), difference in trace element concentrations (Kruskal Wallis) between species for each measured trace element (C) and post-hoc results (Dunn test) for trace elements for which there is a significant difference between spiny lobster species (D). For each species, the mean ellipse is represented by a plain line and uncertainty ellipses are represented by dashed lines (A). Overlaps (B) are presented as mean with their associated CI95%. Numbers in the cells are the associated *p*-values, and the cells' colour intensity is proportional to the *p*-value; only *p*-values < 0.05 are indicated (C). Different letters indicate a significant difference between spiny lobster species (D). NS = Non-significant.

4.3.3. Intraspecific variation in trace element profile according to physiology: effect of size and sex

Hg and Zn were strongly positively correlated with cephalothorax length in all three lobster species (Fig. 4.4A). As was strongly positively correlated with cephalothorax length only in the painted spiny lobster and Mn was negatively correlated with cephalothorax length only in the pronghorn spiny lobster.

Male and female pronghorn spiny lobsters had a very high overlap in trace element profile (88.2% [72.2 – 98.6%] for males in females and 90.7% [72.1 – 99.3%] for females in males) (Fig. 4.4B). Male and female longlegged spiny lobsters also had a high overlap in trace element (69.8% [49.4 – 90.0%] for males in females and 87.9% [66.6 – 98.6%] for females in males). The trace element profile ellipse of female painted spiny lobsters seemed highly included in the one of males (overlaps of 21.3% [7.5 – 45.4%] for males in females and of 93.9% [63.0 – 100.0%] for females in males). For all three species, there were few differences between trace element concentrations in males and females (Fig. 4.4C). Cr concentrations were higher in female pronghorn spiny lobster than in males (0.11 ± 0.07 $\mu g.g^{-1}$ ww *vs* 0.09 ± 0.08 $\mu g.g^{-1}$ ww) and higher in male painted spiny lobster than in female (0.24 ± 0.29 $\mu g.g^{-1}$ ww *vs* 0.02 ± 0.01 $\mu g.g^{-1}$ ww). In addition, Zn concentrations seemed be higher in male longlegged spiny lobsters than in females (29 ± 6 $\mu g.g^{-1}$ ww *vs* 26 ± 7 $\mu g.g^{-1}$ ww).

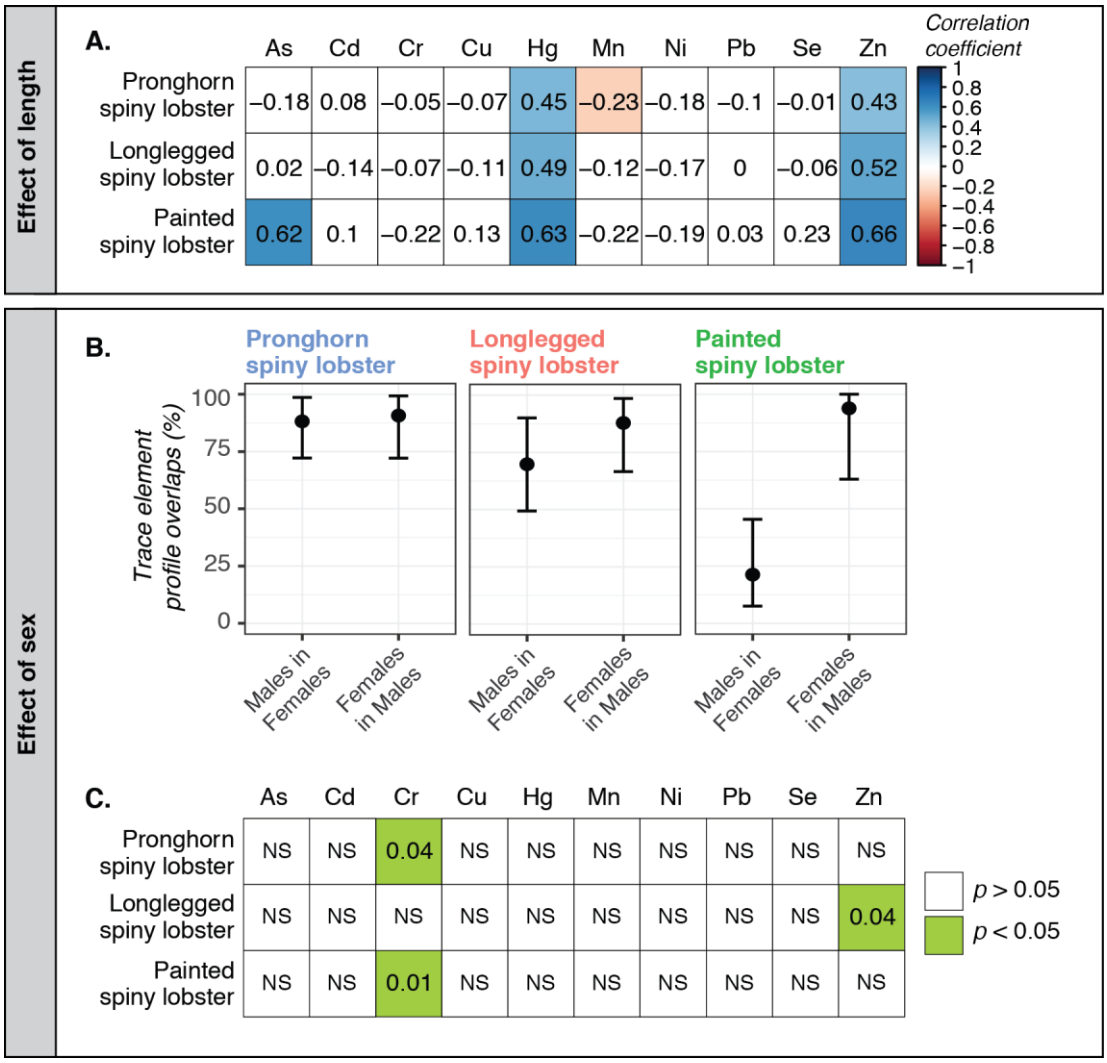

Fig. 4.4. Correlation (Pearson or Kendall) between tail muscle trace element concentrations and spiny lobsters' cephalothorax length (A), probabilities of trace element profile overlap (%) between male and female spiny lobsters of each species (B) and difference of trace element concentrations (t-test or Wilcoxon test) between sexes for each spiny lobster species (C). Coloured cells indicate a significant correlation ($p < 0.05$) between trace element concentrations and cephalothorax length or a significant difference ($p < 0.05$) between males and females, while uncoloured cells indicate a non-significant correlation/difference (A, C). Numbers in the cells are the associated correlation coefficients (for correlation) or the associated *p*-values (for significant difference), and the cells' colour intensity is proportional to the coefficient or the *p*-value (A, C). Only *p*-values < 0.05 are indicated (C). Overlaps are presented as mean with the associated CI95% (B). NS = Non-significant.

4.3.4. Effect of reef habitat type and habitat degradation on intraspecific variation in trace element profile

Trace element ellipses of pronghorn spiny lobsters in carbonate and granite reefs had moderate overlap (57.8% [24.2 – 87.8%] for carbonate in granite and 56.7% [26.3 – 92.1%] for granite in carbonate) (Fig. 4.5A). There was a high overlap between the trace element profiles ellipses of longlegged spiny lobsters from carbonate and from granite reefs (80.9% [55.5 – 97%] for

carbonate in granite reefs and 89.7% [73.0 – 99.3%] for granite in carbonate reefs). Although there was a high uncertainty (i.e. large CI95%) around the mean, the trace element ellipse of painted spiny lobsters from carbonate reefs seemed mainly included in the one of painted spiny lobsters from granite reefs (overlaps of 64.3% [12.5 – 99.3%] for carbonate in granite reefs and 20.5% [4.1 – 60.2%] for granite in carbonate reef).

Pronghorn spiny lobsters from carbonate reefs had higher Cd concentrations (0.084 ± 0.045 $\mu g.g^{-1}$ ww *vs* 0.054 ± 0.086 $\mu g.g^{-1}$ ww) and Pb concentrations (0.039 ± 0.032 $\mu g.g^{-1}$ ww *vs* 0.010 ± 0.011 $\mu g.g^{-1}$ ww) than pronghorn spiny lobsters from granite reefs (Fig. 4.5B). Painted spiny lobsters from carbonate reefs had higher Cr concentrations (0.56 ± 0.36 $\mu g.g^{-1}$ ww *vs* 0.09 ± 0.13 $\mu g.g^{-1}$ ww) while having lower Se concentrations (0.18 ± 0.02 $\mu g.g^{-1}$ ww *vs* 0.31 ± 0.013 $\mu g.g^{-1}$ ww) than those from granite reefs.

Trace element profile ellipses of pronghorn spiny lobsters during the pre- and post-bleaching periods tended to have a high overlap (86.2% [67.5 – 97.5%] for pre- in post-bleaching and 69.3% [50.0 – 86.4%] for post- in pre-bleaching) (Fig. 4.5C). For longlegged spiny lobsters, there also seemed to be a relatively high overlap between trace element profile ellipses during the pre- and during the post-bleaching periods (83.3% [61.9 – 97.3%] for pre- in post-bleaching and 64.8% [47.4 – 85.2%] for post- in pre-bleaching).

During the post-bleaching period (i.e. 2016-2018), longlegged spiny lobsters had higher Ni (0.07 ± 0.04 $\mu g.g^{-1}$ ww *vs* 0.07 ± 0.09 $\mu g.g^{-1}$ ww) and Se concentrations (0.32 ± 0.16 $\mu g.g^{-1}$ ww *vs* 0.24 ± 0.05 $\mu g.g^{-1}$ ww), while having lower Pb concentrations (0.011 ± 0.012 $\mu g.g^{-1}$ ww *vs* 0.073 ± 0.173 $\mu g.g^{-1}$ ww) than during the pre-bleaching period (i.e. 2014-2015) (Fig. 4.5D).

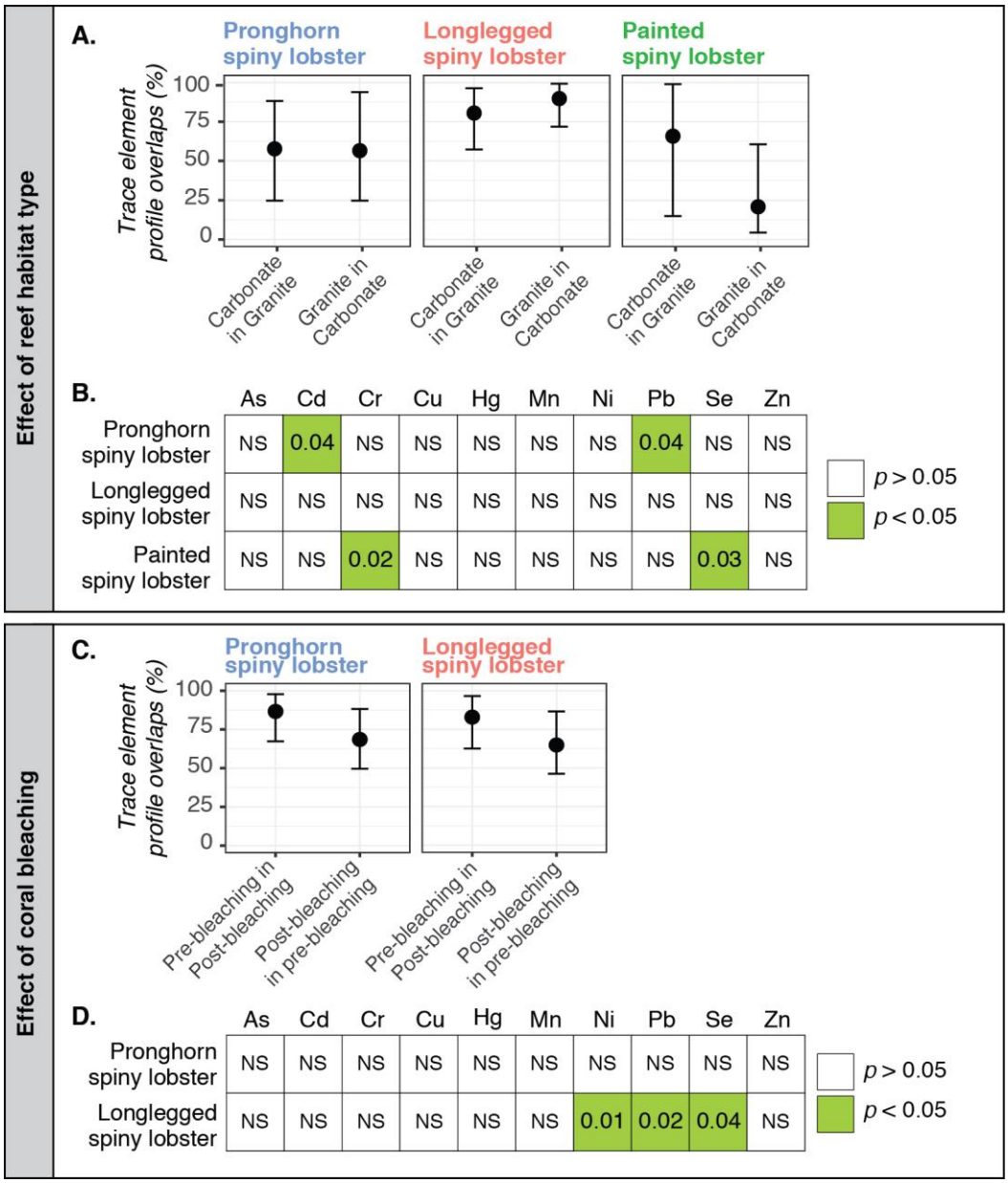

Fig. 4.5. Probabilities of trace element profile overlap (%) (A, C) and difference of trace element concentrations (t-test or Wilcoxon test) (B, D) between reef habitat types (carbonate *vs* granite reefs) and between the pre- (2014-2015) and the post-bleaching (2016-2018) periods for each spiny lobster species. Overlaps are given as mean with their associated CI95% (A, C). Numbers in the cells are the associated *p*-values; only *p*-values < 0.05 are indicated (B, D). NS = Non-significant.

4.3.5. Effect of trophic ecology on trace element bioaccumulation

In all spiny lobster species, As was positively correlated with $\delta^{15}N$, 22:6n-3, 20:1n-7, 20:1n-9 and was negatively correlated with 20:4n-6 and 18:0DMA (Fig. 4.6). Both Cd and Cu were positively correlated with 20:5n-3, and negatively correlated with 20:1n-7, 22:2 NMI (7,13) and iso17:0. Cr was only negatively correlated with 18:0DMA. Hg was positively correlated with $\delta^{15}N$, 18:1n-9 and 20:1n-7, and negatively correlated with 20:5n-3. Mn was positively

correlated with 20:5n-3 and 22:6n-3 and negatively correlated with 20:1n-7 and iso17:0. Ni was positively correlated with 20:4n-6 and 20:5n-3, and negatively correlated with $\delta^{13}C$, $\delta^{15}N$, 18:1n-9, 20:1n-7 and 22:2 NMI (7,13). Pb was positively correlated with 20:1n-7 and iso17:0. Se was positively correlated with 20:5n-3 and 22:6n-3, and negatively correlated with $\delta^{13}C$, 18:1n-9, 20:1n-7 and 22:2 NMI (7,13). Finally, Zn was positively correlated with $\delta^{13}C$, $\delta^{15}N$, 18:1n-9, 20:1n-7 and 20:1n-9, and was negatively correlated with 20:4n-6, 20:5n-3 and 18:0 DMA.

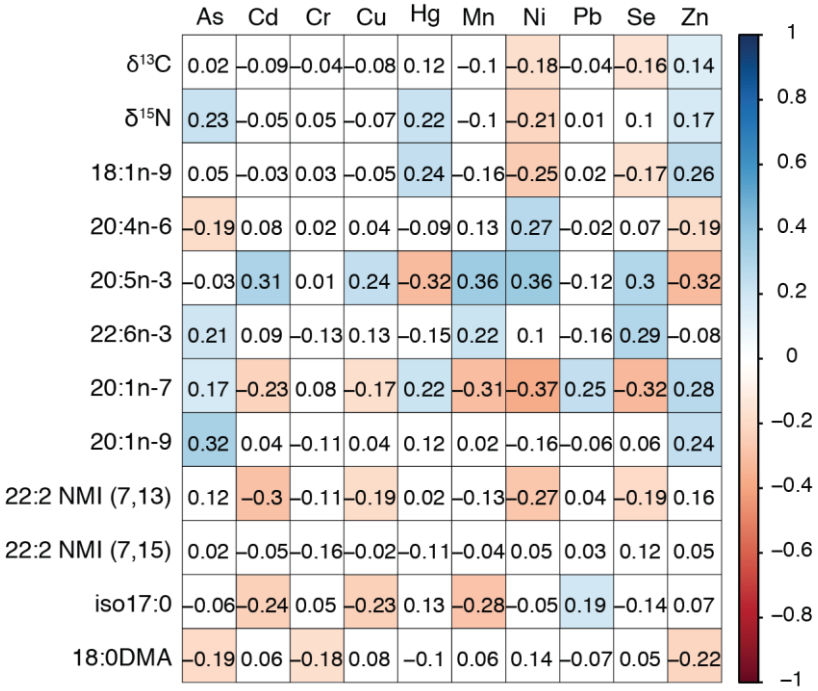

Fig. 4.6. Correlations between trace elements and trophic tracers for in the three spiny lobster species. Coloured cells indicate a significant correlation ($p < 0.05$) between two trophic tracers, while uncoloured cells indicate a non-significant correlation. Numbers in the cells are the associated correlation coefficients and the cells' colour intensity is proportional to the coefficient.

4.4. DISCUSSION

4.4.1. Size and physiology as key factors influencing trace element profiles in spiny lobster species

In fish species, the size and physiology (e.g. physiological needs of the individuals, and type and level of activity of detoxifying mechanisms in the species) of a consumer are usually considered as the main factors influencing trace element bioaccumulation in the consumer's tissues, either by direct bioaccumulation of some trace metals along time, or through metabolism by the

presence of regulation mechanisms (e.g. Kojadinovic *et al*. 2007; Barone *et al.* 2013). Similarly, here we observed that spiny lobsters' size and metabolism strongly influenced their trace element profiles and concentrations. In all three species, correlation results suggested a strong link between spiny lobsters' cephalothorax length and Hg and Zn concentrations. The bioaccumulation capacity of Hg in marine organisms including crustaceans, through MeHg accumulation, has been extensively reviewed (e.g. Neff 2002) and explains this correlation. The bioaccumulation of Zn with size in spiny lobsters, however, may reflect decapod crustaceans-specific physiological needs. Indeed, Zn is essential for decapod crustaceans' metabolism, being co-factor of many enzymes (e.g. carbonic anhydrase, involved in anionic exchange in red blood cells) (Rainbow 2007), and these crustaceans are known to regulate Zn concentrations in their body to certain thresholds (Rainbow and Luoma 2011). In the rockpool prawn *Palaemon elegans*, regulated body concentrations of Zn reported in the litterature are around 80 ± 5 $\mu g.g^{-1}$ ww (Rainbow and Luoma 2011), suggesting that Zn concentrations measured in spiny lobsters here might be in the range of their regulation capacity, with the uptake rate not exceeding the excretion rate. Thus, it is likely that the increase of Zn concentrations with size observed here reflects an increase in Zn physiological needs with growth in spiny lobsters.

Reef habitat type and coral degradation seemed to have few effects on trace element profiles of spiny lobsters, given the high overlaps of profile ellipses between carbonate and granite reefs and between the pre- and post-bleaching periods. Such a finding was a bit surprising, as it was demonstrated that both factors influenced spiny lobsters' trophic ecology (Sabino *et al.* 2021), which in turn is known to influence, at least partially, trace element exposure of marine organisms. Although it is possible that spiny lobsters ate different prey of similar trace element profiles and/or with similar content in trace element bioavailable fractions, this can also suggest that physiology, through regulation mechanisms, has a significant role in controlling trace element concentrations in spiny lobsters. By favouring either trace element retention under insufficient intake or excretion under high intake, regulation mechanisms could thus have blurred differences in trace element intake between both reef habitat types and between the pre- and post-bleaching periods. This is supported by the few identified differences in single trace elements that were for non-essential trace elements (i.e. Cd and Pb).

4.4.2. Influence of size on trophic ecology: indirect influence on trace element profiles

In all ecosystems, body size is recognized as an important factor influencing trophic structure, as it determines interaction between potential prey and predators, with larger consumers being able to eat larger prey (Arim *et al*. 2010). This led to the hypothesis that there is a correlation between a consumer's length and its trophic position (i.e. $\delta^{15}N$ values) (Jennings *et al*. 2002). Indirectly, this can affect trace element bioaccumulation and thus the trace element profile of a consumer. Such mechanism could have influenced interspecific differences in trace element profiles among the three spiny lobster species.

The pronghorn spiny lobster was separated from longlegged spiny lobsters by As and, although not visible on trace element profile ellipses, this species also had the highest Zn concentration compared to both the longlegged and painted spiny lobsters. In spiny lobsters, both As and Zn were positively correlated with trophic position (i.e. $\delta^{15}N$) and with animal trophic markers (i.e. only 20:1n-7 and 20:1n-9 for As, 18:1n-9, 20:1n-7 and 20:1n-9 for Zn; Sabino *et al*. 2021). Such results suggest a link between carnivory and bioaccumulation of As and Zn, which was strongly supported by pronghorn spiny lobsters' dietary pattern. Indeed, this species was shown to have a higher level of carnivory in its diet than both other species (Sabino *et al*. 2021). Such a difference in dietary pattern was suggested to be linked to the larger size of pronghorn spiny lobsters compared to individuals of the two other species (Sabino *et al.* 2021). In addition, previous studies showed that the size range of prey that can be consumed by spiny lobster is function of their size (e.g. Haley *et al*. 2011; Blamey and Branch 2012). Here, the larger size of the pronghorn spiny lobster may allow it to have access to larger and more carnivore prey, which influences its own carnivory level. Spiny lobsters' cephalothorax length could thus have indirectly influenced their trace element profiles by influencing their diet.

The influence of a consumer's size on its diet could also have influenced differences in trace element profiles between male and female painted spiny lobsters. Male painted spiny lobsters were separated from females by many trace elements like Cd, Cr, Cu, Mn, Pb and Se (Appendix 4.2). Although there is a sexual dimorphism between male and female spiny lobsters (Robinson *et al*. 2009), these trace elements are not particularly known to bioaccumulate with age, suggesting that these differences in trace element between sexes were mainly due to differences in trophic ecology. Females were separated from males by fatty acid trophic

markers of animal prey (i.e. NMI fatty acids, 18:1n-9 and 20:1n-9; Iverson 2009; Sabino *et al.* 2021) (Appendix 4.5), suggesting a higher level of carnivory for females, and Cd, Cu, Mn and Se were positively correlated with primary producer trophic markers like 20:4n-6, 20:5n-3 and 22:6n-3 (Meyer *et al*. 2019). In addition, although there was no significant difference in cephalothorax length between male and female painted spiny lobsters, females still tended to have a higher cephalothorax length than males. Thus, it is possible that, due to their larger size, female painted spiny lobsters have a slightly higher level of carnivory than males of the same species, and thus they would have a lower intake of trace elements like Cd, Cu, Mn and Se.

4.4.3. Variation in trace element profiles among spiny lobsters as the result of trophic ecology divergences

As mentioned before, in the marine environment, trace elements are mainly transferred to consumers through the trophic pathway, as shown for fish and molluscs (Wang 2002). The individual ecology of a given organism, including feeding ecosystem, trophic level, or the type of prey consumed, will thus affect the content of trace elements that are not regulated by this organism (Wang 2002; Copaja *et al*. 2017). This suggests that a change of an individual trace element concentration or a change in the trace element profile of a given organism is the result of a modification of the consumer's trophic ecology, either due to different trace element profiles or to difference in trace element bioavailability among consumed prey. Here, computing trace element profile ellipses showed partial segregation between the three spiny lobster species, with some trace elements being in higher concentrations in one species among the others. As the three species have a common classification (i.e. Paniluridae), it is unlikely that such differences result from significant differences in physiology (e.g. presence of different detoxifying processes), suggesting, as expected, that trophic ecology greatly influenced spiny lobsters' trace element profiles. This was confirmed by comparing the differences among trace element profiles of the three spiny lobster species to their FA and isotopic trophic niches identified in Sabino *et al*. (2021). Indeed, trophic niches showed partial resource segregation that explained directly interspecific difference in trace element profiles among the three spiny lobster species.

The painted spiny lobster was separated from the other two species mainly by Cr, Mn and Ni, and the longlegged spiny lobster the highest intraspecific variability in Pb concentrations. This may be due to painted spiny lobsters feeding more on primary producers

(e.g. macroalgae) than do longlegged spiny lobsters. Fleshy algae has been found in the guts of some spiny lobsters in other areas (e.g. Blamey *et al*. 2019), and recent work on Seychelles spiny lobsters suggested that painted spiny lobsters fed more on algae than longlegged and pronghorn spiny lobsters (Sardenne *et al*. 2021). Moreover, when tracing dietary patterns through the use of fatty acids, it is sometimes difficult to discriminate between primary and secondary (i.e. through consumption of herbivores) consumption of primary producers (Dalsgaard *et al*. 2003), and such difference may thus have not appeared when computing fattya acid niches for the three species (Sabino *et al.* 2021). Here, Mn and Ni were positively correlated with primary producer markers (i.e. 20:5n-3 and 22:6n-3 for Mn and 20:4n-6 and 20:5n-3 for Ni; Meyer *et al*. 2019; Sabino *et al*. 2021), while being negatively correlated with animal markers (i.e. 20:1n-7 for Mn and δ^{15}N, 18:1n-9, 20:1n-7 and 22:2 NMI (7,13) for Ni; Iverson 2009; Sabino *et al*. 2021). Both Mn and Ni are known to be in high concentrations in primary producers, including macroalgae (Malea and Kevrekidis 2014; Bonanno and Orlando-Bonaca 2018). Thus, higher concentrations of Mn and Ni in painted spiny lobsters supports higher proportion of primary producers like macroalgae in their diet, compared to longlegged and pronghorn spiny lobsters. Finally, Pb was positively correlated with animal trophic markers (i.e. 20:1n-7; Sabino *et al.* 2021) and bacteria trophic markers (i.e. iso17:0; Kelly and Scheibling 2012). This suggests a link between Pb bioaccumulation and consumption of benthic detritivores, such as polychaetes. This is supported by the previously determined spiny lobsters' diet, as polychaetes are known to be eaten in small proportions by spiny lobsters in some areas (e.g. the coast off Western Australia, MacArthur *et al*. 2011). In addition, polychaetes have been previously identified as transfer vector of trace elements like Pb from sediment to their predators (Castiglioni *et al*. 2018). Although it was not visible on the fatty acid niches computed in Sabino *et al*. (2021), longlegged spiny lobsters seemed to have higher mean proportions of iso17:0 in their hepatopancreas than both other species, which could indicate that some individuals of longlegged spiny lobsters ate higher proportions of polychaetes than other spiny lobster individuals. This could have led to a higher variability in Pb concentration among longlegged spiny lobster individuals compared to individuals of both other species.

Although reef habitat type and the 2016 coral bleaching event seemed to have no significant effect on trace element profiles of the three spiny lobster species, differences were identified for individual trace element concentrations. For painted spiny lobsters, individuals from granite reefs had higher Se but lower Cr concentrations, most probably due to diet

divergences between the two reef types. Here, Se was negatively correlated with animal fatty acid trophic markers like 18:1n-9, 20:1n-7 and 22:2 NMI (7,13) and positively correlated with primary producer fatty acid trophic marker like 20:5n-3 and 20:6n-3 (Meyer *et al.* 2019; Sabino *et al.* 2021), while Cr was negatively correlated with fatty acids trophic markers of bivalve molluscs and carnivorous gastropods (18:0DMA; Budge *et al*. 2006). This suggests that painted spiny lobsters from granite reefs may be less carnivore than those in carbonate reefs. Indeed, by feeding more on primary producers or primary producer-feeders (e.g. filter-feeder bivalve molluscs) and less on more carnivore prey, their Se intake would be higher and their Cr intake would be lower. Assuming spiny lobsters do not have the ability to regulate Se and Cr in their body, this would thus cause a higher Se bioaccumulation and lower Cr bioaccumulation. This process could not be supported by $\delta^{15}N$ values in painted spiny lobsters from both reef habitat types, as those from granite reefs had higher $\delta^{15}N$ values than those from carbonate reefs (Appendix 4.9). However, this could be caused by the biochemical processes at the base of each food web. Nitrogen fixation is known to make a significant contribution to nitrogen supply in coral reefs (Lesser *et al.* 2007), which results in lower $\delta^{15}N$ values in those habitats (Wada *et al*. 2012). It is thus highly probable that a difference of isotopic baseline masks difference of trophic position between painted spiny lobsters from both habitat types.

The 2016 bleaching event also led to modifications of the concentrations of some trace elements in longlegged spiny lobsters. During the post-bleaching period, longlegged spiny lobsters had significantly higher concentrations of Ni and Se, while having significantly lower concentrations of Pb. In addition, some individuals of longlegged spiny lobsters also seemed to have higher concentrations of Cu during this period (Appendix 4.4). As Cu, Ni and Se were positively correlated with primary producer trophic markers (i.e. 20:4n-6, 20:5n-3, 22:6n-3; Meyer *et al.* 2019) and Pb was positively correlated with bacteria trophic markers, this suggests that longlegged spiny lobster fed more on macroalgae and/or herbivores and less on detritivores during the post-bleaching period compared to the pre-bleaching period. This is supported by $\delta^{13}C$ values of longlegged spiny lobsters, which were lower during the post-bleaching period (Appendix 4.9). Indeed, algal turf are known to be highly depleted in ^{13}C compared to sedimentary organic matter (Briand *et al*. 2016). Shifts from coral-dominated to algal turf-dominated benthic covers have been observed in many degraded coral reefs (Haas *et al*. 2010; Vermeij *et al*. 2010; Barott *et al*. 2012). As Seychelles coral reefs were severely impacted by the 2016 bleaching event (Obura *et al*. 2017), subsequent degradation may have

favoured development of algal turf among corals (O'Brien and Scheibling 2018). This is also supported by $\delta^{15}N$ values of longlegged spiny lobsters, which were slightly higher during the post-bleaching period compared to the pre-bleaching period (Appendix 4.9). This modification did not result in a significant change in trace element biomagnification, even for Hg which is known to biomagnify (Lavoie *et al.* 2013), thus hinting to no difference in trophic position. This suggests a change in the isotopic $\delta^{15}N$ baseline, and thus a certain level of shift from corals, where nitrogen fixation makes a significant contribution to nitrogen supply (Lesser *et al*. 2007), to algal turf cover.

It is now evident that, through its variation according to many factors (i.e. at the species level, between habitat reef types and as a result of habitat degradation), trophic ecology has a high influence on the variation of trace element profiles and/or individual trace element concentration in spiny lobsters. The level of carnivory especially seemed to have a negative effect on the bioaccumulation of many trace elements. This could be the result of both bioreduction in the food web and of the fact that spiny lobsters are scavengers and are thus able to feed on body parts of large animal prey (Rainbow 1998). Contrary to detoxifying organs (e.g. liver or hepatopancreas), tissues like muscles are not particularly rich in trace elements, and a low trace element intake from food is expected when only muscle is consumed (Rainbow 1998). Thus, by feeding on body parts of animal prey like fish, some spiny lobsters would have a higher level of carnivory (i.e. higher proportions of FA animal markers and higher $\delta^{15}N$ values) but a lower trace element intake.

4.5. CHAPTER HIGHLIGHTS

Chap. 2 – Main findings

• **Individual size**, **physiology** and **trophic ecology** have a **major role in controlling trace element bioaccumulation** in spiny lobsters.

• **Trace element bioaccumulation** seems to be **controlled by physiology first**, especially for trace elements for which there is a regulation mechanism. However, it is also the **result of the co-influence of size, physiology and trophic ecology**.

• **Size** can have **a direct influence on trace element bioaccumulation** (e.g. Hg and Zn in the case of spiny lobsters), but can also **indirectly influence trace element bioaccumulation** by structuring benthic food webs and thus **influencing the trophic ecology** of benthic marine consumers.

4.6. METHODOLOGICAL CONSIDERATIONS

Computing trace element profile ellipses for levels of the same factor and calculating their overlaps to use as proxy of their similarity first seemed to be an attractive way to investigate the potential effect of categorical variables on trace element bioaccumulation. Indeed, it allows to visually assess difference in trace element profiles through the computing of the ellipses, and the similarity can be quantified through overlap calculation. However, this chapter showed that measure of the overlap failed to capture the extent of all differences, especially when there was a difference in the bioaccumulation of a small number of trace elements (e.g. for each species, only one trace element differed in concentration between males and females). Such an approach would thus only be interesting when investigating diet using FA trophic markers, because the purpose then is to identify major changes in diet. However, when studying trace element bioaccumulation, it is often interesting to see differences in even one trace element, as on given factor (e.g. sex, habitat, diet) will not affect all studied trace elements.

As a consequence, in the following chapters, methods investigating differences in bioaccumulation individually for each investigated trace element, like classical statistics (t-test/Wilcoxon test or ANOVA/Kruskal-Wallis tests) or modelling methods (GLMs or GAMs), will

be preferred. When used with trace element concentrations, multivariate methods will only help visualising trace element profiles.

5. CHAPTER 3 – TRACE ELEMENT BIOACCUMULATION IN TROPICAL DEMERSAL SYSTEMS: CASE OF THE EMPEROR RED SNAPPER

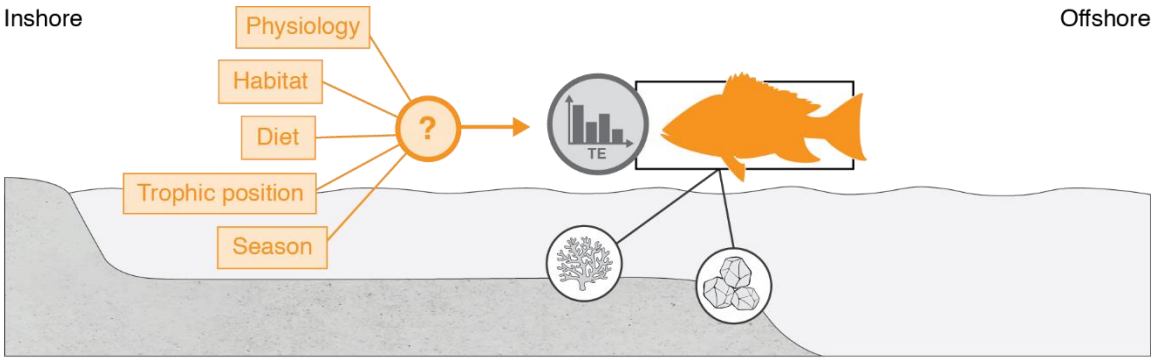

Content

This chapter constitutes a paper in preparation for Environmental Research *and presented in Supp. Doc. 3.*

5.1. CONTEXT AND OBJECTIVES

Lutjanid fishes, also called red snappers, share common and particular features like life-history traits and reproductive biology. They are long-lived species (up to 53 years), with a slow growth rate, a late maturation and a low mortality rate (Martinez-Andrade 2003). They also inhabit a wide diversity of habitats throughout their life. Snappers' eggs and larvae are pelagic, while juveniles settle in nursery grounds (i.e. mangroves or coral/rocky reefs) until they reach maturity (Allen 1985), and adults inhabit a wide range of demersal habitats on continental shelfs or at the continental slope (Martinez-Andrade 2003). Most snappers live in shallow to intermediate depths (Allen 1985), with large individuals generally being associated with deeper waters than juveniles (Martinez-Andrade 2003). As an example, in the Seychelles, adult emperor red snappers (*Lutjanus sebae*) are generally caught in depths above 100 m (Mees 1992). Throughout their adult life stage, snappers will also undertake regular migrations to form spawning aggregations during seasonal reproduction. For emperor red snappers in the Seychelles, these aggregations occur on the Mahé Plateau during inter-monsoon seasons (Robinson *et al*. 2004).

Red snappers are of major importance for many small-scale fisheries worldwide, essentially in tropical and subtropical countries (Cawthorn and Mariani 2017; Amorim *et al*. 2019). In countries where capture fisheries resources are the main source of proteins and micronutrients, like in SIDS, these fisheries support the livelihoods and food security of local populations (Cawthorn and Mariani 2017; Hicks *et al*. 2019). However, their particular biological and ecological features (i.e. long life, slow growth rate, late maturation and formation of spawning aggregation) make them particularly prone to overfishing (Marriott *et al.* 2007; Grandcourt *et al*. 2008). In the Seychelles, snappers' catch per unit effort decreased from 1990 to 2016 (36 to 16 $kg.day^{-1}$), mainly due to spatial expansion of fishing grounds, longer fishing trips and increase in boat size, and concerns have been raised concerning overfishing (Robinson *et al*. 2004, 2020). Yet, the trophic ecology and life-history traits of snappers in the Seychelles, including emperor red snapper are poorly known.

In spite of the importance of capture fisheries resources in the fight against micronutrient deficiency (Béné *et al.* 2015; Hicks *et al.* 2019), little is known about the essential and non-essential trace element content of snappers in SIDS, with most studies only reporting

Hg concentrations in these species (Ahmad *et al*. 2015; Anual *et al.* 2018; Suratno *et al.* 2019). In the Seychelles, where the emperor red snapper (*Lutjanus sebae*) is the main species captured by the demersal fishery (Seychelles Fishing Authority 2019), Hg concentrations were reported to be 0.192 ± 0.105 $\mu g.g^{-1}$ ww in this species (Sardenne *et al*. 2017), which falls in the range of values measured elsewhere in the Indo-Pacific (Malaysia: 0.334 $\mu g.g^{-1}$ dw ≈ 0.084 $\mu g.g^{-1}$ ww, Ahmad *et al*. 2015, and 0.118 $\mu g.g^{-1}$ ww, Anual *et al*. 2018; Indonesia: 0.88 ± 0.34 $\mu g.g^{-1}$ dw ≈ 0.22 $\mu g.g^{-1}$ ww, Suratno *et al.* 2019).

The long lifespan of snappers and their demersal feeding behaviour could make them prone to bioaccumulate high concentrations of non-essential trace elements like Hg, which is known to accumulate along time in muscle and liver (Goutte *et al*. 2015), or Cd and Pb which are in high concentrations in sediments and could thus be transferred to snappers through the trophic pathway (Rejomon *et al*. 2010; Velusamy *et al*. 2014). Ontogenetic changes in habitat and diet, and local movements due to migration to spawning grounds, could also influence trace element bioaccumulation in emperor red snapper by influencing their trophic ecology. Particularly, the sexual dimorphism observed in emperor red snappers from the Seychelles (Mees 1992), may induce different bioaccumulation rates between males and females. Finally, seasonal variations in primary production and environmental parameters (e.g. water temperature and salinity) could also affect trace element concentrations and thus availability for human diets around the year. Yet, in spite of the importance of intrinsic (e.g. size, age, physiological needs) and extrinsic factors (e.g. trophic ecology) in controlling trace element concentrations in capture fisheries species, including red snappers, very few studies investigated this topic (but see Metian *et al*. 2013).

As the trophic ecology, and particularly ontogenetic changes, of emperor red snappers in the Seychelles is poorly known, it was first explored in this chapter using stable isotopes of carbon and nitrogen. Then, the effects of size, trophic ecology and sex on trace element bioaccumulation in emperor red snapper will be investigated. Seasonal variation in trace element concentrations will also be examined in order to identify a potential role of the seasonal reproduction.

5.2. METHODOLOGY

5.2.1. Dataset

Among the 78 emperor red snappers sampled as part of the SEYFISH project and used in chapter 1, sex has been determined by visual observation for all fish except for one individual. Thus, 77 individuals (i.e. 31 males and 46 females; 10 individuals caught during pre-NWM and during pre-SEM, 57 caught during NWM) were used in this chapter. Emperor red snappers were caught around and on the Mahé Plateau by fishers and during scientific cruises onboard the Research Vessel l'Amitie during 2014 and 2018 (Fig. 4.1).

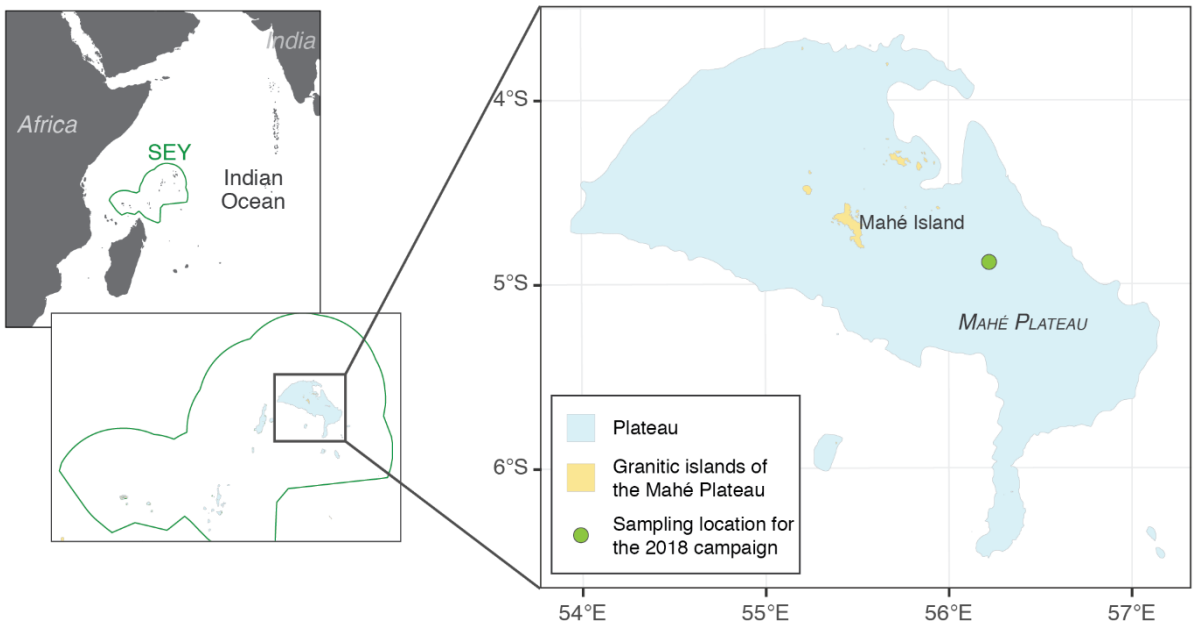

Fig. 4.1. Locations of the fishing area for emperor red snappers analysed in this chapter. SEY = Seychelles.

5.2.2. Classical and multivariate statistics

Size difference between sexes was tested using Wilcoxon test and difference among seasons was tested using Kruskal-Wallis followed by Dunn post-hoc test. As there was no significant difference between sexes or among seasons (Appendix 5.1), while $\delta^{13}C$ and $\delta^{15}N$ values in fish are known to be influenced by fish size (Jennings *et al.* 2002), the effects of continuous variables (i.e. fork length, $\delta^{13}C$ and $\delta^{15}N$ values) and of categorical variables (i.e. sex and season) on trace element bioaccumulation in emperor red snappers were investigated separately.

In order to bring insight into the trophic ecology of sampled emperor red snappers, the relationships between fork length and stable isotope values, and between $\delta^{13}C$ and $\delta^{15}N$ values, were investigated using Kendall correlation tests. Difference ($p < 0.05$) in stable isotope values between sexes and among seasons were also tested using Wilcoxon tests and Kruskal-Wallis followed by Dunn test, respectively.

Non-metrical multidimensional scaling (nMDS) ordination of Bray-Curtis similarity matrix was performed to visually assess the difference in trace element profiles between sexes and among seasons. For each trace element, Wilcoxon test and Kruskal-Wallis followed by Dunn test were used to test for significant difference ($p < 0.05$) in concentrations among sexes and seasons, respectively.

5.2.3. Modelling the relationship between trace element concentrations and size and $\delta^{13}C$ and $\delta^{15}N$

GAMs and/or GLMs were used to assess the relationship between log-transformed trace element concentrations and emperor red snappers' size (i.e. fork length) and $\delta^{13}C$ and $\delta^{15}N$ values. For this, GAMs were first fitted on log-transformed trace element concentrations, with fork length, $\delta^{13}C$ and $\delta^{15}N$ values as explanatory variables. As both $\delta^{13}C$ and $\delta^{15}N$ values are known to vary according to fish size, their interaction terms with fork length were also added as explanatory variables in the full model. However, for all trace elements, modelled trends with fork length or stable isotope values appeared to be linear, thus GLMs were finally preferred. Among explanatory variables, only those improving the goodness of fit in the model base on the AIC were kept in the final model for each trace element. After selection, full and selected models were compared to a null model using AIC to make sure that fork length, $\delta^{13}C$ and $\delta^{15}N$ did have a role in explaining trace element concentrations.

For all trace elements for which fork length or one of its interactions factors was significant, it was necessary to remove the size effect to investigate the direct effects of $\delta^{13}C$ and $\delta^{15}N$ only. Thus, trace element concentrations were standardized by length using a method similar to the one of Houssard *et al*. (2019). GLMs were first fitted on log-transformed trace element concentrations with fork length alone as explanatory variable. All models were checked for linearity to ensure that there was no need to use a GAM instead. Then, the residuals from the size-based models were used as response variable in GAMs with $\delta^{13}C$ and $\delta^{15}N$ values

only. Again, whenever modelled trends appeared to be linear, GLMs were finally preferred instead of GAMs.

5.3. RESULTS

5.3.1. Stable isotopes: intercorrelation, relationship with size and effect of sex and season

In analysed emperor red snappers, $\delta^{13}C$ and $\delta^{15}N$ values in their muscle tissues were both positively correlated with their fork length, regardless of the sex (Fig. 5.2A, B). $\delta^{13}C$ and $\delta^{15}N$ were also positively correlated with each other regardless of the sex (Fig. 5.2C). There was no difference in $\delta^{13}C$ and $\delta^{15}N$ values among sexes or among seasons (Table 5.1).

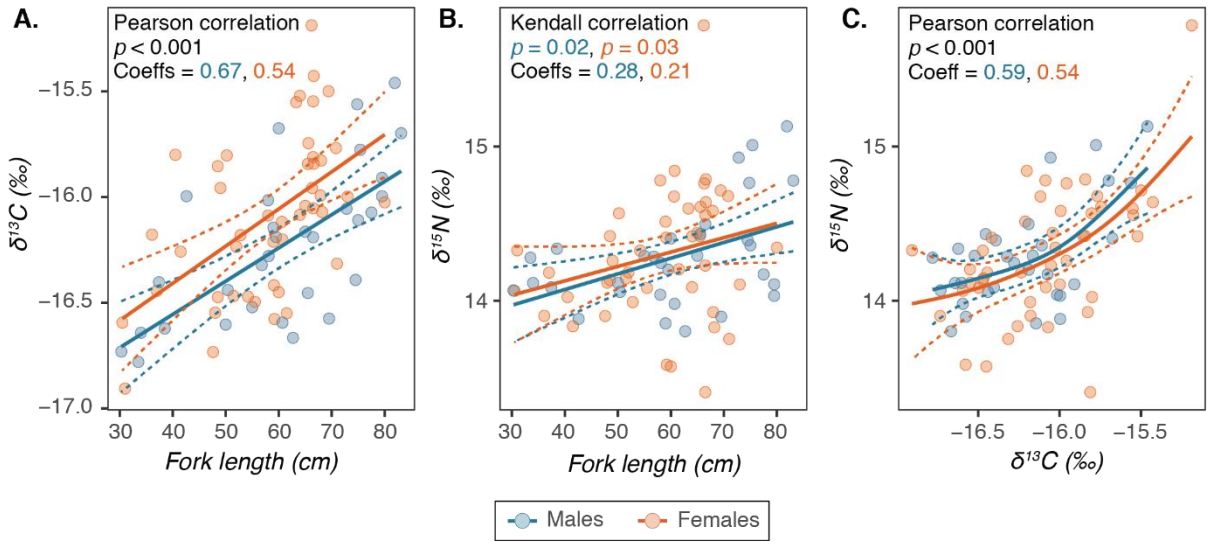

Fig. 5.2. Relationships between fork length (cm) and C and N stable isotope values (‰) (A, B) and between $\delta^{13}C$ and $\delta^{15}N$ values (C), for males and females. Smoothing curves were fitted using the GLM method for linear relationships (A, B) and the GAM method for the non-linear relationship (C) under R software. Dotted curves represent the confidence interval at 95% around the fit.

Table 5.1. $\delta^{13}C$ and $\delta^{15}N$ values (‰) measured in the white muscle tissues of emperor red snappers for each sex and each season. Values are presented as mean ± SD.

	$\delta^{13}C$	$\delta^{15}N$
All individuals (n = 57)	-16.1 ± 0.4	14.3 ± 0.4
Males (n = 31)	-16.2 ± 0.4	14.3 ± 0.3
Females (n = 46)	-16.1 ± 0.4	14.3 ± 0.4
Males		
Pre-NWM (n = 4)	-16.4 ± 0.2	14.2 ± 0.1
NWM (n = 22)	-16.2 ± 0.4	14.3 ± 0.4
Pre-SEM (n = 5)	-16.4 ± 0.2	14.0 ± 0.2
Females		
Pre-NWM (n = 6)	-16.2 ± 0.3	14.3 ± 0.2
NWM (n = 35)	-16.1 ± 0.4	14.3 ± 0.4
Pre-SEM (n = 5)	-15.9 ± 0.1	14.3 ± 0.5
Pre-NWM (n = 10)	-16.2 ± 0.3	14.3 ± 0.1
NWM (n = 57)	-16.1 ± 0.4	14.3 ± 0.4
Pre-SEM (n = 10)	-16.2 ± 0.3	14.1 ± 0.3

5.3.2. Effect of sex and season on trace element bioaccumulation

Trace element profiles were highly similar between sexes (Fig. 5.3A) and there was no significant difference in trace element concentrations between males and females (Fig. 5.4).

Emperor red snappers caught during the pre-NWM season seemed to be separated from those caught during the other two sampling seasons by As (Fig. 5.3B). The profile ellipse of emperor red snappers caught during the pre-SEM season was included in the one of individuals caught during the NWM season. Trace element concentrations were lowest in individuals caught during the pre-NWM season for Cd, Cr, Cu, Mn, Ni, and Zn, in comparison with the NWM season (Dunn test, $p < 0.001$ for Cd and Cr; $p < 0.01$ for Cu and Zn; and $p < 0.05$ for Mn and Ni) and with the pre-SEM season (Dunn test, $p < 0.001$ for Cr and Zn; $p < 0.01$ for Ni; and $p < 0.05$ for Cd, Cu, and Mn), while individuals caught during the pre-SEM had the highest Ni concentrations (Dunn test, $p < 0.001$ with pre-NWM and $p = 0.008$ with NWM) (Fig. 5.4). Individuals caught during the pre-NWM season also had lower Se concentrations than those caught during the NWM season (Dunn test, $p = 0.004$) but higher Hg concentrations than individuals caught during the pre-SEM season (Dunn test, $p = 0.012$).

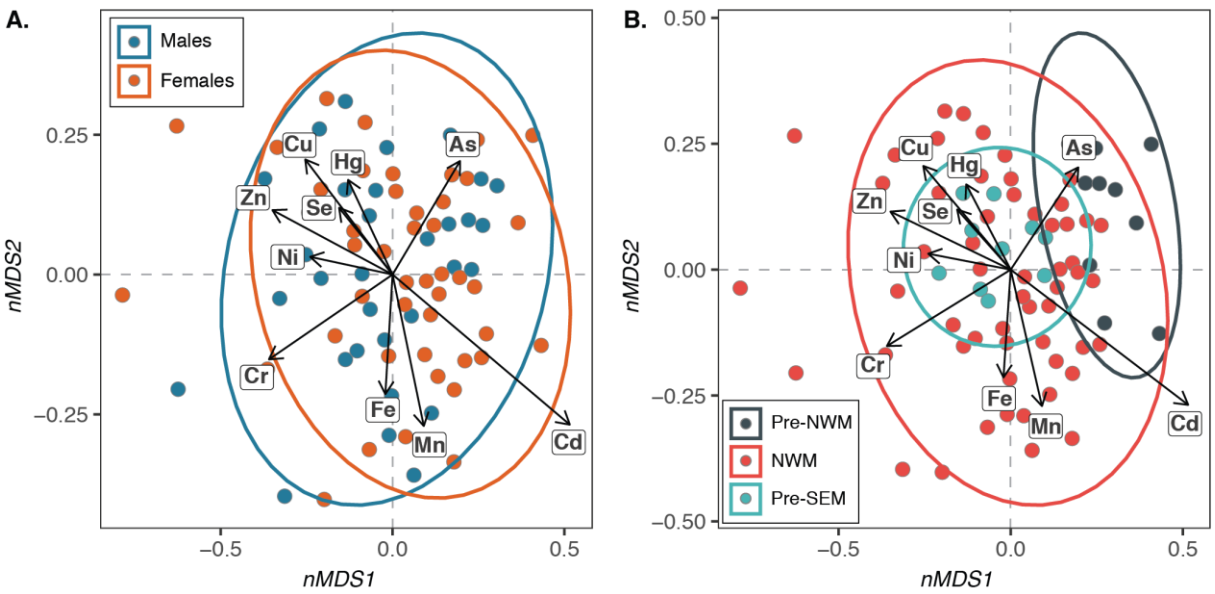

Fig. 5.3. Non-metrical multidimensional scaling (nMDS) ordination of Bray-Curtis similarity matrix of muscle normalised trace element concentrations in emperor red snappers, according to sex (A) and season (B). Probabilistic ellipses at 0.95 are also represented in order to show grouping of points. NWM = Northwest Monsoon, SEM = Southeast Monsoon.

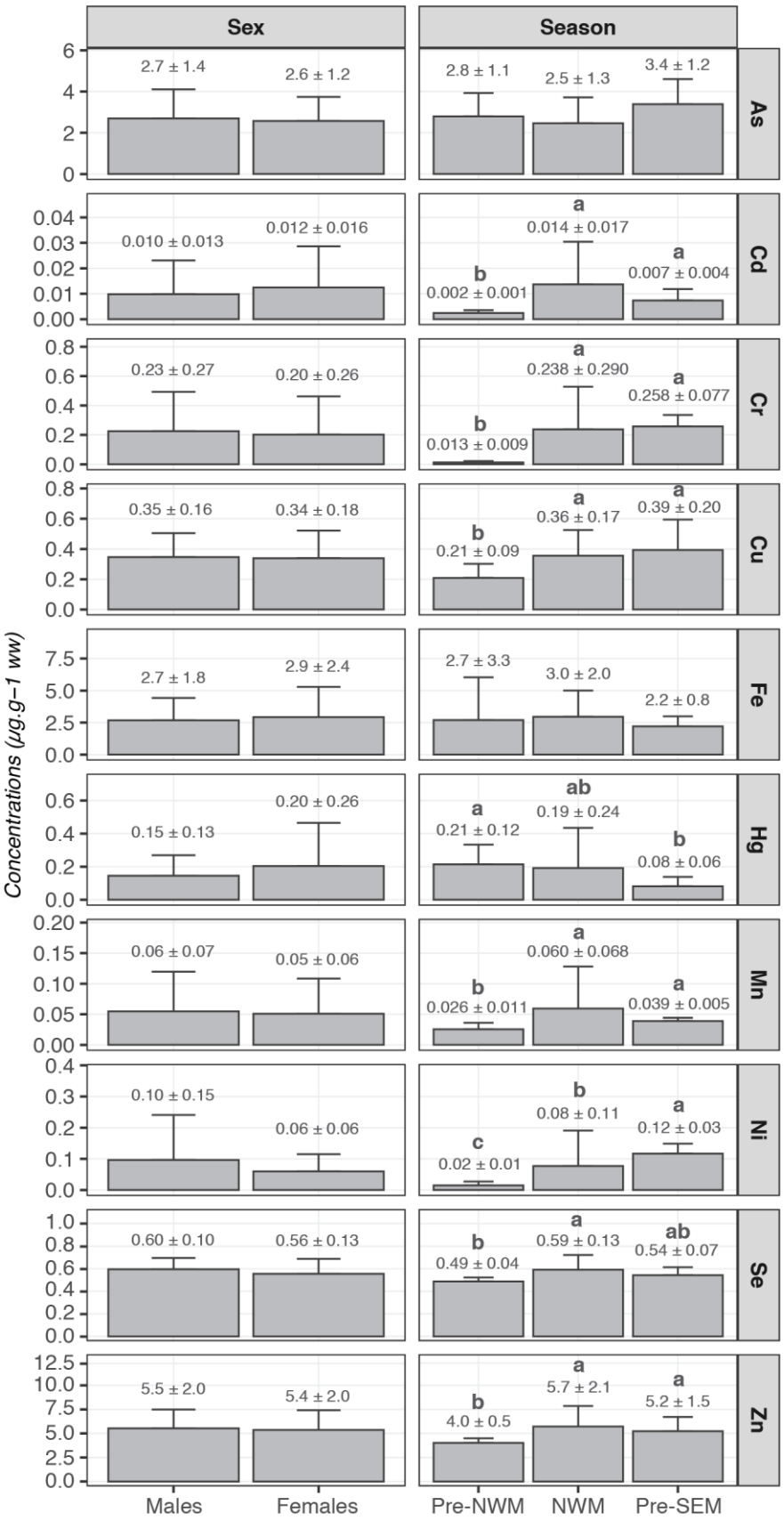

Fig. 5.4. Trace element concentrations (µg.g^{-1} ww) in white muscle tissues of emperor red snappers grouped by sex and season, and presented as mean ± SD (values are also given above each bar). A different letter indicates significant difference (p < 0.05, Wilcoxon or Dunn post-hoc test). NMW = Northwest Monsoon, SEM = Southeast Monsoon.

5.3.3. Relationship between trace element concentrations and size and $\delta^{13}C$ and $\delta^{15}N$ values

Among all models tested to explain trace element concentrations in emperor red snappers, the null model was the best selected model (i.e. with the lowest AIC) for Cr and Fe (Table 5.2). Among all other models, individual size as explanatory variable significantly improved the goodness of fit of the model (i.e. significantly decreased the AIC). However, size was significant ($p < 0.05$) in the model only for As, Cd, Hg with a positive slope, and for Mn and Ni with a negative slope. After removing the size effect, there was a significant relationship between As concentrations and both $\delta^{13}C$ (positive slope) and $\delta^{15}N$ (negative slope) values (Table 5.2). The relationship between concentrations and $\delta^{15}N$ values was also significant for Cu, Hg, Ni, Se and Zn. For these trace elements, a change in relationship trend seems to occur at values between 14.5 and 15.0 ‰ (estimated values of 14.8 ‰ for Cu, 14.9 ‰ for Hg, 15 ‰ for Ni, 14.5 ‰ for Se and 14.6 ‰ for Zn) (Fig. 5.5). Cu and Zn presented the same pattern with, first, a negative relationship with $\delta^{15}N$ values and, then, a weak positive relationship. Se and Zn also presented similar patterns with, first, relatively stable concentrations and then a strong positive relationship with $\delta^{15}N$ values. Finally, Hg seemed to first have a weak negative relationship when $\delta^{15}N$ values are low but a strong positive relationship for values above 15.0 ‰.

Table 5.2. Model results for log-transformed and length-standardised trace element concentrations. For each model explaining log-transformed concentrations, given explanatory variables are those present in the best selected model (i.e. with lowest AIC).

Trace element	Response variable	Model	Explanatory variables	*p* value	GLM – Estimated slope
As	Log(As)	GLM	Fork length	0.006	0.279 ± 0.098
			$\delta^{15}N$	0.135	0.639 ± 0.423
			$\delta^{13}C$:fork length	0.004	0.004 ± 0.001
			$\delta^{15}N$:fork length	0.022	-0.015 ± 0.006
	Residuals(logAs-size)	GLM	$\delta^{13}C$	0.004	0.212 ± 0.071
			$\delta^{15}N$	< 0.001	-0.326 ± 0.069
Cd	Log(Cd)	GLM	Fork length	0.007	0.525 ± 0.191
			$\delta^{13}C$	0.033	-1.514 ± 0.696
			$\delta^{15}N$	0.838	0.036 ± 0.175
			$\delta^{13}C$:fork length	0.008	0.032 ± 0.012
	Residuals(logCd-size)	GLM	$\delta^{13}C$	0.311	0.180 ± 0.176
			$\delta^{15}N$	0.251	0.198 ± 0.172
Cr	Log(Cr)	GAM	Null model	-	-
Cu	Log(Cu)	GLM	Fork length	0.913	-0.017 ± 0.155
			$\delta^{13}C$	0.580	0.179 ± 0.323
			$\delta^{15}N$	1.000	0.001 ± 0.467
			$\delta^{13}C$:fork length	0.565	-0.003 ± 0.006
			$\delta^{15}N$:fork length	0.753	-0.002 ± 0.007
	Residuals(logCu-size)	GAM	$\delta^{13}C$	0.989	-
			$\delta^{15}N$	0.018	-
Fe	Log(Fe)	GAM	Null model	-	-
Hg	Log(Hg)	GLM	Fork length	0.003	0.461 ± 0.151
			$\delta^{15}N$	0.022	1.507 ± 0.646
			$\delta^{13}C$:fork length	0.009	0.006 ± 0.002
			$\delta^{15}N$:fork length	0.014	-0.025 ± 0.009
	Residuals(logHg-size)	GAM	$\delta^{13}C$	0.111	-
			$\delta^{15}N$	0.028	-
Mn	Log(Mn)	GLM	Fork length	0.016	-0.048 ± 0.020
			$\delta^{15}N$:fork length	0.009	0.003 ± 0.001
	Residuals(logMn-size)	GLM	$\delta^{13}C$	0.887	0.015 ± 0.102
			$\delta^{15}N$	0.064	0.186 ± 0.099
Ni	Log(Ni)	GLM	Fork length	0.003	-0.697 ± 0.231
			$\delta^{13}C$	0.002	2.707 ± 0.842
			$\delta^{15}N$	0.023	-0.491 ± 0.212
			$\delta^{13}C$:fork length	0.003	-0.044 ± 0.014
	Residuals(logNi-size)	GAM	$\delta^{13}C$	0.253	-
			$\delta^{15}N$	0.005	-
Se	Log(Se)	GLM	Fork length	0.534	0.035 ± 0.055
			$\delta^{13}C$	0.370	-0.104 ± 0.115
			$\delta^{15}N$	0.822	0.037 ± 0.166
			$\delta^{13}C$:fork length	0.364	0.002 ± 0.002
			$\delta^{15}N$:fork length	0.929	-0.001 ± 0.003
	Residuals(logSe-size)	GAM	$\delta^{13}C$	0.586	-
			$\delta^{15}N$	< 0.001	-
Zn	Log(Zn)	GLM	Fork length	0.639	-0.024 ± 0.051
			$\delta^{13}C$	0.634	0.089 ± 0.185
			$\delta^{15}N$	0.606	-0.024 ± 0.047
			$\delta^{13}C$:fork length	0.566	-0.002 ± 0.003
	Residuals(logZn-size)	GAM	$\delta^{13}C$	0.481	-
			$\delta^{15}N$	0.018	-

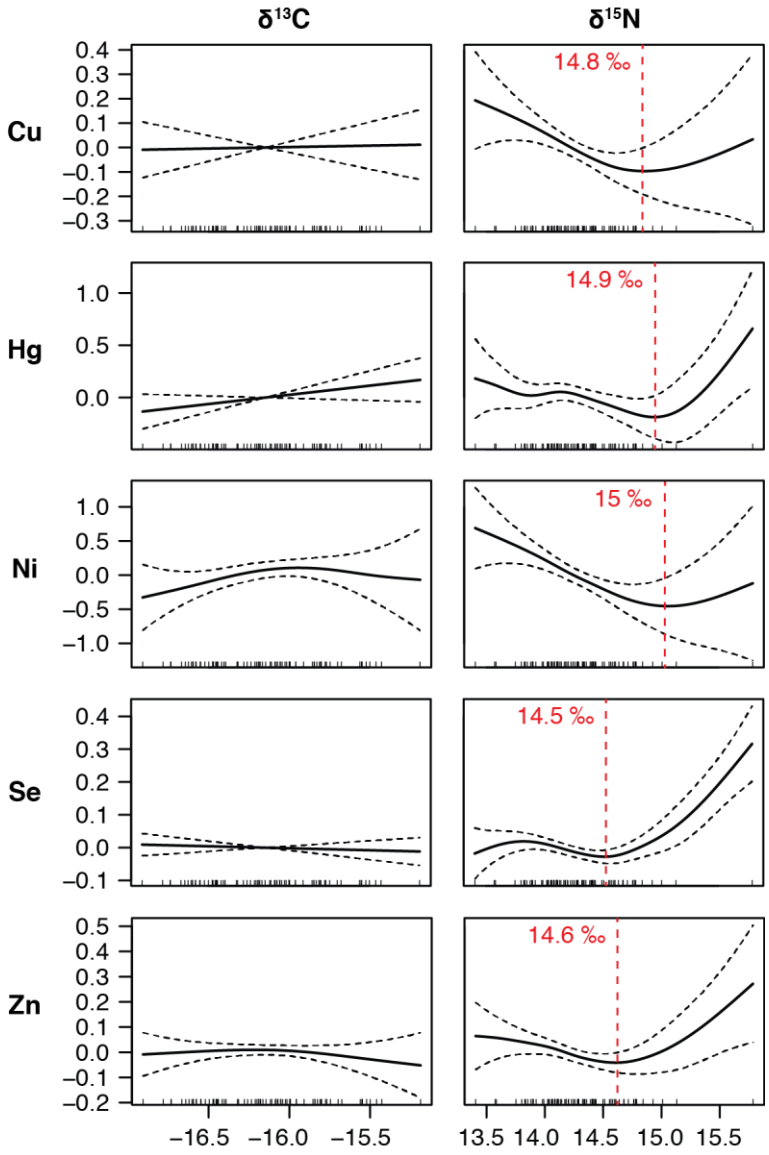

Fig. 5.5. Graphical results of the generalised additive models (GAMs) fitted to the residuals of the size-based models. Smoothers illustrate the partial effect of continuous explanatory variables once the effects of all the other explanatory variables included in the model have been taken into account. The y-axis shows the contribution of the smoother to the predictor function in the model (in arbitrary units). Dashed lines represent the 95% confidence intervals. Whiskers on the x-axis indicate data presence. $\delta^{15}N$ shift values are indicated in red.

5.4. DISCUSSION

5.4.1. Trophic ecology inferred from stable isotopes

Data about the trophic ecology of emperor red snapper in the Seychelles and, more largely, in many areas of the world, are scarce (Mees 1992; Grandcourt *et al.* 2008; Froese and Pauly 2020). Here, it was possible to identify several characteristics using stable isotopes of carbon

and nitrogen, which gave indications on habitat use and diet, as well as temporal and ontogenetic changes in trophic ecology.

Measured $\delta^{13}C$ values in sampled emperor red snappers were comprised between –16.9 ‰ and –15.2 ‰. Generally, it is considered that phytoplankton has $\delta^{13}C$ values between –23 ‰ and –18 ‰, benthic carbon sources have values between –18 ‰ and –13 ‰ and seagrass has values above –13 ‰ (Fry and Sherr 1989). When considering the trophic enrichment factor for $\delta^{13}C$ values (i.e. 1-2 ‰; Fry 2002), measured $\delta^{13}C$ values thus indicate that emperor red snappers mainly depend on benthic sources for carbon. This is in accordance with the fact that emperor red snappers are demersal, their diet being mainly composed of benthic prey (i.e. fishes, crabs, benthic crustaceans and cephalopods) (Froese and Pauly 2020).

Both $\delta^{13}C$ and $\delta^{15}N$ values in emperor red snapper were positively correlated with their size, suggesting ontogenetic changes in habitat use and diet. The positive correlation between size and $\delta^{13}C$, in particular, suggests that larger individuals rely more on demersal/benthic prey than smaller ones, although they are known to be less coastal and to live in deeper waters than smaller individuals. This variation of $\delta^{13}C$ with size probably reflects an ontogenetic change in diet from pelagic carbon source dominated at larval stage to benthic carbon source dominated for adults. Such changes were observed for other reef species like Mullidae (Kolasinski *et al.* 2009), the red snapper *Lutjanus campechanus* (Wells *et al.* 2008), carnivorous reef fishes (Kulbicki *et al.* 2005) and for reef fishes in general (Cocheret De La Morinière *et al.* 2003). In particular, Wells *et al*. (2008) showed a change in diet with growth for *L. campechanus*, from low trophic level prey items in the water column (i.e. zooplankton like pelagic copepods) to high trophic level benthic prey (i.e. benthic crustaceans and fishes). Here, information on the diet of juvenile emperor red snappers and especially on the ontogenetic changes in diet in this species were not available. However, emperor red snappers share common features in habitat and diet with other Lutjanid species, and especially the red snapper *L. campechanus*. This suggests that similar changes in diet could occur for the emperor red snapper *L. sebae*. Such changes would also explain the positive relationship between emperor red snapper size and $\delta^{15}N$ values, as both their values in $\delta^{13}C$ and $\delta^{15}N$ would increase by shifting from a zooplankton-dominated diet at larval stage to a benthic carnivorous prey-dominated diet. In addition, this is coherent with the general hypothesis that size and trophic position are positively correlated in marine ecosystems, that is larger consumers are able to eat larger prey that have a higher trophic

position (Jennings *et al*. 2002). Other studies also observed enrichment in $\delta^{13}C$ and $\delta^{15}N$ values with increasing size and age in different snapper species (Cocheret De La Morinière *et al*. 2003; Wells *et al*. 2008).

The positive correlation between $\delta^{13}C$ and $\delta^{15}N$ completes both previous correlations between size and stable isotope values of carbon and nitrogen. However, the lack of linear relationship between $\delta^{13}C$ and $\delta^{15}N$ suggests a shift in emperor red snappers' isotopic values at some point, thus a shift in the isotopic values of their prey. This may be due to a shift in diet and/or in habitat use. By modelling the relationship between fork length and both $\delta^{13}C$ and $\delta^{15}N$ values in emperor red snappers (Appendix 5.2), it was possible to estimate a size at shift, i.e. 65 cm. This size at shift was close to size at maturity in the Seychelles, which has been estimated around 62-64 cm fork length (Mees 1992). Thus, maturity may play a role in dietary and/or habitat change. Other studies on carnivorous reef fishes found a link between ontogenetic dietary shift and change in habitat and age class, including size at maturity (e.g. Cocheret De La Morinière *et al*. 2003). However, the reason for such a dietary or habitat shift remains unclear, as both are closely linked to each other. A first hypothesis could be a change in habitat when reaching a particular size (e.g. size at maturity) linked to change in habitat requirements. Then, the change in diet would be driven by the change in habitat. A second hypothesis would be a change in diet linked to growth, because larger fishes generally feed on larger prey. This would lead to a change in habitat use to find better-suited prey in terms of size and of energy supply and, in this case, the change in habitat would be driven by ontogenetic changes in diet. However, there are very few studies on the link between maturity and change in habitat use and/or diet (Sheaves 1995). In addition, there is a lack of information on emperor red snappers' habitat use in the Seychelles according to their size and maturity. Thus, more data on habitat use and diet composition according to emperor red snappers' life stage are needed to further explore this hypothesis.

Finally, there was no difference in trophic ecology between males and females, or among seasons. This was expected as there was also no significant difference in size between sexes or among seasons (Appendix 5.1).

5.4.2. Trace element bioaccumulation in emperor red snappers' muscle

By investigating the effects of continuous (i.e. size, habitat use through $\delta^{13}C$ and trophic position through $\delta^{15}N$) and categorical variables (i.e. sex) separately, it was possible to highlight

the effects of several intrinsic and extrinsic factors on trace element bioaccumulation in emperor red snappers. The significance and nature of these effects, that is bioaccumulation, biomagnification or biodilution, was highly dependent on the factor and on the trace element considered.

Among intrinsic factors, sex had no significant effect on trace element bioaccumulation in emperor red snappers, as shown by the very similar trace element profile ellipses between males and females, and by the non-significant difference in trace element concentrations between sexes and for all elements. This suggests that physiological processes involved in reproduction do not affect trace element uptake and/or elimination between males and females. Similar results were found in other species, like the albacore tuna (Chouvelon *et al*. 2017). In this species, the very few differences in trace element concentrations between sexes (mainly Hg) were hypothesized to originate from poor elimination of trace elements during reproduction and to slight differences in the prey composition in their diet. Here, this could partially explain the lack of difference in trace element concentrations between sexes, especially in the case of essential trace elements that are physiologically regulated. In the case of non-essential trace elements like Cd or Hg, similar diets in terms of prey composition between males and females, as suggested by similar $\delta^{13}C$ and $\delta^{15}N$ values, could have led to similar concentrations between sexes. Although male and female emperor red snappers sampled in this study had similar size ranges, Mees (1992) found differences in population dynamics between males and females, with females being smaller than males. Thus, the question is: here, do same-size individuals of different sex have the same age? Indeed, this could have influenced the bioaccumulation of trace elements like Hg, which is known to accumulate in time (Raimundo *et al*. 2013; Chouvelon *et al.* 2017), and could have masked differences of bioaccumulation between sexes.

Size was a major factor influencing trace element concentrations in emperor red snappers' muscle tissues, as revealed by the variables selected in the most parsimonious GLM and GAM models. Except for Cr and Fe for which the null model was the best model, for all other trace elements, fork length or at least one of its interaction factors (i.e. with $\delta^{13}C$ or with $\delta^{15}N$) was present in the selected best models. This indicates direct influence of size on trace element concentrations by either bioaccumulation or biodilution, and indirect influence by affecting trophic ecology, which itself has a direct effect on trace element bioaccumulation.

Such findings are also similar to what is generally observed for other marine species, size being a major driver of trophic structure (Jennings *et al.* 2002). This effect of size on emperor red snappers' trophic ecology was most evident for Cd and Mn. Indeed, the interaction factor between fork length and $\delta^{13}C$ values was significant in explaining Cd concentrations and, after normalizing Cd concentrations by size, the relationship between Cd concentrations and $\delta^{13}C$ values was not significant anymore. The same thing was observed for the relationship between Mn concentrations and $\delta^{15}N$ values, suggesting that, in both cases, these relationships between trace element concentrations and either $\delta^{13}C$ or $\delta^{15}N$ values were mostly driven by the relationship between stable isotope values and size.

Models explaining As concentrations showed they increase with increasing size and $\delta^{13}C$ values (i.e. more benthic signature), but a decrease with increasing $\delta^{15}N$ values (i.e. higher trophic position). The ontogenetic changes in diet and habitat use shown in emperor red snappers (section 4.4.1) could explain these relationships. Decapod crustaceans are known to preferentially accumulate As under the arsenobetaine form (Khokiattiwong *et al*. 2009; Chapter 1), which is one of the most bioavailable forms of As (Zhang *et al.* 2016). Thus, if adult emperor red snappers feed more on large benthic prey, including decapod crustaceans, compared to juveniles, they would potentially bioaccumulate more As while having higher $\delta^{13}C$ values. However, this is in contradiction with the observed increase of $\delta^{15}N$ values with emperor red snappers' size, and more generally with the observed relationships among size, $\delta^{13}C$ and $\delta^{15}N$ values, which were all positively correlated with each other. Thus, here, it is not possible to conclude on the processes that led to a positive link between As concentrations and size and $\delta^{13}C$ values, while leading to a negative link with $\delta^{15}N$ values at the same time.

Although there was no effect of habitat (i.e. $\delta^{13}C$ values) on the concentrations of Cu, Hg, Ni, Se and Zn, there was a significant effect of trophic position (i.e. $\delta^{15}N$ values) with a shift in bioaccumulation trend for $\delta^{15}N$ values between 14.5 and 15.0 ‰. Such a shift could be attributed to the ontogenetic shift in diet and habitat use observed for emperor red snappers analysed here (around $\delta^{15}N$ value of 14.4 ‰) and possibly related to sexual maturity (section 4.4.1). Such hypothesis would be coherent with previous conclusions on ontogenetic changes in emperor red snappers' diet. Indeed, by feeding more on small pelagic prey with a low trophic position, smaller emperor red snappers would bioaccumulate higher concentrations of trace elements known to be in higher levels in primary producers (e.g. Cu and Ni) (Fabregas and

Herrero 1986; Fox and Zimba 2018). In contrast, by feeding on high trophic position prey, including carnivorous fish and benthic crustaceans, larger individuals would bioaccumulate higher concentrations of trace elements that tend to biomagnify like Hg (Wang 2002). In addition, large decapod crustaceans, like crabs, are known to have high concentrations of Zn (Rainbow 2002; Chapter 1), which could thus influence Zn concentrations in emperor red snappers feeding on them. Indeed, although some degree of Zn regulation in the muscle of the mangrove red snapper *Lutjanus argentimaculatus* was observed, suggesting potential of Zn regulation in emperor red snappers' muscle, Zn concentrations in decapod crustaceans can be particularly high (Chapter 1) and Zn intake could have exceeded regulation capacities. Finally, the bioavailability of ingested trace elements is an important factor to consider. As the physicochemical forms of a given trace element can be in different proportions or concentrations in different types of prey, a change in prey composition in emperor red snappers' diet could induce a change in the bioavailability of some trace elements in their food.

Finally, there was no effect of size or of trophic ecology on the bioaccumulation of Cr and Fe, as shown by the null model being the best selected model for both trace elements. This is most probably due to the presence of regulation mechanisms in emperor red snapper metabolism for these trace elements, as they are both essentials to fish physiology (Bury and Grosell 2003; Chanda *et al.* 2015), and to no disequilibrium between uptake rate and detoxification/excretion rates.

5.4.3. Seasonal variation in trace element concentrations

Observed variations in trace element concentrations of emperor red snappers caught during different seasons could have been caused by different phenomenon. The first hypothesis was a link between seasonal change in habitat use and/or diet due to reproduction dynamics (i.e. spawning aggregations) and changes in trace element concentrations in their muscle tissues. However, there was no difference in $\delta^{13}C$ or $\delta^{15}N$ values between seasons. In addition, Mees (1992) observed peaks of reproductive activity during two distinct periods throughout the year (i.e. October/November and March to May), and trace element concentrations variation patterns do not correspond with these periods. It is thus likely that seasonal variations in weather, environmental parameters and trace element bioavailability affected trace element concentrations in emperor red snappers rather than reproductive dynamics. Indeed, environmental parameters such as water temperature, pH and salinity can influence trace

element bioavailability in the water column, and these parameters often vary with seasonal climatic variations (Neff 2002a; Rainbow and Black 2002, 2005).

Generally, except for Hg which was highest in emperor red snappers caught during the pre-NWM season, all trace elements for which concentrations varied according to the season (i.e. Cd, Cr, Cu, Ni, Mn, Se, and Zn) were in highest concentrations in emperor red snappers caught during the NWM and pre-SEM seasons. In the Southern Indian Ocean, the NWM season is characterised by high cyclonic activity which can affect winds and which brings abundant rains in the Seychelles (Chang-Seng 2007). Strong winds during this season could thus have caused resuspension of settled sediments, resulting in higher trace element concentrations and thus their availability in the water column. In addition, the strong rains during this season could also affect water salinity due to high input of freshwater in the ocean, and previous studies showed a negative relationship between salinity and the bioavailability of trace elements like Cd and Zn in the water column (Rainbow and Black 2002, 2005). Although diet is generally the main pathway for trace element intake in marine consumers (Wang 2002), trace elements could have entered the food web through primary producers and travelled up the food web to top predators like the emperor red snapper. Both the NWM and pre-SEM seasons are also particularly warm in the Seychelles (Chang-Seng 2007). To compensate for the low dissolve oxygen in waters caused by high temperatures, fish have to increase their respiratory rate (Saha *et al.* 2016). Trace element intake through the gills, although not being the main pathway, could thus have contributed to increasing trace element concentrations in emperor red snappers' muscle tissues. Finally, although primary production is generally low in Seychelles waters, it is relatively higher during the SEM season, potentially causing phytoplanktonic blooms (ASCLME 2012). Subsequent higher bacterial activity, related to the decomposition of organic matter, may enhance MeHg production and thus Hg bioavailability in the water column (Morel *et al.* 1998). This could explain the highest Hg concentrations measured in emperor red snappers caught during the pre-NWM season.

5.5. CHAPTER HIGHLIGHTS

Chap. 3 – Main findings

• **Sex** seemed to have **no effect on the trophic ecology** of emperor red snapper **and on trace element bioaccumulation** in their muscle tissues.

• **Ontogenetic changes in habitat use and diet** were observed in emperor red snapper, with a **possible effect of maturity stage**.

• **Habitat use, trophic position and**, more generally, **diet**, had a **significant effect on trace element bioaccumulation** in emperor red snappers.

• **Size** had both **direct and indirect effects on trace element bioaccumulation** in emperor red snappers. Indirect effects were mainly related to ontogenetic changes in habitat use and diet.

• **Seasonal variations** in trace element concentrations may be related to **seasonal variations in trace element bioavailability** caused by changes in weather and environmental parameters (i.e. winds, water temperature, salinity, dissolve oxygen and bacterial activity).

6. Chapter 4 – Trace element bioaccumulation in tropical and subtropical pelagic systems: patterns of mercury and selenium concentrations in swordfish from the Indian Ocean

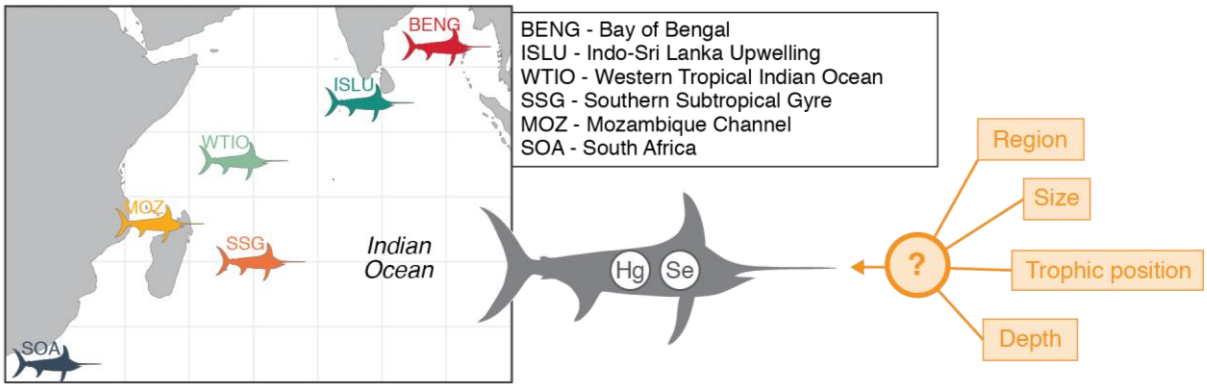

Content

This chapter is included in a paper in preparation for Chemosphere *and presented in Supp. Doc. 4.*

6.1. CONTEXT AND OBJECTIVES

As long-lived top predators in marine pelagic ecosystems (Nakamura 1985), swordfish bioaccumulate high levels of Hg, with reported concentrations higher than in other top predators such as tuna and tuna-like species, and exceeding from time to time the recommended safety limits (Bodin *et al.* 2017). Swordfish is also a highly migratory species (Nakamura 1985) and is thus among the most appropriate bioindicator species for monitoring and understanding broad spatial gradients of Hg contamination in the world's oceans.

In the Indian Ocean, swordfish is the main target of commercial and recreational fisheries, and represents a high income and a high protein source for local populations (FAO 2020). Yet, global data on Hg occurrence in swordfish across the Indian Ocean is still scarce (Esposito *et al*. 2018) while no previous work investigated global patterns of Se concentrations in swordfish from this ocean.

In this chapter, the spatial variation of Hg and Se concentrations in swordfish across the Indian Ocean was assessed, and the influence of ontogenetic parameter (i.e. size) and trophic ecology on these regional variations was examined. I also explore the potential of co-accumulation between Hg and Se in swordfish.

6.2. METHODOLOGY

6.2.1. Sample collection and preparation

A total of 191 swordfish were fished in several regions of the Indian Ocean, between 2007 and 2018 (Fig. 6.1). For each individual, white muscle tissue was retrieved and fishing location (longitude and latitude) and size of the individual were recorded. All samples were analysed for SI ($\delta^{13}C$ and $\delta^{15}N$) and Hg concentrations. Se was only analysed if enough sample powder was left after Hg and SI analyses (13 swordfish from the Bay of Bengal area – BENG, 16 from the Indo-Sri Lanka Upwelling area – ISLU, 45 from the Western Tropical Indian Ocean area – WTIO, 42 from the Southern Subtropical Gyre area – SSG and 1 on the Mozambique Channel and East Coast of South Africa area – MCSA). Samples were freeze-dried during 72h and ground to powder before trace element and stable isotope analysis. Hg and Se were analysed following the method described in section 2.4.1; CRMs were DOLT-5 to validate Hg concentrations, and IAEA-461, DOLT-5 and TORT-3 to validate Se concentrations. Mean recovery rate for Se was

113%. Stable isotopes were prepared and analysed following the methods described in sections 2.5.1.1 and 2.5.3, respectively.

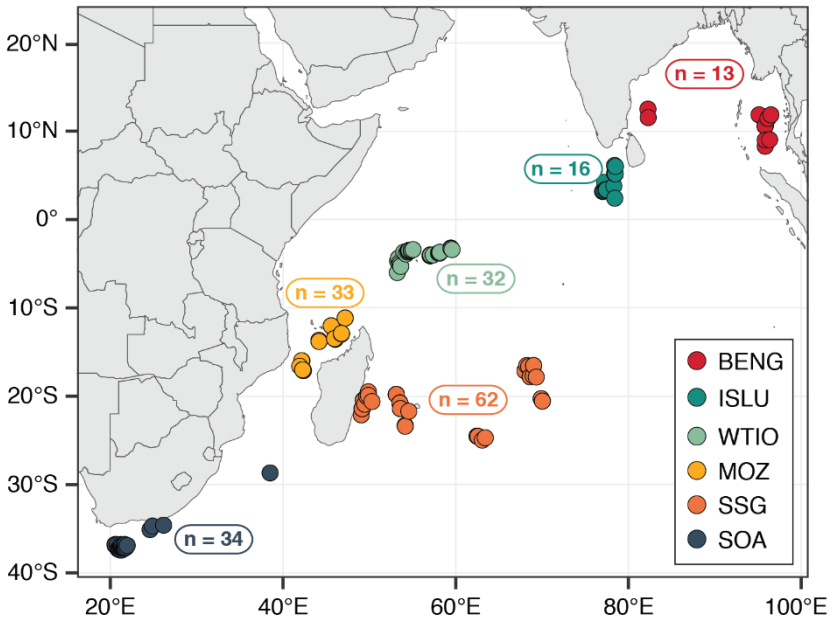

Fig. 6.1. Swordfish fishing sites location and respective areas in the Indian Ocean. BENG = Bay of Bengal; ISLU = Indo-Sri Lanka Upwelling; WTIO = Western Tropical Indian Ocean; SSG = Southern Subtropical Gyre; MOZ = Mozambique Channel; SOA = South Africa.

6.2.2. Mercury data transformation

As Hg is known to bioaccumulate with length (Lavoie *et al.* 2013), concentrations were standardised according to swordfish length in order to investigate the effect of other factors on Hg bioaccumulation. For this, a power-law relationship ($\log(Hg) = a \times (\text{lower jaw-fork length} - b)^c - d$) was fit between log-transformed Hg concentrations (log(Hg)) and swordfish lower jaw-fork length to characterise the bioaccumulative process in swordfish. Residuals from the length-based Hg model (i.e. observed values – predicted values) were extracted and used to calculate length-standardised Hg concentrations (at lower jaw-fork length = 150 cm).

6.2.3. Calculation of trophic position

$\delta^{15}N$ baseline values are highly variable between ecosystems (Wada and Hattori 1976) and use of $\delta^{15}N$ values as proxy of trophic level should be food web-specific. For large-scale data, it is thus recommended to convert $\delta^{15}N$ values to trophic level using an isotopic baseline (Layman *et al.* 2011). Here, trophic position of each swordfish was calculated using Eq. 6.1 (Post 2002),

with $\delta^{15}N_{sc}$ the $\delta^{15}N$ values in the secondary consumer, $\delta^{15}N_{base}$ the $\delta^{15}N$ values at the base, λ the trophic level of the organism used to obtain $\delta^{15}N_{base}$ (i.e. 1 for phytoplankton) and Δ_n the enrichment factor (i.e. 3.4 ‰).

$$\text{Trophic level} = \lambda + (\delta^{15}N_{sc} - \delta^{15}N_{base}) / \Delta_n \qquad \textbf{(Eq. 6.1)}$$

As global $\delta^{15}N$ baselines do not exist in the Indian Ocean, $\delta^{15}N_{base}$ values were modelled for phytoplankton in each recorded fishing location, for each longitude-latitude couple and for each sampling year. Model was based on preindustrial simulations from Somes *et al.* (2017), and results were averaged annually over the upper 130 meters of ocean surface.

6.2.4. Statistical analyses

Concentrations of Hg and Se, theoretically bioavailable Se, swordfish lower jaw-fork length, $\delta^{13}C$ and $\delta^{15}N$ values and trophic levels were compared between areas using ANOVA (i.e. parametric) or Kruskal-Wallis (i.e. non-parametric) and, when a difference was significant ($p < 0.05$), associated post-hoc tests (i.e. Tukey's HSD and Dunn test with Benjamini-Hochberg adjustment respectively).

Generalised additive models (GAM) with a Gaussian distribution and an identity link function were used to assess the effects of several factors (i.e. fish size, trophic level, $\delta^{13}C$ values and fishing location using longitude and latitude) on Hg and Se concentrations. A GAM was also fitted on length-standardised Hg concentrations to investigate effect of ecological factors after removing the length effect. Concurvity was checked for all models and $\delta^{15}N$ values were not included as explaining variable to avoid collinearity with trophic level. Correlations were tested among explaining variables using Kendall tests in order to identify potential interaction terms of interest. According to correlation tests results (Appendix 6.3), in all models, the interaction terms between $\delta^{13}C$ and fishing location (i.e. $\delta^{13}C$+longitude and $\delta^{13}C$+latitude) and between trophic level and latitude were also included as explanatory variables. The interaction term between fish length and trophic level was also added. The best model was selected by using the AIC.

Finally, to characterise the potential of co-accumulation of Hg and Se, correlation (Pearson) was tested between log-transformed Hg and log-transformed Se concentrations. A GAM was also fitted on log-transformed Se concentrations with log-transformed Hg concentrations and associated interactions terms as explaining variables. The best-AIC selected

model was compared to previous model explaining Se concentrations, using deviance explained and AIC, in order to see if adding log-transformed Hg concentrations as explaining variable improved the GAM.

6.3. RESULTS

Across the Indian Ocean, Hg concentrations were lowest in swordfish from the MOZ region (0.37 ± 0.23 $\mu g.g^{-1}$ ww *vs* 0.81 ± 0.68 $\mu g.g^{-1}$ ww in BENG, Dunn test, $p = 0.037$; 1.21 ± 0.83 $\mu g.g^{-1}$ ww in ISLU, $p < 0.001$; 0.77 ± 0.46 $\mu g.g^{-1}$ ww in WTIO, $p = 0.002$; 1.40 ± 0.76 $\mu g.g^{-1}$ ww in SSG, $p < 0.001$; 0.74 ± 0.39 in SOA, $p = 0.001$) (Fig. 6.2A). Hg concentrations in the SSG region were also higher than in the BENG, WTIO and SOA regions (Dunn test, $p = 0.009$ with BENG; $p = 0.001$ with WTIO and SOA).

Se concentrations were highest in swordfish from the BENG region compared to swordfish from the other regions (1.39 ± 0.25 $\mu g.g^{-1}$ ww *vs* 0.91 ± 0.25 $\mu g.g^{-1}$ ww in ISLU, Dunn test, $p = 0.007$; 0.94 ± 0.28 $\mu g.g^{-1}$ ww in WTIO, $p = 0.005$; 0.63 ± 0.31 $\mu g.g^{-1}$ ww in MOZ, $p < 0.001$; 1.04 ± 0.52 $\mu g.g^{-1}$ ww in SSG, $p < 0.005$; 0.65 ± 0.31 $\mu g.g^{-1}$ ww in SOA, $p < 0.001$) (Fig. 6.2B).

Among all swordfish from all sampled regions, there was a significant positive relationship between log-transformed Se and log-transformed Hg concentrations (Fig. 6.2C).

$\delta^{13}C$ values were highest in swordfish from the ISLU region compared to swordfish from the five other regions (–15.8 ± 0.4 ‰ *vs* –17.0 ± 0.4 ‰ in BENG, Dunn test, $p < 0.001$; –6.7 ± 0.5 ‰ in WTIO, $p < 0.001$; –16.6 ± 0.4 ‰ in MOZ, $p = 0.002$; –16.8 ± 0.5 ‰ in SSG, $p < 0.001$; –17.2 ± 0.3 ‰ in SOA, $p < 0.001$) (Fig. 6.2D). These values were also lower in swordfish from the SOA region than in those from the WTIO, MOZ and SSG regions (Dunn test, $p = 0.014$ with WTIO, $p < 0.001$ with MOZ, $p = 0.040$ with SSG).

$\delta^{15}N$ values were significantly higher in swordfish from the WTIO and SSG regions than in swordfish from the BENG and MOZ regions (14.1 ± 0.7 ‰ in WTIO and 14.3 ± 0.9 ‰ in SSG *vs* 13.2 ± 0.7 ‰ in BENG and 13.5 ± 0.9 ‰ in MOZ; Dunn test, $p = 0.002$ between WTIO and BENG, $p = 0.009$ between WTIO and MOZ, $p < 0.001$ between SSG and BENG and between SSG and MOZ) (Fig. 6.2E). Swordfish from the BENG region also had lower $\delta^{15}N$ values than those from the SOA region (13.2 ± 0.7 ‰ *vs* 14.0 ± 0.4 ‰; Dunn test, $p = 0.044$). Swordfish from the ISLU region had intermediate values (13.9 ± 0.7 ‰). Swordfish with the highest trophic levels

were from the SSG region (4.8 ± 0.5 *vs* 2.9 ± 0.3 in BENG, Dunn test, $p < 0.001$; 3.6 ± 0.3 in ISLU, $p < 0.001$; 4.5 ± 0.2 in WTIO, $p = 0.007$; 4.1 ± 0.4 in MOZ, $p < 0.001$; and 4.4 ± 0.1 in SOA, $p < 0.001$) (Fig. 6.2F). Swordfish from the BENG and ISLU regions had the lowest trophic levels (Dunn test, for BENG, $p < 0.001$ with WTIO, $p = 0.001$ with MOZ, $p < 0.001$ with SOA; for ISLU, $p < 0.001$ with WTIO, $p = 0.021$ with MOZ and $p < 0.001$ with SOA).

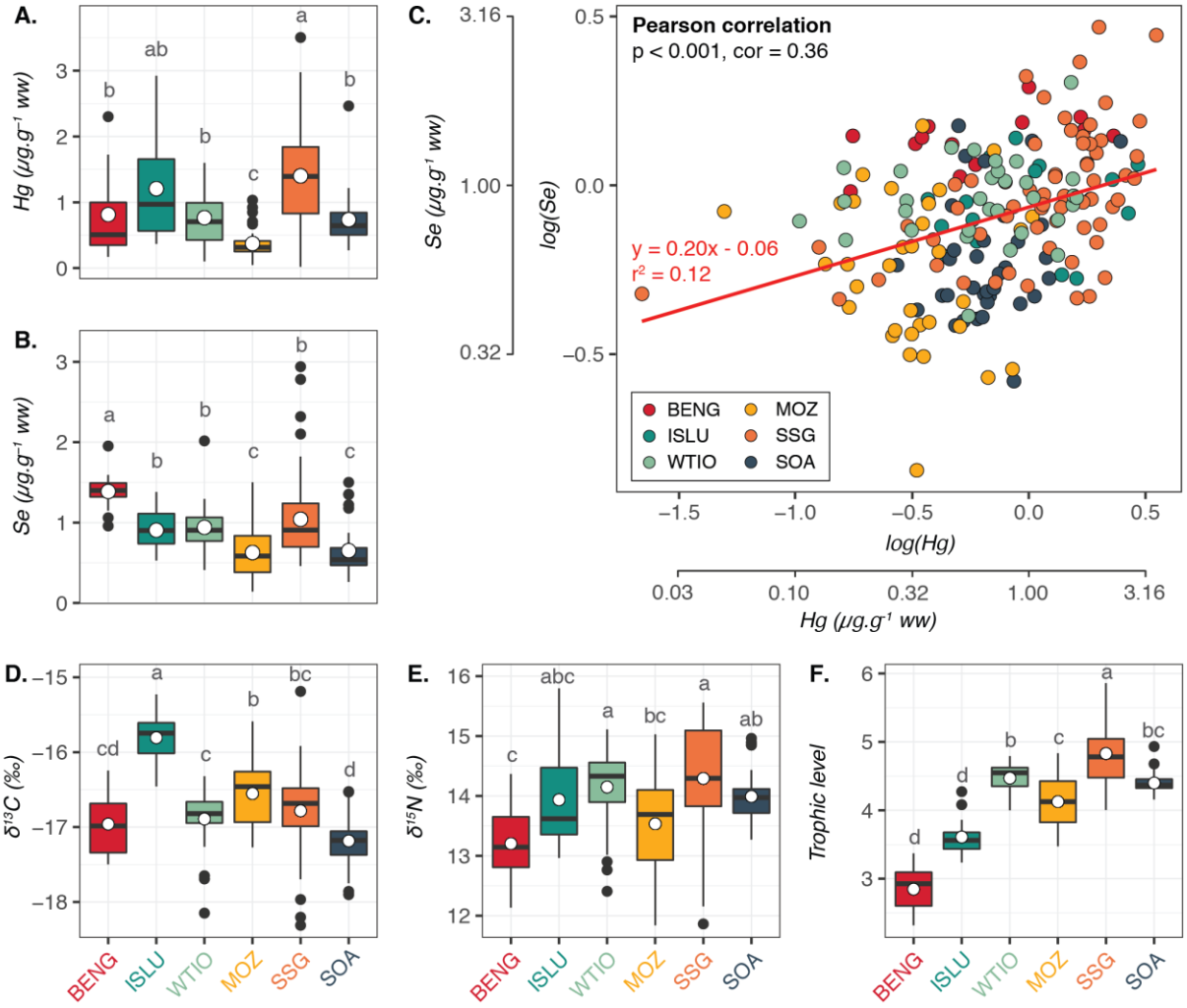

Fig. 6.2. Mercury (Hg) (A) and selenium (Se) concentrations (µg.g^{-1} ww) (B), relationship between log-transformed Se and log-transformed Hg concentrations (C), $\delta^{13}C$ (D) and $\delta^{15}N$ values (‰) (E), and trophic level (F) by sampling region. Mean values are indicated in white; a different letter indicates a significant difference between areas (A, B, D, E, F). The linear regression line is indicated in red (C). Mean (± SD) values for each region are presented in Appendix 6.1; post-hoc test results are presented in Appendix 6.2 (A, B, D, E, F). BENG = Bay of Bengal; ISLU = Indo-Sri Lanka Upwelling; WTIO = Western Tropical Indian Ocean; MOZ = Mozambique Channel; SSG = Southern Subtropical Gyre; SOA = South Africa.

Swordfish from the different Indian Ocean regions significantly differed in lower jaw-fork length (Fig. 6.3B). Swordfish from the ISLU region were the largest (197 ± 46 cm *vs* 111 ±

16 cm in BENG, Dunn test, $p < 0.001$; 142 ± 35 cm in WTIO, $p < 0.001$; 121 ± 29 cm in MOZ, $p < 0.001$; 151 ± 33 cm in SSG, $p = 0.004$; and 155 ± 35 cm in SOA, $p = 0.009$). Those from the BENG and MOZ regions were also smaller than those from the WTIO, SSG and SOA regions (Dunn test, $p = 0.004$ between BENG and WTIO, $p = 0.010$ between MOZ and WTIO and $p < 0.001$ for the other comparisons).

Swordfish from the SSG region had higher length-standardised Hg concentrations than those from the ISLU, WTIO, MOZ and SOA regions (1.41 ± 0.72 µg.g^{-1} ww *vs* 0.74 ± 0.39 µg.g^{-1} ww in ISLU, 0.79 ± 0.25 µg.g^{-1} ww in WTIO, 0.57 ± 0.22 µg.g^{-1} ww in MOZ, and 0.73 ± 0.41 µg.g^{-1} ww in SOA; Dunn test, $p < 0.001$) (Fig. 6.3C). Swordfish from the BENG region had intermediate length-standardised Hg concentrations, while also having high concentrations (1.39 ± 1.01 µg.g^{-1} ww). Finally, swordfish from the MOZ region also had lower length-standardised Hg concentrations than those from the BENG and WTIO regions (Dunn test, $p < 0.001$ with BENG, $p = 0.018$ with WTIO).

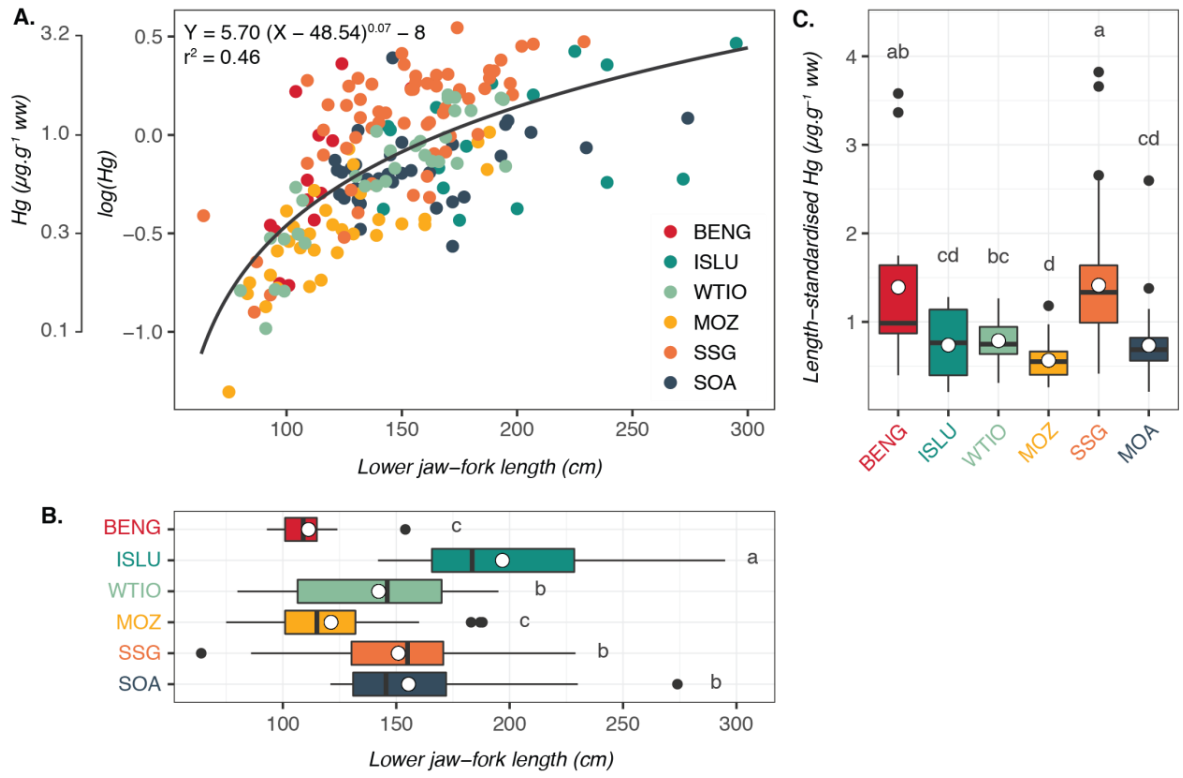

Fig. 6.3. Power-law relationship between log(Hg) and lower jaw-fork length (A), lower jaw-fork length (cm) (B) and length-standardised Hg concentrations (for a 150 cm fish length, µg.g^{-1} ww) for swordfish of each fishing region. Mean values are indicated in white; a different letter indicates a significant difference between regions (B, C). Mean (± SD) values for each region are presented in Appendix 6.1; post-hoc test results are presented in Appendix 6.2 (B, C). BENG = Bay of Bengal; ISLU = Indo-Sri Lanka Upwelling; WTIO = Western Tropical Indian Ocean; MOZ = Mozambique Channel; SSG = Southern Subtropical Gyre; SOA = South Africa.

Best GAM models explaining Hg and Se concentrations in swordfish are presented in Table 6.1. Graphical results (i.e. smoothers) were plotted and are presented in Appendices 6.4 to 6.7. For log-transformed Se concentrations, the model including log-transformed Hg concentrations as explanatory variable had a higher total deviance explained and a lower AIC (-137 *vs* -143) than the model only including lower jaw-fork length, $\delta^{13}C$ values, trophic level, longitude, latitude and their interactions terms.

Table 6.1. Generalised additive model (GAM) results for log-transformed mercury (Hg), log-transformed length-standardised Hg and log-transformed selenium (Se) concentrations.

Trace element	Response variable	Total deviance explained (%)	Explanatory variable used in the best AIC GAM model	*p* value
Hg	log(Hg)	71.7	Lower jaw-fork length	< 0.001
			$\delta^{13}C$	0.031
			Trophic level	0.029
			Latitude	0.005
			Longitude	0.025
			$\delta^{13}C$:Latitude	0.003
			$\delta^{13}C$:Longitude	0.040
			Trophic level:Latitude	0.117
	log(length-standardised Hg)	47.3	$\delta^{13}C$	0.029
			Trophic level	0.018
			Latitude	< 0.001
			Longitude	0.094
			$\delta^{13}C$:Latitude	0.007
			$\delta^{13}C$:Longitude	0.080
			Trophic level:Latitude	< 0.001
Se	log(Se)	43.7	$\delta^{13}C$	0.023
			Trophic level	0.176
			Latitude	0.017
			Longitude	< 0.001
	log(Se) *(with log(Hg) as explanatory variable)*	45.9	$\delta^{13}C$	0.094
			Trophic level	0.036
			Latitude	0.026
			log(Hg)	0.016
			$\delta^{13}C$:Longitude	< 0.001

6.4. DISCUSSION

6.4.1. Factors governing mercury and selenium concentrations in swordfish from the Indian Ocean

Trace element concentrations in marine top predators are well known to vary according to the feeding area of the consumer, either due to regional variations in trace elements' bioavailability

or to potential differences in fish trophic ecology among feeding areas (Wang 2002). This was the case for both Hg and Se bioaccumulation in this study, as shown by GAM results in which geographical origin was one of the main factors explaining Hg and Se concentrations.

Latitude was especially important in explaining both length-standardised Hg and Se bioaccumulation, with a decrease from the BENG region in the north-east to the coast of South Africa (SOA region) in the south-west. Such Hg and Se bioaccumulation patterns may be due in part to regional variations in bioavailability of both trace elements. In oceanic waters, these trace elements originate from both natural and anthropogenic sources, like industry and burning of fossil fuel for Hg (Boening 2000), or irrigation of agricultural lands and coal combustion for Se (Schiavon *et al.* 2017). Then, they both enter the food webs through their bioaccumulation by primary producers and are transferred to higher-level consumers through the trophic pathway (Wang 2002; Schiavon *et al.* 2017). In the case of Se, phytoplankton accumulates this element mainly under the inorganic selenite (Se IV) form and it is further incorporated into selenoproteins (Schiavon *et al*. 2017; Ivanenko 2018). These organic compounds are then transferred to higher-level consumers through primary and secondary consumption (Schiavon *et al*. 2017). In the case of Hg, primary producers accumulate both inorganic and organic forms of Hg, but Hg is mainly transferred to higher-level organisms under the MeHg form (Mason *et al.* 1995). The BENG region generally receives high amount of river discharge (Subramanian 1993), which could have led to high Hg and Se input in the waters of this region. In addition, primary production in this region is known to be lower than in other regions of the Indian Ocean in spite of river discharge, due to strong stratification (Dalabehara and Sarma 2021). This could have led to higher Se bioaccumulation in phytoplankton in this region due to high selenite availability, thus high organic Se compounds production in phytoplankton and thus higher Se bioaccumulation in higher-level organisms. In the case of Hg, MeHg production in subsurface waters (500 m) of the Indian Ocean may have played a large role in the high Hg bioavailability in the BENG region. Modelled MeHg production in this ocean showed a latitudinal gradient, from high production in the BENG region to low production in the MOZ, SSG and SOA regions (Zhang *et al.* 2020). As swordfish usually feed on mesopelagic prey (i.e. depths > 200 m) (Young *et al.* 2006; Potier *et al.* 2007), an interregional difference in MeHg production in mesopelagic waters could have led to different Hg concentrations in swordfish prey (Monteiro *et al.* 1996; Blum *et al.* 2013) and thus to differential Hg bioaccumulation in swordfish tissues.

Although Hg methylation was modelled to be low in the SSG region, length-standardised Hg concentrations were highest in swordfish from this region, suggesting that Hg bioavailability was not the only factor explaining interregional difference in Hg concentration. Such Hg concentration pattern could be explained by swordfish trophic ecology, and particularly trophic position. Both $\delta^{15}N$ and trophic level were present in the best AIC model explaining length-standardised Hg concentrations, confirming Hg biomagnification potential through food webs (Lavoie *et al.* 2013), and swordfish from the SSG region had higher trophic levels than in all other regions. While an interregional difference in diet composition could explain this, it is more likely that it is the result of a difference in trophic structure at the base of the food web due to nutrient limitation conditions. Indeed, while trophic position is thought to be positively correlated to fish size (Jennings *et al.* 2002), swordfish from this region were not the largest among all regions. In addition, in the SSG region, waters are known to be oligotrophic, with low primary production, which was previously shown to affect food web length (Pethybridge *et al.* 2018) and to increase Hg bioaccumulation in high-trophic level consumers (Chouvelon *et al.* 2018). Here, higher Hg bioaccumulation in oligotrophic conditions could be explained by the domination of N_2 fixation, favouring the presence of diazotrophs like cyanobacteria (Gruber and Sarmiento 1997; Longhurst 1998), as showed in the western Pacific Ocean (Médieu *et al*. 2021). As these organisms are smaller (< 2 µm) than diatom and dinoflagellates (usually 20 to 200 µm), they would favour the presence of mesozooplankton (0.2 to 20 mm) in the food web, causing the presence of an extra step at the bottom of the food chain (Sommer *et al*. 2002). In addition, MeHg proportions in phytoplankton was previously shown to increase with decreasing phytoplankton size, suggesting that diazotrophs could be transfer vectors of Hg to zooplankton and to higher trophic levels (Gosnell and Mason 2015; Lee and Fisher 2016). Thus, by feeding both on a longer food web than in other regions of the Indian Ocean and in oligotrophic waters, swordfish from the SSG region would bioaccumulate higher concentrations of Hg.

Across all sampling regions, swordfish size directly affected their Hg bioaccumulation, with a global increase in Hg with increasing lower jaw-fork length. This was expected, as prey selection, itself influencing trace element bioaccumulation in marine predators (e.g. Metian *et al*. 2013; Chouvelon *et al*. 2017), varies according to the predator's body size (Jennings *et al*. 2002). This is what led to the theory that the trophic position of a predator is positively correlated with its size (Jennings *et al.* 2002). Size is also used as a proxy of age and, as we have

shown previously, Hg both biomagnifies along food chains and bioaccumulates through time in organisms.

Depth played a significant role in both Hg and Se bioaccumulation in swordfish. Indeed, $\delta^{13}C$, which is used to discriminate benthic *vs* pelagic feeding habitats (France 1995), was a significant factor influencing Hg and Se concentrations across all sampling regions. Hg concentration, and especially MeHg availability in oceanic waters, has been positively correlated with depth in previous works (e.g. Choy *et al*. 2009). This was linked mainly with a higher microbial activity, and thus a higher Hg methylation rate in deep waters (Blum et al. 2013). As swordfish are able to dive to depths down to more than 1000 meters (Abascal *et al*. 2010), they would bioaccumulate significantly higher Hg concentrations when feeding on deeper-living prey. In contrast, Se concentrations tended to decrease with increasing $\delta^{13}C$ (Appendix 6.6), suggesting a relatively higher Se bioaccumulation when feeding closer to the surface. This is consistent with the high Se bioaccumulation potential and subsequent conversion to selenoproteins in phytoplankton (Schiavon *et al*. 2017; Ivanenko 2018). This suggest that prey living closer to the surface would bioaccumulate higher Se concentrations, and would thus transfer higher Se concentrations to swordfish feeding on these prey.

Here, results thus show interregional variations in Hg and Se bioaccumulation in swordfish from the Indian Ocean, due to local conditions in Hg and Se bioavailability and to local trophic structures. Yet, swordfish is a highly migratory species (Nakamura 1985), and studies on the population structure in the Indian Ocean identified one single panmictic population, with no clear subpopulation at the genetic level (Muths *et al*. 2013; Mahé *et al*. 2016). This suggests that swordfish are able to undertake long migrations in the Indian Ocean, even through the strong current systems of this ocean (Schott *et al.* 2009), but hint to a certain level of residency at the scale of their muscle isotopic and trace element turnover rates (i.e. 3 months), as hypothesized by Ménard *et al*. (2007).

6.4.2. Signs of co-accumulation of mercury and selenium

Due to the antagonist effect between Hg and Se, that is their high binding ability (Raymond and Ralston 2004; Manceau *et al.* 2021), a co-accumulation of these two trace elements can be expected in marine consumers. This bioaccumulation effect is still under debate, as some studies found no significant relationship between both trace elements (e.g. Mikac *et al*. 1985; Chen *et al*. 2001; Kehrig *et al*. 2009), while others found that Se concentrations increased with

increasing Hg concentrations in muscle tissues of marine consumers (e.g. Andersen and Depledge 1997; Faganeli *et al*. 2018; Azad *et al*. 2019). However, it is possible that such positive relationship is dependent on Hg concentrations, with no relationship in species with low Hg concentrations (Azad *et al*. 2019). In this study, log-transformed Se concentrations had a weak but significant positive relationship with log-transformed Hg concentrations, and adding log-transformed Hg concentrations as explanatory variable improved the GAM explaining log-transformed Se concentrations. This suggest a possible co-accumulation of both trace elements in white muscle of swordfish across the Indian Ocean. This would be coherent with previous findings (Azad *et al*. 2019), as swordfish are known to bioaccumulates high concentrations of Hg. Such bioaccumulation process could be the result of both the consumers' physiology and its diet. By binding with Se, Hg would lower Se bioavailability within the consumer's body and, as a result of homeostatic regulation, Se bioaccumulation would increase (Beijer and Jernelov 1978). In addition, fish may receive a part of their dietary Hg as Hg-Se compounds (Khan and Wang 2009), and would thus accumulate both trace elements at the same time. Although we previously showed that Hg and Se bioaccumulation in swordfish from the Indian Ocean could follow inverse or independent trends (e.g. bioaccumulation with depth and with size), implying that co-accumulation is not the main factor influencing both trace element bioaccumulation, correlation and GAM results suggest that the Hg-Se interaction may participate to Hg and Se bioaccumulation in swordfish.

6.5. CHAPTER HIGHLIGHTS

Chap. 4 – Main findings

• In Indian Ocean swordfish, the **main factor** influencing Hg and Se bioaccumulation was **regional origin**, due to **regional differences in trace element bioavailability and in trophic structure at the base of the food web** (i.e. oligotrophy).

• **Feeding depth** also had **some level of effect on both Hg and Se bioaccumulation**, as well as **swordfish size and trophic position** in the case of **Hg**.

• Results showed **signs of co-accumulation** potential **between Hg and Se** in swordfish.

• The identification of **different regional patterns** in Hg and Se concentrations and in stable isotope values **despite swordfish being highly-migratory** suggests that **swordfish may be resident at the scale of their muscle tissue turnover rate**.

7. Chapter 5 – Trace element bioaccumulation in tropical pelagic systems: local variation in swordfish from the Seychelles Economic Exclusive Zone (EEZ)

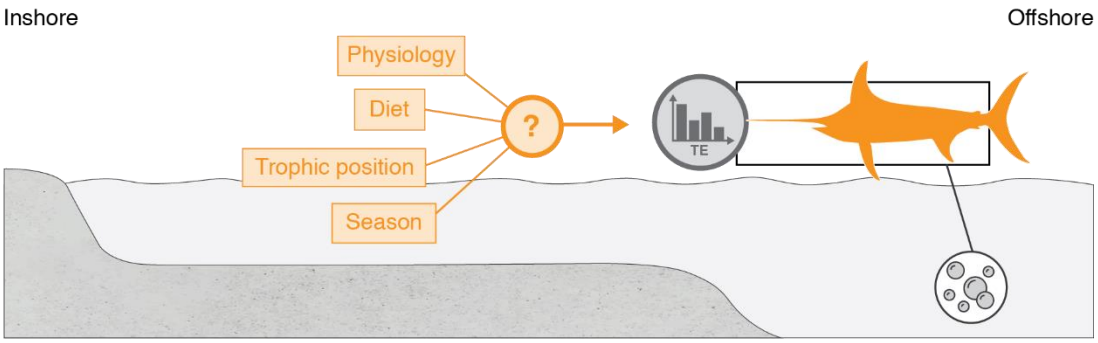

Content

7.1. CONTEXT AND OBJECTIVES

As mentioned in Chapter 4, data on trace element bioaccumulation in swordfish from the Indian Ocean is scarce, and mostly related to Hg only (Kojadinovic *et al.* 2006; Jinadasa *et al.* 2014; Esposito *et al.* 2018). However, the chapter 4 showed the importance of considering the geographical origin of individuals, as well as local dynamics in trophic ecology and trace element bioavailability, especially when one aims at studying trace element bioaccumulation in swordfish at large scale. It is thus necessary to have more information at the local scale to improve global comprehension of trace element bioaccumulation in migratory species like the swordfish.

In the Seychelles, previous works reported trace element concentrations in swordfish muscle tissue (Bodin *et al*. 2017; Hollanda *et al*. 2017), but the factors controlling trace element bioaccumulation in swordfish from this area of the Indian Ocean are still poorly understood. It is expected that the size, physiology (i.e. physiological needs and detoxification processes) and trophic ecology (i.e. trophic position, feeding depth, diet composition) influence trace element bioaccumulation in swordfish, as it was shown in other areas and/or other species (e.g. Kojadinovic *et al.* 2006, 2007; Chouvelon *et al.* 2012, 2017, 2018; Houssard *et al*. 2019; section 1.2). Reproduction dynamics may also have an influence. In the Western Indian Ocean, Poisson and Fauvel (2009) identified seasonal migratory patterns in swordfish movements linked to seasonal reproduction. Such changes in feeding location may seasonally influence trophic ecology and may induce variations in trace element bioavailability in the local environment.

In this chapter, I investigated the effects of size (using lower jaw-fork length), feeding habitat and depth (using $\delta^{13}C$ values), trophic position (using $\delta^{15}N$ values) and diet (using fatty acid profiles) on trace element bioaccumulation in swordfish. Seasonal variations in trace element concentrations were also examined to give insight into a potential effect of reproductive dynamics and migrations. Finally, as sex can influence physiological needs, which are expected to have some level of influence here, its effect on trace element bioaccumulation in swordfish was also tested.

7.2. METHODOLOGY

7.2.1. Dataset

Swordfish were captured in the Seychelles EEZ, around the Mahé Plateau and offshore the Amirantes islands group (Fig. 7.1).

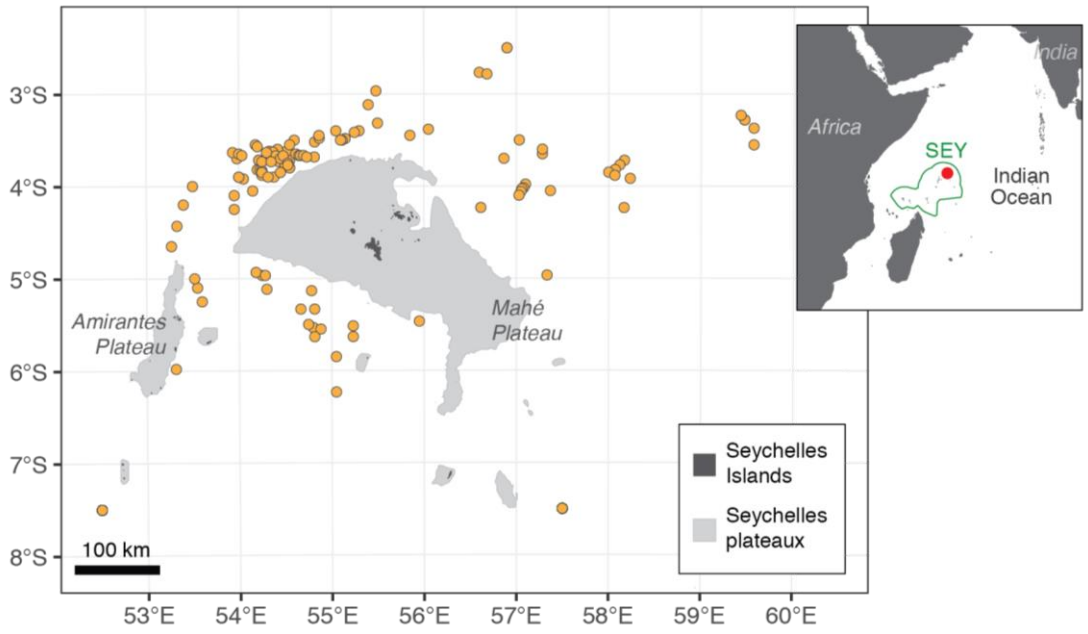

Fig. 7.1. Fishing locations of swordfish caught around the Amirantes Plateau and the Mahé Plateau in the Seychelles economic exclusive zone (EEZ). Red point indicates the location of the Mahé Plateau within the Seychelles EEZ. SEY = Seychelles.

For this chapter, the bioaccumulation of As, Cd, Co, Cu, Fe, Hg, Mn, Pb, Se and Zn (i.e. DF > 70%; Appendix 2.1) was investigated. $\delta^{13}C$ and $\delta^{15}N$ values and fatty acid proportions were used to link trace element bioaccumulation to habitat use and foraging patterns. In order to characterise ontogenetic changes in trophic ecology, all samples analysed for stable isotopes and for which sex was identified (n = 106; 29 males and 77 females) were used. To identify potential variations in diet, all samples analysed for FAs (n = 55) were used. As individuals for which the sex was determined and for which trace elements, stable isotopes and fatty acids were analysed were necessary to characterise trace element bioaccumulation, 48 samples were used for modelling (i.e. 24 males and 24 females; 4 for pre-NWM, 28 for NWM and 8 for pre-SEM and SEM seasons).

7.2.2. Standardisation of trace element concentrations according to swordfish lower jaw-fork length

In order to remove the size effect in subsequent analyses, trace element concentrations were standardised according to swordfish lower jaw-fork length. First, correlations were tested between trace element concentrations and lower jaw-fork length in order to identify the trace elements for which bioaccumulation was influenced, even weakly, by swordfish size. Correlations results are presented in Appendix 7.1. For each trace element for which the correlation was significant, concentrations were standardised by size. For Hg, the same method applied in Chapter 4 (section 6.2.2) was used here to normalise concentrations. For the other trace elements, a linear model was first applied to identify the nature of the relationship (i.e. linear or non-linear). For each linear relationship, a simple linear regression (i.e. form log(trace element) = a * lower jaw-fork length + b) was used. For each non-linear relationship, the same method as for Hg was used. Fitted relationships are presented in Appendix 7.2.

7.2.3. Modelling the relationship between trace element concentrations and size, stable isotope ratios, sex, dietary patterns and season

Generalised additive models (GAM) were used to model the relationship between log-transformed trace element concentrations and swordfish size (through the use of lower jaw-fork length), sex, trophic ecology (through the use of $\delta^{13}C$, $\delta^{15}N$ and fatty acids) and sampling season. As the number of fatty acids with proportions > 0.8% TFA was relatively high (n = 14) and the number of potential fatty acid trophic markers was also high (n = 12), it was not possible to include all of them in the GAM as explanatory variables. Thus, samples were grouped according to measured fatty acid profiles (see section 7.2.4) to create fatty acid trophic groups, which were used as categorical explaining variables.

Lower jaw-fork length and $\delta^{13}C$ and $\delta^{15}N$ values were sometimes significantly different among levels of the same categorical variable (Appendices 7.3 and 7.4), thus associated interactions terms were added to the complete model for each trace element. Correlations were tested between swordfish lower jaw-fork length and stable isotope values in order to characterise their relationship using Pearson and Kendall tests. Among the 48 samples used in this chapter, neither $\delta^{13}C$ nor $\delta^{15}N$ values were significantly correlated with swordfish lower jaw-fork length. However, when using all available samples with measured stable isotope values (n = 106), $\delta^{15}N$ values were positively correlated with lower jaw-fork length, with a non-linear

relationship. As individual size is known to influence its trophic position (i.e. $\delta^{15}N$ values) (Jennings *et al*. 2002), the interaction term between length and $\delta^{15}N$ values was added. Finally, seasonal variations in primary production are known to influence the structure of the associated food webs (McMeans *et al*. 2015), thus it would have been better to add the interaction term between fatty acid trophic groups and season. However, due to a small number of samples in each level (e.g. no individual of fatty acid trophic group 2 sampled during the pre-SEM season), it was not possible to include this interaction factor in the models.

The general forms of the complete models performed for each trace element were thus:

- Log(trace element) ~ lower jaw-fork length + $\delta^{13}C$ + $\delta^{15}N$ + sex + fatty acid trophic group + season + sex:lower jaw-fork length + fatty acid trophic group:lower jaw-fork length + season:lower jaw-fork length + season:$\delta^{13}C$ + season:$\delta^{15}N$ + $\delta^{15}N$:lower jaw-fork length
- Log(length-standardised trace element) ~ $\delta^{13}C$ + $\delta^{15}N$ + sex + fatty acid trophic group + season + season:$\delta^{13}C$ + season:$\delta^{15}N$

For each model, the explained deviance was calculated with the following equation:

Explained deviance = ((Null model deviance – final model residual deviance)/Null model deviance) x 100 **(Eq. 8.1)**

with the null model only containing the intercept terms (Méndez-Fernandez *et al.* 2013).

Correlations between swordfish lower jaw-fork length and stable isotope values were also tested on all samples analysed for stable isotopes (n = 106), independently for each sex using Pearson and Kendall tests (section 7.3.2). Although the relationship between swordfish size and $\delta^{13}C$ values was non-significant for both sexes, there was a significant positive relationship between swordfish size and $\delta^{15}N$ values, with different trends between males and females. Thus, for each selected model explaining log-transformed trace element concentrations, the interaction term between sex, lower jaw-fork length and $\delta^{15}N$ values was added to see if it improved the models.

7.2.4. Identification of dietary patterns among swordfish individuals

In order to identify different foraging patterns among swordfish individuals, samples were grouped according to their fatty acid profiles (i.e. all fatty acids > 0.8% TFA) using Ward's hierarchical clustering method. Inferred fatty acid trophic groups were then compared qualitatively by computing the associated fatty acid trophic niche ellipses. $\delta^{13}C$ and $\delta^{15}N$ values

and lower jaw-fork length were also compared between inferred fatty acid trophic groups using t-tests or Wilcoxon tests (Appendices 7.3 and 7.4) in order to complete trophic ecology analyses.

7.2.5. Fatty acid trophic marker selection and identification for the inference of dietary patterns

Well-known fatty acid trophic markers were used to help identify the different foraging patterns of sampled swordfish associated with identified fatty acid trophic groups. This included trophic markers of diatoms (i.e. 14:0, 16:1n-7, 18:1n-7, 22:5n-3), phytoplankton in general (i.e. 20:4n-6, 20:5n-3, 22:6n-3), mesopelagic prey (i.e. 18:0, 18:1n-9, 22:5n-3, 22:5n-6) and copepod and secondary consumption of zooplankton (i.e. 20:1n-9) (Dalsgaard *et al.* 2003; Meyer *et al*. 2019). As some FAs can be trophic markers of several types of prey, correlations were tested among trophic tracers (i.e. stable isotope values and fatty acid proportions) to discriminate between possible prey of origin for each fatty acid trophic marker. Correlation results are presented in Appendix 7.5.

7.2.6. Characterising the relationship between stable isotopes and swordfish size and effect of sex on these relationships

Correlations between stable isotope values and swordfish lower jaw-fork length were tested using Pearson or Kendall tests, in order to characterise ontogenetic changes in habitat use and trophic position. In addition, there is a well-known sexual dimorphism among swordfish, with females growing faster than males after 3 years of age (Govender *et al.* 2003). Thus, correlations were also tested on males and females separately to identify potential differences in ontogenetic changes between males and females.

7.3. RESULTS

7.3.1. Fatty acid trophic groups

Two groups were inferred from swordfish fatty acid profiles (Fig. 7.2A). Group 1 tended to be separated from Group 2 by positive anomalies of 18:0, 18:1n-9, 20:1n-9 and 24:1n-9, while Group 2 tended to be separated from Group 1 by positive anomalies of 14:0, 16:1n-7, 20:4n-6, 20:5n-3, 22:5n-6 and 22:6n-3 (Fig. 7.2B).

There was no significant difference ($p > 0.05$) in $\delta^{13}C$ values (-16.8 ± 0.6 ‰ for Group 1 *vs* -16.6 ± 0.6 ‰ for Group 2) and in $\delta^{15}N$ values (14.1 ± 0.4 ‰ for Group 1 *vs* 14.1 ± 0.5 ‰ for Group 2). Individuals from Group 1 were larger than individuals from Group 2 (175 ± 26 cm vs 161 ± 25 cm; t-test, p = 0.030, t = 2.2).

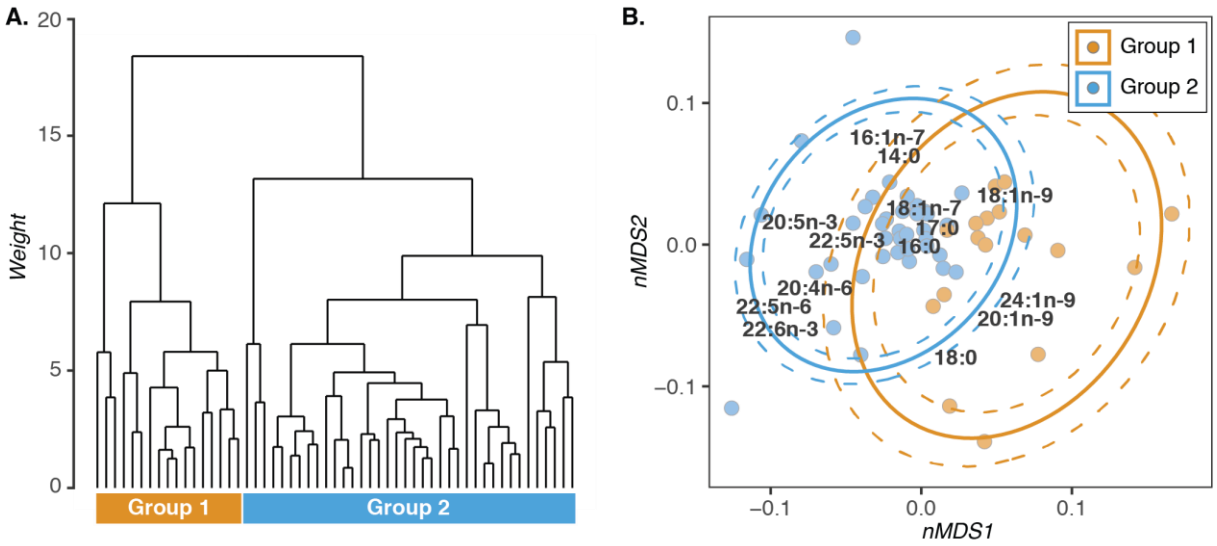

Fig. 7.2. Groups inferred from fatty acid proportions in white muscle tissues of swordfish using only fatty acids > 0.8 % TFA (A) and FA niches of each determined trophic group (B). For each group, the mean ellipse is represented by a plain line and uncertainty ellipses are represented by dashed lines (B).

7.3.2. Relationship between stable isotope values and swordfish size

The relationship between lower jaw-fork length and $\delta^{13}C$ values in swordfish was non-significant, even for males and females separately (Fig. 7.3). However, there was a significant positive correlation between swordfish lower jaw-fork length and their muscle $\delta^{15}N$ values, including for males and females separately (Fig. 7.3). For males, the relationship was non-linear, while it was linear for females.

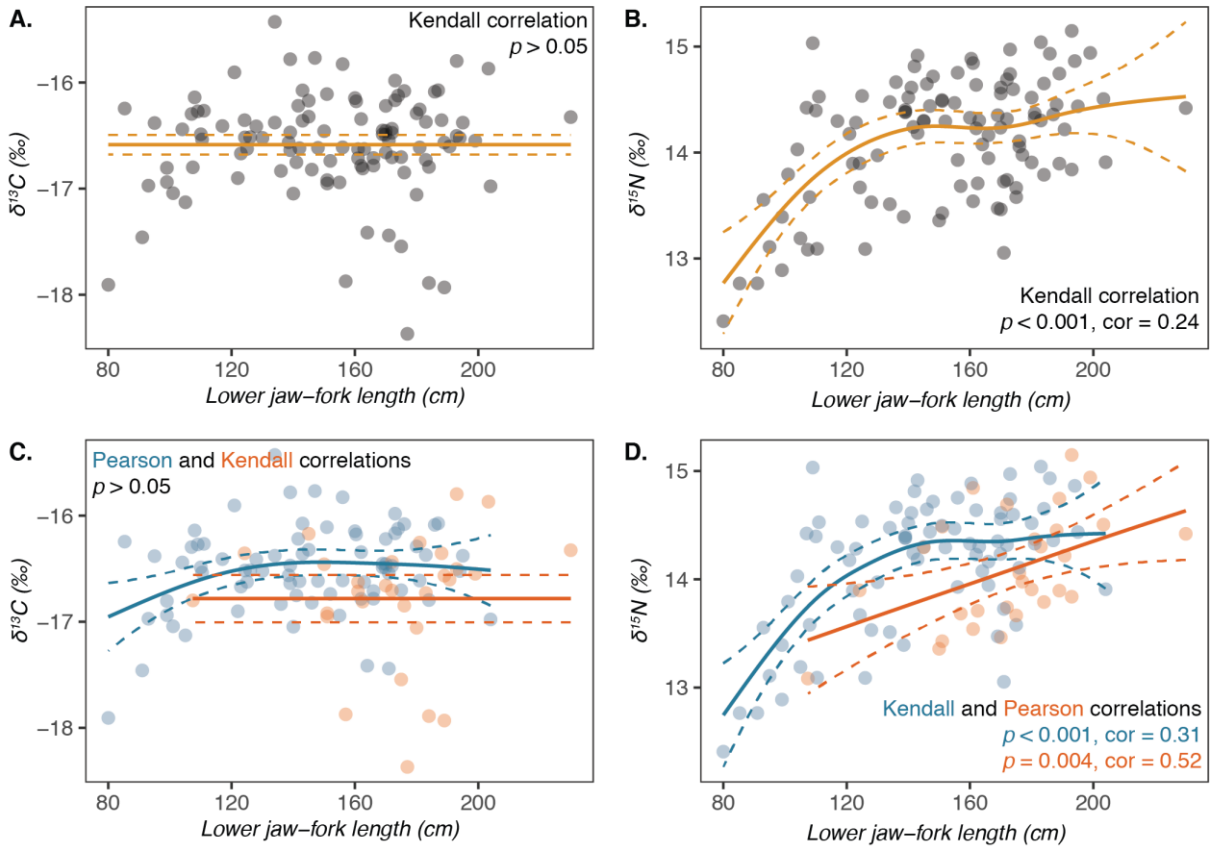

Fig. 7.3. Relationships between lower jaw-fork length (cm) and C and N stable isotope values (‰), for males and females together (A, B) and separately (C, D). Smoothing curves were fitted using the GLM method for linear relationships and the GAM method for the non-linear relationships under R software. Dotted curves represent the confidence interval at 95% around the fit.

7.3.3. Contribution of physiological parameters, trophic ecology and season in explaining trace element bioaccumulation

For each trace element, selected final models for log-transformed concentrations and log-transformed length-standardised concentrations are presented in Table 7.1.

Table 7.1. Explanatory variables used in the selected generalised additive models (GAM) (i.e. with the lowest AIC) and deviance explained by each model. GAMs were fitted on log-transformed concentrations of each trace element. For trace elements for which concentrations were correlated with lower jaw-fork length, GAMs were also fitted on log-transformed length-standardised concentrations. FA = fatty acid.

Trace element	Response variable	Explanatory variable included in the best selected model	*p* value	Model deviance explained (%)
As	log(As)	lower jaw-fork length	< 0.001	74.5
		FA trophic group	< 0.001	
		season	0.002	
		sex:lower jaw-fork length	0.495	
		season:lower jaw-fork length	0.011	
	log(length stand. As)	FA trophic group	< 0.001	34.4
		season	0.007	
Cd	log(Cd)	sex	0.100	61.9
		FA trophic group	< 0.001	
		sex:lower jaw-fork length	0.006	
		season:lower jaw-fork length	0.720	
		season:$\delta^{15}N$	0.002	
	log(length stand. Cd)	FA trophic group	0.002	38.0
		season	0.979	
		season:$\delta^{15}N$	0.026	
Co	log(Co)	$\delta^{15}N$	< 0.001	97.4
		season	< 0.001	
		sex:lower jaw-fork length	0.001	
		season:lower jaw-fork length	< 0.001	
		season:$\delta^{13}C$	0.673	
		season:$\delta^{15}N$	< 0.001	
	log(length stand. Co)	$\delta^{15}N$	0.007	90.7
		season:$\delta^{13}C$	0.008	
Cu	log(Cu)	lower jaw-fork length	0.079	49.1
		season	0.001	
		$\delta^{15}N$:lower jaw-fork length	0.063	
	log(length stand. Cu)	$\delta^{15}N$	0.005	36.8
		Season	0.004	
Fe	log(Fe)	FA trophic group	0.083	52.3
		season	0.807	
		sex:lower jaw-fork length	0.042	
		FA trophic group:lower jaw-fork length	0.054	
		season:$\delta^{13}C$	0.040	
		season:$\delta^{15}N$	0.100	
Hg	log(Hg)	sex	0.205	30.1
		FA trophic group:lower jaw-fork length	< 0.001	
	log(length stand. Hg)	sex	0.023	17.9
		FA trophic group	0.045	
Mn	log(Mn)	lower jaw-fork length	0.002	71.1
		sex	0.057	
		FA trophic group	0.012	
		season	0.189	
		sex:lower jaw-fork length	< 0.001	
		season:$\delta^{13}C$	0.002	
		season:$\delta^{15}N$	0.184	
		$\delta^{15}N$:lower jaw-fork length	0.161	

Table 7.1. Explanatory variables used in the selected generalised additive models (GAM) (i.e. with the lowest AIC) and deviance explained by each model. GAMs were fitted on log-transformed concentrations of each trace element. For trace elements for which concentrations were correlated with lower jaw-fork length, GAMs were also fitted on log-transformed length-standardised concentrations. FA = fatty acid. (continued)

Trace element	Response variable	Explanatory variable included in the best selected model	*p* value	Model deviance explained (%)
Mn	log(length stand. Mn)	FA trophic group	0.117	52.9
		$\delta^{15}N$	0.199	
		season	< 0.001	
		season:$\delta^{13}C$	0.008	
		season:$\delta^{15}N$	0.669	
Pb	log(Pb)	FA trophic group:lower jaw-fork length	0.144	66.1
		season:lower jaw-fork length	< 0.001	
		season:$\delta^{13}C$	0.034	
		season:$\delta^{15}N$	0.020	
		$\delta^{15}N$:lower jaw-fork length	0.055	
Se	log(Se)	FA trophic group	0.585	47.6
		$\delta^{13}C$	0.127	
		season	0.066	
		sex:lower jaw-fork length	0.308	
		FA trophic group:lower jaw-fork length	0.004	
		season:$\delta^{13}C$	0.006	
	log(length stand. Se)	FA trophic group	0.317	28.9
		season:$\delta^{13}C$	0.142	
		season:$\delta^{15}N$	0.157	
Zn	log(Zn)	FA trophic group	0.166	55.8
		$\delta^{13}C$	0.535	
		$\delta^{15}N$	0.588	
		FA trophic group:lower jaw-fork length	0.031	
		season:lower jaw-fork length	0.054	
		season:$\delta^{13}C$	0.069	
		season:$\delta^{15}N$	0.166	
	log(length stand. Zn)	$\delta^{13}C$	0.791	16.2
		season:$\delta^{13}C$	0.345	

In the selected models, As concentrations decreased with increasing lower jaw-fork length (Fig. 7.4A). As concentrations were significantly lower in fatty acid trophic Group 2 than in Group 1 (GAM, $p < 0.001$) and were significantly higher during the pre-NWM season than during the other three seasons (GAM, $p = 0.002$ with NWM, $p = 0.003$ with pre-SEM and $p < 0.001$ with SEM) (Fig. 7.4A). Length-standardised As concentrations were also significantly lower in fatty acid trophic Group 2 than in Group 1 (GAM, $p < 0.001$) (Fig. 7.4B). Length-standardised As concentrations were significantly lower during the pre-SEM and SEM seasons compared to the pre-NWM season (GAM, $p = 0.009$ for pre-SEM, $p = 0.012$ for SEM) and seemed lower than during the NWM season (Fig. 7.4B).

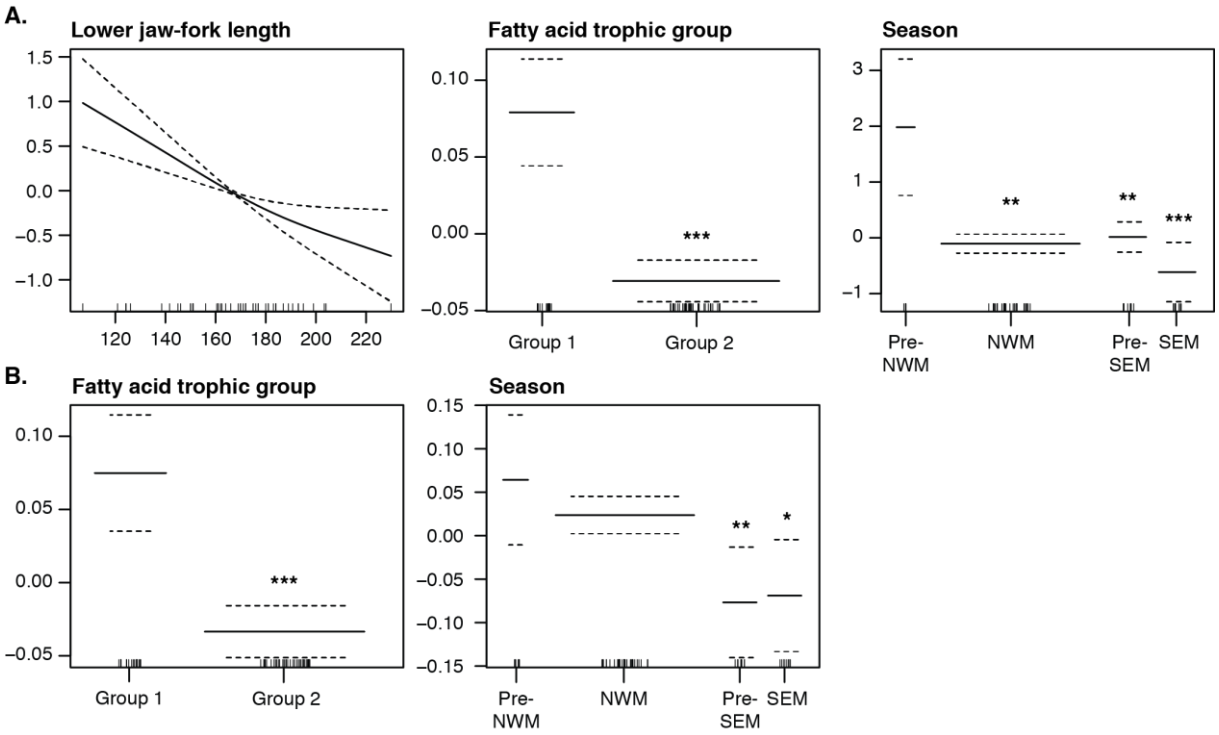

Fig. 7.4. Graphical results of the generalised additive models (GAM) fitted to log-transformed As concentrations (A) and log-transformed length-standardised As concentrations (B) in white muscle of swordfish to identify explanatory variable-related trends in explaining trace element concentration variability. Smoothers illustrate the partial effect of continuous explanatory variables once the effects of all the other explanatory variables included in the model have been considered. For categorical variables, the model also calculates the effect once the effects of all other explanatory variables have been considered; the effect of each category within a factor is calculated to a reference category, which corresponds to the first category for each factor (i.e. the category to the far left). The y-axis shows the contribution of the smoother or of the category to the predictor function in the model (in arbitrary units). Dashed lines represent the 95% confidence intervals. Whiskers on the x-axis indicate data presence. Significant difference: * = $p < 0.05$, ** = $p < 0.01$, *** = $p < 0.001$. NWM = Northwest Monsoon, SEM = Southeast Monsoon.

Cd concentrations tended to be higher in female swordfish than in male swordfish, and they were significantly lower in fatty acid trophic Group 2 than in Group 1 (GAM, $p = 0.002$) (Fig. 7.5A). Length-standardised Cd concentrations were also significantly lower in fatty acid trophic Group 2 than in Group 1 (GAM, $p = 0.005$), and they tended to be lower during the SEM season than during the NWM and pre-SEM seasons (Fig. 7.5B).

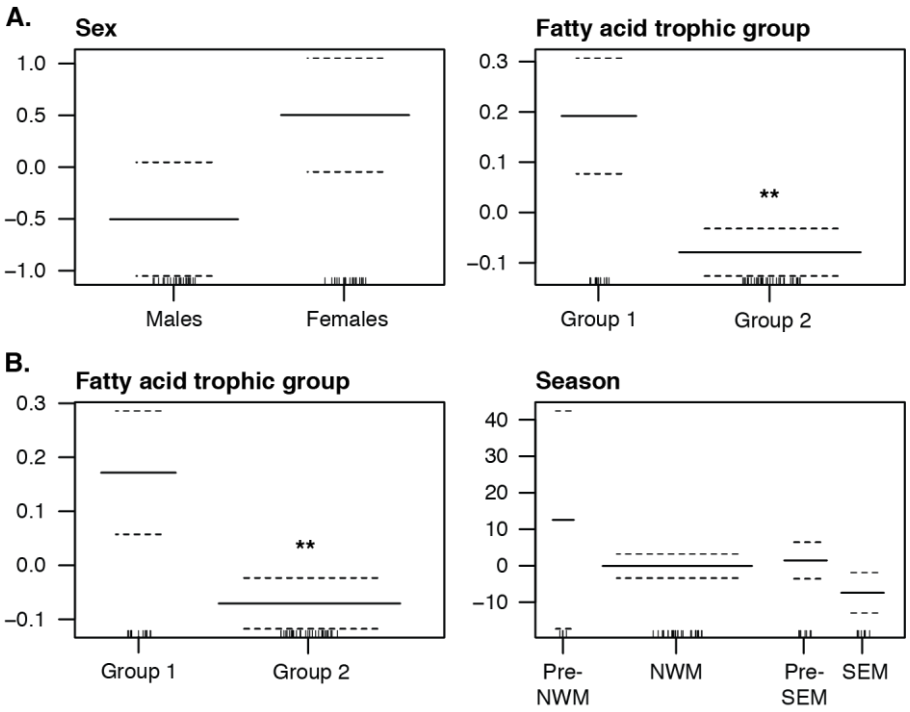

Fig. 7.5. Graphical results of the generalised additive models (GAM) fitted to log-transformed Cd concentrations (A) and log-transformed length-standardised Cd concentrations (B) in white muscle of swordfish to identify explanatory variable-related trends in explaining trace element concentration variability. Plots illustrate the partial effect of categorical explanatory variables once the effects of all the other explanatory variables included in the model have been considered. The effect of each category within a factor is calculated to a reference category, which corresponds to the first category for each factor (i.e. the category to the far left). The y-axis shows the contribution of the smoother or of the category to the predictor function in the model (in arbitrary units). Dashed lines represent the 95% confidence intervals. Whiskers on the x-axis indicate data presence. Significant difference: * = $p < 0.05$, ** = $p < 0.01$, *** = $p < 0.001$. NWM = Northwest Monsoon, SEM = Southeast Monsoon.

Co concentrations were significantly lower during the pre-SEM season than during the pre-NWM season (GAM, $p = 0.009$), and also seemed lower than during the NWM and SEM seasons (Fig 7.6A).

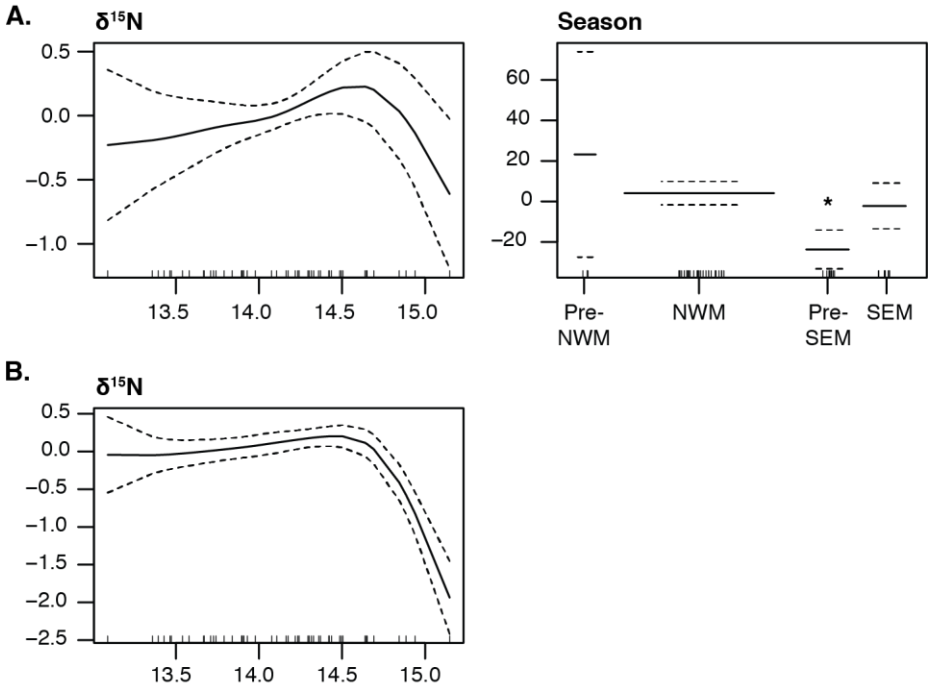

Fig. 7.6. Graphical results of the generalised additive models (GAM) fitted to log-transformed Co concentrations (A) and log-transformed length-standardised Co concentrations (B) in white muscle of swordfish to identify explanatory variable-related trends in explaining trace element concentration variability. Smoothers illustrate the partial effect of continuous explanatory variables once the effects of all the other explanatory variables included in the model have been considered. For categorical variables, the model also calculates the effect once the effects of all other explanatory variables have been considered; the effect of each category within a factor is calculated to a reference category, which corresponds to the first category for each factor (i.e. the category to the far left). The y-axis shows the contribution of the smoother or of the category to the predictor function in the model (in arbitrary units). Dashed lines represent the 95% confidence intervals. Whiskers on the x-axis indicate data presence. Significant difference: * = $p < 0.05$. NWM = Northwest Monsoon, SEM = Southeast Monsoon.

Cu concentrations decreased with increasing lower jaw-fork length, and they seemed lower during the two monsoon seasons (i.e. NWM and SEM) than during the two inter-monsoon seasons (i.e. pre-NWM and pre-SEM) (Fig. 7.7A). Length-standardised Cu concentrations tended to increase with increasing $\delta^{15}N$ values, and they seemed higher during the pre-SEM season than during the other three seasons (Fig. 7.7B).

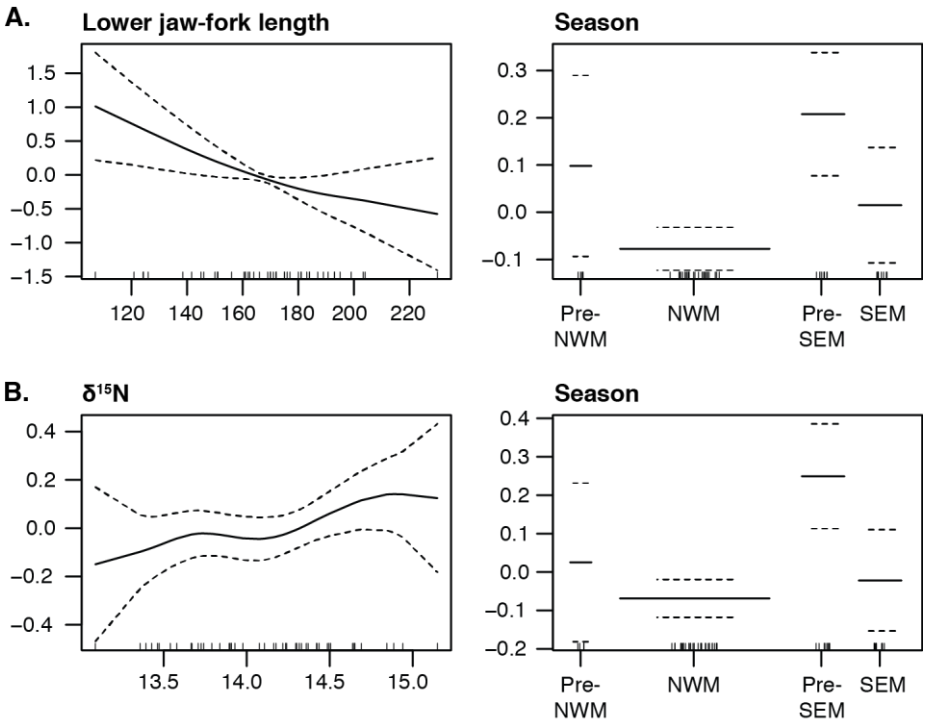

Fig. 7.7. Graphical results of the generalised additive models (GAM) fitted to log-transformed Cu concentrations (A) and log-transformed length-standardised Cu concentrations (B) in white muscle of swordfish to identify explanatory variable-related trends in explaining trace element concentration variability. Smoothers illustrate the partial effect of continuous explanatory variables once the effects of all the other explanatory variables included in the model have been considered. For categorical variables, the model also calculates the effect once the effects of all other explanatory variables have been considered; the effect of each category within a factor is calculated to a reference category, which corresponds to the first category for each factor (i.e. the category to the far left). The y-axis shows the contribution of the smoother or of the category to the predictor function in the model (in arbitrary units). Dashed lines represent the 95% confidence intervals. Whiskers on the x-axis indicate data presence. NWM = Northwest Monsoon, SEM = Southeast Monsoon.

Although differences were not significant, Fe concentrations seemed higher in fatty acid trophic Group 2 than in Group 1 and seemed lower during the SEM season than during the NWM and pre-SEM seasons (Fig. 7.8).

Again, although not significantly different, both Hg and length-standardised Hg concentrations seemed to be lower in female swordfish than in males (Fig. 7.9A, B). Length-standardised Hg concentrations also seemed lower in fatty acid trophic group 2 than in group 1 (Fig. 7.9B).

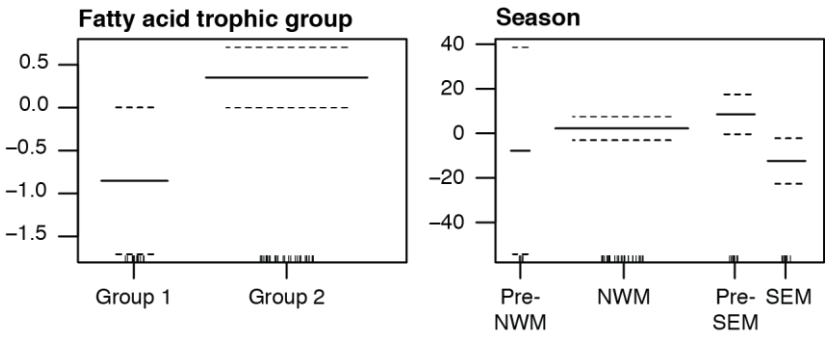

Fig. 7.8. Graphical results of the generalised additive models (GAM) fitted to log-transformed Fe concentrations in white muscle of swordfish to identify explanatory variable-related trends in explaining trace element concentration variability. Plots illustrate the partial effect of categorical explanatory variables once the effects of all the other explanatory variables included in the model have been considered. The effect of each category within a factor is calculated to a reference category, which corresponds to the first category for each factor (i.e. the category to the far left). The y-axis shows the contribution of the smoother or of the category to the predictor function in the model (in arbitrary units). Dashed lines represent the 95% confidence intervals. Whiskers on the x-axis indicate data presence. NWM = Northwest Monsoon, SEM = Southeast Monsoon.

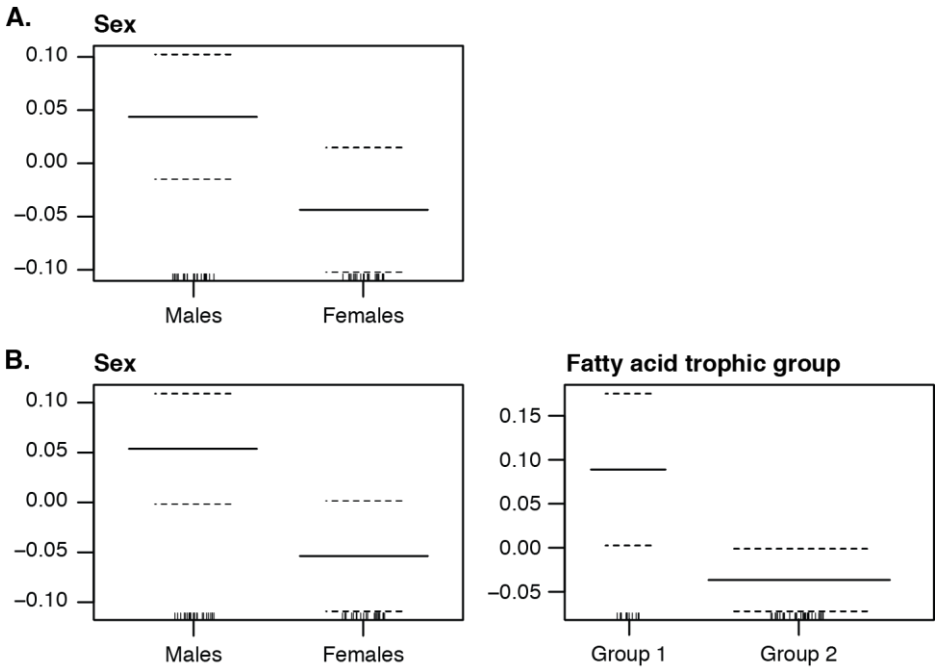

Fig. 7.9. Graphical results of the generalised additive models (GAM) fitted to log-transformed Hg concentrations (A) and log-transformed length-standardised Hg concentrations (B) in white muscle of swordfish to identify explanatory variable-related trends in explaining trace element concentration variability. Plots illustrate the partial effect of categorical explanatory variables once the effects of all the other explanatory variables included in the model have been considered. The effect of each category within a factor is calculated to a reference category, which corresponds to the first category for each factor (i.e. the category to the far left). The y-axis shows the contribution of the smoother or of the category to the predictor function in the model (in arbitrary units). Dashed lines represent the 95% confidence intervals. Whiskers on the x-axis indicate data presence.

Mn concentrations in swordfish white muscle tissues decreased with increasing lower jaw-fork length (Fig. 7.10A). They were significantly higher in female swordfish than in males (GAM, p = 0.033), and seemed higher in fatty acid trophic 1 than in group 2 (Fig. 7.10A). Mn concentrations seemed to be lower during the SEM season than during the NWM and pre-SEM seasons (Fig. 7.10A). Length-standardised Mn concentrations seemed to increase with increasing $\delta^{15}N$ values (Fig. 7.10B). They seemed lower in fatty acid trophic group 2 than in group 1, and during the SEM season compared to the NWM and pre-SEM seasons (Fig. 7.10B).

Se concentrations decreased with increasing $\delta^{13}C$ values (Fig. 7.11A). They were significantly higher in fatty acid trophic 2 than in group 1 (GAM, p = 0.032), and seemed higher during the pre-SEM and SEM seasons than during the NWM season (Fig. 7.11A). Length-standardised Se concentrations seemed lower in fatty acid trophic group 2 than in group 1 (Fig. 7.11B).

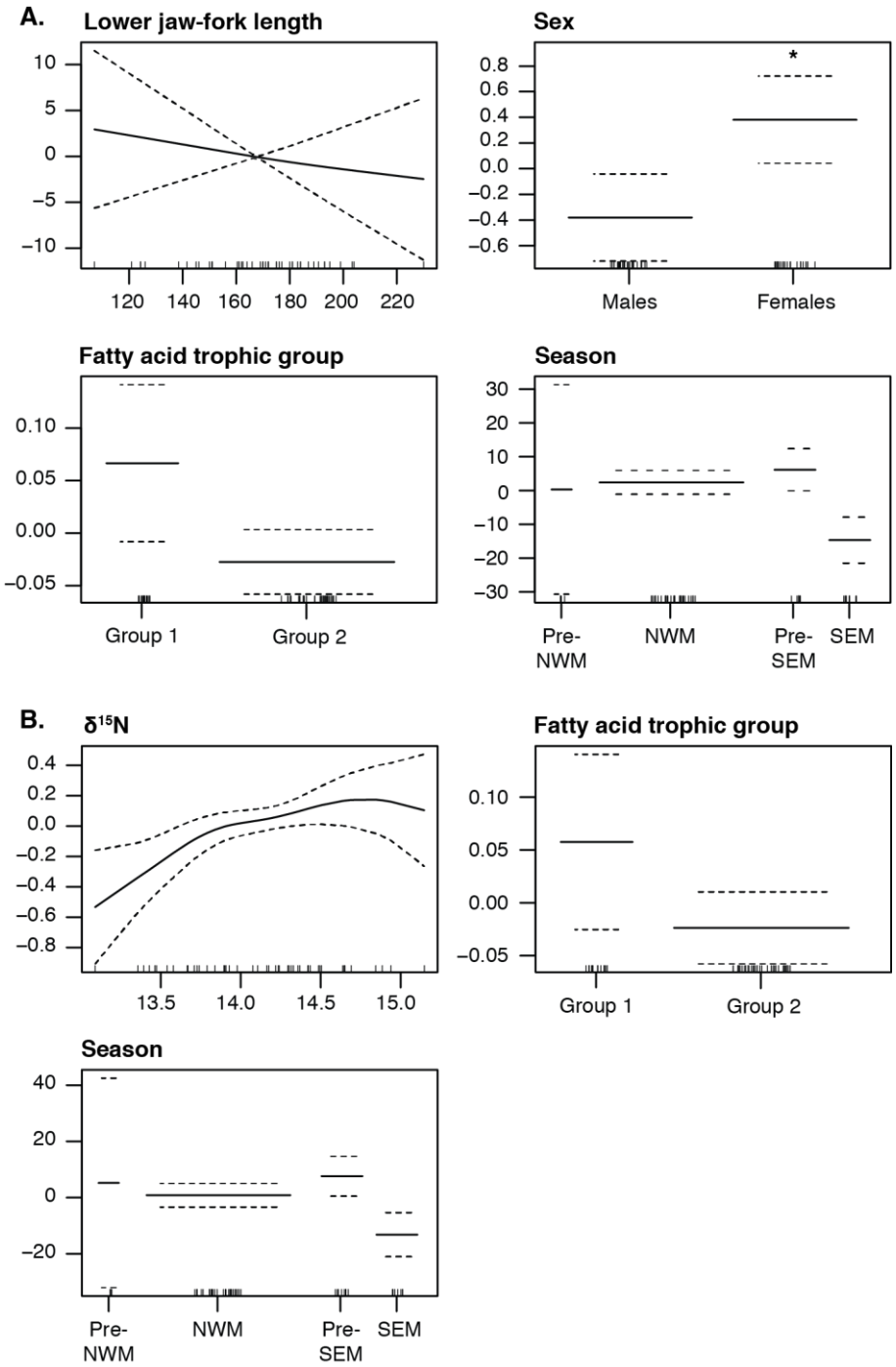

Fig. 7.10. Graphical results of the generalised additive models (GAM) fitted to log-transformed Mn concentrations (A) and log-transformed length-standardised Mn concentrations (B) in white muscle of swordfish to identify explanatory variable-related trends in explaining trace element concentration variability. Smoothers illustrate the partial effect of continuous explanatory variables once the effects of all the other explanatory variables included in the model have been considered. For categorical variables, the model also calculates the effect once the effects of all other explanatory variables have been considered; the effect of each category within a factor is calculated to a reference category, which corresponds to the first category for each factor (i.e. the category to the far left). The y-axis shows the contribution of the smoother or of the category to the predictor function in the model (in arbitrary units). Dashed lines represent the 95% confidence intervals. Whiskers on the x-axis indicate data presence. Significant difference: * = $p < 0.05$. NWM = Northwest Monsoon, SEM = Southeast Monsoon.

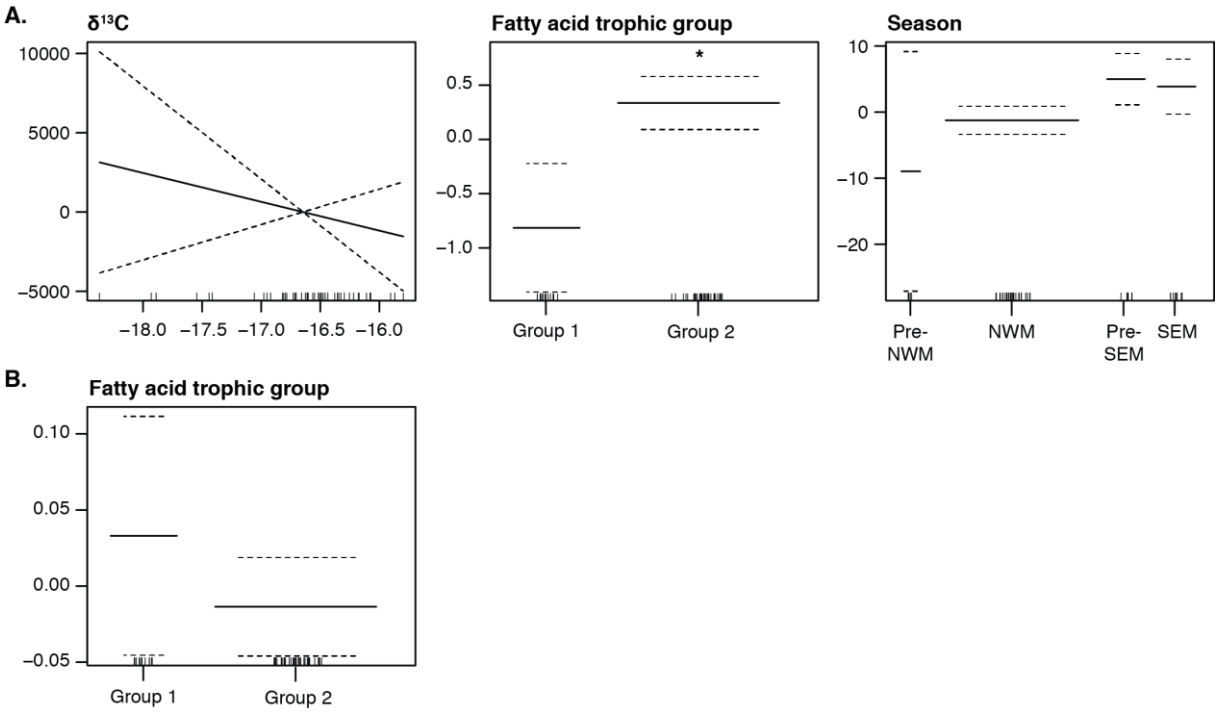

Fig. 7.11. Graphical results of the generalised additive models (GAM) fitted to log-transformed Se concentrations (A) and log-transformed length-standardised Se concentrations (B) in white muscle of swordfish to identify explanatory variable-related trends in explaining trace element concentration variability. Smoothers illustrate the partial effect of continuous explanatory variables once the effects of all the other explanatory variables included in the model have been considered. For categorical variables, the model also calculates the effect once the effects of all other explanatory variables have been considered; the effect of each category within a factor is calculated to a reference category, which corresponds to the first category for each factor (i.e. the category to the far left). The y-axis shows the contribution of the smoother or of the category to the predictor function in the model (in arbitrary units). Dashed lines represent the 95% confidence intervals. Whiskers on the x-axis indicate data presence. Significant difference: * = $p < 0.05$. NWM = Northwest Monsoon, SEM = Southeast Monsoon.

Zn concentrations increased slightly with increasing $\delta^{13}C$ values (Fig. 7.12A). They also increased with increasing $\delta^{15}N$ values to a $\delta^{15}N$ value of around 14.5 ‰ before being constant (Fig. 7.12A). Zn concentrations were significantly in fatty acid trophic group 2 than in group 1 (GAM, $p = 0.004$) (Fig. 7.12A). Length-standardised Zn concentrations decreased slightly with increasing $\delta^{13}C$ values (Fig. 7.12B).

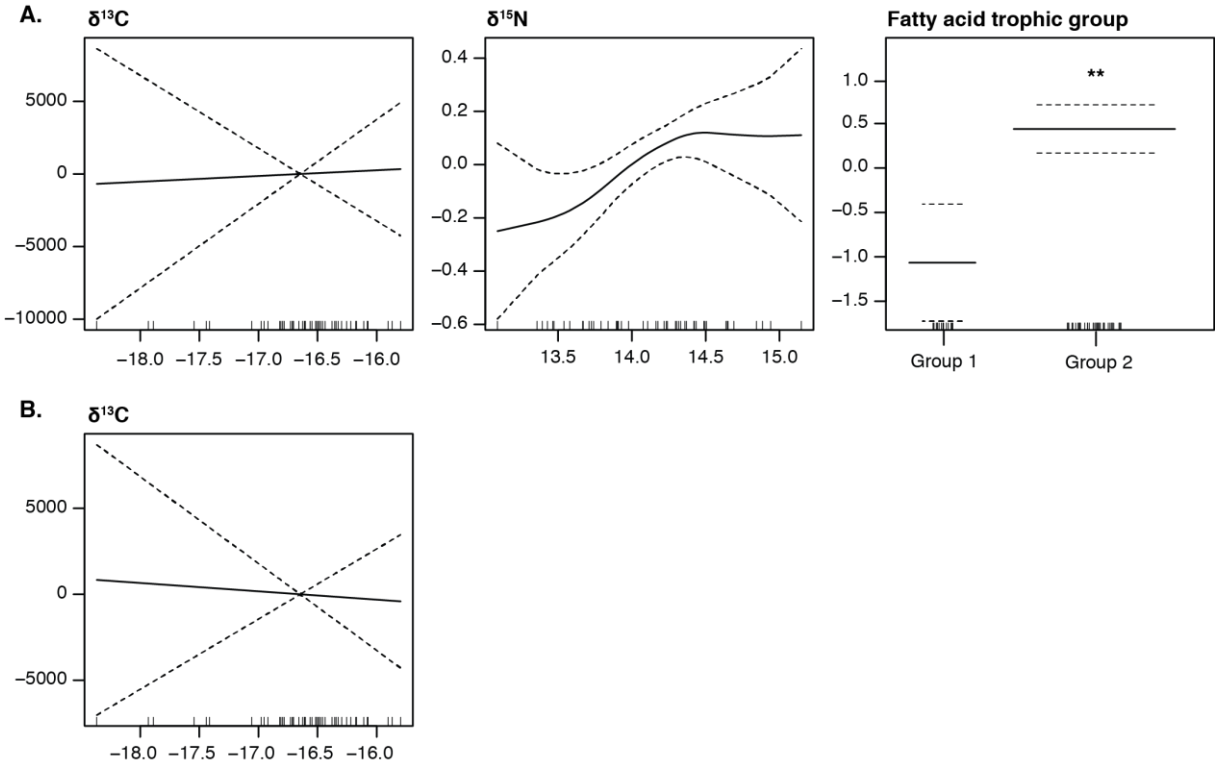

Fig. 7.12. Graphical results of the generalised additive models (GAM) fitted to log-transformed Zn concentrations (A) and log-transformed length-standardised Zn concentrations (B) in white muscle of swordfish to identify explanatory variable-related trends in explaining trace element concentration variability. Smoothers illustrate the partial effect of continuous explanatory variables once the effects of all the other explanatory variables included in the model have been considered. For categorical variables, the model also calculates the effect once the effects of all other explanatory variables have been considered; the effect of each category within a factor is calculated to a reference category, which corresponds to the first category for each factor (i.e. the category to the far left). Significant difference between the reference category and the other categories of the factor is indicated by asterisks. The y-axis shows the contribution of the smoother or of the category to the predictor function in the model (in arbitrary units). Dashed lines represent the 95% confidence intervals. Whiskers on the x-axis indicate data presence. Significant difference: ** = $p < 0.01$.

Adding the interaction terms between sex, lower jaw-fork length and stable isotope values did not improve any of the selected models presented in Table 7.1, as the calculated AICs were either higher or indicated that the best selected models were the most parsimonious (Table 7.2).

Table 7.2. Effect of adding the interaction terms between sex, lower jaw-fork length and $\delta^{13}C$ and/or $\delta^{15}N$ values in the selected generalised additive models (GAM) presented in Table 7.1. The term "best selected model" refers to the variables in the models presented in Table 7.1. For each response variable, the best model (i.e. with the lowest AIC) is indicated in bold. FA = fatty acid.

Response variable	Tested model	Model deviance explained (%)	AIC	Explaining variable	*p* value
log(As)	**~ best selected model**	**74.5**	**-115.4**	-	-
	~ best selected model + sex:$\delta^{15}N$:lower jaw-fork length	77.1	-112.2	lower jaw-fork length	0.030
				FA trophic group	< 0.001
				season	< 0.001
				sex:lower jaw-fork length	0.055
				season:lower jaw-fork length	0.004
				sex:$\delta^{15}N$:lower jaw-fork length	*0.467*
log(Cd)	**~ best selected model**	**61.9**	**1.5**	-	-
	~ best selected model + sex:$\delta^{15}N$:lower jaw-fork length	63.1	3.9	sex	0.010
				FA trophic group	0.003
				sex:lower jaw-fork length	0.723
				season:lower jaw-fork length	0.736
				season:$\delta^{15}N$	0.003
				sex:$\delta^{15}N$:lower jaw-fork length	*0.952*
log(Co)	**~ best selected model**	**97.4**	**-38.5**	-	-
	~ best selected model + sex:$\delta^{15}N$:lower jaw-fork length	97.4	-34.9	$\delta^{15}N$	< 0.001
				season	< 0.001
				sex:lower jaw-fork length	0.001
				season:lower jaw-fork length	< 0.001
				season:$\delta^{13}C$	0.848
				season:$\delta^{15}N$	< 0.001
				sex:$\delta^{15}N$:lower jaw-fork length	*0.200*
log(Cu)	**~ best selected model**	**49.1**	**-17.6**	-	-
	~ best selected model + sex:$\delta^{15}N$:lower jaw-fork length	49.6	-16.0	lower jaw-fork length	0.240
				season	0.001
				$\delta^{15}N$:lower jaw-fork length	0.066
				sex:$\delta^{15}N$:lower jaw-fork length	*0.589*
log(Fe)	**~ best selected model**	**52.3**	**2.0**	-	-
	~ best selected model + sex:$\delta^{15}N$:lower jaw-fork length	52.2	4.1	FA trophic group	0.088
				season	0.814
				sex:lower jaw-fork length	0.047
				FA trophic group:lower jaw-fork length	0.058
				season:$\delta^{13}C$	0.109
				season:$\delta^{15}N$	0.046
				sex:$\delta^{15}N$:lower jaw-fork length	*0.589*
log(Hg)	**~ best selected model**	**30.1**	**-18.8**	-	-
	~ best selected model + sex:$\delta^{15}N$:lower jaw-fork length	22.2	-15.7	sex	0.024
				FA trophic group:lower jaw-fork length	0.068
				sex:$\delta^{15}N$:lower jaw-fork length	*0.690*

Table 7.2. Effect of adding the interaction terms between sex, lower jaw-fork length and $\delta^{13}C$ and/or $\delta^{15}N$ values in the selected generalised additive models (GAM) presented in Table 7.1. The term "best selected model" refers to the variables in the models presented in Table 7.1. For each response variable, the best model (i.e. with the lowest AIC) is indicated in bold. FA = fatty acid. (continued)

Response variable	Tested model	Model deviance explained (%)	AIC	Explaining variable	*p* value
log(Mn)	**~ best selected model**	**71.1**	**-32.5**	-	-
	~ best selected model + sex:$\delta^{15}N$:lower jaw-fork length	72.5	-32.9	lower jaw-fork length	0695
				sex	0.011
				FA trophic group	0.206
				season	< 0.001
				sex:lower jaw-fork length	0.016
				season:$\delta^{13}C$	0.002
				season:$\delta^{15}N$	0.149
				$\delta^{15}N$:lower jaw-fork length	0.037
				sex:$\delta^{15}N$:lower jaw-fork length	*0.228*
log(Pb)	**~ best selected model**	**66.1**	**89.1**	-	-
	~ best selected model + sex:$\delta^{15}N$:lower jaw-fork length	62.1	96.5	FA trophic group:lower jaw-fork length	0.150
				season:lower jaw-fork length	< 0.001
				season:$\delta^{13}C$	0.037
				season:$\delta^{15}N$	0.023
				$\delta^{15}N$:lower jaw-fork length	0.057
				sex:$\delta^{15}N$:lower jaw-fork length	*0.543*
log(Se)	**~ best selected model**	**47.6**	**-34.0**	-	-
	~ best selected model + sex:$\delta^{15}N$:lower jaw-fork length	48.5	-31.2	FA trophic group	0.289
				$\delta^{13}C$	0.216
				season	0.092
				sex:lower jaw-fork length	0.313
				FA trophic group:lower jaw-fork length	0.005
				season:$\delta^{13}C$	0.009
				sex:$\delta^{15}N$:lower jaw-fork length	*0.679*
log(Zn)	**~ best selected model**	**55.8**	**-28.1**	-	-
	~ best selected model + sex:$\delta^{15}N$:lower jaw-fork length	54.8	-24.4	FA trophic group	0.431
				$\delta^{13}C$	0.621
				$\delta^{15}N$	0.887
				FA trophic group:lower jaw-fork length	0.183
				season:lower jaw-fork length	0.069
				season:$\delta^{13}C$	0.085
				season:$\delta^{15}N$	0.238
				sex:$\delta^{15}N$:lower jaw-fork length	*0.817*

7.4. DISCUSSION

7.4.1. Dietary patterns associated with each fatty acid trophic group

The fatty acid profiles measured in swordfish muscle tissues were coherent with the diet of swordfish from the Seychelles. Indeed, fatty acids like 18:0, 18:1n-9, 22:5n-3 and 22:6n-3 are known to be high in mesopelagic fish, crustaceans and/or squids (Meyer *et al.* 2019), and swordfish in the Seychelles are known to feed mainly on mesopelagic prey (Potier *et al.* 2007). However, thanks to the clustering method, two groups with divergences in fatty acid profiles could be identified among the analysed swordfish. As the biochemical composition of consumers largely reflects that of their prey (Iverson 2009), this suggests that these two groups have different foraging ecologies.

Among sampled swordfish, those in group 1 differed from those in group 2 by positive anomalies of 18:0, 18:1n-9, 20:1n-9 and 24:1n-9. The first three fatty acids are known to be animal trophic markers, especially 18:1n-9 and 20:1n-9 which are markers of carnivory (Meyer *et al*. 2019). Although not known as a specific trophic marker, the fatty acid 24:1n-9 was negatively correlated with primary producers fatty acid trophic markers (i.e. 14:0, 16:1n-7, 20:5n-3 and 22:5n-3; Meyer *et al.* 2019), while being positively correlated with animal/carnivorous fatty acid trophic markers (i.e. 18:0 and 20:1n-9; Meyer *et al.* 2019) (Appendix 7.5). In combination with the other fatty acis identified here, this suggests that the 24:1n-9 is a marker of carnivory. In contrast, swordfish from group 2 differed from those from group 1 by positive anomalies of 14:0, 16:1n-7, 20:5n-3, 22:5n-3, 20:4n-6, 22:5n-3 and 22:6n-3, which are mainly trophic markers of primary producers (Meyer *et al.* 2019).

Swordfish used in the present study were large individuals with lower jaw-fork lengths ranging from 107 to 230 cm, while major ontogenetic shifts in the main targeted prey types usually occur at lower jaw-fork length < 100 cm (Young *et al.* 2006). Thus, the differences in fatty acid profiles observed here between the two identified fatty acid trophic groups may have resulted from the consumption of the same prey types but in different proportions, with a fish-dominated diet for smaller individuals and a cephalopod-dominated diet for larger individuals (Young *et al.* 2006). This would be consistent with size differences between the two fatty acid trophic groups, as swordfish from Group 1 were larger than those from Group 2. The higher presence of fatty acid trophic markers of zooplankton (i.e. 20:5n-3 and 22:6n-3, Meyer *et al.* 2019) in swordfish from Group 2 also suggests feeding on zooplanktivorous prey, which is in

accordance with the known ontogenetic changes in swordfish diet. For example, cephalopods preyed upon by swordfish are squids, which feed on crustaceans and fish such as myctophids (mainly zooplanktivorous), with higher proportions of crustaceans for the small individuals (Pierce *et al*. 1994; Cherel and Duhamel 2003). A higher proportion of small and mainly crustacean-eating squids or mainly zooplanktivorous myctophids in the diet of smaller swordfish would be consistent with the seemingly lower level of carnivory in Group 2.

Surprisingly, trophic position in both groups seemed to not follow this logic, as there was no difference in $\delta^{15}N$ values between fatty acid trophic groups. This may be due to temporal variations in nitrogen cycling or to intra-oceanic migrations of swordfish. Indeed, the relationship between $\delta^{15}N$ values and swordfish size was previously shown to be linear (Ménard *et al*. 2007), while here this relationship was non-linear. Although the size range in Ménard *et al*. (2007) was larger than in this chapter (i.e. lower jaw-fork lengths ranging from 68 to 225 cm *vs* 107 to 230 cm), this suggests either temporal variation in trophic position or potential differences in isotopic baselines among individuals. Temporal variations in local oceanographic conditions (e.g. sea surface temperature, midwater oxygen concentrations and nutrient availability) were shown to affect nitrogen cycling and community assemblage, and thus food chain length (Ruiz-Cooley *et al.* 2017). In addition, variations in $\delta^{15}N$ baselines due to different biogeochemical dynamics have been reported across the Indian Ocean (Gruber and Sarmiento 1997; Naqvi *et al*. 2006; Lorrain *et al*. 2015). Thus, annual variations in food web length in the Seychelles due to variations in oceanographic conditions and/or migration of swordfish from another region to the Seychelles waters could have induced this non-linear relationship between $\delta^{15}N$ values and size, and could have masked the difference in trophic position between both FA trophic groups.

7.4.2. Influence of intrinsic factors and of trophic ecology on trace element bioaccumulation

Among all factors, intrinsic factors like size and sex had a major influence on trace element bioaccumulation in swordfish. The interaction between sex and size, in particular, had an effect on half of all analysed trace elements in this chapter (i.e. As, Cd, Co, Fe, Mn, and Se). This can be explained by the differential growth of males and females, with females growing faster than males after 3 years of age (Govender *et al.* 2003). Faster growth also means faster metabolism, which could have caused higher biodilution for elements not prone to bioaccumulation (either

poorly assimilated and/or efficiently excreted) or higher bioaccumulation for elements efficiently assimilated and/or efficiently retained (Auer *et al.* 2015; Rosenfeld *et al.* 2015). This applies particularly for females, depending on the considered trace element and its role in swordfish physiology. Among all models, both Cd and Hg concentrations were also significantly influenced by the factor sex alone, with higher Cd but lower Hg concentrations in females than in males. In the case of Cd, this could be explained by difference in diet between sexes. Along the Australian Coast, Young *et al.* (2006) observed that, for the same size class (> 150 cm), female swordfish included a larger proportion of cephalopods in their diet than males. Although there is no information on differences in swordfish diet between sexes in the Seychelles waters, such a difference could explain the differential bioaccumulation of Cd between sexes. Previous study on dolphins from the Bay of Biscay indicated that individuals including more cephalopods in their diet had clearly higher Cd concentrations in their tissues compared to those feeding less on this type of prey (Lahaye *et al*. 2005). As cephalopods are well-admitted vectors of Cd for their predators (Bustamante *et al.* 1998; Lischka *et al.* 2018), such a difference in the diet should therefore be reflected also in swordfish. In the case of Hg, an age difference between males and females is more likely to explain the higher concentrations in males. Indeed, while cephalopods have also been reported to contain high Hg concentrations (Lischka *et al*. 2018), the bioavailable fraction in cephalopod is usually lower than in fish (i.e. 67-93% *vs* virtually 100% of total Hg, respectively) (Wagemann *et al.* 1997; Bustamante *et al*. 2006). In addition, in muscle tissues, Hg is particularly known to bioaconcentrate along time (e.g. Kojadinovic *et al*. 2007; Goutte *et al*. 2015). As female swordfish grow faster than males after four years of age, for a given size female swordfish are younger than males for a given size, which could explain the higher Hg concentrations found in males.

Similarly to the factor sex, size influenced trace element bioaccumulation in swordfish both directly, through dilution with growth, and indirectly by influencing swordfish trophic ecology. The indirect effect of size was highlighted by the presence of one or more interaction factor(s) between size and stable isotope values or fatty acid trophic group. The direct effect of size was shown only for As, Cu and Mn concentrations, which decreased with increasing size. Although ontogenetic changes in diet and thus in trace element intake were shown to affect trace element bioaccumulation in other species (e.g. emperor red snapper, Chapter 3), such factors poorly explain As, Cu and Mn bioaccumulation trends with size in swordfish. Indeed, both squids and myctophids were reported to have similar Mn concentrations, while squids,

which are the main prey in large swordfish's diet (Young *et al*. 2006), tend to have higher As and Cu concentrations (Figueiredo *et al*. 2020; Lischka *et al*. 2020). Here, dilution during swordfish growth is more likely to explain As, Cu and Mn bioaccumulation trends with size. Previous work showed similar results in swordfish from the Mozambique Channel for Cu and Mn (Kojadinovic *et al.* 2007). Interestingly, in spite of As potential biodilution during growth, its concentration was higher in fatty acid trophic group 1, within larger swordfish, than in fatty acid trophic group 2 within smaller swordfish. Such findings highlight the major influence of diet on trace element bioaccumulation in top predators like swordfish, and especially of the bioavailability of trace elements in their prey, as suggested by previous work (Storelli *et al.* 2005) and by results of this chapter. Indeed, here, As, Cd, Hg and Mn concentrations were higher in fatty acid trophic Group 1 than in Group 2 while Fe, Se and Zn concentrations were lower in fatty acid trophic Group 1 than in Group 2. A cephalopod-dominated diet for swordfish in Group 1, as suggested in section 7.4.1, would be consistent with higher concentrations of As and Cd. As mentioned before, cephalopods have been identified as major source of exposure of Cd for top predators like swordfish (Bustamante *et al.* 1998; Lischka *et al*. 2018), but data on the bioavailability of other trace elements in cephalopod, like for As, Fe, Mn, Se, and Zn, are still scarce. Previous work showed that arsenobetaine, the most bioavailable form of As, was in higher proportion in squids than in fish muscle (Lin *et al.* 2008). Although more studies are needed to determine if squids could indeed be a significant source of As to top predators, this could also explain the higher As concentrations in swordfish with a cephalopod-dominated diet. Finally, Wang *et al.* (2012) showed that the assimilation efficiency of Zn in juvenile black seabream was significantly higher from mullet muscle than from squid viscera. This would explain the higher Zn concentrations in swordfish with a fish-dominated diet (i.e. from FA trophic group 2). These results thus show the importance of trace element bioavailability in top predators' prey and of the resulting effect on the predator assimilation efficiency, in influencing trace element concentrations in top predators' tissues. However, more data are needed to better identify the trace elements for which bioavailability differs from one type of prey to another.

Finally, feeding depth and trophic position had an influence on the bioaccumulation of Co, Cu, Mn and Zn. After removing the size effect, Zn concentrations decreased with increasing $\delta^{13}C$ values, suggesting that Zn bioaccumulation in swordfish is associated with feeding on shallower-living and/or more offshore prey. However, there are not enough data on swordfish

diet according to feeding habitat to conclude on this. After removing the size effect on trace element bioaccumulation, trophic position seemed to influence Co, Cu and Mn bioaccumulation. This could reflect ontogenetic changes in diet, from fish-dominated to cephalopod-dominated (Young *et al.* 2006; Ménard *et al.* 2007), that is a change in trace element exposure and bioavailability in consumed prey.

Interestingly, while higher Hg concentrations are usually associated with higher trophic position and deeper foraging depths, Hg concentrations were not significantly influenced by $\delta^{15}N$ or $\delta^{13}C$ values here. This may reflect the influence of annual variation in oceanographic conditions and/or swordfish migrations across the Indian Ocean, as feeding in different areas with different dynamics in bacterial activity (i.e. MeHg production and thus Hg bioavailability, Morel *et al.* 1998) and/or with different isotopic baselines would probably mask the usual positive relationship between Hg concentrations and stable isotope values. Although the size range of the swordfish sampled here was quite large (i.e. 107 to 230 cm lower jaw-fork length), a larger size range could help confirming such a hypothesis.

7.4.3. Seasonal variation in trace element concentrations

The factor season was a significant factor influencing the bioaccumulation of most of the trace elements analysed here, as shown by the presence of season and/or one or more of its interaction factors with size, $\delta^{13}C$ or $\delta^{15}N$ values in almost all selected models, even those explaining length-standardised concentrations. Seasonal variations in environmental parameters such as seawater temperature, pH and salinity are known to influence trace element bioavailability in the water column (Neff 2002a; Rainbow and Black 2002, 2005). However, such changes generally occur in surface waters, while swordfish are known to feed on mesopelagic prey that is depths below 200 m (Nakamura 1985; Potier *et al*. 2007). In addition, patterns of variations of trace element concentrations observed here do not correspond to changes in environmental parameters. For example, the bioavailability of Cd and Zn was shown to be higher at lower salinity (Rainbow and Black 2002, 2005). As the NWM is the rainy season (Chang-Seng 2007), which leads to high input of freshwater in the ocean, Cd and Zn bioaccumulation should have been highest during this season and/or during the pre-SEM season. Yet, Cd concentrations were highest in swordfish caught during the pre-NWM season, while Zn was not affected by the factor season alone. MeHg production, and thus Hg bioavailability in oceanic waters, was also shown to be enhanced by high bacterial activity

(Morel *et al.* 1998). In the Seychelles, primary production is generally higher during the SEM season, potentially causing phytoplanktonic blooms (ASCLME 2012), and thus subsequent organic matter degradation and bacterial activity. Thus, in relation with a potentially higher MeHg production in deep waters, Hg bioaccumulation should be expected to be higher during the SEM or pre-NWM seasons. Yet, Hg was the only trace element for which bioaccumulation was not influenced by season or one of its interaction factors. Although these results suggest that seasonal changes in trace element bioavailability did not affect trace element concentrations in swordfish here, it is possible that seasonal changes in community composition, linked to changes in oceanographic conditions, had some level of influence. Indeed, oceanographic conditions are known to influence the composition of marine organisms' communities (Jung and Houde 2003; Ambriz-Arreola *et al.* 2018) and, as we saw throughout this thesis, diet composition is an important factor influencing trace element bioaccumulation in marine organisms, including top predators.

Finally, swordfish seasonal migrations in the Indian Ocean could also explain their seasonal variations in trace element concentrations, as suggested by seasonal variations in size and sex ratio (Appendix 7.3 and 7.6). Swordfish are known to be highly migratory species (Nakamura 1985), and studies on the genetic structure of swordfish populations in the Indian Ocean revealed high similarities across this ocean (Jean *et al*. 2006; Muths *et al.* 2013). Authors suggested that there was only one or two genetic populations in the Indian Ocean, which implies mixing of genetic material among swordfish. In addition, reproductive dynamics of swordfish off the coast of Reunion Island hint to possible seasonal migrations between Reunion and Seychelles waters related to spawning (Poisson and Fauvel 2009). Such movement patterns could explain the non-significant difference in trophic position between the two fatty acid trophic groups with seemingly different carnivory levels (section 7.4.1), as well as the non-significant relationship between Hg bioaccumulation and trophic position and feeding depth (section 7.4.2).

7.5. CHAPTER HIGHLIGHTS

Chap. 5 – Main findings

• **Size and sex both influenced directly and indirectly** (i.e. through influence on trophic ecology) **trace element bioaccumulation** in swordfish. The **difference in growth rate between males and females**, in particular, **highly contributed** to the observed differences in trace element concentrations between sexes.

• **Ontogenetic changes and sexual differences in diet** (i.e. fish-dominated *vs* cephalopod-dominated) likely had a **major influence** on intraspecific difference in trace element bioaccumulation. This was **mainly due to difference in trace element concentrations and bioavailability** between fish and cephalopods.

• As observed for Hg in Chapter 4, here **feeding depth and/or trophic position had an effect on the bioaccumulation of some trace elements** (i.e. Co, Cu, Mn and Zn). Surprisingly, **no effect was shown for Hg**, which was not expected. This **may indicate an influence of swordfish movements across the Indian Ocean**. Indeed, swordfish are highly migratory, and studies on the genetic structure of the swordfish population in the Indian Ocean and on their reproductive dynamics in Reunion Island hint to movements across several areas of the Indian Ocean.

8. Chapter 6 – Risk-benefit analysis of a capture fisheries resources-based diet in Small Island Developing States (SIDS): the Seychelles as a case study

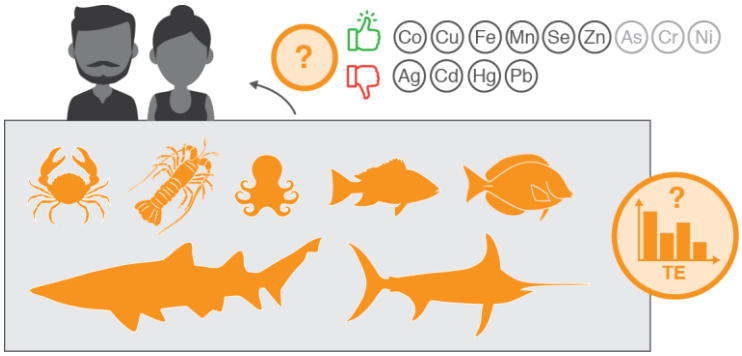

Content

This chapter is partly included in a paper in preparation for Marine Pollution Bulletin *and presented in Supp. Doc. 1.*

8.1. CONTEXT AND OBJECTIVES

As mentioned in the general introduction, seafood are key food items in the fight against micronutrient deficiency, especially in SIDS like the Seychelles, where capture fisheries products are the main source of protein and essential and potentially essential trace elements for local populations (Hicks *et al*. 2019). However, capture fisheries products also contain significant levels of non-essential trace elements that can have adverse effects on human health (Bosch *et al*. 2016). It is thus necessary to consider both essential and non-essential trace elements when studying the contribution of capture fisheries products to healthy human diets. It is important to note that the concentration of a given essential trace element makes its essentiality, that is intakes must remain above a lower limit to avoid deficiency and below an upper limit to avoid toxicity (Goldhaber 2003). Similarly, non-essential trace elements become toxic only above certain levels (Bosch *et al*. 2016).

Among all population categories, growing children and young adults, as well as adult women of childbearing age, are the most at risk to develop essential trace element deficiency and are also the most sensitive to non-essential trace element toxicity. In children, a deficiency in Cu, Fe, Mn and Zn, for example, have been associated with growth retardation and inadequate skeletal growth, while Fe deficiency anaemia also alters cognitive development (Wada 2004; Gupta and Gupta 2014). Among non-essential trace elements, Cd and Hg exposure in children causes decrease in bone density and affects developing of their nervous system, respectively (Bernhoft 2013; Kim *et al*. 2016). Fe deficiency is also one of the first causes of anaemia in adolescent girls and adult women of childbearing age (Jackson and Al-Mousa 2000; Hwalla *et al*. 2004), and Cd and Hg exposure during pregnancy have been associated with low new-born weight and risk of spontaneous abortion (Ikeh-Tawari *et al.* 2013; Bjørklund *et al.* 2019). Finally, new-born trace element supply and/or exposure have been shown to be largely influenced by mothers' dietary habits through breastfeeding (Leotsinidis *et al*. 2005). Given the importance of maintaining sufficient essential trace element levels and of avoiding non-essential trace element exposure for children, young adults and adult women, it is essential to bring insight into their nutrient supply and contaminant exposure through their diet.

After investigating the factors influencing trace element bioaccumulation in Seychelles capture fisheries species in the previous chapters, this chapter thus aims to evaluate, for at-risk Seychellois population categories, (1) the risk related to non-essential trace element levels in

these species and (2) the benefit related to essential trace element supply through consumption of capture fisheries products.

8.2. METHODOLOGY

8.2.1. Dataset

Guidelines for recommended daily intakes (RDI) and provisional tolerable intakes (PTI) were only found for As, Cd, Cu, Fe, Hg, Se and Zn. Thus, although all measured trace element concentrations (i.e. Ag, As, Cd, Co, Cr, Cu, Fe, Hg, Mn, Pb, Se and Zn) in the 54 analysed species are presented in Appendix 8.1, only trace elements with known guidelines will be used for the risk-benefit analysis and will be presented in this chapter.

8.2.2. Risk-benefit analysis for Seychellois diets

In order to assess essential and potentially essential trace element intake and risk related to too high concentrations of some trace elements through consumption of capture fisheries products from the Seychelles, measured trace element concentrations were compared to existing guidelines set by the American Food and Nutrition Board of the Institute of Medicine National Academy of Sciences (2019a, b) for the essential trace elements Cu, Fe, Mn, Se and Zn, by Nielsen (1991) for the potentially essential trace element As, and by the Joint FAO/WHO Expert Committee on Food Additives (JECFA 2011b, 2013) for the non-essential trace elements Cd and Hg (Appendix 8.2). The final purpose of this risk-benefit analysis was to attribute a risk or benefit category to the 54 analysed species, similar to what was done by the United States Environmental Protection Agency (US-EPA) and the United States Food and Drug Administration (US-FDA) (US-EPA and US-FDA 2019) for Hg (Appendix 8.3), in order to make the information easier to read at first glance. For this, several steps were followed (Fig. 8.1).

Physiological needs in terms of essential and potentially essential trace elements vary with age, sex and status (i.e. for women, non-pregnant, pregnant or lactating), and non-essential trace element sensitivity varies with weight which itself varies with age and sex (JECFA 2011b, 2013; American Food and Nutrition Board of the Institute of Medicine National Academy of Sciences 2019a, b). Three main age classes were thus chosen in order to represent the most vulnerable populations, either in term of trace element deficiency or in term of exposure, that is: **children (2-13 year old)**, **young adults (14-18 year old)** and **adult women (19+ year old, includes pregnant and lactating women)**. Guidelines given by the American Food and

Nutrition Board of the Institute of Medicine National Academy of Sciences (2019a, b) are more precise and are given for the following age classes and status: 2-3 year old, 4-8 year old, 9-13 year old, 14-18 year old, 19+ year old, pregnant women and lactating women. Thus, for both essential and non-essential trace elements, calculations were made for each age subclass. Then, information was summarised into the three corresponding main age classes defined above.

First, it was necessary to determine the average weight of a daily portion for each age subclass (Fig 8.1, step 1.A2). For adult Seychellois, the average rate of marine fish consumption is 57 kg.person^{-1}.year^{-1} (WorldBank 2017), this rate was thus divided by 365 to obtain a daily rate of consumption of 156 kg.person^{-1}. For children, the US-EPA and US-FDA (2019) consider that a child of 2-3 years old eats around 30 g of fish per day, this was thus the portion weight used here for this age subclass. Finally, as the portion weight increases with age to reach its maximum at 11 years old (US-EPA and US-FDA 2019), it was considered that it increased linearly. Thus, the used portion weights for intermediate age subclasses were: 72 g for 4-8 year old, 114 g for 9-13 year old, and 156 g for 14-18 year old.

In order to take into account the effect of the interaction ability between Hg and Se on their respective bioavailability in human diet (Fig. 8.1, Step 1.A3), the molar ratio of Hg over Se (MHg:MSe) and the health benefit value of Se (HBV_{Se}) were calculated using the following formulas (Ralston *et al*. 2015):

$$MHg:MSe = (C_{Hg}/M_{Hg}) / (C_{Se}/M_{Se}) \quad \textbf{(Eq. 8.1)}$$

$$HBV_{Se} = ((MSe - MHg) / MSe) \times (MSe + MHg) \quad \textbf{(Eq 8.2)}$$

with MHg and MSe the number of Hg and Se, respectively, CHg and CSe the concentrations of Hg and Se, respectively; and MHg and MSe the molar masses of Hg and Se, respectively (200.59 g.mol^{-1} for Hg and 78.96 g.mol^{-1} for Se). In human tissues, it is considered that Se and Hg bind in a molar ratio of 1:1 (Ralston *et al*. 2007). Thus, it was possible to estimate concentrations of theoretically bioavailable Hg and Se after interaction with each other, using the following formulas:

$$\text{Concentration of theoretically bioavailable Hg} = (MHg - MSe) \times M_{Hg} \quad \textbf{(Eq. 8.3)}$$

$$\text{Concentration of theoretically bioavailable Se} = (MSe - MHg) \times M_{Se} \quad \textbf{(Eq. 8.4)}$$

To calculate the trace element content in a portion for each age subclass (Fig. 8.1, step 1.B1), measured concentrations of Cd, Cu, Fe, Mn and Zn and estimated concentrations of

bioavailable Hg and Se were thus used. Then, it was possible to calculate the percentage of RDI (for essential and potentially essential trace elements) and of PTI (for essential and non-essential trace elements) covered by 1 portion for each age subclass (Fig. 8.1, step 1.C), using the following formulas:

$$\%RDI = ([TE] \times \text{portion weight}) \times 100 / RDI \quad \textbf{(Eq. 8.5)}$$

$$\%PTI = ([TE] \times \text{portion weight}) \times 100 / PTI \quad \textbf{(Eq. 8.6)}$$

with [TE] the concentrations of the considered trace element; portion weight the weight of the portion for the considered age subclass; RDI the recommended daily intake for the considered element; and PTI the daily provisional tolerable intake for the considered trace element. To summarise data into the three age classes, all data related to the corresponding age subclasses were grouped (i.e. 2-3 year old with 4-8 year old and 9-13 year old for Children; 14-18 year old for Young adults; and women 19+ year old with lactating and pregnant women for Adult women). Then, the mean %RDI or mean %PTI and their associated confidence interval at 95% (CI95%) were calculated for each trace element and each age class. CI95% was calculated as following (with SE the standard error):

$$CI95\% = [\text{mean} - (1.96 \times SE); \text{mean} + (1.96 \times SE)] \quad \textbf{(Eq. 8.7)}$$

After selection of the trace elements of interest (Fig. 8.1, step 2), calculated CI95% were used to attribute a risk and/or benefit category to each analysed species (Fig. 8.1, step 3). For PTI, the CI95% upper bound was used to attribute a risk category to the species for each trace element (Fig. 8.1, step 3.A1). Then, in order to attribute a single risk category to species for each age class, the most limiting category among all trace elements was kept (Fig. 8.1, step 3.A1). For species with %PTI > 90%, a maximum weight was calculated for each age class and each considered trace element, and the most limiting was kept:

$$\text{Max weight (g)} = (0.9 \times PTI) / [TE]_{CI95\% \text{ upper bound}} \quad \textbf{(Eq. 8.8)}$$

with 0.9 x PTI the equivalent of 90% of the given PTI; $[TE]_{CI95\% \text{ upper bound}}$ the CI95% upper bound concentration calculated for the considered trace element. The value of 90% of PTI was chosen because capture fisheries products are not the only food items that may contain trace elements, thus this values takes into account a margin for the rest of the diet. For essential trace elements, the CI95% lower bound was used to attribute a benefit category to each species for each trace element and each age class (Fig. 8.1, Steps 3.B1 and 3.B2). If the lower bound

was below 1% but the mean %RDI was above 1%, the mean value was used to attribute the benefit category.

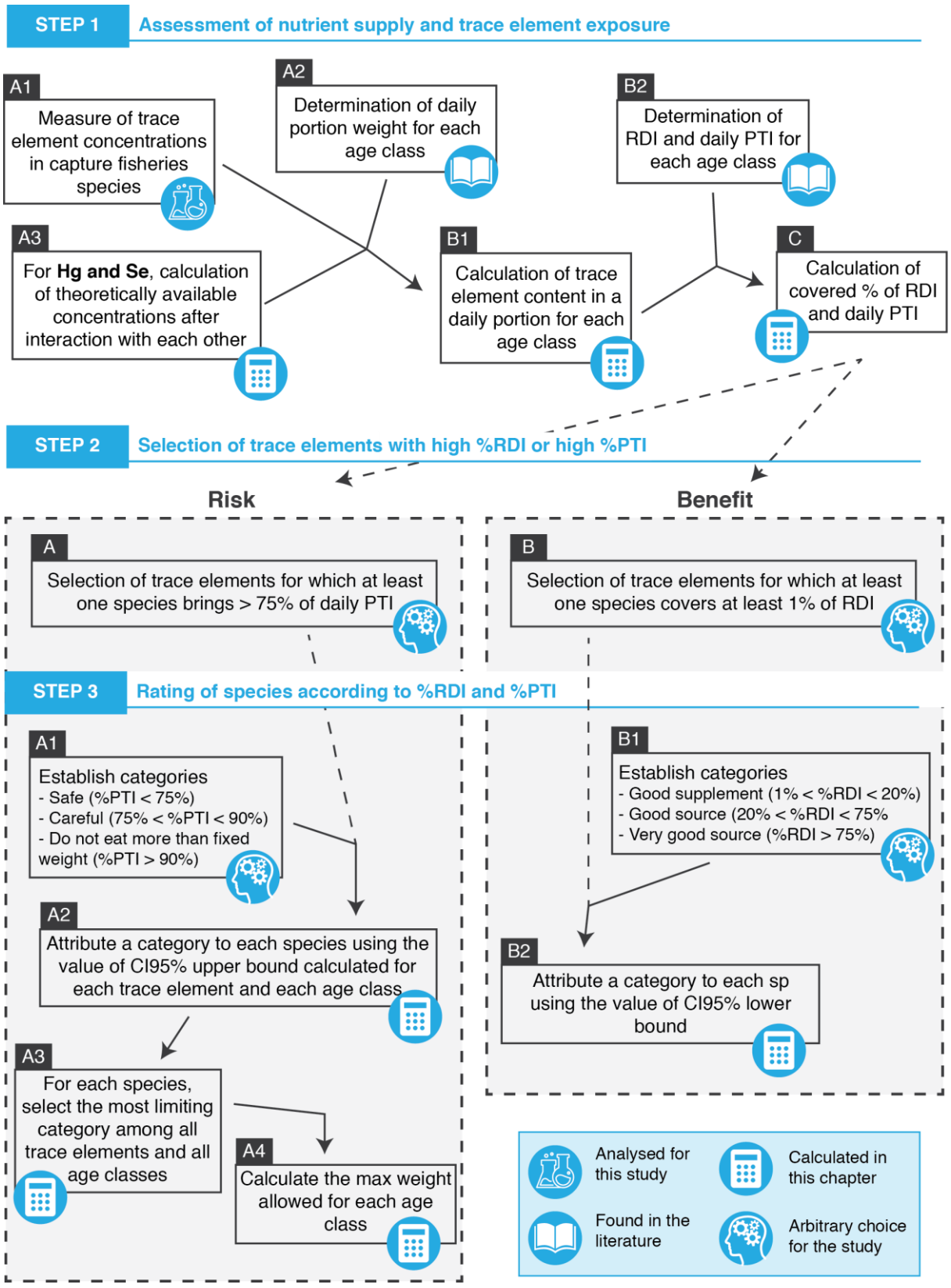

Fig. 8.1. Steps followed to attribute a risk or benefit category to each species. RDI = Recommended daily intake, PTI = Provisional tolerable intake, CI95% = Confidence interval at 95%.

Finally, no PTI was found for As (the one set by the JECFA was withdrawn in 2011, JECFA 2011a), thus this trace element could not be directly integrated in the risk-benefit analysis. However, the most toxic forms of As are its inorganic forms (Molin *et al*. 2015), and previous work determined the proportions of iAs in various capture fisheries species (i.e. 2.2% in crustaceans and 4.2% in fish; Uneyama *et al*. 2007). Thus, for each analysed species, it was possible to estimate the concentration of iAs from the total measured As.

8.3. RESULTS AND DISCUSSION

8.3.1. Interaction between Hg and Se

In all 54 species, the mean MHg:MSe ratio was below 1 indicating that, globally, Se was in molar excess over Hg, and the HBV_{Se} ratio was positive for all analysed species (Table 8.1). As a consequence, the mean concentration of theoretically bioavailable Se was never null, although generally below 1 $\mu g.g^{-1}$ ww (Table 8.1). Three species had particularly low MHg:MSe ratios, i.e. blackeye emperor, pink ear emperor and scalloped hammerhead, which resulted in these species having the highest mean concentrations of theoretically bioavailable Se (above 1 $\mu g.g^{-1}$ ww).

Some individuals of bigeye trevally and bludger had a molar excess of Hg over Se. As a consequence, the concentration of theoretically bioavailable Hg was 0 for all analysed species except for bigeye trevally and bludger (Table 8.1). Those concentrations were however very low (i.e. < 0.01 $\mu g.g^{-1}$ ww).

Results thus indicate that, as a consequence of the very high concentrations of Se in all Seychelles capture fisheries species, there is low risk associated with Hg in Seychellois capture fisheries resources-based diet.

Table 8.1. Molar ratio of Hg above Se (MHg:MSe), HBVSe ratio and estimated concentrations (µg.g^{-1} ww) of theoretically bioavailable Se and Hg. Ratios are presented as mean ± SD [CI95%] and concentrations as mean [CI95%].

Species	MHg:MSe	HBVSe	Theoretically bioavailable Se	Theoretically bioavailable Hg
Octopuses				
Big blue octopus	0.019 ± 0.008 [0.015-0.022]	3.4e-09 ± 0.6e-09 [3.1e-09-3.7e-09]	0.26 [0.24-0.29]	0
Crabs				
Spanner crab	0.024 ± 0.004 [0.020-0.027]	7.0e-09 ± 1.1e-09 [6.0e-09-7.9e-09]	0.54 [0.46-0.61]	0
Spiny lobsters				
Longlegged spiny lobster	0.052 ± 0.035 [0.042-0.063]	3.7e-09 ± 1.7e-09 [3.2e-09-4.2e-09]	0.28 [0.24-0.32]	0
Painted spiny lobster	0.045 ± 0.076 [0.006-0.083]	3.4e-09 ± 1.3e-09 [2.7e-09-4.0e-09]	0.26 [0.21-0.31]	0
Pronghorn spiny lobster	0.052 ± 0.030 [0.043-0.060]	3.7e-09 ± 1.3e-09 [3.3e-09-4.1e-09]	0.28 [0.25-0.31]	0
Goatfishes				
Dash-and-dot goatfish	0.020 ± 0.013 [0.009-0.031]	5.9e-09 ± 1.0e-09 [5.0e-09-6.8e-09]	0.46 [0.38-0.53]	0
Rosy goatfish	0.040 ± 0.024 [0.013-0.067]	5.3e-09 ± 0.9e-09 [4.3e-09-6.3e-09]	0.40 [0.33-0.47]	0
Parrotfishes				
Blue-barred parrotfish	0.006 ± 0.003 [0.004-0.008]	5.4e-09 ± 2.5e-09 [3.9e-09-7.0e-09]	0.43 [0.31-0.55]	0
Shoemaker spinefoot	0.005 ± 0.002 [0.004-0.007]	3.1e-09 ± 1.1e-09 [2.4e-09-3.8e-09]	0.24 [0.19-0.30]	0
Streamlined spinefoot	0.006 ± 0.001 [0.005-0.006]	2.1e-09 ± 6.0e-10 [1.7e-09-2.5e-09]	0.16 [0.13-0.19]	0
Surgeonfishes				
Elongate surgeonfish	0.020 ± 0.007 [0.015-0.026]	5.3e-09 ± 2.2e-09 [3.5e-09-7.0e-09]	0.41 [0.27-0.54]	0
Emperors				
Blackeye emperor	0.031 ± 0.011 [0.016-0.046]	22.2e-09 ± 2.0e-09 [19.4e-09-25.0e-09]	1.70 [1.46-1.94]	0
Blue-lined large-eye bream	0.091 ± 0.027 [0.067-0.115]	12.8e-08 ± 2.8e-09 [10.3e-09-15.2e-09]	0.93 [0.73-1.12]	0
Pink ear emperor	0.049 ± 0.015 [0.033-0.066]	23.8e-09 ± 7.6e-09 [15.2e-09-32.3e-09]	1.79 [1.17-2.40]	0
Slender emperor	0.217 ± 0.095 [0.173-0.261]	7.9e-09 ± 1.9e-09 [7.0e-09-8.8e-09]	0.52 [0.45-0.59]	0
Sky emperor	0.156 ± 0.071 [0.126-0.186]	9.4e-09 ± 2.1e-09 [8.5e-09-10.2e-09]	0.64 [0.58-0.70]	0
Smalltooth emperor	0.191 ± 0.149 [0.099-0.283]	5.8e-09 ± 1.1e-09 [5.1e-09-6.5e-09]	0.40 [0.32-0.48]	0
Spangled emperor	0.090 ± 0.050 [0.064-0.116]	7.4e-09 ± 2.5e-09 [6.1e-09-8.7e-09]	0.54 [0.43-0.64]	0
Yellowtail emperor	0.105 ± 0.101 [0.050-0.159]	13.2e-09 ± 4.4e-09 [10.8e-09-15.5e-09]	0.97 [0.77-1.16]	0
Groupers				
Blacktip grouper	0.089 ± 0.026 [0.060-0.119]	6.2e-09 ± 1.5e-09 [4.5e-09-7.9e-09]	0.45 [0.32-0.59]	0
Brown-marbled grouper	0.219 ± 0.077 [0.113-0.326]	6.4e-09 ± 2.1e-09 [3.5e-09-9.3e-09]	0.42 [0.20-0.64]	0
Brownspotted grouper	0.063 ± 0.057 [0.050-0.075]	7.1e-09 ± 1.2e-09 [6.8e-09-7.3e-09]	0.53 [0.51-0.55]	0
Eightbar grouper	0.162 ± 0.059 [0.105-0.220]	6.5e-09 ± 0.3e-09 [6.2e-09-6.8e-09]	0.44 [0.40-0.48]	0

Table 8.1. Molar ratio of Hg above Se (MHg:MSe), HBVSe ratio and estimated concentrations (μg.g^{-1} ww) of theoretically bioavailable Se and Hg. Ratios are presented as mean ± SD [CI95%] and concentrations as mean [CI95%]. (continued)

Species	MHg:MSe	HBVSe	Theoretically bioavailable Se	Theoretically bioavailable Hg
Honeycomb grouper	0.182 ± 0.114 [0.070-0.294]	4.1e-09 ± 2.0e-09 [2.1e-09-6.0e-09]	0.28 [0.14-0.43]	0
Longspine grouper	0.159 ± 0.028 [0.120-0.198]	4.9e-09 ± 0.3e-09 [4.4e-09-5.4e-09]	0.33 [0.31-0.35]	0
Peacock hind	0.120 ± 0.069 [0.099-0.141]	6.4e-09 ± 3.3e-09 [5.4e-09-7.4e-09]	0.46 [0.38-0.54]	0
Tomato hind	0.109 ± 0.058 [0.078-0.139]	6.6e-09 ± 0.9e-09 [6.2e-09-7.1e-09]	0.48 [0.44-0.51]	0
White-blotched grouper	0.167 ± 0.107 [0.123-0.212]	7.9e-09 ± 2.1e-09 [7.1e-09-8.8e-09]	0.55 [0.48-0.62]	0
Yellow-edged lyretail	0.083 ± 0.058 [0.065-0.101]	7.7e-09 ± 0.9e-09 [7.4e-09-7.9e-09]	0.56 [0.54-0.59]	0
Trevallies				
Bigeye trevally	0.305 ± 0.318 [0.085-0.526]	9.0e-09 ± 6.8e-09 [4.3e-09-13.8e-09]	0.61 [0.28-0.94]	0.005 [0.000-0.014]
Bludger	0.262 ± 0.302 [0.143-0.380]	7.1e-09 ± 3.0e-09 [5.9e-09-8.3e-09]	0.50 [0.40-0.60]	0.001 [0.000-0.002]
Bluefin trevally	0.276 ± 0.185 [0.156-0.397]	5.0e-09 ± 1.0e-09 [4.3e-09-5.7e-09]	0.32 [0.26-0.38]	0
Golden trevally	0.133 ± 0.208 [0.022-0.287]	4.7e-09 ± 1.0e-09 [3.9e-09-5.4e-09]	0.34 [0.26-0.41]	0
Malabar trevally	0.373 ± 0.158 [0.000-0.592]	5.8e-09 ± 0.9e-09 [4.6e-09-7.0e-09]	0.34 [0.21-0.46]	0
Yellowspotted trevally	0.127 ± 0.161 [0.075-0.180]	7.2e-09 ± 2.1e-09 [6.5e-09-7.9e-09]	0.52 [0.46-0.58]	0
Snappers				
Bigeye snapper	0.247	7.0e-09	0.44	0
Deepwater longtail red snapper	0.147 ± 0.071 [0.103-0.191]	7.5e-09 ± 0.7e-09 [7.1e-09-7.9e-09]	0.52 [0.49-0.54]	0
Emperor red snapper	0.116 ± 0.118 [0.090-0.143]	6.2e-09 ± 1.2e-09 [5.9e-09-6.5e-09]	0.44 [0.42-0.46]	0
Green jobfish	0.090 ± 0.079 [0.075-0.104]	7.7e-09 ± 1.9e-09 [7.4e-09-8.1e-09]	0.56 [0.54-0.59]	0
Humpback red snapper	0.169 ± 0.068 [0.135-0.202]	6.7e-09 ± 1.2e-09 [6.1e-09-7.2e-09]	0.45 [0.41-0.49]	0
Humphead snapper	0.146 ± 0.057 [0.095-0.196]	9.4e-09 ± 1.2e-09 [8.4e-09-10.5e-09]	0.65 [0.56-0.74]	0
Two-spot red snapper	0.168 ± 0.104 [0.141-0.195]	8.4e-09 ± 1.7e-09 [8.0e-09-8.8e-09]	0.57 [0.54-0.61]	0
Barracudas				
Pickhandle barracuda	0.200 ± 0.097 [0.163-0.238]	5.8e-09 ± 1.2e-09 [5.4e-09-6.3e-09]	0.39 [0.35-0.42]	0
Mackerels				
Indian mackerel	0.035 ± 0.019 [0.026-0.045]	8.8e-09 ± 2.0e-09 [7.8e-09-9.7e-09]	0.67 [0.60-0.74]	0
Tunas				
Dogtooth tuna	0.199 ± 0.123 [0.108-0.290]	12.8e-09 ± 7.8e-09 [7e-09-18.6e-09]	0.87 [0.42-1.32]	0
Little tunny	0.158 ± 0.036 [0.127-0.190]	6.7e-09 ± 1.2e-09 [5.6e-09-7.7e-09]	0.45 [0.38-0.53]	0
Sharks				
Blacktip shark	0.176	14.1e-09	0.95	0
Great hammerhead	0.617	3.1e-09	0.15	0
Grey reef shark	0.325	9.8e-09	0.58	0

Table 8.1. Molar ratio of Hg above Se (MHg:MSe), HBVSe ratio and estimated concentrations (µg.g^{-1} ww) of theoretically bioavailable Se and Hg. Ratios are presented as mean ± SD [CI95%] and concentrations as mean [CI95%]. (continued)

Species	MHg:MSe	HBVSe	Theoretically bioavailable Se	Theoretically bioavailable Hg
Scalloped hammerhead	0.189 ± 0.096 [0.142-0.236]	15.4e-09 ± 6.1e-09 [12.4e-09-18.4e-09]	1.05 [0.81-1.29]	0
Spinner shark	0.228	4.8e-09	0.31	0
Spot-tail shark	0.072	6.5e-09	0.48	0
Tiger shark	0.639	3.1e-09	0.15	0
Billfishes				
Swordfish	0.421 ± 0.223 [0.383-0.459]	7.6e-09 ± 4.0e-09 [6.9e-09-8.2e-09]	0.46 [0.41-0.50]	0

8.3.2. Risk-benefit of Seychelles capture fisheries products consumption

For all age classes, identified risk through consumption of Seychelles capture fisheries products was related to too high concentrations of Cd and/or Se in three species: spanner crab, blackeye emperor and pink ear emperor (Table 8.2). In particular, there was a risk of excess of Se in children through consumption of blackeye emperor, as a portion of this species brought more than 90% of the PTI value of Se for this age class. For young adults and adult women, although blackeye emperor brought less than 90% of the PTI value for Se, which does not require to give a maximum portion weight to not exceed, caution should be taken when eating this fish in excess. Indeed, it is important to note that this risk-benefit analysis is only focused on capture fisheries resources and does not take into account the rest of the daily diet. Yet, Se concentrations can also be high in food items like meat, eggs and some vegetables and legumes (Navarro-Alarcon and Cabrera-Vique 2008). Thus, by eating other food items rich in Se in addition to a whole portion of blackeye emperor (i.e. 156 g), young adults and adult women could reach or exceed the daily limit recommended by the American Food and Nutrition Board of the Institute of Medicine National Academy of Sciences (2019b).

Here, it is important to note that all trace element forms that are present in capture fisheries species are not necessarily bioavailable. As only the total concentration was measured for each trace element analysed, calculations given in this chapter are only indicative of a potential of risk.

Table 8.2. Capture fisheries species for which caution should be taken when eating them; species not present in this table are considered safe. Trace elements for which there is a potential risk of excess are indicated between brackets beside the corresponding species; maximum weights for each age subcategory are indicated in table notes. Details for covered percentages of daily provisional tolerable intakes (PTI) and corresponding risk category for each species are given in Appendix 8.4.

Risk category	Children (2-13 year old)	Young Adults (14-18 year old)	Adult women (> 18 year old)
Be careful (75% < %PTI < 90%)		Blackeye emperor (Se)	Blackeye emperor (Se)
Do not eat more than given weight (90% < %PTI)	Spanner crab[1] (Cd) Blackeye emperor[2] (Se) Pink ear emperor[3] (Cd, Se)	Spanner crab[1] (Cd) Pink ear emperor[3] (Cd, Se)	Spanner crab[1] (Cd) Pink ear emperor[3] (Cd, Se)

[1] No more than 14 g/day for 2-3 year old, 25 g/day for 4-8 year old, 42 g/day for 9-13 year old, 60 g/day for 14-18 year old and 81 g/day for > 18 year old.
[2] No more than 42 g/day for 2-3 year old, 70 g/day for 4-8 year old and 130 g/day for 9-13 year old.
[3] No more than 34 g/day for 2-3 year old, 56 g/day for 4-8 year old, 100 g/day for 9-13 year old and 150 g/day for > 13 year old.

Concerning benefit related to essential trace element content in Seychelles capture fisheries resources, all investigated species were good sources of Se (even after its interaction with Hg) and As (Table 8.3). Indeed, a portion of all analysed species brought largely more than 100% of As RDI for adults and at least 20% of Se RDI for all age classes. In addition, 19 species brought more than 75% of Se RDI for young adults and adult women and 14 species brought more than 75% of Se RDI for all age classes.

Crustaceans were particularly good sources of Cu and Zn (Table 8.3). The spanner crab and spiny lobsters brought at least 20% of Zn and Cu RDI for all age classes. Both the longlegged and pronghorn spiny lobsters where even very good sources of Cu (i.e. %RDI > 75%) for all age classes. The painted spiny lobster was also a very good source of Cu for young adults and adult women, and the spanner crab for young adults. Interestingly, the big blue octopus was also a good source of Zn, bringing more than 20% of Zn RDI for the three age classes (Table 8.3). All other species could be considered as good supplement for Cu and Zn, as they brought at least 1% of RDI for these trace elements. Some species even brought at least 10% percent of Cu and/or Zn RDI for one age class or more (i.e. big blue octopus, bludger, bigeye snapper, humpback red snapper, Indian mackerel and blacktip shark). These results are highly important for pregnant women, as it has been shown that, in combination with deficiency of other elements like Fe or Ca, Zn deficiency could increase risk of pre-eclampsia, hypertension or

miscarriage during pregnancy (Kim *et al*. 2012; Shen *et al*. 2015) and could affect new-born health (Khoushabi *et al*. 2016).

Except for spot-tail shark for which a %RDI could not be calculated (i.e. measured Fe concentrations were below limit of quantification), all analysed species brought at least 1% of Fe RDI for all age classes (Table 8.3).

All analysed species were poor sources of Mn, as most of them brought less than 1% of Mn RDI for all three age classes (Table 8.3). However, the pink ear emperor, blacktip shark and scalloped hammerhead stood out by bringing between 1 and 2% of RDI for one or more age classes.

Concerning As, the PTI implemented by the JECFA was withdrawn in 2011 (JECFA 2011a). No other PTI was found in the literature, and it was thus not possible to include directly this trace element in the risk analysis, that is to calculate a %PTI and to attribute a risk category. However, in capture fisheries species, it has been reported that the main physicochemical form present is arsenobetaine, an organic form of As, while the main toxic forms are its inorganic forms (Molin *et al*. 2015). Thanks to the review of Uneyama *et al*. (2007) on the proportions of iAs in capture fisheries species, here it was possible to estimate iAs concentrations in Seychelles capture fisheries species (Table 8.4). Among all analysed species, the big blue octopus and crustacean species, which were among the species with the highest As concentrations, also had the highest iAs estimated concentrations (above or close to 1 $\mu g.g^{-1}$ ww), in spite of their lower iAs proportions (i.e. 2.2% in crustaceans and 4.2% in fish, Uneyama *et al*. 2007). Among the other species, 15 had estimated iAs concentrations comprised between 0.1 and 0.4 $\mu g.g^{-1}$ ww, and 34 species had estimated iAs concentrations below 0.1 $\mu g.g^{-1}$ ww.

Table 8.3. Percentage of recommended daily intake (RDI) covered by a daily Seychellois portion (156 g) of capture fisheries products from the Seychelles, presented as mean [CI95%]. Uncoloured cells indicate that one daily portion of the species brings less than 1% of RDI while coloured cells indicate the category in which the species was sorted; values used to sort species into categories are indicated in bold. Species for which a risk was identified are indicated by an asterisk. Very light green = Good supplement (1% < %RDI < 20%), light green = Good source (20% < %RDI < 75%) and green = Very good source (75% < %RDI). C = Children (2-13 years), YA = Young adults (14-18 years) and A = Adult women (> 18 years).

	Essential														Potentially essential
	Cu			Fe			Mn			Theoretically bioavailable Se		Zn			As
Species	C	YA	A	C	YA	A	C	YA	A	C	YA & A	C	YA	A	A
Octopuses															
Big blue octopus	15 [**8**-21]	20 [**17**-23]	17 [**15**-22]	2 [**1**-3]	2 [**2**-3]	2 [**1**-3]	0.4 [**0.2**-0.6]	0.7 [**0.6**-0.7]	0.7 [**0.6**-0.9]	58 [**36**-78]	67 [**54**-81]	24 [**20**-29]	27 [**26**-29]	26 [**24**-29]	33957 [**30317**-37598]
Crabs															
Spanner crab*	97 [**38**-161]	126 [**76**-177]	108 [**67**-175]	**1** [0-1]	1 [**1**-1]	1 [**1**-1]	0.2 [**0.1**-0.3]	0.3 [**0.3**-0.4]	0.3 [**0.3**-0.4]	118 [**69**-169]	137 [**102**-174]	55 [**40**-66]	62 [**56**-67]	59 [**52**-67]	65640 [**52019**-79262]
Spiny lobsters															
Longlegged spiny lobster	134 [**75**-181]	174 [**149**-199]	149 [**132**-197]	2 [**1**-4]	2 [**2**-3]	2 [**1**-3]	0.3 [**0.2**-0.5]	0.5 [**0.5**-0.6]	0.6 [**0.5**-0.8]	61 [**36**-88]	71 [**53**-90]	35 [**26**-42]	40 [**37**-43]	38 [**34**-43]	45259 [**39707**-50811]
Painted spiny lobster	112 [**59**-156]	145 [**118**-172]	124 [**105**-170]	2 [**1**-5]	3 [**2**-4]	3 [**1**-4]	0.4 [**0.2**-0.6]	0.7 [**0.6**-0.8]	0.7 [**0.6**-1.0]	57 [**31**-85]	66 [**46**-88]	26 [**20**-33]	30 [**26**-33]	28 [**24**-33]	46218 [**31635**-60801]
Pronghorn spiny lobster	140 [**82**-182]	182 [**163**-201]	155 [**145**-198]	2 [**1**-4]	3 [**2**-3]	3 [**1**-3]	0.4 [**0.2**-0.6]	0.7 [**0.6**-0.8]	0.7 [**0.7**-0.9]	61 [**37**-85]	71 [**55**-88]	41 [**31**-49]	47 [**44**-49]	45 [**40**-49]	75785 [**69041**-82529]
Goatfishes															
Dash-and-dot goatfish	4 [**2**-5]	5 [**4**-6]	4 [**4**-6]	2 [**1**-5]	3 [**2**-4]	**3** [0-4]	0.3 [**0.1**-0.6]	0.5 [**0.3**-0.7]	0.6 [**0.4**-0.9]	100 [**57**-145]	116 [**85**-150]	6 [**4**-7]	7 [**6**-7]	6 [**5**-7]	12060 [**7768**-16353]
Rosy goatfish	5 [**3**-6]	7 [**6**-7]	6 [**5**-7]	3 [**1**-7]	4 [**2**-5]	**4** [0-5]	0.5 [**0.3**-0.9]	0.9 [**0.7**-1.1]	0.9 [**0.8**-1.3]	88 [**50**-130]	103 [**74**-134]	4 [**3**-5]	5 [**5**-5]	5 [**4**-5]	3500 [**3308**-3692]
Parrotfishes															
Blue-barred parrotfish	6 [**3**-7]	7 [**7**-8]	6 [**6**-8]	1 [**1**-2]	2 [**1**-2]	2 [**1**-2]	0.5 [**0.2**-0.8]	0.8 [**0.6**-1.0]	0.8 [**0.6**-1.3]	94 [**46**-151]	109 [**68**-156]	5 [**3**-6]	6 [**5**-7]	6 [**5**-7]	1748 [**959**-2538]
Shoemaker spinefoot	5 [**3**-6]	6 [**5**-7]	5 [**4**-7]	2 [**1**-5]	3 [**2**-4]	3 [**1**-4]	0.3 [**0.1**-0.5]	0.5 [**0.4**-0.6]	0.5 [**0.4**-0.8]	53 [**28**-82]	62 [**42**-85]	6 [**3**-8]	7 [**5**-8]	6 [**5**-8]	272 [**220**-323]
Streamlined spinefoot	7 [**4**-9]	9 [**8**-10]	8 [**7**-10]	2 [**1**-4]	3 [**2**-3]	3 [**1**-3]	0.4 [**0.1**-1.0]	0.7 [**0.2**-1.2]	0.7 [**0.2**-1.4]	36 [**20**-54]	42 [**29**-55]	4 [**3**-5]	5 [**5**-5]	5 [**4**-5]	320 [**289**-351]

Table 8.3. Percentage of recommended daily intake (RDI) covered by a daily Seychellois portion (156 g) of capture fisheries products from the Seychelles, presented as mean [CI95%]. Uncoloured cells indicate that one daily portion of the species brings less than 1% of RDI while coloured cells indicate the category in which the species was sorted; values used to sort species into categories are indicated in bold. Species for which a risk was identified are indicated by an asterisk. Very light green = Good supplement (1% < %RDI < 20%), light green = Good source (20% < %RDI < 75%) and green = Very good source (75% < %RDI). C = Children (2-13 years), YA = Young adults (14-18 years) and A = Adult women (> 18 years). (continued)

	Essential														Potentially essential
	Cu			Fe			Mn			Theoretically bioavailable Se		Zn			As
Species	C	YA	A	C	YA	A	C	YA	A	C	YA & A	C	YA	A	A
Surgeonfishes															
Elongate surgeonfish	5 [**3**-7]	7 [**6**-8]	6 [**5**-7]	3 [**1**-6]	3 [**2**-5]	4 [**1**-5]	0.2 [**0.1**-0.4]	0.3 [**0.2**-0.5]	0.4 [**0.2**-0.6]	90 [**41**-149]	104 [**61**-154]	6 [**3**-9]	7 [**5**-9]	7 [**5**-9]	2574 [**110**-5038]
Emperors															
Blackeye emperor*	4 [**2**-6]	5 [**4**-7]	5 [**3**-7]	**2** [0-7]	**3** [0-5]	**3** [0-7]	0.2 [**0.1**-0.2]	0.3 [**0.3**-0.3]	0.3 [**0.3**-0.4]	373 [**219**-533]	434 [**326**-549]	6 [**4**-7]	7 [**6**-7]	7 [**6**-7]	2139 [**1582**-2696]
Blue-lined large-eye bream	5 [**2**-9]	7 [**4**-10]	6 [**4**-9]	3 [**1**-7]	4 [**2**-5]	4 [**1**-6]	0.1 [**0.1**-0.2]	0.2 [**0.2**-0.2]	0.2 [**0.2**-0.3]	204 [**110**-308]	237 [**164**-318]	7 [**4**-10]	7 [**5**-10]	7 [**5**-10]	2718 [**2102**-3334]
Pink ear emperor*	8 [**3**-13]	10 [**6**-14]	9 [**6**-14]	4 [**1**-13]	6 [**1**-10]	**6** [0-12]	0.6 [**0.1**-1.6]	1.0 [**0.1**-2.0]	**1.1** [0.1-2.4]	392 [**176**-660]	456 [**261**-681]	6 [**3**-10]	7 [**4**-10]	7 [**4**-10]	1080 [**606**-1554]
Slender emperor	6 [**4**-8]	8 [**7**-9]	7 [**6**-9]	3 [**1**-6]	4 [**3**-5]	4 [**1**-5]	0.2 [**0.1**-0.3]	0.3 [**0.2**-0.3]	0.3 [**0.2**-0.4]	114 [**67**-162]	132 [**100**-167]	5 [**4**-7]	6 [**5**-7]	6 [**5**-7]	3461 [**2986**-3936]
Sky emperor	6 [**4**-8]	8 [**7**-9]	7 [**6**-9]	3 [**1**-6]	4 [**3**-5]	4 [**1**-5]	0.2 [**0.1**-0.4]	0.4 [**0.2**-0.5]	0.4 [**0.2**-0.6]	140 [**87**-192]	163 [**129**-198]	6 [**4**-7]	6 [**6**-7]	6 [**5**-7]	6472 [**5396**-7549]
Smalltooth emperor	5 [**3**-6]	6 [**6**-7]	5 [**5**-7]	3 [**1**-6]	3 [**3**-4]	3 [**1**-4]	0.1 [**0.1**-0.2]	0.2 [**0.2**-0.2]	0.2 [**0.2**-0.3]	88 [**49**-131]	102 [**72**-135]	6 [**4**-7]	7 [**6**-7]	7 [**6**-7]	1542 [**1288**-1795]
Spangled emperor	6 [**3**-8]	8 [**7**-9]	7 [**6**-9]	5 [**1**-13]	6 [**3**-10]	**6** [0-11]	0.5 [**0.2**-0.9]	0.8 [**0.5**-1.1]	0.8 [**0.5**-1.4]	118 [**65**-176]	137 [**97**-182]	6 [**4**-7]	6 [**6**-7]	6 [**5**-7]	1400 [**943**-1858]
Yellowtail emperor	5 [**3**-7]	7 [**6**-8]	6 [**5**-8]	4 [**1**-10]	5 [**3**-7]	6 [**1**-8]	0.2 [**0.1**-0.4]	0.3 [**0.2**-0.5]	0.4 [**0.3**-0.6]	212 [**116**-320]	247 [**172**-330]	5 [**4**-7]	6 [**5**-7]	6 [**5**-7]	2963 [**2337**-3590]
Groupers															
Blacktip grouper	5 [**3**-6]	6 [**5**-7]	5 [**5**-6]	2 [**1**-4]	2 [**2**-3]	2 [**1**-3]	0.2 [**0.1**-0.3]	0.3 [**0.3**-0.4]	0.3 [**0.3**-0.4]	100 [**48**-161]	116 [**72**-167]	6 [**4**-8]	7 [**5**-8]	6 [**5**-8]	720 [**652**-789]
Brown-marbled grouper	3 [**2**-5]	4 [**4**-5]	4 [**3**-5]	**3** [0-9]	**3** [0-7]	**3** [0-9]	0.2 [**0.1**-0.2]	0.3 [**0.2**-0.3]	0.3 [**0.3**-0.4]	92 [**29**-177]	107 [**44**-183]	8 [**3**-15]	9 [**4**-15]	9 [**4**-15]	7949 [**2166**-13732]
Brownspotted grouper	4 [**3**-6]	6 [**5**-6]	5 [**5**-6]	2 [**1**-5]	3 [**2**-4]	3 [**1**-4]	0.3 [**0.1**-0.4]	0.5 [**0.4**-0.5]	0.5 [**0.5**-0.6]	116 [**76**-151]	135 [**113**-156]	6 [**4**-7]	7 [**6**-7]	6 [**6**-7]	614 [**427**-801]
Eightbar grouper	4 [**2**-6]	5 [**4**-6]	4 [**3**-6]	3 [**1**-8]	4 [**3**-6]	4 [**1**-6]	0.2 [**0.1**-0.3]	0.3 [**0.3**-0.4]	0.3 [**0.3**-0.4]	97 [**60**-133]	113 [**89**-137]	8 [**5**-10]	8 [**6**-10]	8 [**6**-10]	1395 [**1036**-1754]

Table 8.3. Percentage of recommended daily intake (RDI) covered by a daily Seychellois portion (156 g) of capture fisheries products from the Seychelles, presented as mean [CI95%]. Uncoloured cells indicate that one daily portion of the species brings less than 1% of RDI while coloured cells indicate the category in which the species was sorted; values used to sort species into categories are indicated in bold. Species for which a risk was identified are indicated by an asterisk. Very light green = Good supplement (1% < %RDI < 20%), light green = Good source (20% < %RDI < 75%) and green = Very good source (75% < %RDI). C = Children (2-13 years), YA = Young adults (14-18 years) and A = Adult women (> 18 years). (continued)

	Essential														Potentially essential
	Cu			Fe			Mn			Theoretically bioavailable Se		Zn			As
Species	C	YA	A	C	YA	A	C	YA	A	C	YA & A	C	YA	A	A
Honeycomb grouper	3 [**1**-5]	3 [**2**-5]	3 [**2**-5]	3 [**1**-8]	4 [**2**-6]	**4** [0-6]	0.3 [**0.1**-0.7]	0.4 [**0.1**-0.8]	0.5 [**0.1**-1.0]	62 [**20**-117]	72 [**30**-121]	6 [**4**-8]	6 [**5**-8]	6 [**5**-8]	2222 [**680**-3764]
Longspine grouper	6 [**2**-10]	7 [**3**-11]	6 [**3**-11]	2 [**1**-4]	3 [**2**-3]	3 [**1**-3]	0.2 [**0.1**-0.5]	0.4 [**0.2**-0.6]	0.4 [**0.2**-0.7]	73 [**47**-97]	85 [**70**-100]	7 [**3**-11]	8 [**5**-11]	7 [**4**-11]	494 [**489**-499]
Peacock hind	5 [**2**-7]	6 [**4**-7]	5 [**4**-7]	4 [**2**-8]	5 [**4**-6]	5 [**2**-6]	0.3 [**0.1**-0.4]	0.4 [**0.4**-0.5]	0.5 [**0.4**-0.7]	101 [**57**-149]	118 [**85**-154]	7 [**5**-9]	8 [**7**-9]	8 [**6**-9]	550 [**388**-712]
Tomato hind	5 [**2**-7]	7 [**5**-8]	6 [**4**-8]	3 [**1**-7]	3 [**2**-5]	**3** [0-6]	0.1 [**0.1**-0.2]	0.2 [**0.1**-0.2]	0.2 [**0.1**-0.3]	104 [**66**-141]	121 [**97**-146]	6 [**3**-8]	6 [**4**-8]	6 [**4**-8]	922 [**685**-1158]
White-blotched grouper	5 [**3**-6]	6 [**6**-7]	5 [**5**-7]	2 [**1**-4]	3 [**2**-3]	3 [**1**-3]	0.2 [**0.1**-0.4]	0.4 [**0.3**-0.5]	0.4 [**0.3**-0.6]	120 [**72**-170]	140 [**107**-175]	7 [**4**-9]	8 [**6**-9]	7 [**6**-9]	4482 [**2729**-6234]
Yellow-edged lyretail	5 [**3**-6]	6 [**5**-7]	5 [**5**-6]	4 [**1**-8]	5 [**4**-6]	5 [**2**-6]	0.3 [**0.1**-0.4]	0.4 [**0.3**-0.5]	0.5 [**0.4**-0.6]	123 [**81**-161]	144 [**120**-166]	7 [**5**-8]	8 [**7**-8]	7 [**6**-8]	603 [**468**-737]
Trevallies															
Bigeye trevally	7 [**4**-10]	9 [**7**-11]	8 [**6**-11]	9 [**3**-21]	11 [**7**-16]	12 [**2**-17]	0.2 [**0.1**-0.5]	0.3 [**0.1**-0.6]	0.3 [**0.1**-0.7]	134 [**42**-259]	156 [**63**-267]	11 [**7**-15]	12 [**9**-15]	12 [**9**-15]	1043 [**587**-1500]
Bludger	9 [**5**-11]	11 [**10**-12]	10 [**9**-12]	7 [**3**-13]	9 [**8**-10]	9 [**4**-9]	0.4 [**0.2**-0.5]	0.6 [**0.5**-0.7]	0.6 [**0.5**-0.8]	109 [**59**-165]	127 [**88**-170]	9 [**6**-11]	10 [**9**-11]	9 [**8**-11]	1748 [**1469**-2027]
Bluefin trevally	6 [**3**-9]	8 [**6**-10]	7 [**6**-10]	4 [**2**-9]	5 [**4**-7]	6 [**2**-6]	0.3 [**0.1**-0.5]	0.5 [**0.4**-0.6]	0.5 [**0.4**-0.7]	70 [**39**-105]	82 [**58**-108]	8 [**6**-10]	9 [**8**-10]	9 [**7**-10]	397 [**337**-457]
Golden trevally	9 [**3**-15]	11 [**6**-17]	10 [**6**-16]	6 [**2**-14]	7 [**4**-10]	7 [**1**-11]	0.3 [**0.1**-0.5]	0.5 [**0.4**-0.6]	0.5 [**0.4**-0.7]	74 [**40**-112]	86 [**59**-116]	7 [**5**-9]	8 [**6**-9]	8 [**6**-9]	995 [**564**-1426]
Malabar trevally	6 [**4**-8]	8 [**8**-8]	7 [**7**-8]	4 [**1**-8]	5 [**3**-6]	5 [**1**-6]	0.2 [**0.1**-0.4]	0.4 [**0.3**-0.4]	0.4 [**0.3**-0.5]	74 [**32**-127]	86 [**48**-131]	8 [**5**-9]	9 [**7**-10]	8 [**7**-10]	1514 [**1356**-1671]
Yellowspotted trevally	6 [**4**-8]	8 [**8**-9]	7 [**7**-9]	5 [**2**-9]	6 [**4**-7]	6 [**2**-7]	0.5 [**0.2**-0.7]	0.7 [**0.7**-0.8]	0.8 [**0.8**-1.0]	114 [**69**-160]	133 [**102**-165]	8 [**6**-9]	9 [**8**-9]	8 [**7**-9]	1015 [**877**-1153]
Snappers															
Bigeye snapper	7 [**4**-8]	**9**	8 [**6**-9]	1 [**1**-2]	**2**	2 [**1**-3]	0.2 [**0.1**-0.3]	**0.3**	0.3 [**0.3**-0.4]	97 [**67**-122]	113 [**99**-126]	17 [**14**-19]	**19**	18 [**18**-19]	**438**
Deepwater longtail red snapper	5 [**3**-7]	7 [**5**-8]	6 [**5**-8]	1 [**1**-3]	2 [**1**-2]	2 [**1**-2]	0.2 [**0.1**-0.3]	0.3 [**0.2**-0.3]	0.3 [**0.2**-0.4]	113 [**73**-149]	132 [**109**-154]	5 [**4**-6]	5 [**5**-6]	5 [**5**-6]	692 [**567**-817]

Table 8.3. Percentage of recommended daily intake (RDI) covered by a daily Seychellois portion (156 g) of capture fisheries products from the Seychelles, presented as mean [CI95%]. Uncoloured cells indicate that one daily portion of the species brings less than 1% of RDI while coloured cells indicate the category in which the species was sorted; values used to sort species into categories are indicated in bold. Species for which a risk was identified are indicated by an asterisk. Very light green = Good supplement (1% < %RDI < 20%), light green = Good source (20% < %RDI < 75%) and green = Very good source (75% < %RDI). C = Children (2-13 years), YA = Young adults (14-18 years) and A = Adult women (> 18 years). (continued)

	Essential														Potentially essential
	Cu			Fe			Mn			Theoretically bioavailable Se		Zn			As
Species	C	YA	A	C	YA	A	C	YA	A	C	YA & A	C	YA	A	A
Emperor red snapper	4 [**2**-5]	5 [**5**-6]	5 [**4**-6]	2 [**1**-4]	3 [**2**-3]	3 [**1**-3]	0.2 [**0.1**-0.3]	0.3 [**0.2**-0.4]	0.3 [**0.3**-0.5]	97 [**64**-127]	113 [**94**-131]	6 [**4**-7]	7 [**6**-7]	7 [**6**-7]	3011 [**2691**-3331]
Green jobfish	6 [**4**-7]	8 [**7**-8]	7 [**6**-8]	3 [**1**-5]	4 [**3**-4]	4 [**2**-4]	0.3 [**0.2**-0.5]	0.6 [**0.5**-0.6]	0.6 [**0.6**-0.7]	124 [**81**-163]	144 [**120**-168]	6 [**4**-7]	7 [**6**-7]	6 [**6**-7]	2667 [**2425**-2910]
Humpback red snapper	8 [**5**-11]	11 [**10**-12]	9 [**9**-12]	7 [**2**-14]	8 [**5**-11]	8 [**2**-11]	0.2 [**0.1**-0.3]	0.3 [**0.3**-0.4]	0.4 [**0.3**-0.5]	99 [**62**-136]	116 [**92**-140]	7 [**5**-9]	8 [**7**-9]	8 [**7**-9]	3948 [**2513**-5384]
Humphead snapper	5 [**3**-8]	7 [**6**-9]	6 [**5**-8]	5 [**2**-11]	6 [**5**-8]	6 [**2**-8]	0.3 [**0.1**-0.7]	0.5 [**0.2**-0.8]	0.5 [**0.2**-1.0]	143 [**84**-205]	167 [**125**-211]	7 [**4**-10]	8 [**6**-10]	7 [**5**-10]	7441 [**4011**-10871]
Two-spot red snapper	5 [**3**-7]	7 [**6**-8]	6 [**6**-8]	4 [**2**-8]	5 [**4**-6]	5 [**2**-6]	0.2 [**0.1**-0.4]	0.4 [**0.3**-0.5]	0.4 [**0.3**-0.6]	126 [**81**-168]	147 [**120**-173]	6 [**4**-7]	6 [**6**-7]	6 [**6**-7]	4474 [**3902**-5046]
Barracudas															
Pickhandle barracuda	5 [**3**-7]	7 [**5**-8]	6 [**5**-8]	4 [**2**-8]	5 [**4**-6]	5 [**2**-6]	0.5 [**0.2**-0.9]	0.8 [**0.6**-1.0]	0.8 [**0.6**-1.3]	85 [**53**-115]	98 [**79**-118]	6 [**4**-8]	7 [**6**-8]	7 [**6**-8]	1354 [**1127**-1580]
Mackerels															
Indian mackerel	9 [**5**-12]	12 [**11**-13]	10 [**10**-13]	6 [**3**-11]	7 [**6**-8]	7 [**4**-7]	0.3 [**0.2**-0.5]	0.5 [**0.5**-0.6]	0.5 [**0.5**-0.7]	147 [**90**-204]	171 [**133**-210]	9 [**6**-13]	11 [**8**-13]	10 [**8**-13]	1685 [**1113**-2257]
Tunas															
Dogtooth tuna	7 [**4**-9]	9 [**7**-10]	7 [**7**-10]	3 [**1**-8]	4 [**2**-6]	**4** [0-6]	0.3 [**0.1**-0.5]	0.5 [**0.3**-0.7]	0.5 [**0.4**-0.8]	190 [**62**-363]	222 [**93**-374]	8 [**6**-10]	9 [**8**-10]	9 [**7**-10]	712 [**530**-894]
Little tunny	10 [**4**-16]	13 [**9**-17]	11 [**8**-17]	11 [**5**-19]	14 [**13**-14]	14 [**7**-12]	0.5 [**0.2**-1.0]	0.9 [**0.6**-1.2]	0.9 [**0.7**-1.4]	100 [**57**-145]	116 [**85**-150]	9 [**6**-11]	10 [**9**-11]	9 [**8**-11]	1728 [**1384**-2072]
Sharks															
Blacktip shark	5 [**3**-6]	**7**	6 [**5**-7]	3 [**2**-6]	**4**	4 [**2**-7]	0.6 [**0.3**-0.8]	**0.9**	**1.0** [0.8-1.1]	208 [**142**-261]	242 [**211**-269]	10 [**8**-11]	**11**	**11**	**2129**
Great hammerhead	3 [**2**-3]	**3**	3 [**2**-3]	2 [**1**-3]	**2**	2 [**1**-4]	0.4 [**0.2**-0.5]	**0.6**	0.6 [**0.5**-0.7]	33 [**22**-41]	38 [**33**-42]	5 [**4**-6]	**6**	5 [**5**-6]	**4044**
Grey reef shark	4 [**3**-5]	**6**	5 [**4**-6]	1 [**1**-2]	**2**	2 [**1**-3]	0.4 [**0.2**-0.5]	**0.6**	0.6 [**0.5**-0.7]	128 [**87**-160]	149 [**130**-165]	5 [**4**-6]	**6**	6 [**5**-6]	**4376**
Scalloped hammerhead	5 [**3**-6]	**6**	5 [**5**-6]	2 [**1**-3]	2 [**2**-2]	2 [**1**-2]	0.8 [**0.4**-1.2]	1.4 [**1.2**-1.5]	1.5 [**1.4**-1.9]	231 [**122**-355]	269 [**181**-367]	7 [**4**-9]	8 [**6**-9]	7 [**6**-9]	7323 [**6010**-8636]

Table 8.3. Percentage of recommended daily intake (RDI) covered by a daily Seychellois portion (156 g) of capture fisheries products from the Seychelles, presented as mean [CI95%]. Uncoloured cells indicate that one daily portion of the species brings less than 1% of RDI while coloured cells indicate the category in which the species was sorted; values used to sort species into categories are indicated in bold. Species for which a risk was identified are indicated by an asterisk. Very light green = Good supplement (1% < %RDI < 20%), light green = Good source (20% < %RDI < 75%) and green = Very good source (75% < %RDI). C = Children (2-13 years), YA = Young adults (14-18 years) and A = Adult women (> 18 years). (continued)

	Essential														Potentially essential
	Cu			Fe			Mn			Theoretically bioavailable Se		Zn			As
Species	C	YA	A	C	YA	A	C	YA	A	C	YA & A	C	YA	A	A
Spinner shark	5 [**3**-5]	**6**	5 [**4**-6]	**1** [0-1]	**1**	1 [**1**-2]	0.4 [**0.2**-0.6]	**0.7**	0.7 [**0.6**-0.9]	68 [**46**-85]	79 [**69**-88]	5 [**4**-5]	**5**	5 [**5**-5]	**7733**
Spot-tail shark	3 [**2**-3]	**3**	3 [**2**-3]	ND	ND	ND	0.5 [**0.3**-0.6]	**0.7**	0.8 [**0.6**-0.9]	104 [**71**-131]	121 [**106**-135]	6 [**5**-7]	**7**	6 [**6**-7]	**9385**
Tiger shark	6 [**4**-7]	**8**	7 [**5**-8]	2 [**1**-3]	**2**	3 [**1**-4]	0.4 [**0.2**-0.5]	**0.6**	0.7 [**0.5**-0.8]	33 [**22**-41]	38 [**33**-43]	8 [**7**-9]	**9**	9 [**8**-9]	**4108**
Billfishes															
Swordfish	6 [**3**-8]	8 [**7**-9]	6 [**6**-8]	3 [**1**-6]	4 [**3**-5]	4 [**2**-4]	0.2 [**0.1**-0.2]	0.3 [**0.2**-0.3]	0.3 [**0.2**-0.4]	100 [**61**-139]	117 [**91**-143]	11 [**8**-14]	13 [**12**-14]	12 [**11**-14]	964 [**891**-1036]

Table 8.4. Estimated concentrations of inorganic As (iAs, $\mu g.g^{-1}$ ww), calculated from measured total As concentrations using the estimated proportions of iAs in various capture fisheries species from Uneyama *et al*. (2007).

Species	Estimated iAs concentrations
Octopuses	
Big blue octopus	1.097 ± 0.247
Crabs	
Spanner crab	1.111 ± 0.263
Spiny lobsters	
Longlegged spiny lobster	0.766 ± 0.318
Painted spiny lobster	0.782 ± 0.488
Pronghorn spiny lobster	1.283 ± 0.399
Goatfishes	
Dash-and-dot goatfish	0.390 ± 0.158
Rosy goatfish	0.113 ± 0.005
Parrotfishes	
Blue-barred parrotfish	0.056 ± 0.041
Rabbitfishes	
Shoemaker spinefoot	0.009 ± 0.003
Streamlined spinefoot	0.010 ± 0.002
Surgeonfishes	
Elongate surgeonfish	0.083 ± 0.099
Emperors	
Blackeye emperor	0.069 ± 0.013
Blue-lined large-eye bream	0.088 ± 0.023
Pink ear emperor	0.035 ± 0.014
Slender emperor	0.112 ± 0.033
Sky emperor	0.209 ± 0.081
Smalltooth emperor	0.050 ± 0.013
Spangled emperor	0.045 ± 0.028
Yellowtail emperor	0.096 ± 0.037
Groupers	
Blacktip grouper	0.023 ± 0.002
Brown-marbled grouper	0.257 ± 0.135
Brownspotted grouper	0.020 ± 0.027
Eightbar grouper	0.045 ± 0.012
Honeycomb grouper	0.072 ± 0.051
Longspine grouper	0.016 ± 0.001
Peacock hind	0.018 ± 0.017
Tomato hind	0.030 ± 0.015

Species	Estimated iAs concentrations
Groupers	
White-blotched grouper	0.145 ± 0.135
Yellow-edged lyretail	0.019 ± 0.014
Trevallies	
Bigeye trevally	0.034 ± 0.021
Bludger	0.056 ± 0.023
Bluefin trevally	0.013 ± 0.003
Golden trevally	0.032 ± 0.019
Malabar trevally	0.049 ± 0.004
Yellowspotted trevally	0.033 ± 0.014
Snappers	
Bigeye snapper	0.014
Deepwater longtail red snapper	0.022 ± 0.007
Emperor red snapper	0.097 ± 0.047
Green jobfish	0.086 ± 0.042
Humpback red snapper	0.128 ± 0.095
Humphead snapper	0.240 ± 0.126
Two-spot red snapper	0.145 ± 0.071
Barracudas	
Pickhandle barracuda	0.044 ± 0.019
Mackerels	
Indian mackerel	0.054 ± 0.039
Tunas	
Dogtooth tuna	0.023 ± 0.008
Little tunny	0.056 ± 0.013
Sharks	
Blacktip shark	0.069
Great hammerhead	0.131
Grey reef shark	0.141
Scalloped hammerhead	0.237 ± 0.087
Spinner shark	0.250
Spot-tail shark	0.303
Tiger shark	0.133
Billfishes	
Swordfish	0.031 ± 0.014

In regards of these results on risk-benefit of Seychelles capture fisheries products consumption in Seychellois diet, this chapter thus show the importance of varying capture fisheries species consumption in diets, and especially in capture fisheries resources-based diets.

Results showed than no species had the highest concentration for all essential trace elements, suggesting that each species has its own benefit and that the best way to tackle micronutrient deficiency is to have a varied diet, even among capture fisheries food items. This is all the more true in case of a seafood-based diet, for which seafood, and especially capture fisheries products, are the main food source for micronutrients (Hicks *et al*. 2019). In addition, results of this chapter showed that some species with very high concentrations of a non-essential trace element also had very high concentrations of one or more essential trace element(s). The spanner crab was the best example, as it was a species associated with a high risk of Cd excess, while it was a good source of Cu, Se and Zn. Another example was the pink ear emperor, which was associated with a risk of Cd and Se excess, but which was also among the 3 species to bring more than 1% of Mn RDI to adult women. In such situation, stopping consumption of such species is often not the best solution, either because the species contains high or very high levels of one or more essential trace element(s), or because the species is among the most affordable and/or most consumed species in local diets. A trade-off is then necessary to keep eating these species but to avoid excess, for example by reducing the portion weight that is daily consumed.

8.3.3. Need to fill in data gaps to better assess trace element intake in Seychellois diet

This chapter allowed to make a first assessment of risk-benefit analysis through capture fisheries product consumption in Seychellois diet. Although this gives baseline indications for a population with a major reliance to capture fisheries resources, knowledge about dietary habits and morphometric parameters of all age categories in Seychellois population needs to be improved. It was especially difficult to find data related to the dietary habits of children and young adults, and portion weights estimated here may not reflect the real capture fisheries products consumption for these age categories. In addition, if detailed morphometric data were found for children and young adults in the Seychelles (Marques-Vidal *et al*. 2008), no data were found for adult women regardless of their status (i.e. non-pregnant, pregnant or lactating). Thus, here, the use of estimates for portion weights and individual weights may have led to a slight underestimation or overestimation of the benefit, but also to an underestimation of the risk.

Although capture fisheries resources contains high levels of some trace elements, either essential, potentially essential or non-essential, these trace elements are also present in other food items (Navarro-Alarcon and Cabrera-Vique 2008; Gupta and Gupta 2014). As an example, beside capture fisheries resources, Se was found to be in high concentrations in bread, red meat, pork meat and eggs in some countries, and in plants grown in Se-rich soils (Navarro-Alarcon and Cabrera-Vique 2008; Gupta and Gupta 2014). Here, the possible dietary interaction with other food items was taken into account by calculating the maximum weight to not exceed for 90% of the PTI for each trace element and each species for which there was a risk of toxicity. However, this threshold was arbitrary chosen in order to keep a margin of error of 10% and was not calculated by using data on Seychellois global diet. As trace element levels in food items seems to be country-dependant, it is necessary to improve knowledge on (1) Seychellois global diet and (2) trace element content in all their food items.

Lastly, capture fisheries resources also contain other essential nutrients (e.g. fatty acids, amino acids and vitamins), as well as toxic contaminants (e.g. persistent organic pollutants) that need to be investigated and taken into account for a full risk-benefit analysis.

8.4. CHAPTER HIGHLIGHTS

Chap. 6 – Main findings

- **Toxicity risk** through feeding on Seychelles capture fisheries products is only related to **Cd in two species** (spanner crab and pink ear emperor), while there is a **risk of excess of Se** for two species (blackeye emperor and pink ear emperor). **All other species are safe to eat**, regardless of the age group or adult women status.
- **All analysed species** can be considered as **good supplement** (1 to 20% of RDI covered by 1 portion) of **Cu, Fe and Zn**, and as **good source** (20 to 75% of RDI covered by 1 portion) **to very good source** (more than 75% of RDI covered by 1 portion) of **Se and As**. **Crustaceans** were **particularly good sources of Cu and Zn**.
- This chapter also showed the **importance of varying capture fisheries food items in a capture fisheries resources-based diet** in order **to stay healthy**.

9. GENERAL DISCUSSION

Content

With the rapid growth of the global population, food security, including food quantity and quality, has become one of the biggest challenges of the 21st century (United Nations 2019). The fight against malnutrition, like micronutrient deficiency, is thus one of the focuses of the UN sustainable development goals (United Nations 2015). This question is all the more important in SIDS like the Seychelles, as they are highly reliant on marine resources for local subsistence due to their particular geographical features (i.e. small land size, insularity and remoteness) (Briguglio 1995). If seafood is recognised as a key food type to insure healthy diets, due to its high essential fatty acid and high essential trace element contents (Figueras *et al*. 2011; Lu *et al*. 2011; Gupta and Gupta 2014), it also contains non-essential trace elements that can cause adverse effects on human health if present in too high concentrations (Bosch *et al*. 2016). As capture fisheries resources are generally the main source of protein and micronutrients in SIDS populations' diets (Weichselbaum *et al*. 2013; Hicks *et al*. 2019), this makes them particularly vulnerable to non-essential trace element exposure. In combination with fishing pressure that already affect the availability of some capture fisheries species, climate change could alter the availability of many other species by altering their population dynamics (Myers *et al.* 2017). Climate change also affects trace element bioaccumulation dynamics in marine food webs, and thus influences trace element concentrations in marine capture fisheries resources (Myers *et al*. 2017). It is thus necessary to better understand current fisheries populations' dynamics and to better understand current trace element bioaccumulation processes to better anticipate potential alterations of capture fisheries resources supply and of trace element profiles in these resources. By decreasing the availability of some capture fisheries species, and/or by decreasing essential trace element concentrations or increasing non-essential trace element concentrations, such alterations could have major consequences on the health of SIDS populations. There have been a growing attention of governments and of the scientific community on these topics in the recent years, with the development of studies on the risk and benefit of capture fisheries resources consumption, in terms of trace element content (e.g. Gladyshev *et al.* 2009; Sirot *et al.* 2012; Ricketts *et al*. 2019). However, studies on the trace element bioaccumulation processes in these resources, and particularly in the Indian Ocean, remain scarce (Kojadinovic *et al*. 2007; Chouvelon *et al.* 2017).

The main objectives of this PhD thesis were thus to characterise essential, potentially essential and non-essential trace element concentrations in Seychelles capture fisheries

resources, but also to bring a better understanding of trace element bioaccumulation processes in Seychelles food webs. This thus brings a baseline for the Seychelles, but also for other SIDS in tropical and subtropical areas, as they share common features in terms of habitat, species composition and ecosystem dynamics.

9.1. TRACE ELEMENT BIOACCUMULATION IN SEYCHELLES FOOD WEBS AND CONSEQUENCES FOR SEYCHELLOIS CAPTURE FISHERIES RESOURCES-BASED DIETS: COMPLEMENTARY INFORMATION FROM DIFFERENT SCALES

As stated in the general introduction, the equilibrium between absorption and excretion is fundamentally important to understand trace element bioaccumulation in marine consumers, as this equilibrium will govern bioaccumulation (i.e. when absorption exceeds excretion), bioreduction and/or biodilution (i.e. when excretion exceeds absorption), or constant concentrations (i.e. when equilibrium is reached between absorption and excretion) (Hodson 1988). Many intrinsic or extrinsic factors have been identified to influence this equilibrium in marine consumers (section 1.2), and among these factors, many scales of influence could be identified. Some factors, like the type and efficiency of detoxifying and excretion mechanisms, are species-dependent (e.g. Rainbow 1998, 2007), while others like diet or trophic position are age- and/or size-dependent (e.g. Cocheret De La Morinière *et al*. 2003; Young *et al.* 2006; Ménard *et al*. 2007; Wells *et al.* 2008), and thus have an influence at the intra-specific level. Extrinsic factors like natural and/or anthropogenic trace element inputs in the ocean will also influence trace element concentrations and bioavailability, and the subsequent bioaccumulation by organisms from a given area (Raimundo *et al*. 2013; Le Croizier *et al*. 2016), thus having an impact at the population level. In light of these elements, it became evident that all scales (i.e. population level, interspecific or intraspecific) were necessary to reconstruct a global vision of trace element bioaccumulation in Seychelles food webs. The first step was thus to try to identify patterns of bioaccumulation in the 54 capture fisheries species analysed here. Thanks to their different physiology, biology and trophic ecology, these 54 species constituted an advanced image of the Seychelles system, which allowed a first highlight of factors governing trace element bioaccumulation in this global system. Then, within each identified pattern, the choice of a model species allowed for the identification of factors influencing trace element bioaccumulation at the intraspecific level.

Among all ecosystems, the **vertical feeding habitat had a major influence on trace element bioaccumulation** in capture fisheries species from the Seychelles. Although this was partly attributed to the trophic proximity of species with reservoirs of trace elements like sediments, as previously shown in other areas by Abdallah (2008) and Velusamy *et al*. (2014), **physiology, trophic position, diet composition and dietary habits also played an important role**. This influence of other factors was particularly well illustrated by the distribution of demersal teleost fish species in two different groups, and by the distribution of the big blue octopus (i.e. benthic cephalopod) and of all benthic teleost fishes among these two groups. In addition, it was **particularly difficult to distinguish the factor(s) responsible for some differences**, like for benthic crustaceans, for which taxonomy, vertical habitat and/or diet type (i.e. benthivore and scavenger) could have significantly influenced trace element bioaccumulation.

In benthic decapod crustaceans, the particularly high concentrations of As, Cu and Zn were first attributed to their metabolism (i.e. preferential accumulation) and, to a lesser extent, to their diet composition. In particular, As was thought to bioaccumulate through preferential accumulation under the arsenobetaine form, but also through feeding on prey with particularly high As concentrations, like macroalgae and bivalve filter-feeders. However, Chapter 2 showed that As bioaccumulation in spiny lobsters was associated with a higher level of carnivory and thus a higher trophic position, while macroalgae are primary producers and bivalve filter-feeders generally have a low trophic position (Wilson *et al.* 2009). In this case, the complex diet of spiny lobsters may have played a role in confounding results. In these species, lower trophic positions were associated with higher feeding on macroalgae, while spiny lobsters with higher trophic positions fed more on decapod crustaceans (i.e. hermit crabs) and echinoderms (i.e. sea urchins) (Sardenne *et al.* 2021). By feeding more on decapod crustaceans, known to preferentially retain As under the bioavailable arsenobetaine form (Neff 2002a; Khokiattiwong *et al.* 2009), and at the same time on sea urchin, which have relatively high $\delta^{15}N$ values compared to other potential prey (Sardenne *et al.* 2021), some spiny lobsters would thus have a higher As contamination level associated with a higher trophic position. In addition, for spiny lobsters and more generally decapod crustaceans, no data on the assimilation efficiency of As from various prey, including primary producers *vs* animal prey, were found in the literature. Yet, it is possible that the assimilation efficiency of As from macroalgae is lower than from animal prey, even though concentrations may be particularly high in primary producers when waters are phosphate-depleted (Littler *et al.* 1991; Metian *et al.* 2008; Hédouin *et al.* 2009;

Chapter 1). This would be consistent with spiny lobsters with a lower trophic position feeding more on macroalgae than their counterparts (Sardenne *et al*. 2021) and having lower As concentrations. This would also be consistent with the known diet of the spanner crab, which can feed on a large diversity of prey, including decapod crustaceans (i.e. other crabs) (Baylon and Tito 2012).

Chapter 2 also confirmed the positive relationship between Zn concentrations and size in decapod crustaceans, suggesting higher physiological needs with growth. However, Chapter 2 also brought complementary information on trace element bioaccumulation in spiny lobsters by allowing the inclusion of more trace elements in analysis of this chapter than of Chapter 1. Pb concentrations, for example, were often below LOQ when considering all analysed species, while they could be measured in almost all spiny lobster individuals (detection frequency of 69% for all analysed species *vs* 99% in spiny lobsters, Appendix 2.1). In spiny lobsters, Pb bioaccumulation was associated with feeding on detritus-feeders like polychaetes. Although Chapter 1 did not allow a clear discrimination among decapod crustacean species in terms of trace element concentrations, Pb concentrations seemed to be higher in spiny lobsters than in the spanner crab (Appendix 8.1), which was not reported to feed on polychaetes (Baylon and Tito 2012). In benthic food webs, this thus highlights the importance of detritivores in processes of trace element trophic transfer from reservoirs (i.e. sediments) to higher trophic levels. This also highlights the importance of the trophic proximity of marine consumers to these reservoirs of trace elements in understanding difference of trace element bioaccumulation among the different marine compartments.

In Chapter 1, interspecific trace element bioaccumulation patterns did not seem to be influenced by the trophic group (i.e. herbivores *vs* carnivores) or the diet type. However, diet composition did have an effect, and especially the presence in the diet of one or more "super-vector" prey, that is a prey which is a particularly good vector of a trace element for upper trophic levels. This was first illustrated above in the diet of spiny lobsters, with the examples of As being highly transferred by decapod crustaceans (due to high arsenobetaine content) and/or bivalves, and of Pb being highly transferred by polychaetes. This was also observed in the diet of swordfish (Chapter 4), which tended to accumulate higher concentrations of Cd when feeding more on cephalopods, previously identified as vectors of this element for top predators (Bustamante *et al*. 1998; Lischka *et al*. 2018). Trace element assimilation efficiency was also an

important factor to take into account for swordfish, as their assimilation efficiency seemed to differ between their prey (i.e. fish *vs* cephalopods; Wang *et al.* 2012). These results show the **importance to consider both the concentrations and the physicochemical forms** of the trace element, **both driving the assimilation efficiency** from a prey type by a given consumer, to better understand trace element flow in a food web.

The clustering in Chapter 1 also did not seem to be influenced by habitat type. However Chapter 2 showed that the bioaccumulation of some trace elements in spiny lobsters was influenced by reef type and by coral reef degradation (i.e. bleaching). However, in this case, habitat type and quality influenced spiny lobsters' diet which, in turn, influenced their trace element bioaccumulation. Thus, rather than a direct effect of habitat linked to diet composition, it is **the suitability of the habitat** that **is questioned**. Although spiny lobsters feed in both rocky and coral reefs, Sabino *et al.* (2021) showed that coral reefs supported a more varied diet in the three spiny lobsters species, as shown by their higher dietary overlap in rocky reefs. They also hypothesised that the degradation of coral reefs linked to bleaching events altered prey availability and thus spiny lobsters' diet composition. Added to the effects on trace element bioaccumulation in spiny lobsters observed in Chapter 2, and in a context of climate change that will weaken coral reefs on the long term (Hoegh-Guldberg 2011; Obura *et al.* 2017), results of this thesis raise several questions: **(1) are rocky reefs alone sufficient to support a suitable diet for spiny lobsters, in order for them to acquire enough essential trace elements for their metabolism and maintenance (i.e. reproductive ability) and to limit non-essential trace element bioaccumulation**, and thus **(2) will spiny lobsters' essential and non-essential trace element concentrations be altered by climate change-induced habitat degradation?** More largely, **will climate change affect the quality of Seychelles coastal ecosystems to the point that it has an effect** on the trace element supply, health and maintenance of coastal reef capture fisheries species, and thus **on essential trace element supply to human capture fisheries resources-based diets?**

Among all factors identified to have an effect on trace element bioaccumulation in Seychelles food webs, **size was prevalent**, affecting the bioaccumulation of almost all trace elements analysed here, either **directly or indirectly**. Unsurprisingly, Hg bioaccumulation was positively correlated with size and thus age for all model species, which was previously shown in other marine consumers (e.g. Chouvelon *et al.* 2011, 2014, 2017; Goutte *et al.* 2015). While

size did not significantly improve the model explaining log-transformed Hg concentrations in swordfish (Chapter 5), these concentrations were positively correlated with swordfish size (Appendix 7.1). In addition, among all analysed species, those from Group 3 had the highest Hg and Se concentrations. If this was mainly attributed to a difference in trophic position, with species from Group 3 having the highest $\delta^{15}N$ values, it is also possible that size played a direct role on Hg bioaccumulation. Indeed, although it is difficult to compare directly crustaceans, cephalopods, teleosts and elasmobranchs in terms of size, species from Group 3 did have particularly large sizes compared to other groups (i.e. smallest common length for blacktip shark with 150 cm total length, to largest common length for tiger shark with 500 cm, Froese and Pauly 2020). Thus, by being able to eat much larger prey that the other capture fisheries species, species from Group 3 would have bioaccumulated higher concentrations of Hg. Due to their high Hg concentrations, Se bioaccumulation would have followed, as suggested in Chapter 1. This hypothesis is supported by results of Chapter 4 which show a potential of co-accumulation between these trace elements.

For the other trace elements analysed here, the effects of size were mostly due to interaction with other factors like physiology and trophic ecology. Apart from rare exceptions, size is known to structure food webs regardless of the habitat type, because a larger predator can eat a larger prey, which led to the theory that larger predators have a higher trophic position (Jennings *et al*. 2000). In this case, Hg was a good example to show the interaction effect between size and trophic position, as it tends to bioaccumulate with size and to biomagnify (e.g. Kojadinovic *et al*. 2007; Chouvelon *et al*. 2012). The interaction between size and physiology was also well illustrated by the bioaccumulation of Zn with size in spiny lobsters, probably due to a rate of storage in granules that was higher than the rate of excretion of granules. But this interaction of size (and age) with physiology and/or trophic ecology was best illustrated by the effects of ontogenetic changes, and more largely of life-history traits, on trace element bioaccumulation in marine consumers. Habitat use and diet are known to vary with age and growth (e.g. Cocheret De La Morinière *et al*. 2003; Young *et al.* 2006; Wells *et al.* 2008). These changes were obvious here for emperor red snapper, for which the trace element bioaccumulation trends of Cu, Hg, Ni, Se, and Zn seemed to change at mature size, and for swordfish for which ontogenetic changes in diet had an effect on the bioaccumulation of Cd, Hg and Zn. The change of metabolic rate through growth could also affect difference of trace element bioaccumulation between sexes, as showed in swordfish.

Along with difference in diet composition between male and female swordfish, this was the only factor causing a difference in trace element bioaccumulation between sexes, suggesting that physiological needs in terms of essential trace elements may not differ between males and females. These results are supported by those of Kojadinovic *et al*. (2007) who found very few differences in trace element profiles between male and female swordfish, and who also showed that the reproduction process itself did not affect trace element concentrations in this species. If such findings are confirmed for other marine consumers, then sex itself (and associated differences in physiology) may not affect trace element bioaccumulation in capture fisheries species.

In addition to the interaction between size and trophic position (i.e. increase of trophic position with increasing size), trophic position alone also had a significant influence on Hg bioaccumulation, as observed elsewhere (Chouvelon *et al*. 2014, 2017; Goutte *et al*. 2015). For the other trace elements, however, it seems that this effect of trophic position, mostly observed at the intraspecific level, depends mainly on the diet composition of marine consumers (and especially of the presence or absence of super-vectors of trace elements in their diet), and on the growth rate of the considered species (i.e. biodilution associated with increase of trophic position during growth). The rare exception observed was Se which, as mentioned above, co-accumulated with Hg and thus biomagnified at high Hg concentrations.

Finally, trace element concentrations in fish species (emperor red snapper and swordfish) varied seasonally due to changes in environmental conditions and/or reproduction-induced seasonal migrations. Here again, it is possible that vertical habitat had some level of effect on these variations. Contrary to emperor red snapper who lives in demersal relatively shallow waters (5-180 m, Froese and Pauly 2020), by being able to dive to deep waters (> 1000 m, Abascal *et al*. 2010), swordfish physiology may be less affected by seasonal changes in sea surface temperatures, changes in salinity due to heavy rain or changes in trace element bioavailability due to resuspension of sediments by wind. However, to understand seasonal variations in trace element bioaccumulation, it is also important to consider other processes controlling trace element bioavailability (e.g. upwelling and gyre occurrence, sea surface temperature, salinity, pH, midwater oxygen concentrations or trace element speciation), as well as the reproductive dynamics of the studied species. Although local migrations within Seychelles waters did not seem to have a direct effect in emperor red snapper, swordfish

migrations through different oceanographic regions of the Indian Ocean did have some level of influence. As shown in Chapter 4, processes controlling trace element bioaccumulation can vary among regions of the same ocean, and spatial variations in trace element concentrations and stable isotope values can be recorded if individuals are resident at the scale of their tissue turnover rate. Thus, the scale of the migrations, and especially local dynamics in regions where marine consumers reside for a time, are important to consider. In addition, Chapter 5 showed that local and seasonal/annual variations in oceanographic conditions could affect the trophic ecology of marine species, and subsequent trace element bioaccumulation.

As a consequence of all factors mentioned above, trace element supply and/or exposure for human diets varied among Seychelles capture fisheries species (Chapter 6). Due to their high As, Cu and Zn, spiny lobsters and more generally decapod crustaceans were good sources of these trace elements for human diets. All species were also very good sources of Se, which lowered Hg toxicity to a point that it was null or close to null, even for top predators known to bioaccumulate very high concentrations of Hg like swordfish (Bodin *et al.* 2017). Care should be taken in interpreting Hg-related toxicity risk, as the estimated Hg and Se concentrations after interaction with each other were based on the hypothesis that all ingested Se will bind to all ingested Hg on a molar ratio 1:1 (Raymond and Ralston 2004). Although this may not be the case, meaning that the theoretically bioavailable Hg concentrations might be underestimated with this method, it is likely that the very high Se concentrations in all Seychelles capture fisheries species will lower Hg toxicity to the point that, even if not null, Hg concentrations should not be toxic. Nevertheless, there is a great need of a better understanding of the binding process between Hg and Se in the human body after seafood ingestion. Globally, the main toxicity risk was linked to high Cd concentrations in two species (i.e. spanner crab and pink ear emperor) and to particularly high and potentially adverse Se concentrations in two species (i.e. blackeye emperor and pink ear emperor). By identifying different patterns of trace element (either essential, potentially essential or non-essential) concentrations in Seychelles capture fisheries species, this chapter highlighted the **importance of varying dietary composition in capture fisheries species to meet RDI**.

Here, it is important to note the importance of scale difference between trace element variation in capture fisheries species, especially for essential trace elements, and consequences of these variations on trace element supply and exposure. In other words, small variations in

essential trace element content in capture fisheries species may not have consequences on micronutrient supply in human diets. Rather, consequences will depend on (1) meeting the smallest supply necessary to remain within the optimal range (see General introduction, Fig. 1.2) and (2) the efficiency of metabolic processes in the human body. Indeed, like in marine organisms, human physiology plays a role in the regulation of trace elements in the human body (Malinouski *et al.* 2014). Associated with a varied and balanced diet, a good-functioning human metabolism could thus regulate trace element uptake and/or excretion in the case of small concentration variations in capture fisheries resources. Contrary to essential trace elements, non-essential trace elements are often not regulated in human metabolism, thus the first preoccupation might be the potential increase of these non-essential trace element concentrations in capture fisheries species. **In a context of climate change, it is thus necessary to identify the essential trace elements for which changes in concentrations will be important. In other words, if we want to understand future micronutrient supply and contaminant exposure in human diets, it is mandatory to quantify the effects of global changes on trace element concentrations.** This point will be further discussed in section 9.2.

In Chapters 1 to 5, we showed that all trace elements were affected by several factors, intrinsic and/or extrinsic, and that the significance of the effect or its nature (bioaccumulation or biodilution) could be element-, species- and even individual-specific. Although intrinsic factors were often key in understanding trace element bioaccumulation dynamics, especially for essential ones, trace element bioaccumulation in capture fisheries species was globally the result of a combination of both intrinsic and extrinsic factors. This thesis thus highlighted the **importance of scale** (i.e. population, inter- or intraspecific level) and the **importance of knowing the biology and ecology** of the studied species, as well as environmental conditions, when studying trace element bioaccumulation in capture fisheries species. Finally, Chapter 6 allowed to identify which species were good sources of essential trace elements in Seychellois capture fisheries resources-based diet, and also highlighted what exposure risk to consider in risk-benefit analyses for Seychellois.

9.2. CLIMATE CHANGE: A NEW VARIABLE IN THE EQUATION

Today, it is generally accepted that climate change has many impacts on the marine environment at several scales, with many of these impacts being known to affect trace element bioaccumulation in marine organisms. Although the purpose of this thesis was to establish a

baseline on trace element concentrations and bioaccumulation processes in Seychelles marine food webs, it is clear that climate change needs to be taken into account to better anticipate nutrient supply and contaminant exposure through capture fisheries resources consumption. This is all the more important in SIDS who, in addition to be highly reliant on marine resources for local subsistence (Briguglio 1995), are particularly vulnerable to climate change-induced environmental changes (Barnett and Waters 2016; Klöck and Nunn 2019). Therefore, the next step is to identify the nature and intensity of the effects of climate change on trace element bioaccumulation in SIDS marine resources. Here again, the Seychelles are a typical case study, as they are predicted to be affected by long-term changes (e.g. increase in rainfall intensity and sea surface temperature) and by extreme climatic events (e.g. El Niño Southern-Oscillation events and tropical cyclones) (Chang-Seng 2007; Khan and Amelie 2015) that could directly or indirectly affect trace element bioaccumulation in marine capture fisheries species. Thus, if this section is not intended to provide an extensive review of all possible climate change effects on trace element bioaccumulation, it will help highlight some of these possible variations by using the results from this thesis.

9.2.1. Modifications of trace element bioaccumulation processes

On a global aspect, global changes induce modifications of environmental parameters, like increase in sea surface temperature, decrease in dissolved oxygen, decrease in pH (i.e. ocean acidification) and variable salinity due to ice melting and changes in evaporation/precipitation rates (Beaugrand and Kirby 2018). As a result of the rapid changes in environmental parameters, climate change have an impact on species by altering their physiology and trophic ecology, and on ecosystem functioning due to habitat degradation and/or loss of biodiversity, to species' biology disruption (e.g. change in reproductive behaviour) and to migration of species that follow parameters optimums (i.e. modification of distributional range) (Beaugrand and Kirby 2018; Clarke *et al.* 2021). Among the factors identified in this thesis influencing trace element bioaccumulation in Seychelles capture fisheries species, all could potentially be influenced by climate change and its effects.

First, physiology was a prevalent factor, as it influenced the bioaccumulation of one or more trace element(s) in all of the 54 species analysed here. This was especially the case for trace elements essentials to marine organisms' physiology, as their bioaccumulation is regulated through metabolic processes, but also for non-essential trace elements for which

some species had a metabolic process implicated in detoxification. Therefore, through modifications of parameters like temperature that will affect the physiology of marine organisms (Little *et al*. 2020), climate change will most probably induce changes in bioaccumulation dynamics of trace elements in marine capture fisheries species. This is supported by results on emperor red snappers (Chapter 3), for which natural (i.e. seasonal) variations in seawater parameters (i.e. temperature, salinity and dissolved oxygen) potentially affected the bioaccumulation of Cd, Cr, Cu, Ni, Mn, Se and Zn. Variation in trace element bioaccumulation, like increased Cd, Co and Hg bioaccumulation or decrease in Ag, Cu and Zn bioaccumulation with increased water temperature, was also observed for other species (e.g. O'Hara 1972; Baines *et al*. 2005; Wang *et al*. 2005; Mubiana and Blust 2007; Curtis *et al*. 2019). While this could not be tested for spiny lobsters, as they were all sampled at the same period (in October/November for all sampling years), decapod crustaceans may also be affected by the changes of environmental parameters. If swordfish seemed to not be majorly affected by changes in sea surface temperature and associated changes in water dissolved oxygen, such changes from one season to another generally only affect surface waters, while swordfish preferentially feed on mesopelagic prey in cold deep waters with low oxygen (Abascal *et al*. 2010). It is thus possible that, through their use of deep habitats and by being more resistant to anoxia than other species, swordfish are less prone to be affected by changes in sea surface parameters. However, on the long-term, climate change is predicted to increase sea bottom temperatures (Coro *et al*. 2020), with an increase of oxygen minimum zones occurrence (Clarke *et al*. 2021), which may affect swordfish's diving capacities and exposure to Hg, and by extension those of deep diving species in the future (Stramma *et al.* 2012). Although not mentioned in this thesis, ocean acidification was also shown to have effect on trace element bioaccumulation in marine organisms through changes of their physiology (e.g. Lacoue-Labarthe *et al*. 2011; Ivanina *et al*. 2013; Shi *et al*. 2016).

By affecting marine organisms' physiology, the increase in water temperature also alters the growth of these organisms (Little *et al*. 2020). Yet, the importance of size was illustrated by results in this thesis, as size was a major factor influencing trace element bioaccumulation in capture fisheries species here. Effects of size were either direct through bioaccumulation/biodilution during growth, or indirect by conditioning diet and/or habitat use of the considered species. Thus by altering fish growth, the predicted climate change-induced increase in water temperature (Coro *et al.* 2020) will probably affect trace element

bioaccumulation by (1) altering bioaccumulation/biodilution processes during growth and/or (2) affecting ontogenetic changes in habitat use and/or diet composition.

On a more general aspect than physiology, water temperature also controls the biology of marine predators, including reproductive behaviour like spawning-induced migrations. For example, in Atlantic bluefin tuna, spawning season shifted from late to early spring due to changes in water temperature, which also affected migrations and thus habitat use (Muhling *et al.* 2011). Similarly to this species, spawning and associated migrations in swordfish are triggered by water temperature (Abid and Idrissi 2006). As seasonal spawning-related migrations possibly had some level of effect on trace element bioaccumulation in swordfish (Chapter 5), it is possible that increase in water temperature will also affect trace element bioaccumulation through modification of seasonal migration patterns. More studies on swordfish movements in the Indian Ocean and on the effect of these movements on trace element bioaccumulation are thus needed to confirm or refute this hypothesis.

Finally, the increase in water temperature will also indirectly affect trace element bioaccumulation in marine organisms by altering oceanic mixing (Beaugrand and Kirby 2018), which itself will change trace element bioavailability in the water column. The most evident consequence of water column stratification is limited macro- and micronutrient mitigation, thus potentially decreasing trace element bioavailability for primary producers in surface waters and upper trophic levels (Beaugrand and Kirby 2018). However, in the special case of Hg bioaccumulation, bacterial activity was shown to be important in controlling MeHg bioavailability in seawater and subsequent bioaccumulation and biomagnification in food webs (Chapters 3 to 5). By favouring water column stratification, climate change will also favour the occurrence of oxygen minimum zones, which will enhance bacterial activity and Hg methylation in these zones (Krabbenhoft and Sunderland 2013). With higher bioavailability of Hg (in its methylated form) in the water column, and with higher Hg bioaccumulation rates in marine organisms due to higher water temperatures (Curtis *et al*. 2019), climate change is therefore expected to increase Hg concentrations in capture fisheries species in the future (Alava *et al.* 2017), with projected increases of 8-20% by the end of the 21st century (Alava *et al.* 2018).

Water temperature is not the only environmental parameter that will influence trace element bioavailability in seawater. Trace element bioavailability is also dependent on the physicochemical form of trace elements, itself being dependent on seawater physicochemical

properties, linked in part to salinity (Neff 2002a). Here, a seasonal decrease in salinity linked to high rainfalls potentially affected bioaccumulation of Cd, Cr, Cu, Ni, Mn, Se and Zn in emperor red snapper (Chapter 3). This was supported by previous findings showing that seawater salinity influenced Cd and Zn bioavailability (Rainbow and Black 2002, 2005; Wang and Rainbow 2008). With the predicted climate change-induced increase in extreme weather events in some areas (Kibria *et al.* 2021), including the Seychelles (Chang-Seng 2007; Khan and Amelie 2015), it is possible that differences in salinity between seasons will increase due to either higher temperatures during the warmest season and increased evaporation, or to increased rainfalls during the rainy season which will locally increase input of freshwater. Climate change-induced extreme weather events also include phenomena like storms and cyclones that are able to locally affect wind force (Kibria *et al*. 2021). As strong winds could possibly affect trace element bioavailability by resuspension of sediments (Saha *et al*. 2016; Chapter 3), an increase in the force and/or frequency of storms/cyclones could also indirectly influence trace element bioaccumulation in capture fisheries species.

Habitat degradation caused by climate change may also alter trace element bioaccumulation dynamics in marine food webs, and especially in species which are highly dependent on habitat structure and complexity. Here, coral bleaching had some level of effect on Cd, Cr, Ni, Pb, and Se bioaccumulation in spiny lobsters (Chapter 2). This raised the question of habitat suitability, that is, in the future, will marine habitats be in sufficient health to provide food quality prey to marine consumers? Indeed, if bleaching events are predicted to increase in frequency due to climate change, thereby weakening coral ecosystems in the long-term (Hoegh-Guldberg 2011), coral reefs are not the only ecosystems that are threatened by global change (e.g. Pratchett *et al*. 2011; Thorner *et al.* 2014; Bruno *et al*. 2018). Although the effect of tropical marine habitat loss on trace element bioaccumulation in marine consumers depending on these habitats are still poorly known, it is likely there will be an effect. By altering habitats and, subsequently, species diversity (e.g. Beaugrand and Kirby 2018; Robinson *et al*. 2019; Clarke *et al*. 2021), climate change alters the prey composition of marine consumers' diet and/or induces changes in food web length (i.e. effect on trophic position). In Chapters 1 to 5, diet composition and/or trophic position were shown to have an effect on trace element bioaccumulation. In addition, the bioaccumulation of some trace elements (e.g. Cd and Zn) could increase as ingestion rate the consumer decreases (Xu and Wang 2002). Climate change

may therefore also alter trace element bioaccumulation in capture fisheries species by altering prey availability and/or food web structure through habitat degradation/loss.

As exposed in this section, through changes in environmental parameters and by altering marine ecosystems health and biodiversity, climate change will change trace element bioaccumulation dynamics in marine food webs at many levels. This will therefore affect essential trace element supply and non-essential trace element exposure in capture fisheries resources-based diets. For now, it is difficult to quantify these effects on tropical species and ecosystems, as most studies on this topic were conducted in polar or temperate areas (Poloczanska *et al*. 2016). Moreover, tropical species may be more or less sensitive than polar and temperate ones to some environmental changes. As an example, tropical species generally display narrow ranges of thermal tolerance compared to temperate species (Nguyen *et al.* 2011; Madeira *et al.* 2012), which could make them more sensitive to climate change-driven rising in water temperature. Thus, there is an urgent need of more studies on the effects of environmental parameter changes on tropical species, and on the extent of these effects on trace element bioaccumulation processes in tropical food webs. As a first step, observing seasonal variations in trace element bioaccumulation in combination with variation in environmental parameters could, as suggested by results in this thesis, participate to identify the environmental factors for which variation influences trace element bioaccumulation in capture fisheries species. But more importantly, it could allow for the identification of trace elements for which this influence is significant, which is crucial to better understand future nutritional supply and contaminant exposure through capture fisheries resources-based diets.

9.2.2. What consequences on the benefit-risk of capture fisheries resources consumption?

One of the challenges of the 21st century is to understand the extent of the influence of factors driving trace element bioaccumulation in marine tropical capture fisheries species to better understand future nutrient supply and contaminant exposure in SIDS populations. The previous section highlighted the potential effects of climate change on tropical species, considering results from this thesis and what was found in the literature. In this section, the question addressed is: what consequences on the realation between risk and benefit in capture fisheries resources-based diets?

Nowadays, the effects of climate change on capture fisheries species nutritional quality are still difficult to quantify. If there has been an increasing awareness on climate change-related capture fisheries resources security problems during the last decades, the "quantity" aspect due to decline in fishing stocks has been a more ancient preoccupation and has been more extensively reviewed than the "quality" aspect due to changes in micronutrient content (e.g. Tirado *et al*. 2010; Ding *et al*. 2017; Rizal and Anna 2019 ***vs*** Alava *et al*. 2017; Myers *et al*. 2017). In addition, what stands out from the literature (and from this thesis) is that the link between trace element bioaccumulation in capture fisheries species and trace element supply (benefit) or exposure (risk) is difficult to make and rarely done. Indeed, as this was the case in this thesis, trace element bioaccumulation processes and risk-benefit of capture fisheries resources consumption are generally treated separately (e.g. Anan *et al.* 2005; Abdallah 2008; Rejomon *et al.* 2010; Vieira *et al*. 2011). Yet, studies on trace element bioaccumulation in capture fisheries species, including studies on the effects of global changes on this bioaccumulation, could allow to quantify variations in trace element concentrations (e.g. Baines *et al.* 2005; Baines and Fisher 2008). This would bring key information to anticipate micronutrient supply and contaminant exposure through capture fisheries resources consumption in the coming decades.

Global change-driven factors that could affect trace element bioaccumulation in capture fisheries species were identified in the previous section, but no real consensus could be drawn. Indeed, these effects seem to be trace element-, species- and even life stage-specific (Table 9.1). As an example, ocean acidification was shown to decrease Cd bioaccumulation in the eggs of the common cuttlefish and of the squid *Loligo vulgaris* (Lacoue-Labarthe *et al.* 2009, 2011), and in the hard clam *Mercenaria mercenaria* (Ivanina *et al*. 2013), while Cd bioaccumulation increased in four other bivalve species (Shi *et al*. 2016; Cao *et al*. 2018). In addition, interaction between several global change-driven factors could produce unexpected effects on trace element bioaccumulation in capture fisheries species, here again likely to be trace element- and species-specific (Table 9.1). From this information, two main scenarios can be drawn: (1) compensations of the different variations in trace element bioaccumulation among capture fisheries species or (2) global decrease in essential and potentially essential trace element concentrations coupled with a global increase in non-essential trace element concentrations. Although a third scenario in which there would be a global increase in essential and potentially essential trace element concentrations and a global decrease in non-essential

trace element concentrations cannot be totally excluded, no study hinting to such possible evolution was found, thus it will not be discussed here.

Table 9.1. Examples of identified variations in trace element bioaccumulation due to global change-driven variations in temperature, pH and salinity.

Global change-driven factor variation	Effect on trace elements	Model species	Reference(s)
Temperature ↗	↗ Cd	Fiddler crab (*Uca pugnax*)	O'Hara (1972)
	↗ Cd, Zn	Green mussel (*Perna viridis*)	Wang *et al*. (2005)
	↗ Cd, Co ↘ Ag, Se, Zn	Mussel (*Mytilus edulis*)	Baines *et al.* (2005); Baines and Fisher (2008)
	↗ Cd, Pb ↘ Cu	Mussel (*Mytilus edulis*)	Mubiana and Blust (2007)
	↗ Fe, Mn, Zn	Guilthead seabream (*Sparus aurata*)	Guinot *et al*. (2012)
	↗ Hg	Killifish (*Fundulus heteroclitus*)	Dijkstra *et al.* (2013)
	↗ Hg and MeHg	Chinese muddy loach (*Misgurnus mizolepis*)	Pack *et al.* (2014)
	↗ Hg (i.e. MeHg)	Juvenile seabass (*Dicentrarchus labrax*)	Maulvault *et al.* (2016)
	↘ iAs	Japanese carpet shell clam (*Ruditapes philippinarium*) and Mediterranean mussel (*Mytilus galloprovincialis*)	Maulvault *et al*. (2018)
	↗ Zn	Turbot (*Scophthalmus maximus*)	Pouil *et al.* (2018)
	↗ Hg (i.e. MeHg)	*Leptocheirus plumulosus* (estuarine amphipod)	Curtis *et al*. (2019)
pH ↘	↗ Ag, Zn ↘ Cd	Eggs of common cuttlefish (*Sepia officinalis*)	Lacoue-Labarthe *et al.* (2009)
	↗ Ag, Zn ↘ Cd, Mn	Eggs of squid (*Loligo vulgaris*)	Lacoue-Labarthe et al. (2011)
	↗ Cu ↘ Cd	Hard clam (*Mercenaria mercenaria*)	Ivanina *et al.* (2013)
	↗ Cd	Mussel (*Mytilus edulis*), blood cockle (*Tegillarca granosa*) and Asiatic hard clam (*Meretrix meretrix*)	Shi *et al*. (2016)
	↗ Cd	Oyster (*Crassostrea gigas*)	Cao *et al*. (2018)
Salinity ↘	↗ Cd ↘ Zn	Common shore crab (*Carcinus maenas*), Chinese mitten crab (*Eriocheir sinensis*) and velvet swimming crab (*Necora puber*)	Rainbow and Black (2002, 2005)
	↗ Mn	Turbot (*Scophthalmus maximus*)	Pouil *et al*. (2020)
Temperature ↗ & pH ↘	↗ Cu, Zn ↘ Fe, Se	Oysters (*Magallana gigas* and *Ostrea edulis*)	Lemasson *et al.* (2019)

❖ SCENARIO 1: COMPENSATION AMONG CAPTURE FISHERIES SPECIES

In Chapter 6, we showed the importance of varying the consumption of capture fisheries species in order to meet the RDI of the highest number of micronutrients, and to limit contaminant exposure. In this first scenario, we thus suppose that a decrease in one or more essential or potentially essential trace element concentration(s) in a capture fisheries species can be compensated by an increase of the same trace element(s) concentration(s) in another capture fisheries species. But, for this compensation to be effective, several conditions should be respected:

(1) The decrease/increase process should occur in two species with similar accessibility, in terms of region (i.e. to avoid being dependent on imports, Gephart *et al.* 2016), in terms of fishing gear (i.e. artisanal fishers should not have to invest heavily in new gears), in terms of ecological cost (i.e. the species in which there is an increase in essential/potentially essential trace element concentrations should not be already overfished or particularly vulnerable to overfishing), and in terms of market price (i.e. consumers should not spend more money to remain healthy).

(2) The increase in an essential or potentially essential trace element concentration in a capture fisheries species should not occur in a species with an already very high concentration in this trace element (Lemasson *et al*. 2019). As an example, in Chapter 6, the very high Se concentrations in all analysed species were shown to be both an advantage, because RDI were met even when Hg concentrations were high, and a disadvantage because there is a risk of adverse effects following an excess of consumption for two species. Thus, this increase in trace element concentrations should not expose human populations to too high essential trace element concentrations, and thus to risk of exceeding recommended thresholds of toxic effects.

(3) The increase in an essential or potentially essential trace element concentration in a capture fisheries species should not co-occur with an increase in non-essential trace element concentration to limit the risk of exposure to a minimum.

Concerning the last condition however, it is likely that an increase in at least one non-essential trace element concentration will occur in capture fisheries species due to global change (Table 9.1). In addition, Baines *et al*. (2005) found that changes in assimilation

efficiencies of trace elements in the mussel *Mytilus edulis* were higher for non-essential trace elements than for essential and potentially essential trace elements. This was explained by the biological role and thus metabolic regulation of essential/potentially essential trace elements in *Mytilus edulis*. While more studies on the quantification of global change-driven variations in trace element concentrations are needed, this suggests that the equilibrium between micronutrient supply and contaminant exposure could become unbalanced in the future, which would disrupt the "compensation effect". This is all the more true for trace elements with an interaction ability, like Hg and Se. In Chapter 6, Se was shown to have a protective effect against Hg in Seychelles capture fisheries species, because it was in molar excess over Hg. However, if the increase in Hg concentrations due to global change is higher than the change in Se concentrations, Hg could reach molar excess, thus increasing Hg exposure risk and potential Se deficiency.

- **SCENARIO 2: GLOBAL ESSENTIAL/POTENTIALLY ESSENTIAL TRACE ELEMENT DECREASE AND GLOBAL NON-ESSENTIAL TRACE ELEMENT INCREASE**

Again, Chapter 6 showed the importance of a varied capture fisheries resources-based diet in order to stay healthy. However, climate change is predicted to alter species diversity in marine ecosystems (Chapter 2 and section 9.2.1), thus probably reducing the number of species that can be exploited by fisheries. In Bernhardt and O'Connor (2021), the authors show that capture fisheries species dietary quality, and especially micronutrient content, is intrinsically linked to species richness. In other words, thanks to species richness, a human consumer can gain more nutritional benefit through capture fisheries resources consumption without necessarily consuming more of them (Fig. 9.1).

Again, although there is a great need of more studies on the combined effects of global changes on trace element concentrations in capture fisheries species, loss of species richness due to degradation and/or loss of marine ecosystems has reached a consensus. In particular, coral reefs are key ecosystems in SIDS including the Seychelles, as they provide food for small-scale fisheries (Spalding *et al*. 2001), and these ecosystems and their associated marine species are among the most vulnerable to climate change (e.g. Graham *et al*. 2006, 2011; Graham and Nash 2013). In this context, loss of species richness in Seychelles marine systems due to loss of

coral reefs is likely to happen, which will have consequences on micronutrient supply and contaminant exposure in Seychellois' diet.

Yet, the interaction effects of all global changes and their consequences on trace element bioaccumulation in marine capture fisheries species are still poorly known. Better understanding and quantification of these effects would help SIDS to evaluate the extent to which their populations' diets will be affected in terms of micronutrient supply and contaminant exposure.

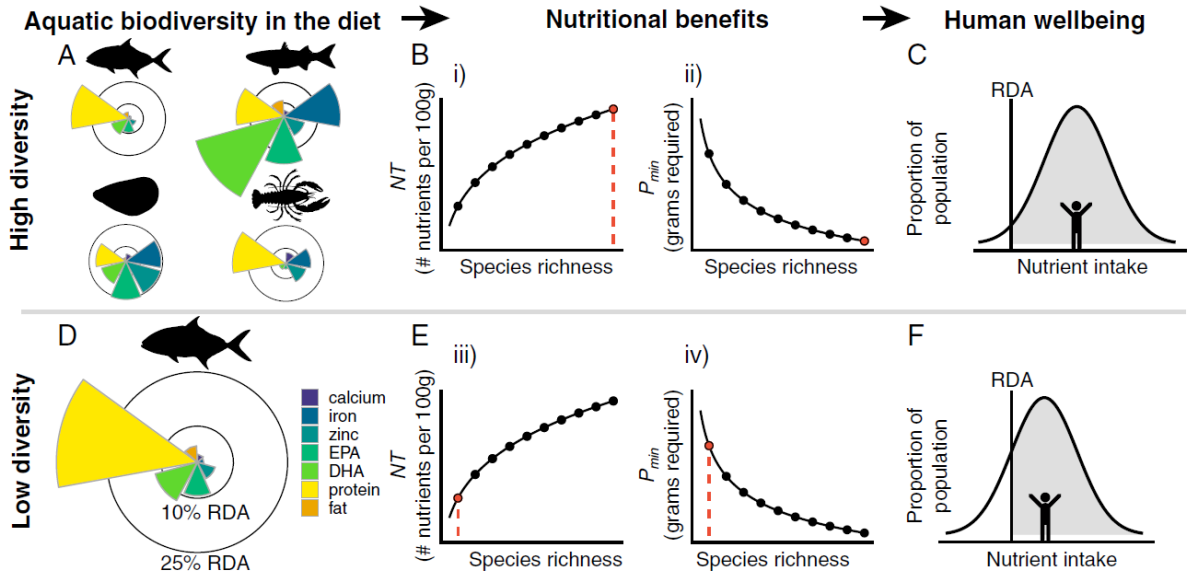

Fig. 9.1. Aquatic biodiversity increases human well-being because edible species have distinct and complementary multinutrient profiles (A) and differ in mean micro- and macronutrient content (shown here relative to 10 and 25% thresholds of recommended dietary allowance, RDA, guidelines) for representative finfish (*Abramis brama*, *Mullus surmuletus*), mollusc (*Mytilus galloprovincialis*), and crustacean species (*Nephrops norvegicus*). Biodiversity-ecosystem functioning theory predicts that nutritional benefits, including the number of nutrient RDA targets met per 100 g portion and minimum portion size, are enhanced with increasing seafood species richness. Orange dots in B and E correspond to potential diets of high and low biodiversity levels. Seafood consumers with limited access to seafood each day may not reach RDA targets if diets are low in diversity (D-F vs A-C; grey shading indicated proportion of population that meets nutrient requirements). DHA = docosahexaenoic acid, EPA = eicosapentaenoic acid. (Taken from Bernhardt and O'Connor 2021).

9.3. CAVEATS AND LIMITS: WHAT TO IMPROVE?

This thesis dissertation allowed for the identification of many factors influencing trace element bioaccumulation, but also allowed to identify gaps of knowledge that need to be improved.

Many gaps will need to be addressed by the worldwide scientific community, but others can be addressed at the local Seychelles scale.

❖ DATASET CONSOLIDATION: IMPROVING SAMPLE SIZE

This thesis established a baseline on trace element concentrations and bioaccumulation in a wide variety of capture fisheries species, from different functional groups and habitats, and with different diets and trophic positions (Chapters 1 and 6). However, intraspecific variations were not considered for some species due to a too small sample size (e.g. only one individual available for blackeye emperor and some elasmobranch species, and no species of bivalves). Yet, Chapter 6 showed the importance of considering this intraspecific variability when assessing the risk-benefit of capture fisheries resources consumption. This was especially true in the case of non-essential trace elements, which wan be toxic above thresholds, and for which there was sometimes a factor 10 between the CI95% lower and upper bounds for the percentage of covered PTI (e.g. Cd in shoemaker spinefoot, Appendix 8.4B). The next step should thus be the analysis of more individuals for these species with low sample size, in order to obtain a more robust database and to complete analyses made in this thesis. Given the effects of ontogenetic changes in size, habitat use and/or diet on trace element concentrations in capture fisheries species, the analysis of several size ranges for each species would also bring valuable information on the individuals that are safe to eat. On this aspect, continuing the partnership with local fishers for sampling procedures is crucial, as they represent useful collaborators in tropical countries where there is a widespread lack of access to scientific vessels (Wehrtmann *et al*. 2012).

❖ COMMENT ON THE ANALYSED TISSUES

In this thesis, the tissues analysed for trace element concentrations and used to study trace element bioaccumulation were the edible parts (section 2.2) of the selected species which were mostly muscular tissues. In studies on trace element bioaccumulation, however, tissues involved in the digestive process (e.g. liver or digestive glands/hepatopancreas) are usually preferred as they are the main organs for the metabolisation, storage and detoxification processes of trace elements, and thus they often bioaccumulate higher trace element concentrations than other tissue types (Ciardullo *et al*. 2008; Metian *et al.* 2013; Raimundo *et*

al. 2013). However, in most species, such tissues are discarded and no consumed. Thus, although the use of digestive tissues is useful in biomonitoring studies, as the main edible parts, muscle tissues were the most appropriate for this thesis as the main aim was to better understand essential trace element availability and non-essential trace element exposure in Seychellois' capture fisheries resources-based diet. In addition, in a context of climate change which may alter trace element bioaccumulation in all marine organisms' tissues, it is essential to understand processes of bioaccumulation in capture fisheries species edible parts to better anticipate future micronutrient supply- and contaminant exposure-related issues.

❖ EMBLEMATIC SPECIES: IMPROVING KNOWLEDGE ON THEIR BIOLOGY AND ECOLOGY

While this thesis contributed to bring more information on the trophic ecology of some emblematic species from the Seychelles (Sabino *et al.* 2021; Chapters 2 to 5), there are still gaps of knowledge on many species, and especially on the emperor red snapper. Their population structure in the Seychelles has already been studied (Mees 1992; Grandcourt *et al*. 2008), however literature revealed very few information about their biology, trophic ecology and life-history traits (Robinson *et al*. 2004). Data on this species are also scarce in many other areas of the world, with mainly large focuses on the snapper group (e.g. Cocheret De La Morinière *et al.* 2003; Martinez-Andrade 2003; Kimirei *et al.* 2013) or focus on other snapper species (e.g. McPherson and Squire 1992; Wells *et al.* 2008). Yet, Chapter 3 highlighted the importance of knowing such details to better understand trace element bioaccumulation in capture fisheries species, and subsequent trace element intake in human diets. Ontogenetic changes in habitat and diet, in particular, are crucial elements to know in order to understand trace element bioaccumulation dynamics in time in emperor red snappers' edible tissues.

It is thus crucial to improve knowledge on the biology, trophic ecology and life-history traits of Seychelles emblematic species, with a particular interest in the emperor red snapper, for which many key information are still lacking.

❖ INDIVIDUAL SIZE: NEED OF A BETTER PROXY OF AGE?

Chapters 1, 3, 4 and 5 showed the importance of a reliable proxy of age when studying trace element bioaccumulation. Indeed, as showed many times in this thesis, bioaccumulation

dynamics of some trace elements vary in time, with the most obvious example being Hg. In this respect, size can be a good proxy when studying trace element bioaccumulation at the intraspecific scale, and when all individuals of the same species have a relatively uniform growth. However, it becomes difficult to use it when different populations of the same species have differential growth rates (e.g. among sexes or among regions), or when comparing trace element bioaccumulation among different species. In addition, climate change is predicted to affect the growth of capture fisheries species (see section 9.2.1), thus altering their size.

Although methods of age estimation vary according to capture fisheries species' morphological characteristics, the most common methods are based on the same principle that is the identification of annuli/banding patterns on hard parts in teleost fishes and cephalopods (i.e. scales, otoliths and bones or statoliths, gladii, stylets and beaks, respectively) (Panfili *et al*. 2002; Arkhipkin *et al*. 2018), calcified parts in elasmobranch fishes (i.e. vertebrae, dorsal spines, caudal thorns and neural arches) (Cailliet and Goldman 2004; Cailliet *et al.* 2006) or chitinised structure in decapod crustaceans (i.e. gastric mill) (Kilada and Driscoll 2017). In combination with validation analyses, these methods of age estimation are usually considered highly reliable. However, they are often time-consuming and/or expensive, which limits the number of individuals that can be aged and thus can increase bias due to small sample size (Worthington *et al.* 1995). Due to limited resources in SIDS, this suggests low feasibility in this region.

A solution could be the combination of an expensive and time-consuming method on a small sample size, with a less robust but more cost-effective method on a large sample size, to assess the age and size structure of a capture fisheries species' population (Worthington *et al*. 1995; Hanson and Stafford 2017). For species with a sexual dimorphism, such study should be sex-specific to consider the differential growth rate between males and females. Then, this age and size structure study could be used to estimate the age of an individual from its size. Although this would not bring a precise age determination for each sampled individual, this would give an idea of the age difference between two populations of the same species (e.g. between males and females). In studies like this PhD thesis that include trace elements bioaccumulating in time, like Hg, this would bring valuable information that would help discriminating between factors influencing trace element bioaccumulation.

❖ IMPROVING RISK-BENEFIT ASSESSMENT: TOWARDS A BETTER ASSESSMENT OF TRACE ELEMENT INTAKE

Chapter 6 was a baseline assessment of essential and potentially essential trace element supply and non-essential trace element exposure in Seychellois capture fisheries resources-based diet. In this respect, some aspects of this baseline risk-benefit assessment need to be improved to better assess and to better understand trace element intake in Seychellois' diet.

As mentioned in Chapter 6 (section 8.3.3), more data on daily capture fisheries resources consumption by children and young adults are needed, since trace element intake depends on the daily portion consumed. It is also necessary to collect more data on adult Seychellois morphometrics, and especially for adult women who are among the most vulnerable to non-essential trace element exposure through pregnancy and lactation, as threshold calculations often depend on the capture fisheries resources consumer's weight (e.g. Cd and Hg; JECFA 2011b, 2013). In addition, improving knowledge on Seychellois whole diet is of high interest, as it would bring more information on (1) the place of capture fisheries species in the whole diet and thus on (2) the contribution of capture fisheries species in terms of trace element intake. This is especially important as trace elements, including non-essential ones, are present in all food items in variable concentrations (Gupta and Gupta 2014). In addition to improve this knowledge, other points need to be addressed, like the effects of cooking methods on trace element concentrations and bioaccessibility in capture fisheries species, or the interaction ability between Hg and Se, which both have an effect on trace elements bioavailability.

All trace elements were analysed in raw capture fisheries products edible parts, thus the cooking method was also not taken into account in this risk-benefit analysis. Yet, trace element concentrations have been shown to be influenced by cooking methods (reviewed in Domingo 2011). The nature of the effect (i.e. increase or decrease in concentrations and bioaccessibility), however, seems to be dependent on the cooking method, the trace element considered and its biochemical form and/or the capture fisheries species (Perello *et al*. 2008; Domingo 2011; Schmidt *et al*. 2015, 2018; Gheisari *et al*. 2016). As most studies have been conducted on species from temperate areas (Domingo 2011), there is a great need of more data on capture fisheries species from tropical and subtropical areas.

In order to assess the potential bioavailability of the non-essential trace element Hg and of the essential trace element Se in Chapter 6, I used the molar ration of Hg above Se (i.e.

MHg:MSe) to estimate the Hg and Se content that could interact with each other. This method is based on two hypotheses: (1) all ingested Hg can interact with all ingested Se, regardless of the physicochemical form of the element, and (2) Hg and Se bind at a molar ratio of 1:1. However, many questions on the mechanisms involved in this interaction remain unanswered, and recent studies tend to question the relevance of the MHg:MSe ratio in assessing Hg risk and Se benefit (Gerson *et al*. 2020; Gochfeld and Burger 2021). This could involve the use of the HBV_{Se} value to estimate potential of interaction between both trace elements and subsequent potential Se availability, but this would also require the establishment of a method for Hg, as the HBV_{Se} is more adapted to estimate Se benefit rather than Hg risk (Ralston *et al*. 2015). It may also be necessary to determine the form under which Hg and Se are present in capture fisheries species' edible parts. Indeed, their respective forms have different binding affinities, which could cause different effects on Se bioavailability according to the forms that are present (Manceau *et al.* 2021).

❖ COMPLETING RISK-BENEFIT ASSESSMENT: TOWARDS SUSTAINABLE CONSUMPTION GUIDELINES

Chapter 6 was only related to risk-benefit of capture fisheries products in Seychellois' diet. This analysis thus did not consider stock status of analysed species, their vulnerability to climate change or the impact of fishing techniques on the marine environment. Yet, food safety is not only related to food quality in terms of nutrients and contaminants, but also to ensuring the sustainability of fishing stocks, that is "responsible consumption and production" (United Nations 2015). There is an increasing awareness on the question of the sustainability of fisheries and, more largely, capture fisheries resources production (Tuomisto 2018; Tlusty *et al*. 2019; McKuin *et al*. 2021), with authors beginning to take into account the impacts of fishing techniques on the environment and on the climate in consumption guidelines assessments (Hallström *et al.* 2019). After determining the risk-benefit of Seychelles capture fisheries products consumption for Seychellois, assessing the impact of Seychelles fisheries on fishing stocks, marine ecosystems and greenhouse gas emission should thus be the next step to achieve sustainability in the Seychelles.

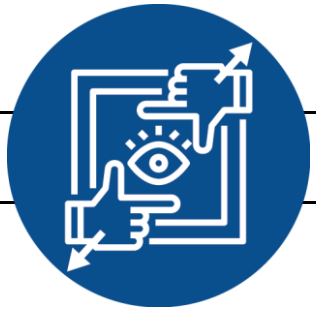

10. CONCLUSION AND PERSPECTIVES

This PhD thesis is the first baseline assessment of essential, potentially essential and non-essential trace element concentrations in capture fisheries species in the Seychelles and, more largely, in the Indian Ocean, to include such a high diversity of species with different trophic ecologies. Thanks to the use of taxonomic and morphometric data as well as ecological tracers like stable isotopes and fatty acids in combination with trace element data, it was possible to investigate the main factors influencing trace element bioaccumulation in these capture fisheries species, both at the inter- and intraspecific level. The use of model species was particularly useful to investigate intraspecific differences in trace element bioaccumulation in all three main marine compartments considered (i.e. benthic, demersal and pelagic). Investigating trace element bioaccumulation at both the inter- and intraspecific levels highlighted the importance of considering different scales (i.e. ecosystem, community, species, population and subpopulation) to better understand trace element bioavailability, intake and uptake in capture fisheries species, and thus trace element flow in and among systems. Finally, comparisons of trace element concentrations to allowed safety thresholds and/or recommended daily intakes for a first assessment of potential toxicity risks and nutritional benefits linked to capture fisheries resources consumption in Seychellois' diet.

Tropical areas include key ecosystems like coral reefs, mangroves and seagrass beds that provide many services for local population, including biomass productivity for small-scale fisheries (Mukherjee *et al*. 2014; Nordlund *et al.* 2018; Woodhead *et al*. 2019; Sanchez-Vidal *et al.* 2021). Yet, the associated species and their response to anthropogenic disturbances remain largely unknown for ecosystems in tropical areas compared to temperate and polar areas. By investigating the effects of coral reef degradation on spiny lobsters' trophic ecology and on their trace element concentrations, and by investigating ontogenetic changes in emperor red snappers' trophic ecology, this thesis contributed to increase knowledge on some reef-associated species. However, many aspects remain to be studied, like the interdependencies of several ecosystems (i.e. some ecosystems are ecologically linked through key species' ontegenetic changes in habitat and/or diet), or the life-history traits, biology and trophic ecology of key species that remain poorly known (e.g. emperor red snapper).

In this thesis, GLMs and GAMs were used to model trace element concentrations according to several intrinsic and extrinsic variables in key capture fisheries species. Although these modelling methods brought insight into factors controlling trace element

bioaccumulation in these key species, they are species-specific and thus do not allow to consider interspecific interactions. In this respect, ecosystem modelling approaches are useful tools. In particular, the "Ecopath with Ecosim" approach, which can be used for the exploration of past and future impacts of fishing and environmental disturbances on ecosystems, includes an "Ecotracer" routine that allows for the predictions of changes in the concentrations of certain compounds (Christensen and Walters 2004). This approach could thus allow to model contaminant concentrations in capture fisheries species after ecosystem perturbation (McGill *et al.* 2017). Such modelling approach could therefore be particularly useful in SIDS, where preoccupations regarding marine resources include the effects of anthropogenic and anthropogenic-induced perturbations on the functioning of ecosystems, and the associated consequences on seafood safety.

Although the purpose of this thesis was to better understand trace element flow in Seychelles food webs, results suggest that some trace elements (i.e. those that are not regulated) have the potential to be used as tracers themselves, in combination with other types of tracers (e.g. stable isotopes and fatty acids). These trace elements could be used to detect the presence of a certain type of organism in food webs (e.g. polychaetes for Pb in benthic systems, or cephalopods for Cd in pelagic systems), or to discriminate metapopulation structures across a wide area (e.g. Hg and Se in swordfish across the Indian Ocean). As mentioned in the general introduction, combining different types of trophic tracers can help reducing misinterpretations linked to the influence of environmental and biological processes on these trophic tracers (Ramos and González-Solís 2012; Sardenne *et al*. 2017; Sabino *et al*. 2021). Combining trace elements as trophic tracers with other tracers like stable isotopes and fatty acids could thus help to better understand interspecific interactions among marine organisms in tropical systems, as it was done in other areas (e.g. Chouvelon *et al*. 2011, 2014; Méndez-Fernandez *et al.* 2013).

In a context of human-induced global changes altering marine habitats and their biodiversity, as well as ecological processes including trace element bioaccumulation in marine organisms, baseline studies like this thesis are key foundation stones in the establishment of capture fisheries resources consumption guidelines in SIDS. Indeed, a better knowledge of ecosystem functioning and of trace element bioaccumulation processes and concentrations ultimately allows for (1) a better management and/or protection of key ecosystems and (2) for

the improvement of capture fisheries resources consumption guidelines. Although the assessment of the effects of climate change on trace element bioaccumulation in capture fisheries species was not the primary purpose of this thesis, the general discussion provided hypotheses on how trace element bioaccumulation and subsequent contaminant exposure and micronutrient supply could be altered by global changes, given the actual knowledge of the scientific community. This thus brings lines of research for future studies on trace element bioaccumulation in capture fisheries species in SIDS.

If establishing a baseline on trace element concentrations in capture fisheries resources is important, many things remain to be done before reaching sustainability in the consumption of these resources. This thesis was focused on trace element content, either essential, potentially essential or non-essential, but capture fisheries resources also contain significant levels of other nutrients like proteins and essential fatty acids, and of other contaminants like persistent organic pollutants (Weichselbaum *et al.* 2013) and plastics (Rochman *et al.* 2015; Godswill and Gospel 2019). It is thus important to increase knowledge on the occurrence of these compounds in capture fisheries resources from SIDS in order to have a global view of what are the risks and benefits associated with the consumption of these resources. In particular, this would allow the use of indexes integrating several types of contaminants (e.g. Cano-Sancho *et al.* 2015) or integrating both nutrient and contaminant content (e.g. Gladyshev *et al.* 2009; Sirot *et al.* 2012; Ricketts *et al*. 2019). In addition, nutrient and contaminant uptake is influenced by their bioavailability in food items, which can be modified by the cooking method. Thus, more data on nutrient and contaminant bioaccessibility in capture fisheries resources depending on the cooking methods are also needed. Such data would (1) contribute to better understand nutrient supply and contaminant exposure in capture fisheries resources-based diets when compared with cooking habits of local populations, and (2) would also allow local authorities to establish guidelines on the best cooking method(s) to insure optimal nutrient supply and low contaminant exposure. As sustainability also includes “responsible consumption and production” (United Nations 2015), data on fishing stocks, on capture fisheries species’ vulnerability to global changes and on the impact of fisheries on the environment (e.g. fishing gear and techniques, greenhouse gas emission) should also be included in capture fisheries resources consumption guidelines (Tuomisto 2018).

11. REFERENCES

Abascal FJ, Mejuto J, Quintans M, Ramos-Cartelle A (2010) Horizontal and vertical movements of swordfish in the Southeast Pacific. *ICES J Mar Sci* **67**:466–474. doi: 10.1093/icesjms/fsp252

Abdallah MAM (2008) Trace element levels in some commercially valuable fish species from coastal waters of Mediterranean Sea, Egypt. *J Mar Syst* **73**:114–122. doi: 10.1016/j.jmarsys.2007.09.006

Abdi H (2004) Multivariate analysis. In: *The SAGE encyclopedia of Social Science Research* (Eds. Lewis-Beck MS, Bryman A, Liao TF). SAGE Publications, pp 700–702. doi: 10.4135/9781412950589.n607

Abid N, Idrissi M (2006) Swordfish. In: *ICCAT Manual*, pp 181–198. URL: https://www.iccat.int/Documents/SCRS/Manual/CH2/2_1_9_SWO_ENG.pdf

Afandi I, Talba S, Benhra A, Benbrahim S, Chfiri R, Labonne M, Masski H, Laë R, Tito De Morais L, Bekkali M, Bouthir FZ (2018) Trace metal distribution in pelagic fish species from the north-west African coast (Morocco). *Int Aquat Res* **10**:191–205. doi: 10.1007/s40071-018-0192-7

Ahmad NI, Noh MFM, Mahiyuddin WRW, Jaafar H, Ishak I, Azmi WNFW, Veloo Y, Hairi MH (2015) Mercury levels of marine fish commonly consumed in Peninsular Malaysia. *Environ Sci Pollut Res* **22**:3672–3686. doi: 10.1007/s11356-014-3538-8

Akaike H (1981) Likelihood of a model and information criteria. *J Econom* **16**:3–14. doi: 10.1016/0304-4076(81)90071-3

Alais C, Linden G, Miclo L (2008) Biochimie alimentaire, 6e édition. Dunod. 272p.

Alava JJ, Cheung WWL, Ross PS, Sumaila UR (2017) Climate change-contaminant interactions in marine food webs: Towards a conceptual framework. *Glob Chang Biol* **23**:3984–4001. doi: https://doi.org/10.1111/gcb.13667

Alava JJ, Cisneros-Montemayor AM, Sumaila UR, Cheung WWL (2018) Projected amplification of food web bioaccumulation of MeHg and PCBs under climate change in the Northeastern Pacific. *Sci Rep* **8**:1–12. doi: 10.1038/s41598-018-31824-5

Alfaro AC, Thomas F, Sergent L, Duxbury M (2006) Identification of trophic interactions within an estuarine food web (northern New Zealand) using fatty acid biomarkers and stable isotopes. *Estuar Coast Shelf Sci* **70**:271–286. doi: 10.1016/j.ecss.2006.06.017

Allen G-R (1985) FAO species catalogue. Vol 6. Snappers of the world. An annotated and illustrated catalogue of lutjanid species known to date. *FAO Fish* **6**:24–29. doi: ISBN 92-5-103125-8

Ambriz-Arreola I, Gómez-Gutiérrez J, Franco-Gordo M del C, Plascencia-Palomera V, Gasca R, Kozak ER, Lavaniegos BE (2018) Seasonal succession of tropical community structure, abundance, and biomass of five zooplankton taxa in the central Mexican Pacific. *Cont Shelf Res* **168**:54–67. doi: 10.1016/j.csr.2018.08.007

American Food and Nutrition Board of the Institute of Medicine National Academy of Sciences (2019a) Dietary Reference Intakes (DRIs): Recommended dietary allowances and adequate intakes, elements. URL: https://ods.od.nih.gov/Health_Information/Dietary_ Reference_Intakes.aspx.

American Food and Nutrition Board of the Institute of Medicine National Academy of Sciences (2019b) Dietary Reference Intakes (DRIs): Tolerable upper intake levels, elements. URL: https://www.ncbi.nlm.nih.gov/books/NBK545442/table/appJ_tab9/?report=objectonly.

Amorim P, Sousa P, Jardim E, Menezes GM (2019) Sustainability status of data-limited fisheries: Global challenges for snapper and grouper. *Front Mar Sci* **6**:1–17. doi: 10.3389/fmars.2019.00654

Anan Y, Kunito T, Tanabe S, Mitrofanov I, Aubrey DG (2005) Trace element accumulation in fishes collected from coastal waters of the Caspian Sea. *Mar Pollut Bull* **51**:882–888. doi: 10.1016/j.marpolbul.2005.06.038

Andersen JL, Depledge MH (1997) A survey of total mercury and methylmercury in edible fish and invertebrates from Azorean waters. *Mar Environ Res* **44**:331–350. doi: 10.1016/S0141-1136(97)00011-1

Anual ZF, Maher W, Krikowa F, Hakim L, Ahmad NI, Foster S (2018) Mercury and risk assessment from consumption of crustaceans, cephalopods and fish from West Peninsular Malaysia. *Microchem J* **140**:214–221. doi: 10.1016/j.microc.2018.04.024

Arim M, Abades SR, Laufer G, Loureiro M, Marquet PA (2010) Food web structure and body size: Trophic position

and resource acquisition. *Oikos* **119**:147–153. doi: 10.1111/j.1600-0706.2009.17768.x

Arkhipkin AI, Bizikov VA, Doubleday ZA, Laptikhovsky V V., Lishchenko F V., Perales-Raya C, Hollyman PR (2018) Techniques for estimating the age and growth of molluscs: Cephalopoda. *J Shellfish Res* **37**:783–792. doi: 10.2983/035.037.0409

Arts MT, Brett MT, Kainz MJ (2009) Lipids in aquatic ecosystems. Springer Science, 377p. doi: 10.1007/978-0-387-89366-2

ASCLME (2012) National Marine Ecosystem Diagnostic Analysis. Seychelles. Contribution to the Agulhas and Somali Current Large Marine Ecosystems Project (supported by UNDP with GEF grant financing). 64p. URL: https://nairobiconvention.org/clearinghouse/node/298

Auer SK, Salin K, Rudolf AM, Anderson GJ, Metcalfe NB (2015) Flexibility in metabolic rate confers a growth advantage under changing food availability. *J Anim Ecol* **84**:1405–1411. doi: 10.1111/1365-2656.12384

Azad AM, Frantzen S, Bank MS, Nilsen BM, Duinker A, Madsen L, Maage A (2019) Effects of geography and species variation on selenium and mercury molar ratios in Northeast Atlantic marine fish communities. *Sci Total Environ* **652**:1482–1496. doi: 10.1016/j.scitotenv.2018.10.405

Baines SB, Fisher NS (2008) Modeling the effect of temperature on bioaccumulation of metals by a marine bioindicator organism, mytilus edulis. *Environ Sci Technol* **42**:3277–3282. doi: 10.1021/es702336q

Baines SB, Fisher NS, Kinney EL (2005) Influence of temperature on dietary metal uptake in Arctic and temperate mussels. *Mar Ecol Prog Ser* **289**:201–213. doi: 10.3354/meps289201

Baki MA, Hossain M, Akter J, Quraishi SB, Shojib FH, Atique Ullah AKM, Khan F (2018) Concentration of heavy metals in seafood (fishes, shrimp, lobster and crabs) and human health assessment in Saint Martin Island, Bangladesh. *Ecotoxicol Environ Saf* **159**:153–163. doi: 10.1016/j.ecoenv.2018.04.035

Ballantyne JS (1997) Jaws: The inside story. The metabolism of elasmobranch fishes. *Comp Biochem Physiol B* **118**:703–742. doi: 10.1016/S0305-0491(97)00272-1

Barneche DR, Allen AP (2018) The energetics of fish growth and how it constrains food-web trophic structure. *Ecol Lett* **21**:836–844. doi: 10.1111/ele.12947

Barnett J, Waters E (2016) Rethinking the vulnerability of Small Island States: Climate change and development in the Pacific Islands. In: *The Palgrave Handbook of International Development* (Eds. Grugel J, Hammel D). Palgrave Macmillan UK, pp 731–748.

Barone G, Giacominelli-Stuffler R, Storelli MM (2013) Comparative study on trace metal accumulation in the liver of two fish species (Torpedinidae): Concentration-size relationship. *Ecotoxicol Environ Saf* **97**:73–77. doi: 10.1016/j.ecoenv.2013.07.004

Barott KL, Williams GJ, Vermeij MJA, Harris J, Smith JE, Rohwer FL, Sandin SA (2012) Natural history of coral-algae competition across a gradient of human activity in the Line Islands. *Mar Ecol Prog Ser* **460**:1–12. doi: 10.3354/meps09874

Baylon JC, Tito OD (2012) Natural diet and feeding habit of the red frog crab (*Ranina ranina*) from Southwestern Mindanao, Philippines. *Philipp Agric Sci* **95**:370–377.

Beaugrand G, Kirby RR (2018) How do marine pelagic species respond to climate change? Theories and observations. *Ann Rev Mar Sci* **10**:169–197. doi: 10.1146/annurev-marine-121916-063304

Beijer K, Jernelov A (1978) Ecological aspects of mercury-selenium interactions in the marine environment. *Environ Health Perspect* **25**:43–45. doi: 10.1289/ehp.782543

Béné C, Barange M, Subasinghe R, Pinstrup-Andersen P, Merino G, Hemre G-I, Williams M (2015) Feeding 9 billion by 2050 – Putting fish back on the menu. *Food Secur* **7**:261–274. doi: 10.1007/s12571-015-0427-z

Bernhardt JR, O'Connor MI (2021) Aquatic biodiversity enhances multiple nutritional benefits to humans. *Proc Natl Acad Sci USA* **118**:1–11. doi: 10.1073/pnas.1917487118

Bernhoft RA (2012) Mercury toxicity and treatment: A review of the literature. *J Environ Public Health* **2012**:1–10. doi: 10.1155/2012/460508

Bernhoft RA (2013) Cadmium toxicity and treatment. *Sci World J* **2013**:1–7. doi: 10.1155/2013/394652

Bienfang PK, Trapido-Rosenthal H, Laws EA (2013) Bioaccumulation/Biomagnifications in Food Chains. In: *Environmental Toxicology* (Ed. Laws E.). Springer, New York, NY. doi: 10.1007/978-1-4614-5764-0_3Bistoquet K, Marguerite M, Lucas T, Morel S, Elizabeth NJ, Michaud P, Tsuji S (2018) Development of the fishery satellite account in the Seychelles. 7p. URL: https://www.iotc.org/documents/WPDCS/14/29-SYC-SatAccount

Bivand R, Keitt T, Rowlingson B (2019) rgdal: Bindings for the "Geospatial" Data Abstraction Library.

Bjørklund G, Chirumbolo S, Dadar M, Pivina L, Lindh U, Butnariu M, Aaseth J (2019) Mercury exposure and its effects on fertility and pregnancy outcome. *Basic Clin Pharmacol Toxicol* **125**:317–327. doi: 10.1111/bcpt.13264

Blamey LK, Branch GM (2012) Regime shift of a kelp-forest benthic community induced by an "invasion" of the rock lobster Jasus lalandii. *J Exp Mar Bio Ecol* **420**–421:33–47. doi: 10.1016/j.jembe.2012.03.022

Blamey LK, de Lecea AM, Jones LDS, Branch GM (2019) Diet of the spiny lobster Jasus paulensis from the Tristan da Cunha archipelago: Comparisons between islands, depths and lobster sizes. *Estuar Coast Shelf Sci* **219**:262–272. doi: 10.1016/j.ecss.2019.02.021

Blum JD, Popp BN, Drazen JC, Anela Choy C, Johnson MW (2013) Methylmercury production below the mixed layer in the North Pacific Ocean. *Nat Geosci* **6**:879–884. doi: 10.1038/ngeo1918

Bodin N, Budzinski H, Le Ménach K, Tapie N (2009) ASE extraction method for simultaneous carbon and nitrogen stable isotope analysis in soft tissues of aquatic organisms. *Anal Chim Acta* **643**:54–60. doi: 10.1016/j.aca.2009.03.048

Bodin N, Lesperance D, Albert R, Hollanda S, Michaud P, Degroote M, Churlaud C, Bustamante P (2017) Trace elements in oceanic pelagic communities in the western Indian Ocean. *Chemosphere* **174**:354–362. doi: 10.1016/j.chemosphere.2017.01.099

Boening DW (2000) Ecological effects, transport, and fate of mercury: A general review. *Chemosphere* **40**:1335–1351. doi: 10.1016/S0045-6535(99)00283-0

Bonanno G, Orlando-Bonaca M (2018) Trace elements in Mediterranean seagrasses and macroalgae. A review. *Sci Total Environ* **618**:1152–1159. doi: 10.1016/j.scitotenv.2017.09.192

Borcard D, Gillet F, Legendre P (2018) Numerical ecology with R, 2nd edition. Springer International Publishing, 435p. doi: 10.1007/978-3-319-71404-2

Bosch AC, O'Neill B, Sigge GO, Kerwath SE, Hoffman LC (2016) Heavy metals in marine fish meat and consumer health: A review. *J Sci Food Agric* **96**:32–48. doi: 10.1002/jsfa.7360

Brewster JD, Giraldo C, Choy ES, MacPhee SA, Hoover C, Lynn B, McNicholl DG, Majewski A, Rosenberg B, Power M, Reist JD, Loseto LL (2017) A comparison of the trophic ecology of Beaufort Sea Gadidae using fatty acids and stable isotopes. *Polar Biol* **41**:149–162. doi: 10.1007/s00300-017-2178-0

Briand MJ, Bonnet X, Guillou G, Letourneur Y (2016) Complex food webs in highly diversified coral reefs: Insights from $\delta^{13}C$ and $\delta^{15}N$ stable isotopes. *Food Webs* **8**:12–22. doi: 10.1016/j.fooweb.2016.07.002

Briguglio L (1995) Small island developing states and their economic vulnerabilities. *World Dev* **23**:1615–1632. doi: 10.1016/0305-750X(95)00065-K

Bruno JF, Carr LA, O'Connor MI (2015) Exploring the role of temperature in the ocean through metabolic scaling. *Ecology* **96**:3126–3140. doi: 10.1890/14-1954.1

Bruno JF, Bates AE, Cacciapaglia C, Pike EP, Amstrup SC, Van Hooidonk R, Henson SA, Aronson RB (2018) Climate change threatens the world's marine protected areas. *Nat Clim Chang* **8**:499–503. doi: 10.1038/s41558-018-0149-2

Budge SM, Iverson SJ, Koopman HN (2006) Studying trophic ecology in marine ecosystems using fatty acids: A primer on analysis and interpretation. *Mar Mammal Sci* **22**:759–801. doi: 10.1111/j.1748-7692.2006.00079.x

Bury N, Grosell M (2003) Iron acquisition by teleost fish. *Comp Biochem Physiol - C Toxicol Pharmacol* **135**:97–105. doi: 10.1016/S1532-0456

Bustamante P, Caurant F, Fowler SW, Miramand P (1998) Cephalopods as a vector for the transfer of cadmium to top marine predators in the north-east Atlantic Ocean. *Sci Total Environ* **220**:71–80. doi: 10.1016/S0048-9697(98)00250-2

Bustamante P, Lahaye V, Durnez C, Churlaud C, Caurant F (2006) Total and organic Hg concentrations in cephalopods from the North Eastern Atlantic waters: Influence of geographical origin and feeding ecology. *Sci Total Environ* **368**:585–596. doi: 10.1016/j.scitotenv.2006.01.038

Cabrita ARJ, Maia MRG, Oliveira HM, Sousa-Pinto I, Almeida AA, Pinto E, Fonseca AJM (2016) Tracing seaweeds as mineral sources for farm-animals. *J Appl Phycol* **28**:3135–3150. doi: 10.1007/s10811-016-0839-y

Cailliet GM, Goldman KJ (2004) Age determination and validation in chondrichthyan fishes. In: *Biology of Sharks and Their Relatives, 1st edition* (Eds. Carrier JC, Musick J, Heithaus M). CRC Press, pp 399–448. doi: 10.1201/9780203491317.pt3

Cailliet GM, Smith WD, Mollet HF, Goldman KJ (2006) Age and growth studies of chondrichthyan fishes: The need for consistency in terminology, verification, validation, and growth function fitting. *Environ Biol Fishes* **77**:211–228. doi: 10.1007/s10641-006-9105-5

Cano-Sancho G, Sioen I, Vandermeersch G, Jacobs S, Robbens J, Nadal M, Domingo JL (2015) Integrated risk index for seafood contaminants (IRISC): Pilot study in five European countries. *Environ Res* **143**:109–115. doi: 10.1016/j.envres.2015.03.006

Cao R, Liu Y, Wang Q, Dong Z, Yang D, Liu H, Ran W, Qu Y, Zhao J (2018) Seawater acidification aggravated cadmium toxicity in the oyster *Crassostrea gigas*: Metal bioaccumulation, subcellular distribution and multiple physiological responses. *Sci Total Environ* **642**:809–823. doi: 10.1016/j.scitotenv.2018.06.126

Carravieri A, Bustamante P, Labadie P, Budzinski H, Chastel O, Cherel Y (2020) Trace elements and persistent organic pollutants in chicks of 13 seabird species from Antarctica to the subtropics. *Environ Int* **134**:105225. doi: 10.1016/j.envint.2019.105225

Castiglioni D, Rezende CE, Muniz P, Muir AI, Garcia-Alonso J (2018) Trace metals bioavailability approach in intertidal estuarine sediments and bioaccumulation in associated Nereidid polychaetes. *Bull Environ Contam Toxicol* **100**:472–476. doi: 10.1007/s00128-018-2301-0

Cawthorn DM, Mariani S (2017) Global trade statistics lack granularity to inform traceability and management of diverse and high-value fishes. *Sci Rep* **7**:1–11. doi: 10.1038/s41598-017-12301-x

Chanda S, Paul BN, Ghosh K, Giri SS (2015) Dietary essentiality of trace minerals in aquaculture: A Review. *Agric Rev* **36**:100–112. doi: 10.5958/0976-0741.2015.00012.4

Chang-Seng D (2007) Climate Variability and climate change assessment for the Seychelles. 56p. URL: https://www.unisdr.org/files/18929_18929climatevariabiltyandclimatecha.pdf

Charrad M, Ghazzali N, Boiteau V, Niknafs A (2014) NbClust: An R package for determining the relevant number of clusters in a data set. *J Stat Softw* **61**:1–36.

Chen YW, Belzile N, Gunn JM (2001) Antagonistic effect of selenium on mercury assimilation by fish populations near Sudbury metal smelters? *Limnol Oceanogr* **46**:1814–1818. doi: 10.4319/lo.2001.46.7.1814

Cherel Y, Duhamel G (2003) Diet of the squid *Moroteuthis ingens* (Teuthoidea: Onychoteuthidae) in the upper slope waters of the Kerguelen Islands. *Mar Ecol Prog Ser* **250**:197–203. doi: 10.3354/meps250197

Chouvelon T, Spitz J, Cherel Y, Caurant F, Sirmel R, Mèndez-Fernandez P, Bustamante P (2011) Inter-specific and ontogenic differences in $\delta^{13}C$ and $\delta^{15}N$ values and Hg and Cd concentrations in cephalopods. *Mar Ecol Prog Ser* **433**:107–120. doi: 10.3354/meps09159

Chouvelon T, Spitz J, Caurant F, Mèndez-Fernandez P, Autier J, Lassus-Débat A, Chappuis A, Bustamante P (2012) Enhanced bioaccumulation of mercury in deep-sea fauna from the Bay of Biscay (north-east Atlantic) in relation to trophic positions identified by analysis of carbon and nitrogen stable isotopes. *Deep Res Part I*

Oceanogr Res Pap 65:113–124. doi: 10.1016/j.dsr.2012.02.010

Chouvelon T, Caurant F, Cherel Y, Simon-Bouhet B, Spitz J, Bustamante P (2014) Species- and size-related patterns in stable isotopes and mercury concentrations in fish help refine marine ecosystem indicators and provide evidence for distinct management units for hake in the Northeast Atlantic. *ICES J Mar Sci* 71:1073–1087. doi: 10.1093/icesjms/fst199

Chouvelon T, Brach-Papa C, Auger D, Bodin N, Bruzac S, Crochet S, Degroote M, Hollanda SJ, Hubert C, Knoery J, Munschy C, Puech A, Rozuel E, Thomas B, West W, Bourjea J, Nikolic N (2017) Chemical contaminants (trace metals, persistent organic pollutants) in albacore tuna from western Indian and south-eastern Atlantic Oceans: Trophic influence and potential as tracers of populations. *Sci Total Environ* 596–597:481–495. doi: 10.1016/j.scitotenv.2017.04.048

Chouvelon T, Cresson P, Bouchoucha M, Brach-Papa C, Bustamante P, Crochet S, Marco-Miralles F, Thomas B, Knoery J (2018) Oligotrophy as a major driver of mercury bioaccumulation in medium-to high-trophic level consumers: A marine ecosystem-comparative study. *Environ Pollut* 233:844–854. doi: 10.1016/j.envpol.2017.11.015

Chouvelon T, Strady E, Harmelin-Vivien M, Radakovitch O, Brach-Papa C, Crochet S, Knoery J, Rozuel E, Thomas B, Tronczynski J, Chiffoleau JF (2019) Patterns of trace metal bioaccumulation and trophic transfer in a phytoplankton-zooplankton-small pelagic fish marine food web. *Mar Pollut Bull* 146:1013–1030. doi: 10.1016/j.marpolbul.2019.07.047

Choy CA, Popp BN, Kaneko JJ, Drazen JC (2009) The influence of depth on mercury levels in pelagic fishes and their prey. *Proc Natl Acad Sci USA* 106:13865–13869. doi: 10.1073/pnas.0900711106

Christensen V, Walters CJ (2004) Ecopath with Ecosim: Methods, capabilities and limitations. *Ecol Modell* 172:109–139. doi: 10.1016/j.ecolmodel.2003.09.003

Ciardullo S, Aureli F, Coni E, Guandalini E, Iosi F, Raggi A, Rufo G, Cubadda F (2008) Bioaccumulation potential of dietary arsenic, cadmium, lead, mercury, and selenium in organs and tissues of rainbow trout (*Oncorhyncus mykiss*) as a function of fish growth. *J Agric Food Chem* 56:2442–2451. doi: 10.1021/jf703572t

Clarke TM, Reygondeau G, Wabnitz C, Robertson R, Ixquiac-Cabrera M, López M, Ramírez Coghi AR, del Río Iglesias JL, Wehrtmann I, Cheung WWL (2021) Climate change impacts on living marine resources in the Eastern Tropical Pacific. *Divers Distrib* 27:65–81. doi: 10.1111/ddi.13181

Cocheret De La Morinière E, Pollux BJA, Nagelkerken I, Van Der Velde G (2003) Diet shifts of Caribbean grunts (Haemulidae) and snappers (Lutjanidae) and the relation with nursery-to-coral reef migrations. *Estuar Coast Shelf Sci* 57:1079–1089. doi: 10.1016/S0272-7714(03)00011-8

Connan M, McQuaid CD, Bonnevie BT, Smale MJ, Cherel Y (2014) Combined stomach content, lipid and stable isotope analyses reveal spatial and trophic partitioning among three sympatric albatrosses from the Southern Ocean. *Mar Ecol Prog Ser* 497:259–272. doi: 10.3354/meps10606

Copaja S V., Pérez CA, Vega-Retter C, Véliz D (2017) Heavy metal content in chilean fish related to habitat use, tissue type and river of origin. *Bull Environ Contam Toxicol* 99:695–700. doi: 10.1007/s00128-017-2200-9

Copper Development Association (2019) Copper in human health. URL: https://www.copper.org/consumers/health/cu_health_uk.html. Accessed 29 May 2019

Coro G, Pagano P, Ellenbroek A (2020) Detecting patterns of climate change in long-term forecasts of marine environmental parameters. *Int J Digit Earth* 13:567–585. doi: 10.1080/17538947.2018.1543365

Costa-Pereira R, Araújo MS, Souza FL, Ingram T (2019) Competition and resource breadth shape niche variation and overlap in multiple trophic dimensions. *Proc R Soc B Biol Sci* 286:1–9. doi: 10.1098/rspb.2019.0369

Curtis AN, Bourne K, Borsuk ME, Buckman KL, Demidenko E, Taylor VF, Chen CY (2019) Effects of temperature, salinity, and sediment organic carbon on methylmercury bioaccumulation in an estuarine amphipod. *Sci Total Environ* 687:907–916. doi: 10.1016/j.scitotenv.2019.06.094

Dalabehara HB, Sarma VVSS (2021) Physical forcing controls spatial variability in primary production in the Indian

Ocean. *Deep Res Part II Top Stud Oceanogr* **183**:104906. doi: 10.1016/j.dsr2.2020.104906

Dalsgaard J, St. John M, Kattner G, Müller-Navarra D, Hagen W (2003) Fatty acid trophic markers in the pelagic marine environment. *Adv Mar Biol* **46**:225–340. doi: 10.1016/S0065-2881(03)46005-7

De Niro M, Epstein S (1978) Influence of diet on the distribution of carbon isotopes in animals. *Geochim Cosmochim Acta* **42**:495–506. doi: 10.1016/0016-7037(78)90199-0

Di Bona KR, Love S, Rhodes NR, McAdory D, Sinha SH, Kern N, Kent J, Strickland J, Wilson A, Beaird J, Ramage J, Rasco JF, Vincent JB (2011) Chromium is not an essential trace element for mammals: Effects of a "low-chromium" diet. *J Biol Inorg Chem* **16**:381–390. doi: 10.1007/s00775-010-0734-y

Dijkstra JA, Buckman KL, Ward D, Evans DW, Dionne M, Chen CY (2013) Experimental and natural warming elevates mercury concentrations in estuarine fish. *PLoS One* **8**:1–9. doi: 10.1371/journal.pone.0058401

Ding Q, Chen X, Hilborn R, Chen Y (2017) Vulnerability to impacts of climate change on marine fisheries and food security. *Mar Policy* **83**:55–61. doi: 10.1016/j.marpol.2017.05.011

Domingo JL (2011) Influence of cooking processes on the concentrations of toxic metals and various organic environmental pollutants in food: A review of the published literature. *Crit Rev Food Sci Nutr* **51**:29–37. doi: 10.1080/10408390903044511

Dunnington D (2018) ggspatial: Spatial Data Framework for ggplot2.

Esposito M, De Roma A, La Nucara R, Picazio G, Gallo P (2018) Total mercury content in commercial swordfish (*Xiphias gladius*) from different FAO fishing areas. *Chemosphere* **197**:14–19. doi: 10.1016/j.chemosphere.2018.01.015

Fabregas J, Herrero C (1986) Marine microalgae as a potential source of minerals in fish diet. *Aquaculture* **51**:237–243. doi: 10.1007/bf01982726

Faganeli J, Falnoga I, Horvat M, Klun K, Lipej L, Mazej D (2018) Selenium and mercury interactions in apex predators from the gulf of trieste (Northern Adriatic Sea). *Nutrients* **10**:1–11. doi: 10.3390/nu10030278

FAO (2020) Species facts sheet – *Xiphias gladius*. URL: http://www.fao.org/fishery/species/ 2503/en.

Figueiredo C, Baptista M, Grilo T, Caetano M, Markaida U, Raimundo J, Rosa R (2020) Bioaccumulation of trace elements in myctophids in the oxygen minimum zone ecosystem of the Gulf of California. *Oceans* **1**:34–46. doi: 10.3390/oceans1010004

Figueras M, Olivan M, Busquets S, Lopez-Soriano F, Argiles J (2011) Effects of eicosapentaenoic acid (EPA) treatment on insulin sensitivity in an animal model of diabetes: Improvemnt of the inflammatory status. *Obesity* **19**:362–369. doi: 10.1038/oby.2010.194

Folch J, Lees M, Sloane-Stanley GH (1957) A simple method for the isolation and purification of total lipids from animal tissues. *J Biol Chem* **226**:497–509. doi: 10.1016/S0021-9258(18)64849-5

Fox JM, Zimba P V. (2018) Minerals and trace elements in microalgae. In: *Microalgae in Health and Disease Prevention* (Eds. Levine I, Fleurence J). Elsevier, pp 177–193. doi 10.1016/B978-0-12-811405-6.00008-6

France RL (1995) Carbon-13 enrichment in benthic compared to planktonic algae: food web implications. *Mar Ecol Prog Ser* **124**:307–312. doi: 10.3354/meps124307

Frank A, Danielsson R, Jones B (2000) Experimental copper and chromium deficiency and additional molybdenum supplementation in goats. II. Concentrations of trace and minor elements in liver, kidneys and ribs: Haematology and clinical chemistry. *Sci Total Environ* **249**:143–170. doi: 10.1016/S0048-9697(99)00518-5

Froese R, Pauly D (2020) FishBase. World Wide Web electronic publication. URL: www.fishbase.org.

Fry B (2002) Stable isotopic indicators of habitat use by Mississippi River fish. *J North Am Benthol Soc* **21**:676–685. doi: 10.2307/1468438

Fry B, Sherr EB (1989) $\delta^{13}C$ measurements as indicators of carbon flow in marine and freshwater ecosystems. In: *Stable Isotopes in Ecological Research. Ecological Studies (Analysis and Synthesis)* (Eds. Rundel PW, Ehleringer JR, Nagy KA). Springer, pp 196–229. doi: 10.1007/978-1-4612-3498-2_12

Gephart JA, Rovenskaya E, Dieckmann U, Pace ML, Brännström Å (2016) Vulnerability to shocks in the global seafood trade network. *Environ Res Lett* **11**:035008. doi: 10.1088/1748-9326/11/3/035008

Gerson JR, Walters DM, Eagles-Smith CA, Bernhardt ES, Brandt JE (2020) Do two wrongs make a right? Persistent uncertainties regarding environmental selenium-mercury interactions. *Environ Sci Technol* **54**:9228–9234. doi: 10.1021/acs.est.0c01894

Gheisari E, Raissy M, Rahimi E (2016) The effect of different cooking methods on lead and cadmium contents of shrimp and lobster. *J Food Biosci Technol* **6**:53–58. doi: 10.37896/jxu14.8/076

Gladyshev MI, Sushchik NN, Anishchenko O V., Makhutova ON, Kalachova GS, Gribovskaya I V. (2009) Benefit-risk ratio of food fish intake as the source of essential fatty acids vs. heavy metals: A case study of Siberian grayling from the Yenisei River. *Food Chem* **115**:545–550. doi: 10.1016/j.foodchem.2008.12.062

Gochfeld M, Burger J (2021) Mercury interactions with selenium and sulfur and the relevance of the Se:Hg molar ratio to fish consumption advice. *Environ Sci Pollut Res* **28**:18407–17420. doi: 10.1007/s11356-021-12361-7

Godswill C, Gospel C (2019) Impacts of plastic pollution on the sustainability of seafood value chain and human health. *Int J Adv Acad Res Sci* **5**:2488–9849.

Goldhaber SB (2003) Trace element risk assessment: Essentiality vs. toxicity. *Regul Toxicol Pharmacol* **38**:232–242. doi: 10.1016/S0273-2300(02)00020-X

Gómez-Batista M, Metian M, Teyssie JL, Alonso-Hernández C, Warnau M (2007) Bioaccumulation of dissolved arsenic in the oyster *Crassostrea virginica*: A radiotracer study. *Environ Bioindic* **2**:237–244. doi: 10.1080/15555270701693570

Gosnell KJ, Mason RP (2015) Mercury and methylmercury incidence and bioaccumulation in plankton from the central Pacific Ocean. *Mar Chem* **177**:772–780. doi: 10.1016/j.marchem.2015.07.005

Goutte A, Cherel Y, Churlaud C, Ponthus JP, Massé G, Bustamante P (2015) Trace elements in Antarctic fish species and the influence of foraging habitats and dietary habits on mercury levels. *Sci Total Environ* **538**:743–749. doi: 10.1016/j.scitotenv.2015.08.103

Govender A, Van Der Elst R, James N (2003) Swordfish: Global lessons. 39p. doi: 10.13140/RG.2.1.1418.4720

Government of Seychelles (2013) Seychelles damage, loss, and needs assessment (DaLA) - 2013 floods. 56p. URL: http://documents.worldbank.org/curated/en/689161468106741988/Seychelles-Damage-Loss-and-Needs-Assessment-DaLA-2013-floods-a-report-by-the-Government-of-Seychelles

Goyer RA (1997) Toxic and essential metal interactions. *Annu Rev Nutr* **17**:37–50. doi: 10.1146/annurev.nutr.17.1.37

Graham NAJ, Nash KL (2013) The importance of structural complexity in coral reef ecosystems. *Coral Reefs* **32**:315–326. doi: 10.1007/s00338-012-0984-y

Graham NAJ, Wilson SK, Jennings S, Polunin NVC, Bijoux JP, Robinson J (2006) Dynamic fragility of oceanic coral reef ecosystems. *Proc Natl Acad Sci USA* **103**:8425–8429. doi: 10.1073/pnas.0600693103

Graham NAJ, Chabanet P, Evans RD, Jennings S, Letourneur Y, Aaron Macneil M, Mcclanahan TR, Öhman MC, Polunin NVC, Wilson SK (2011) Extinction vulnerability of coral reef fishes. *Ecol Lett* **14**:341–348. doi: 10.1111/j.1461-0248.2011.01592.x

Grandcourt EM, Hecht T, Booth AJ, Robinson J (2008) Retrospective stock assessment of the Emperor red snapper (*Lutjanus sebae*) on the Seychelles Bank between 1977 and 2006. *ICES J Mar Sci* **65**:889–898. doi: 10.1093/icesjms/fsn064

Gruber N, Sarmiento JL (1997) Global patterns of marine nitrogen fixation and denitrification. *Global Biogeochem Cycles* **11**:235–266. doi: 10.1029/97GB00077

Guinot D, Ureña R, Pastor A, Varó I, Ramo J del, Torreblanca A (2012) Long-term effect of temperature on bioaccumulation of dietary metals and metallothionein induction in Sparus aurata. *Chemosphere* **87**:1215–1221. doi: 10.1016/j.chemosphere.2012.01.020

Gupta UC, Gupta SC (2014) Sources and deficiency diseases of mineral nutrients in human health and nutrition: A review. *Pedosphere* **24**:13–38. doi: 10.1016/S1002-0160(13)60077-6

Haas A, el-Zibdah M, Wild C (2010) Seasonal monitoring of coral-algae interactions in fringing reefs of the Gulf of Aqaba, Northern Red Sea. *Coral Reefs* **29**:93–103. doi: 10.1007/s00338-009-0556-y

Haley CN, Blamey LK, Atkinson LJ, Branch GM (2011) Dietary change of the rock lobster *Jasus lalandii* after an "invasive" geographic shift: Effects of size, density and food availability. *Estuar Coast Shelf Sci* **93**:160–170. doi: 10.1016/j.ecss.2011.04.015

Hallström E, Bergman K, Mifflin K, Parker R, Tyedmers P, Troell M, Ziegler F (2019) Combined climate and nutritional performance of seafoods. *J Clean Prod* **230**:402–411. doi: 10.1016/j.jclepro.2019.04.229

Hanson SD, Stafford CP (2017) Modeling otolith weight using fish age and length: Applications to age determination. *Trans Am Fish Soc* **146**:778–790. doi: 10.1080/00028487.2017.1310138

Hawkes C, Fanzo J, Udomkesmalee E, Achadi E, Ahuja A, Bhutta Z, De-Regil LM, Fracassi P, Grummer-Strawn LM, Hayashi C, Kimani-Murage E, Martin-Prével Y, Menon P, Oenema S, Randel J, Requejo J, Swimburn B (2017) Global Nutrition Report - Nourishing the SDGs. 115p. URL: https://globalnutritionreport.org/reports/2017-global-nutrition-report/

Hazon N, Wells A, Pillans RD, Good JP, Anderson WG, Franklin CE (2003) Urea based osmoregulation and endocrine control in elasmobranch fish with special reference to euryhalinity. *Comp Biochem Physiol - B Biochem Mol Biol* **136**:685–700. doi: 10.1016/S1096-4959(03)00280-X

Heath-Brown N (2016) The statesman's yearbook 2016 - The politics, cultures and economies of the world. Palgrave Macmillan, 1564p.

Hédouin L, Bustamante P, Churlaud C, Pringault O, Fichez R, Warnau M (2009) Trends in concentrations of selected metalloid and metals in two bivalves from the coral reefs in the SW lagoon of New Caledonia. *Ecotoxicol Environ Saf* **72**:372–381. doi: 10.1016/j.ecoenv.2008.04.004

Hédouin L, Batista MG, Metian M, Buschiazzo E, Warnau M (2010) Metal and metalloid bioconcentration capacity of two tropical bivalves for monitoring the impact of land-based mining activities in the New Caledonia lagoon. *Mar Pollut Bull* **61**:554–567. doi: 10.1016/j.marpolbul.2010.06.036

Herut B, Kress N (1997) Particulate metals contamination in the Kishon River estuary, Israel. *Mar Pollut Bull* **34**:706–711. doi: 10.1016/S0025-326X(97)00018-0

Hesslein RH, Hallard KA, Rarnlal P (1993) Replacement of sulfur, carbon and nitrogen in tissues of growing broad whitefish (*Coregonus nasus*) in response to a change in diet traced by $\delta^{34}S$, $\delta^{13}C$ and $\delta^{15}N$. *Can J Fish Aquat Sci* **50**:2071–2076. doi: 10.1139/f93-230

Hicks CC, Cohen PJ, Graham NAJ, Nash KL, Allison EH, Lima CD, Mills DJ, Roscher M, Thilsted SH, Thorne-Lyman AL, Macneil MA (2019) Harnessing global fisheries to tackle micronutrient deficiencies. *Nature* **574**:95–98. doi: 10.1038/s41586-019-1592-6

Hill CH, Matrone G (1970) Chemical parameters in the study of in vivo and in vitro interactions of transition elements. *Fed Proc* **29**:1474–1481.

Hodson P V. (1988) The effect of metal metabolism on uptake, disposition and toxicity in fish. *Aquat Toxicol* **11**:3–18. doi: 10.1016/0166-445X(88)90003-3

Hoegh-Guldberg O (2011) Coral reef ecosystems and anthropogenic climate change. *Reg Environ Chang* **11**:215–227. doi: 10.1007/s10113-010-0189-2

Hollanda S, Bodin N, Churlaud C, Bustamante P (2017) Mercury and selenium levels in Swordfish (*Xiphias gladius*) fished in the exclusive economic zone of the Republic of Seychelles. *Int J Environ Ecol Eng* **11**:23–26.

Holthuis LB (1991) FAO species catalogue Vol. 13. Marine lobsters of the world An annotated and illustrated catalogue of species of interest to fisheries known to date. *FAO Fish Synopsis* **13**:1–4. URL: http://www.fao.org/publications/card/fr/c/5b06cf31-81fe-54f7-ac3c-5d4380638296/

Horn F, Lindenmeier G, Moc I, Grillhösl C, Berghold S, Schneider N, Münster B (2005) Biochimie humaine.

Flammarion, 596p.

Houssard P, Point D, Tremblay-Boyer L, Allain V, Pethybridge H, Masbou J, Ferriss BE, Baya PA, Lagane C, Menkes CE, Letourneur Y, Lorrain A (2019) a model of mercury distribution in tuna from the western and central Pacific Ocean: Influence of physiology, ecology and environmental factors. *Environ Sci Technol* **53**:1422–1431. doi: 10.1021/acs.est.8b06058

Hwalla N, Adra N, Jackson RT (2004) Iron deficiency is an important contributor to anemia among reproductive age women in Lebanon. *Ecol Food Nutr* **43**:77–92. doi: 10.1080/03670240490274101

Ikeh-Tawari EP, Anetor JI, Charles-Davies MA (2013) Cadmium level in pregnancy, influence on neonatal birth weight and possible amelioration by some essential trace elements. *Toxicol Int 20:108–112*. doi: 10.4103/0971-6580.111558

Intès A, Laboute P, Menou JL (1979) Les langoustes coralliennes aux Seychelles : prospection. 20p. URL: http://www.documentation.ird.fr/hor/fdi:010026859

Ivanenko N V. (2018) The role of microorganisms in transformation of selenium in marine waters. *Russ J Mar Biol* **44**:87–93. doi: 10.1134/S1063074018020049

Ivanina A V., Beniash E, Etzkorn M, Meyers TB, Ringwood AH, Sokolova IM (2013) Short-term acute hypercapnia affects cellular responses to trace metals in the hard clams *Mercenaria mercenaria*. *Aquat Toxicol* **140**–141:123–133. doi: 10.1016/j.aquatox.2013.05.019

Iverson SJ (2009) Tracing aquatic food webs using fatty acids: from qualitative indicators to quantitative determination. In: *Lipids in Aquatic Ecosystems* (Eds. Kainz M, Brett MT, Arts MT). Springer, pp 281–308. doi: 10.1007/978-0-387-89366-2_12

Jackson RT, Al-Mousa Z (2000) Iron deficiency is a more important cause of anemia than hemoglobinopathies in Kuwaiti adolescent girls. *J Nutr* **130**:1212–1216. doi: 10.1093/jn/130.5.1212

Jaishankar M, Tseten T, Anbalagan N, Mathew BB, Beeregowda KN (2014) Toxicity, mechanism and health effects of some heavy metals. *Interdiscip Toxicol* **7**:60–72. doi: 10.2478/intox-2014-0009

Jaschinski S, Brepohl DC, Sommer U (2011) Seasonal variation in carbon sources of mesograzers and small predators in an eelgrass community: Stable isotope and fatty acid analyses. *Mar Ecol Prog Ser* **431**:69–82. doi: 10.3354/meps09143

Jean C, Bourjea J, Jouen E, Taquet M (2006) Stock structure of the swordfish (*Xiphias gladius*) in the southwest Indian Ocean : A preliminary study. *Bull Mar Sci* **79**:521–526.

JECFA (2011a) Arsenic. URL: https://apps.who.int/food-additives-contaminants-jecfa-database/chemical.aspx?chemID=1863.

JECFA (2011b) Mercury. URL: https://apps.who.int/food-additives-contaminants-jecfa-database/chemical.aspx?chemID=1806.

JECFA (2013) Cadmium. URL: https://apps.who.int/food-additives-contaminants-jecfa-database/chemical.aspx?chemID=1376.

Jeffree RA, Warnau M, Teyssié JL, Markich SJ (2006) Comparison of the bioaccumulation from seawater and depuration of heavy metals and radionuclides in the spotted dogfish *Scyliorhinus canicula* (Chondrichthys) and the turbot *Psetta maxima* (Actinopterygii: Teleostei). *Sci Total Environ* **368**:839–852. doi: 10.1016/j.scitotenv.2006.03.026

Jeffree RA, Oberhansli F, Teyssie JL (2010) Phylogenetic consistencies among chondrichthyan and teleost fishes in their bioaccumulation of multiple trace elements from seawater. *Sci Total Environ* **408**:3200–3210. doi: 10.1016/j.scitotenv.2010.04.015

Jennings S, Marshall SS, Cuet P, Naim O (2000) Chapter 13 - The Seychelles. In: *Coral reefs of the Indian Ocean* (Eds. McClanahan TR, Sheppard CRC, Obura DO). Oxford University Press, pp 383–410. doi: 10.1016/B978-0-12-389601-8.50009-6

Jennings S, Pinnegar JK, Polunin NVC, Warr KJ (2002) Linking size-based and trophic analyses of benthic community

structure. *Mar Ecol Prog Ser* **226**:77–85. doi: 10.3354/meps226077

Jinadasa BKKK, Ahmad SBN, Edirisinghe EMRKB, Wicramasinghe I (2014) Mercury content in yellowfin tuna (*Thunnus albacares*) and swordfish (*Xiphias gladius*) and estimation of mercury intake. *J food Secur* **2**:23–16. doi: 10.12691/jfs-2-1-3

Jochum M, Schneider FD, Crowe TP, Brose U, O'Gorman EJ (2012) Climate-induced changes in bottom-up and top-down processes independently alter a marine ecosystem. *Philos Trans R Soc B Biol Sci* **367**:2962–2970. doi: 10.1098/rstb.2012.0237

Jung S, Houde ED (2003) Spatial and temporal variabilities of pelagic fish community structure and distribution in Chesapeake Bay, USA. *Estuar Coast Shelf Sci* **58**:335–351. doi: 10.1016/S0272-7714(03)00085-4

Juszczak P, Tax DMJ, Duin RPW (2002) Feature scaling in support vector data description. *Proc ASCI, 8th Annu Conf Adv Sch Comput Imaging* 95–102.

Kehrig HDA, Seixas TG, Palermo EA, Baêta AP, Castelo-Branco CW, Malm O, Moreira I (2009) The relationships between mercury and selenium in plankton and fish from a tropical food web. *Environ Sci Pollut Res* **16**:10–24. doi: 10.1007/s11356-008-0038-8

Kelly JR, Scheibling RE (2012) Fatty acids as dietary tracers in benthic food webs. *Mar Ecol Prog Ser* **446**:1–22. doi: 10.3354/meps09559

Khan A, Amelie V (2015) Assessing climate change readiness in Seychelles: implications for ecosystem-based adaptation mainstreaming and marine spatial planning. *Reg Environ Chang* **15**:721–733. doi: 10.1007/s10113-014-0662-4

Khan MAK, Wang F (2009) Mercury-selenium compounds and their toxicological significance: Toward a molecular understanding of the mercury-selenium antagonism. *Environ Toxicol Chem* **28**:1567–1577. doi: 10.1897/08-375.1

Khokiattiwong S, Kornkanitnan N, Goessler W, Kokarnig S, Francesconi KA (2009) Arsenic compounds in tropical marine ecosystems: Similarities between mangrove forest and coral reef. *Environ Chem* **6**:226–234. doi: 10.1071/EN09009

Khoushabi F, Shadan M, Miri A, SharifiRad J (2016) Determination of maternal serum zinc, iron, calcium and magnesium during pregnancy in pregnant women and umbilical cord blood and their association with outcome of pregnancy. *Mater Socio Medica* **28**:104–107. doi: 10.5455/msm.2016.28.104-107

Kibria G, Nugegoda D, Rose G, Haroon AKY (2021) Climate change impacts on pollutants mobilization and interactive effects of climate change and pollutants on toxicity and bioaccumulation of pollutants in estuarine and marine biota and linkage to seafood security. *Mar Pollut Bull* **167**:112364. doi: 10.1016/j.marpolbul.2021.112364

Kilada R, Driscoll JG (2017) Age determination in crustaceans: A review. *Hydrobiologia* **799**:21–36. doi: 10.1007/s10750-017-3233-0

Kim J, Kim YJ, Lee R, Moon JH, Jo I (2012) Serum levels of zinc, calcium, and iron are associated with the risk of preeclampsia in pregnant women. *Nutr Res* **32**:764–769. doi: 10.1016/j.nutres.2012.09.007

Kim KH, Kabir E, Jahan SA (2016) A review on the distribution of Hg in the environment and its human health impacts. *J Hazard Mater* **306**:376–385. doi: 10.1016/j.jhazmat.2015.11.031

Kim SL, Koch PL (2012) Methods to collect, preserve, and prepare elasmobranch tissues for stable isotope analysis. *Environ Biol Fishes* **95**:53–63. doi: 10.1007/s10641-011-9860-9

Kimirei IA, Nagelkerken I, Trommelen M, Blankers P, van Hoytema N, Hoeijmakers D, Huijbers CM, Mgaya YD, Rypel AL (2013) What drives ontogenetic niche shifts of fishes in coral reef ecosystems? *Ecosystems* **16**:783–796. doi: 10.1007/s10021-013-9645-4

Klöck C, Nunn PD (2019) Adaptation to climate change in Small Island Developing States: A systematic literature review of Academic Research. *J Environ Dev* **28**:196–218. doi: 10.1177/1070496519835895

Kojadinovic J, Potier M, Le Corre M, Cosson RP, Bustamante P (2006) Mercury content in commercial pelagic fish and its risk assessment in the Western Indian Ocean. *Sci Total Environ* **366**:688–700. doi: 10.1016/j.scitotenv.2006.02.006

Kojadinovic J, Potier M, Le Corre M, Cosson RP, Bustamante P (2007) Bioaccumulation of trace elements in pelagic

fish from the Western Indian Ocean. *Environ Pollut* **146**:548–566. doi: 10.1016/j.envpol.2006.07.015

Kolasinski J, Frouin P, Sallon A, Rogers K, Bruggemann HJ, Potier M (2009) Feeding ecology and ontogenetic dietary shift of yellowstripe goatfish *Mulloidichthys flavolineatus* (Mullidae) at Reunion Island, SW Indian ocean. *Mar Ecol Prog Ser* **386**:181–195. doi: 10.3354/meps08081

Koolman J, Röhm K-H (2011) Atlas de poche de biochimie humaine, 4e édition. Lavoisier, 529p.

Krabbenhoft DP, Sunderland EM (2013) Global changes and mercury. *Nature* **341**:1457–1458. doi: 10.1126/science.1242838

Kulbicki M, Bozec YM, Labrosse P, Letourneur Y, Mou-Tham G, Wantiez L (2005) Diet composition of carnivorous fishes from coral reef lagoons of New Caledonia. *Aquat Living Resour* **18**:231–250. doi: 10.1051/alr:2005029

Lacoue-Labarthe T, Martin S, Oberhänsli F, Teyssié JL, Markich S, Ross J, Bustamante P (2009) Effects of increased pCO_2 and temperature on trace element (Ag, Cd and Zn) bioaccumulation in the eggs of the common cuttlefish, *Sepia officinalis*. *Biogeosciences* **6**:2561–2573. doi: 10.5194/bg-6-2561-2009

Lacoue-Labarthe T, Réveillac E, Oberhänsli F, Teyssié JL, Jeffree R, Gattuso JP (2011) Effects of ocean acidification on trace element accumulation in the early-life stages of squid *Loligo vulgaris*. *Aquat Toxicol* **105**:166–176. doi: 10.1016/j.aquatox.2011.05.021

Lahaye V, Bustamante P, Spitz J, Dabin W, Das K, Pierce GJ, Caurant F (2005) Long-term dietary segregation of common dolphins. *Mar Ecol Prog Ser* **305**:275–285. doi: 10.3354/meps305275

Larsen R, Eilertsen KE, Elvevoll EO (2011) Health benefits of marine foods and ingredients. *Biotechnol Adv* **29**:508–518. doi: 10.1016/j.biotechadv.2011.05.017

Lavoie RA, Jardine TD, Chumchal MM, Kidd KA, Campbell LM (2013) Biomagnification of mercury in aquatic food webs: A worldwide meta-analysis. *Environ Sci Technol* **47**:13385–13394. doi: 10.1021/es403103t

Layman CA, Araujo MS, Boucek R, Hammerschlag-Peyer CM, Harrison E, Jud ZR, Matich P, Rosenblatt AE, Vaudo JJ, Yeager LA, Post DM, Bearhop S (2011) Applying stable isotopes to examine food-web structure: An overview of analytical tools. *Biol Rev* **87**:545–562. doi: 10.1111/j.1469-185X.2011.00208.x

Le Croizier G, Schaal G, Gallon R, Fall M, Le Grand F, Munaron JM, Rouget ML, Machu E, Le Loc'h F, Laë R, De Morais LT (2016) Trophic ecology influence on metal bioaccumulation in marine fish: Inference from stable isotope and fatty acid analyses. *Sci Total Environ* **573**:83–95. doi: 10.1016/j.scitotenv.2016.08.035

Lee B-G, Griscon SB, Lee J-S, Choi HJ, Koh C-H, Luoma SN, Fisher NS (2000) Influences of dietary uptake and reactive sulfides on metal bioavailability from aquatic sediments. *Science* **287**:282–284. doi: 10.1126/science.287.5451.282

Lee CS, Fisher NS (2016) Methylmercury uptake by diverse marine phytoplankton. *Limnol Oceanogr* **61**:1626–1639. doi: 10.1002/lno.10318

Lemasson AJ, Hall-Spencer JM, Kuri V, Knights AM (2019) Changes in the biochemical and nutrient composition of seafood due to ocean acidification and warming. *Mar Environ Res* **143**:82–92. doi: 10.1016/j.marenvres.2018.11.006

Leotsinidis M, Alexopoulos A, Kostopoulou-Farri E (2005) Toxic and essential trace elements in human milk from Greek lactating women: Association with dietary habits and other factors. *Chemosphere* **61**:238–247. doi: 10.1016/j.chemosphere.2005.01.084

Lesser MP, Falcón LI, Rodríguez-Román A, Enríquez S, Hoegh-Guldberg O, Iglesias-Prieto R (2007) Nitrogen fixation by symbiotic cyanobacteria provides a source of nitrogen for the scleractinian coral *Montastraea cavernosa*. *Mar Ecol Prog Ser* **346**:143–152. doi: 10.3354/meps07008

Li Y, Zhang Y, Hussey NE, Dai X (2016) Urea and lipid extraction treatment effects on $\delta^{15}N$ and $\delta^{13}C$ values in pelagic sharks. *Rapid Commun Mass Spectrom* **30**:1–8. doi: 10.1002/rcm.7396

Lin HT, Chen SW, Shen CJ, Chu C (2008) Arsenic speciation in fish on the market. *J Food Drug Anal* **16**:70–75. doi: 10.38212/2224-6614.2343

Lischka A, Lacoue-Labarthe T, Hoving HJT, JavidPour J, Pannell JL, Merten V, Churlaud C, Bustamante P (2018) High cadmium and mercury concentrations in the tissues of the orange-back flying squid, *Sthenoteuthis pteropus*, from the tropical Eastern Atlantic. *Ecotoxicol Environ Saf* **163**:323–330. doi: 10.1016/j.ecoenv.2018.07.087

Lischka A, Lacoue-Labarthe T, Bustamante P, Piatkowski U, Hoving HJT (2020) Trace element analysis reveals bioaccumulation in the squid *Gonatus fabricii* from polar regions of the Atlantic Ocean. *Environ Pollut* **256**:113389. doi: 10.1016/j.envpol.2019.113389

Little AG, Loughland I, Seebacher F (2020) What do warming waters mean for fish physiology and fisheries? *J Fish*

Biol **97**:328–340. doi: 10.1111/jfb.14402

Littler MM, Littler DS, Titlyanov EA (1991) Comparisons of N- and P-limited productivity between high granitic islands versus low carbonate atolls in the Seychelles Archipelago: A test of the relative-dominance paradigm. *Coral Reefs* **10**:199–209. doi: 10.1007/BF00336775

Logan JM, Lutcavage ME (2010) Stable isotope dynamics in elasmobranch fishes. *Hydrobiologia* **644**:231–244. doi: 10.1007/s10750-010-0120-3

Logan JM, Jardine TD, Miller TJ, Bunn SE, Cunjak RA, Lutcavage ME (2008) Lipid corrections in carbon and nitrogen stable isotope analyses: comparison of chemical extraction and modelling methods. *J Anim Ecol* **77**:838–846. doi: 10.1111/j.1365-2656.2008.01394.x

Longhurst AR (1998) Chapter 10 - The Indian Ocean. In: *Ecological Geography of the Sea* (Ed. Longhurst AR). Academic Press, pp 275-325. doi: 10.1080/00377996.1953.9957307

Lorrain A, Graham BS, Popp BN, Allain V, Olson RJ, Hunt BP V, Potier M, Fry B, Galván-magaña F, Menkes CER, Kaehler S, Ménard F (2015) Nitrogen isotopic baselines and implications for estimating foraging habitat and trophic position of yellowfin tuna in the Indian and Pacific Oceans. *Deep Res Part II Top Stud Oceanogr* **113**:1–11. doi: 10.1016/j.dsr2.2014.02.003

Lu J, Borthwick F, Hassalani Z, Wang Y, Mangat R, Ruth M, Shi D, Jaeschke A, Russell JC, Field CJ, Proctor SD, Vine DF (2011) Chronic dietary n-3 PUFA intervention improves dyslipidaemia and subsequent cardiovascular complications in the JCR:LA-cp rat model on the metabolic syndrome. *Br J Nutr* **105**:1572–1582. doi: 10.1017/S0007114510005453

MacArthur LD, Phillips DL, Hyndes GA, Hanson CE, Vanderklift MA (2011) Habitat surrounding patch reefs influences the diet and nutrition of the western rock lobster. *Mar Ecol Prog Ser* **436**:191–205. doi: 10.3354/meps09256

Madeira D, Narciso L, Cabral HN, Vinagre C (2012) Thermal tolerance and potential impacts of climate change on coastal and estuarine organisms. *J Sea Res* **70**:32–41. doi: 10.1016/j.seares.2012.03.002

Mahé K, Evano H, Mille T, Muths D, Bourjea J (2016) Otolith shape as a valuable tool to evaluate the stock structure of swordfish *Xiphias gladius* in the Indian Ocean. *African J Mar Sci* **38**:457–464. doi: 10.2989/1814232X.2016.1224205

Malea P, Kevrekidis T (2014) Trace element patterns in marine macroalgae. *Sci Total Environ* **495**:144–157. doi: 10.1016/j.scitotenv.2014.06.134

Malinouski M, Hasan NM, Zhang Y, Seravalli J, Lin J, Avanesov A, Lutsenko S, Gladyshev VN (2014) Genome-wide RNAi ionomics screen reveals new genes and regulation of human trace element metabolism. *Nat Commun* **5**:1–11. doi: 10.1038/ncomms4301

Manceau A, Azemard S, Hédouin L, Vassileva E, Lecchini D, Fauvelot C, Swarzenski PW (2021) Chemical forms of mercury in blue marlin billfish: Implications for human exposure. *Environ Sci Technol Lett* **8**:405–411. doi: https://doi.org/10.1021/acs.estlett.1c00217

Marques-Vidal P, Madeleine G, Romain S, Gabriel A, Bovet P (2008) Secular trends in height and weight among children and adolescents of the Seychelles, 1956-2006. *BMC Public Health* **8**:1–9. doi: 10.1186/1471-2458-8-166

Marriott RJ, Mapstone BD, Beng GA (2007) Age-specific demographic parameters, and their implications for management of the red bass, *Lutjanus bohar* (Forsskal 1775): A large, long-lived reef fish. *Fish Res* **83**:204–215. doi: http://dx.doi.org/10.1016/j.fishres.2006.09.016

Martinez-Andrade F (2003) A comparison of life histories and ecological aspects among snappers (Pisces: Lutjanidae). Graduate Faculty of the Louisiana State University, 201p.

Mason RP, Reinfelder JR, Morel FMM (1995) Bioaccumulation of mercury and methylmercury. *Water, Air Soil Pollut* **80**:915–921. doi: 10.1007/BF01189744

Mathews T, Fisher NS (2009) Dominance of dietary intake of metals in marine elasmobranch and teleost fish. *Sci Total Environ* **407**:5156–5161. doi: 10.1016/j.scitotenv.2009.06.003

Mathews T, Fisher NS, Jeffree RA, Teyssié JL (2008) Assimilation and retention of metals in teleost and elasmobranch fishes following dietary exposure. *Mar Ecol Prog Ser* **360**:1–12. doi: 10.3354/meps07462

Maulvault AL, Custódio A, Anacleto P, Repolho T, Pousão P, Nunes ML, Diniz M, Rosa R, Marques A (2016) Bioaccumulation and elimination of mercury in juvenile seabass (*Dicentrarchus labrax*) in a warmer environment. *Environ Res* **149**:77–85. doi: 10.1016/j.envres.2016.04.035

Maulvault AL, Camacho C, Barbosa V, Alves R, Anacleto P, Fogaça F, Kwadijk C, Kotterman M, Cunha SC, Fernandes JO, Rasmussen RR, Sloth JJ, Aznar-Alemany Ò, Eljarrat E, Barceló D, Marques A (2018) Assessing the effects of seawater temperature and pH on the bioaccumulation of emerging chemical contaminants in marine bivalves. *Environ Res* **161**:236–247. doi: 10.1016/j.envres.2017.11.017

McConnaughey T, McRoy CP (1979) Food-Web structure and the fractionation of Carbon isotopes in the Bering Sea. *Mar Biol* **53**:257–262. doi: 10.1007/BF00952434

McGill LM, Gerig BS, Chaloner DT, Lamberti GA (2017) An ecosystem model for evaluating the effects of introduced Pacific salmon on contaminant burdens of stream-resident fish. *Ecol Modell* **355**:39–48. doi: 10.1016/j.ecolmodel.2017.03.027

McKuin B, Watson JT, Stohs S, Campbell JE (2021) Rethinking sustainability in seafood: Synergies and trade-offs between fisheries and climate change. *Elementa* **9**:1–21. doi: 10.1525/elementa.2019.00081

McMeans BC, McCann KS, Humphries M, Rooney N, Fisk AT (2015) Food web structure in temporally-forced ecosystems. *Trends Ecol Evol* **30**:662–672. doi: 10.1016/j.tree.2015.09.001

McPherson GR, Squire L (1992) Age and growth of three dominant *Lutjanus* species of the Great Barrier Reef inter-reef fishery. *Asian Fish Sci* **5**:25–36.

Médieu A, Point D, Receveur A, Gauthier O, Allain V, Pethybridge H, Menkes CE, Gillikin DP, Revill AT, Somes CJ, Collin J, Lorrain A (2021) Stable mercury concentrations of tropical tuna in the south western Pacific ocean: An 18-year monitoring study. *Chemosphere* **262**:128024. doi: 10.1016/j.chemosphere.2020.128024

Mees C (1992) Seychelles demersal fishery: an analysis of data relating to four key demersal species. 142p. URL: https://aquadocs.org/handle/1834/5114

Ménard F, Lorrain A, Potier M, Marsac F (2007) Isotopic evidence of distinct feeding ecologies and movement patterns in two migratory predators (yellowfin tuna and swordfish) of the western Indian Ocean. *Mar Biol* **153**:141–152. doi: 10.1007/s00227-007-0789-7

Méndez-Fernandez P, Pierce GJ, Bustamante P, Chouvelon T, Ferreira M, González AF, López A, Read FL, Santos MB, Spitz J, Vingada J V., Caurant F (2013) Ecological niche segregation among five toothed whale species off the NW Iberian Peninsula using ecological tracers as multi-approach. *Mar Biol* **160**:2825–2840. doi: 10.1007/s00227-013-2274-9

Mergler D, Anderson HA, Hing Man Chan L, Mahaffey KR, Murray M, Sakamoto M, Stern AH (2007) Methylmercury exposure and health effects in humans: A worldwide concern. *AMBIO A J Hum Environ* **36**:3–11. doi: 10.1579/0044-7447(2007)36

Metian M, Bustamante P, Hédouin L, Warnau M (2008) Accumulation of nine metals and one metalloid in the tropical scallop *Comptopallium radula* from coral reefs in New Caledonia. *Environ Pollut* **152**:543–552. doi: 10.1016/j.envpol.2007.07.009

Metian M, Warnau M, Chouvelon T, Pedraza F, Rodriguezy Baena AM, Bustamante P (2013) Trace element bioaccumulation in reef fish from New Caledonia: Influence of trophic groups and risk assessment for consumers. *Mar Environ Res* **88**:26–36. doi: 10.1016/j.marenvres.2013.03.001

Meyer L, Pethybridge H, Nichols PD, Beckmann C, Huveneers C (2019) Abiotic and biotic drivers of fatty acid tracers in ecology: A global analysis of chondrichthyan profiles. *Funct Ecol* **33**:1243–1255. doi: 10.1111/1365-2435.13328

Miao X-S, Woodward LA, Swenson C, Li QX (2001) Comparative concentrations of metals in marine species from French Frigate Shoals, North Pacific Ocean. *Mar Pollut Bull* **42**:1049–1054. doi: 10.1016/S0025-326X(01)00067-4

Mikac N, Picer M, Stegnar P, Tušek-Žnidarić M (1985) Mercury distribution in a polluted marine area, ratio of total mercury, methyl mercury and selenium in sediments, mussels and fish. *Water Res* **19**:1387–1392. doi: 10.1016/0043-1354(85)90305-7

Milinki E, Molnar SZ, Kiss A, Virag D, Penzes-Konya E (2011) Study of micronutrient accumulating characteristics of microalgae. *Acta Bot Hungaria* **53**:159–167. doi: 10.1556/ABot.53.2011.1

Molin M, Ulven SM, Meltzer HM, Alexander J (2015) Arsenic in the human food chain, biotransformation and toxicology - Review focusing on seafood arsenic. *J Trace Elem Med Biol* **31**:249–259. doi: 10.1016/j.jtemb.2015.01.010

Monteiro LR, Costa V, Furness RW, Santos RS (1996) Mercury concentrations in prey fish indicate enhanced bioaccumulation in mesopelagic environments. *Mar Ecol Prog Ser* **141**:21–25. doi: 10.3354/meps141021

Morel FMM, Kraepiel AML, Amyot M (1998) The chemical cycle and bioaccumulation of mercury. *Annu Rev Ecol Syst* **29**:543–566. doi: 10.1146/annurev.ecolsys.29.1.543

Moustahfid H, Marsac F, Gangopadhyay A (2018) Chapter 12: Climate change impacts, vulnerabilities and adaptations: Western Indian Ocean marine fisheries. In: *Impacts of climate change on fisheries and aquaculture – Synthesis of current knowledge, adaptation and mitigation options* (Eds. Barange M, Bahri T, Beveridge MCM, Cochrane KL, Funge-Smith S, Poulain F). FAO, Rome, pp 251–279. URL: http://www.fao.org/3/i9705en/i9705en.pdf

Mubiana VK, Blust R (2007) Effects of temperature on scope for growth and accumulation of Cd, Co, Cu and Pb by the marine bivalve *Mytilus edulis*. *Mar Environ Res* **63**:219–235. doi: 10.1016/j.marenvres.2006.08.005

Mudgal V, Madaan N, Mudgal A, Singh RB, Mishra S (2010) Effect of toxic metals on human health. *Open Nutraceuticals J* **3**:94–99. doi: 10.2174/1876396001003010094

Muhling BA, Lee SK, Lamkin JT, Liu Y (2011) Predicting the effects of climate change on bluefin tuna (*Thunnus thynnus*) spawning habitat in the Gulf of Mexico. *ICES J Mar Sci* **68**:1051–1062. doi: 10.1093/icesjms/fsr008

Mukherjee N, Sutherland WJ, Dicks L, Hugé J, Koedam N, Dahdouh-Guebas F (2014) Ecosystem service valuations of mangrove ecosystems to inform decision making and future valuation exercises. *PLoS One* **9**:1–9. doi: 10.1371/journal.pone.0107706

Murry BA, Farrell JM, Teece MA, Smyntek PM (2006) Effect of lipid extraction on the interpretation of fish community trophic relationships determined by stable carbon and nitrogen isotopes. *Can J Fish Aquat Sci* **63**:2167–2172. doi: 10.1139/F06-116

Murthagh F, Legendre P (2014) Ward's Hierarchical Agglomerative Clustering method: Which algorithms implement Ward's Criterion? *J Classif* **31**:274–295. doi: 10.1007/s00357-014-9161-z

Muths D, Le Couls S, Evano H, Grewe P, Bourjea J (2013) Multi-genetic marker approach and spatio-temporal analysis suggest there is a single panmictic population of Swordfish *Xiphias gladius* in the Indian Ocean. *PLoS One* **8**:e63558. doi: 10.1371/journal.pone.0063558

Myers SS, Smith MR, Guth S, Golden CD, Vaitla B, Mueller ND, Dangour AD, Huybers P (2017) Climate change and global food systems: Potential impacts on food security and undernutrition. *Annu Rev Public Health* **38**:259–277. doi: 10.1146/annurev-publhealth-031816-044356

Nair M, Jayalakshmy K V., Balachandran KK, Joseph T (2006) Bioaccumulation of toxi metals by fish in a semi-enclosed tropical ecosystem. *Environ Forensics* **7**:197–206. doi: 10.1080/15275920600840438

Nakamura I (1985) Vol. 5 Billfishes of the world – An annotated and illustrated catalogue of marlins, sailfishes, spearfishes and swordfishes known to date. *FAO Fish Synopsis* **5**:1–4. doi: 10.1016/S0921-4526(05)00705-2

Naqvi SWA, Naik H, Pratihary A, Souza WD, Narvekar P V, Jayakumar DA, Devol AH (2006) Coastal versus open-ocean denitrification in the Arabian Sea. *Biogeosciences* **3**:621–633.

Nassiri Y, Rainbow PS, Smith BD, Nassiri Y, Amiard-Triquet C, Rainglet F (2000) Trace-metal detoxification in the ventral caeca of *Orchestia gammarellus* (Crustacea: Amphipoda). *Mar Biol* **136**:477–484. doi: 10.1007/s002270050707

Navarro-Alarcon M, Cabrera-Vique C (2008) Selenium in food and the human body: A review. *Sci Total Environ* **400**:115–141. doi: 10.1016/j.scitotenv.2008.06.024

Neff JM (2002a) Bioaccumulation mechanisms. In: *Bioaccumulation in marine organisms* (Ed. Neff JM). Elsevier, pp 37–56. doi: 10.1016/b978-008043716-3/50003-8

Neff JM (2002b) Mercury in the ocean. In: *Bioaccumulation in marine organisms* (Ed. Neff JM). Elsevier, pp 103–130. doi: 10.1016/B978-008043716-3/50007-5

Nguyen KDT, Morley SA, Lai CH, Clark MS, Tan KS, Bates AE, Peck LS (2011) Upper temperature limits of tropical marine ectotherms: Global warming implications. *PLoS One* **6**:6–13. doi: 10.1371/journal.pone.0029340

Nielsen FH (1991) Nutritional requirements for boron, silicon, vanadium, nickel, and arsenic: Current knowledge and speculation. *FASEB J* **5**:2661–2667. doi 10.1096/fasebj.5.12.1916090

Nordlund LM, Jackson EL, Nakaoka M, Samper-Villarreal J, Beca-Carretero P, Creed JC (2018) Seagrass ecosystem services – What's next? *Mar Pollut Bull* **134**:145–151. doi: 10.1016/j.marpolbul.2017.09.014

O'Brien JM, Scheibling RE (2018) Turf wars: Competition between foundation and turf-forming species on temperate and tropical reefs and its role in regime shifts. *Mar Ecol Prog Ser* **590**:1–17. doi: 10.3354/meps12530

O'Hara J (1972) The influence of temperature and salinity on the toxixity of cadmium to the Fiddler crab, *Uca*

pucilator. *Fish Bull* **71**:149–153.

Obura D, Gudka M, Rabi FA, Gian SB, Bijoux J, Freed S, Maharavo J, Mwaura J, Porter S, Sola E, Wickel J, Yahya S, Ahamada S (2017) Coral reef status report for the Western Indian Ocean. 271p. doi: 10.13140/RG.2.2.20642.07366

Ogle DH, Wheeler P, Dinno A (2018) FSA: Fisheries Stock Analysis.

Ohio State University (2015) Ohio State University extension fact sheet: Iron. URL: https://ohioline.osu.edu/factsheet/HYG-5559. Accessed 29 May 2019

Oksanen J, Blanchet FG, Friendly M, Kindt R, Legendre P, McGlinn D, Michin PR, O'Hara RB, Simpson GL, Solymos P, Stevens HH, Szoecs E, Wagner H (2019) vegan: Community Ecology Package.

Pack EC, Lee SH, Kim CH, Lim CH, Sung DG, Kim MH, Park KH, Lim KM, Choi DW, Kim SW (2014) Effects of environmental temperature change on mercury absorption in aquatic organisms with respect to climate warming. *J Toxicol Environ Heal - Part A Curr Issues* **77**:1477–1490. doi: 10.1080/15287394.2014.955892

Palomares MLD, Pauly D (2020) SeaLifeBase. World Wide Web electronic publication. URL: www.sealifebase.org.

Panfili J, Pontual H de, Troadec H, Wright PJ (2002) Manual of fish sclerochronology. Editions Ifremer, 464p. doi: 10.4324/9780080967691-8

Pebesma EJ (2018) Simple Features for R: Standardized Support for Spatial Vector Data.

Pebesma EJ, Bivand RS (2005) Classes and methods for spatial data in R.

Penicaud V, Lacoue-labarthe T, Bustamante P (2017) Metal bioaccumulation and detoxification processes in cephalopods : A review. *Environ Res* **155**:123–133. doi: 10.1016/j.envres.2017.02.003

Perello G, Martí-Cid R, Llobet JM, Domingo JL (2008) Effects of various cooking processes on the concentrations of arsenic, cadmium, mercury, and lead in foods. *J Agric Food Chem* **56**:11262–11269. doi: 10.1021/jf802411q

Perkins MJ, McDonald RA, van Veen FJF, Kelly SD, Rees G, Bearhop S (2014) Application of Nitrogen and Carbon stable isotopes ($\delta^{15}N$ and $\delta^{13}C$) to quantify food chain length and trophic structure. *PLoS One* **9**:e93281. doi: 10.1371/journal.pone.0093281

Pethybridge H, Choy CA, Logan JM, Allain V, Lorrain A, Bodin N, Somes CJ, Young J, Ménard F, Langlais C, Duffy L, Hobday AJ, Kuhnert P, Fry B, Menkes C, Olson RJ (2018) A global meta-analysis of marine predator nitrogen stable isotopes: Relationships between trophic structure and environmental conditions. *Glob Ecol Biogeogr* **27**:1043–1055. doi: 10.1111/geb.12763

Pierce GJ, Boyle PR, Hastie LC, Santos MB (1994) Diets of squid *Loligo forbesi* and *Loligo vulgaris* in the northeast Atlantic. *Fish Res* **21**:149–163. doi: 10.1016/0165-7836(94)90101-5

Pillans RD, Good JP, Gary Anderson W, Hazon N, Franklin CE (2005) Freshwater to seawater acclimation of juvenile bull sharks (*Carcharhinus leucas*): Plasma osmolytes and Na^+/K^+-ATPase activity in gill, rectal gland, kidney and intestine. *J Comp Physiol B Biochem Syst Environ Physiol* **175**:37–44. doi: 10.1007/s00360-004-0460-2

Poisson F, Fauvel C (2009) Reproductive dynamics of swordfish (*Xiphias gladius*) in the southwestern Indian Ocean (Reunion Island).Part 1: Oocyte development, sexual maturity and spawning. *Aquat Living Resour* **22**:45–58. doi: 10.1051/alr/2009007

Poloczanska ES, Burrows MT, Brown CJ, Molinos JG, Halpern BS, Hoegh-Guldberg O, Kappel C V., Moore PJ, Richardson AJ, Schoeman DS, Sydeman WJ (2016) Responses of marine organisms to climate change across oceans. *Front Mar Sci* **3**:1–21. doi: 10.3389/fmars.2016.00062

Post DM (2002) Using stable isotopes to estimate trophic position: Models, methods, and assumptions. *Ecology* **83**:703–718. doi: 10.2307/3071875

Post DM, Layman CA, Arrington DA, Takimoto G, Quattrochi J, Montaña CG (2007) Getting to the fat of the matter: Models, methods and assumptions for dealing with lipids in stable isotope analyses. *Oecologia* **152**:179–189. doi: 10.1007/s00442-006-0630-x

Potier M, Marsac F, Cherel Y, Lucas V, Sabatié R, Maury O, Ménard F (2007) Forage fauna in the diet of three large pelagic fishes (lancetfish, swordfish and yellowfin tuna) in the western equatorial Indian Ocean. *Fish Res* **83**:60–72. doi: 10.1016/j.fishres.2006.08.020

Pouil S, Oberhänsli F, Bustamante P, Metian M (2018) Investigations of temperature and pH variations on metal trophic transfer in turbot (*Scophthalmus maximus*). *Environ Sci Pollut Res* **25**:11219–11225. doi: 10.1007/s11356-017-8691-4

Pouil S, Oberhänsli F, Bustamante P, Metian M (2020) Trophic transfer of trace elements in a euryhaline fish, the

turbot *Scophthalmus maximus*: Contrasting effects of salinity on two essential elements. *Mar Pollut Bull* **154**:111065. doi: 10.1016/j.marpolbul.2020.111065

Pratchett MS, Hoey AS, Wilson SK, Messmer V, Graham NAJ (2011) Changes in biodiversity and functioning of reef fish assemblages following coral bleaching and coral loss. *Diversity* **3**:424–452. doi: 10.3390/d3030424

Qiao Q, Le Manach S, Sotton B, Huet H, Duvernois-Berthet E, Paris A, Duval C, Ponger L, Marie A, Blond A, Mathéron L, Vinh J, Bolbach G, Djediat C, Bernard C, Edery M, Marie B (2016) Deep sexual dimorphism in adult medaka fish liver highlighted by multi-omic approach. *Sci Rep* **6**:1–12. doi: 10.1038/srep32459

R Core Team (2018) R: A language and environment for statistical computing.

Raimundo J, Vale C, Caetano M, Giacomello E, Anes B, Menezes GM (2013) Natural trace element enrichment in fishes from a volcanic and tectonically active region (Azores archipelago). *Deep Res Part II Top Stud Oceanogr* **98**:137–147. doi: 10.1016/j.dsr2.2013.02.009

Rainbow PS (1998) Phylogeny of trace metal accumulation in crustaceans. In: *Metal metabolism in aquatic environments* (Eds. Langston WJ, Bebianno MJ). Springer-Science, pp 285–319. doi: 10.1007/978-1-4757-2761-6_9

Rainbow PS (2002) Trace metal concentrations in aquatic invertebrates: Why and so what? *Environ Pollut* **120**:497–507. doi: 10.1016/S0269-7491(02)00238-5

Rainbow PS (2007) Trace metal bioaccumulation: Models, metabolic availability and toxicity. *Environ Int* **33**:576–582. doi: 10.1016/j.envint.2006.05.007

Rainbow PS, Black WH (2002) Effects of changes in salinity and osmolality on the rate of uptake of zinc by three crabs of different ecologies. *Mar Ecol Prog Ser* **244**:205–217. doi: 10.3354/meps244205

Rainbow PS, Black WH (2005) Physicochemistry or physiology: Cadmium uptake and effects of salinity and osmolality in three crabs of different ecologies. *Mar Ecol Prog Ser* **286**:217–229. doi: 10.3354/meps286217

Rainbow PS, Luoma SN (2011) Metal toxicity, uptake and bioaccumulation in aquatic invertebrates – Modelling zinc in crustaceans. *Aquat Toxicol* **105**:455–465. doi: 10.1016/j.aquatox.2011.08.001

Ralston NVC, Blackwell JL, Raymond LJ (2007) Importance of molar ratios in selenium-dependent protection against methylmercury toxicity. *Biol Trace Elem Res* **119**:255–268. doi: 10.1007/s12011-007-8005-7

Ralston NVC, Ralston CR, Raymond LJ (2015) Selenium Health Benefit Values: Updated criteria for mercury risk assessments. *Biol Trace Elem Res* **171**:262–269. doi: 10.1007/s12011-015-0516-z

Ramos R, González-Solís J (2012) Trace me if you can: The use of intrinsic biogeochemical markers in marine top predators. *Front Ecol Environ* **10**:258–266. doi: 10.1890/110140

Ratte HT (1999) Bioaccumulation and toxicity of silver compounds: A review. *Environ Toxicol Chem* **18**:89–108. doi: 10.1897/1551-5028(1999)018<0089:BATOSC>2.3.CO;2

Raymond LJ, Ralston NVC (2004) Mercury:selenium interactions and health implications. *Seychelles Med Dent J* **7**:72–77. doi: 10.1016/j.neuro.2020.09.020

Rejomon G, Nair M, Joseph T (2010) Trace metal dynamics in fishes from the southwest coast of India. *Environ Monit Assess* **167**:243–255. doi: 10.1007/s10661-009-1046-y

Ricketts P, Voutchkov M, Chan HM (2019) Risk-benefit assessment for total mercury, arsenic, selenium, and Omega-3 fatty acids exposure from fish consumption in Jamaica. *Biol Trace Elem Res* **197**:262-270. doi: 10.1007/s12011-019-01965-3

Rizal A, Anna Z (2019) Climate change and its possible food security implications toward Indonesian marine and fisheries. *World News Nat Sci* **22**:119–128.

Robinson J, Isidore M, Marguerite MA, Öhman MC, Payet RJ (2004) Spatial and temporal distribution of reef fish spawning aggregations in the Seychelles - An interview-based survey of srtisanal fishers. *West Indian Ocean J Mar Sci* **3**:63–69. doi: 10.1007/s10641-006-9161-x

Robinson J, Aumeeruddy R, Isidore M, Payet R, Marguerite M, Laval M, Domingue G, Lucas V (2006) Country review: Seychelles. In: *Review of the state of world marine capture fisheries management: Indian Ocean* (Eds. De Young C, Fishery Policy Analyst, Fishery Policy and Planning Division, FAO Fisheries Department). FAO, pp 425–436. URL: http://www.fao.org/docrep/009/a0477e/a0477e11.htm

Robinson J, Dorizo J, Assan C (2009) The Seychelles Spiny Lobster Fishery - Fishery and Stock Status: 2005-2008. 22p. URL: http://hdl.handle.net/1834/7198

Robinson JPW, Wilson SK, Jennings S, Graham NAJ (2019) Thermal stress induces persistently altered coral reef fish assemblages. *Glob Chang Biol* **25**:2739–2750. doi: 10.1111/gcb.14704

Robinson JPW, Robinson J, Gerry C, Govinden R, Freshwater C, Graham NAJ (2020) Diversification insulates fisher catch and revenue in heavily exploited tropical fisheries. *Sci Adv* **6**:1–10. doi: 10.1126/sciadv.aaz0587

Rochman CM, Tahir A, Williams SL, Baxa D V., Lam R, Miller JT, Teh FC, Werorilangi S, Teh SJ (2015) Anthropogenic debris in seafood: Plastic debris and fibers from textiles in fish and bivalves sold for human consumption. *Sci Rep* **5**:1–10. doi: 10.1038/srep14340

Rosenfeld J, Van Leeuwen T, Richards J, Allen D (2015) Relationship between growth and standard metabolic rate: Measurement artefacts and implications for habitat use and life-history adaptation in salmonids. *J Anim Ecol* **84**:4–20. doi: 10.1111/1365-2656.12260

Ruiz-Cooley RI, Gerrodette T, Fiedler PC, Chivers SJ, Danil K, Ballance LT (2017) Temporal variation in pelagic food chain length in response to environmental change. *Sci Adv* **3**:1–9. doi: 10.1126/sciadv.1701140

Sabino MA, Govinden R, Pethybridge H, Blamey L, Le Grand F, Sardenne F, Rose M, Bustamante P, Bodin N (2021) Habitat degradation increases interspecific trophic competition between three spiny lobster species in Seychelles. *Estuar Coast Shelf Sci* **256**:107368. doi: 10.1016/j.ecss.2021.107368

Saha N, Mollah MZI, Alam MF, Safiur Rahman M (2016) Seasonal investigation of heavy metals in marine fishes captured from the Bay of Bengal and the implications for human health risk assessment. *Food Control* **70**:110–118. doi: 10.1016/j.foodcont.2016.05.040

Sanchez-Vidal A, Canals M, de Haan WP, Romero J, Veny M (2021) Seagrasses provide a novel ecosystem service by trapping marine plastics. *Sci Rep* **11**:1–7. doi: 10.1038/s41598-020-79370-3

Sardenne F, Hollanda S, Lawrence S, Albert-Arrisol R, Degroote M, Bodin N (2017) Trophic structures in tropical marine ecosystems: A comparative investigation using three different ecological tracers. *Ecol Indic* **81**:315–324. doi: 10.1016/j.ecolind.2017.06.001

Sardenne F, Bodin N, Barret L, Blamey L, Govinden R, Gabriel K, Mangroo R, Munaron J-M, Le Loc'h F, Bideau A, Le Grand F, Sabino M, Bustamante P, Rowat D (2021) Diets of spiny lobsters from Mahé Island reefs, Seychelles reefs inferred by trophic tracers. *Reg Stud Mar Sci* **42**:101640. doi: 10.1016/j.rsma.2021.101640

Scherer PE, Hill JA (2016) Obesity, diabetes, and cardiovascular diseases. *Circ Res* **118**:1703–1705. doi: 10.1161/CIRCRESAHA.116.308999

Schiavon M, Ertani A, Parrasia S, Vecchia FD (2017) Selenium accumulation and metabolism in algae. *Aquat Toxicol* **189**:1–8. doi: 10.1016/j.aquatox.2017.05.011

Schmidt L, Bizzi CA, Duarte FA, Muller EI, Krupp E, Feldmann J, Flores EMM (2015) Evaluation of Hg species after culinary treatments of fish. *Food Control* **47**:413–419. doi: 10.1016/j.foodcont.2014.07.040

Schmidt L, Figueroa JAL, Dalla Vecchia P, Duarte FA, Mello PA, Caruso JA, Flores EMM (2018) Bioavailability of Hg and Se from seafood after culinary treatments. *Microchem J* **139**:363–371. doi: 10.1016/j.microc.2018.03.009

Schott FA, Xie S-P, McCreary JP (2009) Indian ocean circulation and climate variability. *Rev Geophys* **47**:1–46. doi: 10.1029/2007RG000245

Sébastien L, Josse J, Husson F (2008) FactoMineR: An R package for Multivariate Analysis. *J Stat Softw* **25**:1–18. doi: 10.18637/jss.v025.i01

Seychelles Fishing Authority (2014) Fishery independent indices for the Seychelles lobster resource. 27p. URL: http://hdl.handle.net/1834/14833

Seychelles Fishing Authority (2018) Seychelles Fishing Authority - Strategic Plan 2018-2020. 135p. URL: http://hdl.handle.net/1834/14808

Seychelles Fishing Authority (2019) Annual Report 2015-2016. 133p. URL: http://hdl.handle.net/1834/17743

Sezer N, Kılıç Ö, Sıkdokur E, Çayır A, Belivermiş M (2020) Impacts of elevated pCO_2 on Mediterranean mussel (*Mytilus galloprovincialis*): Metal bioaccumulation, physiological and cellular parameters. *Mar Environ Res* **160**:104987. doi: 10.1016/j.marenvres.2020.104987

Shamlaye C, Davidson PW, Myers GJ (2004) The Seychelles Child Development Study : two decades of collaboration. *Seychelles Med Dent J* **7**:92–99. doi: 10.1016/j.neuro.2020.09.023

Sheaves M (1995) Large lutjanid and serranid fishes in tropical estuaries: Are they adults or juveniles? *Mar Ecol Prog Ser* **129**:31–40. doi: 10.3354/meps129031

Shen PJ, Gong B, Xu FY, Luo Y (2015) Four trace elements in pregnant women and their relationships with adverse pregnancy outcomes. *Eur Rev Med Pharmacol Sci* **19**:4690–4697.

Shi W, Zhao X, Han Y, Che Z, Chai X, Liu G (2016) Ocean acidification increases cadmium accumulation in marine

bivalves: A potential threat to seafood safety. *Sci Rep* **6**:1–8. doi: 10.1038/srep20197

Sirot V, Leblanc JC, Margaritis I (2012) A risk-benefit analysis approach to seafood intake to determine optimal consumption. *Br J Nutr* **107**:1812–1822. doi: 10.1017/S0007114511005010

Skerrett PJ, Willett WC (2010) Essentials of healthy eating: A guide. *J Midwifery Women's Heal* **55**:492–501. doi: 10.1016/j.jmwh.2010.06.019

Somes CJ, Schmittner A, Muglia J, Oschlies A (2017) A three-dimensional model of the marine nitrogen cycle during the last glacial maximum constrained by sedimentary isotopes. *Front Mar Sci* **4**:1–24. doi: 10.3389/fmars.2017.00108

Sommer U, Stibor H, Katechakis A, Sommer F, Hansen T (2002) Pelagic food web configurations at different levels of nutrient richness and their implications for the ratio fish production: Primary production. *Hydrobiologia* **484**:11–20. doi: http://dx.doi.org/10.1023/A:1021340601986

Sotiropoulos MA, Tonn WM, Wassenaar LI (2004) Effects of lipid extraction on stable carbon and nitrogen isotope analyses of fish tissues : Potential consequences for food web studies. *Ecol Freshw Fish* **13**:155–160. doi: 10.1111/j.1600-0633.2004.00056.x

Spalding MD, Ravilious C, Green EP (2001) World atlas of coral reefs. UNEP-WCMC, 424p. URL: https://archive.org/details/worldatlasofcora01spal/page/2/mode/2up

Storelli MM, Giacominelli-Stuffler R, Storelli A, Marcotrigiano GO (2005) Accumulation of mercury, cadmium, lead and arsenic in swordfish and bluefin tuna from the Mediterranean Sea: A comparative study. *Mar Pollut Bull* **50**:1004–1007. doi: 10.1016/j.marpolbul.2005.06.041

Stramma L, Prince ED, Schmidtko S, Luo J, Hoolihan JP, Visbeck M, Wallace DWR, Brandt P, Körtzinger A (2012) Expansion of oxygen minimum zones may reduce available habitat for tropical pelagic fishes. *Nat Clim Chang* **2**:33–37. doi: 10.1038/nclimate1304

Subramanian V (1993) Sediment load of Indian rivers. *Curr Sci* **64**:928–930.

Suratno, Puspitasari R, Rositasari R, Oktaviyani S (2019) Total mercury of marine fishes in Natuna Islands area, Indonesia: Risk assessment for human consumption. *IOP Conf Ser Earth Environ Sci* **277**:012025. doi: 10.1088/1755-1315/277/1/012025

Swanson HK, Lysy M, POwer M, Stasko AD, Johnson JD, Reist JD (2015) A new probabilistic method for quantifying n-dimensional ecological niches and niche overlap. *Ecology* **96**:318–324. doi: 10.1890/14-0235.1

Syversen T, Kaur P (2012) The toxicology of mercury and its compounds. *J Trace Elem Med Biol* **26**:215–226. doi: 10.1016/j.jtemb.2012.02.004

Taylor HH, Anstiss JM (1999) Copper and haemocyanin dynamics in aquatic invertebrates. *Mar Freshw Res Res* **50**:907–931. doi: 10.1071/MF99117

Thorner J, Kumar L, Smith SDA (2014) Impacts of climate-change-driven sea level rise on intertidal rocky reef habitats will be variable and site specific. *PLoS One* **9**:1–7. doi: 10.1371/journal.pone.0086130

Tirado MC, Clarke R, Jaykus LA, McQuatters-Gollop A, Frank JM (2010) Climate change and food safety: A review. *Food Res Int* **43**:1745–1765. doi: 10.1016/j.foodres.2010.07.003

Tlusty MF, Tyedmers P, Bailey M, Ziegler F, Henriksson PJG, Béné C, Bush S, Newton R, Asche F, Little DC, Troell M, Jonell M (2019) Reframing the sustainable seafood narrative. *Glob Environ Chang* **59**:101991. doi: 10.1016/j.gloenvcha.2019.101991

Trustwell AS, Mann J (2017) Introducing human nutrition. In: *Essentials of Human nutrition, 5th edition* (Eds. Mann J, Trustwell AS). Oxford University Press, pp 3–12. URL: https://books.google.fr/books?hl=fr&lr=&id=a6t0DgAAQBAJ&oi=fnd&pg=PP1&dq=%22essential+nutrients%22+%22human%22&ots=cr4qB5zNvV&sig=cppgl_OWOAfX8bEhrKcuhoRvZmw#v=onepage&q&f=false

Tuomisto HL (2018) Importance of considering environmental sustainability in dietary guidelines. *Lancet Planet Heal* **2**:e331–e332. doi: 10.1016/S2542-5196(18)30174-8

Twining BS, Baines SB (2013) The trace metal composition of marine phytoplankton. *Ann Rev Mar Sci* **5**:191–215. doi: 10.1146/annurev-marine-121211-172322

Twining BS, Rauschenberg S, Morton PL, Vogt S (2015) Metal contents of phytoplankton and labile particulate material in the North Atlantic Ocean. *Prog Oceanogr* **137**:261–283. doi: 10.1016/j.pocean.2015.07.001

Uneyama C, Toda M, Yamamoto M, Morikawa K (2007) Arsenic in various foods: Cumulative data. *Food Addit Contam* **24**:447–534. doi: 10.1080/02652030601053121

United Nations (2015) The 2030 agenda for sustainable development. 41p. doi: 10.1201/b20466-7

United Nations (2019) World population prospects 2019: Demographic profiles. 1238p. URL: http://www.ncbi.nlm.nih.gov/pubmed/12283219

US-EPA, US-FDA (2019) EPA-FDA Fish Advice: Technical Information. URL: https://www.epa.gov/fish-tech/epa-fda-fish-advice-technical-information.

Uthus EO (2003) Arsenic essentially: A role affecting methionine metabolism. *J Trace Elem Exp Med* **16**:345–355. doi: 10.1002/jtra.10044

Velusamy A, Satheesh Kumar P, Ram A, Chinnadurai S (2014) Bioaccumulation of heavy metals in commercially important marine fishes from Mumbai Harbor, India. *Mar Pollut Bull* **81**:218–224. doi: 10.1016/j.marpolbul.2014.01.049

Vermeij MJA, van Moorselaar I, Engelhard S, Hörnlein C, Vonk SM, Visser PM (2010) The effects of nutrient enrichment and herbivore abundance on the ability of turf algae to overgrow coral in the Caribbean. *PLoS One* **5**:1–8. doi: 10.1371/journal.pone.0014312

Vieira C, Morais S, Ramos S, Delerue-Matos C, Oliveira MBPP (2011) Mercury, cadmium, lead and arsenic levels in three pelagic fish species from the Atlantic Ocean: Intra- and inter-specific variability and human health risks for consumption. *Food Chem Toxicol* **49**:923–932. doi: 10.1016/j.fct.2010.12.016

Vincent JB (2017) New evidence against chromium as an essential trace element. *J Nutr* **147**:2212–2219. doi: 10.3945/jn.117.255901

Wada E, Hattori A (1976) Natural abundance of ^{15}N in particulate organic matter in the North Pacific Ocean. *Geochim Cosmochim Acta* **40**:249–251. doi: 10.1016/0016-7037(76)90183-6

Wada E, Ohki K, Yoshikawa S, Parker PL, Baalen C Van, Matsumoto GI, Aita MN, Saino T (2012) Ecological aspects of carbon and nitrogen isotope ratios of cyanobacteria. *Plankt Benthos Res* **7**:135–145. doi: 10.3800/pbr.7.135

Wada O (2004) What are trace elements? Their deficiency and excess states. *Japan Med Assoc J* **47**:351–358.

Wagemann R, Trebacz E, Hunt R, Boila G (1997) Percent methylmercury and organic mercury in tissues of marine mammals and fish using different experimental and calculation methods. *Environ Toxicol Chem* **16**:1859–1866. doi: 10.1897/1551-5028(1997)016<1859:PMAOMI>2.3.CO;2

Wang F, Wu Y, Chen Z, Zhang G, Zhang J, Zheng S, Kattner G (2019) Trophic interactions of mesopelagic fishes in the South China Sea illustrated by stable isotopes and fatty acids. *Front Mar Sci* **5**:1–12. doi: 10.3389/fmars.2018.00522

Wang J, Chuang CY, Wang WX (2005) Metal and oxygen uptake in the green mussel *Perna viridis* under different metabolic conditions. *Environ Toxicol Chem* **24**:2657–2664. doi: 10.1897/05-109R.1

Wang WX (2002) Interactions of trace metals and different marine food chains. *Mar Ecol Prog Ser* **243**:295–309. doi: 10.3354/meps243295

Wang WX, Rainbow PS (2008) Comparative approaches to understand metal bioaccumulation in aquatic animals. *Comp Biochem Physiol - C Toxicol Pharmacol* **148**:315–323. doi: 10.1016/j.cbpc.2008.04.003

Wang WX, Onsanit S, Dang F (2012) Dietary bioavailability of cadmium, inorganic mercury, and zinc to a marine fish: Effects of food composition and type. *Aquaculture* **356–357**:98–104. doi: 10.1016/j.aquaculture.2012.05.031

Ward JH (1963) Hierarchical grouping to optimize an objective function. *J Am Stat Assoc* **58**:236–244. doi: 10.2307/2282967

Webb M (1979) The chemistry, biochemistry and biology of cadmium. Elsevier, 465p.

Wehrtmann IS, Arana PM, Barriga E, Gracia A, Pezzuto PR (2012) Deep-water shrimp fisheries in Latin America: A review. *Lat Am J Aquat Res* **40**:497–535. doi: 10.3856/vol40-issue3-fulltext-2

Wei T, Simko V (2017) R package "corrplot": Visualization of a Correlation Matrix.

Weichselbaum E, Coe S, Buttriss J, Stanner S (2013) Fish in the diet: A review. *Nutr Bull* **38**:128–177. doi: 10.1111/nbu.12021

Wells RJD, Cowan JH, Fry B (2008) Feeding ecology of red snapper *Lutjanus campechanus* in the northern Gulf of Mexico. *Mar Ecol Prog Ser* **361**:213–225. doi: 10.3354/meps07425

WHO (2020) Fact sheet - Obesity and overweight. URL: https://www.who.int/news-room/fact-sheets/detail/obesity-and-overweight.

Wickham H (2016) ggplot2: Elegant Graphics for Data Analysis.

Williams KC (2007) Nutritional requirements and feeds development for post-larval spiny lobster: A review. *Aquaculture* **263**:1–14. doi: 10.1016/j.aquaculture.2006.10.019

Wilson RM, Chanton J, Lewis G, Nowacek D (2009) Combining organic matter source and relative trophic position determinations to explore trophic structure. *Estuaries and Coasts* **32**:999–1010. doi: 10.1007/s12237-009-9183-7

Winder M, Sommer U (2012) Phytoplankton response to a changing climate. *Hydrobiologia* **698**:5–16. doi: 10.1007/s10750-012-1149-2

Wood CM, Walsh PJ, Kajimura M, McClelland GB, Chew SF (2010) The influence of feeding and fasting on plasma metabolites in the dogfish shark (*Squalus acanthias*). *Comp Biochem Physiol - A Mol Integr Physiol* **155**:435–444. doi: 10.1016/j.cbpa.2009.09.006

Wood SN (2011) Fast stable restricted maximum likelihood and marginal likelihood estimation of semiparametric generalized linear models. *J R Stat Soc* **73**:3–36. doi: 10.1111/j.1467-9868.2010.00749.x

Woodhead AJ, Hicks CC, Norström A V., Williams GJ, Graham NAJ (2019) Coral reef ecosystem services in the Anthropocene. *Funct Ecol* **33**:1023–1034. doi: 10.1111/1365-2435.13331

WorldBank (2017) Third South West Indian Ocean Fisheries Governance and Shared Growth Project (SWIOFish3). 18p. URL: https://documents1.worldbank.org/curated/en/660191570638647407/pdf/Project-Information-Document-Integrated-Safeguards-Data-Sheet-Municipal-Investment-Program-P166580.pdf

Worthington DG, Fowler AJ, Doherty PJ (1995) Determining the most efficient method of age determination for estimating the age structure of a fish population. *Can J Fish Aquat Sci* **52**:2320–2326. doi: 10.1139/f95-224

Xu Y, Wang WX (2002) Exposure and potential food chain transfer factor of Cd, Se and Zn in marine fish *Lutjanus argentimaculatus*. *Mar Ecol Prog Ser* **238**:173–186. doi: 10.3354/meps238173

Young J, Lansdell M, Riddoch S, Revill A (2006) Feeding ecology of broadbill swordfish, *Xiphias gladius*, off eastern Australia in relation to physical and environmental variables. *Bull Mar Sci* **79**:793–809.

Zand N, Christides T, Loughrill E (2015) Dietary intake of minerals. In: *Handbook of mineral elements in food* (Eds. de la Guardia M, Garrigues S). Wiley-Blackwell, pp 23–39. doi 10.1002/9781118654316.ch2

Zeller D, Pauly D (2019) Viewpoint: Back to the future for fisheries, where will we choose to go? *Glob Sustain* **2**:1–8. doi: 10.1017/sus.2019.8

Zhang W, Wang WX, Zhang L (2016) Comparison of bioavailability and biotransformation of inorganic and organic arsenic to two marine fish. *Environ Sci Technol* **50**:2413–2423. doi: 10.1021/acs.est.5b06307

Zhang Y, Soerensen AL, Schartup AT, Sunderland EM (2020) A global model for methylmercury formation and uptake at the base of marine food webs. *Global Biogeochem Cycles* **34**:1–21. doi: 10.1029/2019GB006348

Zhao Y (2012) R and data mining. Academic Press, 256p. doi: 10.1016/C2011-0-06686-3

Zoroddu MA, Aaseth J, Crisponi G, Medici S, Peana M, Nurchi VM (2019) The essential metals for humans: A brief overview. *J Inorg Biochem* **195**:120–129. doi: 10.1016/j.jinorgbio.2019.03.013

Zuur AF, Ieno EN, Smith GM (2007) Analysing ecological data. Springer, 672p. doi: 10.1007/978-0-387-45972-1

12. APPENDICES

Appendix 2.1. Recovery rates (%) in certified materials (A) and detection frequency (%) in all samples for all trace elements analysed by induced coupled plasma (ICP). Detection frequencies are presented for all analysed species and for each model species.

A.

Trace element	IAEA-407	IAEA-436	IAEA-452	IAEA-461	DOLT-5	TORT-3
Ag	NC	NC	NC	NC	82.8 ± 8.3	NC
As	98.9 ± 7.0	113.6	101.1 ± 0.3	99.4 ± 0.5	97.7 ± 5.0	105.8 ± 5.7
Cd	89.4 ± 6.9	103.1	99.7 ± 0.8	102.6 ± 1.6	99.1 ± 3.6	98.9 ± 5.0
Co	NC	101.1	NC	95.0 ± 4.9	96.4 ± 5.3	100.2 ± 3.1
Cr	92.3 ± 12.3	NC	86.7 ± 0.5	77.5 ± 0.4	NC	94.9 ± 9.3
Cu	99.3 ± 3.2	NC	95.7 ± 2.4	88.5 ± 0.2	97.9 ± 2.2	91.3 ± 6.4
Fe	106.7 ± 31.7	99.2	84.2 ± 2.4	83.7 ± 1.3	100.2 ± 10.2	93.3 ± 8.1
Mn	95.6 ± 18.4	90.2	91.2 ± 0.2	86.5 ± 0.2	NC	94.0 ± 7.7
Ni	NC	112.2	NC	90.8 ± 0.4	NC	95.0 ± 6.6
Pb	74.2	NC	86.7 ± 1.0	89.7 ± 0.3	94.9 ± 7.8	95.7 ± 11.4
Se	127.6 ± 15.1	94.0	NC	124.2 ± 4.6	108.2 ± 6.2	114.1 ± 12.8
V						
Zn	104.6 ± 3.0	NC	100.8	102.1 ± 0.2	104.7 ± 7.0	101.2 ± 5.5

B.

Trace element	All capture fisheries species	Spiny lobsters	Emperor red snapper	Swordfish
Ag	10	45	4	4
As	96	100	100	100
Cd	83	96	78	100
Co	55	43	14	76
Cr	69	77	81	48
Cu	100	100	100	100
Fe	90	51	91	99
Hg	100	100	100	100
Mn	99	100	100	100
Ni	80	89	78	60
Pb	69	99	54	81
Se	96	99	100	100
V	0	0	0	0
Zn	100	100	100	100

Appendix 2.2. Percentage of moisture (mean ± SD) measured for each analysed species and calculated conversion factor for conversion from dry weight to wet weight.

Family	Scientific name	English name	Moisture (%)	Conversion coefficient
Octopodidae	*Octopus cyaneus*	Big blue octopus	NA	ND
Raninidae	*Ranina ranina*	Spanner crab	NA	ND
Palinuridae	*Panulirus longipes*	Longlegged spiny lobster	74.5 ± 3.3	3.9
	Panulirus penicillatus	Pronghorn spiny lobster	73.8 ± 2.7	3.8
	Panulirus versicolor	Painted spiny lobster	76.2 ± 6.3	4.2
Carcharhinidae	*Carcharhinus amblyrhynchos*	Grey reef shark	NA	ND
	Carcharhinus brevipinna	Spinner shark	NA	ND
	Carcharhinus limbatus	Blacktip shark	NA	ND
	Carcharhinus sorrah	Spot-tail shark	NA	ND
	Galeocerdo cuvier	Tiger shark	NA	ND
Sphyrnidae	*Sphyrna mokarran*	Great hammerhead	NA	ND
	Sphyrna lewini	Scalloped hammerhead	NA	ND
Acanthuridae	*Acanthurus mata*	Elongate surgeonfish	79.9	5
Siganidae	*Siganus sutor*	Shoemaker spinefoot	78.5 ± 1.7	4.7
	Siganus argenteus	Streamlined spinefoot	NA	ND
Sphyraenidae	*Sphyraena jello*	Pickhandle barracuda	78.5 ± 1.4	4.7
Carangidae	*Caranx sexfasciatus*	Bigeye trevally	76.1 ± 1	4.2
	Gnathanodon speciosus	Golden trevally	77.6 ± 0.7	4.5
	Carangoides malabaricus	Malabar trevally	NA	ND
	Carangoides fulvoguttatus	Yellowspotted trevally	76.1 ± 0.7	4.2
	Carangoides gymnostethus	Bludger	74 ± 4.1	3.8
	Caranx melampygus	Bluefin trevally	78.1 ± 0.3	4.6
Lethrinidae	*Gymnocranius grandoculis*	Blue-lined large-eye bream	78 ± 0.9	4.6
	Lethrinus crocineus	Yellowtail emperor	79.1 ± 1.9	4.8
	Lethrinus microdon	Smalltooth emperor	76.7 ± 1	4.3
	Lethrinus nebulosus	Spangled emperor	75.2 ± 3.7	4
	Lethrinus variegatus	Slender emperor	77.2 ± 1.3	4.4
	Lethrinus enigmaticus	Blackeye emperor	79.5	4.9
	Lethrinus mahsena	Sky emperor	77.6 ± 1.9	4.5
	Lethrinus lentjan	Pink ear emperor	76.8	4.3
Lutjanidae	*Aprion virescens*	Green jobfish	75.7 ± 1.7	4.1
	Etelis coruscans	Deepwater longtail red snapper	NA	ND
	Lutjanus bohar	Two-spot red snapper	75.5 ± 3.1	4.1
	Lutjanus gibbus	Humpback red snapper	74.3 ± 0.4	3.9
	Lutjanus lutjanus	Bigeye snapper	NA	ND
	Lutjanus sebae	Emperor red snapper	77.9 ± 0.5	4.5
	Lutjanus sanguineus	Humphead snapper	77.9 ± 1.1	4.5
Mullidae	*Parupeneus barberinus*	Dash-and-dot goatfish	77.7 ± 0.7	4.5
	Parupeneus rubescens	Rosy goatfish	78.7 ± 0.5	4.7
Scaridae	*Scarus ghobban*	Blue-barred parrotfish	NA	ND
Serranidae	*Cephalopholis argus*	Peacock hind	77.3 ± 1.8	4.4
	Epinephelus fasciatus	Blacktip grouper	NA	ND
	Epinephelus merra	Honeycomb grouper	77.8 ± 0.2	4.5

	Epinephelus chlorostigma	Brownspotted grouper	78.5 ± 1.7	4.7
	Cephalopholis sonnerati	Tomato hind	77.9 ± 0.6	4.5
	Epinephelus fuscoguttatus	Brown-marbled grouper	77.9 ± 0.2	4.5
	Epinephelus octofasciatus	Eightbar grouper	76.4 ± 1.6	4.2
	Epinephelus multinotatus	White-blotched grouper	76.4 ± 1.4	4.2
	Epinephelus longispinis	Longspine grouper	78.9 ± 0.1	4.7
	Variola louti	Yellow-edged lyretail	78 ± 1.5	4.5
Scombridae	*Gymnosarda unicolor*	Dogtooth tuna	75 ± 1.5	4
	Euthynnus alletteratus	Little tunny	76.6	4.3
	Rastrelliger kanagurta	Indian mackerel	74.1 ± 1.4	3.9
Xiphiidae	*Xiphias gladius*	Swordfish	NA	ND

Appendix 2.3. Detailed process of model choice for mathematical correction of $\delta^{13}C$ values in non-lipid-free swordfish samples.

In order to model the relationship between $\Delta\delta^{13}C$ (i.e. $\delta^{13}C_{lipid\text{-}free}$ - $\delta^{13}C_{bulk}$) and $C{:}N_{bulk}$ in non-lipid-free swordfish samples, several models were tested. The first tested model was based on the McConnaughey and McRoy (1979) model:

$$\Delta\delta^{13}C = D\ (\theta + \frac{3.90}{1+\frac{287}{L}}) \quad \textbf{(Eq. 1)}$$

where L is the lipid content measured or calculated as $L = \frac{93}{1+(0.246*C:Nbulk-0.775)^{-1}}$, D is the protein-lipid discrimination and θ a constant adjusted to the dataset.

The second tested model was developed by Logan *et al.* (2008), from the model of McConnaughey and McRoy (1979):

$$\Delta\delta^{13}C = \frac{D * C:N_{bulk}+a}{C:N_{bulk}+b} \quad \textbf{(Eq. 2)}$$

where D is the protein-lipid discrimination. The y-asymptote corresponds to D, while the model estimate $C{:}N_{lipid\text{-}free}$ is represented by –a/D (x-intercept). The y-intercept, a/b, is the $\delta^{13}C$ difference when $C{:}N_{bulk}$ equals to 0.

The third tested model was based on the Fry (2002) equation:

$$\Delta\delta^{13}C = P - \frac{P*F}{C:N_{bulk}} \quad \textbf{(Eq. 3)}$$

where P represents the protein-lipid discrimination and F represents the $C{:}N_{lipid\text{-}free}$.

A log-linear model was also tested, with the relationship between the difference between $\delta^{13}C_{lipid\text{-}free}$ and $\delta^{13}C_{bulk}$ and the $C{:}N_{bulk}$ following the below formula:

$$\Delta\delta^{13}C = \beta_0 + \beta_1 \ln(C{:}N_{bulk}) \quad \textbf{(Eq. 4)}$$

where the model estimate of $C{:}N_{lipid\text{-}free}$ is represented by $e^{(-\beta0/\beta1)}$ Logan *et al.* (2008).

Finally, the above models were compared to a classic linear model:

$$\Delta\delta^{13}C = a + b * C{:}N_{bulk} \quad \textbf{(Eq. 5)}$$

Cross-validation was used to assess the predictive performance of each model. First, each model was trained with a random subset of the data (i.e. 2/3 of the dataset), and optimal parameters were calculated for this subset. For this, the *nls* function of the *nlstools* package in R was used. As starting values were needed in order to obtain the optimal parameter values,

the parameter estimates given in Logan *et al*. (2008) were used for equations 2.2 to 2.5 (Table 1). For equation 2.6, the regression was first modelled on all the dataset and the calculated intercept and slope were used as starting values. Once the parameters were obtained, corrected values of $\delta^{13}C$ were calculated from the validation dataset (i.e. 1/3 of the complete dataset) and compared to measured $\delta^{13}C_{lipid\text{-}free}$ using paired Wilcoxon's tests. The mean square error (MSE) and mean absolute error (MAE) were also calculated. The process of cross-validation on random dataset was repeated 500 times. For each equation, the percentage of good predictions was also calculated, based on the number of acceptable p-values (i.e. $p > 0.05$) among the 500 iterations.

Table 1 Parameters estimates given in Logan *et al.* (2008) and used as starting values for the estimation of optimal parameter values.

Equation	Parameters estimates
1	D = 7.209 ± 0.148 ; θ = 0.015 ± 0.006
2	D = 7.415 ± 0.558 ; a = -22.732 ± 1.572 ; b = 0.746 ± 0.573
3	P = 6.699 ± 0.119 ; F = 3.098 ± 0.018
4	β_0 = -4.763 ± 0.142 ; β_1 = 4.401 ± 0.099

Visually, equations 1, 2 and 3 were the best models describing the data (Fig. 1). **Equation 2 (Logan *et al*. 2008)** had the highest proportion of good predictions, but also the lowest MSE and MAE (Table 2), and **was thus selected as the best model**. The equation used to correct $\delta^{13}C_{bulk}$ for lipid content before further data treatment was the following:

$$\delta^{13}C_{corrected} = \frac{7.05 * C{:}N_{bulk} - 22.4}{C{:}N_{bulk} - 0.44} + \delta^{13}C_{bulk}$$

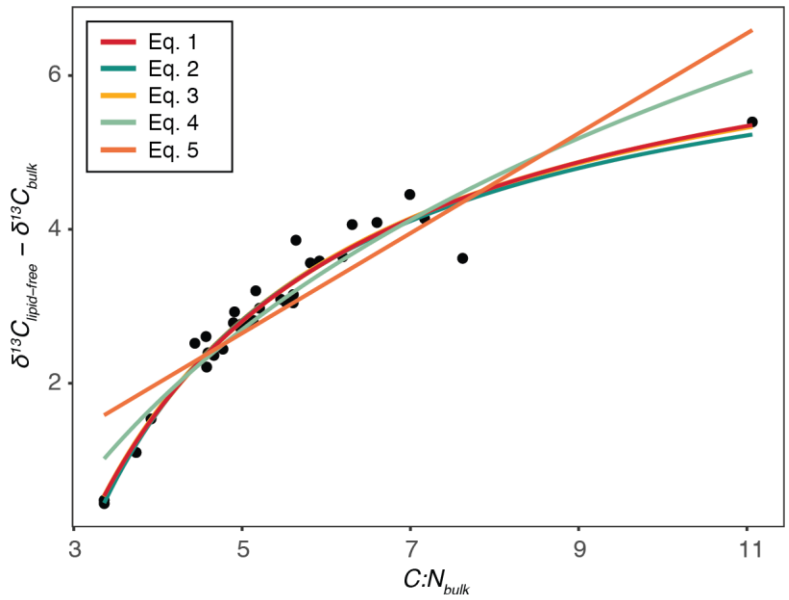

Fig. 1 Model fits to differences in swordfish muscle bulk $\delta^{13}C$ and lipid-free $\delta^{13}C$ plotted against bulk C:N ratio.

Table 2 Model parameters and assessment of the prediction of the five models using a cross-validation procedure.

Model	Estimated parameters	$\delta^{13}C_{corr} - \delta^{13}C_{lipid-free}$ (‰)	Wilcoxon test – p value	MSE	MAE	Good predictions (%)
Eq 2.2	D = 7.69 ± 0.01 θ = 0.007 ± 0.001	0.0004 ± 0.0039	0.49 ± 0.01	0.233 ± 0.003	0.178 ± 0.002	92.8
Eq 2.3	D = 7.05 ± 0.00 a = -22.4 ± 0.0 b = -0.44 ± 0.00	0.0008 ± 0.0026	0.59 ± 0.01	0.211 ± 0.003	0.163 ± 0.002	99.0
Eq 2.4	P = 7.46 ± 0.00 F = 3.12 ± 0.00	0.001 ± 0.003	0.58 ± 0.01	0.218 ± 0.003	0.164 ± 0.002	97.4
Eq 2.5	β_0 = -4.11 ± 0.00 β_1 = 4.23 ± 0.00	0.004 ± 0.004	0.57 ± 0.01	0.314 ± 0.003	0.235 ± 0.003	95.4
Eq 2.6	a = -0.6 ± 0.0 b = 0.65 ± 0.00	0.004 ± 0.006	0.46 ± 0.01	0.468 ± 0.005	0.348 ± 0.004	92.0

Appendix 4.1. Summary of the number of individuals analysed for different tissues and tracers for each species of spiny lobster grouped by sex, habitat type (carbonate and granite reefs) and time period of habitat degradation (pre- and post-bleaching periods). The total number of sampled individuals is 106. TM = tail muscle, TE = trace elements, SI = stable isotopes, H = hepatopancreas, FA = fatty acids.

	Tissue – Tracer	Pronghorn spiny lobster	Longlegged spiny lobster	Painted spiny lobster
Males	TM – TE & SI	33	30	11
	H – FA	23	19	3
Females	TM – TE & SI	14	14	4
	H – FA	8	7	4
Carbonate reefs	TM – TE & SI	5	10	3
	H – FA	4	3	-
Granite reefs	TM – TE & SI	42	34	12
	H – FA	27	23	7
Pre-bleaching (2014-2015)	TM – TE & SI	16	17	2
	H – FA	-	-	-
Post-bleaching (2016-2017)	TM – TE & SI	31	27	13
	H – FA	31	26	7

Appendix 4.2. Trace element profiles of pronghorn, longlegged and painted spiny lobsters according to sex. Mean ellipses are represented by a plain line and uncertainty ellipses are represented by dashed lines.

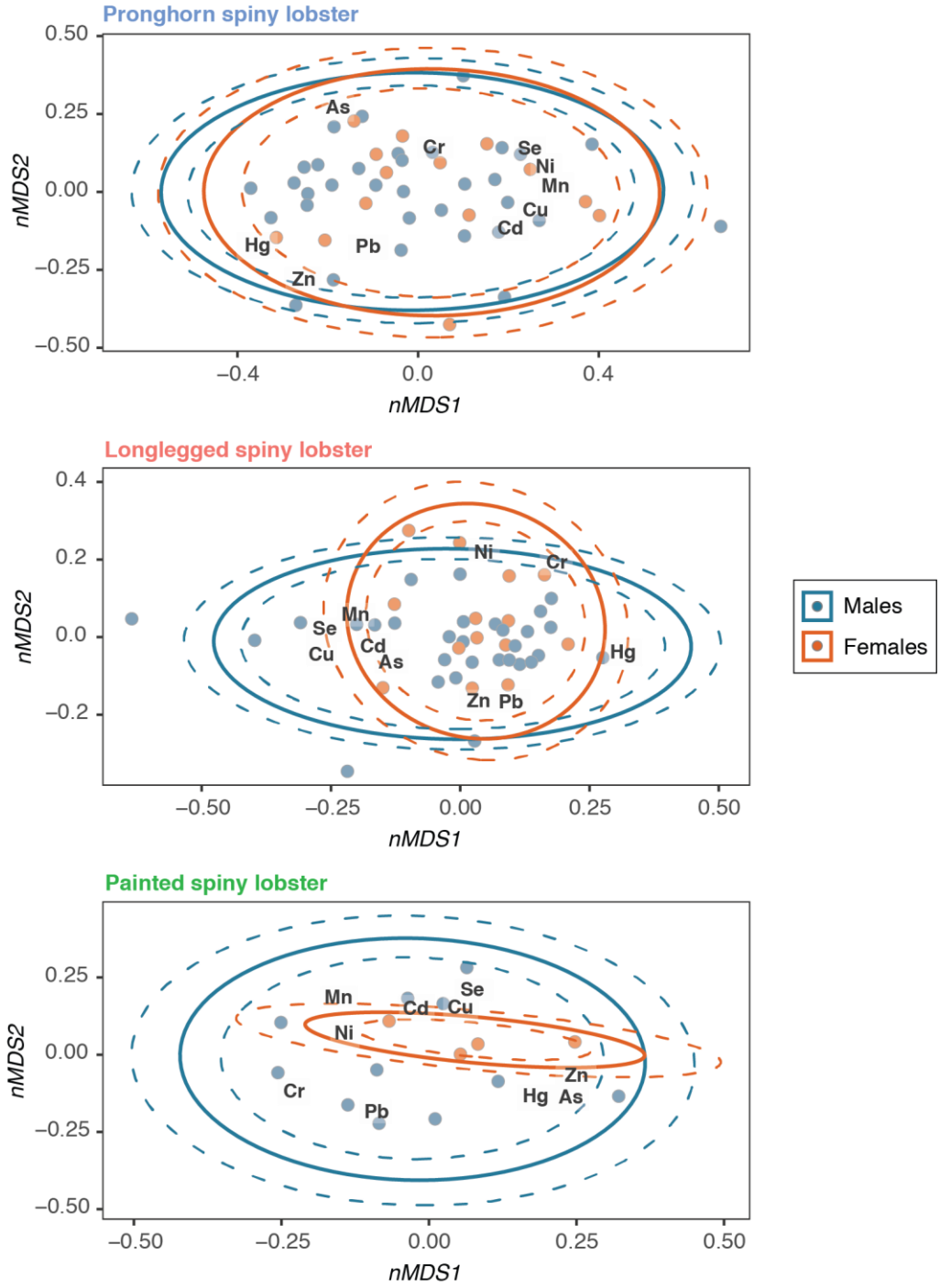

Appendix 4.3. Trace element profiles of pronghorn, longlegged and painted spiny lobsters according to reef habitat type. Mean ellipses are represented by a plain line and uncertainty ellipses are represented by dashed lines.

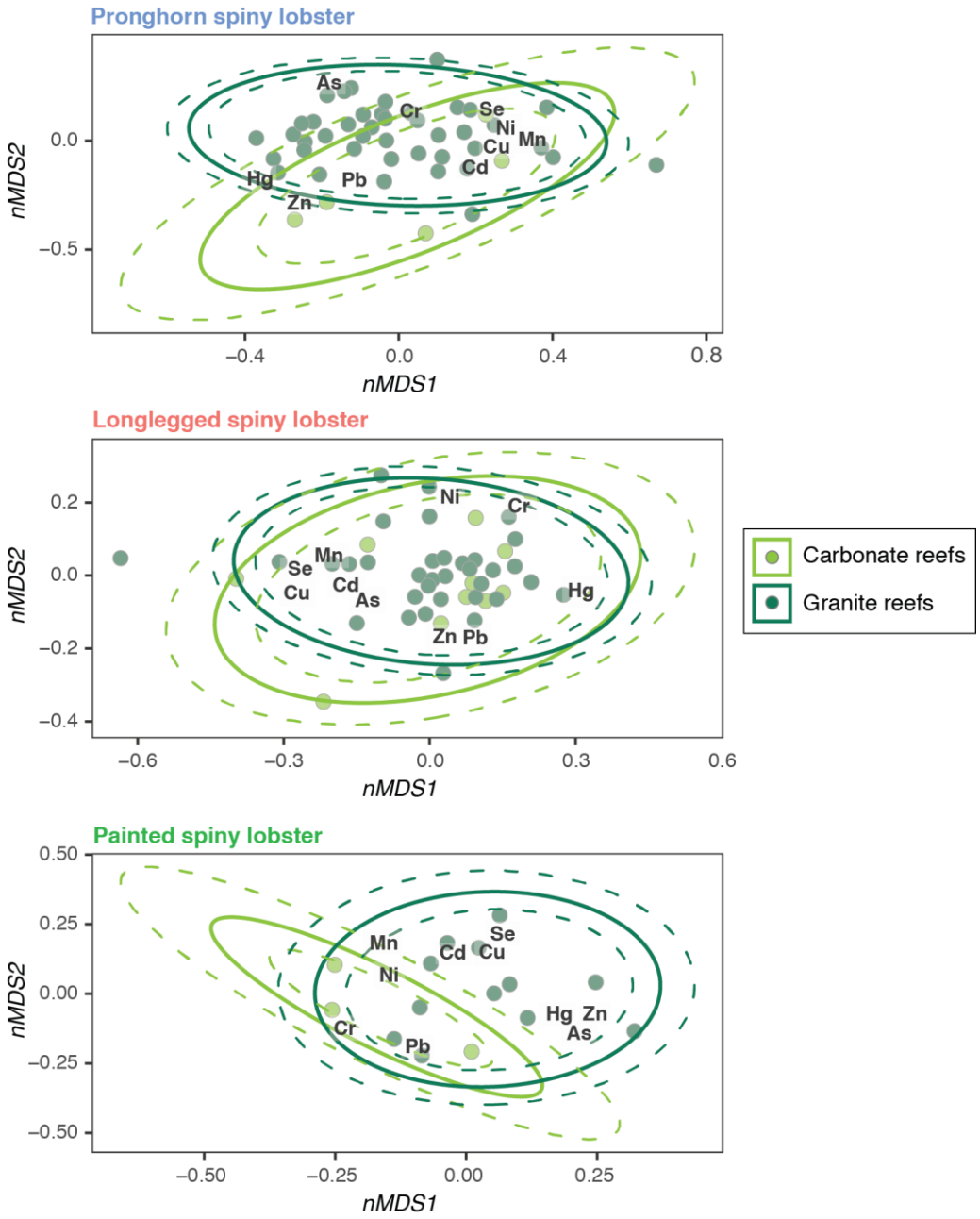

Appendix 4.4. Trace element profiles of pronghorn and longlegged spiny lobsters according to the period of coral reef degradation, i.e. pre- (2014-2015) and post-2016 bleaching event (2016-2018) periods. Mean ellipses are represented by a plain line and uncertainty ellipses are represented by dashed lines.

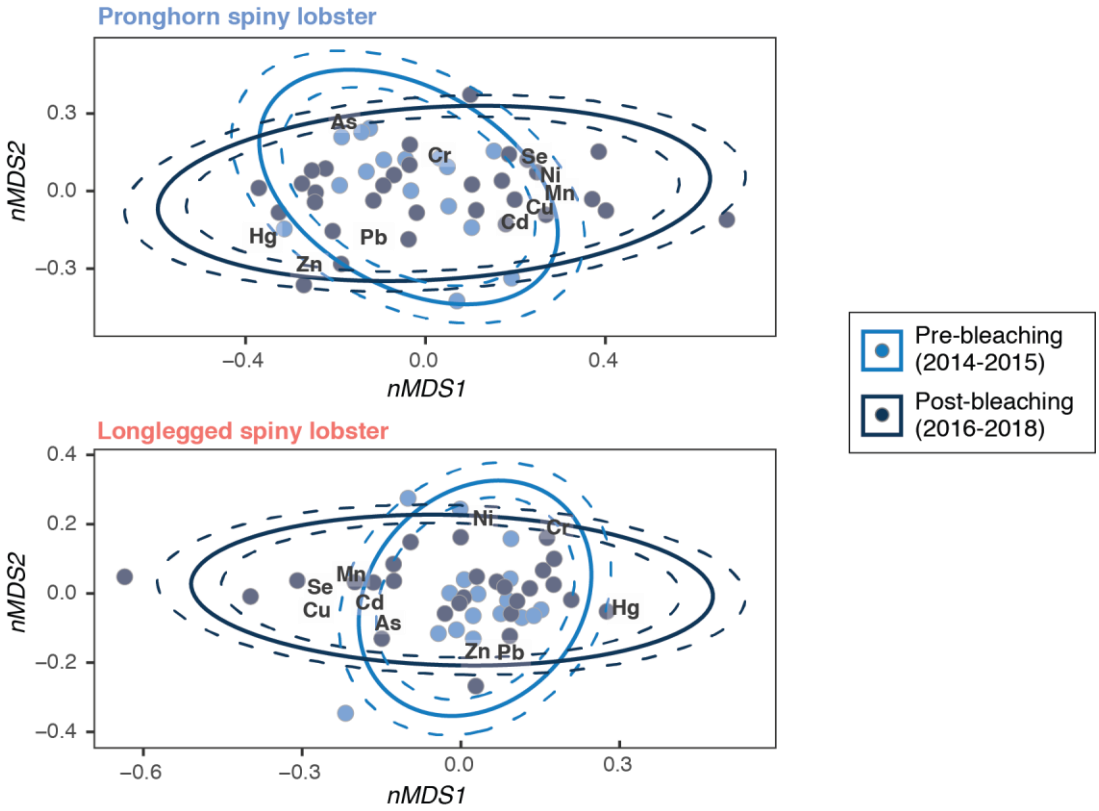

Appendix 4.5. Fatty acid niches of pronghorn (A), longlegged (C) and painted (E) spiny lobsters according to sex and associated overlaps (%) between sexes (B, D, F). Mean ellipses are represented by a plain line and uncertainty ellipses are represented by dashed lines (A, C, F). Overlaps are given as mean with their associated CI95% (B, D, F).

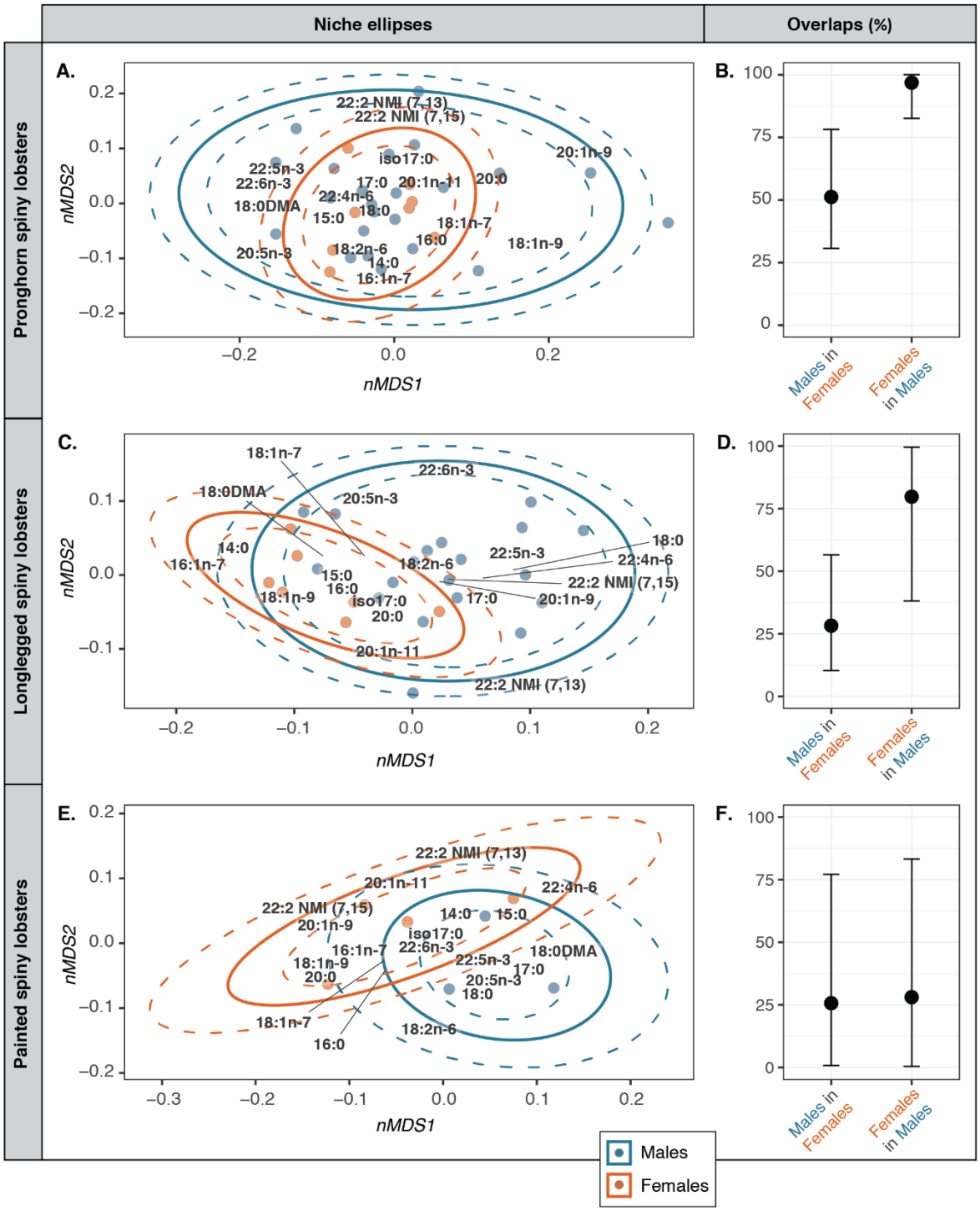

Appendix 4.6. Isotopic niches of pronghorn (A), longlegged (C) and painted (E) spiny lobsters according to sex and associated overlaps (%) between sexes (B, D, F). Mean ellipses are represented by a plain line and uncertainty ellipses are represented by dashed lines (A, C, F). Mean (± SD) $\delta^{13}C$ and $\delta^{15}N$ values (‰) are also indicated (A, C, F). Overlaps are given as mean with their associated CI95% (B, D, F).

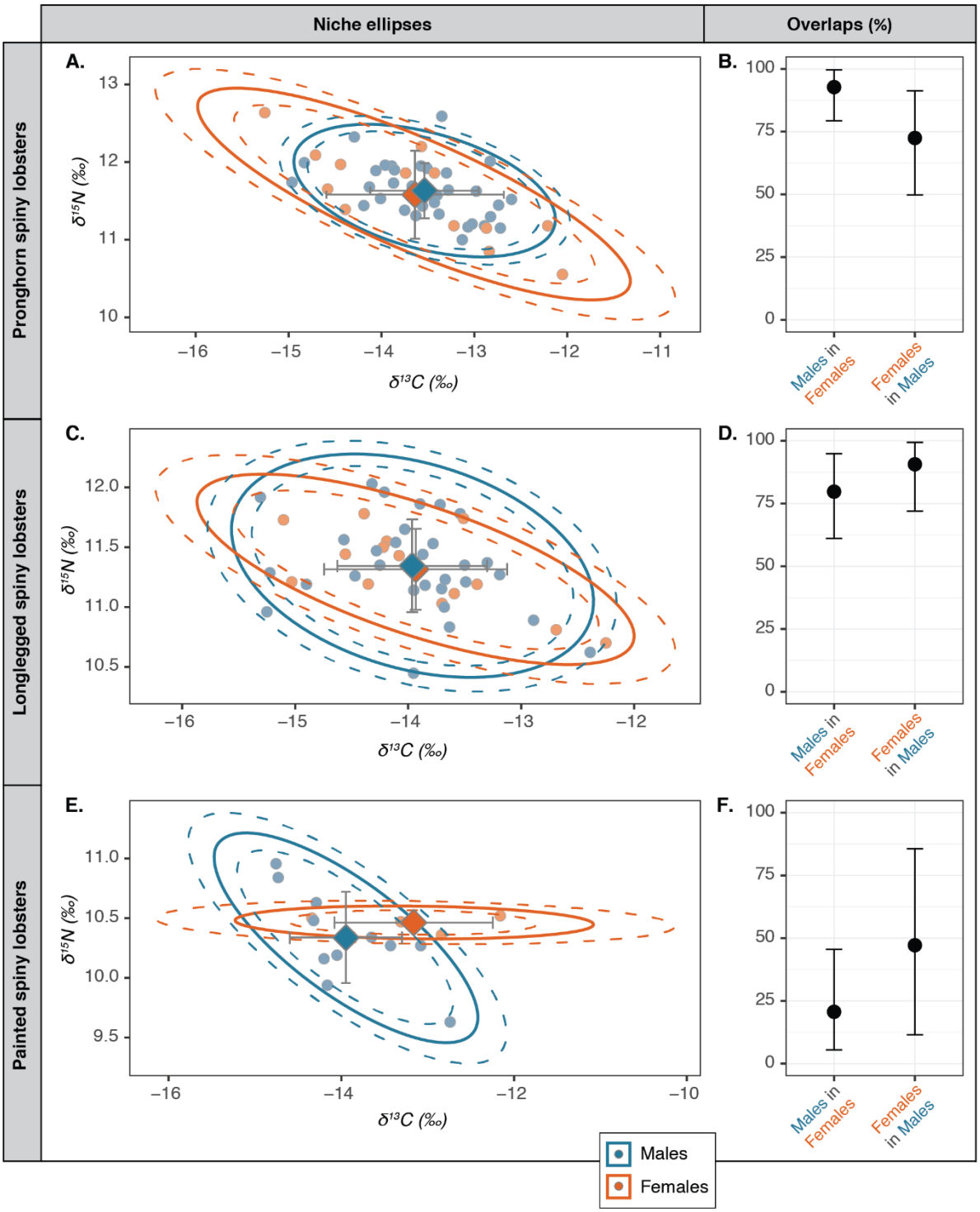

Appendix 4.7. Isotopic niches of pronghorn (A), longlegged (C) and painted (E) spiny lobsters according to reef habitat type and associated overlaps (%) between reef types (B, D, F). Mean ellipses are represented by a plain line and uncertainty ellipses are represented by dashed lines (A, C, E). Overlaps are given as mean with their associated CI95% (B, D, F).

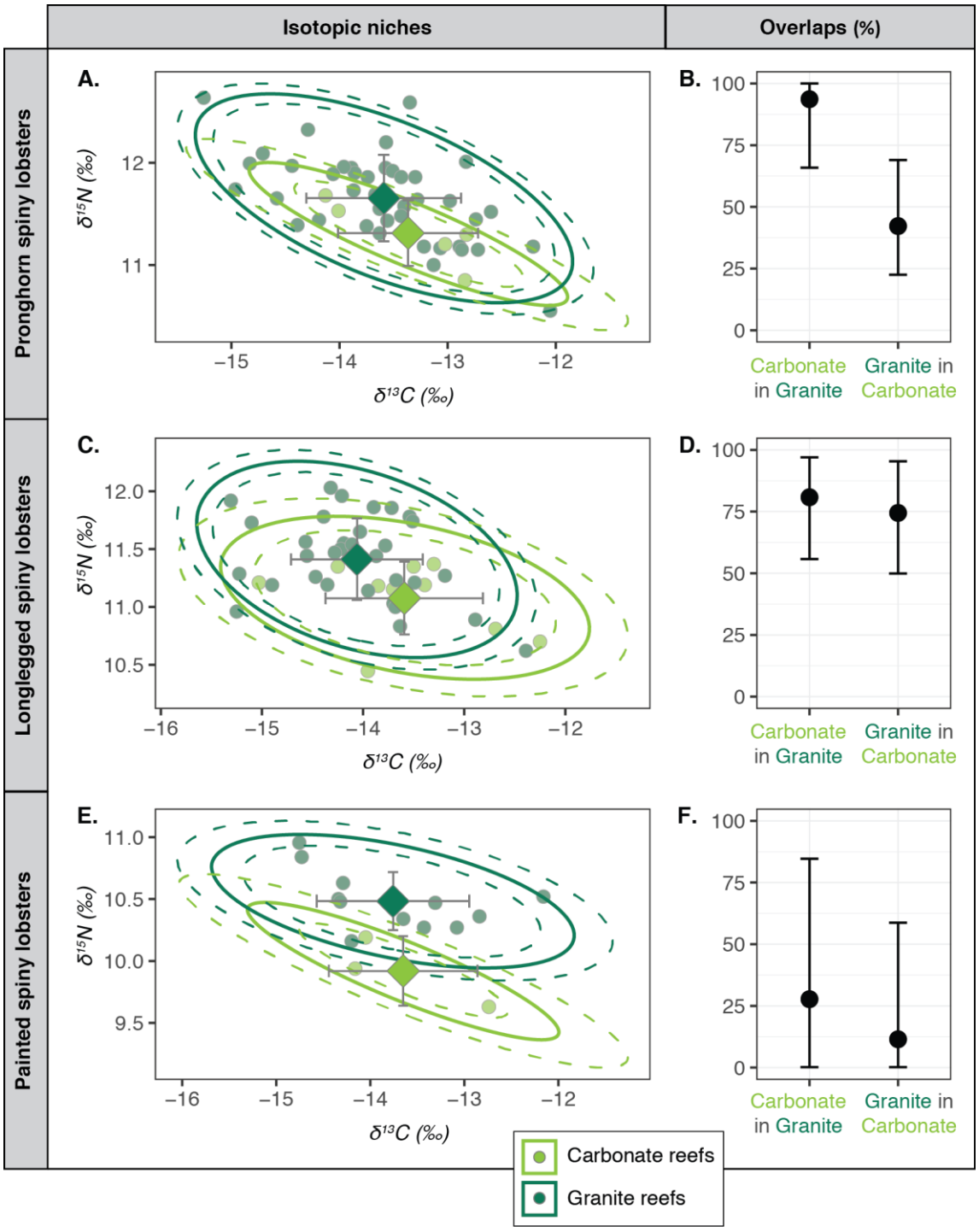

Appendix 4.8. Isotopic niches of pronghorn (A) and longlegged (C) spiny lobsters according to the period of coral reef degradation (i.e. pre- (2014-2015) and post-2016 bleaching event (2016-2018) periods) and associated overlaps (%) between periods (B, D). Mean ellipses are represented by a plain line and uncertainty ellipses are represented by dashed lines (A, C). Overlaps are given as mean with their associated CI95% (B, D).

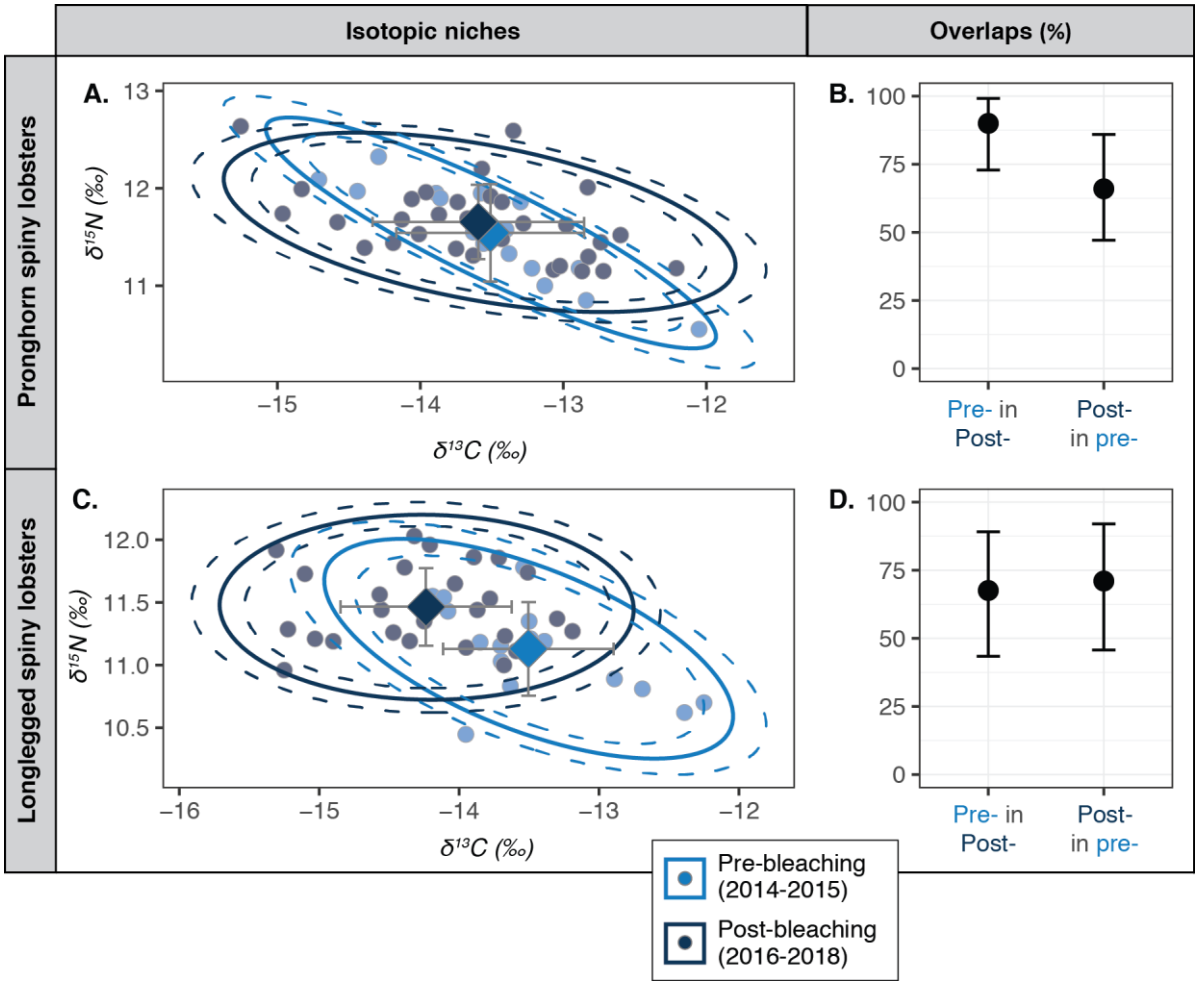

Appendix 4.9. $\delta^{13}C$ and $\delta^{15}N$ values (‰) measured in the tail muscle tissues of each spiny lobster species grouped by sex, reef habitat type (carbonate and granite reefs) and time period of habitat degradation (pre- and post-bleaching periods). Data are presented as mean ± SD. A different letter indicates a significant differences (t-test or Wilcoxon test) between levels of the same factor (i.e. sex, reef habitat type and time period of reef degradation) for the same isotopic ratio measured in the same species.

	Pronghorn spiny lobster		Longlegged spiny lobster		Painted spiny lobster	
	$\delta^{13}C$	$\delta^{15}N$	$\delta^{13}C$	$\delta^{15}N$	$\delta^{13}C$	$\delta^{15}N$
Males	-13.5 ± 0.6	11.6 ± 0.4	-14.0 ± 0.7	11.3 ± 0.4	-13.9 ± 0.6	10.3 ± 0.4
Females	-13.6 ± 1.0	11.6 ± 0.6	-13.9 ± 0.8	11.3 ± 0.3	-13.2 ± 0.9	10.5 ± 0.1
Carbonate reefs	-13.4 ± 0.6	11.3 ± 0.3	13.6 ± 0.8[b]	11.1 ± 0.3	-13.7 ± 0.8	9.9 ± 0.3[b]
Granite reefs	-13.6 ± 0.7	11.7 ± 0.4	-14.1 ± 0.7[a]	11.4 ± 0.4	-13.8 ± 0.8	10.5 ± 0.2[a]
Pre-bleaching (2014-2015)	-13.5 ± 0.7	11.5 ± 0.5	-13.5 ± 0.6[b]	11.1 ± 0.4	-13.8 ± 0.8	10.1 ± 0.7
Post-bleaching (2016-2017)	-13.6 ± 0.7	11.7 ± 0.4	-14.2 ± 0.6[a]	11.5 ± 0.3	-13.5 ± 1.1	10.4 ± 0.3

Appendix 5.1. Fork length (cm) of sampled emperor red snappers by sex and season. Mean values (± SD) by sex and season are also indicated above each corresponding boxplot.

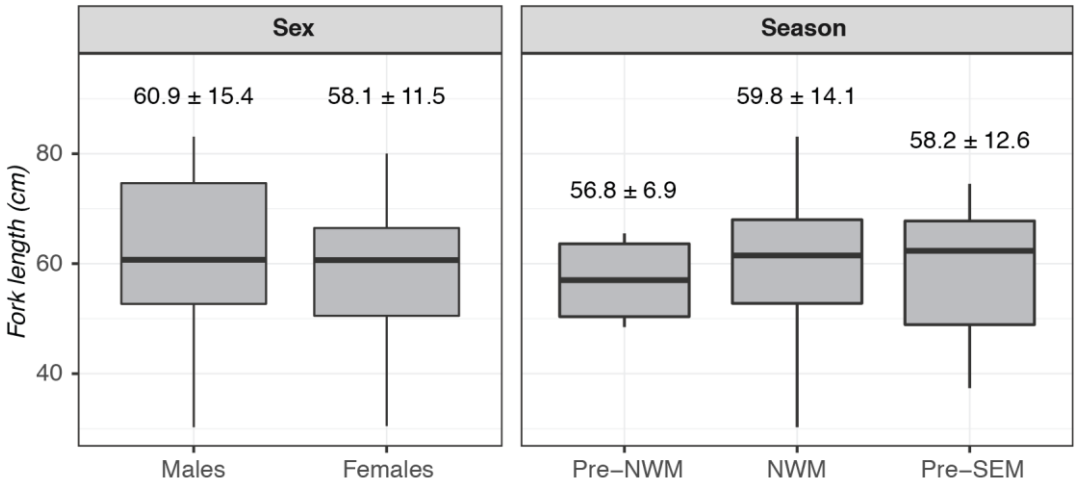

Appendix 5.2. Method used to estimate the size around which a shift in the relationship between $\delta^{13}C$ and $\delta^{15}N$ values was observed in emperor red snapper.

Step 1: The $\delta^{13}C$ value at which the shift was observed was graphically determined by using the fitted curve representing the relationship between $\delta^{13}C$ and $\delta^{15}N$ values (Fig. 1).

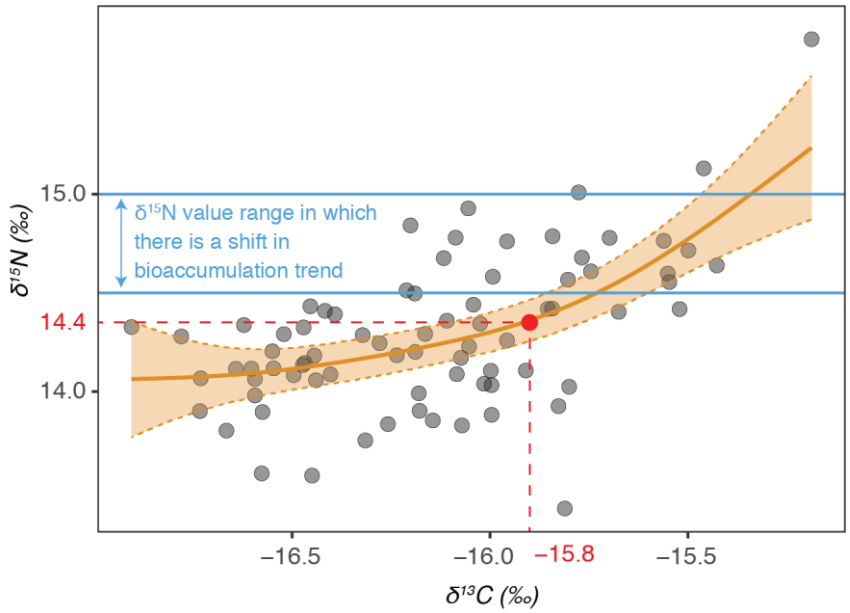

Fig. 1. Relationships between $\delta^{13}C$ and $\delta^{15}N$ values. Smoothing curve was fitted using the GAM method under R software. Dotted curves represent the confidence interval at 95% around the fit. Red point represent the estimated point at which there is a shift in trend in the relationship. The $\delta^{15}N$ range of value in which there is a change in bioconcentration trend for Cu, Hg, Ni, Se and Zn is also indicated in blue.

Step 2: The corresponding $\delta^{15}N$ value was calculated using a GAM model. The model was first fitted on $\delta^{15}N$ values with $\delta^{13}C$ values as explaining variable. Then, the predict function of the stats included R package was used to estimate the $\delta^{15}N$ value for a $\delta^{13}C$ value = –15.8 ‰ (i.e. shift point). The obtained $\delta^{15}N$ shift value was 14.4 ‰.

Step 3: Then, a GAM model was fitted on emperor red snappers' fork lengths with $\delta^{13}C$ and $\delta^{15}N$ values as explaining variables. The form of the equation was: fork length ~ s($\delta^{13}C$) + s($\delta^{15}N$). Finally, similarly to step 2, the size at shift was determined by using the *predict* function in R, with $\delta^{13}C$ = –15.8 ‰ and $\delta^{15}N$ = 14.4 ‰. The obtained fork length at shift was 65.1 cm.

Appendix 6.1. Lower jaw-fork length (cm), raw mercury (Hg), length-standardised Hg and selenium (Se) concentrations (µg.g^{-1} ww), $\delta^{13}C$ and $\delta^{15}N$ values (‰), and calculated trophic levels in each sampling region of the Indian Ocean. Data are presented as mean ± SD, with the minimum and maximum values in each region between brackets. BENG = Bay of Bengal; ISLU = Indo-Sri Lanka Upwelling; WTIO = Western Tropical Indian Ocean; MOZ = Mozambique Channel; SSG = Southern Subtropical Gyre; SOA = South Africa.

Region	Lower jaw-fork length (cm)	Hg (µg.g^{-1} ww)	Length-stand. Hg (µg.g^{-1} ww)	Se (µg.g^{-1} ww)	$\delta^{13}C$ (‰)	$\delta^{15}N$ (‰)	Calculated trophic level
BENG	111 ± 16	0.81 ± 0.68	1.39 ± 1.01	1.39 ± 0.25	–17.0 ± 0.4	13.2 ± 0.7	2.9 ± 0.3
	(93 – 154)	(0.17 – 2.30)	(0.40 – 3.58)	(0.96 – 1.95)	(–17.5 – –16.2)	(12.1 – 14.4)	(2.3 – 3.4)
ISLU	197 ± 46	1.21 ± 0.83	0.74 ± 0.39	0.91 ± 0.25	–15.8 ± 0.4	13.9 ± 0.7	3.6 ± 0.3
	(142 – 295)	(0.37 – 2.92)	(0.21 – 1.28)	(0.53 – 1.38)	(–16.5 – –15.2)	(13.0 – 15.8)	(3.2 – 4.3)
WTIO	142 ± 35	0.77 ± 0.46	0.79 ± 0.25	0.94 ± 0.28	–6.7 ± 0.5	14.1 ± 0.7	4.5 ± 0.2
	(80 – 195)	(0.10 – 1.60)	(0.31 – 1.26)	(0.41 – 2.02)	(–18.1 – –16.3)	(12.4 – 15.1)	(4.0 – 4.5)
MOZ	121 ± 29	0.37 ± 0.23	0.57 ± 0.22	0.63 ± 0.31	–16.6 ± 0.4	13.5 ± 0.9	4.1 ± 0.4
	(75 – 188)	(0.05 – 1.03)	(0.26 – 1.18)	(0.14 – 1.50)	(–17.3 – –16.5)	(11.8 – 15.0)	(3.5 – 4.8)
SSG	151 ± 33	1.40 ± 0.76	1.41 ± 0.72	1.04 ± 0.52	–16.8 ± 0.5	14.3 ± 0.9	4.8 ± 0.5
	(64 – 229)	(0.02 – 3.50)	(0.42 – 3.82)	(0.46 – 2.94)	(–18.3 – –15.2)	(11.9 – 15.6)	(4.0 – 5.9)
SOA	155 ± 35	0.74 ± 0.39	0.73 ± 0.41	0.65 ± 0.31	–17.2 ± 0.3	14.0 ± 0.4	4.4 ± 0.1
	(121 – 274)	(0.27 – 2.46)	(0.21 – 2.60)	(0.26 – 1.50)	(–17.9 – –16.5)	(13.3 – 15.0)	(4.1 – 4.9)

Appendix 6.2. Post-hoc test results for interregional comparisons of Hg concentrations (A), Se concentrations (B), $\delta^{13}C$ values (C) and $\delta^{15}N$ values (D) measured in the white muscle of sampled swordfish, for interregional comparison of calculated trophic level (E), length-standardised Hg concentrations (G) and theoretically bioavailable Se concentrations (H), and of measured swordfish lower jaw-fork length (F). For each interregional comparison, used post-hoc is indicated in the top left. Significant differences are indicated in bold. BENG = Bay of Bengal; ISLU = Indo-Sri Lanka Upwelling; WTIO = Western Tropical Indian Ocean; MOZ = Mozambique Channel; SSG = Southern Subtropical Gyre; SOA = South Africa.

A.

Hg concentrations					
Dunn test	BENG	ISLU	WTIO	MOZ	SSG
ISLU	0.158				
WTIO	0.913	0.143			
MOZ	**0.037**	**< 0.001**	**0.002**		
SSG	**0.009**	0.399	**0.001**	**< 0.001**	
SOA	0.893	0.155	0.895	**0.001**	**0.001**

B.

Se concentrations					
Dunn test	BENG	ISLU	WTIO	MOZ	SSG
ISLU	**0.007**				
WTIO	**0.005**	0.953			
MOZ	**< 0.001**	**0.006**	**< 0.001**		
SSG	**0.003**	0.908	0.951	**< 0.001**	
SOA	**< 0.001**	**0.006**	**< 0.001**	0.920	**< 0.001**

C.

$\delta^{13}C$ values					
Dunn test	BENG	ISLU	WTIO	MOZ	SSG
ISLU	**< 0.001**				
WTIO	0.595	**< 0.001**			
MOZ	**0.017**	**0.002**	**0.014**		
SSG	0.179	**< 0.001**	0.252	0.090	
SOA	0.175	**< 0.001**	**0.014**	**< 0.001**	**< 0.001**

D.

$\delta^{15}N$ values					
Dunn test	BENG	ISLU	WTIO	MOZ	SSG
ISLU	0.109				
WTIO	**0.002**	0.185			
MOZ	0.255	0.391	**0.009**		
SSG	**< 0.001**	0.068	0.543	**< 0.001**	
SOA	**0.044**	0.773	0.200	0.202	**0.040**

E.

Trophic level					
Dunn test	BENG	ISLU	WTIO	MOZ	SSG
ISLU	0.329				
WTIO	< 0.001	< 0.001			
MOZ	0.001	0.021	0.005		
SSG	< 0.001	< 0.001	0.007	< 0.001	
SOA	< 0.001	< 0.001	0.322	0.056	< 0.001

F.

Lower jaw-fork length					
Dunn test	BENG	ISLU	WTIO	MOZ	SSG
ISLU	< 0.001				
WTIO	0.004	< 0.001			
MOZ	0.333	< 0.001	0.010		
SSG	< 0.001	0.004	0.328	< 0.001	
SOA	< 0.001	0.009	0.342	< 0.001	0.865

G.

Length-standardised Hg concentrations					
Dunn test	BENG	ISLU	WTIO	MOZ	SSG
ISLU	0.053				
WTIO	0.105	0.536			
MOZ	< 0.001	0.179	0.018		
SSG	0.441	< 0.001	< 0.001	< 0.001	
SOA	0.018	0.898	0.400	0.127	< 0.001

Appendix 6.3. Correlation (Kendall test) between swordfish sampling coordinates (i.e. latitude and longitude) and $\delta^{13}C$ values measured in swordfish white muscle tissues and swordfish lower jaw-fork length and trophic level. Coloured cells indicate a significant correlation ($p < 0.05$) between two variables, while uncoloured cells indicate a non-significant correlation. Numbers in the cells are the associated correlation coefficients and the cell's colour intensity is proportional to the coefficient.

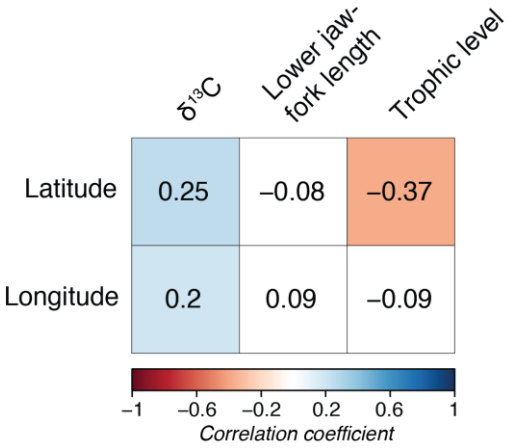

Appendix 6.4. Graphical results of the generalised additive models (GAM) fitted to log-transformed Hg concentrations in white muscle of swordfish from the Indian Ocean. Smoothers illustrate the partial effect of continuous explanatory variables once the effects of all the other explanatory variables included in the model have been considered. The y-axis shows the contribution of the smoother to the predictor function in the model (in arbitrary units). Dashed lines represent the 95% confidence intervals. Whiskers on the x-axis indicate data presence.

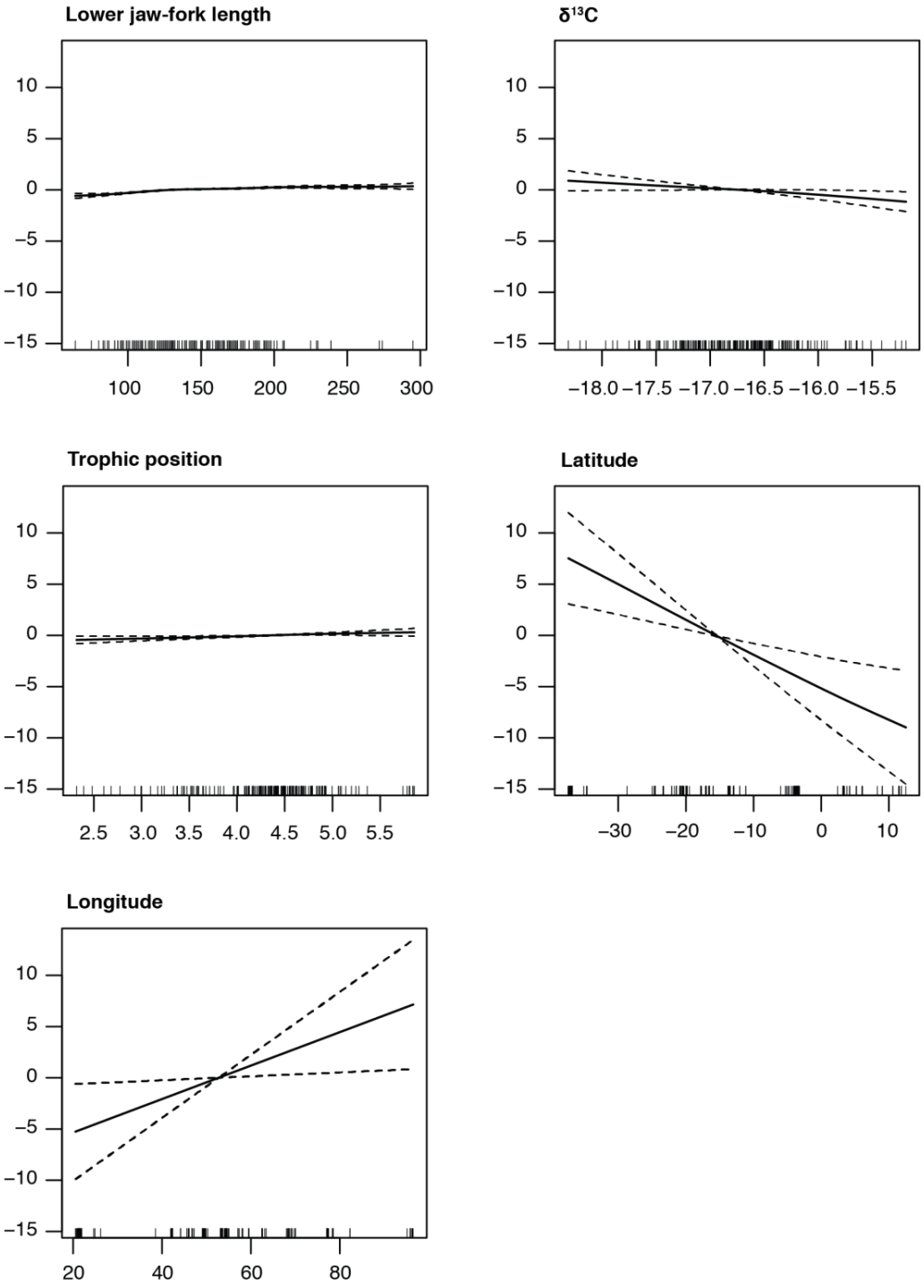

Appendix 6.5. Graphical results of the generalised additive models (GAM) fitted to log-transformed length-standardised Hg concentrations in white muscle of swordfish from the Indian Ocean. Smoothers illustrate the partial effect of continuous explanatory variables once the effects of all the other explanatory variables included in the model have been considered. The y-axis shows the contribution of the smoother to the predictor function in the model (in arbitrary units). Dashed lines represent the 95% confidence intervals. Whiskers on the x-axis indicate data presence.

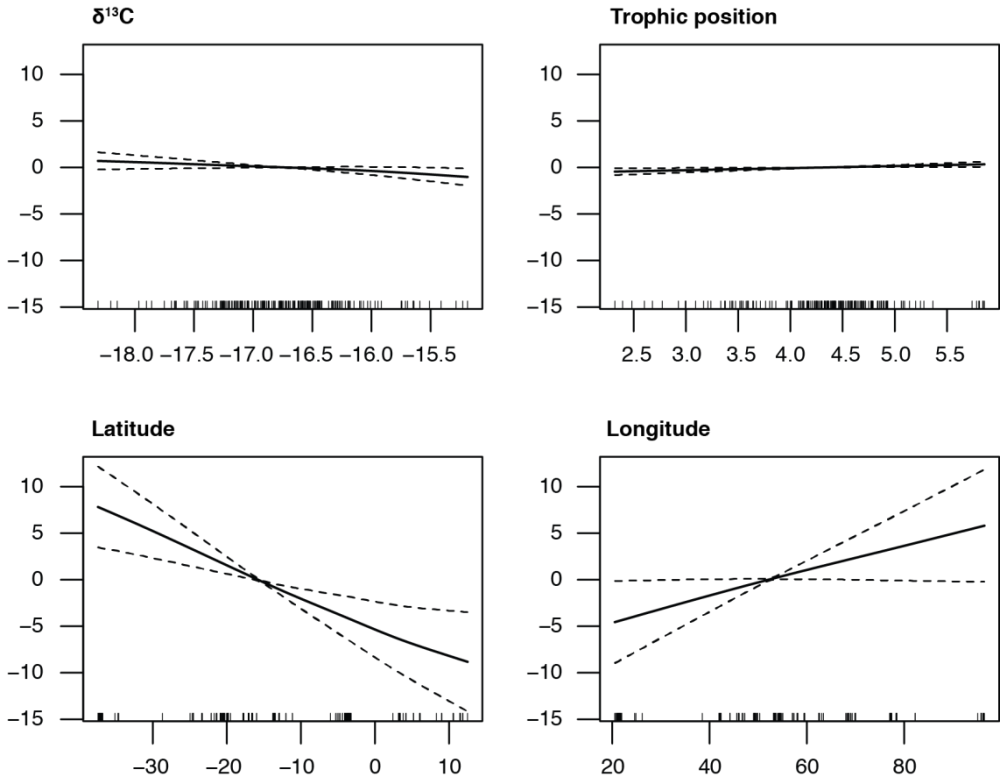

Appendix 6.6. Graphical results of the generalised additive models (GAM) fitted to log-transformed Se concentrations in white muscle of swordfish from the Indian Ocean. Smoothers illustrate the partial effect of continuous explanatory variables once the effects of all the other explanatory variables included in the model have been considered. The y-axis shows the contribution of the smoother to the predictor function in the model (in arbitrary units). Dashed lines represent the 95% confidence intervals. Whiskers on the x-axis indicate data presence.

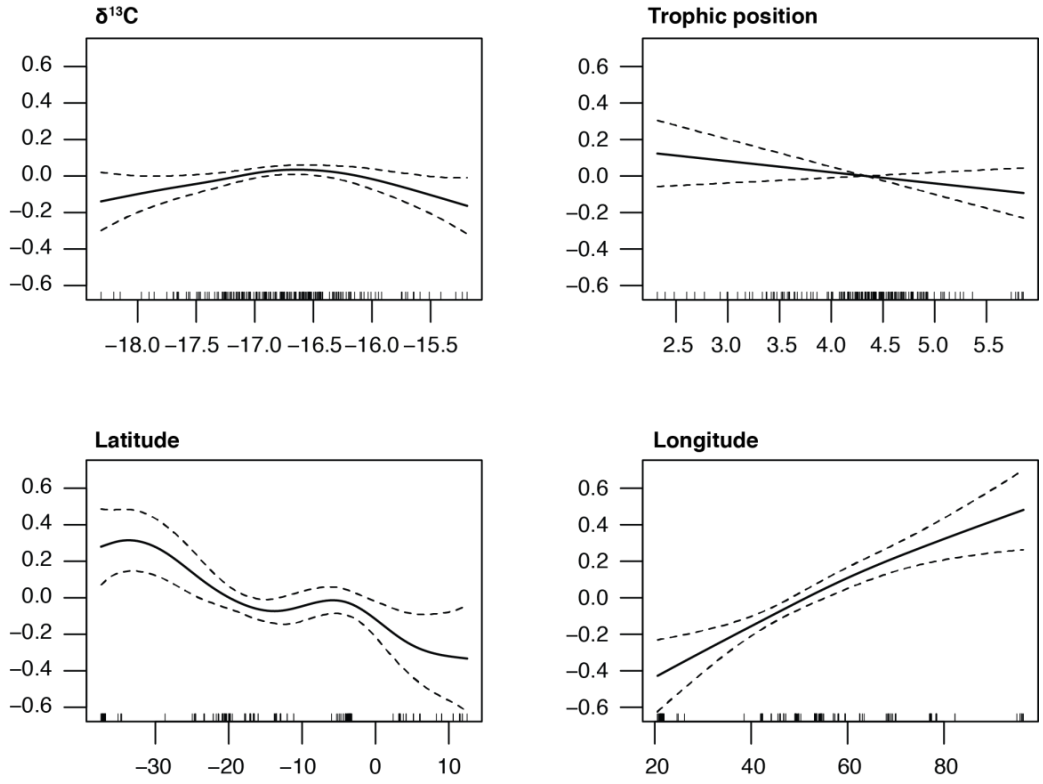

Appendix 6.7. Graphical results of the generalised additive models (GAM) fitted to log-transformed Se concentrations in white muscle of swordfish from the Indian Ocean, with log-transformed Hg concentrations as explaining variable. Smoothers illustrate the partial effect of continuous explanatory variables once the effects of all the other explanatory variables included in the model have been considered. The y-axis shows the contribution of the smoother to the predictor function in the model (in arbitrary units). Dashed lines represent the 95% confidence intervals. Whiskers on the x-axis indicate data presence.

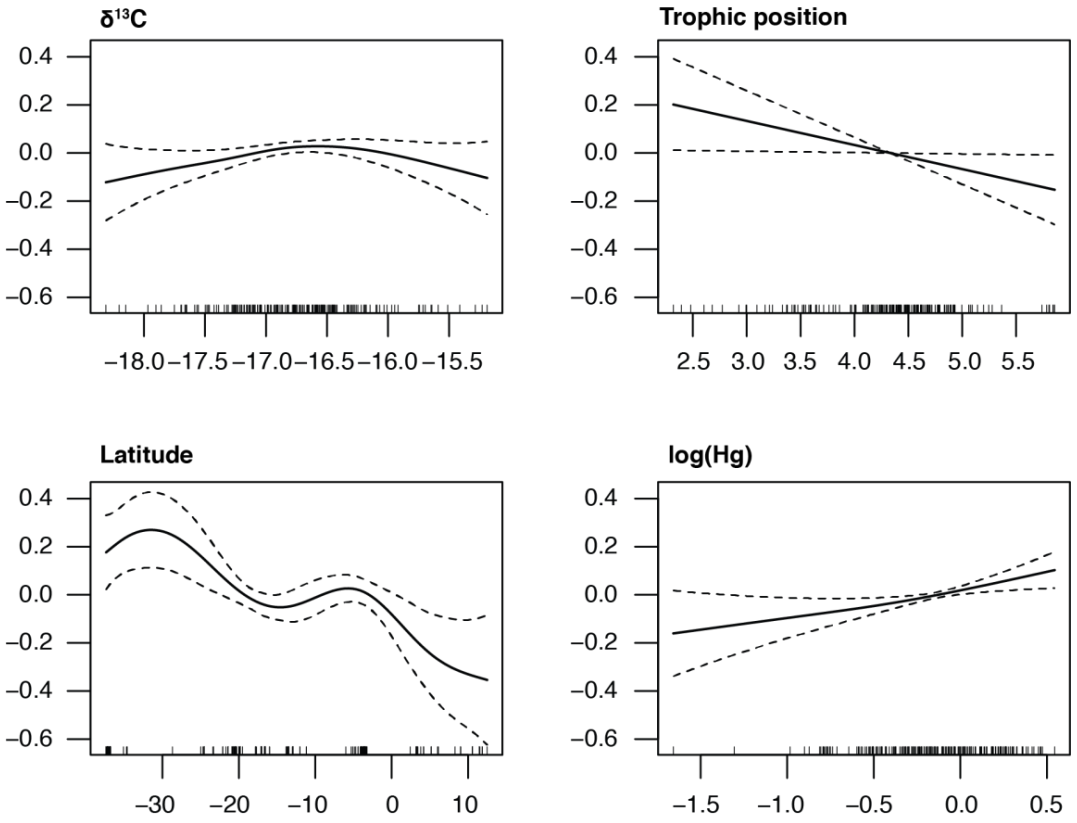

Appendix 7.1. Correlation (Kendall test) between log-transformed trace element concentrations and lower jaw-fork length in swordfish. Coloured cells indicate a significant correlation ($p < 0.05$) between log-transformed trace element concentrations and lower jaw-fork length, while uncoloured cells indicate a non-significant correlation. Numbers in the cells are the associated correlation coefficients and the cells' colour intensity is proportional to the coefficient.

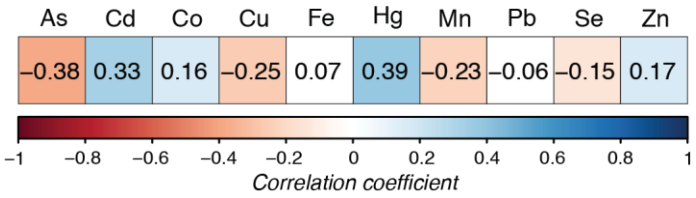

Appendix 7.2. Fitted relationships between log-transformed trace element concentrations and lower jaw-fork length (cm) in swordfish from the Seychelles. Relationships were fitted only for trace elements significantly correlated with lower jaw-fork length.

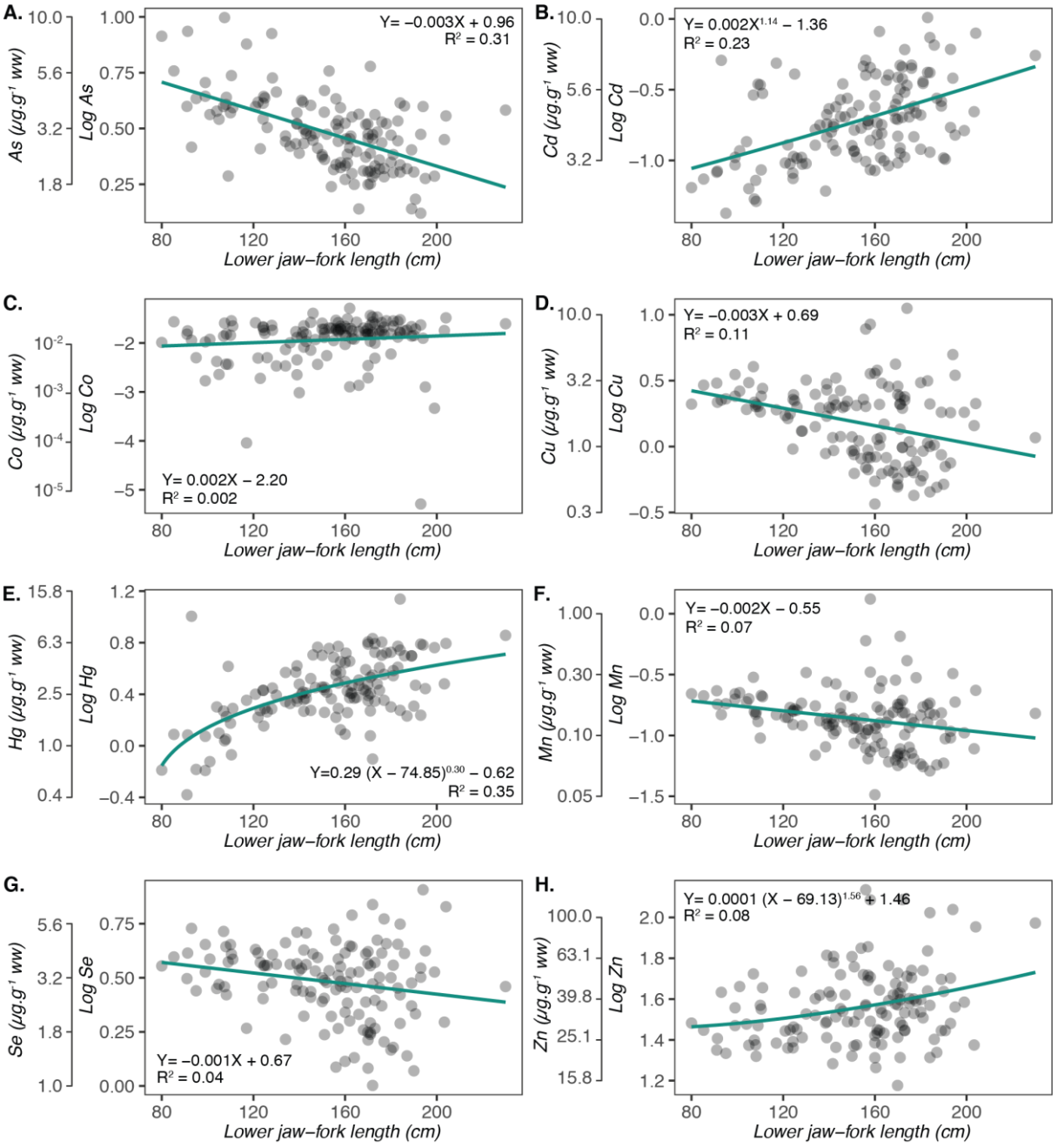

Appendix 7.3. Swordfish lower jaw-fork length (cm) by sex (A), fatty acid (FA) trophic group (B) and season (C). A different letter indicates a significant difference ($p < 0.05$) between levels of the same factor. NWM = Northwest Monsoon, SEM = Southeast Monsoon.

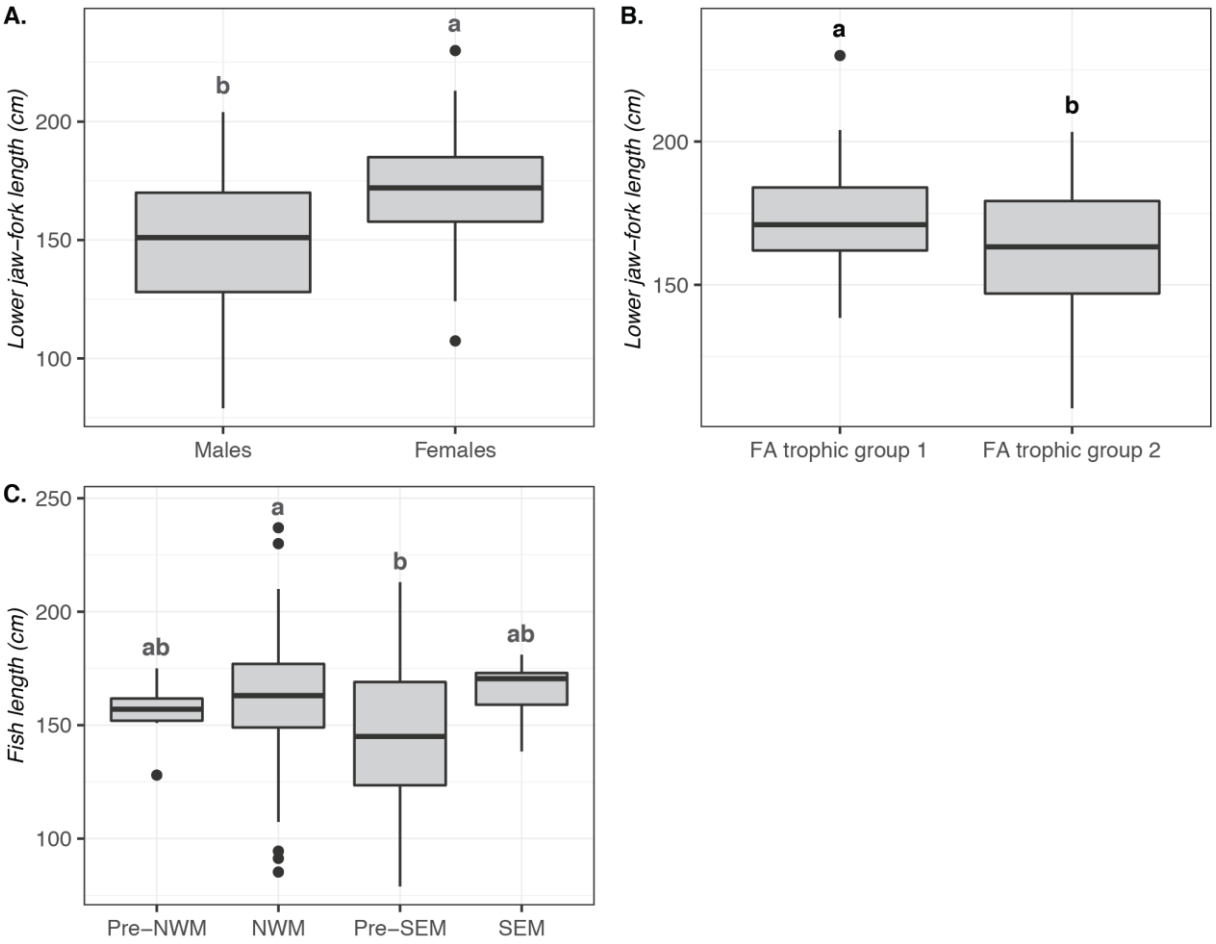

Appendix 7.4. $\delta^{13}C$ and $\delta^{15}N$ values (‰) measured in swordfish muscle tissues by sex (A), fatty acid (FA) trophic group (B) and season (C). A different letter indicates a significant difference ($p < 0.05$) between levels of the same factor. NWM = Northwest Monsoon, SEM = Southeast Monsoon.

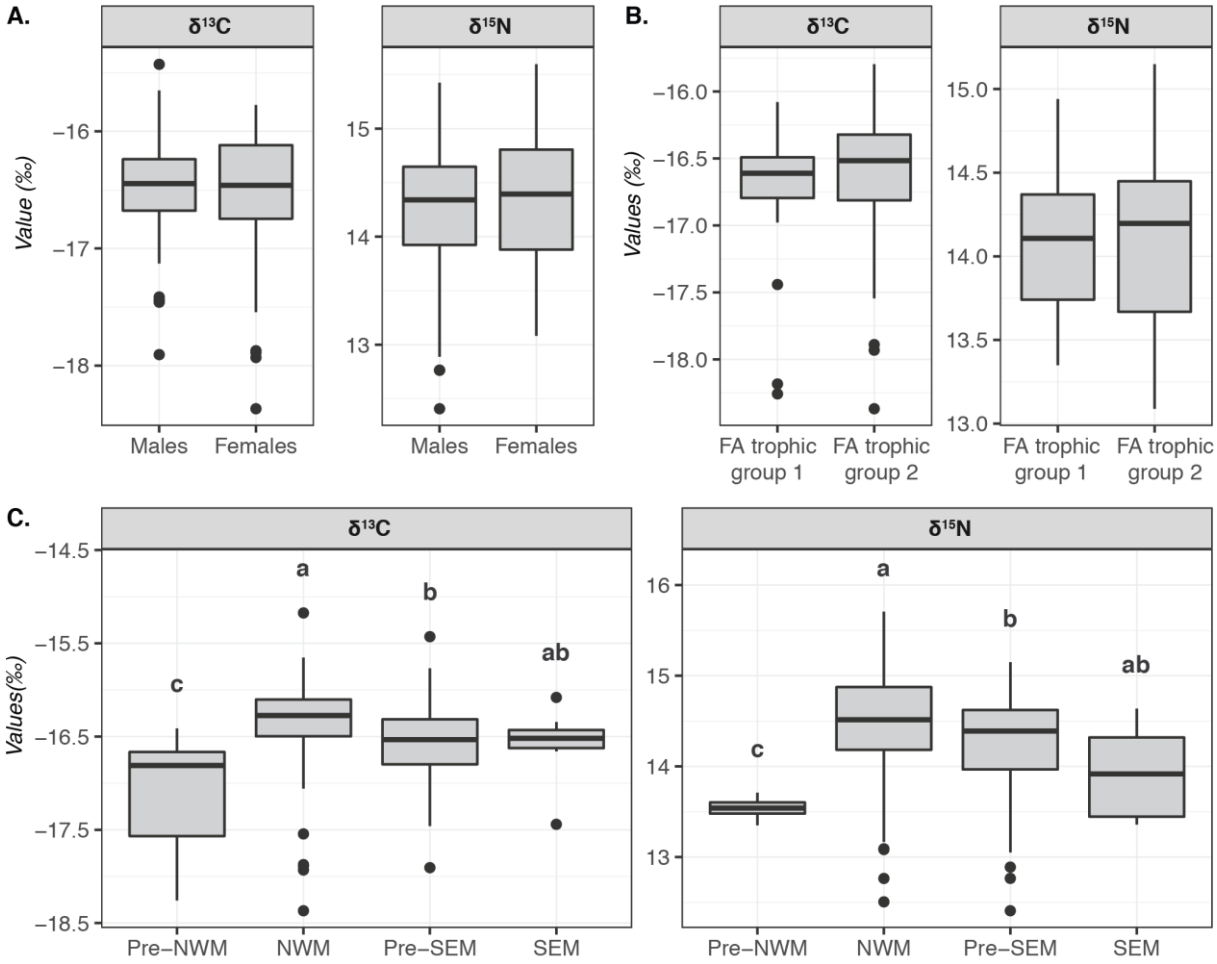

Appendix 7.5. Correlations among biochemical tracers in swordfish muscle tissues. Coloured cells indicate a significant correlation ($p < 0.05$) between one trace element and one biochemical tracer, while uncoloured cells indicate a non-significant correlation. Numbers in the cells are the associated coefficients (Pearson for parametric and Kendall for non-parametric) and the cells' colour intensity is proportional to the coefficient.

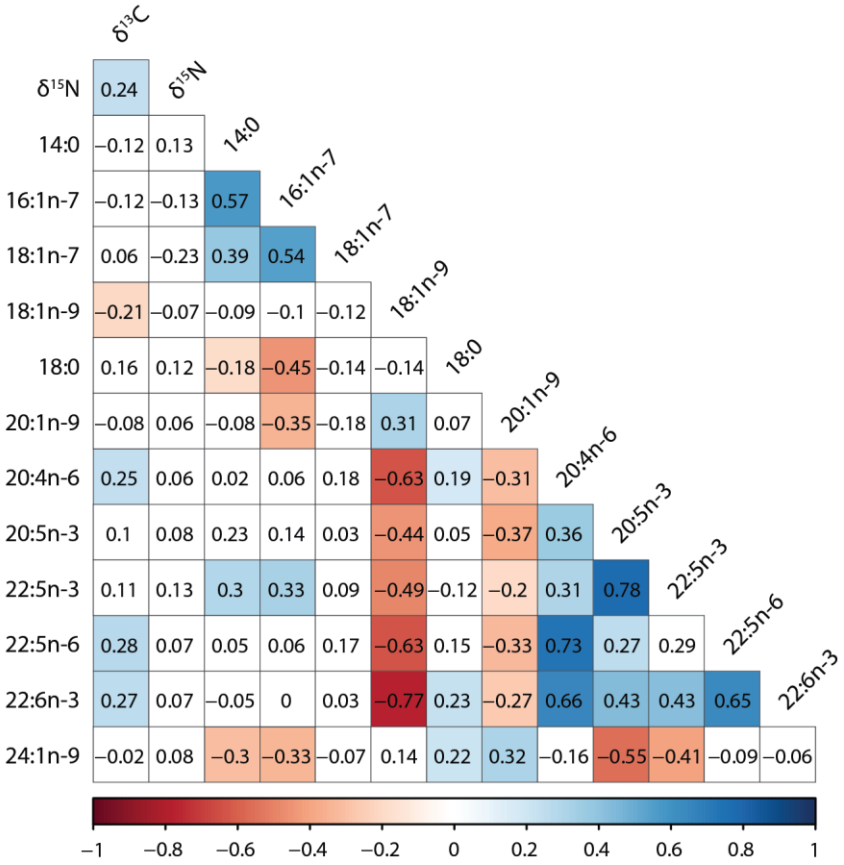

Appendix 7.6. Sex ratio (Females above males) for each season. Calculated sex ratios are given above each corresponding point. NWM = Northwest Monsoon, SEM = Southeast Monsoon.

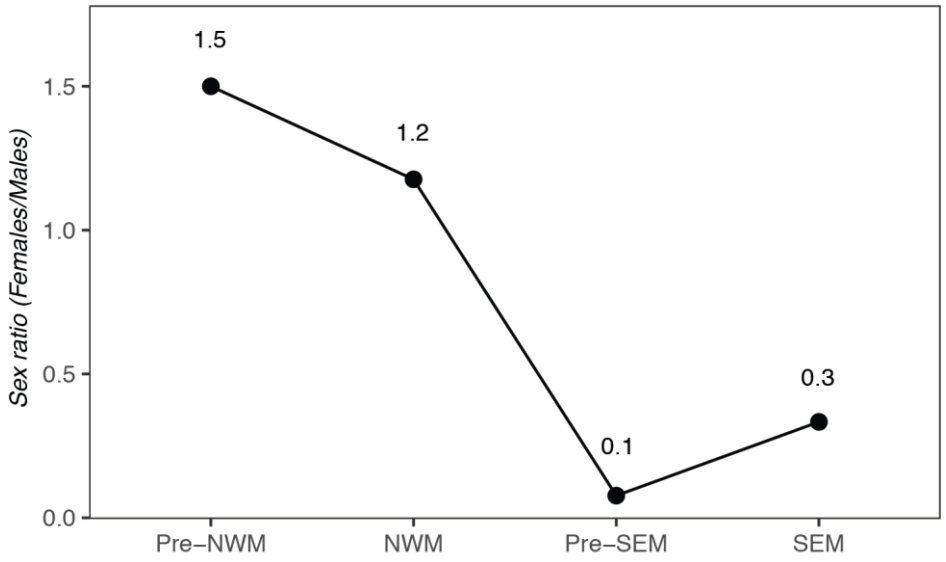

Appendix 8.1 Trace element concentrations (µg.g^{-1} ww) in the muscles of 54 capture fisheries species from the Seychelles. Data are presented as mean ± SD. N = Number of samples, LOQ = Limit of quantification.

	Essential						Potentially essential			Non-essential			
Species	**Co**	**Cu**	**Fe**	**Mn**	**Se**	**Zn**	**As**	**Cr**	**Ni**	**Ag**	**Cd**	**Hg**	**Pb**
Octopuses													
Big blue octopus	0.003 ± 0.001	1.12 ± 0.35	1.9 ± 1.0	0.09 ± 0.02	0.27 ± 0.05	19.3 ± 2.5	26.1 ± 5.9	0.11 ± 0.06	0.03 ± 0.01	<LOQ	0.018 ± 0.011	0.013 ± 0.006	0.003 ± 0.001
Crabs													
Spanner crab	0.009 ± 0.003	7.21 ± 3.29	1.0 ± 0.1	0.04 ± 0.01	0.55 ± 0.09	43.5 ± 4.2	50.5 ± 12.0	<LOQ	0.08 ± 0.03	0.039 ± 0.011	0.443 ± 0.235	0.032 ± 0.004	0.003 ± 0.001
Spiny lobsters													
Longlegged spiny lobster	0.005 ± 0.002	9.93 ± 4.92	2.3 ± 1.1	0.08 ± 0.04	0.29 ± 0.14	28.1 ± 6.5	34.8 ± 14.5	0.13 ± 0.11	0.07 ± 0.06	0.019 ± 0.042	0.079 ± 0.173	0.034 ± 0.020	0.035 ± 0.111
Painted spiny lobster	0.005 ± 0.002	8.27 ± 3.05	2.8 ± 1.6	0.10 ± 0.03	0.27 ± 0.10	20.9 ± 5.2	35.6 ± 22.2	0.24 ± 0.26	0.11 ± 0.07	0.013 ± 0.019	0.071 ± 0.153	0.025 ± 0.038	0.008 ± 0.009
Pronghorn spiny lobster	0.005 ± 0.002	10.37 ± 3.77	2.6 ± 2.0	0.10 ± 0.04	0.29 ± 0.10	32.8 ± 7.2	58.3 ± 18.1	0.12 ± 0.11	0.05 ± 0.04	0.016 ± 0.022	0.060 ± 0.086	0.034 ± 0.012	0.013 ± 0.017
Goatfishes													
Dash-and-dot goatfish	0.004 ± 0.002	0.28 ± 0.04	2.6 ± 1.3	0.08 ± 0.03	0.46 ± 0.08	4.6 ± 0.7	9.3 ± 3.8	0.09 ± 0.02	0.06 ± 0.04	<LOQ	0.013 ± 0.006	0.019 ± 0.014	0.004 ± 0.001
Rosy goatfish	0.004 ± 0.001	0.37 ± 0.03	3.4 ± 1.2	0.13 ± 0.02	0.42 ± 0.07	3.4 ± 0.2	2.7 ± 0.1	0.22 ± 0.13	0.09 ± 0.04	<LOQ	0.010 ± 0.001	0.044 ± 0.029	0.004 ± 0.002
Parrotfishes													
Blue-barred parrotfish	0.005 ± 0.002	0.42 ± 0.06	1.6 ± 0.3	0.11 ± 0.05	0.39 ± 0.16	4.0 ± 0.9	1.3 ± 1.0	0.05 ± 0.03	0.02 ± 0.01	<LOQ	0.007 ± 0.006	0.007 ± 0.004	0.007 ± 0.003
Rabbitfishes													
Shoemaker spinefoot	0.047 ± 0.051	0.34 ± 0.09	2.9 ± 1.4	0.07 ± 0.03	0.24 ± 0.09	4.6 ± 1.7	0.2 ± 0.1	0.14 ± 0.09	0.28 ± 0.16	0.005	0.047 ± 0.058	0.003 ± 0.001	0.005 ± 0.001
Streamlined spinefoot	0.012 ± 0.007	0.52 ± 0.09	2.5 ± 0.6	0.10 ± 0.11	0.16 ± 0.05	3.5 ± 0.2	0.2 ± 0.1	<LOQ	0.02 ± 0.01	<LOQ	0.002 ± 0.001	0.002 ± 0.001	0.003
Surgeonfishes													
Elongate surgeonfish	0.011 ± 0.008	0.38 ± 0.07	3.3 ± 1.4	0.05 ± 0.02	0.42 ± 0.17	4.9 ± 1.8	2.0 ± 2.4	0.11 ± 0.05	0.11 ± 0.12	<LOQ	0.017 ± 0.011	0.021 ± 0.008	0.004 ± 0.001
Emperors													
Blackeye emperor	0.002 ± 0.001	0.30 ± 0.07	2.6 ± 1.8	0.04 ± 0.01	1.75 ± 0.16	4.8 ± 0.3	1.6 ± 0.3	0.08 ± 0.01	0.13 ± 0.04	<LOQ	0.010 ± 0.003	0.136 ± 0.037	<LOQ
Blue-lined large-eye bream	0.004 ± 0.001	0.40 ± 0.17	3.6 ± 1.6	0.03 ± 0.01	1.02 ± 0.22	5.2 ± 1.8	2.1 ± 0.5	0.24 ± 0.1.0	0.06 ± 0.06	<LOQ	0.023 ± 0.012	0.229 ± 0.061	0.004 ± 0.002
Pink ear emperor	0.005 ± 0.001	0.59 ± 0.20	5.4 ± 3.6	0.15 ± 0.12	1.88 ± 0.60	4.8 ± 1.8	0.8 ± 0.3	0.25 ± 0.11	0.05 ± 0.03	<LOQ	0.158 ± 0.079	0.254 ± 0.105	0.003 ± 0.001

Slender emperor	0.004 ± 0.001	0.46 ± 0.11	3.6 ± 2.3	0.04 ± 0.01	0.66 ± 0.15	4.2 ± 1.1	2.7 ± 0.8	0.26 ± 0.24	0.06 ± 0.08	0.008 ± 0.005	0.015 ± 0.012	0.352 ± 0.150	0.006 ± 0.002
Sky emperor	0.004 ± 0.003	0.47 ± 0.13	3.6 ± 2.4	0.05 ± 0.05	0.76 ± 0.17	4.6 ± 1.4	5.0 ± 1.9	0.23 ± 0.21	0.09 ± 0.07	0.002	0.034 ± 0.038	0.314 ± 0.172	0.006 ± 0.003
Smalltooth emperor	0.004 ± 0.001	0.36 ± 0.04	3.3 ± 1.3	0.03 ± 0.01	0.48 ± 0.07	4.8 ± 0.7	1.2 ± 0.3	0.14 ± 0.10	0.05 ± 0.02	0.003	0.010 ± 0.009	0.215 ± 0.154	0.005 ± 0.001
Spangled emperor	0.009 ± 0.009	0.45 ± 0.13	6.1 ± 6.2	0.11 ± 0.09	0.58 ± 0.18	4.4 ± 0.8	1.1 ± 0.7	0.5 ± 0.42	0.05 ± 0.05	0.043 ± 0.029	0.008 ± 0.003	0.126 ± 0.062	0.026 ± 0.034
Yellowtail emperor	0.007 ± 0.006	0.40 ± 0.09	5.2 ± 3.5	0.05 ± 0.03	1.05 ± 0.33	4.3 ± 1.1	2.3 ± 0.9	0.35 ± 0.32	0.13 ± 0.14	<LOQ	0.020 ± 0.014	0.215 ± 0.115	0.005 ± 0.004
Groupers													
Peacock hind	0.021 ± 0.024	0.34 ± 0.27	5.1 ± 3.3	0.06 ± 0.04	0.51 ± 0.26	5.7 ± 2.6	0.4 ± 0.4	0.21 ± 0.11	0.14 ± 0.17	0.007	0.012 ± 0.008	0.094 ± 0.067	0.014 ± 0.027
Tomato hind	0.007 ± 0.003	0.37 ± 0.18	3.3 ± 3.1	0.03 ± 0.02	0.53 ± 0.06	4.5 ± 2.5	0.7 ± 0.3	0.41 ± 0.37	0.06 ± 0.06	<LOQ	0.011 ± 0.007	0.141 ± 0.054	0.003 ± 0.001
Blacktip grouper	<LOQ	0.34 ± 0.03	2.2 ± 0.5	0.05 ± 0.01	0.50 ± 0.12	4.6 ± 0.9	0.6 ± 0.1	0.06 ± 0.03	0.04 ± 0.02	<LOQ	0.006 ± 0.005	0.108 ± 0.011	0.003
Honeycomb grouper	0.078 ± 0.089	0.20 ± 0.09	3.8 ± 1.8	0.06 ± 0.05	0.33 ± 0.16	4.5 ± 1.0	1.7 ± 1.2	0.13 ± 0.05	0.06 ± 0.01	<LOQ	0.029 ± 0.018	0.119 ± 0.037	0.005 ± 0.001
Brownspotted grouper	0.006 ± 0.004	0.33 ± 0.11	3.0 ± 2.8	0.07 ± 0.04	0.56 ± 0.09	4.7 ± 1.5	0.5 ± 0.6	0.14 ± 0.11	0.05 ± 0.05	0.002 ± 0.001	0.009 ± 0.008	0.083 ± 0.067	0.035 ± 0.053
Brown-marbled grouper	0.005 ± 0.001	0.26 ± 0.03	3.1 ± 2.6	0.04 ± 0.01	0.53 ± 0.16	6.6 ± 2.8	6.1 ± 3.2	0.22 ± 0.23	0.05 ± 0.02	<LOQ	0.010	0.280 ± 0.017	0.003 ± 0.001
Eightbar grouper	0.004 ± 0.001	0.28 ± 0.08	4.1 ± 1.6	0.05 ± 0.01	0.53 ± 0.02	6.0 ± 1.4	1.1 ± 0.3	0.34 ± 0.20	0.03 ± 0.01	<LOQ	0.021 ± 0.011	0.216 ± 0.076	<LOQ
White-blotched grouper	0.004 ± 0.001	0.36 ± 0.11	2.6 ± 1.6	0.06 ± 0.04	0.65 ± 0.16	5.4 ± 2.5	3.4 ± 3.2	0.34 ± 0.40	0.05 ± 0.04	0.063 ± 0.042	0.008 ± 0.005	0.256 ± 0.156	0.012 ± 0.008
Longspine grouper	0.004 ± 0.001	0.41 ± 0.16	2.5 ± 0.2	0.05 ± 0.02	0.40 ± 0.03	5.5 ± 1.6	0.4 ± 0.1	0.10 ± 0.05	0.02	<LOQ	0.011 ± 0.001	0.161 ± 0.041	<LOQ
Yellow-edged lyretail	0.006 ± 0.004	0.34 ± 0.10	4.5 ± 3.4	0.06 ± 0.04	0.61 ± 0.07	5.3 ± 1.6	0.5 ± 0.3	0.47 ± 0.47	0.10 ± 0.08	<LOQ	0.005 ± 0.003	0.128 ± 0.088	0.021 ± 0.052
Trevallies													
Bigeye trevally	0.004	0.53 ± 0.18	11.0 ± 6.1	0.05 ± 0.05	0.78 ± 0.49	8.6 ± 2.7	0.8 ± 0.5	0.43 ± 0.28	0.06 ± 0.07	<LOQ	0.028 ± 0.018	0.438 ± 0.236	0.018 ± 0.025
Bluefin trevally	0.008 ± 0.007	0.46 ± 0.15	5.3 ± 1.5	0.07 ± 0.02	0.44 ± 0.06	6.3 ± 1.2	0.3 ± 0.1	0.28 ± 0.12	0.10 ± 0.11	<LOQ	0.022 ± 0.026	0.311 ± 0.206	0.004 ± 0.001
Golden trevally	0.006 ± 0.004	0.65 ± 0.39	6.9 ± 4.2	0.07 ± 0.02	0.39 ± 0.06	5.5 ± 1.3	0.8 ± 0.4	0.23 ± 0.23	0.10 ± 0.07	<LOQ	0.041 ± 0.020	0.135 ± 0.216	0.023 ± 0.018
Malabar trevally	0.005 ± 0.001	0.46 ± 0.01	4.4 ± 1.0	0.05 ± 0.01	0.54 ± 0.01	6.0 ± 0.5	1.2 ± 0.1	0.13	0.11 ± 0.03	<LOQ	0.009 ± 0.001	0.510 ± 0.210	0.006 ± 0.002
Yellowspotted trevally	0.011 ± 0.015	0.47 ± 0.13	5.5 ± 3.8	0.11 ± 0.03	0.58 ± 0.17	6.1 ± 1.7	0.8 ± 0.3	0.26 ± 0.19	0.13 ± 0.13	0.042 ± 0.054	0.009 ± 0.008	0.184 ± 0.239	0.005 ± 0.003
Bludger	0.009 ± 0.008	0.63 ± 0.14	8.5 ± 2.7	0.08 ± 0.03	0.63 ± 0.16	6.9 ± 1.6	1.3 ± 0.5	0.39 ± 0.26	0.22 ± 0.15	<LOQ	0.044 ± 0.034	0.345 ± 0.361	0.004 ± 0.001
Snappers													

Green jobfish	0.005 ± 0.003	0.44 ± 0.12	3.5 ± 2.3	0.08 ± 0.04	0.62 ± 0.14	4.8 ± 1.4	2.1 ± 1.0	0.37 ± 0.35	0.08 ± 0.10	0.033 ± 0.022	0.014 ± 0.023	0.136 ± 0.127	0.014 ± 0.019
Deep water longtail red snapper	<LOQ	0.37 ± 0.11	1.8 ± 0.5	0.04 ± 0.01	0.61 ± 0.07	3.8 ± 0.4	0.5 ± 0.2	0.06 ± 0.03	0.02 ± 0.01	<LOQ	0.007 ± 0.002	0.233 ± 0.133	0.009 ± 0.004
Two-spot red snapper	0.007 ± 0.009	0.40 ± 0.13	5.1 ± 3.6	0.05 ± 0.05	0.69 ± 0.14	4.5 ± 1.1	3.4 ± 1.7	0.47 ± 0.42	0.09 ± 0.12	0.030 ± 0.017	0.018 ± 0.028	0.295 ± 0.203	0.017 ± 0.021
Humpback red snapper	0.005 ± 0.001	0.61 ± 0.12	7.9 ± 5.3	0.05 ± 0.02	0.55 ± 0.09	5.6 ± 1.1	3.0 ± 2.3	0.45 ± 0.47	0.07 ± 0.05	<LOQ	0.039 ± 0.027	0.235 ± 0.110	0.006 ± 0.004
Bigeye snapper	<LOQ	0.5	1.7	0.05	0.59	13.5	0.3	0.09	0.02	<LOQ	<LOQ	0.370	0.005
Emperor red snapper	0.005 ± 0.006	0.30 ± 0.15	2.7 ± 1.8	0.05 ± 0.05	0.50 ± 0.11	4.8 ± 1.8	2.3 ± 1.1	0.23 ± 0.24	0.08 ± 0.09	0.007 ± 0.006	0.012 ± 0.014	0.157 ± 0.191	0.009 ± 0.007
Humphead snapper	0.01 ± 0.011	0.40 ± 0.09	6.1 ± 1.9	0.07 ± 0.05	0.76 ± 0.09	5.5 ± 1.6	5.7 ± 3.0	0.90 ± 0.63	0.42 ± 0.81	<LOQ	0.069 ± 0.059	0.278 ± 0.097	0.005 ± 0.002
Barracudas													
Pickhandle barracuda	0.005 ± 0.002	0.38 ± 0.21	4.8 ± 2.3	0.11 ± 0.09	0.49 ± 0.10	5.0 ± 1.4	1.0 ± 0.5	0.41 ± 0.23	0.05 ± 0.03	<LOQ	0.024 ± 0.045	0.254 ± 0.144	0.003 ± 0.001
Mackerels													
Indian mackerel	0.008 ± 0.005	0.69 ± 0.13	6.9 ± 1.5	0.07 ± 0.01	0.69 ± 0.16	7.5 ± 3.3	1.3 ± 0.9	0.10 ± 0.06	0.04 ± 0.02	<LOQ	0.025 ± 0.032	0.065 ± 0.041	0.005 ± 0.002
Tunas													
Dogtooth tuna	0.004 ± 0.001	0.49 ± 0.10	3.8 ± 2.3	0.07 ± 0.03	1.06 ± 0.62	6.4 ± 1.0	0.5 ± 0.2	0.17 ± 0.16	0.02 ± 0.01	<LOQ	0.018 ± 0.022	0.491 ± 0.360	0.003
Little tunny	0.007 ± 0.002	0.74 ± 0.27	13.1 ± 0.7	0.13 ± 0.05	0.54 ± 0.10	6.9 ± 1.1	1.3 ± 0.3	0.28 ± 0.16	0.07 ± 0.06	<LOQ	0.078 ± 0.040	0.218 ± 0.071	0.005 ± 0.002
Sharks													
Grey reef shark	<LOQ	0.32	1.6	0.08	0.86	4.1	3.4	<LOQ	0.02	<LOQ	0.003	0.712	0.004
Spinner shark	<LOQ	0.34	1.1	0.10	0.4	3.6	5.9	0.03	0.01	<LOQ	<LOQ	0.232	0.004
Blacktip shark	<LOQ	0.38	4.1	0.13	1.15	8.1	1.6	0.15	0.03	<LOQ	0.003	0.513	0.004
Spot-tail shark	<LOQ	0.19	<LOQ	0.11	0.51	4.7	7.2	0.08	<LOQ	<LOQ	<LOQ	0.093	<LOQ
Tiger shark	0.004	0.44	2.4	0.09	0.41	6.5	3.2	0.04	0.02	<LOQ	<LOQ	0.673	0.006
Great hammerhead	<LOQ	0.20	2.4	0.08	0.39	4.0	3.1	0.06	<LOQ	<LOQ	<LOQ	0.613	0.004
Scalloped hammerhead	0.010 ± 0.009	0.35 ± 0.03	1.9 ± 0.6	0.19 ± 0.04	1.26 ± 0.46	5.3 ± 2.1	5.6 ± 2.1	0.06 ± 0.02	0.02 ± 0.01	<LOQ	0.003 ± 0.001	0.534 ± 0.185	0.005 ± 0.004
Billfishes													
Swordfish	0.005 ± 0.002	0.43 ± 0.34	3.8 ± 3.7	0.04 ± 0.03	0.74 ± 0.28	9.1 ± 4.6	0.7 ± 0.3	0.16 ± 0.16	0.03 ± 0.03	0.003 ± 0.001	0.055 ± 0.040	0.734 ± 0.440	0.045 ± 0.097

Appendix 8.2. Daily provisional tolerable intakes (PTI) calculated from the guidelines given by the JECFA (2011b, 2013)(B) and Recommended daily intakes (RDI) and daily PTI for essential trace elements given by the American Food and Nutrition Board of the Institute of Medicine National Academy of Sciences (2019a, b). Mean weights for children and young adults were taken from Marques-Vidal et al. (2008) and mean weight for adult women was taken from US-EPA and US-FDA (2019); PTI values in calculations are indicated in bold (A). yo = years old, kg bw = kilogram of body weight.

A.

			Cd			Hg		
Age class	Age subclass	Mean weight (kg)	Literature value (µg/kg bw/month)	In µg/month	In µg/day	Literature value (µg/kg bw/week)	In µg/week	In µg/day
Children	2-3 yo	12	25	300	**10**	4	48	**7**
	4-8 yo	22		550	**18**		88	**13**
	9-13 yo	36		900	**30**		144	**21**
Young adults	14-18 yo	52		1300	**43**		208	**30**
Adult women	19+ yo	70		1750	**58**		280	**40**

B.

		RDI (µg.g^{-1})					PTI (µg.g^{-1})				
Age class	Age subclass	Cu	Fe	Mn	Se	Zn	Cu	Fe	Mn	Se	Zn
Children	2-3 yo	340	7,000	1,200	20	3,000	1,000	40,000	2,000	90	7,000
	4-8 yo	440	10,000	1,500	30	5,000	3,000	40,000	3,000	150	12,000
	9-13 yo	700	8,000	1,900	40	8,000	5,000	40,000	6,000	280	23,000
Young adults	14-18 yo	890	15,000	2,200	55	11,000	8,000	45,000	9,000	400	34,000
Adult women	19+ yo	900	18,000	1,800	55	9,000	10,000	45,000	11,000	400	40,000
	19+ yo and pregnant	1,000	27,000	2,000	60	11,000					
	19+ yo and lactating	1,300	9,000	2,600	70	12,000					

Appendix 8.3. Extract of advice chart about eating fish from the US-EPA and US-FDA (2019).

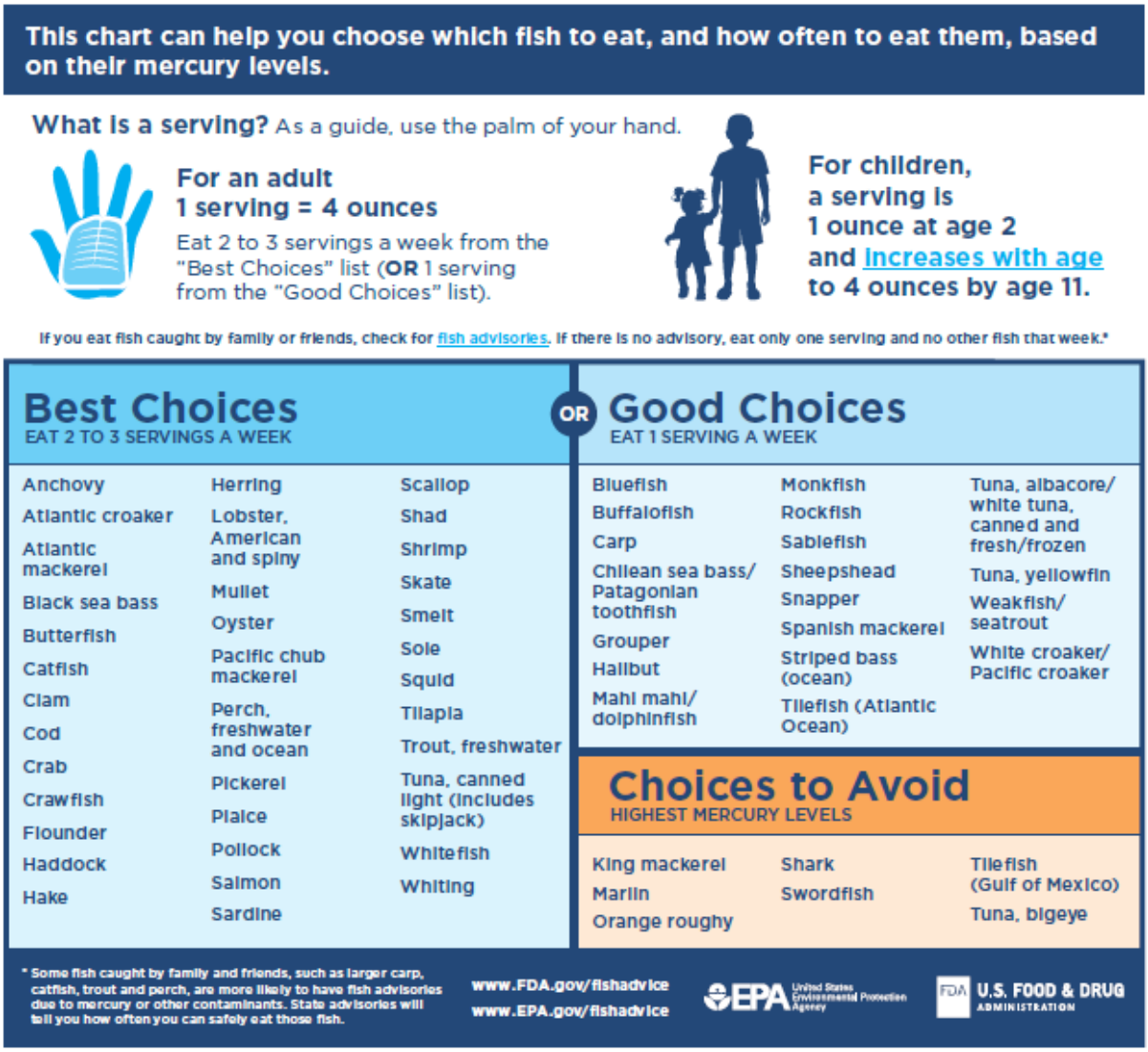

Appendix 8.4. Percentage of daily provisional tolerable intake (%PTI) covered by a daily Seychellois portion (156 g) of capture fisheries products from the Seychelles for essential (A) and non-essential trace elements (B). %PTI are presented as mean [CI95%] and iAs estimated concentrations are presented as mean ± SD. Uncoloured cells indicate that the daily portion is safe to eat for the age category (%PTI < 75%) and coloured cells indicate the risk category; values used to sort species into risk categories are indicated in bold. Yellow = Be careful (75% < %PTI < 90%) and orange = Do not eat more than given weight (90% < %PTI). C = Children (2-13 years), YA = Young adults (14-18 years) and A = Adult women (> 18 years).

A.

	Cu			Fe		Mn			Theoretically bioavailable Se		Zn		
Species	C	YA	A	C	YA & A	C	YA	A	C	YA & A	C	YA	A
Octopuses													
Big blue octopus	2.9 [2.2-**3.9**]	2.2 [1.9-**2.5**]	1.8 [1.5-**2.0**]	0.35 [0.11-**0.69**]	0.67 [0.51-**0.84**]	0.18 [0.12-**0.25**]	0.16 [0.14-**0.18**]	0.13 [0.12-**0.15**]	11 [8-**14**]	10 [9-**11**]	10 [8-**12**]	9 [8-**9**]	8 [7-**8**]
Crabs													
Spanner crab	18.4 [9.9-**30.3**]	14.1 [8.4-**19.7**]	11.2 [6.7-**15.7**]	0.18 [0.07-**0.30**]	0.35 [0.33-**0.37**]	0.09 [0.05-**0.12**]	0.08 [0.06-**0.09**]	0.06 [0.05-**0.07**]	22 [15-**30**]	21 [18-**24**]	22 [17-**28**]	20 [18-**22**]	17 [16-**18**]
Spiny lobsters													
Longlegged spiny lobster	25.4 [19.3-**34.1**]	19.4 [16.5-**22.2**]	15.5 [13.2-**17.8**]	0.42 [0.15-**0.75**]	0.80 [0.69-**0.91**]	0.15 [0.10-**0.21**]	0.13 [0.11-**0.15**]	0.11 [0.09-**0.13**]	11 [8-**15**]	11 [9-**12**]	14 [11-**18**]	13 [12-**14**]	11 [10-**12**]
Painted spiny lobster	21.2 [15.3-**29.4**]	16.1 [13.1-**19.1**]	12.9 [10.5-**15.3**]	0.50 [0.15-**1.02**]	0.96 [0.68-**1.24**]	0.18 [0.12-**0.27**]	0.17 [0.14-**0.19**]	0.14 [0.11-**0.16**]	10 [7-**15**]	10 [8-**12**]	11 [8-**14**]	10 [8-**11**]	8 [7-**9**]
Pronghorn spiny lobster	26.6 [21.2-**34.4**]	20.2 [18.1-**22.3**]	16.2 [14.5-**17.9**]	0.46 [0.15-**0.89**]	0.89 [0.70-**1.08**]	0.19 [0.13-**0.26**]	0.17 [0.15-**0.19**]	0.14 [0.12-**0.15**]	11 [8-**15**]	11 [10-**12**]	17 [13-**21**]	15 [14-**16**]	13 [12-**14**]
Goatfishes													
Dash-and-dot goatfish	0.7 [0.6-**1.0**]	0.6 [0.5-**0.6**]	0.4 [0.4-**0.5**]	0.47 [0.11-**1.07**]	0.90 [0.50-**1.30**]	0.15 [0.07-**0.25**]	0.13 [0.08-**0.18**]	0.11 [0.07-**0.15**]	19 [13-**25**]	18 [15-**21**]	2 [2-**3**]	2 [2-**2**]	2 [2-**2**]
Rosy goatfish	1.0 [0.8-**1.2**]	0.7 [0.7-**0.8**]	0.6 [0.5-**0.6**]	0.61 [0.15-**1.37**]	1.17 [0.68-**1.66**]	0.24 [0.15-**0.36**]	0.22 [0.18-**0.26**]	0.18 [0.14-**0.21**]	16 [11-**23**]	16 [13-**18**]	2 [1-**2**]	2 [1-**2**]	1 [1-**1**]
Parrotfishes													
Blue-barred parrotfish	1.1 [0.9-**1.4**]	0.8 [0.8-**0.9**]	0.7 [0.6-**0.7**]	0.29 [0.10-**0.51**]	0.55 [0.48-**0.62**]	0.22 [0.12-**0.35**]	0.20 [0.14-**0.25**]	0.16 [0.11-**0.21**]	17 [10-**26**]	17 [12-**21**]	2 [1-**3**]	2 [2-**2**]	2 [1-**2**]
Rabbitfishes													
Shoemaker spinefoot	0.9 [0.7-**1.2**]	0.7 [0.6-**0.8**]	0.5 [0.4-**0.6**]	0.52 [0.15-**1.09**]	1.01 [0.69-**1.33**]	0.13 [0.07-**0.21**]	0.12 [0.09-**0.15**]	0.10 [0.07-**0.12**]	10 [6-**14**]	9 [7-**12**]	2 [1-**3**]	2 [2-**3**]	2 [1-**2**]
Streamlined spinefoot	1.3 [1.1-**1.7**]	1.0 [0.9-**1.1**]	0.8 [0.7-**0.9**]	0.45 [0.16-**0.82**]	0.87 [0.75-**0.99**]	0.19 [0.04-**0.40**]	0.17 [0.05-**0.29**]	0.14 [0.04-**0.24**]	7 [4-**9**]	6 [5-**8**]	2 [1-**2**]	2 [2-**2**]	1 [1-**1**]
Surgeonfishes													
Elongate surgeonfish	1.0 [0.7-**1.3**]	0.7 [0.6-**0.8**]	0.6 [0.5-**0.7**]	0.60 [0.17-**1.27**]	1.16 [0.78-**1.54**]	0.09 [0.05-**0.15**]	0.08 [0.05-**0.11**]	0.07 [0.04-**0.09**]	17 [9-**26**]	16 [11-**21**]	2 [1-**4**]	2 [2-**3**]	2 [1-**2**]
Emperors													
Blackeye emperor	0.8 [0.5-**1.2**]	0.6 [0.4-**0.8**]	0.5 [0.3-**0.6**]	0.47 [0.00-**1.47**]	0.90 [0.02-**1.79**]	0.08 [0.06-**0.10**]	0.07 [0.06-**0.07**]	0.06 [0.05-**0.06**]	69 [49-**93**]	66 [57-**76**]	2 [2-**3**]	2 [2-**2**]	2 [2-**2**]

Blue-lined large-eye bream	1.0 [0.6-**1.6**]	0.8 [0.5-**1.1**]	0.6 [0.4-**0.9**]	0.65 [0.17-**1.43**]	1.26 [0.78-**1.74**]	0.05 [0.03-**0.07**]	0.04 [0.04-**0.05**]	0.04 [0.03-**0.04**]	38 [24-**54**]	36 [29-**44**]	3 [2-**4**]	2 [2-**3**]	2 [1-**3**]
Pink ear emperor	1.5 [0.8-**2.5**]	1.1 [0.7-**1.6**]	0.9 [0.6-**1.3**]	0.96 [0.09-**2.70**]	1.86 [0.43-**3.29**]	0.28 [0.02-**0.66**]	0.25 [0.03-**0.48**]	0.21 [0.02-**0.39**]	73 [39-**115**]	70 [46-**94**]	2 [1-**4**]	2 [1-**3**]	2 [1-**3**]
Slender emperor	1.2 [0.9-**1.5**]	0.9 [0.8-**1.0**]	0.7 [0.6-**0.8**]	0.65 [0.19-**1.33**]	1.26 [0.89-**1.62**]	0.07 [0.05-**0.11**]	0.07 [0.05-**0.08**]	0.05 [0.04-**0.06**]	21 [15-**28**]	20 [17-**23**]	2 [2-**3**]	2 [2-**2**]	2 [1-**2**]
Sky emperor	1.2 [0.9-**1.6**]	0.9 [0.8-**1.0**]	0.7 [0.6-**0.8**]	0.65 [0.20-**1.32**]	1.26 [0.90-**1.61**]	0.10 [0.04-**0.18**]	0.09 [0.05-**0.13**]	0.07 [0.04-**0.10**]	26 [19-**33**]	25 [23-**27**]	2 [2-**3**]	2 [2-**2**]	2 [2-**2**]
Smalltooth emperor	0.9 [0.8-**1.2**]	0.7 [0.7-**0.8**]	0.6 [0.5-**0.6**]	0.59 [0.18-**1.16**]	1.13 [0.84-**1.41**]	0.06 [0.04-**0.08**]	0.05 [0.05-**0.06**]	0.04 [0.04-**0.05**]	16 [11-**23**]	16 [13-**19**]	2 [2-**3**]	2 [2-**2**]	2 [2-**2**]
Spangled emperor	1.2 [0.9-**1.6**]	0.9 [0.7-**1.0**]	0.7 [0.6-**0.8**]	1.09 [0.21-**2.67**]	2.11 [0.97-**3.24**]	0.22 [0.10-**0.38**]	0.19 [0.12-**0.27**]	0.16 [0.09-**0.22**]	22 [14-**31**]	21 [17-**25**]	2 [2-**3**]	2 [2-**2**]	2 [2-**2**]
Yellowtail emperor	1.0 [0.8-**1.3**]	0.8 [0.7-**0.9**]	0.6 [0.5-**0.7**]	0.94 [0.25-**2.04**]	1.81 [1.14-**2.48**]	0.09 [0.05-**0.15**]	0.08 [0.06-**0.11**]	0.07 [0.05-**0.09**]	39 [26-**56**]	38 [30-**45**]	2 [2-**3**]	2 [2-**2**]	2 [1-**2**]
Groupers													
Blacktip grouper	0.9 [0.7-**1.1**]	0.7 [0.6-**0.7**]	0.5 [0.5-**0.6**]	0.39 [0.12-**0.79**]	0.75 [0.54-**0.96**]	0.09 [0.06-**0.12**]	0.08 [0.07-**0.09**]	0.06 [0.06-**0.07**]	18 [11-**28**]	18 [13-**23**]	2 [2-**3**]	2 [2-**3**]	2 [1-**2**]
Brown-marbled grouper	0.7 [0.5-**0.9**]	0.5 [0.4-**0.6**]	0.4 [0.3-**0.5**]	0.56 [0.00-**1.91**]	1.07 [0.00-**2.33**]	0.07 [0.05-**0.10**]	0.06 [0.06-**0.07**]	0.05 [0.05-**0.06**]	17 [7-**31**]	16 [8-**25**]	3 [1-**6**]	3 [1-**5**]	3 [1-**4**]
Brownspotted grouper	0.8 [0.7-**1.0**]	0.6 [0.6-**0.7**]	0.5 [0.5-**0.5**]	0.53 [0.17-**1.02**]	1.02 [0.81-**1.24**]	0.13 [0.09-**0.18**]	0.12 [0.10-**0.13**]	0.09 [0.08-**0.11**]	21 [17-**26**]	21 [20-**21**]	2 [2-**3**]	2 [2-**2**]	2 [2-**2**]
Eightbar grouper	0.7 [0.5-**1.1**]	0.5 [0.4-**0.7**]	0.4 [0.3-**0.6**]	0.73 [0.19-**1.61**]	1.41 [0.86-**1.96**]	0.09 [0.06-**0.12**]	0.08 [0.07-**0.09**]	0.07 [0.06-**0.07**]	18 [13-**23**]	17 [16-**19**]	3 [2-**4**]	3 [2-**3**]	2 [2-**3**]
Honeycomb grouper	0.5 [0.2-**0.9**]	0.4 [0.2-**0.6**]	0.3 [0.2-**0.5**]	0.68 [0.15-**1.57**]	1.31 [0.71-**1.90**]	0.12 [0.01-**0.27**]	0.11 [0.02-**0.20**]	0.09 [0.01-**0.16**]	11 [5-**20**]	11 [5-**17**]	2 [2-**3**]	2 [2-**2**]	2 [1-**2**]
Longspine grouper	1.1 [0.4-**1.9**]	0.8 [0.4-**1.3**]	0.6 [0.3-**1.0**]	0.44 [0.17-**0.76**]	0.86 [0.78-**0.93**]	0.10 [0.04-**0.19**]	0.09 [0.04-**0.14**]	0.07 [0.04-**0.11**]	14 [10-**17**]	13 [12-**14**]	3 [1-**5**]	3 [1-**4**]	2 [1-**3**]
Peacock hind	0.9 [0.6-**1.3**]	0.7 [0.5-**0.8**]	0.5 [0.4-**0.7**]	0.92 [0.31-**1.74**]	1.78 [1.44-**2.12**]	0.12 [0.08-**0.18**]	0.11 [0.09-**0.13**]	0.09 [0.07-**0.11**]	19 [13-**26**]	18 [15-**21**]	3 [2-**4**]	3 [2-**3**]	2 [2-**3**]
Tomato hind	1.0 [0.6-**1.4**]	0.7 [0.5-**0.9**]	0.6 [0.4-**0.7**]	0.59 [0.12-**1.40**]	1.14 [0.57-**1.70**]	0.05 [0.03-**0.08**]	0.05 [0.03-**0.06**]	0.04 [0.03-**0.05**]	19 [15-**25**]	19 [17-**20**]	2 [1-**3**]	2 [1-**3**]	2 [1-**2**]
White-blotched grouper	0.9 [0.7-**1.2**]	0.7 [0.6-**0.8**]	0.6 [0.5-**0.6**]	0.46 [0.14-**0.92**]	0.89 [0.66-**1.12**]	0.11 [0.06-**0.17**]	0.10 [0.07-**0.12**]	0.08 [0.06-**0.10**]	22 [16-**30**]	21 [19-**24**]	3 [2-**4**]	2 [2-**3**]	2 [2-**3**]
Yellow-edged lyretail	0.9 [0.7-**1.1**]	0.7 [0.6-**0.7**]	0.5 [0.5-**0.6**]	0.81 [0.26-**1.58**]	1.55 [1.18-**1.92**]	0.12 [0.07-**0.18**]	0.10 [0.08-**0.13**]	0.09 [0.07-**0.10**]	23 [18-**28**]	22 [21-**23**]	3 [2-**3**]	2 [2-**3**]	2 [2-**2**]
Trevallies													
Bigeye trevally	1.4 [0.9-**2.0**]	1.0 [0.8-**1.3**]	0.8 [0.6-**1.0**]	1.99 [0.51-**4.36**]	3.83 [2.36-**5.30**]	0.09 [0.02-**0.19**]	0.08 [0.02-**0.14**]	0.06 [0.02-**0.11**]	25 [9-**45**]	24 [11-**37**]	4 [3-**6**]	4 [3-**5**]	3 [3-**4**]
Bludger	1.6 [1.3-**2.1**]	1.2 [1.1-**1.3**]	1.0 [0.9-**1.1**]	1.53 [0.56-**2.72**]	2.95 [2.59-**3.31**]	0.16 [0.10-**0.23**]	0.14 [0.12-**0.16**]	0.12 [0.10-**0.13**]	20 [13-**29**]	19 [15-**23**]	4 [3-**5**]	3 [3-**3**]	3 [2-**3**]
Bluefin trevally	1.2 [0.8-**1.7**]	0.9 [0.7-**1.1**]	0.7 [0.6-**0.9**]	0.95 [0.32-**1.78**]	1.83 [1.50-**2.17**]	0.13 [0.08-**0.20**]	0.12 [0.09-**0.14**]	0.10 [0.08-**0.12**]	13 [9-**18**]	12 [10-**15**]	3 [2-**4**]	3 [3-**3**]	2 [2-**3**]

Golden trevally	1.7 [0.8-**2.8**]	1.3 [0.7-**1.8**]	1.0 [0.6-**1.5**]	1.24 [0.28-**2.86**]	2.39 [1.31-**3.48**]	0.13 [0.08-**0.19**]	0.12 [0.09-**0.14**]	0.09 [0.07-**0.11**]	14 [9-**20**]	13 [10-**16**]	3 [2-**4**]	3 [2-**3**]	2 [2-**3**]
Malabar trevally	1.2 [1.0-**1.5**]	0.9 [0.9-**0.9**]	0.7 [0.7-**0.8**]	0.78 [0.23-**1.62**]	1.51 [1.05-**1.97**]	0.10 [0.06-**0.15**]	0.09 [0.07-**0.11**]	0.07 [0.06-**0.09**]	14 [7-**22**]	13 [8-**18**]	3 [2-**4**]	3 [2-**3**]	2 [2-**3**]
Yellowspotted trevally	1.2 [1.0-**1.6**]	0.9 [0.8-**1.0**]	0.7 [0.7-**0.8**]	0.99 [0.32-**1.92**]	1.90 [1.47-**2.33**]	0.20 [0.14-**0.27**]	0.18 [0.17-**0.20**]	0.15 [0.14-**0.16**]	21 [15-**28**]	20 [18-**23**]	3 [2-**4**]	3 [3-**3**]	2 [2-**3**]
Snappers													
Bigeye snapper	1.3 [1.1-**1.5**]	**1.0**	**0.8**	0.30 [0.12-**0.47**]	**0.58**	0.09 [0.07-**0.11**]	**0.08**	**0.07**	18 [15-**21**]	**17**	7 [6-**8**]	**6**	**5**
Deepwater longtail red snapper	1.0 [0.7-**1.3**]	0.7 [0.6-**0.9**]	0.6 [0.5-**0.7**]	0.32 [0.11-**0.60**]	0.61 [0.50-**0.73**]	0.07 [0.04-**0.10**]	0.06 [0.05-**0.07**]	0.05 [0.04-**0.06**]	21 [16-**26**]	20 [19-**21**]	2 [2-**2**]	2 [2-**2**]	1 [1-**2**]
Emperor red snapper	0.8 [0.6-**1.0**]	0.6 [0.5-**0.7**]	0.5 [0.4-**0.5**]	0.48 [0.17-**0.88**]	0.93 [0.79-**1.07**]	0.09 [0.05-**0.14**]	0.08 [0.06-**0.10**]	0.07 [0.05-**0.08**]	18 [14-**22**]	17 [17-**18**]	2 [2-**3**]	2 [2-**2**]	2 [2-**2**]
Green jobfish	1.1 [0.9-**1.4**]	0.9 [0.8-**0.9**]	0.7 [0.6-**0.7**]	0.63 [0.23-**1.11**]	1.20 [1.06-**1.35**]	0.15 [0.11-**0.20**]	0.14 [0.12-**0.15**]	0.11 [0.10-**0.12**]	23 [18-**28**]	22 [21-**23**]	2 [2-**3**]	2 [2-**2**]	2 [2-**2**]
Humpback red snapper	1.6 [1.3-**2.0**]	1.2 [1.1-**1.3**]	0.9 [0.9-**1.0**]	1.41 [0.40-**2.97**]	2.72 [1.83-**3.62**]	0.09 [0.06-**0.14**]	0.08 [0.07-**0.10**]	0.07 [0.06-**0.08**]	18 [14-**24**]	18 [16-**19**]	3 [2-**4**]	3 [2-**3**]	2 [2-**2**]
Humphead snapper	1.0 [0.7-**1.5**]	0.8 [0.6-**0.9**]	0.6 [0.5-**0.8**]	1.10 [0.34-**2.21**]	2.12 [1.56-**2.69**]	0.14 [0.04-**0.28**]	0.12 [0.05-**0.20**]	0.10 [0.04-**0.16**]	27 [19-**36**]	25 [22-**29**]	3 [2-**4**]	3 [2-**3**]	2 [2-**3**]
Two-spot red snapper	1.0 [0.8-**1.3**]	0.8 [0.7-**0.8**]	0.6 [0.6-**0.7**]	0.92 [0.31-**1.72**]	1.77 [1.44-**2.10**]	0.10 [0.06-**0.15**]	0.09 [0.07-**0.11**]	0.07 [0.06-**0.09**]	23 [18-**29**]	22 [21-**24**]	2 [2-**3**]	2 [2-**2**]	2 [2-**2**]
Barracudas													
Pickhandle barracuda	1.0 [0.7-**1.4**]	0.7 [0.6-**0.9**]	0.6 [0.5-**0.7**]	0.87 [0.29-**1.62**]	1.67 [1.36-**1.97**]	0.22 [0.12-**0.35**]	0.19 [0.13-**0.25**]	0.16 [0.11-**0.21**]	16 [12-**20**]	15 [14-**16**]	3 [2-**3**]	2 [2-**3**]	2 [2-**2**]
Mackerels													
Indian mackerel	1.8 [1.4-**2.2**]	1.3 [1.2-**1.5**]	1.1 [1.0-**1.2**]	1.25 [0.47-**2.18**]	2.40 [2.16-**2.65**]	0.14 [0.10-**0.19**]	0.13 [0.12-**0.14**]	0.10 [0.09-**0.11**]	27 [20-**36**]	26 [23-**29**]	4 [3-**5**]	3 [3-**4**]	3 [2-**4**]
Tunas													
Dogtooth tuna	1.2 [1.0-**1.7**]	1.0 [0.8-**1.1**]	0.8 [0.7-**0.9**]	0.69 [0.16-**1.56**]	1.32 [0.74-**1.90**]	0.14 [0.07-**0.22**]	0.12 [0.09-**0.16**]	0.10 [0.07-**0.13**]	35 [14-**63**]	34 [16-**51**]	3 [2-**4**]	3 [3-**3**]	3 [2-**3**]
Little tunny	1.9 [1.1-**2.9**]	1.4 [1.0-**1.9**]	1.2 [0.8-**1.5**]	2.36 [0.93-**3.92**]	4.54 [4.31-**4.76**]	0.24 [0.13-**0.40**]	0.22 [0.15-**0.29**]	0.18 [0.12-**0.24**]	19 [13-**25**]	18 [15-**21**]	4 [3-**5**]	3 [3-**4**]	3 [2-**3**]
Sharks													
Blacktip shark	1.0 [0.9-**1.2**]	**0.7**	**0.6**	0.74 [0.31-**1.18**]	**1.43**	0.25 [0.20-**0.31**]	**0.23**	**0.19**	39 [32-**46**]	**37**	4 [3-**5**]	**4**	**3**
Great hammerhead	0.5 [0.4-**0.6**]	**0.4**	**0.3**	0.42 [0.18-**0.67**]	**0.81**	0.16 [0.13-**0.20**]	**0.15**	**0.12**	6 [5-**7**]	**6**	2 [2-**2**]	**2**	**2**
Grey reef shark	0.8 [0.7-**1.0**]	**0.6**	**0.5**	0.30 [0.12-**0.47**]	**0.57**	0.16 [0.13-**0.20**]	**0.15**	**0.12**	24 [19-**28**]	**23**	2 [2-**2**]	**2**	**2**
Scalloped hammerhead	0.9 [0.8-**1.1**]	0.7 [0.7-**0.7**]	0.5 [0.5-**0.6**]	0.34 [0.12-**0.62**]	0.65 [0.55-**0.75**]	0.37 [0.26-**0.51**]	0.34 [0.30-**0.37**]	0.27 [0.25-**0.30**]	43 [27-**62**]	41 [32-**50**]	3 [2-**4**]	2 [2-**3**]	2 [2-**2**]
Spinner shark	0.9 [0.8-**1.0**]	**0.7**	**0.5**	0.20 [0.08-**0.31**]	**0.38**	0.19 [0.15-**0.24**]	**0.17**	**0.14**	13 [10-**15**]	**12**	2 [2-**2**]	**2**	**1**

Spot-tail shark	0.5 [0.4-**0.6**]	**0.4**	**0.3**	ND	ND	0.20 [0.16-**0.25**]	**0.18**	**0.15**	19 [16-**23**]	**19**	2 [2-**3**]	**2**	**2**
Tiger shark	1.1 [1.0-**1.3**]	**0.9**	**0.7**	0.43 [0.18-**0.68**]	**0.83**	0.17 [0.13-**0.21**]	**0.16**	**0.13**	6 [5-**7**]	**6**	3 [3-**4**]	**3**	**3**
Billfishes													
Swordfish	1.1 [0.9-**1.5**]	0.8 [0.7-**1.0**]	0.7 [0.6-**0.8**]	0.69 [0.24-**1.27**]	1.33 [1.11-**1.55**]	0.07 [0.05-**0.10**]	0.06 [0.05-**0.07**]	0.05 [0.04-**0.06**]	19 [14-**24**]	18 [16-**20**]	5 [4-**6**]	4 [4-**5**]	4 [3-**4**]

B.

	Non-essential					
	Cd			**Theoretically bioavailable Hg**		
Species	**C**	**YA**	**A**	**C**	**YA**	**A**
Octopuses						
Big blue octopus	6 [4-**9**]	7 [5-**8**]	5 [3-**6**]	**0**	**0**	**0**
Crabs						
Spanner crab	159 [71-**256**]	160 [85-**234**]	119 [63-**174**]	**0**	**0**	**0**
Spiny lobsters						
Longlegged spiny lobster	28 [8-**51**]	28 [10-**47**]	21 [7-**35**]	**0**	**0**	**0**
Painted spiny lobster	25 [0-**59**]	26 [0-**54**]	19 [0-**40**]	**0**	**0**	**0**
Pronghorn spiny lobster	21 [11-**33**]	21 [13-**30**]	16 [9-**23**]	**0**	**0**	**0**
Goatfishes						
Dash-and-dot goatfish	5 [2-**7**]	5 [3-**7**]	4 [2-**5**]	**0**	**0**	**0**
Rosy goatfish	4 [3-**5**]	4 [3-**4**]	3 [2-**3**]	**0**	**0**	**0**
Parrotfishes						
Blue-barred parrotfish	3 [1-**4**]	3 [1-**4**]	2 [1-**3**]	**0**	**0**	**0**
Rabbitfishes						
Shoemaker spinefoot	17 [3-**33**]	17 [3-**30**]	12 [2-**23**]	**0**	**0**	**0**
Streamlined spinefoot	1 [1-**1**]	1 [1-**1**]	1 [1-**1**]	**0**	**0**	**0**
Surgeonfishes						
Elongate surgeonfish	6 [2-**10**]	6 [3-**9**]	5 [2-**7**]	**0**	**0**	**0**
Emperors						

Blackeye emperor	3 [1-**6**]	3 [2-**5**]	3 [1-**4**]	**0**	**0**	**0**
Blue-lined large-eye bream	8 [4-**13**]	8 [4-**12**]	6 [3-**9**]	**0**	**0**	**0**
Pink ear emperor	57 [21-**98**]	57 [25-**89**]	42 [18-**66**]	**0**	**0**	**0**
Slender emperor	5 [3-**8**]	5 [3-**7**]	4 [3-**5**]	**0**	**0**	**0**
Sky emperor	12 [5-**20**]	12 [7-**18**]	9 [5-**14**]	**0**	**0**	**0**
Smalltooth emperor	4 [1-**6**]	4 [2-**6**]	3 [1-**4**]	**0**	**0**	**0**
Spangled emperor	3 [2-**4**]	3 [2-**4**]	2 [2-**3**]	**0**	**0**	**0**
Yellowtail emperor	7 [4-**11**]	7 [5-**10**]	5 [3-**7**]	**0**	**0**	**0**
Groupers						
Blacktip grouper	2 [0-**4**]	2 [0-**4**]	2 [0-**3**]	**0**	**0**	**0**
Brown-marbled grouper	4 [3-**4**]	**4**	**3**	**0**	**0**	**0**
Brownspotted grouper	3 [2-**4**]	3 [2-**4**]	2 [2-**3**]	**0**	**0**	**0**
Eightbar grouper	8 [3-**13**]	8 [4-**11**]	6 [3-**9**]	**0**	**0**	**0**
Honeycomb grouper	10 [3-**18**]	10 [4-**17**]	8 [3-**12**]	**0**	**0**	**0**
Longspine grouper	4 [3-**4**]	4 [4-**4**]	3 [3-**3**]	**0**	**0**	**0**
Peacock hind	4 [3-**6**]	4 [4-**5**]	3 [3-**4**]	**0**	**0**	**0**
Tomato hind	4 [2-**6**]	4 [3-**5**]	3 [2-**4**]	**0**	**0**	**0**
White-blotched grouper	3 [2-**4**]	3 [2-**4**]	2 [2-**3**]	**0**	**0**	**0**
Yellow-edged lyretail	2 [1-**2**]	2 [2-**2**]	1 [1-**2**]	**0**	**0**	**0**
Trevallies						
Bigeye trevally	10 [5-**16**]	10 [6-**14**]	7 [4-**11**]	2.5 [0.0-**8.0**]	2.5 [0.0-**7.4**]	1.9 [0.0-**5.5**]
Bludger	16 [9-**23**]	16 [11-**21**]	12 [8-**15**]	0.4 [0.0-**1.2**]	0.4 [0.0-**1.1**]	0.3 [0.0-**0.8**]
Bluefin trevally	8 [2-**15**]	8 [2-**14**]	6 [1-**10**]	**0**	**0**	**0**
Golden trevally	15 [8-**22**]	15 [9-**20**]	11 [7-**15**]	**0**	**0**	**0**
Malabar trevally	3 [2-**4**]	3 [3-**4**]	2 [2-**3**]	**0**	**0**	**0**
Yellowspotted trevally	3 [2-**4**]	3 [2-**4**]	2 [2-**3**]	**0**	**0**	**0**
Snappers						
Bigeye snapper	ND	ND	ND	**0**	**0**	**0**
Deepwater longtail red snapper	2 [2-**3**]	2 [2-**3**]	2 [1-**2**]	**0**	**0**	**0**
Emperor red snapper	4 [3-**6**]	4 [3-**6**]	3 [2-**4**]	**0**	**0**	**0**
Green jobfish	5 [3-**7**]	5 [4-**7**]	4 [3-**5**]	**0**	**0**	**0**

Humpback red snapper	14 [8-**21**]	14 [9-**19**]	10 [7-**14**]	**0**	**0**	**0**
Humphead snapper	25 [5-**47**]	25 [6-**43**]	19 [5-**32**]	**0**	**0**	**0**
Two-spot red snapper	7 [3-**10**]	7 [4-**9**]	5 [3-**7**]	**0**	**0**	**0**
Barracudas						
Pickhandle barracuda	9 [2-**16**]	9 [3-**15**]	7 [2-**11**]	**0**	**0**	**0**
Mackerels						
Indian mackerel	9 [3-**16**]	9 [4-**15**]	7 [3-**11**]	**0**	**0**	**0**
Tunas						
Dogtooth tuna	7 [1-**14**]	7 [1-**12**]	5 [1-**9**]	**0**	**0**	**0**
Little tunny	28 [13-**44**]	28 [16-**40**]	21 [12-**30**]	**0**	**0**	**0**
Sharks						
Blacktip shark	1 [1-**1**]	**1**	**1**	**0**	**0**	**0**
Great hammerhead	ND	ND	ND	**0**	**0**	**0**
Grey reef shark	1 [1-**1**]	**1**	**1**	**0**	**0**	**0**
Scalloped hammerhead	1 [1-**1**]	1 [1-**1**]	1 [1-**1**]	**0**	**0**	**0**
Spinner shark	ND	ND	ND	**0**	**0**	**0**
Spot-tail shark	ND	ND	ND	**0**	**0**	**0**
Tiger shark	ND	ND	ND	**0**	**0**	**0**
Billfishes						
Swordfish	20 [14-**24**]	20 [17-**22**]	15 [13-**16**]	**0**	**0**	**0**

13. SUPPLEMENTARY DOCUMENTS

Content

- SUPPLEMENTARY DOCUMENT 1 -

The role of tropical capture fisheries in trace element delivery for a Small Island Developing State community, the Seychelles

Magali A. SABINO[1,2], Nathalie BODIN[1,3,4], Rodney GOVINDEN[1], Rona ALBERT[1], Carine CHURLAUD[2], Heidi PETHYBRIDGE[5], Paco BUSTAMANTE[2,6]

[1] Seychelles Fishing Authority (SFA), Fishing Port, Victoria, Mahé, Republic of Seychelles

[2] Littoral Environnement et Sociétés (LIENSs), UMR 7266 CNRS - La Rochelle Université, 2 rue Olympe de Gouges, 17000 La Rochelle, France

[3] Institute for Research and Development (IRD), Fishing Port, Victoria, Mahé, Seychelles

[4] Sustainable Ocean Seychelles (SOS), BeauBelle, Mahé, Republic of Seychelles

[5] CSIRO Oceans and Atmosphere, Hobart, Tasmania, Australia

[6] Institut Universitaire de France (IUF), 1 rue Descartes 75005 Paris, France

Submitted in *Marine Pollution Bulletin*

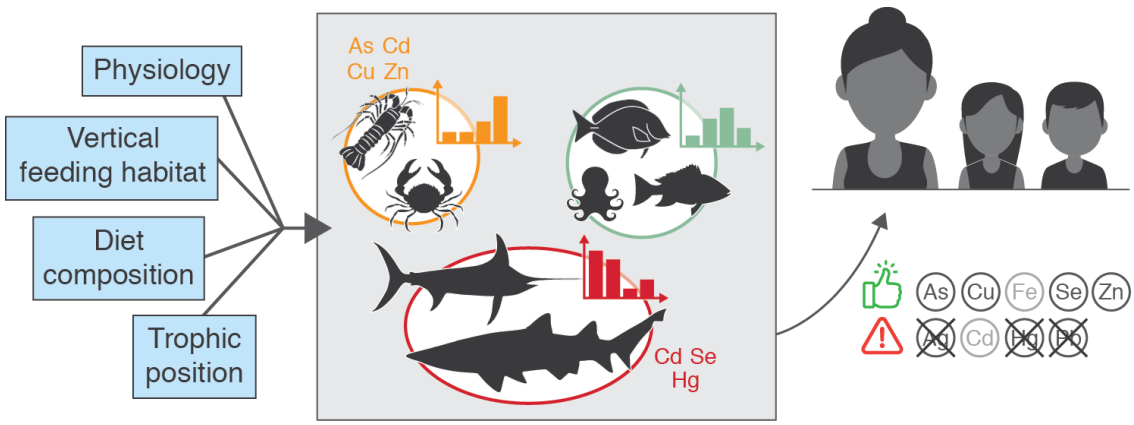

Abstract

Due to its high content in some essential and potentially essential trace elements, seafood is critical in promoting healthy human diets, but it can also contain non-essential trace elements that can potentially harm consumers. Studying trace element concentrations in seafood is thus of utmost interest for policy-makers, especially in Small Island Developing States with seafood-based diets, like the Seychelles. In this study, we measured the concentrations of 13 trace elements in the edible parts of 54 capture fisheries species from Seychelles coastal and offshore waters to provide baseline information and examine factors that influence differences in concentrations among species. Both taxonomy-dependent processes (i.e. metabolic requirements, regulation processes) and ecological factors (i.e. vertical feeding habitat, feeding, and trophic guild) affected interspecific differences in trace element concentrations among capture fisheries species. A benefit-risk assessment showed that the capture fisheries species analysed were good sources of As, Cu, Se and Zn for children, young adult and adult women's diets (at least 10% of daily needs covered by one portion). Crustacean species were found to be high in As, Cu and Zn (i.e. > 30 $\mu g.g^{-1}$ ww, > 8 $\mu g.g^{-1}$ ww, and > 20 $\mu g.g^{-1}$ ww, respectively). Although there was a degree of risk of excess of Se in children's diet identified, there was low risk related to exposure to Ag, Cd, Hg and Pb, with only two species (i.e. spanner crab and pink ear emperor) with a risk regarding Cd. Here, we thus provide important baseline information on micronutrient supply and contaminant exposure for an SIDS community, the Seychelles, and is a foundation stone in supplying nutritional information to SIDS governments for the development of guidelines on seafood consumption for their populations.

Keywords: Micronutrient; Metals; Bioaccumulation; Marine resources; Nutritional health assessment; Food security

1. Introduction

Globally, seafood consumption has long been known to play an important role in a healthy and balanced diet, as it provides numerous essential macro- and micronutrients in human diets (Larsen *et al.* 2011; Weichselbaum *et al.* 2013). Whilst much attention has been given to seafood regarding its content in essential fatty acids like long chain omega-3, seafood can also provide important levels of essential trace elements such as copper (Cu), iron (Fe), selenium (Se) and zinc (Zn) (Weichselbaum *et al*. 2013), which are co-factors of many proteins and enzymes (Koolman and Röhm 2011). For instance, fish is a good source of heme Fe, which is more readily absorbed than other forms of Fe and has a role in the transport of oxygen as part of haemoglobin (Ohio State University 2015), as well as a good source of Se, a component of important antioxidant enzymes (Weichselbaum *et al.* 2013). Selenoproteins are also known to have a protective effect against mercury (Hg), due their binding affinity with each other (Ralston *et al*. 2008). As a consequence of their high micronutrient content, seafood consumption is thought to be critical in promoting food security and healthy diets (Béné *et al.* 2015), and it could have the largest impact of all foods in the fight against micronutrient deficiency (Hicks *et al*. 2019).

Although the most common essential trace elements-related nutritional problems are associated with low intakes and thus mineral deficiency, problems can also arise from too high intakes resulting in trace element toxicity (Goldhaber 2003). Indeed, the essentiality of a trace element for human metabolism depends on the dose, with some essential trace elements having narrow concentration ranges for which they are neither in deficiency or in excess (e.g. Se) (Preda *et al.* 2016). In addition, seafood contains significant levels of non-essential trace elements, like cadmium (Cd), Hg and lead (Pb), which are toxic even at low concentrations and can thus have adverse effects on human health (Mudgal *et al*. 2010). Children and pregnant women are particularly susceptible to these effects, as pre- and postnatal exposure to non-essential trace elements like Hg can alter the nervous and cognitive development (Bosch *et al*. 2016). In order to better understand nutritional intakes, it is thus crucial to increase knowledge on essential and non-essential trace element contents in seafood.

Documenting the nutritional quality of seafood items, especially from capture fisheries, is all the more important in Small Island Developing States (SIDS) like the Seychelles (Western Indian Ocean). One of the particularities of SIDS is their high reliance on marine resources for local subsistence and for their economy, due to their small land size (i.e. limited terrestrial resources), insularity and remoteness (Briguglio 1995). As a consequence, capture fisheries resources are the main source of proteins and micronutrients for local populations of SIDS (Hicks *et al*. 2019). As an example, Seychelles have one of the highest rate of marine fish consumption in the world (57 $kg.person^{-1}.year^{-1}$) (WorldBank 2017). In this country, trace element concentrations in pelagic species have been documented, showing that they were good sources of Fe, Se and Zn (Bodin *et al.* 2017). In addition, these fish were low in Cd, Hg and Pb

exposure risk due low concentrations of Cd and Pb and to the protective effect of Se against Hg (Bodin *et al*. 2017; Hollanda *et al.* 2017). However, there is a lack of data on the vast majority of species that are exploited, particularly in demersal and reef species which constitute a significant part of the seafood diet of SIDS population like Seychelles (Robinson *et al.* 2020).

Trace element concentrations in marine organisms depend on many physiological processes that can be species- (e.g. Bustamante *et al.* 1998; Metian *et al*. 2008), age- (e.g. Raimundo *et al*. 2013; Goutte *et al*. 2015) or size-dependent (e.g. Kojadinovic *et al*. 2007; Barone *et al*. 2013), and on many ecological factors such as habitat and diet (Chouvelon *et al*. 2012; Metian *et al.* 2013; Le Croizier *et al*. 2016). In a context of global change that can affect both the physiology and ecology of marine species (Beaugrand and Kirby 2018; Little *et al*. 2020), anthropogenic modifications of ecosystems could thus indirectly affect levels of essential and non-essential trace elements in marine species. To better understand the future nutrient supply and contaminant exposure through capture fisheries resources consumption in SIDS populations' diet, it is thus particularly helpful to understand the influence of physiological and ecological factors on trace element concentrations in capture fisheries species.

In this context, our study aims to better understand micronutrient delivery and contaminant exposure in Seychelles communities, that is assess the benefit and risk of consumption of the main capture fisheries species, and to identify species' taxonomic and ecological traits influencing these delivery and thus exposure to human consumers. The specific objectives were to (i) report on the concentrations of essential, potentially essential (i.e. trace elements that have been determined as essentials for some mammal species, but not yet for humans, *cf* review of Zoroddu *et al*. 2019) and non-essential trace elements in the edible part of 54 coastal and offshore species from the Seychelles, (ii) investigate the effects of taxonomy and trophic ecology (i.e. habitat type, feeding mode and trophic guild) on trace elements accumulation in those species and (iii) assess the benefits and risks related to capture fisheries resources consumption in human diets.

2. Material and methods

2.1. Sample collection and preparation

A total of 54 marine species, including one cephalopod, four crustaceans, seven elasmobranchs and 42 teleost fish, were collected from the Seychelles waters during 2013-2019 (Table S1). Nearshore species (n = 51) were caught on the Mahé Plateau, where most of the artisanal fishing grounds are located (Robinson *et al.* 2006), and offshore species (n = 3) were caught around the Mahé Plateau (Fig. 1). After their capture, all the organisms were measured (mantle and total lengths for octopus, cephalothorax length for crustaceans, lower jaw-fork length for swordfish, fork length and total length

for other fish species), weighted and dissected to sample a piece of dorsal muscle (around 2 g). Samples were then freeze-dried during 72 hr and ground to powder before trace element and stable isotope analyses.

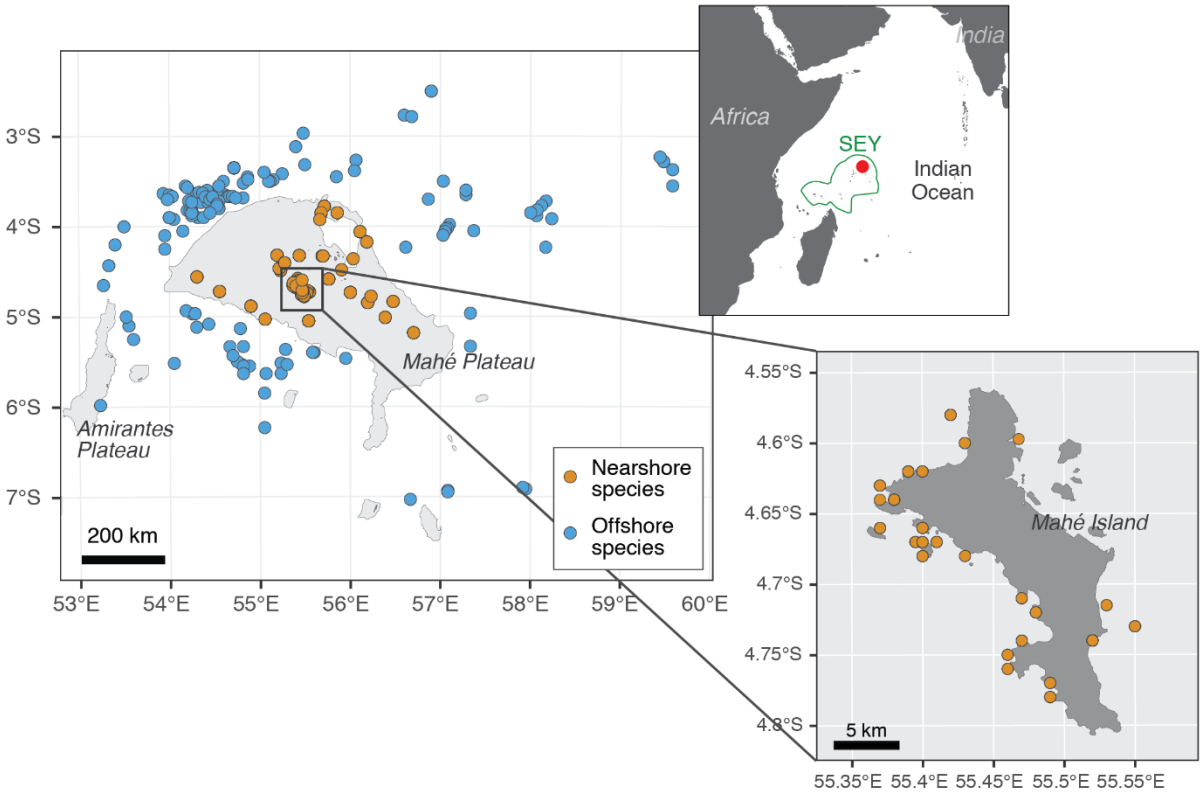

Fig. 1 Fishing locations of the 54 marine species on and around the Mahé Plateau, Seychelles (Western Indian Ocean). Red point indicates the location of the Mahé Plateau within the Seychelles economic exclusive zone. SEY = Seychelles.

2.2. Trace element analysis

A total of 1039 samples were analysed for the concentrations of six essential (i.e. cobalt – Co, Cu, Fe, manganese – Mn, Se, Zn) (reviewed in Zoroddu *et al.* 2019), three potentially essential (i.e. arsenic – As, chromium – Cr, nickel – Ni) (reviewed in Zoroddu *et al.* 2019) and four non-essential trace elements (i.e. silver – Ag, Cd, Hg, Pb) (reviewed in Bosch *et al.* 2016). Except for Hg, all trace elements were analysed by induced coupled plasma (ICP) at the LIENSs laboratory (France), using a Varian Vista-Pro ICP coupled with optical emission spectrometry and a ThermoFisherScientific XSeries 2 ICP coupled with mass spectrometry. Aliquots of 90-200 mg were microwave digested with 6 ml 67-70% of nitric acid and 2 ml 34-37% of hydrochloric acid. Seven control samples (five Certified Reference Materials, CRMs, and two blanks) treated and analysed in the same way as the samples were included in each analytical batch. CRMs were fish homogenate IAEA 407, tuna fish flesh homogenate IAEA 436, scallop (*Pecten maximus*) IAEA 452, marine tropical clam (*Gafrarium tumidum*) IAEA-461, dogfish liver DOLT-5 (National Research Council Canada) and lobster hepatopancreas TORT-3 (National Research Council

Canada). Mean recovery rates in CRMs ranged from 74 to 128%, and detection frequencies (i.e. number of data above limit of quantification, LOQ) in samples ranged from 10 to 100% (Table S2).

Hg was analysed in aliquots of 2-10 mg by atomic absorption spectrophotometer with a Direct Mercury Analyser (Milestone DMA 80) at the SFA facility (Seychelles) or an Advanced Mercury Analyser (Altec AMA 254) at the LIENSs laboratory (France). Hg determination involves progressive heating to 750 °C to burn the matrix and evaporate the metal which is further collected on a gold amalgamator. Hg is then liberated by heating at 950 °C, and measured by atomic absorption spectrophotometry. Hg concentrations were validated by the analysis of CRM DOLT-5 whose masses were adjusted to represent the same amount of Hg as the samples. CRMs were analysed every 10 samples, according to the same conditions as the samples. Blanks were also analysed at the beginning of each set of samples, and the LOQ was 0.1 ng.

2.3. Stable isotope analysis

A total of 1019 samples were analysed for stable isotopes of carbon ($\delta^{13}C$) and nitrogen ($\delta^{15}N$) at the LIENSs laboratory (France). Removal of lipids and urea before the C and N isotope analysis is recommended to avoid biased results due to lipids being more depleted in ^{13}C than other tissue components (Post *et al.* 2007) and to urea being more depleted in ^{15}N (Logan and Lutcavage 2008). In this study, spiny lobsters characterised by their low muscle fat content (mean of 0.74 ± 0.14% wet weight as reported in Sabino *et al.* 2021) were analysed directly for stable isotopes (raw $\delta^{13}C$ and $\delta^{15}N$ values), while $\delta^{13}C$ corresponded to lipid-normalised values for all other species and $\delta^{15}N$ corresponded to urea-normalised values for elasmobranch species.

Lipid-normalisation methods: Except for swordfish, lipids were chemically removed prior to stable isotope analysis. For each sample, between 10 and 12 mg of powdered sample was placed in a glass tube with 4 ml of cyclohexane. The tubes were then agitated during 10 minutes at room temperature and centrifuged during 5 minutes at 4500 rpm before removal of extraction solvent. Agitation, centrifugation and solvent-removal steps were repeated three times before putting tubes for drying in an oven at 45 °C overnight. For swordfish, known for their particularly high muscle fat content (26.2 ± 18.9% dw, Bodin *et al*. 2017), a mathematical lipid-correction was applied on $\delta^{13}C$ values. Indeed, lipid-removal in fatty tissues can affect $\delta^{15}N$ values due to contact with the extraction solvent during an extended period of time (Sotiropoulos *et al.* 2004; Murry *et al*. 2006). For this, we used the following equation: $\delta^{13}C_{corr} = [(D \times C{:}N_{bulk} + a) / (C{:}N_{bulk} + b)] + \delta^{13}C_{bulk}$, with $C{:}N_{bulk}$ and $\delta^{13}C_{bulk}$ the C:N ratio and $\delta^{13}C$ value measured in the sample (Logan *et al*. 2008), and with D = 7.05, a = -22.4 and b = -0.44. Model selection for mathematical correction and constant determination are described in Text S1.

Urea-removal: Urea was removed in muscle tissue samples from all analysed elasmobranch species using deionised water (Kim and Koch 2012; Li *et al*. 2016). For this, after lipid-removal, 1 ml of deionised water was added in each tube containing the samples, and tubes were then vortexed during 30 sec. Samples were left in deionised water for 24 h before centrifugation (5 min at 5000 rpm) and removal of rinsing water with a pipette. These steps were repeated three times before freeze-drying the samples during 24 h prior to stable isotope analysis.

Isotopic Ratio Mass Spectrometry analysis: Between 250 and 500 µg of sample was weighed in tin capsules. The samples were analysed by continuous flow on a Thermo Scientific Flash 2000 elemental analyser coupled to a Delta V Plus interface mass spectrometer. International isotopic standards of known $\delta^{13}C$ and $\delta^{15}N$ were used: USGS-61 and USGS-62. Results are expressed in the δ unit notation as deviations from standards (Vienna Pee Dee Belemnite for $\delta^{13}C$ and atmospheric nitrogen for $\delta^{15}N$) following the formula: $\delta^{13}C$ or $\delta^{15}N = [(Rsample/Rstandard) - 1] \times 1000$, where R is $^{13}C/^{12}C$ or $^{15}N/^{14}N$, respectively. Measurement errors (SD) of SI, calculated on all measured values of $\delta^{13}C$ and $\delta^{15}N$ in isotopic reference materials, were < 0.10 ‰ for both the nitrogen and carbon isotope measurements. This was in accordance with the analytical precision given by the manufacturer (i.e. < 0.10 ‰ for $\delta^{13}C$ and < 0.15 ‰ for $\delta^{15}N$; Thermo Scientific). For each sample, the C:N ratio was calculated, and never exceeded 3.5 proving that reserve lipids were adequately removed, or that there was no need of lipid removal or normalisation (Post *et al*. 2007).

2.4. Benefit-risk assessment

All trace element concentrations were converted from dry weight to wet weight (ww) by using the percentage of moisture determined during the preparation of the samples. When not available, a percentage of moisture of 75% was used (Table S1). To assess essential and potentially essential trace element supply, we calculated the contribution of one serving to recommended daily intakes (RDI); to assess the risk associated with too high intake of essential trace elements and with non-essential trace element exposure, we also calculated the number of servings necessary to reach provisional tolerable intakes (PTI) (Nielsen 1991; EC 2006, 2011; JECFA 2011, 2013; American Food and Nutrition Board of the Institute of Medicine National Academy of Sciences 2019a, b; US-EPA and US-FDA 2019) (Table S3). Three main age classes were chosen in order to represent the most vulnerable populations, either in terms of trace element deficiency or in terms of exposure, that is: children (2-13 year old), young adults (14-18 year old) and adult women (19+ year old, includes pregnant and lactating women). Guidelines given by the American Food and Nutrition Board of the Institute of Medicine National Academy of Sciences (2019a, b) are given for the following age classes and status: 2-3 year old, 4-8 year old, 9-13 year old, 14-18 year old, 19+ year old, pregnant women and lactating women. Thus, for both essential

and non-essential trace elements, calculations were made for each age subclass and were then summarised into the three corresponding main age classes defined above. In the case of potentially essential trace elements, RDI were only found for As and for adults, thus calculations were only made for this trace element for the "adult women" category; no PTI were found for all potentially essential trace elements. However, it is known that the main non-essential and toxic forms of As are inorganic As (iAs) (Sharma and Sohn 2009). Thus, the concentrations of iAs in analysed capture fisheries species were estimated by using the proportions of iAs in seafood calculated by Uneyama *et al*. (2007) (i.e. 4.4% in fish and 2.2% in crustaceans).

To take into account the interaction ability of Se with Hg in the benefit/risk assessment, we also calculated the molar ratio of Hg above Se (MHg:MSe) and the Health Benefit Value of Se (HBVSe) (Ralston *et al*. 2007, 2015). It is considered that Se and Hg bind in a molar ratio of 1:1 in human tissues (Ralston *et al*. 2007), thus we could also estimate the theoretical concentrations of bioavailable Se after interaction with Hg and the associated contribution to RDI and number of servings before reaching PTI. More details on all calculations used in the benefit-risk assessment are available in Text S2.

2.5. Assessment of the influence of intrinsic and extrinsic factors on trace element concentrations

We investigated the potential influence of a number of factors on trace element concentration patterns in capture fisheries species. For this, only trace elements for which the detection frequency was above 70% were selected and data < LOQ were substituted with values drawn randomly from the range]0;LOQ[(Carravieri *et al*. 2020). Then, species were grouped according to their trace element profiles by using hierarchical cluster analysis (Ward's clustering method) on their scaled mean trace element concentrations (Ward 1963; Murthagh and Legendre 2014). Trace element concentrations and stable isotope ($\delta^{13}C$ and $\delta^{15}N$) values were compared among determined groups by using Kruskal-Wallis followed by Dunn post-hoc tests. Finally, we looked at the composition of each group in terms of functional group, habitat type and feeding mode (Table S1). All data treatment were performed under R 3.5.2 software (R Core Team 2018).

3. Results

3.1. Essential, potentially essential and non-essential trace element concentrations

Trace element profiles in Seychelles capture fisheries species were dominated by As, Cu, Fe, Se and Zn (Table 1). Among essential and potentially essential trace elements, Mn and Ni concentrations were very low, with mean concentrations mostly below 0.1 $\mu g.g^{-1}$ ww for both trace elements. Among non-

essential trace elements, Ag concentrations were also very low, with concentrations mostly below 0.05 $\mu g.g^{-1}$ ww and often below LOQ (detection frequency of 10%, Table S2).

Table 1 Trace element concentrations (μg.g^{-1} ww) in the muscle of 54 capture fisheries species from the Seychelles. Data are presented as mean ± SD. N = Number of samples, LOQ = Limit of quantification.

		Essential						Potentially essential			Non-essential			
Species	**N**	**Co**	**Cu**	**Fe**	**Mn**	**Se**	**Zn**	**As**	**Cr**	**Ni**	**Ag**	**Cd**	**Hg**	**Pb**
Octopodidae														
Octopus cyaneus	13	0.003 ± 0.001	1.12 ± 0.35	1.9 ± 1.0	0.09 ± 0.02	0.27 ± 0.05	19.3 ± 2.5	26.1 ± 5.9	0.11 ± 0.06	0.03 ± 0.01	<LOQ	0.018 ± 0.011	0.013 ± 0.006	0.003 ± 0.001
Palinuridae														
Panulirus longipes	44	0.005 ± 0.002	9.93 ± 4.92	2.3 ± 1.1	0.08 ± 0.04	0.29 ± 0.14	28.1 ± 6.5	34.8 ± 14.5	0.13 ± 0.11	0.07 ± 0.06	0.019 ± 0.042	0.079 ± 0.173	0.034 ± 0.020	0.035 ± 0.111
Panulirus penicillatus	47	0.005 ± 0.002	10.37 ± 3.77	2.6 ± 2.0	0.10 ± 0.04	0.29 ± 0.10	32.8 ± 7.2	58.3 ± 18.1	0.12 ± 0.11	0.05 ± 0.04	0.016 ± 0.022	0.060 ± 0.086	0.034 ± 0.012	0.013 ± 0.017
Panulirus versicolor	15	0.005 ± 0.002	8.27 ± 3.05	2.8 ± 1.6	0.10 ± 0.03	0.27 ± 0.10	20.9 ± 5.2	35.6 ± 22.2	0.24 ± 0.26	0.11 ± 0.07	0.013 ± 0.019	0.071 ± 0.153	0.025 ± 0.038	0.008 ± 0.009
Raninidae														
Ranina ranina	5	0.009 ± 0.003	7.21 ± 3.29	1.0 ± 0.1	0.04 ± 0.01	0.55 ± 0.09	43.5 ± 4.2	50.5 ± 12.0	<LOQ	0.08 ± 0.03	0.039 ± 0.011	0.443 ± 0.235	0.032 ± 0.004	0.003 ± 0.001
Mullidae														
Parupeneus barberinus	3	0.004 ± 0.002	0.28 ± 0.04	2.6 ± 1.3	0.08 ± 0.03	0.46 ± 0.08	4.6 ± 0.7	9.3 ± 3.8	0.09 ± 0.02	0.06 ± 0.04	<LOQ	0.013 ± 0.006	0.019 ± 0.014	0.004 ± 0.001
Parupeneus rubescens	3	0.004 ± 0.001	0.37 ± 0.03	3.4 ± 1.2	0.13 ± 0.02	0.42 ± 0.07	3.4 ± 0.2	2.7 ± 0.1	0.22 ± 0.13	0.09 ± 0.04	<LOQ	0.010 ± 0.001	0.044 ± 0.029	0.004 ± 0.002
Scaridae														
Scarus ghobban	6	0.005 ± 0.002	0.42 ± 0.06	1.6 ± 0.3	0.11 ± 0.05	0.39 ± 0.16	4.0 ± 0.9	1.3 ± 1.0	0.05 ± 0.03	0.02 ± 0.01	<LOQ	0.007 ± 0.006	0.007 ± 0.004	0.007 ± 0.003
Siganidae														
Siganus sutor	8	0.047 ± 0.051	0.34 ± 0.09	2.9 ± 1.4	0.07 ± 0.03	0.24 ± 0.09	4.6 ± 1.7	0.2 ± 0.1	0.14 ± 0.09	0.28 ± 0.16	0.005	0.047 ± 0.058	0.003 ± 0.001	0.005 ± 0.001
Siganus argenteus	10	0.012 ± 0.007	0.52 ± 0.09	2.5 ± 0.6	0.10 ± 0.11	0.16 ± 0.05	3.5 ± 0.2	0.2 ± 0.1	<LOQ	0.02 ± 0.01	<LOQ	0.002 ± 0.001	0.002 ± 0.001	0.003
Acanthuridae														
Acanthurus mata	6	0.011 ± 0.008	0.38 ± 0.07	3.3 ± 1.4	0.05 ± 0.02	0.42 ± 0.17	4.9 ± 1.8	2.0 ± 2.4	0.11 ± 0.05	0.11 ± 0.12	<LOQ	0.017 ± 0.011	0.021 ± 0.008	0.004 ± 0.001
Carangidae														
Caranx sexfasciatus	8	0.004	0.53 ± 0.18	11.0 ± 6.1	0.05 ± 0.05	0.78 ± 0.49	8.6 ± 2.7	0.8 ± 0.5	0.43 ± 0.28	0.06 ± 0.07	<LOQ	0.028 ± 0.018	0.438 ± 0.236	0.018 ± 0.025
Caranx melampygus	6	0.008 ± 0.007	0.46 ± 0.15	5.3 ± 1.5	0.07 ± 0.02	0.44 ± 0.06	6.3 ± 1.2	0.3 ± 0.1	0.28 ± 0.12	0.10 ± 0.11	<LOQ	0.022 ± 0.026	0.311 ± 0.206	0.004 ± 0.001
Gnathanodon speciosus	7	0.006 ± 0.004	0.65 ± 0.39	6.9 ± 4.2	0.07 ± 0.02	0.39 ± 0.06	5.5 ± 1.3	0.8 ± 0.4	0.23 ± 0.23	0.10 ± 0.07	<LOQ	0.041 ± 0.020	0.135 ± 0.216	0.023 ± 0.018
Carangoides malabaricus	2	0.005 ± 0.001	0.46 ± 0.01	4.4 ± 1.0	0.05 ± 0.01	0.54 ± 0.01	6.0 ± 0.5	1.2 ± 0.1	0.13	0.11 ± 0.03	<LOQ	0.009 ± 0.001	0.510 ± 0.210	0.006 ± 0.002
Carangoides fulvoguttatus	33	0.011 ± 0.015	0.47 ± 0.13	5.5 ± 3.8	0.11 ± 0.03	0.58 ± 0.17	6.1 ± 1.7	0.8 ± 0.3	0.26 ± 0.19	0.13 ± 0.13	0.042 ± 0.054	0.009 ± 0.008	0.184 ± 0.239	0.005 ± 0.003
Carangoides gymnostethus	24	0.009 ± 0.008	0.63 ± 0.14	8.5 ± 2.7	0.08 ± 0.03	0.63 ± 0.16	6.9 ± 1.6	1.3 ± 0.5	0.39 ± 0.26	0.22 ± 0.15	<LOQ	0.044 ± 0.034	0.345 ± 0.361	0.004 ± 0.001

Lethrinidae														
Gymnocranius grandoculis	5	0.004 ± 0.001	0.40 ± 0.17	3.6 ± 1.6	0.03 ± 0.01	1.02 ± 0.22	5.2 ± 1.8	2.1 ± 0.5	0.24 ± 0.1.0	0.06 ± 0.06	<LOQ	0.023 ± 0.012	0.229 ± 0.061	0.004 ± 0.002
Lethrinus crocineus	13	0.007 ± 0.006	0.40 ± 0.09	5.2 ± 3.5	0.05 ± 0.03	1.05 ± 0.33	4.3 ± 1.1	2.3 ± 0.9	0.35 ± 0.32	0.13 ± 0.14	<LOQ	0.020 ± 0.014	0.215 ± 0.115	0.005 ± 0.004
Lethrinus microdon	10	0.004 ± 0.001	0.36 ± 0.04	3.3 ± 1.3	0.03 ± 0.01	0.48 ± 0.07	4.8 ± 0.7	1.2 ± 0.3	0.14 ± 0.10	0.05 ± 0.02	0.003	0.010 ± 0.009	0.215 ± 0.154	0.005 ± 0.001
Lethrinus nebulosus	11	0.009 ± 0.009	0.45 ± 0.13	6.1 ± 6.2	0.11 ± 0.09	0.58 ± 0.18	4.4 ± 0.8	1.1 ± 0.7	0.5 ± 0.42	0.05 ± 0.05	0.043 ± 0.029	0.008 ± 0.003	0.126 ± 0.062	0.026 ± 0.034
Lethrinus variegatus	18	0.004 ± 0.001	0.46 ± 0.11	3.6 ± 2.3	0.04 ± 0.01	0.66 ± 0.15	4.2 ± 1.1	2.7 ± 0.8	0.26 ± 0.24	0.06 ± 0.08	0.008 ± 0.005	0.015 ± 0.012	0.352 ± 0.150	0.006 ± 0.002
Lethrinus enigmaticus	2	0.002 ± 0.001	0.30 ± 0.07	2.6 ± 1.8	0.04 ± 0.01	1.75 ± 0.16	4.8 ± 0.3	1.6 ± 0.3	0.08 ± 0.01	0.13 ± 0.04	<LOQ	0.010 ± 0.003	0.136 ± 0.037	<LOQ
Lethrinus mahsena	20	0.004 ± 0.003	0.47 ± 0.13	3.6 ± 2.4	0.05 ± 0.05	0.76 ± 0.17	4.6 ± 1.4	5.0 ± 1.9	0.23 ± 0.21	0.09 ± 0.07	0.002	0.034 ± 0.038	0.314 ± 0.172	0.006 ± 0.003
Lethrinus lentjan	2	0.005 ± 0.001	0.59 ± 0.20	5.4 ± 3.6	0.15 ± 0.12	1.88 ± 0.60	4.8 ± 1.8	0.8 ± 0.3	0.25 ± 0.11	0.05 ± 0.03	<LOQ	0.158 ± 0.079	0.254 ± 0.105	0.003 ± 0.001
Lutjanidae														
Aprion virescens	107	0.005 ± 0.003	0.44 ± 0.12	3.5 ± 2.3	0.08 ± 0.04	0.62 ± 0.14	4.8 ± 1.4	2.1 ± 1.0	0.37 ± 0.35	0.08 ± 0.10	0.033 ± 0.022	0.014 ± 0.023	0.136 ± 0.127	0.014 ± 0.019
Etelis coruscans	10	<LOQ	0.37 ± 0.11	1.8 ± 0.5	0.04 ± 0.01	0.61 ± 0.07	3.8 ± 0.4	0.5 ± 0.2	0.06 ± 0.03	0.02 ± 0.01	<LOQ	0.007 ± 0.002	0.233 ± 0.133	0.009 ± 0.004
Lutjanus bohar	54	0.007 ± 0.009	0.40 ± 0.13	5.1 ± 3.6	0.05 ± 0.05	0.69 ± 0.14	4.5 ± 1.1	3.4 ± 1.7	0.47 ± 0.42	0.09 ± 0.12	0.030 ± 0.017	0.018 ± 0.028	0.295 ± 0.203	0.017 ± 0.021
Lutjanus gibbus	14	0.005 ± 0.001	0.61 ± 0.12	7.9 ± 5.3	0.05 ± 0.02	0.55 ± 0.09	5.6 ± 1.1	3.0 ± 2.3	0.45 ± 0.47	0.07 ± 0.05	<LOQ	0.039 ± 0.027	0.235 ± 0.110	0.006 ± 0.004
Lutjanus lutjanus	1	<LOQ	0.5	1.7	0.05	0.59	13.5	0.3	0.09	0.02	<LOQ	<LOQ	0.370	0.005
Lutjanus sebae	78	0.005 ± 0.006	0.30 ± 0.15	2.7 ± 1.8	0.05 ± 0.05	0.50 ± 0.11	4.8 ± 1.8	2.3 ± 1.1	0.23 ± 0.24	0.08 ± 0.09	0.007 ± 0.006	0.012 ± 0.014	0.157 ± 0.191	0.009 ± 0.007
Lutjanus sanguineus	5	0.01 ± 0.011	0.40 ± 0.09	6.1 ± 1.9	0.07 ± 0.05	0.76 ± 0.09	5.5 ± 1.6	5.7 ± 3.0	0.90 ± 0.63	0.42 ± 0.81	<LOQ	0.069 ± 0.059	0.278 ± 0.097	0.005 ± 0.002
Serranidae														
Cephalopholis argus	42	0.021 ± 0.024	0.34 ± 0.27	5.1 ± 3.3	0.06 ± 0.04	0.51 ± 0.26	5.7 ± 2.6	0.4 ± 0.4	0.21 ± 0.11	0.14 ± 0.17	0.007	0.012 ± 0.008	0.094 ± 0.067	0.014 ± 0.027
Cephalopholis sonnerati	14	0.007 ± 0.003	0.37 ± 0.18	3.3 ± 3.1	0.03 ± 0.02	0.53 ± 0.06	4.5 ± 2.5	0.7 ± 0.3	0.41 ± 0.37	0.06 ± 0.06	<LOQ	0.011 ± 0.007	0.141 ± 0.054	0.003 ± 0.001
Epinephelus fasciatus	3	<LOQ	0.34 ± 0.03	2.2 ± 0.5	0.05 ± 0.01	0.50 ± 0.12	4.6 ± 0.9	0.6 ± 0.1	0.06 ± 0.03	0.04 ± 0.02	<LOQ	0.006 ± 0.005	0.108 ± 0.011	0.003
Epinephelus merra	4	0.078 ± 0.089	0.20 ± 0.09	3.8 ± 1.8	0.06 ± 0.05	0.33 ± 0.16	4.5 ± 1.0	1.7 ± 1.2	0.13 ± 0.05	0.06 ± 0.01	<LOQ	0.029 ± 0.018	0.119 ± 0.037	0.005 ± 0.001
Epinephelus chlorostigma	74	0.006 ± 0.004	0.33 ± 0.11	3.0 ± 2.8	0.07 ± 0.04	0.56 ± 0.09	4.7 ± 1.5	0.5 ± 0.6	0.14 ± 0.11	0.05 ± 0.05	0.002 ± 0.001	0.009 ± 0.008	0.083 ± 0.067	0.035 ± 0.053
Epinephelus fuscoguttatus	2	0.005 ± 0.001	0.26 ± 0.03	3.1 ± 2.6	0.04 ± 0.01	0.53 ± 0.16	6.6 ± 2.8	6.1 ± 3.2	0.22 ± 0.23	0.05 ± 0.02	<LOQ	0.010	0.280 ± 0.017	0.003 ± 0.001
Epinephelus octofasciatus	4	0.004 ± 0.001	0.28 ± 0.08	4.1 ± 1.6	0.05 ± 0.01	0.53 ± 0.02	6.0 ± 1.4	1.1 ± 0.3	0.34 ± 0.20	0.03 ± 0.01	<LOQ	0.021 ± 0.011	0.216 ± 0.076	<LOQ
Epinephelus multinotatus	21	0.004 ± 0.001	0.36 ± 0.11	2.6 ± 1.6	0.06 ± 0.04	0.65 ± 0.16	5.4 ± 2.5	3.4 ± 3.2	0.34 ± 0.40	0.05 ± 0.04	0.063 ± 0.042	0.008 ± 0.005	0.256 ± 0.156	0.012 ± 0.008
Epinephelus longispinis	2	0.004 ± 0.001	0.41 ± 0.16	2.5 ± 0.2	0.05 ± 0.02	0.40 ± 0.03	5.5 ± 1.6	0.4 ± 0.1	0.10 ± 0.05	0.02	<LOQ	0.011 ± 0.001	0.161 ± 0.041	<LOQ
Variola louti	37	0.006 ± 0.004	0.34 ± 0.10	4.5 ± 3.4	0.06 ± 0.04	0.61 ± 0.07	5.3 ± 1.6	0.5 ± 0.3	0.47 ± 0.47	0.10 ± 0.08	<LOQ	0.005 ± 0.003	0.128 ± 0.088	0.021 ± 0.052

Sphyraenidae														
Sphyraena jello	26	0.005 ± 0.002	0.38 ± 0.21	4.8 ± 2.3	0.11 ± 0.09	0.49 ± 0.10	5.0 ± 1.4	1.0 ± 0.5	0.41 ± 0.23	0.05 ± 0.03	<LOQ	0.024 ± 0.045	0.254 ± 0.144	0.003 ± 0.001
Scombridae														
Gymnosarda unicolor	7	0.004 ± 0.001	0.49 ± 0.10	3.8 ± 2.3	0.07 ± 0.03	1.06 ± 0.62	6.4 ± 1.0	0.5 ± 0.2	0.17 ± 0.16	0.02 ± 0.01	<LOQ	0.018 ± 0.022	0.491 ± 0.360	0.003
Euthynnus alletteratus	5	0.007 ± 0.002	0.74 ± 0.27	13.1 ± 0.7	0.13 ± 0.05	0.54 ± 0.10	6.9 ± 1.1	1.3 ± 0.3	0.28 ± 0.16	0.07 ± 0.06	<LOQ	0.078 ± 0.040	0.218 ± 0.071	0.005 ± 0.002
Rastrelliger kanagurta	17	0.008 ± 0.005	0.69 ± 0.13	6.9 ± 1.5	0.07 ± 0.01	0.69 ± 0.16	7.5 ± 3.3	1.3 ± 0.9	0.10 ± 0.06	0.04 ± 0.02	<LOQ	0.025 ± 0.032	0.065 ± 0.041	0.005 ± 0.002
Carcharhinidae														
Carcharhinus amblyrhynchos	1	<LOQ	0.32	1.6	0.08	0.86	4.1	3.4	<LOQ	0.02	<LOQ	0.003	0.712	0.004
Carcharhinus brevipinna	1	<LOQ	0.34	1.1	0.10	0.4	3.6	5.9	0.03	0.01	<LOQ	<LOQ	0.232	0.004
Carcharhinus limbatus	1	<LOQ	0.38	4.1	0.13	1.15	8.1	1.6	0.15	0.03	<LOQ	0.003	0.513	0.004
Carcharhinus sorrah	1	<LOQ	0.19	<LOQ	0.11	0.51	4.7	7.2	0.08	<LOQ	<LOQ	<LOQ	0.093	<LOQ
Galeocerdo cuvier	1	0.004	0.44	2.4	0.09	0.41	6.5	3.2	0.04	0.02	<LOQ	<LOQ	0.673	0.006
Sphyrnidae														
Sphyrna mokarran	1	<LOQ	0.20	2.4	0.08	0.39	4.0	3.1	0.06	<LOQ	<LOQ	<LOQ	0.613	0.004
Sphyrna lewini	16	0.010 ± 0.009	0.35 ± 0.03	1.9 ± 0.6	0.19 ± 0.04	1.26 ± 0.46	5.3 ± 2.1	5.6 ± 2.1	0.06 ± 0.02	0.02 ± 0.01	<LOQ	0.003 ± 0.001	0.534 ± 0.185	0.005 ± 0.004
Xiphiidae														
Xiphias gladius	131	0.005 ± 0.002	0.43 ± 0.34	3.8 ± 3.7	0.04 ± 0.03	0.74 ± 0.28	9.1 ± 4.6	0.7 ± 0.3	0.16 ± 0.16	0.03 ± 0.03	0.003 ± 0.001	0.055 ± 0.040	0.734 ± 0.440	0.045 ± 0.097

3

3.2. Clustering on capture fisheries species trace element profiles and composition of inferred groups

Four groups were inferred by the hierarchical cluster analysis of mean trace element concentrations in Seychelles capture fisheries species (Fig. 2A). Among all groups, group 1 and group 3 had the highest mean concentrations of Cd (Dunn test, $p < 0.001$) and group 1 and group 4 had the highest mean Ni concentrations (Dunn test, $p = 0.001$ between groups 1 and 2, $p < 0.001$ for all other comparisons) (Fig. 2B, C). Groups 2 and 3 had the lowest mean Cu concentrations (Dunn test, $p < 0.001$). Group 1 also had the highest mean As, Cu, Mn and Zn concentrations (Dunn test, all $p < 0.001$), and the lowest mean Hg, Fe and Se concentrations (Dunn test, all $p < 0.001$). Group 3 also had the highest mean Hg and Se concentrations (Dunn test, both $p < 0.001$) while having the lowest mean Ni and Mn concentrations (Dunn test, both $p < 0.001$). Group 4 also had the highest mean Fe concentration (Dunn test, $p < 0.001$). Finally, group 2 also had the lowest mean Cd (Dunn test, $p < 0.001$) and mean Zn (Dunn test, $p = 0.001$ with group 2, $p < 0.001$ with all other groups) concentrations.

Group 1 was composed only of benthic crustaceans (Fig. 3). Groups 2 and 4 were mainly composed of demersal teleost fish (but group 2 includes the octopus), and group 3 was composed only of pelagic species, including pelagic-neritic and pelagic-oceanic elasmobranch, and teleost fish species. There was no clear clustering among species' habitat type or feeding mode. Indeed, for most habitat types and feeding modes, a given type or mode could be found in at least two groups.

Group 1 had a higher mean $\delta^{13}C$ value than the three other groups (Dunn test, $p < 0.001$) (Fig. 4). Group 3 had the highest mean $\delta^{15}N$ value (Dunn test, $p < 0.001$), while group 1 had the lowest mean $\delta^{15}N$ value (Dunn test, $p < 0.001$) (Fig. 4).

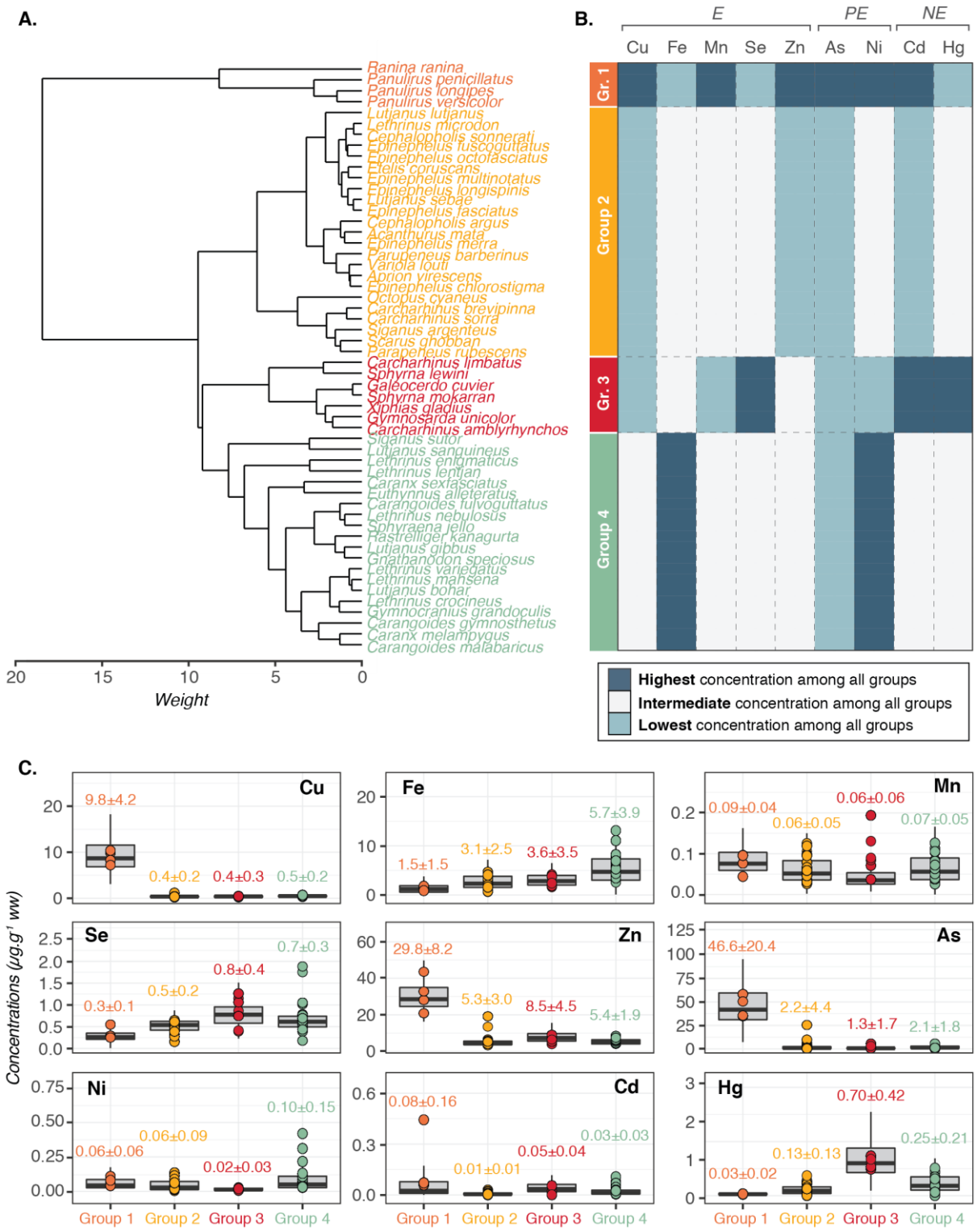

Fig. 2 Groups inferred from cluster analysis of mean trace element concentrations in capture fisheries species from the Seychelles (A), and their trace element profiles (B) and concentrations (C) in each group. Points represent the mean concentration for each species in the group, and the mean concentration in each group (mean ± SD) is indicated above each boxplot in the corresponding colour (C). E = essential, PE = potentially essential, NE = non-essential.

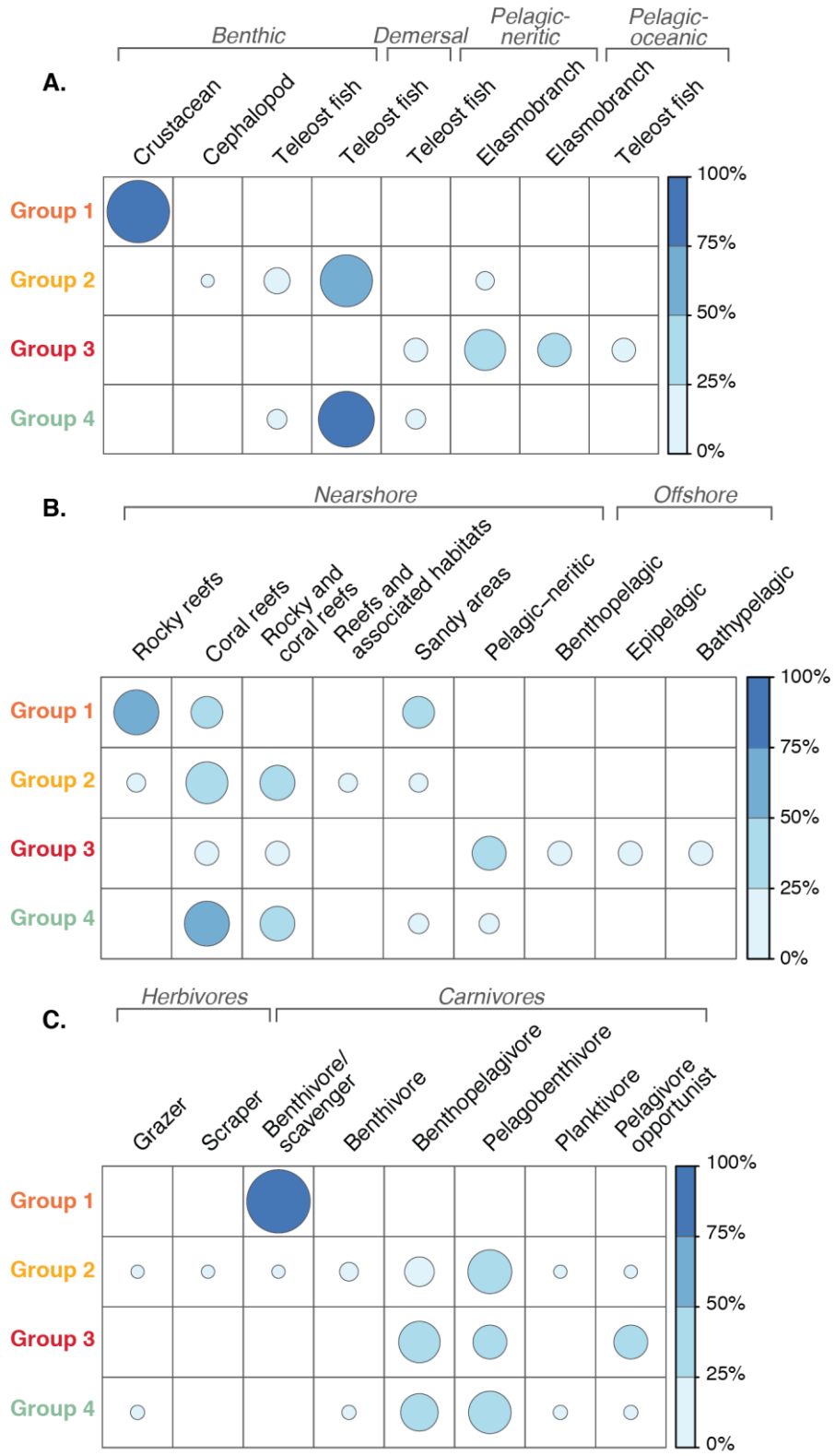

Fig. 3 Compositions of groups inferred from mean trace element concentrations in Seychelles capture fisheries species in terms of functional group (A), habitat type (B) and feeding mode (C). Circles' colour intensity and size are proportional to the percentage of each functional group, habitat type or feeding mode in each trace element profile group.

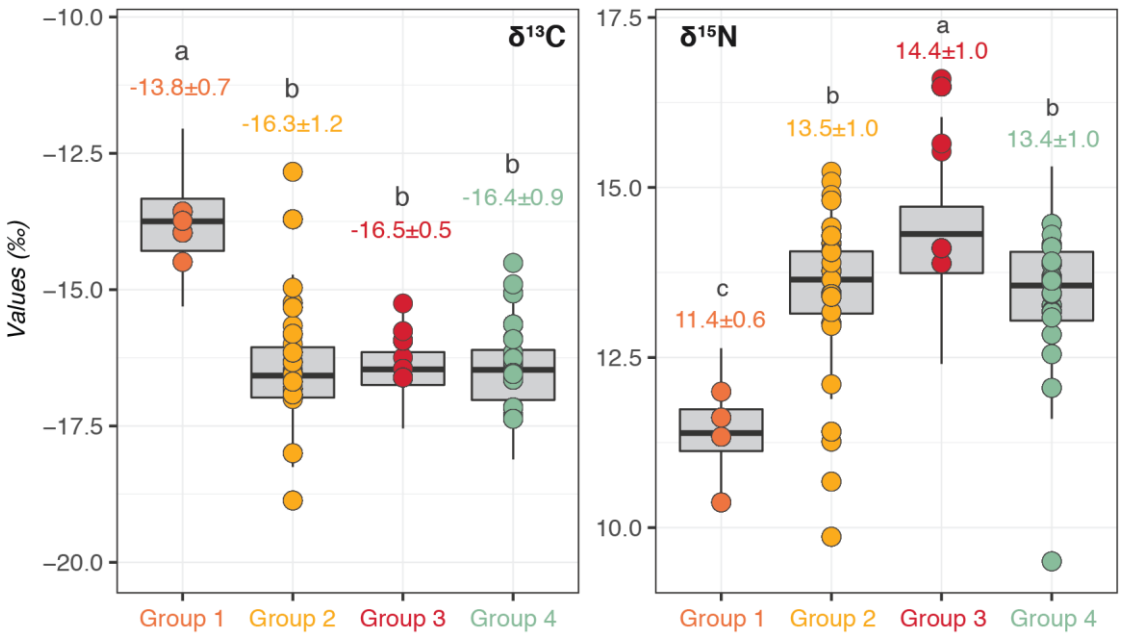

Fig. 4 $\delta^{13}C$ and $\delta^{15}N$ values (‰) measured in the muscle of Seychelles capture fisheries species in each group determined from trace element profiles. Points represent the mean value for each species present in the group, and the mean value in each group (mean ± SD) is indicated above each boxplot in the corresponding colour. A different letter indicates a significant difference between groups.

3.3. Contribution to recommended daily intakes and number of servings before reaching provisional recommended intakes

For all species, one portion provided more than 20% of the Se daily RDI for all age classes, but generally less than 10% of Fe daily needs and less than 1% of Mn daily needs (Table 2A). However, for 11 species (i.e. *Caranx sexfasciatus*, *Gnathanodon speciosus*, *Carangoides fulvoguttatus*, *Carangoides gymnostethus*, *Lethrinus crocineus*, *Lethrinus nebulosus*, *Lethrinus lentjan*, *Lutjanus gibbus*, *Lutjanus sanguineus*, *Euthynnus alletteratus* and *Rastrelliger kanagurta*), a portion could deliver more than 10% of Fe daily RDI for one or more age classes, and especially for children. For nine species (i.e. *Parupeneus rubescens*, *Scarus ghobban*, *Siganus argenteus*, *Lethrinus nebulosus*, *Lethrinus lentjan*, *Sphyraena jello*, *Euthynnus alletteratus*, *Carcharhinus limbatus* and *Sphyrna lewini*), a portion provided more than 1% of Mn daily RDI one or more age classes. Crustacean species (i.e. Paniluridae and Raninidae) provided at least 30% of Cu daily RDI for children and more than 50% of Cu young adult and adult women daily RDI, and Octopodidae delivered more than 10%. Those species, along with *Lutjanus lutjanus*, also provided more than 15% of Zn daily RDI for all three age classes. All other species globally provided less than 10% of Cu daily RDI and of Zn daily RDI. A portion of all species also contributed to more than 100% of adult women As RDI.

For almost all species, the daily numbers of servings before reaching Cu, Fe, Mn and Zn PTI were high (i.e. five servings or above) for all age classes (Table 2B). For Cu and Zn, the minimum number of

servings before reaching PTI was between 3 and 4 for children and for four species only (i.e. *Panulirus longipes*, *Panulirus penicillatus* and *Panulirus versicolor* for Cu; *Ranina ranina* for both Cu and Zn). For Fe, the minimum number of servings before reaching PTI was between 3 and 4 for all three age classes but for two species only (i.e. *Lethrinus enigmaticus* and *Epinephelus fuscoguttatus*). For Se, the minimum daily number of servings before reaching PTI was often below 5 for one or more age classes (i.e. 38 among the 54 analysed species). The monthly number of servings before reaching Cd PTI was high for most species. However, the minimum number of servings before reaching monthly PTI was below 10 for *Gnathanodon speciosus* and it was even below 5 for *Ranina ranina*, *Lethrinus lentjan* and *Euthynnus alletteratus*. For most species, the weekly number of servings before reaching Hg PTI was relatively low (i.e. below 5).

Except for *Octopus cyaneus*, *Panulirus penicillatus* and *Ranina ranina* for which the estimated iAs concentrations were between 1.0 and 1.3 $\mu g.g^{-1}$ ww, all species contained less than 1 $\mu g.g^{-1}$ ww of iAs in their tissues (Table 2B).

In all species, the MHg:MSe ratio was below 1 and the HBV_{Se} was above 0 (Table 3). When considering the interaction of Hg with Se, the contribution of one portion to human daily needs was still high for all species (> 20%) (Table 3). For children, the minimum number of servings before reaching Se daily PTI was still very low (≤ 3 servings) for 18 species (i.e. *Ranina ranina*, two Carangidae species, most Lethrinidae species, *Lutjanus sanguineus*, three Serranidae species, two Scombridae species, *Carcharhinus limbatus* and *Sphyrna lewini*) (Table 3). For young adults and adult women, the minimum number of servings before reaching Se daily PTI was also still low (< 5 servings) for two species (i.e. *Carcharhinus amblyrhynchos* and *Carcharhinus limbatus*).

Table 2 Benefit (A) and risk (B) assessment for consumption of Seychelles capture fisheries species. Contribution to human recommended daily intakes (RDI) (A) and number of servings to reach human provisional tolerable intakes (PTI) (B) are presented as minimum (mean – SD for contribution, mean + SD for number of servings) and maximum (mean + SD for contribution, mean – SD for number of servings). Estimated concentrations of inorganic As (iAs) are presented as mean ± SD (B). C = Children, YA = Young adults, A = Adult women, including lactating and pregnant women.

A.

	Essential														Potentially essential
	Cu			Fe			Mn			Se		Zn			As
Species	C	YA	A	C	YA	A	C	YA	A	C	YA & A	C	YA	A	A
Octopodidae															
Octopus cyaneus	8-21	17-23	15-22	1-3	2-3	1-3	0.2-0.6	0.6-0.7	0.6-0.9	37-83	55-83	18-30	26-29	24-29	30317-37598
Palinuridae															
Panulirus longipes	75-186	149-199	132-197	1-4	2-3	1-3	0.2-0.5	0.5-0.6	0.5-0.8	38-95	56-94	26-43	37-43	34-43	39707-50811
Panulirus penicillatus	82-187	163-201	145-198	1-4	2-3	1-3	0.2-0.6	0.6-0.8	0.7-0.9	39-92	58-91	31-50	44-49	40-50	69041-82529
Panulirus versicolor	59-161	118-172	105-170	1-5	2-4	1-4	0.2-0.7	0.6-0.8	0.6-1.0	33-91	49-90	18-34	26-33	24-33	31635-60801
Raninidae															
Ranina ranina	38-165	76-177	67-175	0-2	1-1	1-1	0.1-0.3	0.3-0.4	0.3-0.4	71-179	105-178	40-68	56-67	52-67	52019-79262
Mullidae															
Parupeneus barberinus	2-5	4-6	4-6	1-5	2-4	0-4	0.1-0.6	0.3-0.7	0.4-0.9	59-153	88-152	4-8	6-7	5-7	7768-16353
Parupeneus rubescens	3-7	6-7	5-7	1-7	2-5	0-5	0.3-0.9	0.7-1.1	0.8-1.3	51-142	76-141	3-5	5-5	4-5	3308-3692
Scaridae															
Scarus ghobban	3-8	7-8	6-8	1-3	1-2	1-2	0.2-0.9	0.6-1.0	0.6-1.3	43-139	64-138	3-7	5-7	5-7	959-2538
Siganidae															
Siganus sutor	3-7	5-7	4-7	1-5	2-4	1-4	0.1-0.5	0.4-0.6	0.4-0.8	28-85	42-85	3-8	5-8	5-8	220-323
Siganus argenteus	4-9	8-10	7-10	1-4	2-3	1-3	0.1-1.0	0.2-1.2	0.2-1.4	20-56	29-55	3-5	5-5	4-5	289-351
Acanthuridae															
Acanthurus mata	3-7	6-8	5-7	1-6	2-5	1-5	0.1-0.4	0.2-0.5	0.2-0.6	42-158	62-157	3-9	5-9	5-9	110-5038
Carangidae															
Caranx sexfasciatus	4-11	7-11	6-11	3-22	7-16	2-17	0.0-0.5	0.1-0.6	0.1-0.7	67-320	99-318	7-15	9-15	9-15	587-1500
Caranx melampygus	3-9	6-10	6-10	2-9	4-7	2-6	0.1-0.5	0.4-0.6	0.4-0.7	60-138	89-137	6-10	8-10	7-10	337-457
Gnathanodon speciosus	3-15	6-17	6-16	2-14	4-10	1-11	0.1-0.5	0.4-0.6	0.4-0.7	51-125	76-124	5-9	6-9	6-9	564-1426
Carangoides malabaricus	4-8	8-8	7-8	1-8	3-6	1-6	0.1-0.4	0.3-0.4	0.3-0.5	79-156	118-155	5-10	7-10	7-10	1356-1671
Carangoides fulvoguttatus	4-8	8-9	7-9	2-10	4-7	2-7	0.2-0.7	0.7-0.8	0.8-1.0	78-180	116-179	6-10	8-9	7-9	877-1153
Carangoides gymnostethus	5-11	10-12	9-12	3-14	8-10	4-9	0.2-0.6	0.5-0.7	0.5-0.8	86-198	128-197	6-11	9-11	8-11	1469-2027
Lethrinidae															
Gymnocranius grandoculis	2-9	4-10	4-9	1-7	2-5	1-6	0.1-0.2	0.2-0.2	0.2-0.3	124-345	184-343	4-10	5-10	5-10	2102-3334
Lethrinus crocineus	3-7	6-8	5-8	1-10	3-7	1-8	0.1-0.4	0.2-0.5	0.3-0.6	131-351	195-349	4-7	5-7	5-7	2337-3590
Lethrinus microdon	3-6	6-7	5-7	1-6	3-4	1-4	0.1-0.2	0.2-0.2	0.2-0.3	66-150	99-150	4-8	6-7	6-7	1288-1795

Lethrinus nebulosus	3-9	7-9	6-9	1-13	3-10	0-11	0.2-0.9	0.5-1.1	0.5-1.4	73-193	108-193	4-7	6-7	5-7	943-1858
Lethrinus variegatus	4-8	7-9	6-9	1-7	3-5	1-5	0.1-0.3	0.2-0.3	0.2-0.4	88-207	131-206	4-7	5-7	5-7	2986-3936
Lethrinus enigmaticus	2-6	4-7	3-7	0-7	0-5	-2-7	0.1-0.3	0.3-0.3	0.3-0.4	230-562	342-559	4-8	6-7	6-8	1582-2696
Lethrinus mahsena	4-9	7-9	6-9	1-7	3-5	1-5	0.1-0.4	0.2-0.5	0.2-0.6	103-238	154-237	4-7	6-7	5-7	5396-7549
Lethrinus lentjan	3-13	6-14	6-14	1-14	1-10	1-12	0.0-1.7	0.1-2.0	0.1-2.4	180-731	268-727	3-10	4-10	4-10	606-1554
Lutjanidae															
Aprion virescens	4-8	7-8	6-8	1-6	3-4	2-4	0.2-0.5	0.5-0.6	0.6-0.7	88-183	131-182	4-7	6-7	6-7	2425-2910
Etelis coruscans	3-7	5-8	5-8	1-3	1-2	1-2	0.1-0.3	0.2-0.3	0.2-0.4	85-185	126-184	4-6	5-6	5-6	567-817
Lutjanus bohar	3-7	6-8	6-8	2-9	4-6	2-6	0.1-0.4	0.3-0.5	0.3-0.6	97-206	145-205	4-7	6-7	6-7	3902-5046
Lutjanus gibbus	5-11	10-12	9-12	2-15	5-11	2-11	0.1-0.4	0.3-0.4	0.3-0.5	75-170	112-169	5-9	7-9	7-9	2513-5384
Lutjanus lutjanus	4-8	9	6-9	1-2	2	1-3	0.1-0.3	0.3	0.3-0.4	88-168	131-167	14-19	19	18-19	438
Lutjanus sebae	2-5	5-6	4-6	1-4	2-3	1-3	0.1-0.3	0.2-0.4	0.3-0.5	72-150	107-150	4-7	6-7	6-7	2691-3331
Lutjanus sanguineus	3-8	6-9	5-8	2-11	5-8	2-8	0.1-0.7	0.2-0.8	0.2-1.0	102-241	152-239	4-10	6-10	5-10	4011-10871
Serranidae															
Cephalopholis argus	2-7	4-7	4-7	2-9	4-6	2-6	0.1-0.5	0.4-0.5	0.4-0.7	65-168	97-167	5-9	7-9	6-9	388-712
Cephalopholis sonnerati	2-8	5-8	4-8	1-7	2-5	0-6	0.0-0.2	0.1-0.2	0.1-0.3	75-161	111-160	3-8	4-8	4-8	685-1158
Epinephelus fasciatus	3-6	5-7	5-6	1-4	2-3	1-3	0.1-0.3	0.3-0.4	0.3-0.4	55-180	81-179	4-8	5-8	5-8	652-789
Epinephelus merra	1-5	2-5	2-5	1-8	2-6	0-6	0.0-0.7	0.1-0.8	0.1-1.0	26-138	39-137	4-8	5-8	5-8	680-3764
Epinephelus chlorostigma	3-6	5-6	5-6	1-5	2-4	1-4	0.1-0.4	0.4-0.5	0.5-0.6	81-166	120-165	4-7	6-7	6-7	427-801
Epinephelus fuscoguttatus	2-5	4-5	3-5	0-10	0-7	0-9	0.1-0.2	0.2-0.3	0.3-0.4	47-212	70-211	3-15	4-15	4-15	2166-13732
Epinephelus octofasciatus	2-6	4-6	3-6	1-8	3-6	1-6	0.1-0.3	0.3-0.4	0.3-0.4	76-156	113-156	5-11	6-10	6-11	1036-1754
Epinephelus multinotatus	3-7	6-7	5-7	1-5	2-3	1-3	0.1-0.4	0.3-0.5	0.3-0.6	88-204	130-203	4-9	6-9	6-9	2729-6234
Epinephelus longispinis	2-10	3-11	3-11	1-4	2-3	1-3	0.1-0.5	0.2-0.6	0.2-0.7	53-125	79-125	3-11	5-11	4-11	489-499
Variola louti	3-6	5-7	5-6	1-8	4-6	2-6	0.1-0.4	0.3-0.5	0.4-0.6	89-181	132-180	5-8	7-8	6-8	468-737
Sphyraenidae															
Sphyraena jello	3-8	5-8	5-8	2-8	4-6	2-6	0.2-0.9	0.6-1.0	0.6-1.3	67-149	100-149	4-8	6-8	6-8	1127-1580
Scombridae															
Gymnosarda unicolor	4-9	7-10	7-10	1-8	2-6	0-6	0.1-0.6	0.3-0.7	0.4-0.8	91-432	135-430	6-10	8-10	7-10	530-894
Euthynnus alletteratus	4-16	9-17	8-17	5-20	13-14	7-12	0.2-1.0	0.6-1.2	0.7-1.4	68-178	102-177	6-11	9-11	8-11	1384-2072
Rastrelliger kanagurta	5-12	11-13	10-13	3-11	6-8	4-7	0.2-0.5	0.5-0.6	0.5-0.7	93-219	138-218	6-13	8-13	8-13	1113-2257
Carcharhinidae															
Carcharhinus amblyrhynchos	3-5	6	4-6	1-2	2	1-3	0.2-0.5	0.6	0.5-0.7	130-246	192-245	4-6	6	5-6	4376
Carcharhinus brevipinna	3-6	6	4-6	0-2	1	1-2	0.2-0.6	0.7	0.6-0.9	60-114	89-114	4-5	5	5-5	7733
Carcharhinus limbatus	3-6	7	5-7	2-6	4	2-7	0.3-0.8	0.9	0.8-1.1	172-328	256-326	8-12	11	11-12	2129
Carcharhinus sorrah	2-3	3	2-3	ND	ND	ND	0.3-0.6	0.7	0.6-0.9	77-146	114-145	5-7	7	6-7	9385
Galeocerdo cuvier	4-7	8	5-8	1-3	2	1-4	0.2-0.5	0.6	0.5-0.8	62-118	92-118	7-9	9	8-9	4108
Sphyrnidae															
Sphyrna mokarran	2-3	3	2-3	1-3	2	1-4	0.2-0.5	0.6	0.5-0.7	59-111	87-111	4-6	6	5-6	4044

Sphyrna lewini	3-6	6-6	5-6	1-3	2-2	1-2	0.4-1.3	1.2-1.5	1.4-1.9	155-425	231-423	4-9	6-9	6-9	6010-8636					
Xiphiidae																				
Xiphias gladius	3-8	7-9	6-8	1-6	3-5	2-4	0.1-0.3	0.2-0.3	0.2-0.4	104-226	155-225	8-14	12-14	11-14	891-1036					

B.

	Essential														Non-essential						
	Cu			Fe			Mn			Se		Zn			Cd			Hg			iAs
Species	**C**	**YA**	**A**	**C**	**YA**	**A**	**C**	**YA**	**A**	**C**	**YA & A**	**C**	**YA**	**A**	**C**	**YA**	**A**	**C**	**YA**	**A**	**(µg.g-1 ww)**
Octopodidae																					
Octopus cyaneus	28-50	42-58	53-73	174-956	143-207	143-207	419-853	581-738	710-902	7-13	9-11	8-13	11-12	13-14	14-34	16-28	21-38	13-26	14-21	19-29	1.10 ± 0.25
Palinuridae																					
Panulirus longipes	4-6	5-7	7-9	161-763	132-165	132-165	574-1112	794-962	971-1176	7-13	9-11	6-9	8-9	9-10	10-25	11-21	15-29	6-10	6-8	8-11	0.77 ± 0.32
Panulirus penicillatus	3-5	5-6	6-8	159-766	131-166	131-166	443-895	614-774	750-946	7-12	9-11	5-8	7-7	8-9	13-33	14-27	19-37	5-9	6-7	8-9	1.28 ± 0.40
Panulirus versicolor	4-8	6-9	7-11	124-853	102-184	102-184	407-881	564-762	689-932	7-15	9-13	8-13	10-12	12-14	14-57	15-47	20-64	10-22	11-18	15-24	0.78 ± 0.49
Raninidae																					
Ranina ranina	3-11	5-12	6-16	331-1415	272-306	272-306	807-1839	1118-1591	1366-1945	3-6	4-5	4-6	5-5	5-6	0-4	0-3	0-4	5-8	5-7	7-9	1.11 ± 0.26
Mullidae																					
Parupeneus barberinus	101-183	156-213	195-267	110-761	90-165	90-165	442-1216	611-1052	747-1286	4-8	5-6	32-57	42-54	50-63	13-44	15-36	20-49	4-38	4-31	6-41	0.39 ± 0.16
Parupeneus rubescens	82-128	127-150	158-187	60-648	50-140	50-140	278-639	385-553	471-676	4-9	5-7	46-73	60-68	71-80	21-37	23-31	31-42	1-13	1-11	1-15	0.11 ± 0.01
Scaridae																					
Scarus ghobban	73-115	112-134	140-167	196-1004	161-217	161-217	284-1097	394-949	481-1160	5-10	6-9	38-66	50-61	59-72	26-99	28-83	38-111	22-73	24-59	32-80	0.06 ± 0.04
Siganidae																					
Siganus sutor	86-158	132-185	164-232	106-673	87-146	87-146	553-1274	766-1102	936-1347	7-18	9-15	30-74	40-69	47-81	7-23	7-19	10-26	56-132	61-108	82-145	0.01 ± 0.01
Siganus argenteus	59-95	91-111	113-139	126-624	104-135	104-135	540-1630	748-1410	914-1724	11-24	14-20	46-69	60-65	71-76	103-144	112-120	151-161	77-120	84-98	113-132	0.01 ± 0.01
Acanthuridae																					

Acanthurus mata	76-141	117-165	146-206	85-577	70-125	70-125	711-1995	984-1727	1202-2110	3-12	4-11	29-62	38-58	45-68	11-43	12-36	16-49	3-25	4-21	5-28	0.08 ± 0.10
Carangidae																					
Caranx sexfasciatus	55-110	84-128	105-160	28-183	23-40	23-40	829-7492	1148-6483	1403-7924	2-7	3-6	16-38	21-35	25-42	8-26	8-21	11-29	0-1	0-1	0-1	0.03 ± 0.02
Caranx melampygus	63-126	97-147	121-184	58-317	48-69	48-69	532-1289	737-1115	901-1363	4-8	5-7	24-43	31-40	37-47	15-51	16-42	22-57	0-2	0-2	1-2	0.01 ± 0.01
Gnathanodon speciosus	40-137	62-160	77-200	32-479	26-104	26-104	528-1310	732-1133	894-1385	5-9	6-8	27-51	35-48	41-56	5-14	5-12	7-16	2-6	2-5	3-6	0.03 ± 0.02
Carangoides malabaricus	69-99	106-116	132-144	57-410	47-89	47-89	655-1623	906-1404	1108-1716	4-6	5-5	25-44	32-41	38-48	22-44	24-36	33-49	0-1	0-1	0-1	0.05 ± 0.01
Carangoides fulvoguttatus	69-113	106-132	132-165	71-354	58-77	58-77	385-735	534-636	652-777	4-6	4-5	27-45	35-42	41-49	39-73	42-61	57-82	2-4	2-3	3-4	0.03 ± 0.01
Carangoides gymnostethus	50-79	77-93	96-116	40-194	33-42	33-42	507-1145	702-991	858-1211	3-6	4-5	23-38	30-36	35-42	7-13	7-11	10-15	1-4	1-3	2-4	0.06 ± 0.02
Lethrinidae																					
Gymnocranius grandoculis	64-166	99-194	123-243	66-622	54-135	54-135	1406-3098	1946-2681	2379-3277	2-4	2-3	27-59	35-55	41-65	8-25	9-21	12-28	1-1	1-1	1-2	0.09 ± 0.02
Lethrinus crocineus	77-131	119-154	148-192	62-471	51-102	51-102	828-1931	1147-1671	1402-2042	2-4	2-3	36-64	47-60	55-71	11-35	12-29	17-40	1-2	1-1	1-2	0.10 ± 0.04
Lethrinus microdon	86-132	132-154	165-192	94-597	77-129	77-129	1210-2545	1676-2202	2048-2692	4-7	5-6	32-53	42-50	50-58	27-88	29-73	39-99	1-3	1-2	1-3	0.05 ± 0.01
Lethrinus nebulosus	67-122	103-143	129-179	67-432	55-94	55-94	381-922	527-798	645-975	3-7	4-6	35-60	46-56	54-66	28-63	30-53	41-71	1-5	1-4	2-5	0.05 ± 0.03
Lethrinus variegatus	67-116	103-135	129-169	101-586	83-127	83-127	1069-2148	1480-1858	1808-2271	3-5	4-5	38-64	50-60	59-70	20-46	21-38	29-52	0-2	0-1	0-2	0.11 ± 0.03
Lethrinus enigmaticus	78-197	119-231	149-289	4-1350	3-292	3-292	994-1798	1377-1556	1683-1902	1-2	1-2	31-52	41-49	48-58	14-54	16-45	21-61	1-2	1-2	1-3	0.07 ± 0.01
Lethrinus mahsena	68-111	104-130	131-162	104-598	86-129	86-129	924-2093	1280-1811	1564-2214	3-5	3-4	35-60	46-56	54-66	10-29	11-24	15-32	0-2	0-2	1-2	0.21 ± 0.08
Lethrinus lentjan	37-111	56-129	71-162	36-505	30-109	30-109	5-1594	5-1379	5-1686	1-2	1-2	24-71	32-67	37-78	1-4	1-3	1-4	0-2	0-1	1-2	0.03 ± 0.01
Lutjanidae																					
Aprion virescens	78-116	120-135	151-169	131-613	108-133	108-133	598-1149	828-994	1012-1215	3-5	4-5	36-55	47-51	55-60	31-51	34-43	46-58	2-5	3-4	3-5	0.09 ± 0.04
Etelis coruscans	69-178	107-208	133-260	176-954	145-206	145-206	1065-2421	1474-2095	1802-2561	3-5	4-5	42-67	54-63	64-74	33-63	37-53	49-71	1-2	1-1	1-2	0.02 ± 0.01
Lutjanus bohar	84-133	129-156	162-195	85-463	70-100	70-100	1028-2395	1424-2073	1740-2534	3-5	4-4	36-57	48-53	56-63	25-46	27-39	36-52	1-1	1-1	1-1	0.14 ± 0.07
Lutjanus gibbus	52-81	80-94	100-118	46-306	38-66	38-66	812-1796	1124-1555	1374-1900	4-6	4-5	28-48	37-44	43-52	6-22	7-18	9-24	1-2	1-1	1-2	0.13 ± 0.09
Lutjanus lutjanus	66-87	102	127	212-804	174	174	905-1448	1253	1531	4-5	4	12-17	16	19	ND	ND	ND	0-1	1	1	0.01

Lutjanus sebae	124-200	191-234	239-293	157-744	129-161	129-161	1259-2554	1743-2210	2131-2702	4-6	5-5	36-57	47-53	56-63	35-62	38-52	52-70	2-4	2-3	3-4	0.10 ± 0.05
Lutjanus sanguineus	70-135	107-157	134-197	47-290	38-63	38-63	469-1705	650-1476	794-1803	2-4	3-4	25-55	33-52	38-61	2-14	3-11	4-15	0-1	0-1	1-2	0.24 ± 0.13
Serranidae																					
Cephalopholis argus	126-230	195-269	243-336	79-414	65-90	65-90	728-1492	1008-1291	1232-1578	4-11	5-9	30-52	39-49	46-57	24-45	26-37	35-50	2-6	3-5	4-7	0.02 ± 0.02
Cephalopholis sonnerati	78-222	119-260	149-325	130-907	107-196	107-196	1518-3954	2102-3422	2569-4182	4-6	5-5	35-82	46-77	54-91	22-52	24-44	32-59	1-2	1-2	2-2	0.03 ± 0.01
Epinephelus fasciatus	89-140	137-163	172-204	115-858	95-186	95-186	804-1686	1114-1459	1361-1784	3-8	4-7	29-63	38-59	44-69	5-161	6-134	8-181	1-2	2-2	2-3	0.02 ± 0.01
Epinephelus merra	37-579	57-678	72-847	65-575	53-125	53-125	49-4189	67-3625	82-4431	1-26	1-22	31-65	40-60	47-71	5-24	5-20	7-27	1-3	1-2	2-3	0.07 ± 0.05
Epinephelus chlorostigma	105-160	162-187	202-234	160-764	132-165	132-165	685-1327	948-1148	1158-1404	4-6	5-5	36-58	47-55	56-64	46-80	50-67	68-90	3-5	3-4	4-6	0.02 ± 0.03
Epinephelus fuscoguttatus	112-198	172-232	215-290	3-1472	3-318	3-318	989-2041	1370-1766	1674-2158	2-8	3-7	12-61	15-57	18-67	25-33	27	36	1-1	1-1	1-1	0.26 ± 0.13
Epinephelus octofasciatus	88-216	135-253	169-316	64-482	53-104	53-104	835-1585	1156-1372	1412-1677	4-6	5-5	21-52	28-49	33-57	6-33	7-27	9-37	1-2	1-1	1-2	0.05 ± 0.01
Epinephelus multinotatus	85-160	130-187	163-234	142-774	117-168	117-168	796-2220	1103-1921	1348-2348	3-6	4-5	31-56	40-52	47-62	35-79	39-66	52-89	1-2	1-1	1-2	0.14 ± 0.14
Epinephelus longispinis	39-178	61-208	76-260	130-589	107-127	107-127	412-2066	570-1788	697-2186	5-8	6-7	19-63	25-59	29-70	23-32	25-27	34-36	1-2	1-2	1-2	0.02 ± 0.01
Variola louti	97-154	150-180	187-224	98-549	80-119	80-119	711-3416	985-2956	1204-3613	3-5	4-4	31-52	41-49	48-58	49-83	54-69	72-93	2-3	2-3	2-4	0.02 ± 0.01
Sphyraenidae																					
Sphyraena jello	93-184	143-215	179-269	73-441	60-95	60-95	428-1052	593-911	725-1113	4-7	5-6	32-55	42-51	49-60	27-63	30-52	40-70	1-2	1-1	1-2	0.04 ± 0.02
Scombridae																					
Gymnosarda unicolor	59-109	91-127	114-159	76-642	63-139	63-139	502-1315	695-1138	849-1390	2-5	2-4	23-42	31-39	36-46	16-61	17-51	23-68	0-1	0-1	0-1	0.02 ± 0.01
Euthynnus alletteratus	37-80	57-93	71-117	26-107	21-23	21-23	271-713	375-617	459-755	3-7	4-6	21-38	28-36	33-42	3-7	3-6	4-7	1-1	1-1	1-2	0.06 ± 0.01
Rastrelliger kanagurta	46-72	71-84	88-105	47-223	39-48	39-48	538-1048	744-907	910-1108	3-5	4-4	21-42	28-39	33-46	15-39	17-32	23-44	3-6	3-5	4-7	0.05 ± 0.04
Carcharhinidae																					
Carcharhinus amblyrhynchos	103-136	159	198	213-808	175	175	497-796	689	842	2-3	3	40-56	53	62	78-102	85	114	0-0	0	0	0.14
Carcharhinus brevipinna	98-129	151	189	324-1230	266	266	423-677	586	716	5-7	6	46-64	60	70	ND	ND	ND	1-1	1	1	0.25
Carcharhinus limbatus	87-114	134	167	85-323	70	70	319-510	442	540	2-3	2	21-29	27	32	88-115	96	129	0-0	0	1	0.07
Carcharhinus sorrah	172-226	264	330	ND	ND	ND	395-633	547	669	4-6	5	35-50	46	54	ND	ND	ND	2-3	2	3	0.30

Galeocerdo cuvier	75-99	115	144	146-556	120	120	465-744	644	787	5-7	6	26-36	33	39	ND	ND	ND	0-0	0	0	0.13
Sphyrnidae																					
Sphyrna mokarran	170-224	262	327	149-567	123	123	494-790	684	835	5-8	7	42-59	55	65	ND	ND	ND	0-0	0	0	0.13
Sphyrna lewini	92-131	142-153	177-191	175-873	144-189	144-189	198-407	274-352	335-430	2-3	2-3	30-53	40-50	47-58	89-139	97-116	131-156	0-1	0-0	0-1	0.24 ± 0.09
Xiphiidae																					
Xiphias gladius	105-174	162-203	202-254	118-536	97-116	97-116	1389-2665	1923-2306	2351-2819	3-5	4-4	20-32	26-30	31-35	6-10	7-9	9-12	0-1	0-0	0-1	0.03 ± 0.01

Table 3 Molar ratio of Hg above Se (MHg:MSe), health benefit value of Se (HBVSe) and estimated concentration of theoretically bioavailable Se after its interaction with Hg, and associated contribution to recommended daily intakes (RDI) and number of servings before reaching provisional intakes (PTI) for each Seychelles capture fisheries species. An MHg:MSe < 1 indicates a dominance of Se above Hg and an HBVSe > 1 indicates an Se benefit (Ralston et al. 2007, 2015). C = Children, YA = Young adults, A = Adult women, including lactating and pregnant women.

			Theoretically bioavailable Se				
	MHg:MSe	HBVSe	Estimated concentration ($\mu g.g^{-1}$ ww)	Contribution to RDI (%)		Number of servings to reach PTI	
Species				C	YA & A	C	YA & A
Octopodidae							
Octopus cyaneus	0.019 ± 0.008	$3.4x10^{-09} \pm 6.0x10^{-10}$	0.26 ± 0.05	36-81	54-81	7-13	68-81
Palinuridae							
Panulirus longipes	0.052 ± 0.035	$3.7x10^{-09} \pm 1.7x10^{-09}$	0.28 ± 0.14	36-91	53-90	8-14	67-90
Panulirus penicillatus	0.052 ± 0.030	$3.7x10^{-09} \pm 1.3x10^{-09}$	0.28 ± 0.11	37-88	55-88	8-13	70-88
Panulirus versicolor	0.045 ± 0.076	$3.4x10^{-09} \pm 1.3x10^{-09}$	0.26	31-88	46-88	8-16	58-88
Raninidae							
Ranina ranina	0.024 ± 0.004	$7.0x10^{-09} \pm 1.1x10^{-09}$	0.54 ± 0.09	69-175	102-174	3-7	130-174
Mullidae							
Parupeneus barberinus	0.020 ± 0.013	$5.9x10^{-09} \pm 1.0x10^{-09}$	0.46	57-150	85-150	4-8	108-150
Parupeneus rubescens	0.040 ± 0.024	$5.3x10^{-09} \pm 9.0x10^{-10}$	0.40 ± 0.06	50-135	74-134	4-9	94-134
Scaridae							
Scarus ghobban	0.006 ± 0.003	$5.4x10^{-09} \pm 2.5x10^{-09}$	0.43	46-156	68-156	4-10	87-156
Siganidae							
Siganus sutor	0.005 ± 0.002	$3.1x10^{-09} \pm 1.1x10^{-09}$	0.24	28-85	42-85	7-18	53-85
Siganus argenteus	0.006 ± 0.001	$2.1x10^{-09} \pm 6.0x10^{-10}$	0.16	20-55	29-55	11-24	37-55
Acanthuridae							
Acanthurus mata	0.020 ± 0.007	$5.3x10^{-09} \pm 2.2x10^{-09}$	0.41 ± 0.17	41-155	61-154	4-13	78-154
Carangidae							
Caranx sexfasciatus	0.305 ± 0.318	$9.0x10^{-09} \pm 6.8x10^{-09}$	0.61 ± 0.48	42-268	63-267	0-31	80-267
Caranx melampygus	0.276 ± 0.185	$5.0x10^{-09} \pm 1.0x10^{-09}$	0.32 ± 0.09	39-109	58-108	6-12	73-108
Gnathanodon speciosus	0.133 ± 0.208	$4.7x10^{-09} \pm 1.0x10^{-09}$	0.34 ± 0.10	40-116	59-116	5-13	75-116
Carangoides malabaricus	0.373 ± 0.158	$5.8x10^{-09} \pm 9.0x10^{-10}$	0.34 ± 0.09	32-132	48-131	4-13	61-131
Carangoides fulvoguttatus	0.127 ± 0.161	$7.2x10^{-09} \pm 2.1x10^{-09}$	0.52	69-166	102-165	4-7	130-165
Carangoides gymnostethus	0.262 ± 0.302	$7.1x10^{-09} \pm 3.0x10^{-09}$	0.50 ± 0.26	59-171	88-170	0-30	112-170
Lethrinidae							
Gymnocranius grandoculis	0.091 ± 0.027	$1.28x10^{-08} \pm 2.8x10^{-09}$	0.93 ± 0.22	110-319	164-318	2-4	208-318
Lethrinus crocineus	0.105 ± 0.101	$1.32x10^{-08} \pm 4.4x10^{-09}$	0.97 ± 0.36	116-332	172-330	2-5	219-330
Lethrinus microdon	0.191 ± 0.149	$5.8x10^{-09} \pm 1.1x10^{-09}$	0.40 ± 0.12	49-136	72-135	5-10	92-135
Lethrinus nebulosus	0.090 ± 0.050	$7.4x10^{-09} \pm 2.5x10^{-09}$	0.54	65-182	97-182	3-8	123-182
Lethrinus variegatus	0.217 ± 0.095	$7.9x10^{-09} \pm 1.9x10^{-09}$	0.52 ± 0.15	67-167	100-167	4-7	127-167
Lethrinus enigmaticus	0.031 ± 0.011	$2.22x10^{-08} \pm 2.0x10^{-09}$	1.70 ± 0.17	219-552	326-549	1-2	415-549
Lethrinus mahsena	0.156 ± 0.071	$9.4x10^{-09} \pm 2.1x10^{-09}$	0.64 ± 0.13	87-198	129-198	3-6	165-198
Lethrinus lentjan	0.049 ± 0.015	$2.38x10^{-08} \pm 7.6x10^{-09}$	1.79	176-684	261-681	1-2	332-681
Lutjanidae							
Aprion virescens	0.090 ± 0.079	$7.7x10^{-09} \pm 1.9x10^{-09}$	0.56	81-169	120-168	4-6	152-168
Etelis coruscans	0.147 ± 0.071	$7.5x10^{-09} \pm 7x10^{-10}$	0.52 ± 0.04	73-155	109-154	4-6	138-154
Lutjanus bohar	0.168 ± 0.104	$8.4x10^{-09} \pm 1.7x10^{-09}$	0.57	81-174	120-173	4-6	153-173
Lutjanus gibbus	0.169 ± 0.068	$6.7x10^{-09} \pm 1.2x10^{-09}$	0.45	62-141	92-140	4-7	117-140

Lutjanus lutjanus	0.247	$7x10^{-09}$	0.44	67-126	99-126	5-7	6
Lutjanus sebae	0.116 ± 0.118	$6.2x10^{-09}$ ± $1.2x10^{-09}$	0.44 ± 0.08	64-131	94-131	5-8	120-131
Lutjanus sanguineus	0.146 ± 0.057	$9.4x10^{-09}$ ± $1.2x10^{-09}$	0.65 ± 0.10	84-212	125-211	3-5	159-211
Serranidae							
Cephalopholis argus	0.120 ± 0.069	$6.4x10^{-09}$ ± $3.3x10^{-09}$	0.46	57-155	85-154	5-13	108-154
Cephalopholis sonnerati	0.109 ± 0.058	$6.6x10^{-09}$ ± $9x10^{-10}$	0.48 ± 0.07	66-146	97-146	4-7	124-146
Epinephelus fasciatus	0.089 ± 0.026	$6.2x10^{-09}$ ± $1.5x10^{-09}$	0.45 ± 0.12	48-167	72-167	3-9	91-167
Epinephelus merra	0.182 ± 0.114	$4.1x10^{-09}$ ± $2x10^{-09}$	0.28 ± 0.15	20-122	30-121	0-39	39-121
Epinephelus chlorostigma	0.063 ± 0.057	$7.1x10^{-09}$ ± $1.2x10^{-09}$	0.53 ± 0.10	76-157	113-156	4-6	143-156
Epinephelus fuscoguttatus	0.219 ± 0.077	$6.4x10^{-09}$ ± $2.1x10^{-09}$	0.42 ± 0.16	29-184	44-183	2-12	55-183
Epinephelus octofasciatus	0.162 ± 0.059	$6.5x10^{-09}$ ± $3x10^{-10}$	0.44 ± 0.04	60-138	89-137	4-7	114-137
Epinephelus multinotatus	0.167 ± 0.107	$7.9x10^{-09}$ ± $2.1x10^{-09}$	0.55 ± 0.17	72-176	107-175	3-8	136-175
Epinephelus longispinis	0.159 ± 0.028	$4.9x10^{-09}$ ± $3x10^{-10}$	0.33 ± 0.01	47-101	70-100	6-10	89-100
Variola louti	0.083 ± 0.058	$7.7x10^{-09}$ ± $9x10^{-10}$	0.56 ± 0.07	81-167	120-166	4-6	153-166
Sphyraenidae							
Sphyraena jello	0.200 ± 0.097	$5.8x10^{-09}$ ± $1.2x10^{-09}$	0.39 ± 0.08	53-119	79-118	5-9	100-118
Scombridae							
Gymnosarda unicolor	0.199 ± 0.123	$1.28x10^{-08}$ ± $7.8x10^{-09}$	0.87 ± 0.61	62-376	93-374	2-6	118-374
Euthynnus alletteratus	0.158 ± 0.036	$6.7x10^{-09}$ ± $1.2x10^{-09}$	0.45 ± 0.08	57-150	85-150	4-8	108-150
Rastrelliger kanagurta	0.035 ± 0.019	$8.8x10^{-09}$ ± $2x10^{-09}$	0.67 ± 0.15	90-211	133-210	3-5	169-210
Carcharhinidae							
Carcharhinus amblyrhynchos	0.325	$9.8x10^{-09}$	0.58	87-166	130-165	4-5	4
Carcharhinus brevipinna	0.228	$4.8x10^{-09}$	0.31	46-88	69-88	7-10	8
Carcharhinus limbatus	0.176	$1.41x10^{-08}$	0.95	142-270	211-269	2-3	3
Carcharhinus sorrah	0.072	$6.5x10^{-09}$	0.48	71-135	106-135	4-6	5
Galeocerdo cuvier	0.639	$3.1x10^{-09}$	0.15	22-43	33-43	14-20	17
Sphyrnidae							
Sphyrna mokarran	0.617	$3.1x10^{-09}$	0.15	22-43	33-42	14-20	17
Sphyrna lewini	0.189 ± 0.096	$1.54x10^{-08}$ ± $6.1x10^{-09}$	1.05 ± 0.49	122-368	181-367	2-4	231-367
Xiphiidae							
Xiphias gladius	0.421 ± 0.223	$7.6x10^{-09}$ ± $4x10^{-09}$	0.46	61-144	91-143	6-18	116-143

4. Discussion

In this study, we report on the concentrations of essential and non-essential trace elements in a wide range of tropical capture fisheries species from the Seychelles, caught in both nearshore and offshore waters. We highlight the importance of taxonomy-related physiological processes and trophic ecology (i.e. vertical feeding habitat, feeding mode and trophic guild) in explaining interspecific difference in trace element concentrations in capture fisheries species. We also bring key information to better understand micronutrient supply and contaminant exposure in Seychellois diet, showing that Seychelles fisheries resources are a good source of As and Se, but can also bring substantial levels of Cu, Fe and Zn to human diets. Crustacean and cephalopod species, in particular, are good sources of Cu and Zn. In addition, although there is a risk of Se excess in children's diet for some capture fisheries species, there is low health risk related to Ag, Cd, Hg and Pb exposure in seafood-based diets, with only two

species (i.e. the spanner crab, *Ranina ranina*, and the pink ear emperor, *Lethrinus lentjan*) presenting a risk of Cd poisoning if eaten in excess.

4.1. Intrinsic and extrinsic factors influencing trace element concentrations in capture fisheries species

In marine organisms, trace element accumulation is influenced by the combination of intrinsic (e.g. physiology) (Kojadinovic *et al*. 2007; Rainbow 2007) and extrinsic factors (e.g. trophic ecology) (Metian *et al.* 2013; Chouvelon *et al.* 2017), and by the availability of trace elements in the consumers' environment and/or diet (Bustamante *et al.* 1998; Raimundo *et al.* 2013). In our study, these factors were also key to explaining the results which demonstrated that the trophic pathway is the dominant route for trace element exposure for marine organisms (Wang 2002; Mathews and Fisher 2009).

Here, crustacean species were grouped together in the clustering, being the species with the highest As, Cu and Zn concentrations, and the lowest Fe, Hg and Se concentrations. Decapod crustaceans are known to have high Cu and Zn uptake rates from food due to high physiological needs for these elements (Rainbow 2002). Zn is well-known to be a cofactor in numerous enzymes (Rainbow 2002) while Cu constitutes an essential compound of hemocyanin, a protein involved in the transport of oxygen in the blood of crustaceans (Taylor and Anstiss 1999). In addition, decapod crustaceans are known to detoxify trace elements by storing them into trace element-rich granules (Rainbow 1998) and previous work reported that the most common granules were those containing Cu and Zn (Nassiri *et al.* 2000). The low concentrations of other trace elements in the muscle of the three crustacean species analysed in our study could also be explained by the morphology of these species: as their body is covered by an impermeable cuticle, trace element uptake from water is highly limited for decapod crustaceans (Rainbow 1998). The trophic pathway would thus be the main pathway for these crustaceans' exposure to trace elements, as shown for cephalopods, elasmobranchs and teleost fishes (e.g. Bustamante *et al*. 2002, 2004, Mathews and Fisher 2009). This suggests that their food items contain low levels of Fe, Hg and Se and/or these elements are poorly assimilated and retained. In the case of Hg, usually known to biomagnify through food webs (Wang 2002), this would be consistent with the trophic positions of the crustacean species analysed in this study, which seemed to be lower than all other species (i.e. they had the lowest $\delta^{15}N$ values). Although we could not calculate their absolute trophic positions due to a lack of isotopic baseline in the Seychelles, this was supported by previously estimated trophic positions of these species compared to pelagic and demersal species (Sardenne *et al*. 2017). In addition, all species analysed here were scavengers and thus fed partially on large pieces of animal tissue (Palomares and Pauly 2020). Although digestive tissues like liver or digestive gland are known to be trace elements-rich, being detoxifying organs, muscle generally has a limited role both in

terms of detoxification and storage (Afandi *et al*. 2018). For scavenging decapod crustaceans, low trace element intake is thus expected from their food, which would partly explain their low concentrations in some trace elements (Rainbow 1998).

In crustacean species analysed in this study, As concentrations were also remarkably high compared to elasmobranchs and teleost fishes (21 to 36 times higher). Decapod crustaceans, like the spiny lobster and crab species analysed here, are known to preferentially retain As in the form of arsenobetaine (Khokiattiwong *et al*. 2009), which could explain high As concentrations in these species. However, concentrations exceeding the maximum values reported in crustaceans (i.e. 95.3 $\mu g.g^{-1}$ ww) suggest a link with the bioavailability of As in their food items. Indeed, the four crustacean species analysed here are known to feed partly on invertebrates like bivalves (Baylon and Tito 2012; Sardenne *et al.* 2021), while *Panulirus penicillatus*, *P. longipes* and *P. versicolor* have been reported to also feed on macrolagae (Sardenne *et al*. 2021). Although bivalves generally display low As uptake from seawater (Gómez-Batista *et al*. 2007; Hédouin *et al.* 2010), As accumulation can be very high when there is a disequilibrium between phosphorous (P) and nitrogen (N). As can replace P in phytoplankton growing in enriched-N waters, leading to As bioaccumulation to high levels as shown in some filter-feeder bivalves from New Caledonia (Metian *et al*. 2008; Hédouin *et al*. 2009).. Such processes could also occur in waters surrounding the granitic islands of the Mahé Plateau, especially around Mahé Island, where crustaceans were caught. Indeed, due to local rainfall dynamics and to sewage discharge, waters in this area tend to be enriched in N, further destabilising the N:P ratio (Littler *et al*. 1991). The subsequent enhanced As accumulation in both primary producers and bivalves could thus travel up the food chain to crustaceans feeding on them, thus enhancing As accumulation in their tissues. This deserves further investigation to determine if As highly accumulates in bivalves from the Seychelles coastal waters and effectively transfers from bivalves to crustaceans, or if dietary As could originate from another prey in decapod crustaceans' diet. Analyses of the physicochemical forms under which As is present in crustacean species' prey (i.e. proportions of arsenobetaine and iAs) are also needed.

Although taxonomy significantly played a role in trace element accumulation for crustaceans, there was no clear clustering between elasmobranch and teleost fishes. Previous work on trace elements accumulation in these species showed differences in trace elements uptake from seawater (Jeffree *et al*. 2006, 2010), while assimilation efficiency from food was generally similar between elasmobranchs and teleosts (Mathews *et al*. 2008). Our results thus support the hypothesis that the main pathway for trace element uptake in these species is from food and not from the dissolved phase (Mathews and Fisher 2009).

Habitat and diet types poorly explained trace element patterns in the clustering, but species were mainly grouped according to their vertical feeding habitats (i.e. benthic, demersal and pelagic),

suggesting that trace element exposure varies according to the considered marine compartment. This is supported by trace element dynamics in the marine environment, as sediments are known to be reservoir of trace elements (Neff 2002). Benthic species, feeding on prey living on the seafloor, are thus more exposed to trace element intake through the trophic pathway (Wang 2002). In addition, by feeding close to the seafloor, demersal species are more prone to feed on benthic feeders and thus are expected to be more exposed to trace element uptake than pelagic species (Rejomon *et al.* 2010). It is also possible that trophic position played a role in trace element accumulation in each marine compartment. Pelagic species, in group 3, had the highest Hg and Se concentrations among all groups and were among the species with the highest $\delta^{15}N$ values. As Hg is known to biomagnify through food webs (Lavoie *et al*. 2013), and as Se was suggested to co-accumulate with Hg especially in case of high Hg concentrations (Azad *et al*. 2019), it was thus expected that pelagic species in this study had the highest Hg and Se concentrations.

4.2. Benefit-risk assessment: Seychelles capture fisheries in human diets

Given the importance of seafood in a healthy diet, and especially in SIDS like the Seychelles where capture fisheries resources are key food items in local populations' diets, our study brings key information to better understand micronutrient supply and contaminant exposure in human diets.

Among all analysed species, crustaceans (i.e. spiny lobsters and the spanner crab *Ranina ranina*) were particularly good sources of the essential trace elements Cu and Zn, as they brought at least 30% of Cu daily needs and at least 15% of Zn daily needs for children, young adults and adult women. Although having lower levels of Zn than crustaceans, the cephalopod species (i.e. the big blue octopus *Octopus cyaneus*) and two teleost fish species (i.e. the bigeye snapper *Lutjanus lutjanus* and the swordfish *Xiphias gladius*) were still a good source of Zn in adult women diets, bringing at least 10 % of their daily needs. In addition, although one portion of most species did not contribute highly to daily Fe needs in human diets regardless of the age class (less than 10% for most species), contribution could reach more than 10% of Fe daily needs for some species due to high intraspecific variability. In this way, some individuals of bigeye trevally (*Caranx sexfasciatus*), golden trevally (*Gnathanodon speciosus*), spangled emperor (*Lethrinus nebulosus*), pink ear emperor (*Lethrinus lentjan*), humpback red snapper (*Lutjanus gibbus*) and little tunny (*Euthynnus alleteratus*) could bring more than 10% of Fe daily needs for young adults and adult women. This is highly important for pregnant women, as it has been shown that, in combination with deficiency in other elements like Ca, Fe and/or Zn deficiency could increase risk of pre-eclampsia, hypertension or miscarriage during pregnancy (Kim *et al*. 2012; Shen *et al*. 2015), and could affect new-born health (Khoushabi *et al*. 2016). Although these teleost fish species were high in Hg content (i.e. maximum number of servings before reaching weekly PTI below 1), which is known

to have negative effects on foetal development (Mahaffey 2004), the MHg:MSe ratio for these species was well below 1, suggesting very low risk of Hg poisoning. Thus, these species could be good candidates to help fight Fe and/or Zn deficiency in pregnant women.

In spite of the high Cu and Zn levels in crustaceans and in the octopus, there was no risk of poisoning linked with these trace elements, as the lowest number of servings per day for both Cu and Zn was three servings for children, five servings for young adults and six servings for adult women, which is unlikely to happen.

All species were particularly good sources of As for adult women and of Se for all age classes, but were very poor food sources of Mn (globally, one portion ≤ 1 % of all age classes daily needs). Although no safety limit was found for As, its most toxic forms are known to be the inorganic forms (Sharma and Sohn 2009), which are in low concentrations in seafood (i.e. 4.4 % in fish and 2.2 % in crustaceans) (Uneyama *et al*. 2007). The estimated iAs content in our study was thus low for all species, with concentrations below or close to 1 $\mu g.g^{-1}$ ww, suggesting low risk of toxicity. However, due to very high Se concentrations, the minimum number of servings before reaching daily PTI was still low, even after interaction with Hg, and especially for children (i.e. one third of analysed species had minimum number of servings ≤ 3 for children). Thus, special care on the quantity eaten should be taken for these species given the risk of Se excess, especially in children's diet. Further study is needed here to determine the mean weight of a daily portion for each children age subclass, in order to refine risk linked to an excess of Se for this age class.

For all analysed species, the number of servings before reaching Cd PTI was high (mostly > 10 servings per month) for all age classes. However, for the species with the highest Cd concentrations (i.e. spanner crab, *Ranina ranina*) and for the pink ear emperor (Lethrinus lentjan), the number of servings before reaching PTI was very low for all three age classes (< 5 servings), suggesting risk of poisoning if eaten in excessive amount. Although Hg concentrations were high in some species, the MHg:MSe ratio was < 1 and the HBVSe was > 0 in all species. Thus, our results suggest that there is a very low risk of Hg poisoning for all age classes through Seychelles capture fisheries consumption. In the context of fish export to Europe and to USA, however, caution should be taken for some species. Indeed, some species had individuals above the safety limits implemented by the European Union (Cd, Hg and Pb; Fig. S1), above which seafood cannot be sold (EC 2006, 2011). In addition, most species had individuals above the Hg recommendations in the United States (Fig. S2) (US-EPA and US-FDA 2019).

5. Conclusion

In this study, we provide important baseline information on micronutrient supply and contaminant exposure for an SIDS community, the Seychelles, through the consumption of their main capture fisheries species. By identifying intraspecific difference in essential and potentially essential trace element supply and in risk of poisoning for both essential and non-essential trace elements, we highlighted the importance of varying capture fisheries resource consumption to stay healthy. This was particularly true for children who seemed more exposed to Se than adult women. We also showed the importance of capture fisheries characteristics (i.e. presence/absence of regulation and/or detoxifying mechanisms, vertical feeding habitat, diet composition and trophic position) in the understanding of such intraspecific difference in micronutrient supply and contaminant exposure.

This study is a foundation stone in supplying nutritional information to SIDS governments for the development of policies, initiatives and guidelines on seafood consumption for their populations. However, much remains to be done in the establishment of sustainable guidelines. In a context of climate change and marine resource decrease, it is crucial to also consider the environmental footprint of capture fisheries, that is the status of each species' fishing stock, their sensitivity to climate change and the greenhouse gas emissions related to production techniques (Hallström *et al.* 2019; Tlusty *et al.* 2019; Chapa *et al.* 2020).

Funding The present work is a contribution to the SEYFISH project ("Nutrients and Contaminants in Seychelles fisheries resources") with the financial support of the French Research Institute for Sustainable Development (IRD) and the European Fisheries Partnership Agreement (EU-FPA).

Acknowledgements The authors would like to thank all fishermen and crews who assisted with sampling. A special thank goes to the SFA staff (in alphabetic order, Achille Pascal, Andrew Souffre, Calvin Gerry, Clara Belmont, Dora Lesperance, Kettyna Gabriel, Maria Rose, Marie-Corinne Balett, Natifa Pillay, Rahim Woodcock, Rodney Melanie, Ronny Antat, Stephanie Hollanda, Stephanie Marie), the R.V. L'Amitié crew (Christian Decommardmond, Fred Mondon, Gerard Ernesta, Robert Dookley, Yashim Marday) and the Seychelles Maritime Academy for the invaluable help in collecting and processing the samples. The authors are also grateful to Ariane Reynier-Caërou, Adeline Angles, Maxime Degroote, Maud Brault-Favrou, Gaël Guillou, and Thomas Lacoue-Labarthe for their support in the laboratory analyses. Thanks are due to the CPER (Contrat de Projet Etat-Région) and the FEDER (Fonds Européen de Développement Régional) for funding the IRMS of LIENSs laboratory. The IUF (Institut Universitaire de France) is acknowledged for its support to Paco Bustamante as a Senior Member. This article was written as part of the SEYFISH project, for which Nathalie Bodin was the PI.

Data availability The dataset analysed in the current study is available from the corresponding author on reasonable request. The R code used to compute the cluster analysis and to represent the dendrogram and associated heatplot is available on Github: https://github.com/magalisabino/TraceElement_Cluster_Analysis.

References

Afandi I, Talba S, Benhra A, Benbrahim S, Chfiri R, Labonne M, Masski H, Laë R, Tito De Morais L, Bekkali M, Bouthir FZ (2018) Trace metal distribution in pelagic fish species from the north-west African coast (Morocco). Int Aquat Res 10:191–205. doi: 10.1007/s40071-018-0192-7

American Food and Nutrition Board of the Institute of Medicine National Academy of Sciences (2019a) Dietary Reference Intakes (DRIs): Recommended dietary allowances and adequate intakes, elements. URL: https://ods.od.nih.gov/Health_Information/Dietary_Reference_Intakes.aspx.

American Food and Nutrition Board of the Institute of Medicine National Academy of Sciences (2019b) Dietary Reference Intakes (DRIs): Tolerable upper intake levels, elements. URL: https://www.ncbi.nlm.nih.gov/books/NBK545442/table/appJ_tab9/?report=objectonly.

Azad AM, Frantzen S, Bank MS, Nilsen BM, Duinker A, Madsen L, Maage A (2019) Effects of geography and species variation on selenium and mercury molar ratios in Northeast Atlantic marine fish communities. Sci Total Environ 652:1482–1496. doi: 10.1016/j.scitotenv.2018.10.405

Barone G, Giacominelli-Stuffler R, Storelli MM (2013) Comparative study on trace metal accumulation in the liver of two fish species (Torpedinidae): Concentration-size relationship. Ecotoxicol Environ Saf 97:73–77. doi: 10.1016/j.ecoenv.2013.07.004

Baylon JC, Tito OD (2012) Natural diet and feeding habit of the red frog crab (*Ranina ranina*) from Southwestern Mindanao, Philippines. Philipp Agric Sci 95:370–377.

Beaugrand G, Kirby RR (2018) How do marine pelagic species respond to climate change? Theories and observations. Ann Rev Mar Sci 10:169–197. doi: 10.1146/annurev-marine-121916-063304

Béné C, Barange M, Subasinghe R, Pinstrup-Andersen P, Merino G, Hemre G-I, Williams M (2015) Feeding 9 billion by 2050 – Putting fish back on the menu. Food Secur 7:261–274. doi: 10.1007/s12571-015-0427-z

Bodin N, Lesperance D, Albert R, Hollanda S, Michaud P, Degroote M, Churlaud C, Bustamante P (2017) Trace elements in oceanic pelagic communities in the Western Indian Ocean. Chemosphere 174:354–362. doi: 10.1016/j.chemosphere.2017.01.099

Bosch AC, O'Neill B, Sigge GO, Kerwath SE, Hoffman LC (2016) Heavy metals in marine fish meat and consumer health: A review. J Sci Food Agric 96:32–48. doi: 10.1002/jsfa.7360

Briguglio L (1995) Small island developing states and their economic vulnerabilities. World Dev 23:1615–1632. doi: 10.1016/0305-750X(95)00065-K

Bustamante P, Caurant F, Fowler SW, Miramand P (1998) Cephalopods as a vector for the transfer of cadmium to top marine predators in the north-east Atlantic Ocean. Sci Total Environ 220:71–80. doi: 10.1016/S0048-9697(98)00250-2

Carravieri A, Bustamante P, Labadie P, Budzinski H, Chastel O, Cherel Y (2020) Trace elements and persistent organic pollutants in chicks of 13 seabird species from Antarctica to the subtropics. Environ Int 134:105225. doi: 10.1016/j.envint.2019.105225

Chapa J, Farkas B, Bailey RL, Huang JY (2020) Evaluation of environmental performance of dietary patterns in the United States considering food nutrition and satiety. Sci Total Environ 722:137672. doi: 10.1016/j.scitotenv.2020.137672

Chouvelon T, Spitz J, Caurant F, Mèndez-Fernandez P, Autier J, Lassus-Débat A, Chappuis A, Bustamante P (2012) Enhanced bioaccumulation of mercury in deep-sea fauna from the Bay of Biscay (north-east Atlantic) in relation to trophic positions identified by analysis of carbon and nitrogen stable isotopes. Deep Res Part I Oceanogr Res Pap 65:113–124. doi: 10.1016/j.dsr.2012.02.010

Chouvelon T, Brach-Papa C, Auger D, Bodin N, Bruzac S, Crochet S, Degroote M, Hollanda SJ, Hubert C, Knoery J, Munschy C, Puech A, Rozuel E, Thomas B, West W, Bourjea J, Nikolic N (2017) Chemical contaminants (trace metals, persistent organic pollutants) in albacore tuna from western Indian and south-eastern Atlantic

Oceans: Trophic influence and potential as tracers of populations. Sci Total Environ 596–597:481–495. doi: 10.1016/j.scitotenv.2017.04.048

Copper Development Association (2019) Copper in human health. URL: https://www.copper.org/consumers/health/cu_health_uk.html. Accessed 29 May 2019

EC (2006) 1881/2006. Setting maximum levels for certain contaminants in foodstuffs. Off J Eur Communities 364:5–24.

EC (2011) COMMISSION REGULATION (EU) No 420/2011 of 29 April 2011 amending Regulation (EC) No 1881/2006 setting maximum levels for certain contaminants in foodstuffs. Off J Eur Union L111:3–6.

Goldhaber SB (2003) Trace element risk assessment: Essentiality *vs*. toxicity. Regul Toxicol Pharmacol 38:232–242. doi: 10.1016/S0273-2300(02)00020-X

Gómez-Batista M, Metian M, Teyssie JL, Alonso-Hernández C, Warnau M (2007) Bioaccumulation of dissolved arsenic in the oyster *Crassostrea virginica*: A radiotracer study. Environ Bioindic 2:237–244. doi: 10.1080/15555270701693570

Goutte A, Cherel Y, Churlaud C, Ponthus JP, Massé G, Bustamante P (2015) Trace elements in Antarctic fish species and the influence of foraging habitats and dietary habits on mercury levels. Sci Total Environ 538:743–749. doi: 10.1016/j.scitotenv.2015.08.103

Hallström E, Bergman K, Mifflin K, Parker R, Tyedmers P, Troell M, Ziegler F (2019) Combined climate and nutritional performance of seafoods. J Clean Prod 230:402–411. doi: 10.1016/j.jclepro.2019.04.229

Hédouin L, Bustamante P, Churlaud C, Pringault O, Fichez R, Warnau M (2009) Trends in concentrations of selected metalloid and metals in two bivalves from the coral reefs in the SW lagoon of New Caledonia. Ecotoxicol Environ Saf 72:372–381. doi: 10.1016/j.ecoenv.2008.04.004

Hédouin L, Batista MG, Metian M, Buschiazzo E, Warnau M (2010) Metal and metalloid bioconcentration capacity of two tropical bivalves for monitoring the impact of land-based mining activities in the New Caledonia lagoon. Mar Pollut Bull 61:554–567. doi: 10.1016/j.marpolbul.2010.06.036

Hicks CC, Cohen PJ, Graham NAJ, Nash KL, Allison EH, Lima CD, Mills DJ, Roscher M, Thilsted SH, Thorne-Lyman AL, Macneil MA (2019) Harnessing global fisheries to tackle micronutrient deficiencies. Nature 574:95–98. doi: 10.1038/s41586-019-1592-6

Hollanda S, Bodin N, Churlaud C, Bustamante P (2017) Mercury and selenium levels in Swordfish (*Xiphias gladius*) fished in the exclusive economic zone of the Republic of Seychelles. Int J Environ Ecol Eng 11:23–26.

JECFA (2011) Mercury. URL: https://apps.who.int/food-additives-contaminants-jecfa-database/chemical.aspx?chemID=1806.

JECFA (2013) Cadmium. URL: https://apps.who.int/food-additives-contaminants-jecfa-database/chemical.aspx?chemID=1376.

Jeffree RA, Warnau M, Teyssié JL, Markich SJ (2006) Comparison of the bioaccumulation from seawater and depuration of heavy metals and radionuclides in the spotted dogfish *Scyliorhinus canicula* (Chondrichthys) and the turbot *Psetta maxima* (Actinopterygii: Teleostei). Sci Total Environ 368:839–852. doi: 10.1016/j.scitotenv.2006.03.026

Jeffree RA, Oberhansli F, Teyssie JL (2010) Phylogenetic consistencies among chondrichthyan and teleost fishes in their bioaccumulation of multiple trace elements from seawater. Sci Total Environ 408:3200–3210. doi: 10.1016/j.scitotenv.2010.04.015

Khokiattiwong S, Kornkanitnan N, Goessler W, Kokarnig S, Francesconi KA (2009) Arsenic compounds in tropical marine ecosystems: Similarities between mangrove forest and coral reef. Environ Chem 6:226–234. doi: 10.1071/EN09009

Khoushabi F, Shadan M, Miri A, SharifiRad J (2016) Determination of maternal serum zinc, iron, calcium and magnesium during pregnancy in pregnant women and umbilical cord blood and their association with outcome of pregnancy. Mater Socio Medica 28:104–107. doi: 10.5455/msm.2016.28.104-107

Kim J, Kim YJ, Lee R, Moon JH, Jo I (2012) Serum levels of zinc, calcium, and iron are associated with the risk of preeclampsia in pregnant women. Nutr Res 32:764–769. doi: 10.1016/j.nutres.2012.09.007

Kim SL, Koch PL (2012) Methods to collect, preserve, and prepare elasmobranch tissues for stable isotope analysis. Environ Biol Fishes 95:53–63. doi: 10.1007/s10641-011-9860-9

Kojadinovic J, Potier M, Le Corre M, Cosson RP, Bustamante P (2007) Bioaccumulation of trace elements in pelagic fish from the Western Indian Ocean. Environ Pollut 146:548–566. doi: 10.1016/j.envpol.2006.07.015

Koolman J, Röhm K-H (2011) Atlas de poche de biochimie humaine, 4e édition. Lavoisier

Larsen R, Eilertsen KE, Elvevoll EO (2011) Health benefits of marine foods and ingredients. Biotechnol Adv 29:508–518. doi: 10.1016/j.biotechadv.2011.05.017

Lavoie RA, Jardine TD, Chumchal MM, Kidd KA, Campbell LM (2013) Biomagnification of mercury in aquatic food webs: A worldwide meta-analysis. Environ Sci Technol 47:13385–13394. doi: 10.1021/es403103t

Le Croizier G, Schaal G, Gallon R, Fall M, Le Grand F, Munaron JM, Rouget ML, Machu E, Le Loc'h F, Laë R, De Morais LT (2016) Trophic ecology influence on metal bioaccumulation in marine fish: Inference from stable isotope and fatty acid analyses. Sci Total Environ 573:83–95. doi: 10.1016/j.scitotenv.2016.08.035

Li Y, Zhang Y, Hussey NE, Dai X (2016) Urea and lipid extraction treatment effects on $\delta^{15}N$ and $\delta^{13}C$ values in pelagic sharks. Rapid Commun Mass Spectrom 30:1–8. doi: 10.1002/rcm.7396

Little AG, Loughland I, Seebacher F (2020) What do warming waters mean for fish physiology and fisheries? J Fish Biol 97:328–340. doi: 10.1111/jfb.14402

Littler MM, Littler DS, Titlyanov EA (1991) Comparisons of N- and P-limited productivity between high granitic islands versus low carbonate atolls in the Seychelles Archipelago: A test of the relative-dominance paradigm. Coral Reefs 10:199–209. doi: 10.1007/BF00336775

Logan JM, Lutcavage ME (2008) A comparison of carbon and nitrogen stable isotope ratios of fish tissues following lipid extractions with non-polar and traditional chloroform/methanol solvent systems. Rapid Commun Mass Spectrom 22:1081–1086. doi: 10.1002/rcm.3471

Logan JM, Jardine TD, Miller TJ, Bunn SE, Cunjak RA, Lutcavage ME (2008) Lipid corrections in carbon and nitrogen stable isotope analyses: Comparison of chemical extraction and modelling methods. J Anim Ecol 77:838–846. doi: 10.1111/j.1365-2656.2008.01394.x

Mahaffey KR (2004) Fish and shellfish as dietary sources of methylmercury and the ω-3 fatty acids, eicosahexaenoic acid and docosahexaenoic acid: Risks and benefits. Environ Res 95:414–428. doi: 10.1016/j.envres.2004.02.006

Mathews T, Fisher NS (2009) Dominance of dietary intake of metals in marine elasmobranch and teleost fish. Sci Total Environ 407:5156–5161. doi: 10.1016/j.scitotenv.2009.06.003

Mathews T, Fisher NS, Jeffree RA, Teyssié JL (2008) Assimilation and retention of metals in teleost and elasmobranch fishes following dietary exposure. Mar Ecol Prog Ser 360:1–12. doi: 10.3354/meps07462

Metian M, Bustamante P, Hédouin L, Warnau M (2008) Accumulation of nine metals and one metalloid in the tropical scallop *Comptopallium radula* from coral reefs in New Caledonia. Environ Pollut 152:543–552. doi: 10.1016/j.envpol.2007.07.009

Metian M, Warnau M, Chouvelon T, Pedraza F, Rodriguezy Baena AM, Bustamante P (2013) Trace element bioaccumulation in reef fish from New Caledonia: Influence of trophic groups and risk assessment for consumers. Mar Environ Res 87–88:26–36. doi: 10.1016/j.marenvres.2013.03.001

Mudgal V, Madaan N, Mudgal A, Singh RB, Mishra S (2010) Effect of toxic metals on human health. Open Nutraceuticals J 3:94–99. doi: 10.2174/1876396001003010094

Murry BA, Farrell JM, Teece MA, Smyntek PM (2006) Effect of lipid extraction on the interpretation of fish community trophic relationships determined by stable carbon and nitrogen isotopes. Can J Fish Aquat Sci 63:2167–2172. doi: 10.1139/F06-116

Nassiri Y, Rainbow PS, Smith BD, Nassiri Y, Amiard-Triquet C, Rainglet F (2000) Trace-metal detoxification in the ventral caeca of *Orchestia gammarellus* (Crustacea: Amphipoda). Mar Biol 136:477–484. doi: 10.1007/s002270050707

Neff JM (2002) Bioaccumulation Mechanisms. In: Bioaccumulation in Marine Organisms (Ed. Neff JM). Elsevier, Oxford, UK, pp 37–56

Nielsen FH (1991) Nutritional requirements for boron, silicon, vanadium, nickel, and arsenic: Current knowledge and speculation. FASEB J 5:2661–2667.

Ohio State University (2015) Ohio State University extension fact sheet: Iron. URL: https://ohioline.osu.edu/factsheet/HYG-5559.

Palomares MLD, Pauly D (2020) SeaLifeBase. World Wide Web electronic publication. URL: www.sealifebase.org.

Post DM, Layman CA, Arrington DA, Takimoto G, Quattrochi J, Montaña CG (2007) Getting to the fat of the matter: Models, methods and assumptions for dealing with lipids in stable isotope analyses. Oecologia 152:179–189. doi: 10.1007/s00442-006-0630-x

Preda C, Vasiliu I, Bredetean O, Gabriela CD, Ungureanu MC, Leustean EL, Grigorovici A, Oprisa C, Vulpoi C (2016) Selenium in the environment: Essential or toxic to human health? Environ Eng Manag J 15:913–921. doi:

10.30638/eemj.2016.099

R Core Team (2018) R: A language and environment for statistical computing.

Raimundo J, Vale C, Caetano M, Giacomello E, Anes B, Menezes GM (2013) Natural trace element enrichment in fishes from a volcanic and tectonically active region (Azores archipelago). Deep Res Part II Top Stud Oceanogr 98:137–147. doi: 10.1016/j.dsr2.2013.02.009

Rainbow PS (1998) Phylogeny of trace metal accumulation in crustaceans. In: Metal Metabolism in Aquatic Environments (Eds. Langston WJ, Bebianno MJ). Springer-Science, London, UK, pp 285–319

Rainbow PS (2002) Trace metal concentrations in aquatic invertebrates: Why and so what? Environ Pollut 120:497–507. doi: 10.1016/S0269-7491(02)00238-5

Rainbow PS (2007) Trace metal bioaccumulation: Models, metabolic availability and toxicity. Environ Int 33:576–582. doi: 10.1016/j.envint.2006.05.007

Ralston NVC, Blackwell JL, Raymond LJ (2007) Importance of molar ratios in selenium-dependent protection against methylmercury toxicity. Biol Trace Elem Res 119:255–268. doi: 10.1007/s12011-007-8005-7

Ralston NVC, Ralston CR, Blackwell JL, Raymond LJ (2008) Dietary and tissue selenium in relation to methylmercury toxicity. Neurotoxicology 29:802–811. doi: 10.1016/j.neuro.2008.07.007

Ralston NVC, Ralston CR, Raymond LJ (2015) Selenium Health Benefit values: Updated criteria for mercury risk assessments. Biol Trace Elem Res 171:262–269. doi: 10.1007/s12011-015-0516-z

Rejomon G, Nair M, Joseph T (2010) Trace metal dynamics in fishes from the southwest coast of India. Environ Monit Assess 167:243–255. doi: 10.1007/s10661-009-1046-y

Robinson J, Aumeeruddy R, Isidore M, Payet R, Marguerite M, Laval M, Domingue G, Lucas V (2006) Country review: Seychelles. In: Review of the state of world marine capture fisheries management: Indian Ocean (Eds. De Young C, Fishery Policy Analyst, Fishery Policy and Planning Division, FAO Fisheries Department). FAO, pp 425–436

Robinson JPW, Robinson J, Gerry C, Govinden R, Freshwater C, Graham NAJ (2020) Diversification insulates fisher catch and revenue in heavily exploited tropical fisheries. Sci Adv 6:1–10. doi: 10.1126/sciadv.aaz0587

Sabino MA, Govinden R, Pethybridge H, Blamey L, Le Grand F, Sardenne F, Rose M, Bustamante P, Bodin N (2021) Habitat degradation increases interspecific trophic competition between three spiny lobster species in Seychelles. Estuar Coast Shelf Sci 256:107368. doi: 10.1016/j.ecss.2021.107368

Sardenne F, Hollanda S, Lawrence S, Albert-Arrisol R, Degroote M, Bodin N (2017) Trophic structures in tropical marine ecosystems: A comparative investigation using three different ecological tracers. Ecol Indic 81:315–324. doi: 10.1016/j.ecolind.2017.06.001

Sardenne F, Bodin N, Barret L, Blamey L, Govinden R, Gabriel K, Mangroo R, Munaron J-M, Le Loc'h F, Bideau A, Le Grand F, Sabino M, Bustamante P, Rowat D (2021) Diets of spiny lobsters from Mahé Island reefs, Seychelles reefs inferred by trophic tracers. Reg Stud Mar Sci 42:101640. doi: 10.1016/j.rsma.2021.101640

Sharma VK, Sohn M (2009) Aquatic arsenic: Toxicity, speciation, transformations, and remediation. Environ Int 35:743–759. doi: 10.1016/j.envint.2009.01.005

Shen PJ, Gong B, Xu FY, Luo Y (2015) Four trace elements in pregnant women and their relationships with adverse pregnancy outcomes. Eur Rev Med Pharmacol Sci 19:4690–4697.

Sotiropoulos MA, Tonn WM, Wassenaar LI (2004) Effects of lipid extraction on stable carbon and nitrogen isotope analyses of fish tissues : Potential consequences for food web studies. Ecol Freshw Fish 13:155–160. doi: 10.1111/j.1600-0633.2004.00056.x

Taylor HH, Anstiss JM (1999) Copper and haemocyanin dynamics in aquatic invertebrates. Mar Freshw Res 50:907–931. doi: 10.1071/MF99117

Tlusty MF, Tyedmers P, Bailey M, Ziegler F, Henriksson PJG, Béné C, Bush S, Newton R, Asche F, Little DC, Troell M, Jonell M (2019) Reframing the sustainable seafood narrative. Glob Environ Chang 59:101991. doi: 10.1016/j.gloenvcha.2019.101991

Uneyama C, Toda M, Yamamoto M, Morikawa K (2007) Arsenic in various foods: Cumulative data. Food Addit Contam 24:447–534. doi: 10.1080/02652030601053121

US-EPA, US-FDA (2019) EPA-FDA Fish Advice: Technical Information. URL: https://www.epa.gov/fish-tech/epa-fda-fish-advice-technical-information.

Wang WX (2002) Interactions of trace metals and different marine food chains. Mar Ecol Prog Ser 243:295–309. doi: 10.3354/meps243295

Weichselbaum E, Coe S, Buttriss J, Stanner S (2013) Fish in the diet: A review. Nutr Bull 38:128–177. doi:

10.1111/nbu.12021

WorldBank (2017) Third South West Indian Ocean Fisheries Governance and Shared Growth Project (SWIOFish3). Washington, DC

Zoroddu MA, Aaseth J, Crisponi G, Medici S, Peana M, Nurchi VM (2019) The essential metals for humans: A brief overview. J Inorg Biochem 195:120–129. doi: 10.1016/j.jinorgbio.2019.03.013

Supplementary data

Table S1 Analysed species and associated details. Length (presented as mean ± SD) refers to dorsal mantle length for cephalopods, carapace length for crustaceans, lower jaw-fork length for swordfish, and fork length for other teleost fish and for elasmobranchs. Vertical habitat, trophic groups, habitat and diet types were determined from SeaLifeBase (Palomares and Pauly 2020) and FishBase (Froese and Pauly 2020). N TE = number of samples analysed for trace elements, N SI = number of samples analysed for C and N stable isotopes.

Family	Scientific name	English name	N TE	N SI	Length (cm)	Moisture (%)	$\delta^{13}C$ (‰)	$\delta^{15}N$ (‰)	Fishing location	Functional group	Habitat type	Trophic group	Diet type
Octopodidae	*Octopus cyaneus*	Big blue octopus	17	17	13.5 ± 2.8	ND	-15.4 ± 1.0	11.5 ± 0.6	Nearshore	Benthic cephalopod	Coral reefs	Carnivore	Benthivore/scavenger
Palinuridae	*Panulirus longipes*	Longlegged spiny lobster	44	44	7.8 ± 1.0	74.5 ± 3.3	-14.0 ± 0.7	11.3 ± 0.4	Nearshore	Benthic crustacean	Rocky reefs	Carnivore	Benthivore/scavenger
	Panulirus penicillatus	Pronghorn spiny lobster	47	47	9.8 ± 1.8	73.8 ± 2.7	-13.6 ± 0.7	11.6 ± 0.4	Nearshore	Benthic crustacean	Rocky reefs	Carnivore	Benthivore/scavenger
	Panulirus versicolor	Painted spiny lobster	15	15	8.2 ± 1.8	76.2 ± 6.3	-13.7 ± 0.8	10.4 ± 0.3	Nearshore	Benthic crustacean	Coral reefs	Carnivore	Benthivore/scavenger
Raninidae	*Ranina ranina*	Spanner crab	5	5	9.7 ± 1.1	ND	-14.5 ± 0.4	12.0 ± 0.5	Nearshore	Benthic crustacean	Sandy areas	Carnivore	Benthivore/scavenger
Mullidae	*Parupeneus barberinus*	Dash-and-dot goatfish	5	5	26.9 ± 3.3	77.7 ± 0.7	-13.6 ± 2.1	11.9 ± 1.6	Nearshore	Benthic teleost fish	Sandy areas	Carnivore	Benthivore
	Parupeneus rubescens	Rosy goatfish	3	3	25.5 ± 5.2	78.7 ± 0.5	-15.0 ± 0.5	14.8 ± 0.6	Nearshore	Benthic teleost fish	Sandy areas	Carnivore	Benthivore
Scaridae	*Scarus ghobban*	Blue-barred parrotfish	10	10	28.4 ± 2.9	ND	-15.6 ± 1.4	10.2 ± 1.3	Nearshore	Benthic teleost fish	Coral reefs	Herbivore	Scraper
Siganidae	*Siganus sutor*	Shoemaker spinefoot	9	9	25.5 ± 2.0	78.5 ± 1.7	-16.8 ± 2.2	9.7 ± 0.8	Nearshore	Benthic teleost fish	Coral reefs	Herbivore	Grazer
	Siganus argenteus	Streamlined spinefoot	10	10	26.0 ± 1.5	ND	-18.9 ± 2.2	9.9 ± 0.6	Nearshore	Benthic teleost fish	Coral reefs	Herbivore	Grazer
Acanthuridae	*Acanthurus mata*	Elongate surgeonfish	6	6	38.0 ± 13.6	79.9	-16.9 ± 1.5	11.3 ± 1.0	Nearshore	Demersal teleost fish	Rocky and coral reefs	Carnivore	Planktivore
Carangidae	*Caranx sexfasciatus*	Bigeye trevally	8	8	58.5 ± 8.3	76.1 ± 1.0	-16.6 ± 0.4	13.9 ± 0.3	Nearshore	Demersal teleost fish	Coral reefs	Carnivore	Pelagobenthivore
	Caranx melampygus	Bluefin trevally	9	9	49.3 ± 11.6	78.1 ± 0.3	-16.5 ± 0.4	13.8 ± 0.5	Nearshore	Demersal teleost fish	Coral reefs	Carnivore	Pelagobenthivore
	Gnathanodon speciosus	Golden trevally	7	7	52.3 ± 14.0	77.6 ± 0.7	-17.4 ± 0.4	12.8 ± 0.1	Nearshore	Demersal teleost fish	Coral reefs	Carnivore	Pelagobenthivore
	Carangoides malabaricus	Malabar trevally	2	2	67.5 ± 6.4	ND	-15.9 ± 0.3	14.3 ± 0.1	Nearshore	Demersal teleost fish	Rocky and coral reefs	Carnivore	Benthopelagivore
	Carangoides fulvoguttatus	Yellowspotted trevally	36	36	59.1 ± 16.2	76.1 ± 0.7	-16.7 ± 0.3	14.1 ± 0.4	Nearshore	Demersal teleost fish	Rocky and coral reefs	Carnivore	Pelagobenthivore
	Carangoides gymnostethus	Bludger	25	25	56.3 ± 15.9	74.0 ± 4.1	-17.2 ± 0.3	13.6 ± 0.4	Nearshore	Demersal teleost fish	Rocky and coral reefs	Carnivore	Pelagobenthivore

Lethrinidae	*Gymnocranius grandoculis*	Blue-lined large-eye bream	5	5	51.9 ± 6.2	78.0 ± 0.9	-15.9 ± 0.5	14.2 ± 0.2	Nearshore	Demersal teleost fish	Rocky and coral reefs	Carnivore	Benthopelagivore
	Lethrinus crocineus	Yellowtail emperor	13	13	33.1 ± 4.5	79.1 ± 1.9	-15.1 ± 0.9	13.3 ± 0.3	Nearshore	Demersal teleost fish	Coral reefs	Carnivore	Benthopelagivore
	Lethrinus microdon	Smalltooth emperor	10	10	44.6 ± 3.4	76.7 ± 1.0	-16.3 ± 0.4	14.1 ± 0.7	Nearshore	Demersal teleost fish	Coral reefs	Carnivore	Benthopelagivore
	Lethrinus nebulosus	Spangled emperor	14	14	42.4 ± 6.4	75.2 ± 3.7	-16.2 ± 1.7	12.7 ± 0.5	Nearshore	Demersal teleost fish	Rocky and coral reefs	Carnivore	Benthopelagivore
	Lethrinus variegatus	Slender emperor	18	17	29.3 ± 1.8	77.2 ± 1.3	-16.3 ± 0.6	13.2 ± 0.4	Nearshore	Benthic teleost fish	Sandy areas	Carnivore	Benthivore
	Lethrinus enigmaticus	Blackeye emperor	2	2	33.5 ± 0.7	79.5	-14.9 ± 0.1	13.6 ± 0.1	Nearshore	Demersal teleost fish	Coral reefs	Carnivore	Benthopelagivore
	Lethrinus mahsena	Sky emperor	21	21	34.5 ± 5.3	77.6 ± 1.9	-15.6 ± 1.0	13.4 ± 0.5	Nearshore	Demersal teleost fish	Coral reefs	Carnivore	Benthopelagivore
	Lethrinus lentjan	Pink ear emperor	3	3	41.8 ± 5.8	76.8	-14.9 ± 0.8	13.9 ± 0.7	Nearshore	Demersal teleost fish	Sandy areas	Carnivore	Benthopelagivore
Lutjanidae	*Aprion virescens*	Green jobfish	113	113	56.0 ± 9.6	75.7 ± 1.7	-16.8 ± 0.4	13.4 ± 0.5	Nearshore	Demersal teleost fish	Coral reefs	Carnivore	Pelagobenthivore
	Etelis coruscans	Deepwater longtail red snapper	10	10	57.3 ± 11.3	ND	-18.0 ± 0.2	13.6 ± 0.3	Nearshore	Demersal teleost fish	Rocky reefs	Carnivore	Pelagobenthivore
	Lutjanus bohar	Two-spot red snapper	56	56	52.6 ± 14.9	75.5 ± 3.1	-16.3 ± 0.5	13.7 ± 0.5	Nearshore	Demersal teleost fish	Coral reefs	Carnivore	Pelagobenthivore
	Lutjanus gibbus	Humpback red snapper	16	16	35.8 ± 3.9	74.3 ± 0.4	-16.7 ± 0.3	13.2 ± 0.2	Nearshore	Demersal teleost fish	Coral reefs	Carnivore	Pelagobenthivore
	Lutjanus lutjanus	Bigeye snapper	1	1	39.5	ND	-16.0	14.9	Nearshore	Demersal teleost fish	Coral reefs	Carnivore	Pelagobenthivore
	Lutjanus sebae	Emperor red snapper	78	78	58.9 ± 13.3	77.9 ± 0.5	-16.2 ± 0.4	14.3 ± 0.4	Nearshore	Demersal teleost fish	Rocky and coral reefs	Carnivore	Pelagobenthivore
	Lutjanus sanguineus	Humphead snapper	5	5	62.2 ± 5.3	77.9 ± 1.1	-16.5 ± 0.4	13.1 ± 0.6	Nearshore	Demersal teleost fish	Rocky and coral reefs	Carnivore	Pelagobenthivore
Serranidae	*Cephalopholis argus*	Peacock hind	42	42	21.0 ± 6.2	77.3 ± 1.8	-13.7 ± 1.1	13.0 ± 0.6	Nearshore	Demersal teleost fish	Coral reefs	Carnivore	Pelagobenthivore
	Cephalopholis sonnerati	Tomato hind	14	14	41.4 ± 4.1	77.9 ± 0.6	-16.9 ± 0.2	14.2 ± 0.4	Nearshore	Demersal teleost fish	Rocky and coral reefs	Carnivore	Pelagobenthivore
	Epinephelus fasciatus	Blacktip grouper	3	3	ND	ND	-17.0 ± 0.1	13.0 ± 0.2	Nearshore	Demersal teleost fish	Coral reefs	Carnivore	Pelagobenthivore
	Epinephelus merra	Honeycomb grouper	4	4	33.8 ± 1.6	77.8 ± 0.2	-15.2 ± 0.2	13.2 ± 0.1	Nearshore	Demersal teleost fish	Coral reefs	Carnivore	Benthopelagivore
	Epinephelus chlorostigma	Brownspotted grouper	76	76	35.1 ± 3.9	78.5 ± 1.7	-16.8 ± 0.3	13.8 ± 0.3	Nearshore	Demersal teleost fish	Reefs and associated habitats	Carnivore	Pelagobenthivore
	Epinephelus fuscoguttatus	Brown-marbled grouper	2	2	70.8 ± 3.2	77.9 ± 0.2	-15.7 ± 0.4	14.1 ± 0.2	Nearshore	Demersal teleost fish	Coral reefs	Carnivore	Benthopelagivore
	Epinephelus octofasciatus	Eightbar grouper	4	4	68.0 ± 3.9	76.4 ± 1.6	-16.5 ± 0.4	14.4 ± 0.3	Nearshore	Demersal teleost fish	Rocky reefs	Carnivore	Pelagobenthivore

	Epinephelus multinotatus	White-blotched grouper	22	21	64.7 ± 11.7	76.4 ± 1.4	-16.5 ± 0.4	13.4 ± 0.5	Nearshore	Demersal teleost fish	Reefs and associated habitats	Carnivore	Pelagobenthivore
	Epinephelus longispinis	Longspine grouper	2	2	42.5 ± 3.5	78.9 ± 0.1	-16.3 ± 0.1	13.9 ± 0.1	Nearshore	Demersal teleost fish	Rocky and coral reefs	Carnivore	Benthopelagivore
	Variola louti	Yellow-edged lyretail	38	38	46.0 ± 6.6	78.0 ± 1.5	-16.7 ± 0.4	13.4 ± 0.5	Nearshore	Demersal teleost fish	Rocky and coral reefs	Carnivore	Pelagobenthivore
Sphyraenidae	*Sphyraena jello*	Pickhandle barracuda	26	26	61.0 ± 10.3	78.5 ± 1.4	-16.4 ± 0.3	14.5 ± 0.4	Nearshore	Demersal teleost fish	Coral reefs	Carnivore	Pelagobenthivore
Scombridae	*Gymnosarda unicolor*	Dogtooth tuna	7	7	87.1 ± 13.5	75.0 ± 1.5	-16.5 ± 0.2	13.9 ± 0.4	Nearshore	Pelagic-neritic teleost fish	Coral reefs	Carnivore	Pelagobenthivore
	Euthynnus alletteratus	Little tunny	5	5	49.0 ± 3.3	76.6	-17.3 ± 0.2	13.4 ± 0.4	Nearshore	Pelagic-neritic teleost fish	Pelagic-neritic	Carnivore	Pelagivore opportunist
	Rastrelliger kanagurta	Indian mackerel	17	17	25.6 ± 0.6	74.1 ± 1.4	-17.4 ± 0.2	12.1 ± 0.3	Nearshore	Pelagic-neritic teleost fish	Pelagic-neritic	Carnivore	Planktivore
Carcharhinidae	*Carcharhinus amblyrhynchos*	Grey reef shark	1	1	74.0	ND	-16.2	15.6	Nearshore	Pelagic-neritic elasmobranch	Pelagic-neritic	Carnivore	Benthopelagivore
	Carcharhinus brevipinna	Spinner shark	1	1	78.0	ND	-16.5	15.2	Nearshore	Pelagic-neritic elasmobranch	Rocky and coral reefs	Carnivore	Pelagivore opportunist
	Carcharhinus limbatus	Blacktip shark	1	1	139.0	ND	-15.3	16.6	Nearshore	Pelagic-neritic elasmobranch	Rocky and coral reefs	Carnivore	Pelagivore opportunist
	Carcharhinus sorrah	Spot-tail shark	1	1	66.0	ND	-15.8	15.1	Nearshore	Pelagic-neritic elasmobranch	Rocky and coral reefs	Carnivore	Benthopelagivore
	Galeocerdo cuvier	Tiger shark	1	1	169.0	ND	-15.8	15.6	Offshore	Pelagic-oceanic elasmobranch	Benthopelagic	Carnivore	Benthopelagivore
Sphyrnidae	*Sphyrna mokarran*	Great hammerhead	1	1	77.0	ND	-15.8	15.5	Offshore	Pelagic-oceanic elasmobranch	Epipelagic	Carnivore	Benthopelagivore
	Sphyrna lewini	Scalloped hammerhead	16	16	45.4 ± 25.0	ND	-15.9 ± 0.1	16.5 ± 0.3	Nearshore	Pelagic-neritic elasmobranch	Pelagic-neritic	Carnivore	Pelagobenthivore
Xiphiidae	*Xiphias gladius*	Swordfish	132	114	152.9 ± 29.4	ND	-16.7 ± 0.5	14.1 ± 0.6	Offshore	Pelagic-oceanic teleost fish	Bathypelagic	Carnivore	Pelagivore opportunist

Table S2 Recovery rates (mean ± SD) in certified reference materials and detection frequencies in all samples for trace elements analysed by induced coupled plasma (ICP). NC = Not certified.

Trace element	Recovery rates (%)						Detection frequencies (%)
	IAEA-407	IAEA-436	IAEA-452	IAEA-461	DOLT-5	TORT-3	
Ag	NC	NC	NC	NC	82.8 ± 8.3	NC	10
As	98.9 ± 7.0	113.6	101.1 ± 0.3	99.4 ± 0.5	97.7 ± 5.0	105.8 ± 5.7	96
Cd	89.4 ± 6.9	103.1	99.7 ± 0.8	102.6 ± 1.6	99.1 ± 3.6	98.9 ± 5.0	83
Co	NC	101.1	NC	95.0 ± 4.9	96.4 ± 5.3	100.2 ± 3.1	55
Cr	92.3 ± 12.3	NC	86.7 ± 0.5	77.5 ± 0.4	NC	94.9 ± 9.3	68
Cu	99.3 ± 3.2	NC	95.7 ± 2.4	88.5 ± 0.2	97.9 ± 2.2	91.3 ± 6.4	100
Fe	106.7 ± 31.7	99.2	84.2 ± 2.4	83.7 ± 1.3	100.2 ± 10.2	93.3 ± 8.1	90
Mn	95.6 ± 18.4	90.2	91.2 ± 0.2	86.5 ± 0.2	NC	94.0 ± 7.7	100
Ni	NC	112.2	NC	90.8 ± 0.4	NC	95.0 ± 6.6	99
Pb	74.2	NC	86.7 ± 1.0	89.7 ± 0.3	94.9 ± 7.8	95.7 ± 11.4	80
Se	127.6 ± 15.1	94.0	NC	124.2 ± 4.6	108.2 ± 6.2	114.1 ± 12.8	70
Zn	104.6 ± 3.0	NC	100.8	102.1 ± 0.2	104.7 ± 7.0	101.2 ± 5.5	100

Table S3 Mean weight (kg) (Marques-Vidal et al. 2008; US-EPA and US-FDA 2019) and portion weights (g) (WorldBank 2017; US-EPA and US-FDA 2019) used to calculate contributions to recommended daily intakes (RDI) and numbers of servings before reaching provisional tolerable intakes (PTI) (A), RDI and PTI for essential trace elements (American Food and Nutrition Board of the Institute of Medicine National Academy of Sciences 2019a, b) (B), and PTI given by the Joint FAO/WHO Expert Committee on Food Additives (JECFA 2011, 2013) for non-essential trace elements.

A.

Age class	Age subclass	Mean weight (kg)	Portion weight (g)
Children	2-3 years	12	30
	4-8 years	22	72
	9-13 years	36	114
Young Adults	14-19 years	52	156
Adult women	> 19 years	70	156
	> 19 years + pregnant	70	156
	> 19 years + lactating	70	156

B.

		RDI					PTI				
Age class	Age subclass	Cu (µg/d)	Fe (mg/d)	Mn (mg/d)	Se (µg/d)	Zn (mg/d)	Cu (µg/d)	Fe (mg/d)	Mn (mg/d)	Se (µg/d)	Zn (mg/d)
Children	2-3 years	340	7	1.2	20	3	1000	40	2	90	7
	4-8 years	440	10	1.5	30	5	3000	40	3	150	12
	9-13 years	700	8	1.9	40	8	5000	40	6	280	23
Young Adults	14-19 years	890	15	2.2	55	11	8000	45	9	400	34
Adult women	> 19 years	900	18	1.8	55	8	10000	45	11	400	40
	> 19 years + pregnant	1000	27	2	60	11	10000	45	11	400	40
	> 19 years + lactating	1300	9	2.6	70	12	10000	45	11	400	40

C.

Age class	Age subclass	Cd[1] (µg/month)	Hg[2] (µg/week)
Children	2-3 years	300	48
	4-8 years	550	88
	9-14 years	900	144
Young adults	14-19 years	1300	208
Adult women	> 19 years	1750	280
	> 19 years + pregnant	1750	280
	> 19 years + lactating	1750	280

[1] Cd PTI given by the JECFA (2013) was of 25 µg/kg body weight/month.
[2] Hg PTI given by the JECFA (2011b) was of 4 µg/kg body weight/week.

Table S4 Parameters used to estimate Cd, Hg and Pb exposure for Europeans (A) and Hg exposure for Americans in a context of Seychelles capture fisheries products export to Europe and to the USA. In the USA, Hg provisional tolerable intake (PTI) given by the US-EPA and US-FDA (2019) was of 0.1 µg/kg body weight/day (B). For each age class, Hg PTI was thus calculated for the mean weight of each category (CDC 2012; US-EPA and US-FDA 2019); portion weights were also defined by the US-EPA and US-FDA (2019) (B).

A.

Trace element	Species considered	Provisional tolerable intake ($\mu g.g^{-1}$ ww)
Cd	Tuna (*Thunnus* species, *Euthynnus* species, *Katsuwonus pelamis*)	0.1
	Swordfish	0.3
	Fish (excluding species listed above)	0.05
	Crustaceans	0.5
	Cephalopods	1
Hg	Tuna (*Thunnus* species, *Euthynnus* species, *Katsuwonus pelamis*), swordfish and shark	1
	Fish (excluding species listed above)	0.5
	Crustaceans	0.5
Pb	Fish	0.3
	Crustaceans	0.5
	Cephalopods	1

B.

Age subclasses as defined by the US-EPA and the US-FDA	Mean weight (kg)	Portion weight	Hg PTI (µg/day)
2-3 years	15	1 ounce ≈ 28 g	1.5
4-7 years	22	2 ounces ≈ 57 g	2.2
8-10 years	36	3 ounces ≈ 85 g	3.6
11-19 years	60	4 ounces ≈ 113 g	6.0
Women > 19 years, including pregnant and lactating women	75	4 ounces ≈ 113 g	7.5

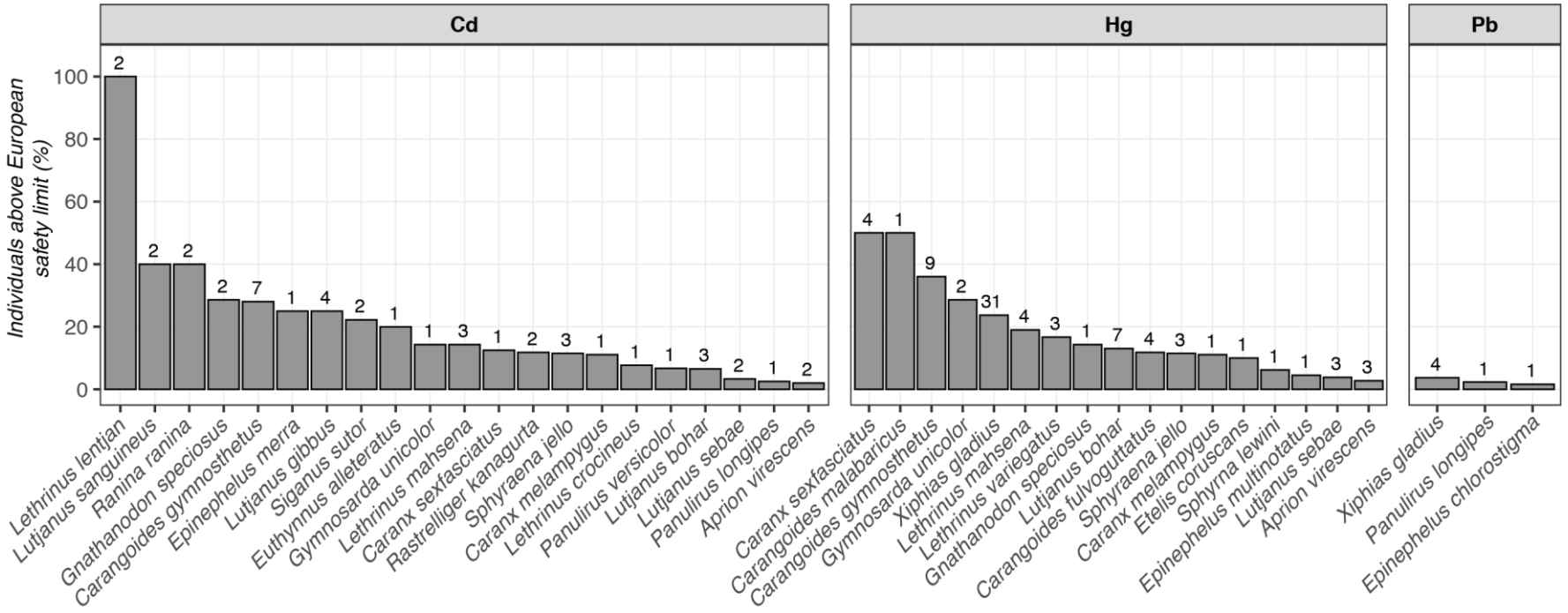

Fig. S1 Percentage of samples for which the concentrations of non-essential trace elements were above the European Commission safety limits (EC 2006, 2011). As the total number of sampled individuals was highly variable, the number of samples above safety limits is also indicated above each bar.

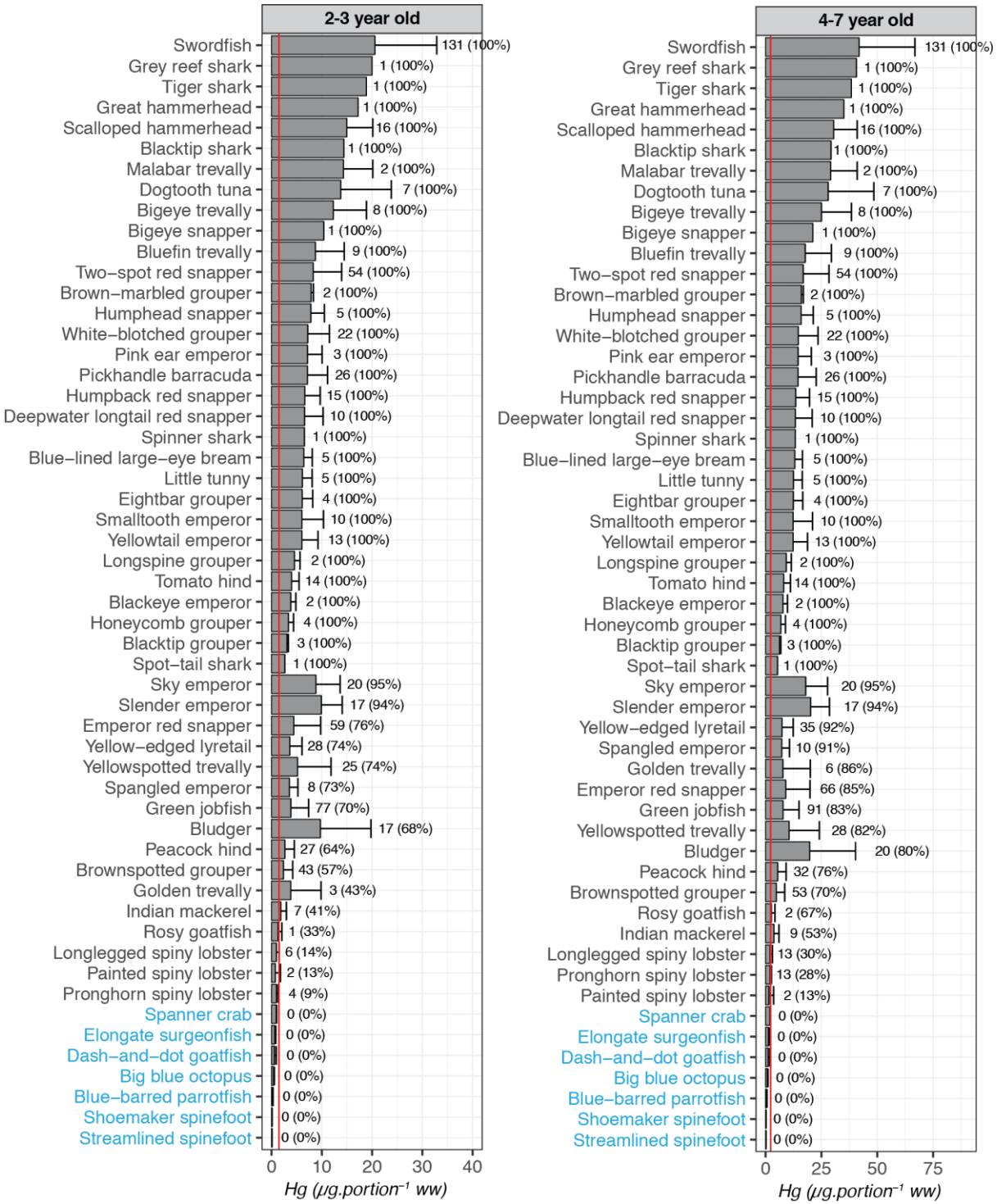

Fig. S2 Mercury (Hg) concentrations in a portion of each analysed species for each age class determined by the US-EPA and US-FDA (2019). Red lines indicate the safety limit for each age class, given in Table S4 (US-EPA and US-FDA 2019); the number of individuals above this limit are given above each bar and corresponding proportions are given between brackets. Species for which no individual was above the limit, regardless of the age class, are indicated in blue.

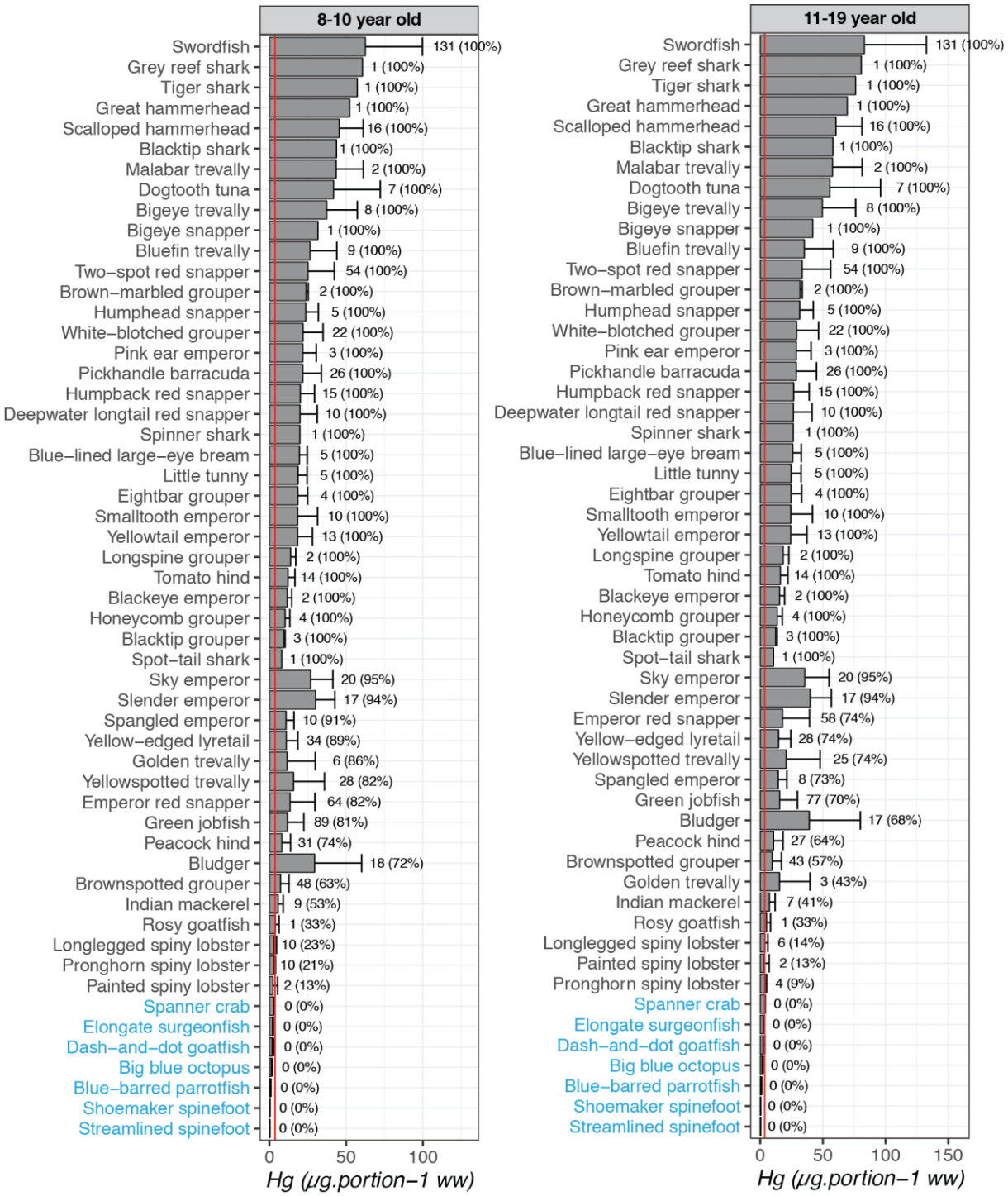

Fig. S2 Mercury (Hg) concentrations in a portion of each analysed species for each age class determined by the US-EPA and US-FDA (2019). Red lines indicate the safety limit for each age class, given in Table S4 (US-EPA and US-FDA 2019); the number of individuals above this limit are given above each bar and corresponding proportions are given between brackets. Species for which no individual was above the limit, regardless of the age class, are indicated in blue. (continued)

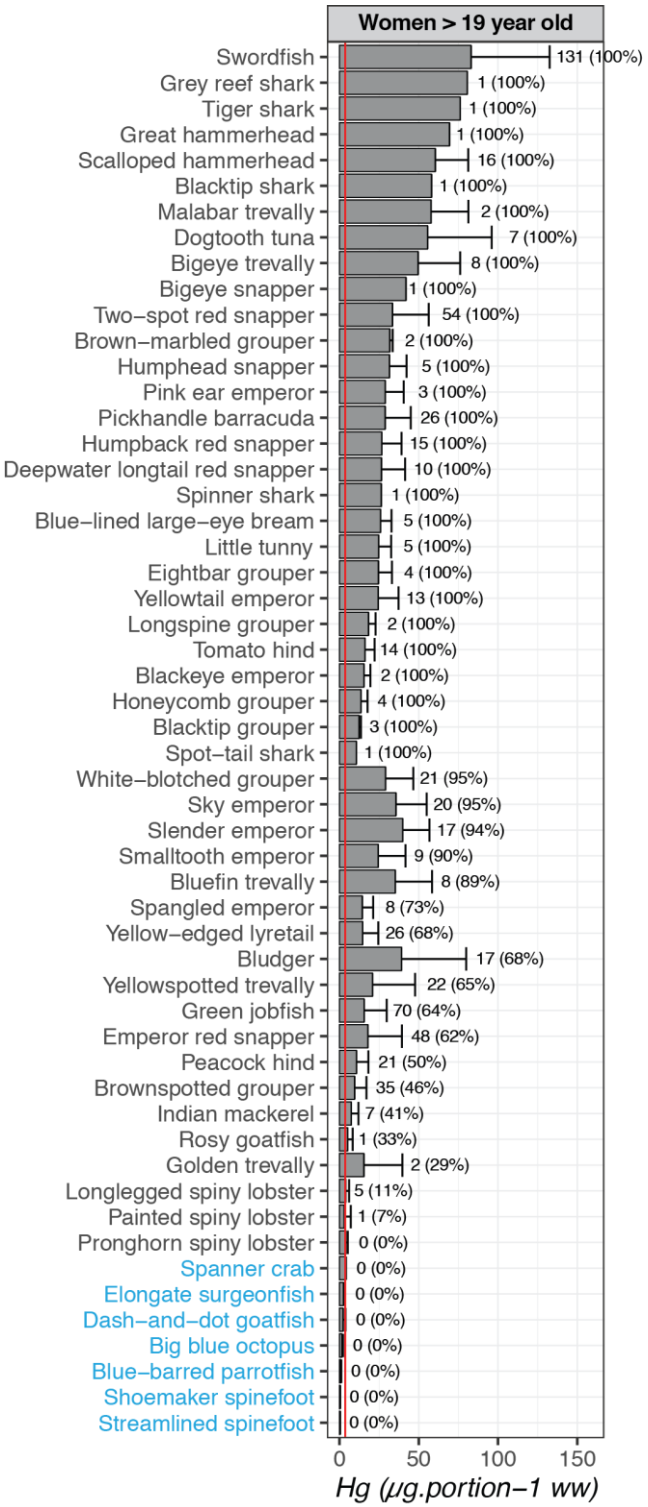

Fig. S2 Mercury (Hg) concentrations in a portion of each analysed species for each age class determined by the US-EPA and US-FDA (2019). Red lines indicate the safety limit for each age class, given in Table S4 (US-EPA and US-FDA 2019); the number of individuals above this limit are given above each bar and corresponding proportions are given between brackets. Species for which no individual was above the limit, regardless of the age class, are indicated in blue. (continued)

Text S1

The mathematical correction method consists of mathematical models that predict lipid-corrected isotope values using stable isotope analysis of bulk tissue and different covariates, including a proxy of lipid content. By first characterising the relationship between the difference in $\delta^{13}C$ between lipid-free and bulk values in a sample and the sample's lipid content or its proxy (generally the C:N ratio in the bulk sample), it is then possible to establish the correction equation to obtain a corrected value of $\delta^{13}C$ (Logan *et al*. 2008).

To allow for $\delta^{13}C$ correction in swordfish muscle tissues, 32 swordfish muscle tissue samples were analysed for stable isotopes of carbon and nitrogen before (i.e. measure of $\delta^{13}C_{bulk}$ and $C{:}N_{bulk}$) and after lipid removal (i.e. measure of $\delta^{13}C_{lipid\text{-}free}$). In order to model the relationship between $\Delta\delta^{13}C$ (i.e. $\delta^{13}C_{lipid\text{-}free}$ - $\delta^{13}C_{bulk}$) and $C{:}N_{bulk}$, several models were tested. The first tested model was based on the McConnaughey and McRoy (1979) model:

$$\Delta\delta^{13}C = D\ (\theta + \frac{3.90}{1+\frac{287}{L}}) \quad \textbf{(Eq. 1)}$$

where L is the lipid content measured or calculated as $L = \frac{93}{1+(0.246*C:Nbulk-0.775)^{-1}}$, D is the protein-lipid discrimination and θ a constant adjusted to the dataset.

The second tested model was developed by Logan *et al.* (2008), from the model of McConnaughey and McRoy (1979):

$$\Delta\delta^{13}C = \frac{D * C:N_{bulk}+a}{C:N_{bulk}+b} \quad \textbf{(Eq. 2)}$$

where D is the protein-lipid discrimination. The y-asymptote corresponds to D, while the model estimate $C{:}N_{lipid\text{-}free}$ is represented by –a/D (x-intercept). The y-intercept, a/b, is the $\delta^{13}C$ difference when $C{:}N_{bulk}$ equals to 0.

The third tested model was based on the Fry (2002) equation:

$$\Delta\delta^{13}C = P - \frac{P*F}{C:N_{bulk}} \quad \textbf{(Eq. 3)}$$

where P represents the protein-lipid discrimination and F represents the $C{:}N_{lipid\text{-}free}$.

A log-linear model was also tested, with the relationship between the difference between $\delta^{13}C_{lipid\text{-}free}$ and $\delta^{13}C_{bulk}$ and the $C{:}N_{bulk}$ following the below formula:

$$\Delta\delta^{13}C = \beta_0 + \beta_1 \ln(C{:}N_{bulk}) \quad \textbf{(Eq. 4)}$$

where the model estimate of $C{:}N_{lipid\text{-}free}$ is represented by $e^{(-\beta 0/\beta 1)}$ Logan *et al.* (2008).

Finally, the above models were compared to a classic linear model:

$$\Delta\delta^{13}C = a + b * C{:}N_{bulk} \quad \textbf{(Eq. 5)}$$

Cross-validation was used to assess the predictive performance of each model. First, each model was trained with a random subset of the data (i.e. 2/3 of the dataset), and optimal parameters were calculated for this subset. For this, the *nls* function of the *nlstools* package in R was used. As starting values were needed in order to obtain the optimal parameter values, the parameter estimates given in Logan *et al.* (2008) were used for equations 1 to 4 (Table 1). For equation 5, the regression was first modelled on all the dataset and the calculated intercept and slope were used as starting values. Once the parameters were obtained, corrected values of $\delta^{13}C$ were calculated from the validation dataset (i.e. 1/3 of the complete dataset) and compared to measured $\delta^{13}C_{lipid\text{-}free}$ using paired Wilcoxon's tests. The mean square error (MSE) and mean absolute error (MAE) were also calculated. The process of cross-validation on random dataset was repeated 500 times. For each equation, the percentage of good predictions was also calculated, based from the number of acceptable p-values (i.e. $p > 0.05$) among the 500 iterations.

Table 1 Parameters estimates given in Logan *et al*. (2008) and used as starting values for the estimation of optimal parameter values.

Equation	Parameters estimates
1	D = 7.209 ± 0.148 ; θ = 0.015 ± 0.006
2	D = 7.415 ± 0.558 ; a = -22.732 ± 1.572 ; b = 0.746 ± 0.573
3	P = 6.699 ± 0.119 ; F = 3.098 ± 0.018
4	β_0 = -4.763 ± 0.142 ; β_1 = 4.401 ± 0.099

Visually, equations 1, 2 and 3 were the best models describing the data (Fig. 1). **Equation 2 (Logan *et al.* 2008)** had the highest proportion of good predictions, but also the lowest MSE and MAE (Table 2), and **was thus selected as the best model**. The equation used to correct $\delta^{13}C_{bulk}$ for lipid content before further data treatment was the following:

$$\delta^{13}C_{corrected} = \frac{\mathbf{7.05} * \boldsymbol{C{:}N_{bulk}} - \mathbf{22.4}}{\boldsymbol{C{:}N_{bulk}} - \mathbf{0.44}} + \delta^{13}C_{bulk}$$

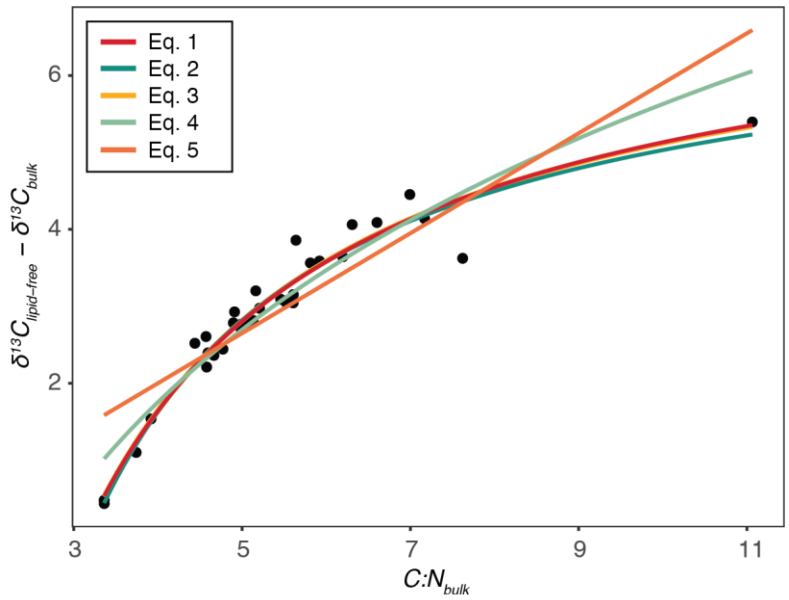

Fig. 1 Model fits to differences in swordfish muscle bulk $\delta^{13}C$ and lipid-free $\delta^{13}C$ plotted against bulk C:N ratio.

Table 2 Model parameters and assessment of the prediction of the five models using a cross-validation procedure. MSE = mean square error, MAE = mean absolute error.

Model	Estimated parameters	$\delta^{13}C_{corr} - \delta^{13}C_{lipid-free}$ (‰)	Wilcoxon test – p value	MSE	MAE	Good predictions (%)
Eq. 1	D = 7.69 ± 0.01 θ = 0.007 ± 0.001	0.0004 ± 0.0039	0.49 ± 0.01	0.233 ± 0.003	0.178 ± 0.002	92.8
Eq. 2	D = 7.05 ± 0.00 a = -22.4 ± 0.0 b = -0.44 ± 0.00	0.0008 ± 0.0026	0.59 ± 0.01	0.211 ± 0.003	0.163 ± 0.002	99.0
Eq. 3	P = 7.46 ± 0.00 F = 3.12 ± 0.00	0.001 ± 0.003	0.58 ± 0.01	0.218 ± 0.003	0.164 ± 0.002	97.4
Eq. 4	β_0 = -4.11 ± 0.00 β_1 = 4.23 ± 0.00	0.004 ± 0.004	0.57 ± 0.01	0.314 ± 0.003	0.235 ± 0.003	95.4
Eq. 5	a = -0.6 ± 0.0 b = 0.65 ± 0.00	0.004 ± 0.006	0.46 ± 0.01	0.468 ± 0.005	0.348 ± 0.004	92.0

Text S2

1. Essential trace element supply and risk associated with too high intake

In order to assess essential trace element benefit through seafood consumption, measured concentrations of Co, Cu, Fe, Mn, Se and Zn were compared to recommended daily intakes (RDI) set by the American Food and Nutrition Board of the Institute of Medicine National Academy of Sciences (2019a). Calculations were made for all age subclasses and status given in the guidelines (i.e. 2-3 year old, 4-8 year old, 9-13 year old, 14-18 year old, 19+ year old, pregnant women and lactating women) and were then summarised into the three chosen main age classes (i.e. children, 2-13 year old; young adults, 14-18 year old; and adult women, 19+ year old, includes pregnant and lactating women). For this, the percentage of contribution to RDI was calculated for each sampled individual of each species with the following equation:

$$\%RDI = ([TE] \times portion\ weight) \times 100 / RDI \qquad \textbf{(Eq. 1)}$$

with [TE] the concentrations of the considered trace element; portion weight the weight of the portion for the considered age subclass; and RDI the recommended daily intake for the considered trace element. To summarise data into the three age classes, all data related to the corresponding age subclasses were grouped (i.e. 2-3 year old with 4-8 year old and 9-13 year old for Children; 14-18 year old for Young adults; and women 19+ year old with lactating and pregnant women for Adult women). Then, the confidence interval at 95% (CI95%) was calculated for each trace element and each age class as following:

$$CI95\% = [mean - (1.96 \times SE); mean + (1.96 \times SE)] \qquad \textbf{(Eq. 2)}$$

with SE the standard error.

As essential trace elements are toxic above certain levels, these concentrations were also compared to provisional tolerable intakes (PTI) set by the American Food and Nutrition Board of the Institute of Medicine National Academy of Sciences (2019b). Again, calculations were made for all age subclasses and status given in the guidelines, and were then summarised into the three chosen main age classes. The number of servings necessary before reaching PTI was calculated for each sampled individual of each species with the following equation:

$$Number\ of\ servings = PTI / ([TE] * portion\ weight) \qquad \textbf{(Eq. 3)}$$

with PTI the daily provisional tolerable intake for the considered trace element; [TE] the concentrations of the considered trace element; and portion weight the weight of the portion for the considered age subclass. Then, like for %RDI data, all data related to the corresponding age subclasses were grouped and the CI95% was calculated for each trace element and each age class. CI95% using Eq. 2.

All parameters used in Eq. 1 and 3 are presented in Table S3.

2. Potentially essential trace element supply

In the case of potentially essential trace elements, no RDI or PTI were found for Cr and Ni. As concentrations were compared to the RDI presented in Nielsen (1991) (i.e. 12 µg/day for adults) and the mean [CI95%] contribution to RDI (%) was calculated for adults as described above (i.e. using Eq. 1 and 2). Parameters used in Eq. 1 are presented in Table S3. No PTI was found for As, as the PTI set by the JECFA was withdrawn in 2011 (JECFA 2011a). However, it is known that the main toxic forms of As are inorganic As (iAs) (Sharma and Sohn 2009). Thus, the concentrations of iAs in analysed seafood species were estimated by using the proportions of iAs in seafood calculated by Uneyama *et al*. (2007) (i.e. 4.4% in fish and 2.2% in crustaceans).

3. Non-essential trace element exposure

In order to assess non-essential trace element exposure, Cd and Hg concentrations were compared to PTI set by the Joint FAO/WHO Expert Committee on Food Additives (JECFA 2011b, 2013). In order to be consistent with the method used for essential trace elements, calculations were again made for all age subclasses and status given in the guidelines (i.e. 2-3 year old, 4-8 year old, 9-13 year old, 14-18 year old, 19+ year old, pregnant women and lactating women) and were then summarised into the three chosen main age classes (i.e. children, 2-13 year old; young adults, 14-18 year old; and adult women, 19+ year old, includes pregnant and lactating women). Again, number of servings before reaching PTI were calculated for each analysed individual of each species using Eq. 3; data related to each age class were grouped together and the CI95% was calculated using Eq. 2. Parameters used in Eq. 3 are presented in Table S3.

In a context of fish export to Europe and to the United States, non-essential trace elements were also compared to limits set by the European Commission (EC 2006, 2011) and by the United States Environmental Protection Agency and the United States Food and Drug Administration (US-EPA and US-FDA 2019). Again, the US-EPA-FDA limit for Hg was expressed as $\mu g.bw^{-1}$, thus used limits were for the age classes defined by the US-EPA and US-FDA (2019) and presented in Table S4.

4. Interaction between mercury (Hg) and selenium (Se)

In order to take into account the interaction ability of Hg with Se, the molar ratio of Hg above Se (MHg:MSe) and the Health Benefit Value of Se (HBVSe) were calculated according to the following equations (Ralston *et al.* 2007, 2015):

$$MHg:MSe = (C_{Hg}/M_{Hg}) / (C_{Se}/M_{Se}) \qquad \textbf{(Eq. 4)}$$

$$HBVSe = [(Mse - MHg)/MSe] \times (MSe + MHg) \quad \textbf{(Eq. 5)}$$

with MHg and MSe the number of moles of Hg and Se respectively; C_{Hg} and C_{Se} the concentrations of Hg and Se, respectively; and M_{Hg} and M_{Se} the molar masses of Hg and Se, respectively (200.59 $g.mol^{-1}$ for Hg and 78.96 $g.mol^{-1}$ for Se).

It is considered that Se and Hg bind in a molar ratio of 1:1 in human tissues (Ralston *et al.* 2007). Thus, the concentration of theoretically bioavailable Se after interaction with Hg was estimated using the following equation:

$$\text{Concentration of theoretically bioavailable Se} = (MSe - MHg) \times M_{Se} \quad \textbf{(Eq. 6)}$$

For each species, contribution to RDI and number of servings necessary to reach PTI associated to concentrations of theoretically bioavailable Se were calculated using the method described above (Eq. 1, 2 and 3). All parameters used in Eq. 1 and 3 to assess Se benefit and exposure are presented in Table S3.

References of supplementary data

American Food and Nutrition Board of the Institute of Medicine National Academy of Sciences (2019a) Dietary Reference Intakes (DRIs): Recommended dietary allowances and adequate intakes, elements. URL: https://ods.od.nih.gov/Health_Information/Dietary_Reference_Intakes.aspx.

American Food and Nutrition Board of the Institute of Medicine National Academy of Sciences (2019b) Dietary Reference Intakes (DRIs): Tolerable upper intake levels, elements. URL: https://www.ncbi.nlm.nih.gov/books/NBK545442/table/appJ_tab9/?report=objectonly.

CDC (2012) Anthropometric reference data for children and adults : United States, 2007-2010.

EC (2006) 1881/2006. Setting maximum levels for certain contaminants in foodstuffs. Off J Eur Communities 364:5–24.

EC (2011) COMMISSION REGULATION (EU) No 420/2011 of 29 April 2011 amending Regulation (EC) No 1881/2006 setting maximum levels for certain contaminants in foodstuffs. Off J Eur Union L111:3–6.

Froese R, Pauly D (2020) FishBase. World Wide Web electronic publication. URL: www.fishbase.org.

Fry B (2002) Stable isotopic indicators of habitat use by Mississippi River fish. J North Am Benthol Soc 21:676–685.

JECFA (2011a) Arsenic. URL: https://apps.who.int/food-additives-contaminants-jecfa-database/chemical.aspx?chemID=1863.

JECFA (2011b) Mercury. URL: https://apps.who.int/food-additives-contaminants-jecfa-database/chemical.aspx?chemID=1806.

JECFA (2013) Cadmium. URL: https://apps.who.int/food-additives-contaminants-jecfa-database/chemical.aspx?chemID=1376.

Logan JM, Jardine TD, Miller TJ, Bunn SE, Cunjak RA, Lutcavage ME (2008) Lipid corrections in carbon and nitrogen stable isotope analyses: comparison of chemical extraction and modelling methods. J Anim Ecol 77:838–846. doi: 10.1111/j.1365-2656.2008.01394.x

Marques-Vidal P, Madeleine G, Romain S, Gabriel A, Bovet P (2008) Secular trends in height and weight among children and adolescents of the Seychelles, 1956-2006. BMC Public Health 8:1–9. doi: 10.1186/1471-2458-8-166

McConnaughey T, McRoy CP (1979) Food-web structure and the fractionation of Carbon isotopes in the bering sea. Mar Biol 53:257–262. doi: 10.1007/BF00952434

Nielsen FH (1991) Nutritional requirements for boron, silicon, vanadium, nickel, and arsenic: Current knowledge and speculation. FASEB J 5:2661–2667.

Palomares MLD, Pauly D (2020) SeaLifeBase. World Wide Web electronic publication. URL: www.sealifebase.org.

Ralston NVC, Blackwell JL, Raymond LJ (2007) Importance of molar ratios in selenium-dependent protection against methylmercury toxicity. Biol Trace Elem Res 119:255–268. doi: 10.1007/s12011-007-8005-7

Ralston NVC, Ralston CR, Raymond LJ (2015) Selenium Health Benefit values: Updated criteria for mercury risk assessments. Biol Trace Elem Res 171:262–269. doi: 10.1007/s12011-015-0516-z

Sharma VK, Sohn M (2009) Aquatic arsenic: Toxicity, speciation, transformations, and remediation. Environ Int 35:743–759. doi: 10.1016/j.envint.2009.01.005

Uneyama C, Toda M, Yamamoto M, Morikawa K (2007) Arsenic in various foods: Cumulative data. Food Addit Contam 24:447–534. doi: 10.1080/02652030601053121

US-EPA, US-FDA (2019) EPA-FDA Fish Advice: Technical Information. URL: https://www.epa.gov/fish-tech/epa-fda-fish-advice-technical-information.

WorldBank (2017) Third south west indian ocean fisheries governance and shared growth project (SWIOFish3). Washington, DC

- SUPPLEMENTARY DOCUMENT 2 -

Habitat degradation increases interspecific trophic competition between three spiny lobster species in Seychelles

Magali A. SABINO[1,2], Rodney GOVINDEN[1], Heidi PETHYBRIDGE[3], Laura BLAMEY[4], Fabienne LE GRAND[5], Fany SARDENNE[5], Maria ROSE[1], Paco BUSTAMANTE[2,6], Nathalie BODIN[1,7,8*]

[1] Seychelles Fishing Authority (SFA), Fishing Port, Victoria, Mahé, Republic of Seychelles

[2] Littoral Environnement et Sociétés (LIENSs), UMR 7266 CNRS - La Rochelle Université, 2 rue Olympe de Gouges, 17000 La Rochelle, France

[3] CSIRO Oceans and Atmosphere, Hobart, Tasmania, Australia

[4] CSIRO Oceans and Atmosphere, Brisbane, Queensland, Australia

[5] Univ Brest, CNRS, IRD, Ifremer, LEMAR, IUEM, F-29280, Plouzané, France

[6] Institut Universitaire de France (IUF), 1 rue Descartes 75005 Paris, France

[7] Institute for Research and Development (IRD), Fishing Port, Victoria, Mahé, Seychelles

[8] Sustainable Ocean Seychelles (SOS), BeauBelle, Mahé, Republic of Seychelles

*Email: natbod@gmail.com

Published in *Estuarine, Coastal and Shelf Science* (2021 - n°256, 107368)
doi: 10.1016/j.ecss.2021.107368

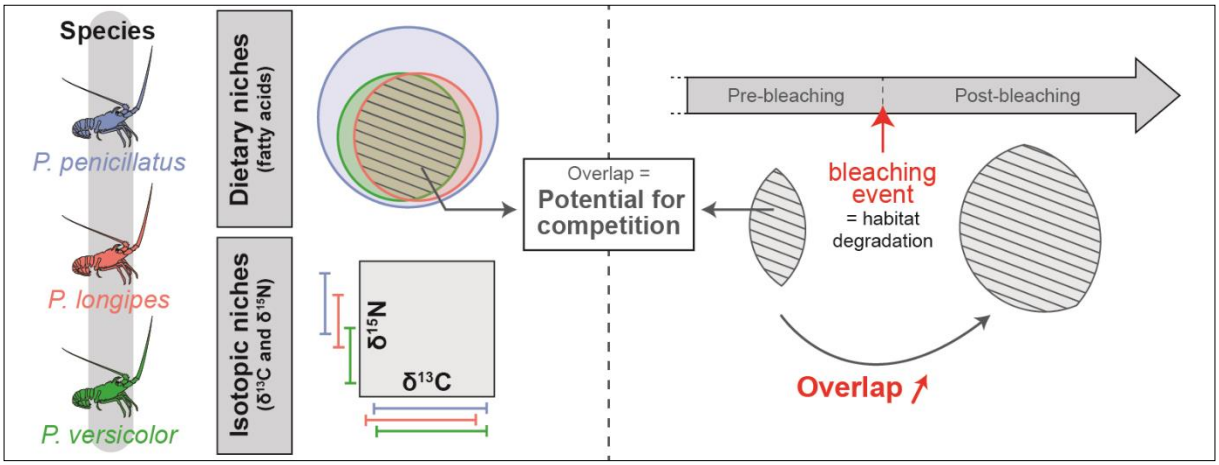

Abstract

Spiny lobsters (*Panulirus penicillatus*, *P. longipes* and *P. versicolor*) are heavily dependent on habitats like coral reefs, known to be highly vulnerable to climate change-driven degradation. Yet, little is known about their trophic ecology and their adaptive capacity to a changing environment. In this study, we used fatty acids (FA) analysed in the hepatopancreas and $\delta^{13}C$ and $\delta^{15}N$ stable isotopes analysed in the tail muscle of three spiny lobster species from the Seychelles coastal waters to (1) infer habitat usage, dietary patterns and potential for resource competition and (2) investigate the effects of reef type and coral bleaching on their trophic niche metrics. We found that there was a potential for interspecific competition between the three species, shown by their high dietary overlap (mean FA niche overlap ranging from 71.2% to 99.5% for *P. longipes* and *P. versicolor* in *P. penicillatus*) and similar habitat use ($\delta^{13}C$ value ranges). *P. penicillatus*, the largest of the three psecies, was more a generalist than the two other species (i.e. had a larger FA niche) and *P. versicolor* seemed to feed on smaller/earlier life stage prey than *P. longipes* (based on differences in $\delta^{15}N$ values). The potential for resource competition of Seychelles spiny lobsters appeared higher in granite than carbonate reefs, and in post-2016 coral bleaching reefs. Our results suggest that *P. penicillatus* could have a greater adaptive capacity to climate change due to its higher dietary plasticity and that competition between Seychelles spiny lobsters may increase in the future as the frequency and severity of bleaching events is predicted to increase with climate change.

Keywords: Resource partitioning; Climate change; Coral bleaching; Decapod crustaceans; Benthic predators; Western Indian Ocean

1. Introduction

The stability, resilience and productivity of high-value marine invertebrate populations are heavily dependent on prey and habitat quality (Österblom et al. 2008). Accurately identifying the habitat use and trophic niche of such species is thus of great importance to better understand stock dynamics. Sympatric species, sharing similar ecological needs such as habitat and food preferences, are interesting case studies as their population dynamics may also be influenced by interspecific interactions (Mason et al. 2011). Sympatric consumers are thought to co-exist stably when resources are sufficient (Carvalho and Davoren 2020) while possibly displaying high levels of interspecific competition when resource supply is limited (Nie et al. 2019). Identifying and quantifying interspecific diet and habitat-niche relationships are therefore key objectives to understand sympatric species' resource partitioning and characterise their potential for competition (Costa-Pereira et al. 2019).

Spiny lobsters provide an important economic resource in different areas of the world (Phillips 2013). In the Seychelles (Western Indian Ocean), catches mainly include *Panulirus penicillatus* (pronghorn spiny lobster), *Panulirus longipes* (longlegged spiny lobster) and *Panulirus versicolor* (painted spiny lobster) (Seychelles Fishing Authority 2016). Despite management policies in place, stocks have remained unstable, with unpredictable catch variability from one fishing season to another (e.g. 30.1 kg by fishing trip during the 1994/1995 fishing season *vs* 10.1 kg by fishing trip during the 2012/2013 fishing season) (Seychelles Fishing Authority 2016). In an attempt to sustainably manage the fishery, seasonal closures are implemented to allow stocks to recover (e.g. 2017/2018 and 2018/2019 fishing seasons) (Seychelles Fishing Authority 2018).

Habitat quality, including the type and complexity of coverage, is fundamentally important for spiny lobsters in respect of their foraging and antipredation strategies (Holthuis 1991; MacArthur et al. 2011). Spiny lobsters are non-gregarious nocturnal species that are found mainly in coastal environments, such as coral and rocky reefs, where they usually use the crevices to hide from predators during the day, while they leave their den at dusk to feed and mate during the night (Holthuis 1991). However, coastal reefs are under high human pressure in the Seychelles due to increasing coastal development and global climate change (Khan and Amelie 2015). In the last 25 years, coral reefs and granitic reefs supporting encrusting corals have been degraded through multiple bleaching events, with the 2016 bleaching event affecting around 50% of hard corals in the Seychelles (Obura et al. 2017). As spiny lobsters are considered generalist feeders, their diet composition is thought to be highly dependent on prey availability, depending on their habitat characteristics (Blamey et al. 2019). A modification of prey and habitat quality and availability through habitat degradation could thus have altered spiny lobsters' diet and level of interspecific competition, further influencing stock dynamics.

Yet, there is a lack of knowledge on spiny lobsters' foraging behaviour in the Western Indian Ocean, particularly in the Seychelles region, and their adaptive capacity to habitat change.

Trophic ecology of marine species can be studied through the use of ecological tracers like stable isotopes (SI) of carbon ($\delta^{13}C$) and nitrogen ($\delta^{15}N$) and fatty acid (FA) trophic markers. $\delta^{13}C$ allows for the identification of primary production sources while $\delta^{15}N$ gives information about the trophic position of an organism (Post 2002). The FA profiles observed in the digestive tissues of a consumer reflect the FA composition of ingested prey and thus can give insights into the consumer's diet (Iverson 2009). By studying spatial and temporal changes in the biochemical composition of consumers, it is possible to examine intraspecific and interspecific variations in their trophic ecology. For this, trophic niches inferred from SI or FA data are particularly useful as their metrics (i.e. niche size and probability of niche overlap) give both intra- and interspecific information. Typically, a species' niche size can be used as a proxy for the diversity of biochemically distinct prey eaten by this species (i.e. intraspecific variability), while the probability of overlap between two species gives indications on the degree of similarity of the biochemical composition of their prey (i.e. interspecific variability) (Costa-Pereira et al. 2019). Many studies successfully combined SI and FA to study trophic overlap between co-occurring species (e.g. Connan et al. 2014; Sardenne et al. 2016; Brewster et al. 2017).

Our study assessed the FA and SI composition of three species of spiny lobsters from the Seychelles coastal waters with the main aim to examine interspecific differences and spatio-temporal patterns in their habitat use, dietary inferences and trophic niche metrics. A particular focus was to examine the effects of habitat type and habitat degradation through coral bleaching on the potential for resource competition (i.e. dietary overlap) between the three species.

2. Material and methods

2.1. Study area and sample collection

Panulirus penicillatus, P. longipes and *P. versicolor* were sampled as part of the annual Participatory Lobster Monitoring Program led by the Seychelles Fishing Authority (SFA) in collaboration with local fishers (Seychelles Fishing Authority 2014). A total of 105 spiny lobsters (47 *P. penicillatus*, 43 *P. longipes* and 15 *P. versicolor*), were caught in several fishing areas on the west coast of the island of Mahé, Seychelles, during five sampling campaigns in October/November from 2014 to 2018 (Fig. 1). The spiny lobsters were caught at dusk, when they leave reef crevices and thus are the most catchable, using snorkel gear and flashlights. The date, GPS location and carapace length (to the nearest 0.1 cm) were recorded for each individual. Finally, a piece of tail muscle and the hepatopancreas were retrieved, stored in amber glass at -20°C for a maximum of eight days before being transferred to -80 °C at the SFA

Research laboratory. Hepatopancreas tissue samples remained at -80°C for FA analysis, and tail muscle tissues were freeze-dried over 72 h and stored in a dry environment for SI analysis. Detailed numbers of the spiny lobsters' tissues sampled and analysed for FA and SI tracers across years and different habitat types (carbonate and granite reefs) are given in the supplementary material (Table S1).

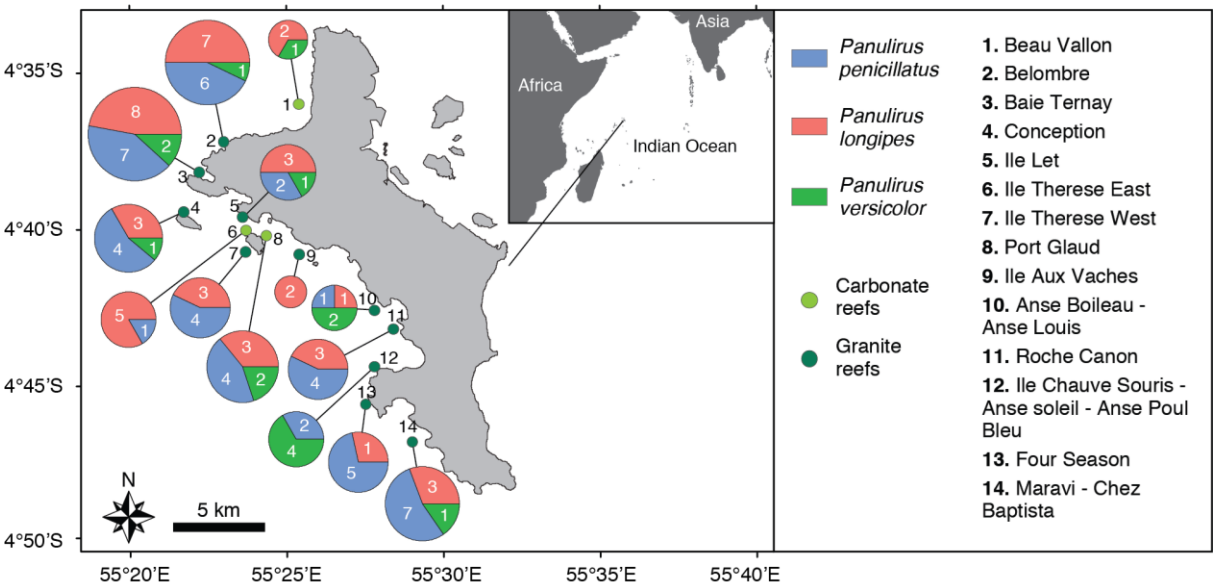

Fig. 1 Sampling locations of the three spiny lobster species caught from the west coast of Mahé (Seychelles, Western Indian Ocean) during 2014-2018. The number of individuals caught per species is indicated in the corresponding chart; size of charts is proportional to the total number of spiny lobsters per site.

2.2. Fatty acid analyses

A total of 64 hepatopancreas samples were analysed for FA at the LIPIDOCEAN platform of the LEMAR (France). Lipids were extracted from around 200 mg of wet tissue using 6 mL of chloroform:methanol (2:1 v/v) in glass vials. Samples were then vortexed, sonicated in an ultrasonic bath for 15 min and stored at -20 °C (maximum 24 h). Fatty acid methyl ester (FAME) were prepared using 1 mL of lipid extract in which 20 µL of an internal standard (tricosanoic acid, C23:0, 0.115 µg/µL) was added to allow FA quantification. Samples were then trans-esterified with 800 µL of methanolic sulphuric acid (3.4% v/v) at 100 °C for 10 min. After cooling, formed FAMEs were retrieved by adding 800 µL of hexane and washed with hexane-saturated distilled water (1.5 mL). FAMEs were separated using a gas chromatograph (Varian CP3800) with auto-sampler equipped with both polar and non-polar capillary columns (ZB-WAX, 30 m length x 0.25 mm i.d. x 0.25 µm film thickness, Phenomenex; and ZB-5 30 m length x 0.25 mm i.d. x 0.25 µm film thickness, Phenomenex), a splitless injector and a flame ionization detector. Oven temperature was raised to 150 °C at 50 °C/min, then to 170 °C at 3.5 °C/min, to 185 °C at 1.5 °C/min, to 225 °C at 2.4 °C/min, and finally to 250 °C at 5.5 °C/min. The identification of FAMEs was carried out by comparison of retention times with four commercially available standards

(37-components, BAME, PUFA no. 1, and PUFA no. 3 FAME mix; Supelco). The concentration for each FA was converted from the area of the chromatogram peaks by using the C23:0 peak area as reference. The analytical variability (mean CV) was 8.1 %, calculated using Supelco 37-component FAME mix.

FAs were labelled according to their traditional C:Xn-Y nomenclature where C is the number of carbons, X is the number of double bonds, and Y is the position of the first double bond from the terminal methyl end of the molecule. In non-methyl interrupted (NMI) FA, double bonds are not separated by only one methyl group, thus they are labelled as C:X NMI (n), where C is the number of carbons, X the number of double bonds and n the position(s) of the double bonds from the terminal methyl end of the molecule. FAs were expressed as percentage of total FA (% TFA), and means are presented with their standard error (mean ± SE).

2.3. Stable isotope analyses

A total of 105 tail muscle samples were analysed for SI of carbon and nitrogen at the LIENSs laboratory (France). As Seychelles spiny lobsters have low total fat content (mean of 0.74 ± 0.14% wet weight, measured for five *P. penicillatus* and five *P. longipes* in this study), no lipid removal before SI analysis or no lipid correction on isotopic data was applied. Samples were ground to powder and aliquots of 0.3-0.5 mg were placed in tin capsules. Carbon and nitrogen SI ratios were determined with a continuous-flow mass spectrometer Thermo Scientific Delta V Advantage coupled to an elemental analyser Thermo Scientific Flash 2000. Measurements of international isotopic standards of known $\delta^{13}C$ and $\delta^{15}N$ were conducted: USGS-61 and USGS-62. Results are expressed in the δ unit notation as deviations from standards (Vienna Pee Dee Belemnite for $\delta^{13}C$ and atmospheric nitrogen for $\delta^{15}N$) following the formula: $\delta^{13}C$ or $\delta^{15}N = [(R_{sample}/R_{standard}) - 1] \times 1000$, where R is $^{13}C/^{12}C$ or $^{15}N/^{14}N$, respectively. Measurement errors (SD) of SI, calculated on all measured values of $\delta^{13}C$ and $\delta^{15}N$ in isotopic reference materials, were < 0.10 ‰ for both the nitrogen and carbon isotope measurements. For each sample, the carbon-to-nitrogen (C:N) ratio never exceeded 3.5 confirming that there was no need for lipid normalisation on spiny lobsters' carbon stable isotope values (Post et al. 2007).

2.4. Statistics

All statistical tests and data analyses were performed using R 3.5.2 software (R Core Team 2018). Prior to any univariate analysis, data were tested for normality and homoscedasticity. An analysis of variance (ANOVA) or a Kruskal-Wallis test was used to compare carapace lengths and $\delta^{13}C$ and $\delta^{15}N$ values between species. When a difference was significant ($P < 0.05$), a post-hoc test was performed (Tukey's HSD after ANOVA and Dunn test with Benjamini-Hochberg adjustment after Kruskal-Wallis).

ANOVA, Kruskal-Wallis and Tukey's HSD were computed using the included *stats* package in R, while Dunn post-hoc test was computed using the *FSA* R package.

To compare trophic niches between species, FA and SI niches were computed and their sizes and overlaps were calculated using the *nicheROVER* R package (see Swanson et al. 2015 for details on the method). This package uses a model developed in a Bayesian framework to calculate probabilistic niche metrics (i.e. niche size and probabilities of overlap) as opposed to the more traditional geometric-based computations. This method is insensitive to sample size and can account for statistical uncertainty. FA and SI niches were computed separately, and niche metrics were calculated using 1000 iterations of ellipses. More specifically, niche overlaps were expressed in percentage of the niche of each species and represent the probability of species A being found in the niche of species B. As FA profiles contained a high number of dimensions (i.e. 23 FAs above trace levels, > 0.8% TFA), non-metric multidimensional scaling (nMDS) ordinations using a Bray-Curtis dissimilarity matrix were first generated using the *metaMDS* function from the R *vegan* package. Then, nMDS coordinates of dimensions 1 and 2 were used to compute FA niches. For SI, $\delta^{15}N$ and $\delta^{13}C$ values were used to calculate isotopic niches. For visual representation, mean ellipses coordinates were calculated using the mean coordinates of the 1000 ellipses from the Bayesian model. For representation of statistical uncertainty, coordinates of the ellipses for the confidence interval at 95% (CI95% ellipses) were also calculated using the mean coordinates of the 2.5% smallest ellipses, and the 2.5% largest ellipses.

To identify potential prey implicated in interspecific trophic overlap and in trophic segregation, we used well known FA trophic markers, including trophic markers of bacteria (iso-branched FA and 18:1n-7), microalgae (16:1n-7, 20:5n-3 and 22:6n-3), macroalgae (18:1n-9, 18:2n-6, 20:4n-6, 20:5n-3 and 22:6n-3) and bivalve molluscs and carnivorous gastropods (NMI FAs and dimethyl acetal – DMA) (Budge et al. 2006; Meyer et al. 2019). As some given trophic markers can originate from different prey types (Meyer et al. 2019), we used parametric (Pearson) and non-parametric (Kendall) correlation tests on SI and FA trophic markers to discriminate between potential prey origins. Correlation plots for each species were computed using the *corrplot* R package (Fig. S1).

The effects of reef habitat type (carbonate *vs* granite) and habitat degradation (i.e. before and after coral bleaching event) on spiny lobsters' trophic ecology was investigated using SI niche metrics. For this, isotopic niche sizes and overlaps were compared between individuals caught on carbonate and granite reefs for the three spiny lobster species, and between the pre- (i.e. 2014-2015) and post-2016 bleaching event periods (i.e. 2016-2018) between *P. penicillatus* and *P. longipes* only (due to low sample sizes for *P. versicolor*). Regarding FA niches, the number of available data only allowed for the comparison of niche sizes and overlaps between sampling years following the 2016 bleaching event (i.e. 2016, 2017 and 2018), for *P. penicillatus* and *P. longipes* only.

Finally, we used associated probability to compare niche metrics between species or among factors (i.e. reef habitat type, time period of reef degradation and sampling year during the post-bleaching period). For each iteration of the model, we gave a value of 1 if one niche metric value was greater than the other, 0 if not. The mean value calculated for the 1000 iterations represented the probability that one metric value was greater than the other. A probability > 0.95 would be associated with a high certainty.

3. Results

3.1. Size of sampled spiny lobsters

Over the sampling period, *Panulirus penicillatus* was significantly larger than the two other species (Dunn test, $P < 0.001$ with *P. longipes*; $P = 0.001$ for *P. versicolor*) (Fig. 2). There was no significant difference in carapace length between *P. longipes* and *P. versicolor* ($P > 0.05$). For each species, there was no significant difference in carapace length over the sampling years ($P > 0.05$).

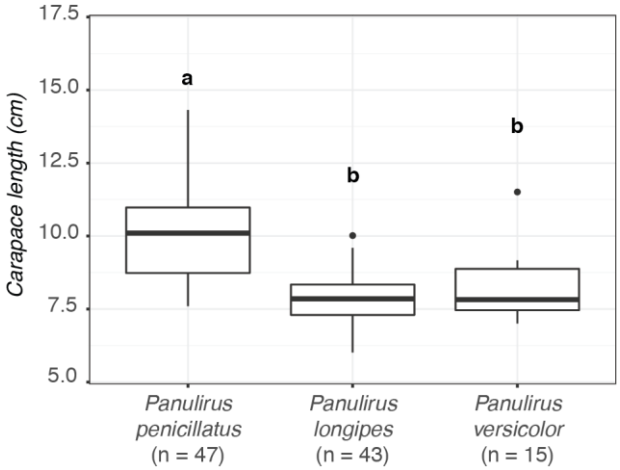

Fig. 2 Carapace length (cm) of sampled spiny lobsters according to the species. A different letter indicates a significant difference ($P < 0.05$).

3.2. Fatty acid niches

For all three species, FA profiles in the hepatopancreas were characterised by dominance of the polyunsaturated FAs, followed by saturated FAs then monounsaturated FAs (Table 1). Among polyunsaturated FAs, 20:4n-6 was the dominant FA, with low proportions of 20:5n-3 and 22:6n-3. Monounsaturated FAs were dominated by 18:1n-9 and saturated FAs were dominated by 16:0 and 18:0.

Panulirus penicillatus had the lowest mean 20:4n-6 proportion (Tukey's HSD, $P < 0.001$) but the highest mean proportion of 18:1n-9 (Dunn test, $P < 0.001$ with *P. versicolor*; $P = 0.03$ with *P. longipes*) (Table 1). This species also had a higher mean 20:1n-7 proportion than *P. versicolor* (Dunn test, $P = 0.03$)

and a higher mean 20:1n-9 proportion than *P. longipes* (Dunn test, $P < 0.001$). Concerning NMI FA, *P. penicillatus* had a higher 22:2 NMI (7,13) mean proportion than *P. longipes* (Tukey's HSD, $P = 0.02$) and the lowest 22:2 NMI (7,15) mean proportion (Dunn test, $P = 0.02$).

Table 1 Fatty acid (FA) profiles analysed in the hepatopancreas of *Panulirus penicillatus*, *P. longipes* and *P. versicolor* across all sampling sites and time periods expressed as % of total FA and presented as mean ± SE. The category "other" refers to the sum of FA compounds detected below trace level (< 0.8%). Different letters indicate significant difference ($P < 0.05$, Tukey's HSD or Dunn post-hoc tests). ∑SFA = sum of saturated FA, ∑MUFA = sum of monounsaturated FA, ∑PUFA = sum of polyunsaturated FA, NMI = non-methyl interrupted, DMA = dimethyl acetal.

Fatty acid	*P. penicillatus* (n = 31)	*P. longipes* (n = 27)	*P. versicolor* (n = 7)
Saturated			
14:0	2.5 ± 0.3	2.2 ± 0.1	1.8 ± 0.2
15:0	1.1 ± 0.1	1.16 ± 0.04	1.2 ± 0.1
16:0	17.4 ± 0.4	17.0 ± 0.4	17.6 ± 0.8
17:0	1.6 ± 0.1^{b}	2.0 ± 0.1^{a}	1.4 ± 0.1^{b}
18:0	9.9 ± 0.2^{ab}	11.4 ± 0.4^{a}	9.5 ± 0.5^{b}
20:0	1.2 ± 0.1^{a}	1.01 ± 0.04^{ab}	0.8 ± 0.1^{b}
∑SFA	31.7 ± 0.5	36.2 ± 0.5	30.8 ± 1.0
Monounsaturated			
16:1n-7	4.4 ± 0.2	4.5 ± 0.2	4.4 ± 0.3
18:1n-7	3.6 ± 0.1	3.5 ± 0.1	3.7 ± 0.1
18:1n-9	10.5 ± 0.6^{a}	7.4 ± 0.3^{b}	7.6 ± 0.7^{b}
20:1n-7	1.0 ± 0.1^{a}	0.69 ± 0.03^{ab}	0.7 ± 0.1^{b}
20:1n-9	1.3 ± 0.1^{a}	0.66 ± 0.02^{b}	1.0 ± 0.1^{a}
20:1n-11	2.8 ± 0.2	2.94 ± 0.13	2.4 ± 0.3
∑MUFA	24.4 ± 0.6^{a}	20.5 ± 0.4^{b}	20.4 ± 1.0^{b}
Polyunsaturated			
18:2n-6	1.29 ± 0.04^{b}	1.5 ± 0.1^{a}	1.5 ± 0.1^{ab}
20:2n-6	1.3 ± 0.1	1.18 ± 0.03	1.24 ± 0.03
20:4n-6	8.5 ± 0.3^{b}	10.9 ± 0.3^{a}	11.3 ± 0.9^{a}
20:5n-3	7.1 ± 0.4	7.6 ± 0.3	7.8 ± 0.5
22:4n-6	1.8 ± 0.1	1.8 ± 0.1	2.3 ± 0.3
22:5n-3	2.2 ± 0.1	2.5 ± 0.1	2.7 ± 0.1
22:6n-3	4.3 ± 0.4	4.0 ± 0.2	4.1 ± 0.4
∑PUFA	38.2 ± 0.8^{b}	40.5 ± 0.8^{ab}	42.6 ± 1.5^{a}
Branched FA, NMI FA and DMA			
iso17:0	0.83 ± 0.04^{b}	1.01 ± 0.03^{a}	0.8 ± 0.1^{ab}
22:2 NMI (7,13)	1.5 ± 0.1^{a}	1.1 ± 0.1^{b}	1.2 ± 0.2^{ab}
22:2 NMI (7,15)	0.74 ± 0.05^{b}	0.86 ± 0.04^{a}	1.2 ± 0.2^{a}
18:0DMA	2.3 ± 0.1	2.4 ± 0.1	2.5 ± 0.3
Other[1]	11.0 ± 0.3	10.8 ± 0.2	11.3 ± 0.2

[1] Includes the SFA 19:0, 21:0, 22:0, 24:0, the MUFA 16:1n-5, 16:1n-9, 17:1n-7, 18:1n-5, 18:1n-11, 22:1n-7, 22:1n-9, 22:1n-11, 24:1n-9, the PUFA 16:2n-4, 16:3n-4, 16:3n-6, 16:4n-3, 18:3n-3, 18:3n-4, 18:3n-6, 18:4n-3, 20:3n-3, 20:3n-6, 20:4n-3, 22:6n-3,

the branched FA iso15:0, ante15:0, iso16:0, the NMI FA 20:2 NMI (5,11), 20:2 NMI (5,13), 22:3 NMI (7,13,16) and the DMA 16:1n-7DMA, 16:0DMA.

Panulirus penicillatus displayed the largest FA niche (niche size of 0.18 [CI95%: 0.13 – 0.27]; associated probability of 1) with little-to-no overlap in CI95% with the other two species, while *P. longipes* and *P. versicolor* displayed similar niche sizes (0.04 [0.03 – 0.05] and 0.06 [0.03 – 0.13] respectively) (Fig. 3A). *P. penicillatus* was separated from the two other species by monounsaturated FAs such as 18:1n-9, 20:1n-7 and 20:1n-9, and by the NMI FAs 22:2 NMI (7,13) and 22:2 NMI (7,15) (Fig. 3A). Both *P. longipes* and *P. versicolor* FA niches were included in *P. penicillatus* FA niche. There was a high overlap between *P. longipes* and *P. versicolor* niches (89.38% [72.40 – 99.70%] for *P. longipes* in *P. versicolor* niche and 71.02% [45.29 – 93.80%] for *P. versicolor* in *P. longipes* niche) (Fig. 3B). By contrast, there was moderate niche overlap between *P. penicillatus* and the two other species (35.05% [21.30 – 52.01%] in *P. longipes* niche and 46.64% [25.10 – 74.90%] in *P. versicolor* niche).

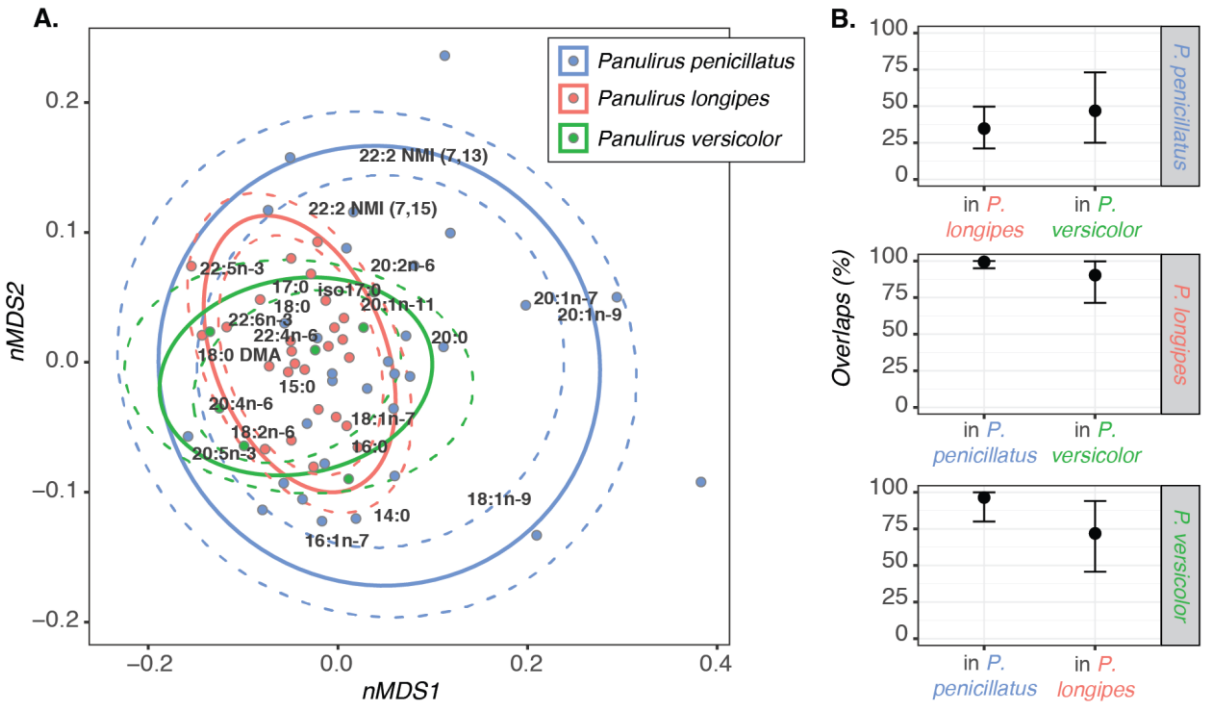

Fig. 3 Non-metric multidimensional scaling (nMDS) ordination of Bray-Curtis similarity matrix of hepatopancreas tissue fatty acid composition in the three spiny lobster species (A) and probabilities of niche overlap (%) between species (B). For each species, the mean ellipse is represented by a plain line and CI95% ellipses are represented by dashed lines (A). Overlaps (B) are presented as mean with their associated CI95%.

3.3. Isotopic niches

Among the three lobster species, *P. penicillatus* displayed the highest $\delta^{15}N$ values, *P. longipes* had intermediate values and *P. versicolor* showed the lowest $\delta^{15}N$ values (Tukey's HSD, P = 0.002

between *P. penicillatus* and *P. longipes*; $P < 0.001$ between *P. penicillatus* and *P. versicolor*; $P < 0.001$ between *P. longipes* and *P. versicolor*) (Table 2). Only *P. penicillatus* and *P. longipes* displayed a significant difference in $\delta^{13}C$ values (Tukey's HSD, $P = 0.03$), with *P. penicillatus* having higher values than *P. longipes* (Table 2).

Table 2 Mean (± SD) $\delta^{13}C$ and $\delta^{15}N$ values (‰) analysed in the tail muscle of *Panulirus penicillatus*, *P. longipes* and *P. versicolor* across all sampling sites and time periods. Different letters indicate significant difference ($P < 0.05$, Tukey's HSD or Dunn post-hoc tests).

Stable isotope ratio	*P. penicillatus* (n = 47)	*P. longipes* (n = 43)	*P. versicolor* (n = 15)
$\delta^{13}C$	-13.6 ± 0.1^{a}	-14.0 ± 0.1^{b}	-13.7 ± 0.2^{ab}
$\delta^{15}N$	11.6 ± 0.1^{a}	11.3 ± 0.1^{b}	10.4 ± 0.1^{c}

All three species had similar SI niche sizes (4.33 ‰^{2} [3.30 – 5.73 ‰^{2}] for *P. penicillatus*, 4.32 ‰^{2} [3.21 – 5.82 ‰^{2}] for *P. longipes* and 4.05 ‰^{2} [2.45 – 6.38 ‰^{2}] for *P. versicolor*) (Fig. 4A). There was a high overlap between *P. penicillatus* and *P. longipes* isotopic niches (75.1% [61.0 – 93.2%] for *P. penicillatus* in *P. longipes* and 78.1% [58.7 – 90.2%] for *P. longipes* in *P. penicillatus*) (Fig. 4B). *P. versicolor* had moderate overlap with *P. longipes* (20.9% [6.4 – 59.0%] for *P. versicolor* in *P. longipes* and 25.6% [4.5 – 58.4%] for *P. longipes* in *P. versicolor*) and little overlap with *P. penicillatus* (4.6% [0.1 – 18.8%] for *P. versicolor* in *P. penicillatus* and 4.8% [0.2 – 21.4%] for *P. penicillatus* in *P. versicolor*).

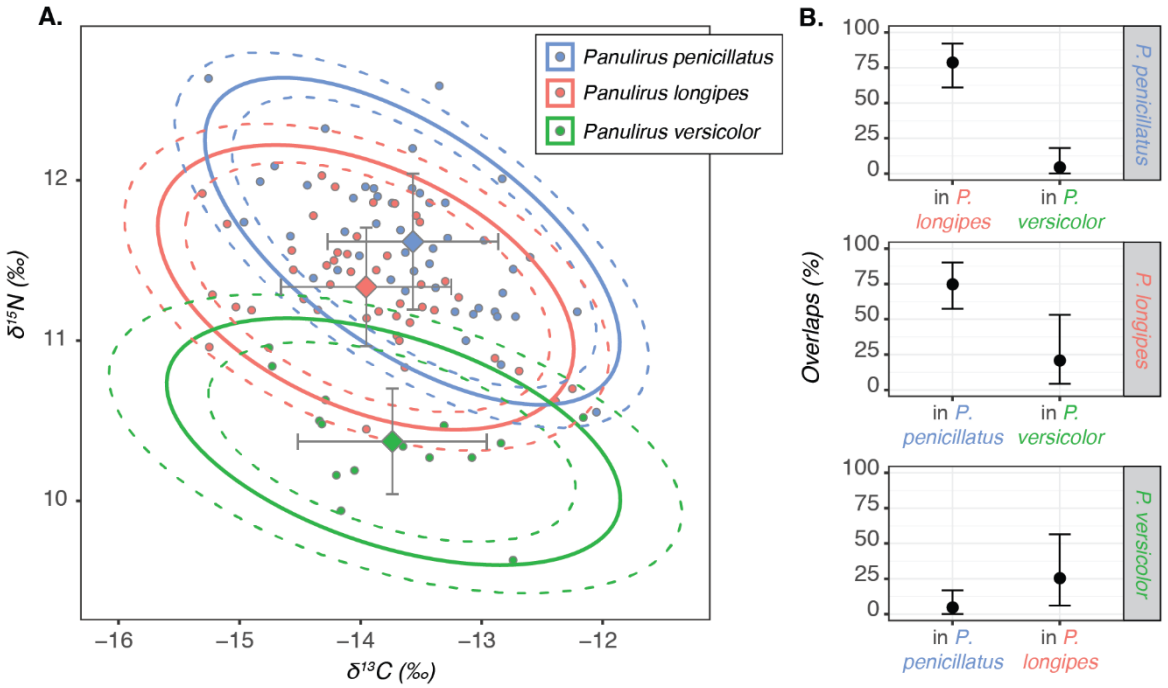

Fig. 4 $\delta^{13}C$ and $\delta^{15}N$ values (‰) in the tail muscle of the three spiny lobster species (A) and niche overlaps (%) between species (B). For each species, the mean ± SD for stable isotope values is also given, and the mean ellipse

and CI95% ellipses are represented by a plain line and dashed lines, respectively (A). Overlaps (B) are presented as mean with their associated CI95 %.

3.4. Effect of habitat type and habitat degradation due to coral bleaching on spiny lobsters' trophic niche metrics

The isotopic niche size of *P. penicillatus* was larger in granite reefs than in carbonate reefs (4.4 ‰^{2} [3.2 – 5.8 ‰^{2}] and 1.6 ‰^{2} [0.7 – 3.6 ‰^{2}] respectively; associated probability of 0.99) with little overlap in CI95% between the two habitat types (Fig. 5A). In spite of the uncertainty around the mean (i.e. high overlap in CI95%), it also appeared that the isotopic niche of *P. versicolor* was larger in granite reefs than in carbonate reefs (2.9 ‰^{2} [1.6 – 5.3‰^{2}] and 1.4 ‰^{2} [0.5 – 3.8 ‰^{2}] respectively; associated probability of 0.90). Except for the isotopic niche overlap of *P. penicillatus* in *P. longipes*, interspecific overlap of isotopic niches seemed to be higher in granite reefs than in carbonate reefs (2.2% [0.1 – 9.8%] and 0.0% respectively for *P. penicillatus* in *P. versicolor*, associated probability of 0.97; 76.3% [58.3 – 92.0%] and 37.8% [14.9 – 76.1%] respectively for *P. longipes* in *P. penicillatus*, associated probability of 0.96; 9.5% [1.4 – 26.5%] and 0.6% [0.0 – 5.2%] respectively for *P. longipes* in *P. versicolor*, associated probability of 0.97; 3.9% [0.0 – 19.8%] and 0.0% respectively for *P. versicolor* in *P. penicillatus*, associated probability of 0.90; 21.1% [1.7 – 59.9%] and 2.5% [0.0 – 31.7%] respectively for *P. versicolor* in *P. longipes*; associated probability of 0.95) (Fig. 5A).

The isotopic niche size of *P. penicillatus* appeared greater during the post-bleaching period (4.5 ‰^{2} [3.2 – 6.4 ‰^{2}]) than during the pre-bleaching period (2.6 ‰^{2} [1.6 – 4.2 ‰^{2}]; associated probability of 0.97), with moderate overlap in CI95% (Fig. 5B). The isotopic niche overlap between *P. longipes* and *P. penicillatus* also seemed higher during the post-bleaching period (78.2% [56.0 – 94.4%]) than during the pre-bleaching period (55.5% [30.9 – 80.6%]; associated probability of 0.91) with moderate overlap in CI95% (Fig. 5B). After the 2016 bleaching event, the FA niche size of *P. longipes* was greater in 2017 (0.042 [0.023 – 0.077]) and in 2018 (0.049 [0.026 – 0.090]) than in 2016 (0.012 [0.006 – 0.024]; associated probabilities of 0.99 between 2017 and 2016 and of 1 between 2018 and 2016), with little-to-no overlap in CI95% between 2016 and both other years (Fig. 5C). The FA niche overlap between *P. penicillatus* and *P. longipes* also seemed larger in 2017 (26.3% [8.2 – 50.6%] for *P. penicillatus* in *P. longipes*) and in 2018 (48.1% [22.8 – 77.5%] for *P. penicillatus* in *P. longipes*) than in 2016 (10.1% [2.3 – 24.7%] for *P. penicillatus* in *P. longipes*; associated probabilities of 0.92 between 2017 and 2016, of 1 between 2018 and 2016) (Fig. 5C).

For all calculated trophic niche metrics of Fig. 5, niche ellipses are presented in Fig. S2. Isotopic niches according to the sampling year (i.e. 2014 to 2018) for *P. penicillatus* and *P. longipes* only (due to low sample sizes for *P. versicolor*) and their associated metrics are presented in Fig. S3. Spiny lobsters'

FA niches in carbonate and granite reefs did not allow for any interpretation but are however presented in Fig. S4 for information purposes.

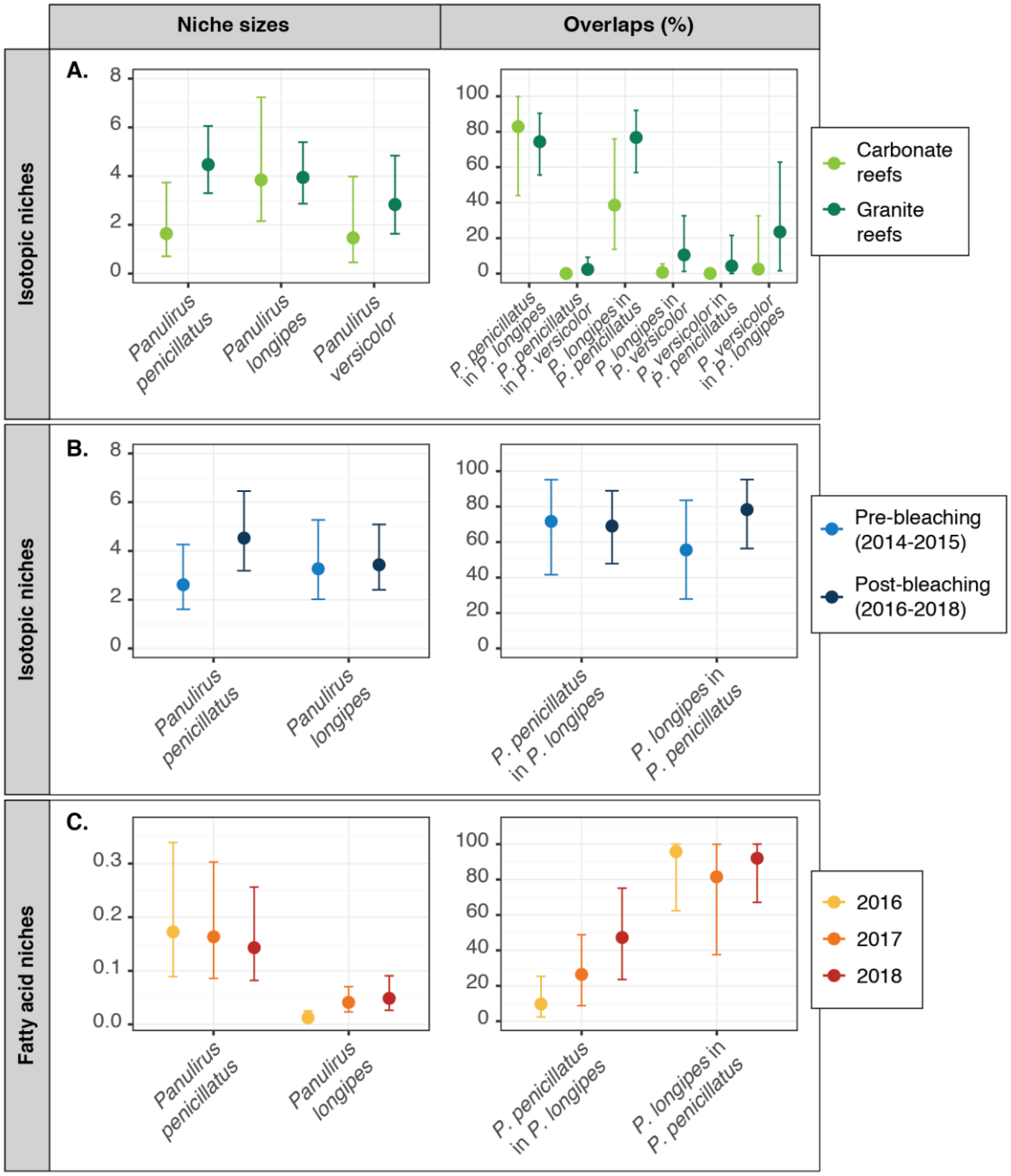

Fig. 5 Inter- and intraspecific differences in the trophic niche sizes and overlaps of spiny lobster species related to (A) different reef habitat types, (B) pre- and post-bleaching periods for isotopic niches, and (C) sampling years after 2016 coral bleaching event for FA niches. Niche sizes and overlaps are presented as mean with their associated CI95 %.

4. Discussion

The present study revealed novel insights into the trophic ecology and interspecific competition between three sympatric spiny lobster species (*Panulirus penicillatus*, *P. longipes* and *P. versicolor*) from the Seychelles coastal waters. We highlighted a substantial potential for dietary overlap between the three species, as revealed by both interspecific FA and isotopic niche overlaps. The use of FA trophic markers further assisted in inferring the dietary source of this overlap. Use of SI in complement to FAs allowed for inference of habitat use and suggested that resources may partially be segregated between the three spiny lobster species that could allow for their coexistence. However, isotopic niche overlap was higher in the less vulnerable-to-degradation reef type and coral bleaching increased FA and isotopic niche overlaps. We thus suggest that climate change-driven coral reef degradation might increase the risk of competition between these spiny lobster species through the reduction of coral reef structural complexity and thus prey availability.

4.1. Characterisation of trophic overlap and potential for competition

As the biochemical composition of consumers largely reflects that of their prey (Iverson 2009), similar FA and SI trophic niches characterise similar dietary patterns. Our study found high habitat use and dietary similarities between the three Seychelles spiny lobster species, consistently with previous reported findings (Sardenne et al. 2021). The $\delta^{13}C$ value ranges and FA profiles of the three species were distinctive of benthic consumers (high in 20:4n-6 with low-to-moderate levels of 20:5n-3 and 22:6n-3). The presence of iso-branched FA (i.e. iso17:0) along with high proportions of 18:1n-7 in the hepatopancreas also suggested a food web partially based on bacteria, known to support benthic food webs, at least in part (Kelly and Scheibling 2012).

Dietary similarities between Seychelles spiny lobsters were characterised by the presence of several FA trophic markers in the hepatopancreas, allowing for the identification of prey implicated in the dietary overlap. First, trophic markers of bacteria (i.e. iso17:0 and 18:1n-7) could indicate consumption of benthic detritivores, such as polychaetes, known to be eaten in small proportions by spiny lobsters in some areas (e.g. the coast off Western Australia, MacArthur et al. 2011). Fleshy algae FA trophic markers (i.e. 18:2n-6, 20:4n-6 and 22:5n-3, Meyer et al. 2019) suggest either direct consumption of fleshy algae, which can support benthic food webs in shallow coastal waters (Kelly and Scheibling 2012) and it was found in the gut contents of some spiny lobsters (Blamey et al. 2019), or consumption of herbivorous prey, such as echinoderms, which are among the most common prey found in the guts of spiny lobsters (Butler and Kintzing 2016). Here, the predominance of primary or secondary consumption of fleshy algae in spiny lobsters' diet was difficult to determine. $\delta^{13}C$ values in macroalgae are highly variable (from -27 to -8 ‰, Fry and Sherr 1989) and, after taking into account the trophic

fractionation factor (1-2 ‰, Post 2002), both primary and secondary consumption could occur according to our isotopic data. It is possible that it depends on the characteristics of the sampling sites. Typically, secondary consumption of fleshy algae would predominate on reefs where herbivores are abundant and macroalgae are limited, while primary consumption, whether intentional or accidental through feeding on epiphyte fauna found on the algae (Williams 2007), would predominate on reefs where macroalgae are abundant.

The presence of a diverse number of FA trophic markers and variability in isotopic values in this study suggest that Seychelles spiny lobsters are generalist feeders, which is in accordance with previous studies on spiny lobsters' diet (Williams 2007; Blamey et al. 2019). This could be an advantage for these species' survival, as dietary plasticity would help them overcome fluctuations in food availability (Korpimäki et al. 2020). However, we suggest that competition between spiny lobsters could occur in this area or could emerge in the near future, if shared resources (e.g. prey, habitat) become limited. Coexistence and avoidance of competition would therefore be closely linked to ecosystem health and to resource segregation mechanisms.

4.2. Resource partitioning among spiny lobsters

Partial resource segregation between the three spiny lobster species was also identified in this study, as suggested by the difference in FA niche size between *P. penicillatus* and the other two species and by differences in trophic position between the three species.

Panulirus penicillatus had a much larger FA niche in comparison with the two other species, suggesting a difference in the ingested proportions of certain types of prey. Its FA niche differed from FA niches of both other species largely due to positive anomalies of several FA trophic markers like 18:1n-9, 20:1n-7, 20:1n-9, 22:2 NMI (7,13) and 22:2 NMI (7,15). In coastal benthic systems, 18:1n-9 can originate from several dietary sources, such as macroalgae, mangrove detritus or animal tissues (Meyer et al. 2019). Here, 18:1n-9 was negatively correlated with trophic markers of macroalgae and mangrove materials (20:4n-6 and 22:5n-3, Fig. S1; Meyer et al. 2019), suggesting animal origin. This was also the case for 20:1n-7 and 20:1n-9, both negatively correlated with trophic markers of macroalgae, mangrove material and seagrass (20:4n-6, 22:5n-3 and 18:2n-6, Fig. S1; Meyer et al. 2019). The FA 20:1n-9 is known to indicate secondary consumption of zooplankton, for example through consumption of carnivorous fish (Pethybridge et al. 2010). Moreover, NMI FAs are trophic markers of bivalve molluscs and carnivorous gastropods (Iverson 2009), suggesting that *P. penicillatus* eats these prey in higher proportions than the two other spiny lobster species. FA niche results were supported by isotopic niche results, as *P. penicillatus* had a higher trophic position than the two other species that is consistent with higher proportions of carnivorous gastropods and fish in its diet. We thus suggest that *P. penicillatus*

may be more of a generalist than *P. longipes* and *P. versicolor*, with a higher level of carnivory. Such a difference in diet could be due to the size range of *P. penicillatus* individuals, which tend to be larger than individuals of the two other species. Previous studies showed that the size range of prey that can be consumed by spiny lobsters is function of their size, with larger individuals being able to eat larger prey (e.g. Haley et al. 2011; Blamey and Branch 2012). Thus, the larger size of *P. penicillatus* may allow it to have access to more resources, resulting in a larger niche size.

Both *P. longipes* and *P. versicolor* had a low isotopic niche overlap, with *P. versicolor* being characterised by significantly lower $\delta^{15}N$ values, while they had a very high FA niche overlap that suggests high dietary similarities. Because all spiny lobsters were caught at the same geographical locations, we suggest that variations in $\delta^{15}N$ values reflect differences in trophic position rather than differences in biochemical processes at the base of food webs (i.e. isotopic baselines). This may be due to size-selective predation, with both species feeding on different size fractions and/or different life stages of the same prey. Such resource partitioning could allow and even promote the stable coexistence of two consumers (de Roos et al. 2008). Moreover, body size is recognised as an important factor influencing trophic structure as it determines interaction between potential prey and predators, with larger consumers being able to eat larger prey. This has led to the theory that there is a positive relationship between a consumer's trophic position and its body size (Jennings et al. 2002). Thus, if *P. versicolor* is specialising on smaller prey (either juveniles or small adults), it would feed on prey with a lower trophic position than those of *P. longipes* (as suggested by our results), while having the same size and feeding on the same prey species than *P. longipes*. Such findings would be of major importance in case of food scarcity, especially if *P. versicolor* feeds on earlier development stages of prey than *P. longipes* and *P. penicillatus*, and not only smaller prey species. Different prey life-history stages are linked by growth and reproduction, and predation on one stage may decrease the abundance of other stages (Murdoch et al. 2003). Thus, prey eaten by *P. versicolor* would not grow and be available for *P. longipes* and *P. penicillatus* to feed on. Given its larger trophic niche, *P. penicillatus* may be able to better overcome this compared to *P. longipes*. Thus, this could accentuate the effects of food scarcity for *P. longipes*, which already has a high level of trophic niche overlap with *P. penicillatus*.

4.3. Effect of habitat type and coral bleaching

The type of reef habitat had an effect on spiny lobsters' isotopic niche overlaps, with higher overlap between lobsters from granite reefs than for those from carbonate reefs, for all studied species. This was most obvious for *P. versicolor*, which had no isotopic niche overlap with *P. penicillatus* from carbonate reefs while there was a possibility of overlap with *P. penicillatus* from granite reefs, and had a higher overlap with *P. longipes* on granite reefs than on carbonate reefs. Although FA niches could not

be computed for this comparison, results suggest a higher potential of competition for prey on granite reefs than on carbonate reefs, especially for *P. versicolor*. This would be consistent with carbonate reefs being recognised as very productive ecosystems, with a high species diversity and structural complexity (Graham and Nash 2013) that would provide sufficient prey of good quality for spiny lobsters to coexist.

Our results also showed a possible effect of habitat degradation on spiny lobsters' diet and foraging dynamics, especially coral reef degradation following the 2016 bleaching event (Obura et al. 2017). The isotopic niche size of *P. penicillatus* seemed to increase after the coral bleaching event, due to higher variability in $\delta^{15}N$ values (Fig. S1), and although we did not have FA data prior to the bleaching event, the FA niche of *P. longipes* has increased during the post-bleaching period. This suggests a possible diversification of prey size class in *P. penicillatus* diet between the pre- and post-bleaching periods and a diversification of *P. longipes* diet after the habitat degradation. Given the large decline in coral cover and as such the loss of reef complexity that provide habitat for a variety of potential prey species, we suggest that such modifications in isotopic and FA niches may be the consequences of a decrease in prey availability. In ecological theory, dietary diversity increases when prey abundance decreases (Tinker et al. 2008) and, as generalist feeders, spiny lobsters are known to adapt their diet according to several factors, such as prey species composition and/or prey availability (Haley et al. 2011; Blamey et al. 2019). This would also be consistent with the loss of species richness that has been reported after loss of coral cover in Seychelles (Robinson et al. 2019). Such drastic changes prey availability may have important consequences on the foraging behaviour of the three spiny lobster species. By influencing spiny lobsters' diet diversity and abundance, the 2016 bleaching event could have increased the risk of competition between the three lobster species. This hypothesis is supported by the increase of isotopic niche overlap between *P. penicillatus* and *P. longipes* between the pre- and post-bleaching periods and by the increase in their FA niche overlap between 2016 and 2018.

The effects of reef habitat type and habitat degradation through coral bleaching on spiny lobsters' diet and foraging dynamics are of high interest for the prediction of fishing stock evolution. Indeed, carbonate reefs are known to be more vulnerable to bleaching and reef degradation than granite reefs (Obura et al. 2017). In addition, granite reefs are quicker to recover than carbonate reefs after degradation, due in part to corals from carbonate reefs being in competition with macroalgae (Obura et al. 2017). Due to climate change and its associated rise in sea surface temperatures, bleaching events are predicted to increase in frequency, thereby weakening corals ecosystems in the long-term (Hoegh-Guldberg 2011). As the reduction of Seychelles spiny lobsters' potential of interspecific competition partly depends on the health and complexity of carbonate reefs, it is likely that the predicted instability of coral reefs could add further instability to the already unstable Seychelles spiny lobster stocks.

5. Conclusion

This study provides important baseline information on Seychelles spiny lobsters' trophic ecology and on their potential for resource competition in the context of a changing climate and associated habitat (i.e. coral reefs) degradation. All three species had biochemical compositions that suggested diets consisting of polychaetes, echinoderms, and fleshy algae. As the species with the largest size range including larger individuals, *P. penicillatus* had the highest trophic position and the largest trophic niche, presumably feeding more on carnivorous gastropods and fish than the two other spiny lobster species. Although having very similar trophic niche than the two other species, *P. versicolor* may feed on smaller prey and/or early life stages. These segregation mechanisms could potentially minimise the effects of competition among these spiny lobster species. Our data also showed that the level of resource segregation was dependent on their habitat. Spiny lobsters' trophic niche overlap was higher on granite reefs than on carbonate reefs, the latter being more degraded following multiple bleaching events. As recent habitat degradation (i.e. following the 2016 coral bleaching event) also led to an increase in trophic niche overlap, this raises questions about the future evolution of competition between these spiny lobster species and, ultimately, their adaptive capacity and population stability.

Although our results provide key information to better understand Seychelles spiny lobsters' trophic interactions and dynamics, further studies are still needed. Most of the available samples were from *P. penicillatus* and *P. longipes*, which did not allow all the analyses to be performed on *P. versicolor* data. Moreover, the FA and SI profiles of a consumer only does not allow quantitative identification of its diet. Information about FA and SI profiles from lobsters' prey collected at different sites and time periods would bring new elements on the spatio-temporal variations in resource sharing and segregation among Seychelles spiny lobster species, and thus help understand the variability in their interspecific competition. In light of our findings, it is crucial to maintain monitoring of trophic ecology and habitat use of spiny lobsters around Seychelles islands if the fishery is to be successfully managed under changing climate.

Acknowledgements The authors would like to thank the lobster fishers who assisted with sampling. A special thank goes to the SFA Research staff (Kettyna Gabriel, Rodney Melanie, Stephanie Marie, Clara Belmont, and Marie-Corinne Balett), the R.V. L'Amitié crew and the Seychelles Maritime School Academy for the invaluable help in processing the samples. The authors are grateful to M. Brault-Favrou and G. Guillou for their support in the stable isotope analyses. Thanks are due to the CPER (Contrat de Projet Etat-Région) and the FEDER (Fonds Européen de Développement Régional) for funding the IRMS of LIENSs laboratory. The IUF (Institut Universitaire de France) is acknowledged for its support to PB as a Senior Member.

Author's contribution Conceptualisation: N Bodin; Funding acquisition: N Bodin, R Govinden; Data acquisition: N Bodin, R Govinden, M Rose, MA Sabino, F Sardenne, F Le Grand; Statistical analysis: MA Sabino, H Pethybridge, L Blamey; Writing – 1st draft: MA Sabino; Review & editing: all co-authors.

Funding The present work is a contribution to the Seychelles Participatory Lobster Monitoring Programme (PLMP) led by the Seychelles Fishing Authority (SFA), with the financial support of the Seychelles Government, the European Fisheries Partnership Agreement (EU-FPA), and the Institute for Research and Development (IRD).

Data availability The dataset analysed in the current study is available from the corresponding author on reasonable request. The R code used to compute FA and isotopic niches and to represent niche ellipses is available on Github: https://github.com/magalisabino/FattyAcid_Isotopic_niche_computing.

Declaration of competing interest The authors declare that they have no conflict of interest.

Ethical approval All applicable international, national, and institutional guidelines for the care and use of animals were followed. All procedures performed in studies involving animals were in accordance with the ethical standards of the Ministry of Environment, Energy, and Climate Change, Seychelles.

References

Blamey LK, Branch GM (2012) Regime shift of a kelp-forest benthic community induced by an "invasion" of the rock lobster *Jasus lalandii*. J Exp Mar Bio Ecol 420–421:33–47. doi: 10.1016/j.jembe.2012.03.022

Blamey LK, de Lecea AM, Jones LDS, Branch GM (2019) Diet of the spiny lobster *Jasus paulensis* from the Tristan da Cunha archipelago: Comparisons between islands, depths and lobster sizes. Estuar Coast Shelf Sci 219:262–272. doi: 10.1016/j.ecss.2019.02.021

Brewster JD, Giraldo C, Choy ES, MacPhee SA, Hoover C, Lynn B, McNicholl DG, Majewski A, Rosenberg B, Power M, Reist JD, Loseto LL (2017) A comparison of the trophic ecology of Beaufort Sea Gadidae using fatty acids and stable isotopes. Polar Biol 41:149–162. doi: 10.1007/s00300-017-2178-0

Budge SM, Iverson SJ, Koopman HN (2006) Studying trophic ecology in marine ecosystems using fatty acids: A primer on analysis and interpretation. Mar Mammal Sci 22:759–801. doi: 10.1111/j.1748-7692.2006.00079.x

Butler MJ, Kintzing MD (2016) An exception to the rule: Top-down control of a coral reef macroinvertebrate community by a tropical spiny lobster. Bull Mar Sci 92:137–152. doi: 10.5343/bms.2015.1045

Carvalho PC, Davoren GK (2020) Niche dynamics of sympatric non-breeding shearwaters under varying prey availability. Ibis 162:701–712. doi: 10.1111/ibi.12783

Connan M, McQuaid CD, Bonnevie BT, Smale MJ, Cherel Y (2014) Combined stomach content, lipid and stable isotope analyses reveal spatial and trophic partitioning among three sympatric albatrosses from the Southern Ocean. Mar Ecol Prog Ser 497:259–272. doi: 10.3354/meps10606

Costa-Pereira R, Araújo MS, Souza FL, Ingram T (2019) Competition and resource breadth shape niche variation and overlap in multiple trophic dimensions. Proc R Soc B Biol Sci 286:1–9. doi: 10.1098/rspb.2019.0369

de Roos AM, Schellekens T, Van Kooten T, Persson L (2008) Stage-specific predator species help each other to

persist while competing for a single prey. Proc Natl Acad Sci U S A 105:13930–13935. doi: 10.1073/pnas.0803834105

Fry B, Sherr EB (1989) δ13C measurements as indicators of carbon flow in marine and freshwater ecosystems. In: Rundel PW, Ehleringer JR, Nagy KA (eds) Stable Isotopes in Ecological Research. Ecological Studies (Analysis and Synthesis). Springer, New-York, USA, pp 196–229. doi: 10.1007/978-1-4612-3498-2_12

Graham NAJ, Nash KL (2013) The importance of structural complexity in coral reef ecosystems. Coral Reefs 32:315–326. doi: 10.1007/s00338-012-0984-y

Haley CN, Blamey LK, Atkinson LJ, Branch GM (2011) Dietary change of the rock lobster *Jasus lalandii* after an "invasive" geographic shift: Effects of size, density and food availability. Estuar Coast Shelf Sci 93:160–170. doi: 10.1016/j.ecss.2011.04.015

Hoegh-Guldberg O (2011) Coral reef ecosystems and anthropogenic climate change. Reg Environ Chang 11:215–227. doi: 10.1007/s10113-010-0189-2

Holthuis LB (1991) FAO species catalogue Vol. 13. Marine lobsters of the world An annotated and illustrated catalogue of species of interest to fisheries known to date. FAO Fish Synopsis 13:1–4. http://www.fao.org/3/t0411e/t0411e00.htm

Iverson SJ (2009) Tracing aquatic food webs using fatty acids: from qualitative indicators to quantitative determination. In: Kainz M, Brett MT, Arts MT (eds) Lipids in Aquatic Ecosystems. Springer New York, New-York, USA, pp 281–308. doi: 10.1007/978-0-387-89366-2_12

Jennings S, Pinnegar JK, Polunin NVC, Warr KJ (2002) Linking size-based and trophic analyses of benthic community structure. Mar Ecol Prog Ser 226:77–85. doi: 10.3354/meps226077

Kelly JR, Scheibling RE (2012) Fatty acids as dietary tracers in benthic food webs. Mar Ecol Prog Ser 446:1–22. doi: 10.3354/meps09559

Khan A, Amelie V (2015) Assessing climate change readiness in Seychelles: implications for ecosystem-based adaptation mainstreaming and marine spatial planning. Reg Environ Chang 15:721–733. doi: 10.1007/s10113-014-0662-4

Korpimäki E, Hongisto K, Masoero G, Laaksonen T (2020) The difference between generalist and specialist: the effects of wide fluctuations in main food abundance on numbers and reproduction of two co-existing predators. J Avian Biol 51:1–13. doi: 10.1111/jav.02508

MacArthur LD, Phillips DL, Hyndes GA, Hanson CE, Vanderklift MA (2011) Habitat surrounding patch reefs influences the diet and nutrition of the Western rock lobster. Mar Ecol Prog Ser 436:191–205. doi: 10.3354/meps09256

Mason NWH, De Bello F, Doležal J, Lepš J (2011) Niche overlap reveals the effects of competition, disturbance and contrasting assembly processes in experimental grassland communities. J Ecol 99:788–796. doi: 10.1111/j.1365-2745.2011.01801.x

Meyer L, Pethybridge H, Nichols PD, Beckmann C, Huveneers C (2019) Abiotic and biotic drivers of fatty acid tracers in ecology: A global analysis of chondrichthyan profiles. Funct Ecol 33:1243–1255. doi: 10.1111/1365-2435.13328

Murdoch WW, Briggs CJ, Nisbet RM (2003) Consumer-resource dynamics. Princeton University Press, Princeton, New Jersey. doi: 10.1515/9781400847259

Nie Y, Zhou W, Gao K, Swaisgood RR, Wei F (2019) Seasonal competition between sympatric species for a key resource: Implications for conservation management. Biol Conserv 234:1–6. doi: 10.1016/j.biocon.2019.03.013

Obura D, Gudka M, Rabi FA, Gian SB, Bijoux J, Freed S, Maharavo J, Mwaura J, Porter S, Sola E, Wickel J, Yahya S, Ahamada S (2017) Coral reef status report for the Western Indian Ocean. doi: 10.13140/RG.2.2.20642.07366

Österblom H, Olsson H, Blenckner T, Furness RW (2008) Junk food in marine ecosystems. Oikos 117:1075–1085. doi: 10.1111/j.0030-1299.2008.16501.x

Pethybridge H, Daley R, Virtue P, Nichols P (2010) Lipid composition and partitioning of deepwater chondrichthyans: Inferences of feeding ecology and distribution. Mar Biol 157:1367–1384. doi: 10.1007/s00227-010-1416-6

Phillips BF (2013) Lobsters: Biology, Management, Aquaculture and Fisheries, 2nd editio. John Wiley & Sons. doi: 10.1002/9781118517444

Post DM (2002) Using stable isotopes to estimate trophic position: models, methods, and assumptions. Ecology 83:703–718. doi: 10.2307/3071875

Post DM, Layman CA, Arrington DA, Takimoto G, Quattrochi J, Montaña CG (2007) Getting to the fat of the matter: Models, methods and assumptions for dealing with lipids in stable isotope analyses. Oecologia 152:179–

189. doi: 10.1007/s00442-006-0630-x

R Core Team (2018) R: A language and environment for statistical computing.

Robinson JPW, Wilson SK, Jennings S, Graham NAJ (2019) Thermal stress induces persistently altered coral reef fish assemblages. Glob Chang Biol 25:2739–2750. doi: 10.1111/gcb.14704

Sardenne F, Bodin N, Chassot E, Amiel A, Fouché E, Degroote M, Hollanda S, Pethybridge H, Lebreton B, Guillou G, Ménard F (2016) Trophic niches of sympatric tropical tuna in the Western Indian Ocean inferred by stable isotopes and neutral fatty acids. Prog Oceanogr 146:75–88. doi: 10.1016/j.pocean.2016.06.001

Sardenne F, Bodin N, Barret L, Blamey L, Govinden R, Gabriel K, Mangroo R, Munaron J-M, Le Loc'h F, Bideau A, Le Grand F, Sabino M, Bustamante P, Rowat D (2021) Diets of spiny lobsters from Mahé Island reefs, Seychelles reefs inferred by trophic tracers. Reg Stud Mar Sci 42:101640. doi: 10.1016/j.rsma.2021.101640

Seychelles Fishing Authority (2014) Fishery independent indices for the Seychelles lobster resource. https://www.oceandocs.org/bitstream/handle/1834/14833/Tech.074.pdf

Seychelles Fishing Authority (2016) Report on the spiny lobster fishery - Summary of fishing activity for the 2015-2016 season. https://www.oceandocs.org/bitstream/handle/1834/9895/Tech.079.pdf

Seychelles Fishing Authority (2018) Lobster survey report 2018. https://www.oceandocs.org/bitstream/handle/1834/15432/Tech.082.pdf

Swanson HK, Lysy M, POwer M, Stasko AD, Johnson JD, Reist JD (2015) A new probabilistic method for quantifying n-dimensional ecological niches and niche overlap. Ecology 96:318–324. doi: 10.1890/14-0235.1

Tinker T, Bentall G, Estes JA (2008) Food limitation leads to behavioral diversification and dietary specialization in sea otters. PNAS 105:560–565. doi: 10.1073/pnas.0709263105

Williams KC (2007) Nutritional requirements and feeds development for post-larval spiny lobster: A review. Aquaculture 263:1–14. doi: 10.1016/j.aquaculture.2006.10.019

Supplementary data

Table S1 Summary of the number of individuals analysed for different tissues and tracers for each species of spiny lobster grouped by sampling year, time period of habitat degradation (pre- and post-bleaching periods), and habitat type (carbonate and granite reefs). The total number of sampled individuals is 106. WM = White muscle, SI = Carbon and nitrogen stable isotopes, H = Hepatopancreas, FA = Fatty acids.

		Tissue - tracers	*Panulirus penicillatus*	*Panulirus longipes*	*Panulirus versicolor*
Pre-bleaching	2014	WM - SI	5	5	-
	2015	WM - SI	11	12	2
Post-bleaching	2016	H - FA	9	7	-
		WM - SI	9	8	4
	2017	H - FA	10	10	-
		WM - SI	10	10	2
	2018	H - FA	12	9	7
		WM - SI	12	9	7
Carbonate reefs		H - FA	4	3	-
		WM - SI	5	10	3
Granite reefs		H - FA	27	23	7
		WM - SI	42	34	12

A.

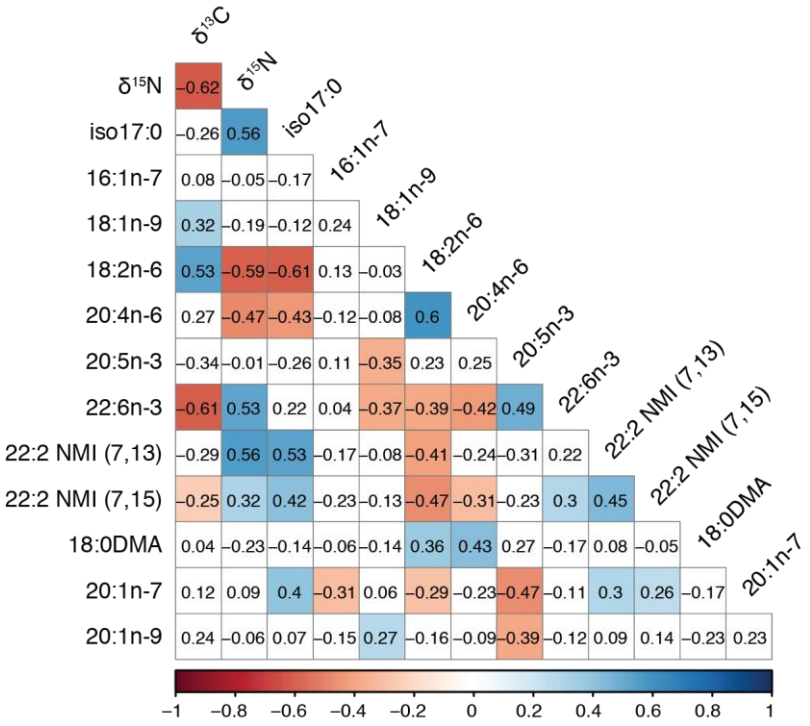
δ13C
δ15N
iso17:0
16:1n-7
18:1n-9
18:2n-6
20:4n-6
20:5n-3
22:6n-3
22:2 NMI (7,13)
22:2 NMI (7,15)
18:0DMA
20:1n-7
20:1n-9
δ15N −0.62
iso17:0 −0.26 0.56
16:1n-7 0.08 −0.05 −0.17
18:1n-9 0.32 −0.19 −0.12 0.24
18:2n-6 0.53 −0.59 −0.61 0.13 −0.03
20:4n-6 0.27 −0.47 −0.43 −0.12 −0.08 0.6
20:5n-3 −0.34 −0.01 −0.26 0.11 −0.35 0.23 0.25
22:6n-3 −0.61 0.53 0.22 0.04 −0.37 −0.39 −0.42 0.49
22:2 NMI (7,13) −0.29 0.56 0.53 −0.17 −0.08 −0.41 −0.24 −0.31 0.22
22:2 NMI (7,15) −0.25 0.32 0.42 −0.23 −0.13 −0.47 −0.31 −0.23 0.3 0.45
18:0DMA 0.04 −0.23 −0.14 −0.06 −0.14 0.36 0.43 0.27 −0.17 0.08 −0.05
20:1n-7 0.12 0.09 0.4 −0.31 0.06 −0.29 −0.23 −0.47 −0.11 0.3 0.26 −0.17
20:1n-9 0.24 −0.06 0.07 −0.15 0.27 −0.16 −0.09 −0.39 −0.12 0.09 0.14 −0.23 0.23
−1 −0.8 −0.6 −0.4 −0.2 0 0.2 0.4 0.6 0.8 1

B.

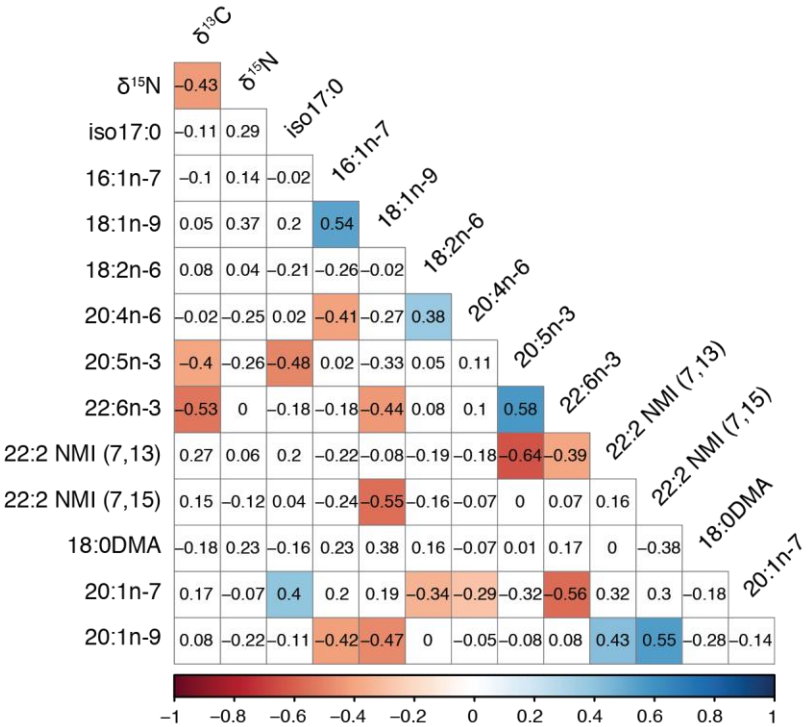
δ13C
δ15N
iso17:0
16:1n-7
18:1n-9
18:2n-6
20:4n-6
20:5n-3
22:6n-3
22:2 NMI (7,13)
22:2 NMI (7,15)
18:0DMA
20:1n-7
20:1n-9
δ15N −0.43
iso17:0 −0.11 0.29
16:1n-7 −0.1 0.14 −0.02
18:1n-9 0.05 0.37 0.2 0.54
18:2n-6 0.08 0.04 −0.21 −0.26 −0.02
20:4n-6 −0.02 −0.25 0.02 −0.41 −0.27 0.38
20:5n-3 −0.4 −0.26 −0.48 0.02 −0.33 0.05 0.11
22:6n-3 −0.53 0 −0.18 −0.18 −0.44 0.08 0.1 0.58
22:2 NMI (7,13) 0.27 0.06 0.2 −0.22 −0.08 −0.19 −0.18 −0.64 −0.39
22:2 NMI (7,15) 0.15 −0.12 0.04 −0.24 −0.55 −0.16 −0.07 0 0.07 0.16
18:0DMA −0.18 0.23 −0.16 0.23 0.38 0.16 −0.07 0.01 0.17 0 −0.38
20:1n-7 0.17 −0.07 0.4 0.2 0.19 −0.34 −0.29 −0.32 −0.56 0.32 0.3 −0.18
20:1n-9 0.08 −0.22 −0.11 −0.42 −0.47 0 −0.05 −0.08 0.08 0.43 0.55 −0.28 −0.14
−1 −0.8 −0.6 −0.4 −0.2 0 0.2 0.4 0.6 0.8 1

C.

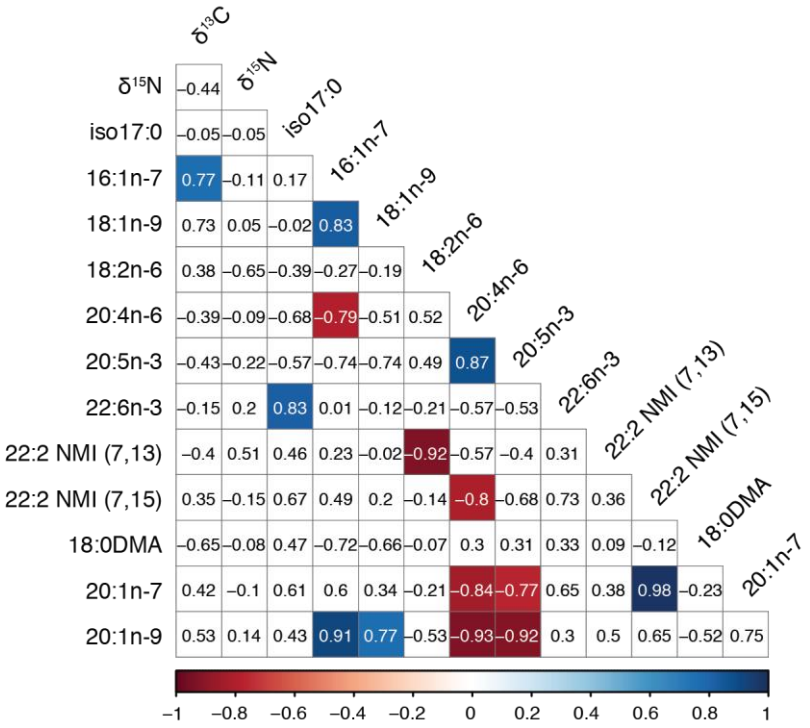

Figure S1 Correlation plots among trophic tracers for (A) *Panulirus penicillatus*, (B) *Panulirus longipes* and (C) *Panulirus versicolor*. Colored cells indicate a significant correlation ($P < 0.05$) between two trophic tracers, while uncolored cells indicate a non-significant correlation. Numbers in the cells are the associated correlation coefficients (Pearson for parametric and Kendall for non-parametric) and the cells' color intensity is proportional to the coefficient. Selected fatty acids are well-known trophic markers that give information on consumed prey (Dalsgaard et al. 2003; Budge et al. 2006; Iverson 2009; Kelly and Scheibling 2012; Meyer et al. 2019).

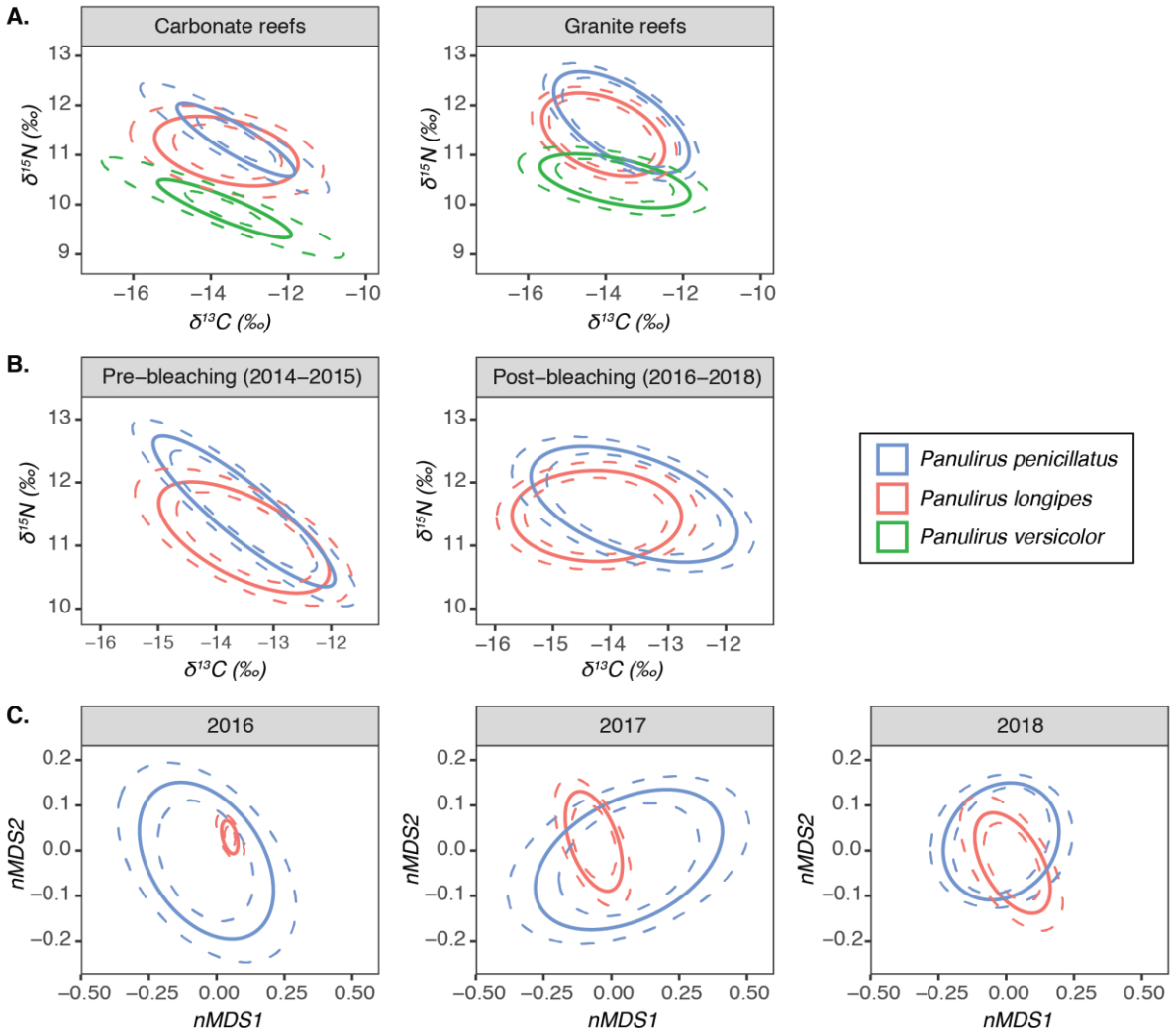

Figure S2 Isotopic niches for the three spiny lobster species by (A) reef habitat type (carbonate *vs* granite reefs; all years 2014-2018 mixed) and (B) pre- and post-2016 coral bleaching event, and (C) fatty acid niches for these species by sampling year (from 2016 to 2018). All niche sizes and niche overlaps are presented in Fig. 5. Mean ellipses are represented by a plain line and uncertainty ellipses (CI 95%) are represented by dashed lines.

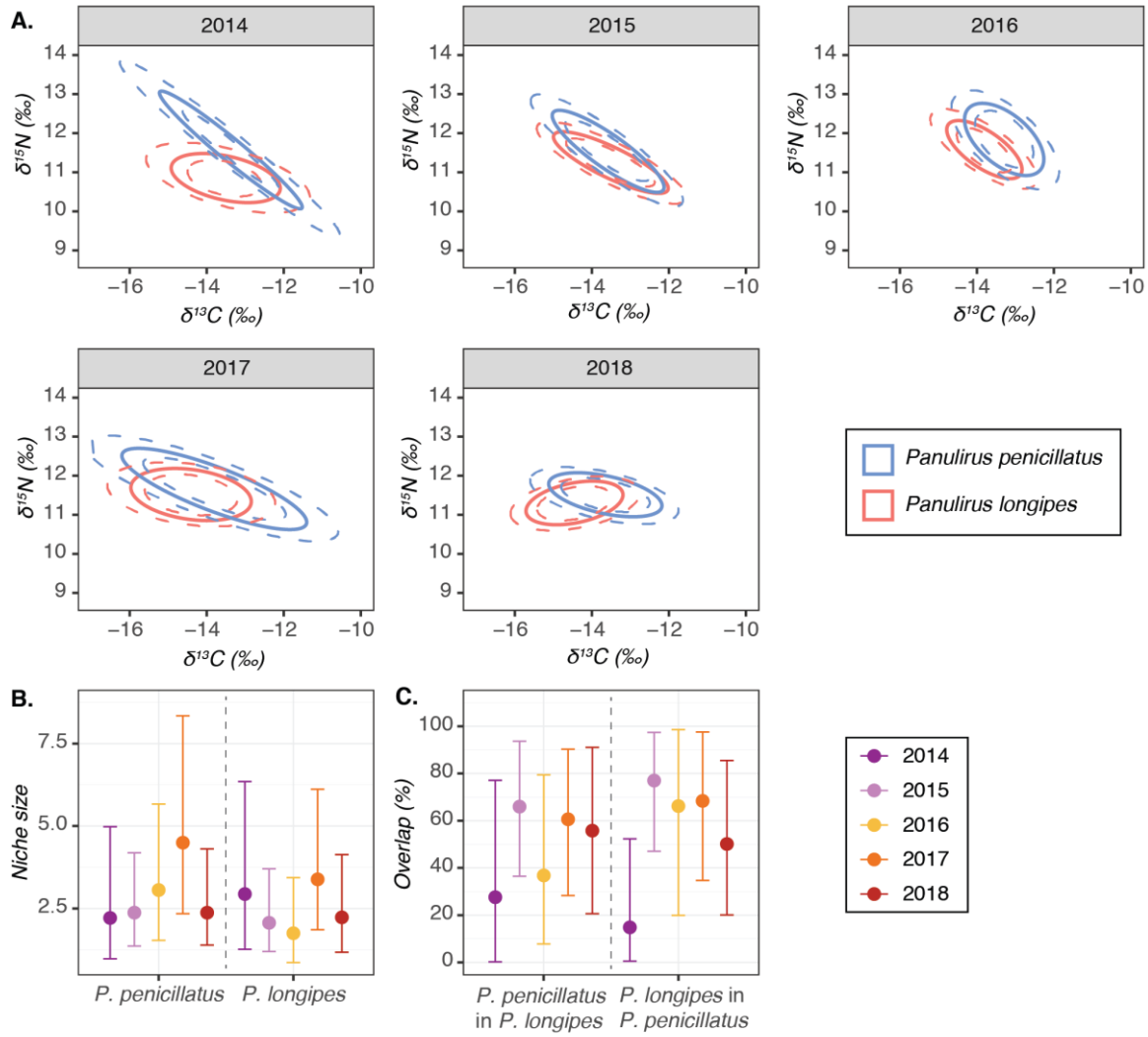

Figure S3 Isotopic niches for *Panulirus penicillatus* and *Panulirus longipes* by sampling year (from 2014 to 2018) (A). The derived lobsters species' niche sizes (B) and overlaps (C) are also provided for each sampling year. The low sample size of *Panulirus versicolor* did not allow for its inclusion in computing. Mean ellipses are represented by a plain line and uncertainty ellipses (CI 95%) are represented by dashed lines. Niche sizes ($‰^2$) and overlaps (%) are presented as mean with their associated confidence interval at 95 %.

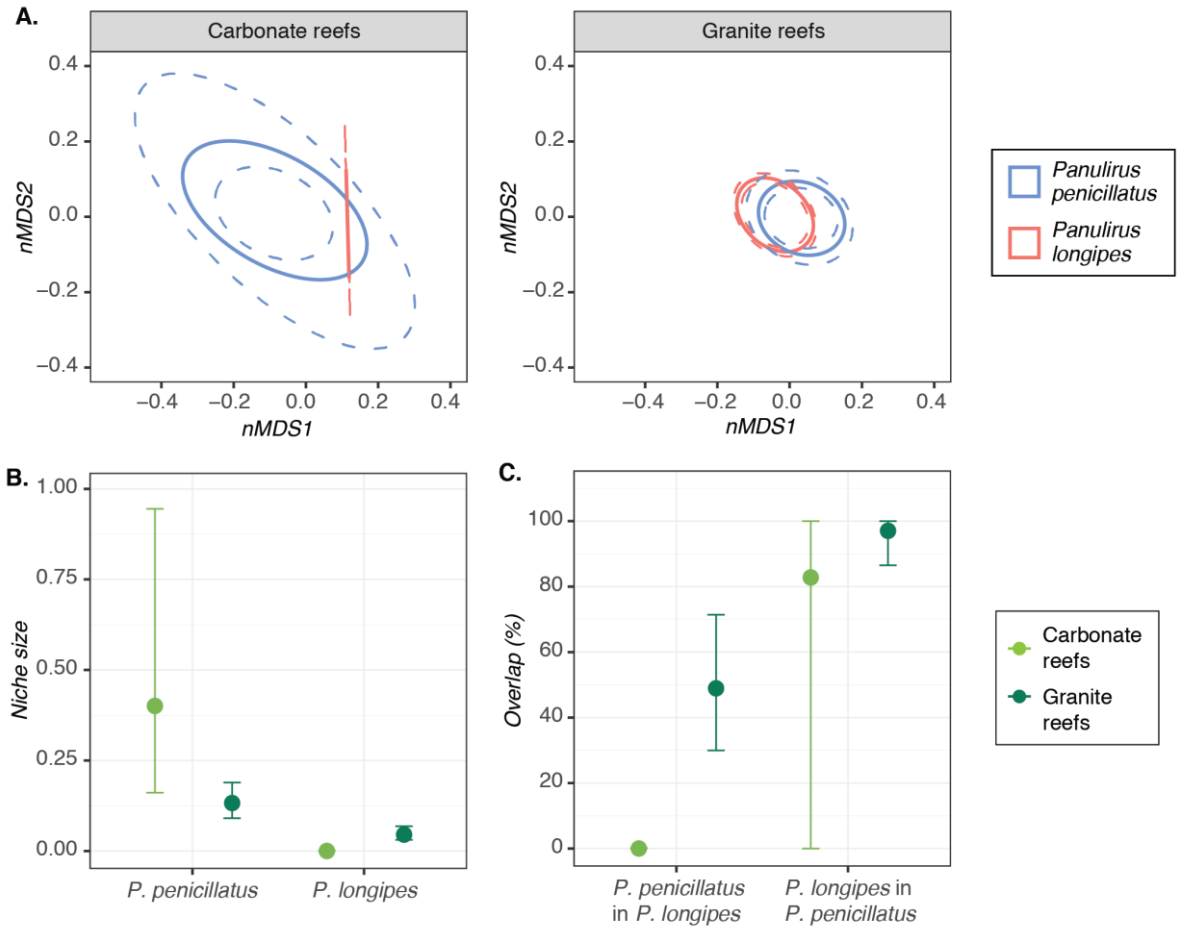

Figure S4 Fatty acid niches for *Panulirus penicillatus* and *Panulirus longipes* by reef habitat type (A). The derived lobster species' niche sizes (B) and overlaps (C) are also provided for each reef habitat. The low sample size of *Panulirus versicolor* did not allow for its inclusion in niche computing. Mean ellipses are represented by a plain line and uncertainty ellipses (CI 95%) are represented by dashed lines. Niche sizes (unitless) and overlaps (%) are presented as mean with their associated confidence interval at 95 %.

References of supplementary data

Budge SM, Iverson SJ, Koopman HN (2006) Studying trophic ecology in marine ecosystems using fatty acids: A primer on analysis and interpretation. Mar Mammal Sci 22:759–801. doi: 10.1111/j.1748-7692.2006.00079.x

Dalsgaard J, St. John M, Kattner G, Müller-Navarra D, Hagen W (2003) Fatty acid trophic markers in the pelagic marine environment. Adv Mar Biol 46:225–340. doi: 10.1016/S0065-2881(03)46005-7

Iverson SJ (2009) Tracing aquatic food webs using fatty acids: from qualitative indicators to quantitative determination. In: Kainz M, Brett MT, Arts MT (eds) Lipids in Aquatic Ecosystems. Springer New York, New-York, USA, pp 281–308. doi: 10.1007/978-0-387-89366-2_12

Kelly JR, Scheibling RE (2012) Fatty acids as dietary tracers in benthic food webs. Mar Ecol Prog Ser 446:1–22. doi: 10.3354/meps09559

Meyer L, Pethybridge H, Nichols PD, Beckmann C, Huveneers C (2019) Abiotic and biotic drivers of fatty acid tracers in ecology: A global analysis of chondrichthyan profiles. Funct Ecol 33:1243–1255. doi: 10.1111/1365-2435.13328

- SUPPLEMENTARY DOCUMENT 3 -

Ontogeny and seasonal variation of environmental parameters influence trace element bioaccumulation in emperor red snappers (*Lutjanus sebae*)

Magali A. SABINO[1,2], Paco BUSTAMANTE[2,3], Rodney GOVINDEN[1], Rona ALBERT[1], Carine CHURLAUD[2], Heidi PETHYBRIDGE[4], Nathalie BODIN[1,5,6]

[1] Seychelles Fishing Authority (SFA), Fishing Port, Victoria, Mahé, Republic of Seychelles

[2] Littoral Environnement et Sociétés (LIENSs), UMR 7266 CNRS - La Rochelle Université, 2 rue Olympe de Gouges, 17000 La Rochelle, France

[3] Institut Universitaire de France (IUF), 1 rue Descartes 75005 Paris, France

[4] CSIRO Oceans and Atmosphere, Brisbane, Queensland, Australia

[5] Institute for Research and Development (IRD), Fishing Port, Victoria, Mahé, Seychelles

[6] Sustainable Ocean Seychelles (SOS), BeauBelle, Mahé, Republic of Seychelles

To be submitted in *Environmental Research*

Abstract

Snappers are highly important for small-scale fisheries in many Small Island Developing Countries. Yet, little is known about trace element bioaccumulation in these species. In the Seychelles, the emperor red snapper (*Lutjanus sebae*) is the main species caught by the demersal fishery. Here, we first investigated ontogenetic changes in trophic ecology in emperor red snappers from the Seychelles using stable isotopes of carbon and nitrogen (i.e. $\delta^{13}C$ and $\delta^{15}N$ values). Then, we examined the effects of size, sex, ontogenetic changes in trophic ecology and season on trace element bioaccumulation in the muscle tissues of emperor red snappers. Ontogenetic changes in habitat use and diet were observed, with a possible effect of maturity stage, and highly influenced the bioaccumulation of Cu, Hg, Ni, Se and Zn in emperor red snapper. On a more general aspect, size, habitat use, trophic position and diet all had different degrees of effect on trace element bioaccumulation in emperor red snappers' muscle tissues. Finally, seasonal variations in trace element concentrations were mainly related to seasonal variations in trace element bioavailability likely due to changes in weather, bacterial activity and environmental parameters (i.e. water temperature, salinity and dissolve oxygen).

Keywords: Demersal; Trophic ecology; Metals; Seychelles

1. Introduction

Lutjanid fishes, also called red snappers, share common and particular features like life-history traits and reproductive biology. They are long-lived species (up to 53 years), with a slow growth rate, a late maturation and a low mortality rate (Martinez-Andrade 2003). They also inhabit a wide diversity of habitats throughout their life. Snappers' eggs and larvae are pelagic, while juveniles settle in nursery grounds (i.e. mangroves or coral/rocky reefs) until they reach maturity (Allen 1985), and adults inhabit a wide range of demersal habitats on continental shelfs or at the continental slope (Martinez-Andrade 2003). Most snappers live in shallow to intermediate depths (Allen 1985), with large individuals generally being associated with deeper waters than juveniles (Martinez-Andrade 2003). As an example, in the Seychelles, adult emperor red snappers (*Lutjanus sebae*) are generally caught in depths above 100 m (Mees 1992). Throughout their adult life stage, snappers will also undertake regular migrations to form spawning aggregations during seasonal reproduction. For emperor red snappers in the Seychelles, these aggregations occur on the Mahé Plateau during inter-monsoon seasons (Robinson *et al*. 2004).

Red snappers are of major importance for many small-scale fisheries worldwide, essentially in tropical and subtropical countries (Cawthorn and Mariani 2017; Amorim *et al*. 2019). In countries where seafood is the main source of proteins and micronutrients, like in Small Island Developing States (SIDS), these fisheries support the livelihoods and food security of local populations (Cawthorn and Mariani 2017; Hicks *et al*. 2019). However, their particular biological and ecological features (i.e. long life, slow growth rate, late maturation and formation of spawning aggregation) make them particularly prone to overfishing (Marriott *et al*. 2007; Grandcourt *et al*. 2008). In the Seychelles, snappers' catch per unit effort decreased from 1990 to 2016 (36 to 16 $kg.day^{-1}$), mainly due to spatial expansion of fishing grounds, longer fishing trips and increase in boat size, and concerns have been raised concerning overfishing (Robinson *et al*. 2004, 2020). Yet, the trophic ecology and life-history traits of snappers in the Seychelles, including emperor red snapper are poorly known.

Seafood, including snapper species, are particularly high in micronutrients like essential trace elements, and are thus thought to be key food items in promoting healthy diets and in the fight against micronutrient deficiency (Béné *et al.* 2015; Hicks *et al.* 2019). However, seafood also contains non-essential trace elements that can have adverse effects on the consumer's health if concentrations are too high (Bosch *et al*. 2016). Yet, little is known about the essential and non-essential trace element content of snappers in SIDS, with most studies only reporting Hg concentrations in these species (Ahmad *et al*. 2015; Anual *et al.* 2018; Suratno *et al.* 2019). In the Seychelles, where the emperor red snapper (*Lutjanus sebae*) is the main species captured by the demersal fishery (Seychelles Fishing Authority 2019), Hg concentrations were reported to be 0.192 ± 0.105 $\mu g.g^{-1}$ ww in this species (Sardenne *et al*.

2017), which falls in the range of values measured elsewhere in the Indo-Pacific (Malaysia: 0.334 $\mu g.g^{-1}$ dw ≈ 0.084 $\mu g.g^{-1}$ ww, Ahmad *et al*. 2015, and 0.118 $\mu g.g^{-1}$ ww, Anual *et al*. 2018; Indonesia: 0.88 ± 0.34 $\mu g.g^{-1}$ dw ≈ 0.22 $\mu g.g^{-1}$ ww, Suratno *et al.* 2019).

The long lifespan of snappers and their demersal feeding behaviour could make them prone to bioaccumulate high concentrations of non-essential trace elements like Hg, which is known to accumulate along time in muscle and liver (Goutte *et al*. 2015), or Cd and Pb which are in high concentrations in sediments and could thus be transferred to snappers through the trophic pathway (Rejomon *et al*. 2010; Velusamy *et al*. 2014). Ontogenetic changes in habitat and diet, and local movements due to migration to spawning grounds, could also influence trace element bioaccumulation in emperor red snapper by influencing their trophic ecology. Particularly, the sexual dimorphism observed in emperor red snappers from the Seychelles (Mees 1992), may induce different bioaccumulation rates between males and females. Finally, seasonal variations in primary production and environmental parameters (e.g. water temperature and salinity) could also affect trace element concentrations and thus availability for human diets around the year. Yet, in spite of the importance of intrinsic (e.g. size, age, physiological needs) and extrinsic factors (e.g. trophic ecology) in controlling trace element concentrations in seafood, including red snappers, very few studies investigated this topic (but see Metian *et al.* 2013).

Here, we investigated the trophic ecology of male and female emperor red snappers in the Seychelles using stable isotopes of carbon and nitrogen (i.e. $\delta^{13}C$ and $\delta^{15}N$ values), in order to bring insight into ontogenetic changes in trophic ecology. Then, we examine the effect of intrinsic (i.e. sex, size and ontogeny) and extrinsic (i.e. trophic ecology, season) factors on trace element bioaccumulation in emperor red snappers from the Seychelles.

2. Material and methods

2.1. Sample collection and preparation

A total of 77 emperor red snapper were caught around the Mahé Plateau (Seychelles, Western Indian Ocean) by fishers and during scientific cruises onboard the Research Vessel l'Amitié during 2014 and 2018 (Table S1). For each individual, a piece of dorsal muscle tissue (around 10-15g) was retrieved, sex was determined by visual observation and fork length was measured to the nearest 0.1 cm. All samples were then stored as soon as possible in a deep-freezer (-80°C) until further specific pre-treatment and analysis. Subsamples (around 2-10g each) for the analysis of trace elements and stable isotopes were freeze-dried over 72 hr and stored in a dry environment prior to any analysis. Water content (77.9 ± 0.5 %) was determined on 8 samples.

2.2. Trace element analysis

Analysis of Ag, As, Cd, Co, Cr, Cu, Fe, Mn, Ni, Pb, Se and Zn were carried out at the UMR LIENSs in La Rochelle (France). Samples were analysed by Induced Coupled Plasma (ICP), using a Varian Vista-Pro ICP coupled with optical emission spectrometry (OES) and a ThermoFisherScientific XSeries 2 ICP coupled with mass spectrometry (MS). Aliquots of the biological samples (90-200 mg) were digested with 6 ml 67-70% of nitric acid (HNO_3) and 2 ml 34-37% of hydrochloric acid (HCl) (Fisher Scientific, trace element grade quality). Acidic digestion of the samples was carried out overnight at room temperature, then using a Milestone microwave (30 min with constantly increasing temperature up to 120°C, then 15 min at this maximal temperature). Each digested sample was completed to 50 ml with milli-Q water. Seven control samples (five Certified Reference Materials, CRMs, and two blanks) treated and analysed in the same way as the samples were included in each analytical batch. CRMs were dogfish liver DOLT-5 (National Research Council Canada) and lobster hepatopancreas TORT-3 (National Research Council Canada). Mean recovery rates for all trace elements ranged from 86 to 113% (Table S2).

Total Hg analyses were carried out at the Seychelles Fishing Authority in Victoria (Seychelles) and UMR LIENSs in La Rochelle (France). Samples were analysed with a Direct Mercury Analyser (Milestone DMA 80) and an Advanced Mercury Analyser (Altec AMA 254) atomic absorption spectrophotometers, respectively. Both devices are based on the same method, which does not require preliminary acidic digestion of the samples. Dry grounded subsamples were thus directly analysed. Hg determination involved progressive heating until 750 °C was reached, that allowed complete burning of the matrix and evaporation of the element. The evaporated element is then fixed on a golden net by amalgamation. Collected Hg on the amalgamator was then liberated by its heating at 950 °C, and measured by atomic absorption spectrophotometry. Each sample was analysed at least twice until the relative standard deviation (RSD) was below 10%.

Hg concentrations were validated by the analysis of a CRM, DOLT-5 (dogfish liver; National Research Council, Canada), every 10 samples. CRM aliquots were treated and analysed according to the same conditions as the samples. Masses of the CRM were adjusted to correspond to the same Hg amounts as in the samples. Blanks were also analysed at the beginning of each set of samples, and the quantification limit was 0.1 ng (5*DL, with DL the detection limit = 3*standard deviation of 8 blanks).

2.3. Stable isotope analysis

Because lipids are usually more depleted in ^{13}C than other tissue components and could thus introduce a bias in the results, reserve lipids must be removed before $\delta^{13}C$ determination (De Niro and Epstein 1978). Lipid content, determined on 8 samples, was of 0.5 ± 0.1 % ww. For all samples, lipids

were thus chemically removed prior to stable isotope analysis. For each sample, between 10 and 12 mg of powdered sample was placed in a glass tube with 4 ml of cyclohexane. Tubes were then agitated during 10 minutes at room temperature and centrifuged during 5 minutes at 4500 rpm before removal of extraction solvent. Agitation, centrifugation and solvent-removal steps were repeated three times before putting tubes for drying in an oven at 45 °C for a night.

For $\delta^{13}C$ and $\delta^{15}N$ determination, between 250 and 500 µg of sample was weighed in tin capsules. The samples were analysed by continuous flow on a Thermo Scientific Flash 2000 elemental analyser coupled to a Delta V Plus interface mass spectrometer. International isotopic standards (USGS-61 and USGS-62) of known $\delta^{13}C$ and $\delta^{15}N$ were used to validate the analytical procedure. Results are expressed in the δ unit notation as deviations from standards (Vienna Pee Dee Belemnite for $\delta^{13}C$ and atmospheric nitrogen for $\delta^{15}N$) following the formula: $\delta^{13}C$ or $\delta^{15}N = [(Rsample/Rstandard) - 1] \times 1000$, where R is $^{13}C/^{12}C$ or $^{15}N/^{14}N$, respectively. Measurement errors (SD) of stable isotope analyses, calculated on all measured values of $\delta^{13}C$ and $\delta^{15}N$ in isotopic reference materials, were < 0.10 ‰ for both the nitrogen and carbon isotope measurements. This was in accordance with the analytical precision given by the manufacturer (i.e. < 0.10 ‰ for $\delta^{13}C$ and < 0.15 ‰ for $\delta^{15}N$; Thermo Scientific). For each sample, the C:N ratio was calculated, and never exceeded 3.5 proving that reserve lipids were adequately removed (Post *et al*. 2007).

2.4. Data analysis

For ecological interpretations, observations below the limit of quantification (LOQ) were substituted with values drawn randomly from the range]0;LOQ[and only trace elements with detection frequencies > 70% (i.e. at least 70% of the measured values are above the LOQ) were used (Table S2) (Carravieri *et al*. 2020). As all measures of V were below LOQ, this element was definitely removed from the database for all analyses.

Prior to any statistical analysis, data were tested for normality and homoscedasticity, using Fligner and Shapiro tests respectively.

Size difference between sexes was tested using Wilcoxon test and difference among seasons was tested using Kruskal-Wallis followed by Dunn post-hoc test with Benjamini-Hochberg adjustment. As there was no significant difference between sexes or among seasons (Fig. S1), while $\delta^{13}C$ and $\delta^{15}N$ values in fish can be influenced by fish size, the effects of continuous variables (i.e. fork length, $\delta^{13}C$ and $\delta^{15}N$ values) and of categorical variables (i.e. sex and season) on trace element bioaccumulation in emperor red snappers were investigated separately.

In order to bring insight into the trophic ecology of sampled emperor red snappers, the relationships between fork length and stable isotope values, and between $\delta^{13}C$ and $\delta^{15}N$ values, were investigated using Kendall correlation tests. Difference ($p < 0.05$) in stable isotope values between sexes and among seasons were also tested using Wilcoxon tests and Kruskal-Wallis followed by Dunn test, respectively.

Non-metrical multidimensional scaling (nMDS) ordination of Bray-Curtis similarity matrix was performed to visually assess the difference in trace element profiles between sexes and among seasons. For each trace element, Wilcoxon test and Kruskal-Wallis followed by Dunn post-hoc test were used to test for significant difference ($p < 0.05$) in concentrations among sexes and seasons, respectively.

2.5. Modelling the relationship between trace element concentrations and size and $\delta^{13}C$ and $\delta^{15}N$ values

Generalised linear models (GLMs) and/or generalised additive models (GAMs) were used to assess the relationship between log-transformed trace element concentrations and emperor red snappers' size (i.e. fork length) and $\delta^{13}C$ and $\delta^{15}N$ values. For this, GAMs were first fitted on log-transformed trace element concentrations, with fork length, $\delta^{13}C$ and $\delta^{15}N$ values as explanatory variables. As both $\delta^{13}C$ and $\delta^{15}N$ values are known to vary according to fish size, their interaction terms with fork length were also added as explanatory variables in the full model. However, for all trace elements, modelled trends with fork length or stable isotope values appeared to be linear, thus GLMs were finally preferred. Although it is usually not recommended to pre-transform the response variable prior to fit a GLM or a GAM, as both include the possibility of within-model transformation through a link function, previous work on trace elements showed that applying a log-transformation prior to fitting models improved the models (e.g. Méndez-Fernandez *et al*. 2013; Chouvelon *et al.* 2014, 2017). Thus, here, all GLMs and GAMs were fitted on log-transformed trace element concentrations with a Gaussian distribution and an identity link function. For each model performed, the complete model was first compared to a null model (i.e. containing only the intercept terms) using the Akaike information criterion (AIC) (Akaike 1981). This allowed to the capacity of the complete model to explain the variability of the response variable. If the null model was better than the complete model (i.e. had a lower AIC), analyses did not go further. If the complete model was better than the null model, a stepwise procedure was used to select the most parsimonious model, again using the AIC. For this, explanatory variables were successively removed from the complete model until all remaining variables significantly improved the model (i.e. no significant lowering of the AIC). When the AIC was not significantly different between two compared models, the simplest model was preferred (Zuur *et al.* 2007). Finally, all selected

models were validated by checking the normality and homoscedasticity of residuals, and the potential presence of outliers (Zuur *et al.* 2007).

For all trace elements for which fork length or one of its interactions factors was significant, it was necessary to remove the size effect to investigate the direct effects of $\delta^{13}C$ and $\delta^{15}N$ only. Thus, trace element concentrations were standardized by length using a method similar to the one of Houssard *et al*. (2019). GLMs were first fitted on log-transformed trace element concentrations with fork length alone as explanatory variable. All models were checked for linearity to ensure that there was no need to use a GAM instead. Then, the residuals from the size-based models were used as response variable in GAMs with $\delta^{13}C$ and $\delta^{15}N$ values only. Again, whenever modelled trends appeared to be linear, GLMs were finally preferred instead of GAMs.

2.6. Software

All statistical analyses and modelling were performed under R 3.5.2 software (R Core Team 2018). Wilcoxon tests and Kruskal-Wallis were computed using the included *stats* R package, while Dunn post-hoc test was computed using the *FSA* R package (Ogle *et al*. 2018). Correlation tests were computed by using the *cor.test* function from the included *stats* R package, in which the wanted method (i.e. Kendall) was specified. nMDS ordinations were generated using the *metaMDS* function from the R *vegan* package (Oksanen *et al*. 2019). GLMs were fitted using the *glm* function from the included *stats* R package and GAMs were fitted using the gam function from the mgcv R package (Wood 2011).

3. Results

3.1. Stable isotopes: intercorrelation, relationship with size and effect of sex and season

In analysed emperor red snappers, $\delta^{13}C$ and $\delta^{15}N$ values in their muscle tissues were both positively correlated with their fork length, regardless of the sex (Fig. 1A, B). $\delta^{13}C$ and $\delta^{15}N$ were also positively correlated with each other regardless of the sex (Fig. 1C). There was no difference in $\delta^{13}C$ and $\delta^{15}N$ values among sexes or among seasons (Table 1).

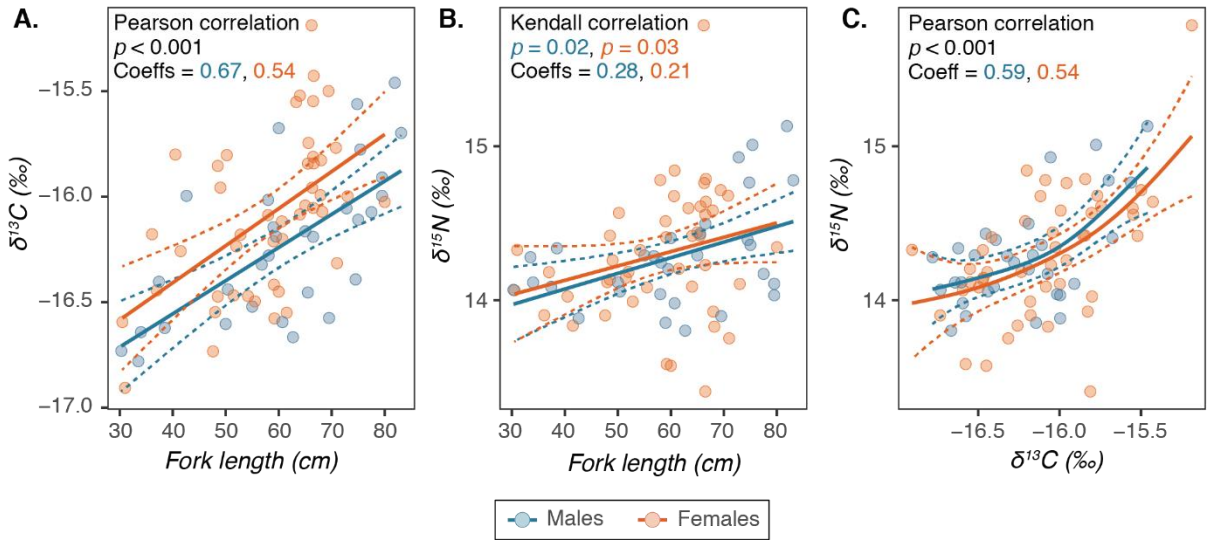

Fig. 1 Relationships between fork length (cm) and C and N stable isotope values (‰) (A, B) and between $\delta^{13}C$ and $\delta^{15}N$ values (C), for males and females. Smoothing curves were fitted using the GLM method for linear relationships (A, B) and the GAM method for the non-linear relationship (C) under R software. Dotted curves represent the confidence interval at 95% around the fit.

Table 1 $\delta^{13}C$ and $\delta^{15}N$ values (‰) measured in the white muscle tissues of emperor red snappers for each sex and each season. Values are presented as mean ± SD.

	$\delta^{13}C$	$\delta^{15}N$
All individuals (n = 57)	-16.1 ± 0.4	14.3 ± 0.4
Males (n = 31)	-16.2 ± 0.4	14.3 ± 0.3
Females (n = 46)	-16.1 ± 0.4	14.3 ± 0.4
Males		
Pre-NWM (n = 4)	-16.4 ± 0.2	14.2 ± 0.1
NWM (n = 22)	-16.2 ± 0.4	14.3 ± 0.4
Pre-SEM (n = 5)	-16.4 ± 0.2	14.0 ± 0.2
Females		
Pre-NWM (n = 6)	-16.2 ± 0.3	14.3 ± 0.2
NWM (n = 35)	-16.1 ± 0.4	14.3 ± 0.4
Pre-SEM (n = 5)	-15.9 ± 0.1	14.3 ± 0.5
Pre-NWM (n = 10)	-16.2 ± 0.3	14.3 ± 0.1
NWM (n = 57)	-16.1 ± 0.4	14.3 ± 0.4
Pre-SEM (n = 10)	-16.2 ± 0.3	14.1 ± 0.3

3.2. Effect of sex and season on trace element bioaccumulation

Trace element profiles were highly similar between sexes (Fig. 2A) and there was no significant difference in trace element concentrations between males and females (Fig. 3).

Emperor red snappers caught during the pre-NWM season seemed to be separated from those caught during the other two sampling seasons by As (Fig. 2B). The profile ellipse of emperor red snappers caught during the pre-SEM season was included in the one of individuals caught during the NWM season. Trace element concentrations were lowest in individuals caught during the pre-NWM season for Cd, Cr, Cu, Mn, Ni and Zn, in comparison with the NWM season (Dunn test, $p < 0.001$ for Cd

and Cr; $p < 0.01$ for Cu and Zn; and $p < 0.05$ for Mn and Ni) and with the pre-SEM season (Dunn test, $p < 0.001$ for Cr and Zn; $p < 0.01$ for Ni; and $p < 0.05$ for Cd, Cu and Mn), while individuals caught during the pre-SEM had the highest Ni concentrations (Dunn test, $p < 0.001$ with pre-NWM and $p = 0.008$ with NWM) (Fig. 3). Individuals caught during the pre-NWM season also had lower Se concentrations than those caught during the NWM season (Dunn test, $p = 0.004$) but higher Hg concentrations than individuals caught during the pre-SEM season (Dunn test, $p = 0.012$).

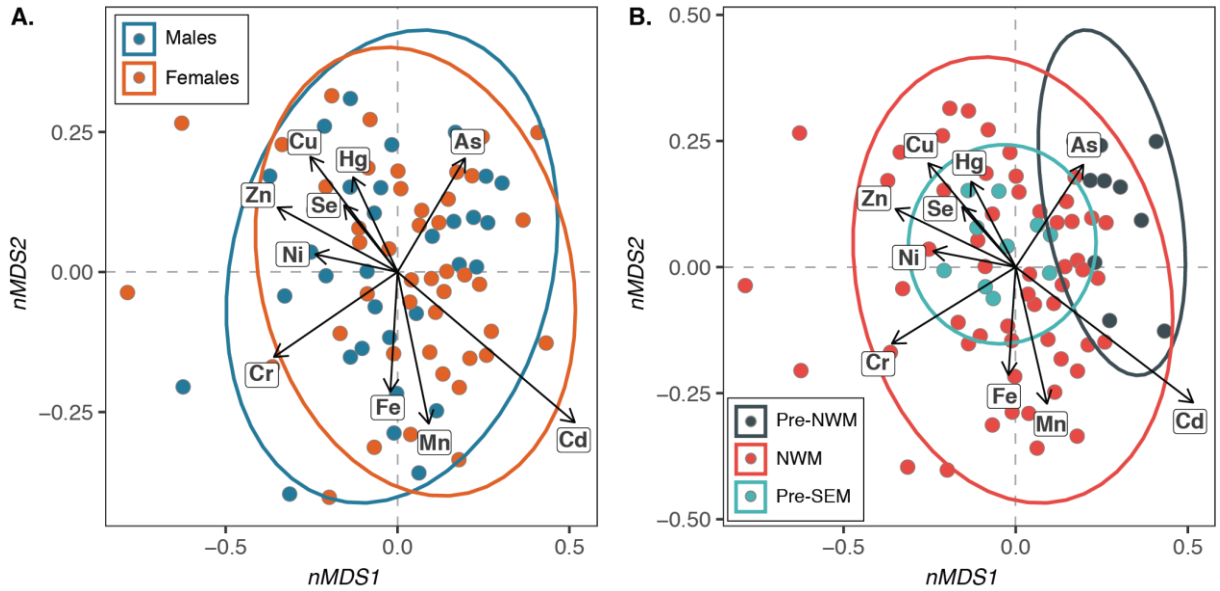

Fig. 2 Non-metrical multidimensional scaling (nMDS) ordination of Bray-Curtis similarity matrix of muscle normalised trace element concentrations in emperor red snappers, according to sex (A) and season (B). Probabilistic ellipses at 0.95 are also represented in order to show grouping of points. NWM = Northwest Monsoon, SEM = Southeast Monsoon.

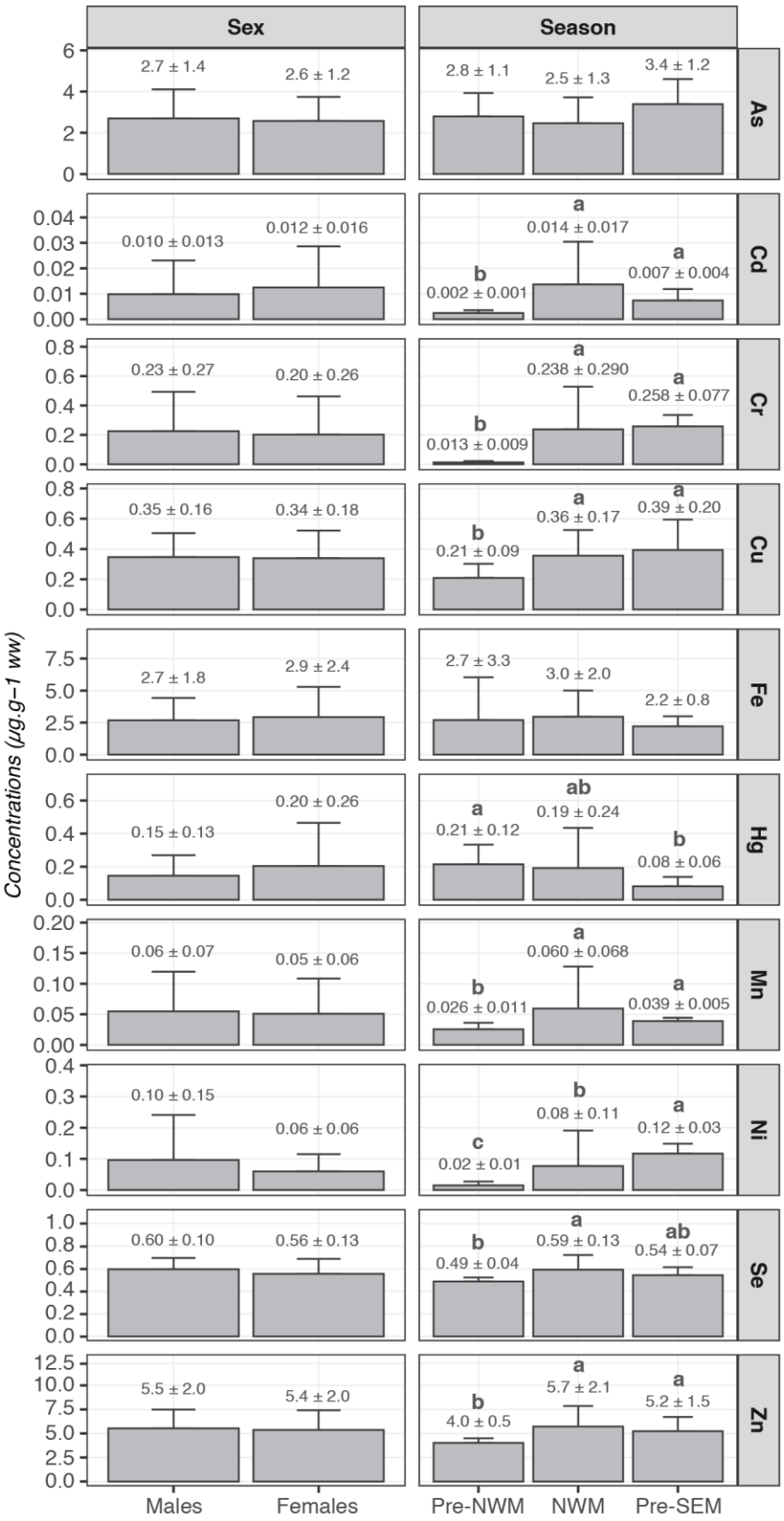

Fig. 3 Trace element concentrations (µg.g-1 ww) in white muscle tissues of emperor red snappers grouped by sex and season, and presented as mean ± SD (values are also given above each bar). A different letter indicates significant difference ($p < 0.05$, Wilcoxon or Dunn post-hoc test). NMW = Northwest Monsoon, SEM = Southeast Monsoon.

3.3. Relationship between trace element concentrations and size and $\delta^{13}C$ and $\delta^{15}N$ values

Among all models tested to explain trace element concentrations in emperor red snappers, the null model was the best selected model (i.e. with the lowest AIC) for Cr and Fe (Table 2). Among all other models, individual size as explanatory variable significantly improved the goodness of fit of the model (i.e. significantly decreased the AIC). However, size was significant ($p < 0.05$) in the model only for As, Cd, Hg with a positive slope, and for Mn and Ni with a negative slope. After removing the size effect, there was a significant relationship between As concentrations and both $\delta^{13}C$ (positive slope) and $\delta^{15}N$ (negative slope) values (Table 2). The relationship between concentrations and $\delta^{15}N$ values was also significant for Cu, Hg, Ni, Se and Zn. For these trace elements, a change in relationship trend seems to occur at values between 14.5 and 15.0 ‰ (estimated values of 14.8 ‰ for Cu, 14.9 ‰ for Hg, 15 ‰ for Ni, 14.5 ‰ for Se and 14.6 ‰ for Zn) (Fig. 4). Cu and Zn presented the same pattern with, first, a negative relationship with $\delta^{15}N$ values and, then, a weak positive relationship. Se and Zn also presented similar patterns with, first, relatively stable concentrations and then a strong positive relationship with $\delta^{15}N$ values. Finally, Hg seemed to first have a weak negative relationship when $\delta^{15}N$ values are low but a strong positive relationship for values above 15.0 ‰.

Table 2 Model results for log-transformed and length-standardised trace element concentrations. For each model explaining log-transformed concentrations, given explanatory variables are those present in the best selected model (i.e. with lowest AIC).

Trace element	Response variable	Model	Explanatory variables	*p* value	GLM – Estimated slope
As	Log(As)	GLM	Fork length	0.006	0.279 ± 0.098
			$\delta^{15}N$	0.135	0.639 ± 0.423
			$\delta^{13}C$:fork length	0.004	0.004 ± 0.001
			$\delta^{15}N$:fork length	0.022	-0.015 ± 0.006
	Residuals(logAs-size)	GLM	$\delta^{13}C$	0.004	0.212 ± 0.071
			$\delta^{15}N$	< 0.001	-0.326 ± 0.069
Cd	Log(Cd)	GLM	Fork length	0.007	0.525 ± 0.191
			$\delta^{13}C$	0.033	-1.514 ± 0.696
			$\delta^{15}N$	0.838	0.036 ± 0.175
			$\delta^{13}C$:fork length	0.008	0.032 ± 0.012
	Residuals(logCd-size)	GLM	$\delta^{13}C$	0.311	0.180 ± 0.176
			$\delta^{15}N$	0.251	0.198 ± 0.172
Cr	Log(Cr)	GAM	Null model	-	-
Cu	Log(Cu)	GLM	Fork length	0.913	-0.017 ± 0.155
			$\delta^{13}C$	0.580	0.179 ± 0.323
			$\delta^{15}N$	1.000	0.001 ± 0.467
			$\delta^{13}C$:fork length	0.565	-0.003 ± 0.006
			$\delta^{15}N$:fork length	0.753	-0.002 ± 0.007
	Residuals(logCu-size)	GAM	$\delta^{13}C$	0.989	-
			$\delta^{15}N$	0.018	-
Fe	Log(Fe)	GAM	Null model	-	-
Hg	Log(Hg)	GLM	Fork length	0.003	0.461 ± 0.151
			$\delta^{15}N$	0.022	1.507 ± 0.646
			$\delta^{13}C$:fork length	0.009	0.006 ± 0.002
			$\delta^{15}N$:fork length	0.014	-0.025 ± 0.009
	Residuals(logHg-size)	GAM	$\delta^{13}C$	0.111	-
			$\delta^{15}N$	0.028	-
Mn	Log(Mn)	GLM	Fork length	0.016	-0.048 ± 0.020
			$\delta^{15}N$:fork length	0.009	0.003 ± 0.001
	Residuals(logMn-size)	GLM	$\delta^{13}C$	0.887	0.015 ± 0.102
			$\delta^{15}N$	0.064	0.186 ± 0.099
Ni	Log(Ni)	GLM	Fork length	0.003	-0.697 ± 0.231
			$\delta^{13}C$	0.002	2.707 ± 0.842
			$\delta^{15}N$	0.023	-0.491 ± 0.212
			$\delta^{13}C$:fork length	0.003	-0.044 ± 0.014
	Residuals(logNi-size)	GAM	$\delta^{13}C$	0.253	-
			$\delta^{15}N$	0.005	-
Se	Log(Se)	GLM	Fork length	0.534	0.035 ± 0.055
			$\delta^{13}C$	0.370	-0.104 ± 0.115
			$\delta^{15}N$	0.822	0.037 ± 0.166
			$\delta^{13}C$:fork length	0.364	0.002 ± 0.002
			$\delta^{15}N$:fork length	0.929	-0.001 ± 0.003
	Residuals(logSe-size)	GAM	$\delta^{13}C$	0.586	-
			$\delta^{15}N$	< 0.001	-
Zn	Log(Zn)	GLM	Fork length	0.639	-0.024 ± 0.051
			$\delta^{13}C$	0.634	0.089 ± 0.185
			$\delta^{15}N$	0.606	-0.024 ± 0.047
			$\delta^{13}C$:fork length	0.566	-0.002 ± 0.003
	Residuals(logZn-size)	GAM	$\delta^{13}C$	0.481	-
			$\delta^{15}N$	0.018	-

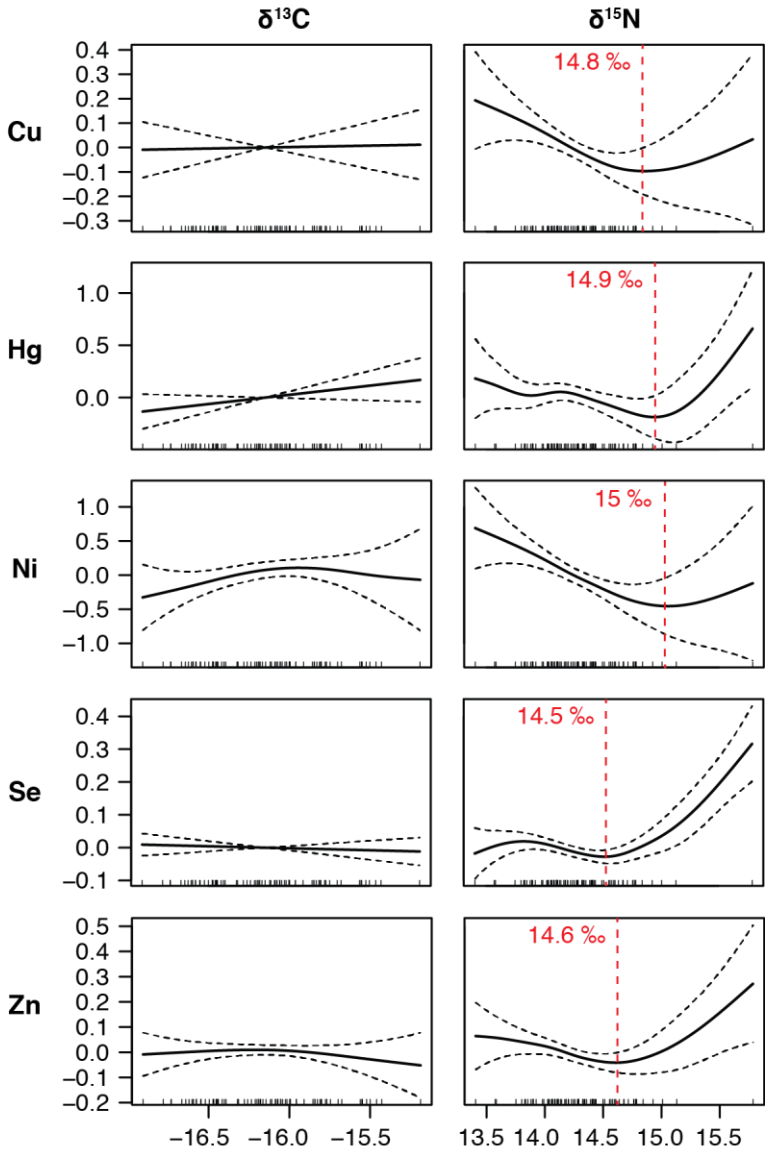

Fig. 4 Graphical results of the generalised additive models (GAMs) fitted to the residuals of the size-based models. Smoothers illustrate the partial effect of continuous explanatory variables once the effects of all the other explanatory variables included in the model have been taken into account. The y-axis shows the contribution of the smoother to the predictor function in the model (in arbitrary units). Dashed lines represent the 95% confidence intervals. Whiskers on the x-axis indicate data presence. Estimated $\delta^{15}N$ shift values are indicated in red.

4. Discussion

4.1. Trophic ecology inferred from stable isotopes

Data about the trophic ecology of emperor red snapper in the Seychelles and, more largely, in many areas of the world, are scarce (Mees 1992; Grandcourt *et al.* 2008; Froese and Pauly 2020). Here, it was possible to identify several characteristics using stable isotopes of carbon and nitrogen, which gave indications on habitat use and diet, as well as temporal and ontogenetic changes in trophic ecology.

Measured $\delta^{13}C$ values in sampled emperor red snappers were comprised between –16.9 ‰ and –15.2 ‰. Generally, it is considered that phytoplankton has $\delta^{13}C$ values between –23 ‰ and –18 ‰,

benthic carbon sources have values between –18 ‰ and –13 ‰ and seagrass has values above –13 ‰ (Fry and Sherr 1989). When considering the trophic enrichment factor for $\delta^{13}C$ values (i.e. 1-2 ‰; Fry 2002), measured $\delta^{13}C$ values thus indicate that emperor red snappers mainly depend on benthic sources for carbon. This is in accordance with the fact that emperor red snappers are demersal, their diet being mainly composed of benthic prey (i.e. fishes, crabs, benthic crustaceans and cephalopods) (Froese and Pauly 2020).

Both $\delta^{13}C$ and $\delta^{15}N$ values in emperor red snapper were positively correlated with their size, suggesting ontogenetic changes in habitat use and diet. The positive correlation between size and $\delta^{13}C$, in particular, suggests that larger individuals rely more on demersal/benthic prey than smaller ones, although they are known to be less coastal and to live in deeper waters than smaller individuals. This variation of $\delta^{13}C$ with size probably reflects an ontogenetic change in diet from pelagic carbon source dominated at larval stage to benthic carbon source dominated for adults. Such changes were observed for other reef species like Mullidae (Kolasinski *et al*. 2009), the red snapper *Lutjanus campechanus* (Wells *et al*. 2008), carnivorous reef fishes (Kulbicki *et al.* 2005) and for reef fishes in general (Cocheret De La Morinière *et al.* 2003). In particular, Wells *et al*. (2008) showed a change in diet with growth for *L. campechanus*, from low trophic level prey items in the water column (i.e. zooplankton like pelagic copepods) to high trophic level benthic prey (i.e. benthic crustaceans and fishes). Here, information on the diet of juvenile emperor red snappers and especially on the ontogenetic changes in diet in this species were not available. However, emperor red snappers share common features in habitat and diet with other Lutjanid species, and especially the red snapper *L. campechanus*. This suggests that similar changes in diet could occur for the emperor red snapper *L. sebae*. Such changes would also explain the positive relationship between emperor red snapper size and $\delta^{15}N$ values, as both their values in $\delta^{13}C$ and $\delta^{15}N$ would increase by shifting from a zooplankton-dominated diet at larval stage to a benthic carnivorous prey-dominated diet. In addition, this is coherent with the general hypothesis that size and trophic position are positively correlated in marine ecosystems, that is larger consumers are able to eat larger prey that have a higher trophic position (Jennings *et al*. 2002). Other studies also observed enrichment in $\delta^{13}C$ and $\delta^{15}N$ values with increasing size and age in different snapper species (Cocheret De La Morinière *et al*. 2003; Wells *et al*. 2008).

The positive correlation between $\delta^{13}C$ and $\delta^{15}N$ completes both previous correlations between size and stable isotope values of carbon and nitrogen. However, the lack of linear relationship between $\delta^{13}C$ and $\delta^{15}N$ suggests a shift in emperor red snappers' isotopic values at some point, thus a shift in the isotopic values of their prey. This may be due to a shift in diet and/or in habitat use. By modelling the relationship between fork length and both $\delta^{13}C$ and $\delta^{15}N$ values in emperor red snappers (Text S1), it was possible to estimate a size at shift, i.e. 65 cm. This size at shift was close to size at maturity in the

Seychelles, which has been estimated around 62-64 cm fork length (Mees 1992). Thus, maturity may play a role in dietary and/or habitat change. Other studies on carnivorous reef fishes found a link between ontogenetic dietary shift and change in habitat and age class, including size at maturity (e.g. Cocheret De La Morinière *et al*. 2003). However, the reason for such a dietary or habitat shift remains unclear, as both are closely linked to each other. A first hypothesis could be a change in habitat when reaching a particular size (e.g. size at maturity) linked to change in habitat requirements. Then, the change in diet would be driven by the change in habitat. A second hypothesis would be a change in diet linked to growth, because larger fishes generally feed on larger prey. This would lead to a change in habitat use to find better-suited prey in terms of size and of energy supply and, in this case, the change in habitat would be driven by ontogenetic changes in diet. However, there are very few studies on the link between maturity and change in habitat use and/or diet (Sheaves 1995). In addition, there is a lack of information on emperor red snappers' habitat use in the Seychelles according to their size and maturity. Thus, more data on habitat use and diet composition according to emperor red snappers' life stage are needed to further explore this hypothesis.

Finally, there was no difference in trophic ecology between males and females, or among seasons. This was expected as there was also no significant difference in size between sexes or among seasons (Fig. S1).

4.2. Trace element bioaccumulation in emperor red snappers' muscle

By investigating the effects of continuous (i.e. size, habitat use through $\delta^{13}C$ and trophic position through $\delta^{15}N$) and categorical variables (i.e. sex) separately, it was possible to highlight the effects of several intrinsic and extrinsic factors on trace element bioaccumulation in emperor red snappers. The significance and nature of these effects, that is bioaccumulation or biodilution, was highly dependent on the factor and on the trace element considered.

Among intrinsic factors, sex had no significant effect on trace element bioaccumulation in emperor red snappers, as shown by the very similar trace element profile ellipses between males and females, and by the non-significant difference in trace element concentrations between sexes and for all elements. This suggests that physiological processes involved in reproduction do not affect trace element uptake and/or elimination between males and females. Similar results were found in other species, like the albacore tuna (Chouvelon *et al*. 2017). In this species, the very few differences in trace element concentrations between sexes (mainly Hg) were hypothesized to originate from poor elimination of trace elements during reproduction and to slight differences in the prey composition in their diet. Here, this could partially explain the lack of difference in trace element concentrations between sexes, especially in the case of essential trace elements that are physiologically regulated. In

the case of non-essential trace elements like Cd or Hg, similar diets in terms of prey composition between males and females, as suggested by similar $\delta^{13}C$ and $\delta^{15}N$ values, could have led to similar concentrations between sexes. Although male and female emperor red snappers sampled in this study had similar size ranges, Mees (1992) found differences in population dynamics between males and females, with females being smaller than males. Thus, the question is: here, do same-size individuals of different sex have the same age? Indeed, this could have influenced the bioaccumulation of trace elements like Hg, which is known to accumulate in time (Raimundo *et al*. 2013; Chouvelon *et al.* 2017), and could have masked differences of bioaccumulation between sexes.

Size was a major factor influencing trace element concentrations in emperor red snappers' muscle tissues, as revealed by the variables selected in the most parsimonious GLM and GAM models. Except for Cr and Fe for which the null model was the best model, for all other trace elements, fork length or at least one of its interaction factors (i.e. with $\delta^{13}C$ or with $\delta^{15}N$) was present in the selected best models. This indicates direct influence of size on trace element concentrations by either bioaccumulation or biodilution, and indirect influence by affecting trophic ecology, which itself has a direct effect on trace element bioaccumulation. Such findings are also similar to what is generally observed for other marine species, size being a major driver of trophic structure (Jennings *et al.* 2002). This effect of size on emperor red snappers' trophic ecology was most evident for Cd and Mn. Indeed, the interaction factor between fork length and $\delta^{13}C$ values was significant in explaining Cd concentrations and, after normalizing Cd concentrations by size, the relationship between Cd concentrations and $\delta^{13}C$ values was not significant anymore. The same thing was observed for the relationship between Mn concentrations and $\delta^{15}N$ values, suggesting that, in both cases, these relationships between trace element concentrations and either $\delta^{13}C$ or $\delta^{15}N$ values were mostly driven by the relationship between stable isotope values and size.

Models explaining As concentrations showed they increase with increasing size and $\delta^{13}C$ values (i.e. more benthic signature), but a decrease with increasing $\delta^{15}N$ values (i.e. higher trophic position). The ontogenetic changes in diet and habitat use shown in emperor red snappers could explain these relationships. Decapod crustaceans are known to preferentially accumulate As under the arsenobetaine form (Khokiattiwong *et al*. 2009), which is one of the most bioavailable forms of As (Zhang *et al.* 2016). Thus, if adult emperor red snappers feed more on large benthic prey, including decapod crustaceans, compared to juveniles, they would potentially accumulate more As while having higher $\delta^{13}C$ values. However, this is in contradiction with the observed increase of $\delta^{15}N$ values with emperor red snappers' size, and more generally with the observed relationships among size, $\delta^{13}C$ and $\delta^{15}N$ values, which were all positively correlated with each other. Thus, here, it is not possible to conclude on the processes that

led to a positive link between As concentrations and size and $\delta^{13}C$ values, while leading to a negative link with $\delta^{15}N$ values at the same time.

Although there was no effect of habitat (i.e. $\delta^{13}C$ values) on the concentrations of Cu, Hg, Ni, Se and Zn, there was a significant effect of trophic position (i.e. $\delta^{15}N$ values) with a shift in bioaccumulation trend for $\delta^{15}N$ values between 14.5 and 15.0 ‰. Such a shift could be attributed to the ontogenetic shift in diet and habitat use observed for emperor red snappers analysed here (around $\delta^{15}N$ value of 14.4 ‰) and possibly related to sexual maturity. Such hypothesis would be coherent with previous conclusions on ontogenetic changes in emperor red snappers' diet. Indeed, by feeding more on small pelagic prey with a low trophic position, smaller emperor red snappers would bioaccumulate higher concentrations of trace elements known to be in higher levels in primary producers (e.g. Cu and Ni) (Fabregas and Herrero 1986; Fox and Zimba 2018). In contrast, by feeding on high trophic position prey, including carnivorous fish and benthic crustaceans, larger individuals would bioaccumulate higher concentrations of trace elements that tend to biomagnify like Hg (Wang 2002). In addition, large decapod crustaceans, like crabs, are known to have high concentrations of Zn (Rainbow 2002), which could thus influence Zn concentrations in emperor red snappers feeding on them. Indeed, although some degree of Zn regulation in the muscle of the mangrove red snapper *Lutjanus argentimaculatus* was observed, suggesting potential of Zn regulation in emperor red snappers' muscle, Zn concentrations in decapod crustaceans can be particularly high (Rainbow 2002) and Zn intake could have exceeded regulation capacities. Finally, the bioavailability of ingested trace elements is an important factor to consider. As the physicochemical forms of a given trace element can be in different proportions or concentrations in different types of prey, a change in prey composition in emperor red snappers' diet could induce a change in the bioavailability of some trace elements in their food.

Finally, there was no effect of size or of trophic ecology on the bioaccumulation of Cr and Fe, as shown by the null model being the best selected model for both trace elements. This is most probably due to the presence of regulation mechanisms in emperor red snapper metabolism for these trace elements, as they are both essentials to fish physiology (Bury and Grosell 2003; Chanda *et al.* 2015), and to no disequilibrium between uptake rate and detoxification/excretion rates.

4.3. Seasonal variation in trace element concentrations

Observed variations in trace element concentrations of emperor red snappers caught during different seasons could have been caused by different phenomenon. The first hypothesis was a link between seasonal change in habitat use and/or diet due to reproduction dynamics (i.e. spawning aggregations) and changes in trace element concentrations in their muscle tissues. However, there was no difference in $\delta^{13}C$ or $\delta^{15}N$ values between seasons. In addition, Mees (1992) observed peaks of

reproductive activity during two distinct periods throughout the year (i.e. October/November and March to May), and trace element concentrations variation patterns do not correspond with these periods. It is thus likely that seasonal variations in weather, environmental parameters and trace element bioavailability affected trace element concentrations in emperor red snappers rather than reproductive dynamics. Indeed, environmental parameters such as water temperature, pH and salinity can influence trace element bioavailability in the water column, and these parameters often vary with seasonal climatic variations (Neff 2002; Rainbow and Black 2002, 2005).

Generally, except for Hg which was highest in emperor red snappers caught during the pre-NWM season, all trace elements for which concentrations varied according to the season (i.e. Cd, Cr, Cu, Ni, Mn, Se, and Zn) were in highest concentrations in emperor red snappers caught during the NWM and pre-SEM seasons. In the Southern Indian Ocean, the NWM season is characterised by high cyclonic activity which can affect winds and which brings abundant rains in the Seychelles (Chang-Seng 2007). Strong winds during this season could thus have caused resuspension of settled sediments, resulting in higher trace element concentrations and thus their availability in the water column. In addition, the strong rains during this season could also affect water salinity due to high input of freshwater in the ocean, and previous studies showed a negative relationship between salinity and the bioavailability of trace elements like Cd and Zn in the water column (Rainbow and Black 2002, 2005). Although diet is generally the main pathway for trace element intake in marine consumers (Wang 2002), trace elements could have entered the food web through primary producers and travelled up the food web to top predators like the emperor red snapper. Both the NWM and pre-SEM seasons are also particularly warm in the Seychelles (Chang-Seng 2007). To compensate for the low dissolve oxygen in waters caused by high temperatures, fish have to increase their respiratory rate (Saha *et al.* 2016). Trace element intake through the gills, although not being the main pathway, could thus have contributed to increasing trace element concentrations in emperor red snappers' muscle tissues. Finally, although primary production is generally low in Seychelles waters, it is relatively higher during the SEM season, potentially causing phytoplanktonic blooms (ASCLME 2012). Subsequent higher bacterial activity, related to the decomposition of organic matter, may enhance MeHg production and thus Hg bioavailability in the water column (Morel *et al*. 1998). This could explain the highest Hg concentrations measured in emperor red snappers caught during the pre-NWM season.

Acknowledgements The authors would like to thank all fishes and crews who assisted with sampling. A special thank goes to the SFA staff (in alphabetic order, Achille Pascal, Andrew Souffre, Calvin Gerry, Clara Belmont, Dora Lesperance, Kettyna Gabriel, Maria Rose, Marie-Corinne Balett, Natifa Pillay, Sabrena Lawrence, Stephanie Marie), the R.V. L'Amitié crew (Christian Decommardmond, Fred Mondon,

Gerard Ernesta, Robert Dookley, Yashim Marday) and the Seychelles Maritime School Academy for the invaluable help in collecting and processing the samples. The authors are also grateful to Ariane Reynier-Caërou, Adeline Angles, Maxime Degroote, Maud Brault-Favrou, and Gaël Guillou for their support in the laboratory analyses. Thanks are due to the CPER (Contrat de Projet Etat-Région) and the FEDER (Fonds Européen de Développement Régional) for funding the AMA, the ICPs and the IRMS of LIENSs laboratory. The IUF (Institut Universitaire de France) is acknowledged for its support to Paco Bustamante as a Senior Member.

Funding The present work is a contribution to the SEYFISH project ("Nutrients and Contaminants in Seychelles fisheries resources" with the financial support of the French Research Institute for Sustainable Development (IRD) and the European Fisheries Partnership Agreement (EU-FPA).

References

Ahmad NI, Noh MFM, Mahiyuddin WRW, Jaafar H, Ishak I, Azmi WNFW, Veloo Y, Hairi MH (2015) Mercury levels of marine fish commonly consumed in Peninsular Malaysia. Environ Sci Pollut Res 22:3672–3686. doi: 10.1007/s11356-014-3538-8

Akaike H (1981) Likelihood of a model and information criteria. J Econom 16:3–14. doi: 10.1016/0304-4076(81)90071-3

Allen G-R (1985) FAO species catalogue. Vol 6. Snappers of the world. An annotated and illustrated catalogue of lutjanid species known to date. In: FAO Fish. Synopsis No. 125, Vol. 6. p 28. FAO Fish 6:24–29. doi: ISBN 92-5-103125-8

Amorim P, Sousa P, Jardim E, Menezes GM (2019) Sustainability Status of Data-Limited Fisheries: Global Challenges for Snapper and Grouper. Front Mar Sci 6:1–17. doi: 10.3389/fmars.2019.00654

Anual ZF, Maher W, Krikowa F, Hakim L, Ahmad NI, Foster S (2018) Mercury and risk assessment from consumption of crustaceans, cephalopods and fish from West Peninsular Malaysia. Microchem J 140:214–221. doi: 10.1016/j.microc.2018.04.024

ASCLME (2012) National Marine Ecosystem Diagnostic Analysis. Seychelles. Contribution to the Agulhas and Somali Current Large Marine Ecosystems Project. 64p. URL: https://nairobiconvention.org/clearinghouse/node/298

Béné C, Barange M, Subasinghe R, Pinstrup-Andersen P, Merino G, Hemre G-I, Williams M (2015) Feeding 9 billion by 2050 – Putting fish back on the menu. Food Secur 7:261–274. doi: 10.1007/s12571-015-0427-z

Bosch AC, O'Neill B, Sigge GO, Kerwath SE, Hoffman LC (2016) Heavy metals in marine fish meat and consumer health: A review. J Sci Food Agric 96:32–48. doi: 10.1002/jsfa.7360

Bury N, Grosell M (2003) Iron acquisition by teleost fish. Comp Biochem Physiol - C Toxicol Pharmacol 135:97–105. doi: 10.1016/S1532-0456

Carravieri A, Bustamante P, Labadie P, Budzinski H, Chastel O, Cherel Y (2020) Trace elements and persistent organic pollutants in chicks of 13 seabird species from Antarctica to the subtropics. Environ Int 134:105225. doi: 10.1016/j.envint.2019.105225

Cawthorn DM, Mariani S (2017) Global trade statistics lack granularity to inform traceability and management of diverse and high-value fishes. Sci Rep 7:1–11. doi: 10.1038/s41598-017-12301-x

Chanda S, Paul BN, Ghosh K, Giri SS (2015) Dietary essentiality of trace minerals in aquaculture: A review. Agric Rev 36:100–112. doi: 10.5958/0976-0741.2015.00012.4

Chang-Seng D (2007) Climate Variability and climate change assessment for the Seychelles. 56p. URL: https://www.unisdr.org/files/18929_18929climatevariabiltyandclimatecha.pdf

Chouvelon T, Caurant F, Cherel Y, Simon-Bouhet B, Spitz J, Bustamante P (2014) Species-and size-related patterns in stable isotopes and mercury concentrations in fish help refine marine ecosystem indicators and provide evidence for distinct management units for hake in the Northeast Atlantic. ICES J Mar Sci 71:1073–1087.

doi: 10.1093/icesjms/fst199

Chouvelon T, Brach-Papa C, Auger D, Bodin N, Bruzac S, Crochet S, Degroote M, Hollanda SJ, Hubert C, Knoery J, Munschy C, Puech A, Rozuel E, Thomas B, West W, Bourjea J, Nikolic N (2017) Chemical contaminants (trace metals, persistent organic pollutants) in albacore tuna from western Indian and south-eastern Atlantic Oceans: Trophic influence and potential as tracers of populations. Sci Total Environ 596–597:481–495. doi: 10.1016/j.scitotenv.2017.04.048

Cocheret De La Morinière E, Pollux BJA, Nagelkerken I, Van Der Velde G (2003) Diet shifts of Caribbean grunts (Haemulidae) and snappers (Lutjanidae) and the relation with nursery-to-coral reef migrations. Estuar Coast Shelf Sci 57:1079–1089. doi: 10.1016/S0272-7714(03)00011-8

De Niro M, Epstein S (1978) Influence of diet on the distribution of carbon isotopes in animals. Geochim Cosmochim Acta 42:495–506. doi: 10.1016/0016-7037(78)90199-0

Fabregas J, Herrero C (1986) Marine microalgae as a potential source of minerals in fish diet. Aquaculture 51:237–243. doi: 10.1007/bf01982726

Fox JM, Zimba P V. (2018) Minerals and trace elements in microalgae. In: Microalgae in health and disease prevention (Eds. Levine I, Fleurence J). Elsevier Inc., Oxford, UK, pp 177–193. doi: 10.1016/B978-0-12-811405-6.00008-6

Froese R, Pauly D (2020) FishBase. World Wide Web electronic publication. URL: www.fishbase.org.

Fry B (2002) Stable isotopic indicators of habitat use by Mississippi River fish. J North Am Benthol Soc 21:676–685. doi: 10.2307/1468438

Fry B, Sherr EB (1989) $\delta^{13}C$ measurements as indicators of carbon flow in marine and freshwater ecosystems. In: Stable isotopes in ecological research. (Eds. Rundel PW, Ehleringer JR, Nagy KA). Springer, New-York, USA, pp 196–229. doi: 10.1007/978-1-4612-3498-2_12

Goutte A, Cherel Y, Churlaud C, Ponthus JP, Massé G, Bustamante P (2015) Trace elements in Antarctic fish species and the influence of foraging habitats and dietary habits on mercury levels. Sci Total Environ 538:743–749. doi: 10.1016/j.scitotenv.2015.08.103

Grandcourt EM, Hecht T, Booth AJ, Robinson J (2008) Retrospective stock assessment of the Emperor red snapper (*Lutjanus sebae*) on the Seychelles Bank between 1977 and 2006. ICES J Mar Sci 65:889–898. doi: 10.1093/icesjms/fsn064

Hicks CC, Cohen PJ, Graham NAJ, Nash KL, Allison EH, Lima CD, Mills DJ, Roscher M, Thilsted SH, Thorne-Lyman AL, Macneil MA (2019) Harnessing global fisheries to tackle micronutrient deficiencies. Nature 574:95–98. doi: 10.1038/s41586-019-1592-6

Houssard P, Point D, Tremblay-Boyer L, Allain V, Pethybridge H, Masbou J, Ferriss BE, Baya PA, Lagane C, Menkes CE, Letourneur Y, Lorrain A (2019) A model of mercury distribution in tuna from the western and central Pacific Ocean: Influence of physiology, ecology and environmental factors. Environ Sci Technol 53:1422–1431. doi: 10.1021/acs.est.8b06058

Jennings S, Pinnegar JK, Polunin NVC, Warr KJ (2002) Linking size-based and trophic analyses of benthic community structure. Mar Ecol Prog Ser 226:77–85. doi: 10.3354/meps226077

Khokiattiwong S, Kornkanitnan N, Goessler W, Kokarnig S, Francesconi KA (2009) Arsenic compounds in tropical marine ecosystems: Similarities between mangrove forest and coral reef. Environ Chem 6:226–234. doi: 10.1071/EN09009

Kolasinski J, Frouin P, Sallon A, Rogers K, Bruggemann HJ, Potier M (2009) Feeding ecology and ontogenetic dietary shift of yellowstripe goatfish *Mulloidichthys flavolineatus* (Mullidae) at Reunion Island, SW Indian ocean. Mar Ecol Prog Ser 386:181–195. doi: 10.3354/meps08081

Kulbicki M, Bozec YM, Labrosse P, Letourneur Y, Mou-Tham G, Wantiez L (2005) Diet composition of carnivorous fishes from coral reef lagoons of New Caledonia. Aquat Living Resour 18:231–250. doi: 10.1051/alr:2005029

Marriott RJ, Mapstone BD, Beng GA (2007) Age-specific demographic parameters, and their implications for management of the red bass, *Lutjanus bohar* (Forsskal 1775): A large, long-lived reef fish. Fish Res 83:204–215. doi: http://dx.doi.org/10.1016/j.fishres.2006.09.016

Martinez-Andrade F (2003) A comparison of life histories and ecological aspects among snappers (Pisces: Lutjanidae). Graduate Faculty of the Louisiana State University. 201p. doi: 10.13140/RG.2.1.1697.4569

Mees C (1992) Seychelles demersal fishery: an analysis of data relating to four key demersal species. 142p. URL: https://aquadocs.org/handle/1834/5114

Méndez-Fernandez P, Pierce GJ, Bustamante P, Chouvelon T, Ferreira M, González AF, López A, Read FL, Santos MB, Spitz J, Vingada J V., Caurant F (2013) Ecological niche segregation among five toothed whale species off the NW Iberian Peninsula using ecological tracers as multi-approach. Mar Biol 160:2825–2840. doi: 10.1007/s00227-013-2274-9

Metian M, Warnau M, Chouvelon T, Pedraza F, Rodriguezy Baena AM, Bustamante P (2013) Trace element bioaccumulation in reef fish from New Caledonia: Influence of trophic groups and risk assessment for consumers. Mar Environ Res 87–88:26–36. doi: 10.1016/j.marenvres.2013.03.001

Morel FMM, Kraepiel AML, Amyot M (1998) The chemical cycle and bioaccumulation of mercury. Annu Rev Ecol Syst 29:543–566. doi: 10.1146/annurev.ecolsys.29.1.543

Neff JM (2002) Bioaccumulation Mechanisms. In: Bioaccumulation in marine organisms (Ed. Neff JM). Elsevier, Oxford, UK, pp 37–56. doi: 10.1016/b978-008043716-3/50003-8

Ogle DH, Wheeler P, Dinno A (2018) FSA: Fisheries Stock Analysis.

Oksanen J, Blanchet FG, Friendly M, Kindt R, Legendre P, McGlinn D, Michin PR, O'Hara RB, Simpson GL, Solymos P, Stevens HH, Szoecs E, Wagner H (2019) vegan: Community Ecology Package.

Post DM, Layman CA, Arrington DA, Takimoto G, Quattrochi J, Montaña CG (2007) Getting to the fat of the matter: Models, methods and assumptions for dealing with lipids in stable isotope analyses. Oecologia 152:179–189. doi: 10.1007/s00442-006-0630-x

R Core Team (2018) R: A language and environment for statistical computing.

Raimundo J, Vale C, Caetano M, Giacomello E, Anes B, Menezes GM (2013) Natural trace element enrichment in fishes from a volcanic and tectonically active region (Azores archipelago). Deep Res Part II Top Stud Oceanogr 98:137–147. doi: 10.1016/j.dsr2.2013.02.009

Rainbow PS (2002) Trace metal concentrations in aquatic invertebrates: Why and so what? Environ Pollut 120:497–507. doi: 10.1016/S0269-7491(02)00238-5

Rainbow PS, Black WH (2002) Effects of changes in salinity and osmolality on the rate of uptake of zinc by three crabs of different ecologies. Mar Ecol Prog Ser 244:205–217. doi: 10.3354/meps244205

Rainbow PS, Black WH (2005) Physicochemistry or physiology: Cadmium uptake and effects of salinity and osmolality in three crabs of different ecologies. Mar Ecol Prog Ser 286:217–229. doi: 10.3354/meps286217

Rejomon G, Nair M, Joseph T (2010) Trace metal dynamics in fishes from the southwest coast of India. Environ Monit Assess 167:243–255. doi: 10.1007/s10661-009-1046-y

Robinson J, Isidore M, Marguerite MA, Öhman MC, Payet RJ (2004) Spatial and temporal distribution of reef fish spawning aggregations in the Seychelles - An interview-based survey of srtisanal fishers. West Indian Ocean J Mar Sci 3:63–69. doi: 10.1007/s10641-006-9161-x

Robinson JPW, Robinson J, Gerry C, Govinden R, Freshwater C, Graham NAJ (2020) Diversification insulates fisher catch and revenue in heavily exploited tropical fisheries. Sci Adv 6:1–10. doi: 10.1126/sciadv.aaz0587

Saha N, Mollah MZI, Alam MF, Safiur Rahman M (2016) Seasonal investigation of heavy metals in marine fishes captured from the Bay of Bengal and the implications for human health risk assessment. Food Control 70:110–118. doi: 10.1016/j.foodcont.2016.05.040

Sardenne F, Hollanda S, Lawrence S, Albert-Arrisol R, Degroote M, Bodin N (2017) Trophic structures in tropical marine ecosystems: A comparative investigation using three different ecological tracers. Ecol Indic 81:315–324. doi: 10.1016/j.ecolind.2017.06.001

Seychelles Fishing Authority (2019) Annual Report 2015-2016. Victoria, Mahé, Seychelles. URL: https://aquadocs.org/handle/1834/17743

Sheaves M (1995) Large lutjanid and serranid fishes in tropical estuaries: Are they adults or juveniles? Mar Ecol Prog Ser 129:31–40. doi: 10.3354/meps129031

Suratno, Puspitasari R, Rositasari R, Oktaviyani S (2019) Total mercury of marine fishes in Natuna Islands area, Indonesia: Risk assessment for human consumption. IOP Conf Ser Earth Environ Sci. doi: 10.1088/1755-1315/277/1/012025

Velusamy A, Satheesh Kumar P, Ram A, Chinnadurai S (2014) Bioaccumulation of heavy metals in commercially important marine fishes from Mumbai Harbor, India. Mar Pollut Bull 81:218–224. doi: 10.1016/j.marpolbul.2014.01.049

Wang WX (2002) Interactions of trace metals and different marine food chains. Mar Ecol Prog Ser 243:295–309. doi: 10.3354/meps243295

Wells RJD, Cowan JH, Fry B (2008) Feeding ecology of red snapper *Lutjanus campechanus* in the northern Gulf of Mexico. Mar Ecol Prog Ser 361:213–225. doi: 10.3354/meps07425

Wood S (2011) Fast stable restricted maximum likelihood and marginal likelihood estimation of semiparametric generalized linear models. J R Stat Soc Ser B 73:3–36. doi: 10.1111/j.1467-9868.2010.00749.x

Zhang W, Wang WX, Zhang L (2016) Comparison of bioavailability and biotransformation of inorganic and organic arsenic to two marine fish. Environ Sci Technol 50:2413–2423. doi: 10.1021/acs.est.5b06307

Zuur AF, Ieno EN, Smith GM (2007) Analysing ecological data. Springer, New-York, USA. doi: 10.1007/978-0-387-45972-1

Supplementary data

Table S1 Detailed number of sampled individual according to sex and season. Total number of samples = 77. NWM = Northwest Monsoon; SEM = Southeast Monsoon.

By sex	Males	31
	Females	46
By season	Pre-NWM	10
	NWM	57
	Pre-SEM	10
	SEM	-

Table S2 Recovery rates (mean ± SD) in certified reference materials and detection frequencies in all samples for trace elements analysed by induced coupled plasma (ICP). NC = Not certified.

Trace element	Recovery rates (%)		Detection frequencies (%)
	DOLT-5	TORT-3	
Ag	86 ± 1	NC	4
As	100 ± 2	107 ± 2	100
Cd	100 ± 1	95 ± 1	78
Co	104 ± 2	100 ± 2	14
Cr	NC	88 ± 10	81
Cu	99 ± 2	83 ± 2	100
Fe	96 ± 1	89 ± 1	91
Mn	NC	86 ± 1	100
Ni	NC	99 ± 4	100
Pb	91 ± 9	108 ± 12	78
Se	110 ± 4	113 ± 5	54
Zn	99 ± 2	99 ± 1	100

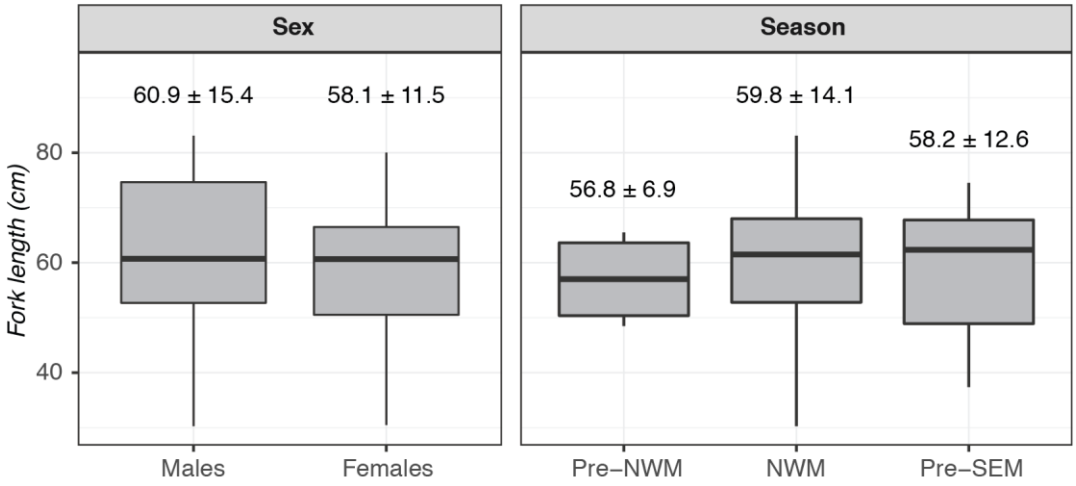

Figure S1 Fork length (cm) of sampled emperor red snappers by sex and season. Mean values (± SD) by sex and season are also indicated above each corresponding boxplot.

Text S1 Method used to estimate the size around which a shift in the relationship between $\delta^{13}C$ and $\delta^{15}N$ values was observed in emperor red snapper.

Step 1: The $\delta^{13}C$ value at which the shift was observed was graphically determined by using the fitted curve representing the relationship between $\delta^{13}C$ and $\delta^{15}N$ values (Fig. 1).

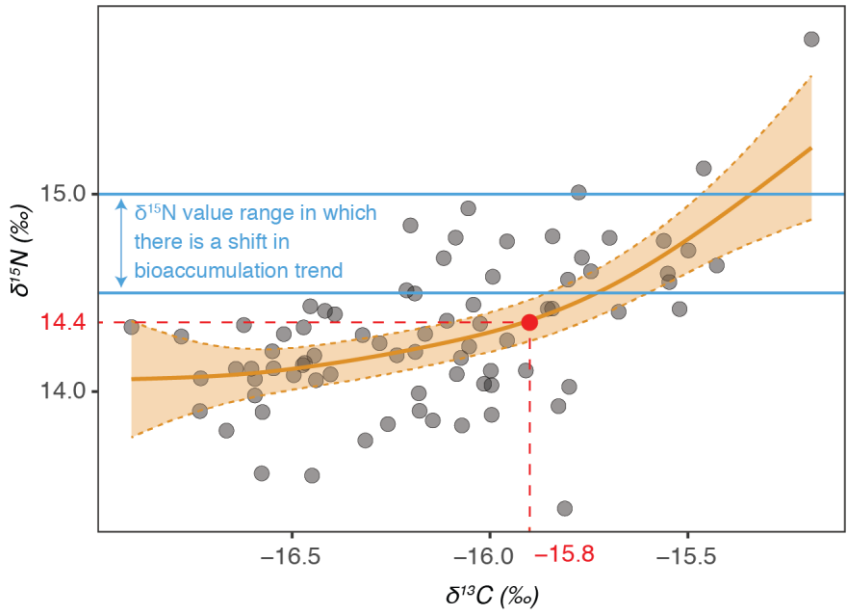

Fig. 1. Relationships between $\delta^{13}C$ and $\delta^{15}N$ values. Smoothing curve was fitted using the GAM method under R software. Dotted curves represent the confidence interval at 95% around the fit. Red point represent the estimated point at which there is a shift in trend in the relationship. The $\delta^{15}N$ range of value in which there is a change in bioaccumulation trend for Cu, Hg, Ni, Se and Zn is also indicated in blue.

Step 2: The corresponding $\delta^{15}N$ value was calculated using a GAM model. The model was first fitted on $\delta^{15}N$ values with $\delta^{13}C$ values as explaining variable. Then, the predict function of the stats included R package was used to estimate the $\delta^{15}N$ value for a $\delta^{13}C$ value = –15.8 ‰ (i.e. shift point). The obtained $\delta^{15}N$ shift value was 14.4 ‰.

Step 3: Then, a GAM model was fitted on emperor red snappers' fork lengths with $\delta^{13}C$ and $\delta^{15}N$ values as explaining variables. The form of the equation was: fork length ~ s($\delta^{13}C$) + s($\delta^{15}N$). Finally, similarly to step 2, the size at shift was determined by using the *predict* function in R, with $\delta^{13}C$ = –15.8 ‰ and $\delta^{15}N$ = 14.4 ‰. The obtained fork length at shift was 65.1 cm.

- SUPPLEMENTARY DOCUMENT 4 -

Regional patterns in mercury (Hg) and selenium (Se) concentration of swordfish in the Indian Ocean

Magali A. SABINO[1,2], Nathalie BODIN[1,3,4], Rodney GOVINDEN[1], Stephanie HOLLANDA[1], Rona ALBERT[1], Natifa PILLAY[1], Carine CHURLAUD[2], Wendy West[5], Evgeny ROMANOV[6], Christopher SOMES[7], Heidi PETHYBRIDGE[8], Paco BUSTAMANTE[2,9]

[1] Seychelles Fishing Authority (SFA), Fishing Port, Victoria, Mahé, Seychelles

[2] Littoral Environnement et Sociétés (LIENSs), UMR 7266 CNRS - La Rochelle Université, 2 rue Olympe de Gouges, 17000 La Rochelle, France

[3] Institute for Research and Development (IRD), Fishing Port, Victoria, Mahé, Seychelles

[4] Sustainable Ocean Seychelles (SOS), BeauBelle, Mahé, Seychelles

[5] Department of Agriculture, Forestry and Fisheries (DAFF), Cape Town, South Africa

[6] CITEB (Centre technique de recherche et de valorisation des milieux aquatiques), Le Port, La Réunion, France

[7] GEOMAR Helmholtz Centre for Ocean Research Kiel, Deusternbrooker Weg 20, Kiel 24105 Germany

[8] CSIRO Oceans and Atmosphere, Castray Esplanade, Battery Point, Hobart, Tasmania 7004 Australia

[9] Institut Universitaire de France (IUF), 1 rue Descartes 75005 Paris, France

To be submitted in *Chemosphere*

Abstract

As highly-migratory long-lived top predators, swordfish are good bioindicator species for monitoring and understanding broad spatial gradients of mercury (Hg) contamination in the world's oceans. In the Indian Ocean, swordfish represent one of the main targets of commercial and recreational pelagic fisheries; yet data on Hg occurrence in Indian Ocean swordfish remain scarce, and little information is available on the co-occurrence of selenium (Se) and its protective role against Hg. In this study, we analysed Hg and Se concentrations in the muscle of swordfish from six regions of the Indian Ocean. We investigated the effect of regional origin, size and trophic ecology (using stable isotope $\delta^{13}C$ values and trophic level) on Hg and Se bioaccumulation. We also assessed the Hg risks and Se benefits for human consumers. Swordfish regional origin was the main factor influencing both Hg and Se concentrations, due to regional variation in trace element bioavailability and in food web trophic structure, although feeding depth also played a substantial role. Results showed evidences of a potential of co-accumulation between Hg and Se, as hypothesised in other studies. Se concentrations were high in swordfish from all regions, bringing at least 40% of children, young adult and adult women daily needs, even after considering the interaction effect with Hg. The MHg:MSe ratios and HBV_{Se} values in all regions suggested low Hg risk for human health.

Keywords: Billfish; Trace elements; Bioaccumulation; Hg risk; Se benefit; Hg-Se interaction

1. Introduction

Over the last decades, mercury (Hg) contamination has become a worldwide concern due to its potential to cause adverse effects on human health and on the environment (Morel *et al*. 1998). While Hg is naturally present in low concentrations in the marine environment due to natural sources (e.g. volcanic activity), anthropogenic activities (e.g. industry, burning of fossil fuel or gold processing from artisanal gold mining) mainly contribute to the increase of Hg concentrations in oceanic waters (Boening 2000). Once deposited into the oceans, the inorganic mercury can be transformed into methylmercury (MeHg) through microbe activity (Costa *et al*. 2012). This organic form of Hg is known to be highly neurotoxic for humans, but it is also the most bioavailable form and is thus readily bioaccumulated in organisms along time and biomagnified through marine food chains (Syversen and Kaur 2012; Bosch *et al*. 2016). As a consequence, marine consumers and especially top predators can bioaccumulate high levels of Hg, and seafood is now considered the main pathway of exposure to MeHg in human diet (Mergler *et al*. 2007).

Seafood is also recognised to be a great food source for trace elements that are essential for human metabolism (Weichselbaum *et al*. 2013). One of them, selenium (Se) is known to have a protective effect against MeHg due to its high binding affinity with Hg (Raymond and Ralston 2004). Once they bind, Se and Hg form an insoluble complex and thus become biologically unavailable (Raymond and Ralston 2004). While this means that Se sequesters Hg and can prevent its adverse effects on human health, this also means that Hg sequesters Se, thus preventing it from being used in human metabolism (Manceau *et al*. 2021). It is thus important to take into account both Hg and Se concentrations when studying Hg risk and Se benefit through fish consumption in the human diet (Ralston *et al*. 2007, 2015; Zhang *et al*. 2014).

In the marine environment, trace elements are mainly transferred to consumers through the trophic pathway (Wang 2002). The individual ecology of a given organism, including feeding area, trophic level, or the type of prey consumed, will thus affect its trace element exposure and content (Wang 2002; Copaja *et al*. 2017). As a consequence, a better understanding of a consumer's trophic ecology is crucial to better understand its trace element concentrations, and to better understand trace elements' intake in human diet through seafood consumption. While there has been extensive research on factors influencing Hg and Se bioaccumulation in marine consumers from the Atlantic (e.g. Payne and Taylor 2010; Vieira *et al*. 2011; Le Croizier *et al*. 2016; Chouvelon *et al*. 2018) and Pacific Oceans (Ferriss and Essington 2011; Ordiano-Flores *et al*. 2011; Metian *et al*. 2013; Houssard *et al.* 2019), very few did so in the Indian Ocean (Kojadinovic *et al.* 2007; Velusamy *et al.* 2014; Carravieri *et al.* 2017, 2020; Chouvelon *et al.* 2017), and never at a global scale.

Trophic ecology can be studied through the use of ecological tracers like stable isotopes (SI) of carbon ($\delta^{13}C$) and nitrogen ($\delta^{15}N$). $\delta^{13}C$ is known to be conservative through the food web, with little variation from one trophic level to another (0.5-1 ‰) (Post 2002). Thus, $\delta^{13}C$ allows the identification of primary production sources and the discrimination between foraging ecosystems (i.e. benthic *vs* pelagic). In turns, $\delta^{15}N$ gives information about the trophic position of an organism, with variation ranging between 3 to 5 ‰ between each trophic level (Post 2002). However, $\delta^{15}N$ baseline values are highly variable between ecosystems (Wada and Hattori 1976; Chouvelon *et al*. 2012) and such use of $\delta^{15}N$ values should be food web-specific. For large-scale data, it is thus recommended to convert $\delta^{15}N$ values to trophic level using an isotopic baseline (Layman *et al*. 2011).

As highly-migratory long-lived top predators in marine pelagic ecosystems (Nakamura 1985), swordfish bioaccumulate high levels of Hg, with reported concentrations higher than in other top predators such as tuna and tuna-like species, and exceeding from time to time the recommended safety limits (Bodin *et al.* 2017). Swordfish is thus among the most appropriate bioindicator species for monitoring and understanding broad spatial gradients of Hg contamination in the world's oceans. In the Indian Ocean, swordfish is the main target of commercial and recreational fisheries, and represents a high income and a high protein source for local populations (FAO 2020). Yet, data on Hg occurrence in swordfish across the Indian Ocean is still scarce (Kojadinovic *et al*. 2006; Esposito *et al*. 2018) while, to the best of our knowledge, no previous work investigated global patterns of Se concentrations in swordfish from this ocean.

In this study, we assessed the spatial variations of Hg and Se concentrations in swordfish across the Indian Ocean, and examined the influence of ontogenetic parameter (i.e. swordfish length) and trophic ecology (SI values) on these regional variations. We also explored the potential of co-accumulation between Hg and Se in swordfish. Finally, we assessed the Hg risks and Se benefits for the diet of human populations depending on swordfish.

2. Material and methods

2.1. Sample collection and preparation

A total of 190 swordfish were caught by commercial vessels from six distinct regions in the Indian Ocean, between 2004 and 2018 (Fig. 1). For each individual, the fishing location (longitude and latitude) and lower jaw-fork length (to the nearest 1 cm) were recorded, and a sample of white muscle was retrieved and stored at -20°C. All samples were then freeze-dried during 72h and ground to powder before analysis of carbon and nitrogen SI ($\delta^{13}C$ and $\delta^{15}N$) and Hg and Se concentrations.

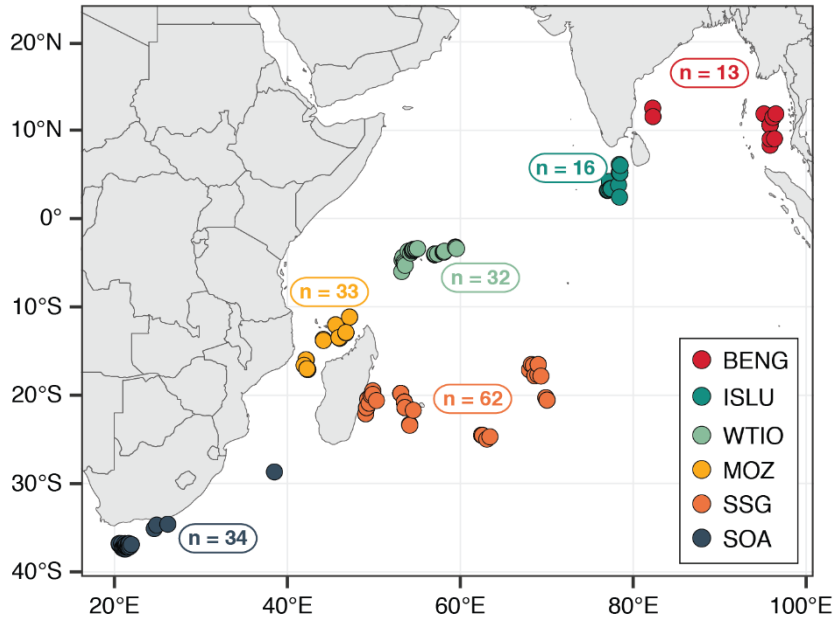

Fig. 1 Swordfish fishing locations and respective areas in the Indian Ocean. BENG = Bay of Bengal; ISLU = Indo-Sri Lanka Upwelling; WTIO = Western Tropical Indian Ocean; MOZ = Mozambique Channel; SSG = Southern Subtropical Gyre; SOA = South Africa.

2.2. Mercury and selenium analysis

As MeHg separation methods are expensive and time-consuming, and as Hg in fish muscle tissues is essentially present under its methylated form (Bloom 1992; Wagemann *et al*. 1997), MeHg separation was not performed prior to Hg analyses. Total Hg was analysed with a Direct Mercury Analyser (Milestone DMA 80) or an Advanced Mercury Analyser atomic absorption spectrophotometer (Altec AMA 254). Both devices are based on the same method, which does not require preliminary acidic digestion of the samples. Dry grounded subsamples from 2 to 10 mg were thus directly analysed. Hg determination involved progressive heating until 750 °C was reached, that allowed complete burning of the matrix and evaporation of the metal. The evaporated metal is then fixed on a golden net by amalgamation. Collected Hg on the amalgamator was then liberated by its heating at 950 °C, and measured by atomic absorption spectrophotometry. Each sample was analysed at least twice until the relative standard deviation (RSD) was below 10 %. Hg concentrations were validated by the analysis of the certified reference material (CRM) DOLT-5 (dogfish liver; National Research Council, Canada), every 10 samples. CRM aliquots were treated and analysed according to the same conditions as the samples. Masses of the CRM were adjusted to correspond to the same Hg amounts as in the samples. Blanks were also analysed at the beginning of each set of samples, and the quantification limit of both DMA and AMA was 0.1 ng (5*DL, with DL the detection limit = 3*standard deviation of 8 blanks).

Se was analysed by Induced Coupled Plasma (ICP), using a Varian Vista-Pro ICP coupled with optical emission spectrometry (OES) and a Thermo Fisher Scientific XSeries 2 ICP coupled with mass

spectrometry (MS). Aliquots of the biological samples (90-200 mg) were digested with 6 ml 67-70% of nitric acid (HNO_3) and 2 ml 34-37% of hydrochloric acid (HCl) (Fisher Scientific, trace element grade quality). Acidic digestion of the samples was carried out overnight at room temperature, then using a Milestone microwave (30 min with constantly increasing temperature up to 120°C, then 15 min at this maximal temperature). Each digested sample was completed to 50 ml with milli-Q water. Seven control samples (five CRMs, and two blanks) treated and analysed in the same way as the samples were included in each analytical batch. CRMs were marine tropical clam (*Gafrarium tumidum*) IAEA-461, dogfish liver DOLT-5 (National Research Council Canada) and lobster hepatopancreas TORT-3 (National Research Council Canada). Mean recovery rates were equal to 113 % for Se.

2.3. Stable isotope analysis

Because lipids are usually more depleted in ^{13}C than other tissue components and could thus introduce a bias in the results, reserve lipids must be removed before $\delta^{13}C$ determination (De Niro and Epstein 1978). Thus, lipid removal was performed prior to SI analysis. Briefly, for each sample, between 10 and 12 mg of powdered sample was placed in a glass tube with 4 ml of cyclohexane. Tubes were then agitated during 10 minutes at room temperature and centrifuged during 5 minutes at 4500 rpm before removal of extraction solvent. Agitation, centrifugation and solvent-removal steps were repeated three times before putting tubes for drying in an oven at 45 °C for a night.

For stable isotope analysis, 0.3-0.5 mg were placed in tin capsules. Carbon and nitrogen ratios were determined with a continuous-flow mass spectrometer Thermo Scientific Delta V Advantage coupled to an elemental analyser Thermo Scientific Flash 2000. Measurements of international isotopic standards of known $\delta^{13}C$ and $\delta^{15}N$ were conducted: USGS-24, IAEA-CH6, IAEA-600, USGS-61 and USGS-62. Results are expressed in the δ unit notation as deviations from standards (Vienna Pee Dee Belemnite for $\delta^{13}C$ and atmospheric nitrogen (air) for $\delta^{15}N$) following the formula: $\delta^{13}C$ or $\delta^{15}N = [(R_{sample}/R_{standard}) - 1] \times 1000$, where R is $^{13}C/^{12}C$ or $^{15}N/^{14}N$, respectively. Measurement errors (SD) of SI were < 0.15 ‰ for both the nitrogen and carbon isotope measurements.

2.4. Mercury data transformation

As Hg is known to bioaccumulate with length (Lavoie *et al*. 2013), concentrations were standardised according to swordfish length in order to investigate the effect of other factors on Hg bioaccumulation. For this, a power-law relationship ($\log(Hg) = a \times (\text{lower jaw-fork length} - b)^c - d$) was fit between log-transformed Hg concentrations (log(Hg)) and swordfish lower jaw-fork length to characterise the bioaccumulative process in swordfish. Residuals from the length-based Hg model (i.e.

observed values – predicted values) were extracted and used to calculate length-standardised Hg concentrations (at lower jaw-fork length = 150 cm).

2.5. Calculation of trophic position

Trophic position of each swordfish was calculated using Eq. 1 (Post 2002), with $\delta^{15}N_{sc}$ the $\delta^{15}N$ values in the secondary consumer, $\delta^{15}N_{base}$ the $\delta^{15}N$ values at the base, λ the trophic level of the organism used to obtain $\delta^{15}N_{base}$ (i.e. 1 for phytoplankton) and Δ_n the enrichment factor (i.e. 3.4 ‰).

$$\text{Trophic level} = \lambda + (\delta^{15}N_{sc} - \delta^{15}N_{base}) / \Delta_n \qquad \textbf{(Eq. 1)}$$

As global $\delta^{15}N$ baselines do not exist in the Indian Ocean, $\delta^{15}N_{base}$ values were modelled for phytoplankton in each recorded fishing location, for each longitude-latitude couple and for each sampling year. Model was based on preindustrial simulations from Somes *et al.* (2017), and results were averaged annually over the upper 130 meters of ocean surface.

2.6. Classical and multivariate statistics

Concentrations of Hg and Se, theoretically bioavailable Se, swordfish lower jaw-fork length, $\delta^{13}C$ and $\delta^{15}N$ values and trophic levels were tested for normality and homoscedasticity. Then, they were compared among areas using ANOVA (i.e. parametric) or Kruskal-Wallis (i.e. non-parametric) and, when a difference was significant ($p < 0.05$), associated post-hoc tests (i.e. Tukey's HSD and Dunn test with Benjamini-Hochberg adjustment respectively) were used.

2.7. Modelling the relationship between mercury and selenium concentrations and explanatory variables

Generalised additive models (GAM) with a Gaussian distribution and an identity link function were used to assess the effects of several factors (i.e. fish size, trophic level, $\delta^{13}C$ values and fishing location using longitude and latitude) on Hg and Se concentrations. A GAM was also fitted on length-standardised Hg concentrations to investigate effect of ecological factors after removing the length effect. Concurvity was checked for all models and $\delta^{15}N$ values were not included as explaining variable to avoid collinearity with trophic level. Correlations were tested among explaining variables using Kendall tests in order to identify potential interaction terms of interest. According to correlation tests results (Fig. S1), in all models, the interaction terms between $\delta^{13}C$ and fishing location (i.e. $\delta^{13}C$+longitude and $\delta^{13}C$+latitude) and between trophic level and latitude were also included as explanatory variables. The interaction term between fish length and trophic level was also added, as

trophic position is thought to be positively correlated to fish size (Jennings *et al*. 2002). Applying GAMs on log-transformed trace element concentrations usually improves modelling (e.g. Méndez-Fernandez *et al.* 2013; Chouvelon *et al.* 2014), thus Hg, standardised Hg and Se concentrations were log-transformed before fitting the GAMs. For each model performed, the complete model was first compared to a null model (i.e. containing only the intercept terms) using the Akaike Information Criterion (AIC) (Akaike 1981). This allowed to evaluate the capacity of the complete model to explain the variability of the response variable. For each model, the complete model was better than the null model, thus a stepwise procedure was used to select the most parsimonious model, again using the AIC. For this, explanatory variables were successively removed from the complete model until all remaining variables significantly improved the model (i.e. no significant lowering of the AIC). When the AIC was not significantly different between two compared models, the simplest model was preferred (Zuur *et al.* 2007). All selected models were validated by checking the normality and homoscedasticity of residuals, and the potential presence of outliers (Zuur *et al.* 2007). For each selected model, the explained deviance was calculated using the method of Méndez-Fernandez *et al*. (2013).

Finally, to characterise the potential of co-accumulation of Hg and Se, correlation (Pearson) was tested between log-transformed Hg and log-transformed Se concentrations. A GAM was also fitted on log-transformed Se concentrations with log-transformed Hg concentrations as explaining variable. The best-AIC selected model was compared to previous model explaining Se concentrations, using deviance explained and AIC, in order to see if adding log-transformed Hg concentrations as explaining variable improved the GAM.

2.8. Assessment of mercury risks and selenium benefits for human consumption

For nutritional interpretation and in order to compare trace element concentrations with nutritional requirements and maximum limits of contaminants for human consumption, all concentrations were converted from dry weight to wet weight (ww), using a conversation ratio with a moisture content of 75% (Bodin *et al*. 2017).

In order to take into account the protective effect of Se against Hg, the molar ratio of Hg over Se (MHg:MSe) and the Health Benefit Value of Se (HBV_{Se}) were calculated according to the formulas in Ralston *et al.* (2015). It is considered that Se and Hg bind in a molar ratio of 1:1 in human tissues (Raymond and Ralston 2004). Thus, we also calculated the concentration of theoretically bioavailable Se after interaction with Hg by subtracting the molar concentration of Hg to the molar concentration of Se.

To assess the risk and benefit of swordfish consumption in human diets, the number of servings before reaching Hg and Se provisional tolerable intakes (JECFA 2011; American Food and Nutrition Board of the Institute of Medicine National Academy of Sciences 2019b), and the percentage of contribution of one serving to recommended daily intakes of Se (American Food and Nutrition Board of the Institute of Medicine National Academy of Sciences 2019a) were also calculated, for both raw Se concentrations and theoretically bioavailable Se concentrations. Calculations were made for populations that are the most vulnerable to nutrient deficiency and contaminant exposure (i.e. 2-13 year old children, 14-19 year old young adults and 19+ year old adult women, including pregnant and lactating women). For each age class, maximum number of servings and percentages of covered recommended daily intake are presented as mean with their associated confidence interval at 95% (CI95%). Parameters used in calculations (i.e. mean weight of each age class, portion weight, recommended daily intakes and provisional tolerable intakes) are presented in Table S1; detailed methods for all calculations are presented in Text S1.

2.9. Software

All statistical analyses and modelling were performed under R 3.5.2 software (R Core Team 2018). Wilcoxon tests and Kruskal-Wallis were computed using the included *stats* R package, while Dunn post-hoc test was computed using the *FSA* R package (Ogle *et al*. 2018). GAMs were fitted using the *gam* function from the *mgcv* R package (Wood 2011).

3. Results

3.1. Characterisation of regional mercury and selenium bioaccumulation

Across the Indian Ocean, Hg concentrations were lowest in swordfish from the MOZ region (0.37 ± 0.23 $\mu g.g^{-1}$ ww *vs* 0.81 ± 0.68 $\mu g.g^{-1}$ ww in BENG, Dunn test, $p = 0.037$; 1.21 ± 0.83 $\mu g.g^{-1}$ ww in ISLU, $p < 0.001$; 0.77 ± 0.46 $\mu g.g^{-1}$ ww in WTIO, $p = 0.002$; 1.40 ± 0.76 $\mu g.g^{-1}$ ww in SSG, $p < 0.001$; 0.74 ± 0.39 in SOA, $p = 0.001$) (Fig. 2A). Hg concentrations in the SSG region were also higher than in the BENG, WTIO and SOA regions (Dunn test, $p = 0.009$ with BENG; $p = 0.001$ with WTIO and SOA).

Se concentrations were highest in swordfish from the BENG region compared to swordfish from the other regions (1.39 ± 0.25 $\mu g.g^{-1}$ ww *vs* 0.91 ± 0.25 $\mu g.g^{-1}$ ww in ISLU, Dunn test, $p = 0.007$; 0.94 ± 0.28 $\mu g.g^{-1}$ ww in WTIO, $p = 0.005$; 0.63 ± 0.31 $\mu g.g^{-1}$ ww in MOZ, $p < 0.001$; 1.04 ± 0.52 $\mu g.g^{-1}$ ww in SSG, $p < 0.005$; 0.65 ± 0.31 $\mu g.g^{-1}$ ww in SOA, $p < 0.001$) (Fig. 2B).

Among all swordfish from all sampled regions, there was a significant positive relationship between log-transformed Se and log-transformed Hg concentrations (Fig. 2C).

$\delta^{13}C$ values were highest in swordfish from the ISLU region compared to swordfish from the five other regions (–15.8 ± 0.4 ‰ *vs* –17.0 ± 0.4 ‰ in BENG, Dunn test, $p < 0.001$; –6.7 ± 0.5 ‰ in WTIO, $p < 0.001$; –16.6 ± 0.4 ‰ in MOZ, $p = 0.002$; –16.8 ± 0.5 ‰ in SSG, $p < 0.001$; –17.2 ± 0.3 ‰ in SOA, $p < 0.001$) (Fig. 2D). These values were also lower in swordfish from the SOA region than in those from the WTIO, MOZ and SSG regions (Dunn test, $p = 0.014$ with WTIO, $p < 0.001$ with MOZ, $p = 0.040$ with SSG).

$\delta^{15}N$ values were significantly higher in swordfish from the WTIO and SSG regions than in swordfish from the BENG and MOZ regions (14.1 ± 0.7 ‰ in WTIO and 14.3 ± 0.9 ‰ in SSG *vs* 13.2 ± 0.7 ‰ in BENG and 13.5 ± 0.9 ‰ in MOZ; Dunn test, $p = 0.002$ between WTIO and BENG, $p = 0.009$ between WTIO and MOZ, $p < 0.001$ between SSG and BENG and between SSG and MOZ) (Fig. 2E). Swordfish from the BENG region also had lower $\delta^{15}N$ values than those from the SOA region (13.2 ± 0.7 ‰ *vs* 14.0 ± 0.4 ‰; Dunn test, $p = 0.044$). Swordfish from the ISLU region had intermediate values (13.9 ± 0.7 ‰). Swordfish with the highest trophic levels were from the SSG region (4.8 ± 0.5 *vs* 2.9 ± 0.3 in BENG, Dunn test, $p < 0.001$; 3.6 ± 0.3 in ISLU, $p < 0.001$; 4.5 ± 0.2 in WTIO, $p = 0.007$; 4.1 ± 0.4 in MOZ, $p < 0.001$; and 4.4 ± 0.1 in SOA, $p < 0.001$) (Fig. 2F). Swordfish from the BENG and ISLU regions had the lowest trophic levels (Dunn test, for BENG, $p < 0.001$ with WTIO, $p = 0.001$ with MOZ, $p < 0.001$ with SOA; for ISLU, $p < 0.001$ with WTIO, $p = 0.021$ with MOZ and $p < 0.001$ with SOA).

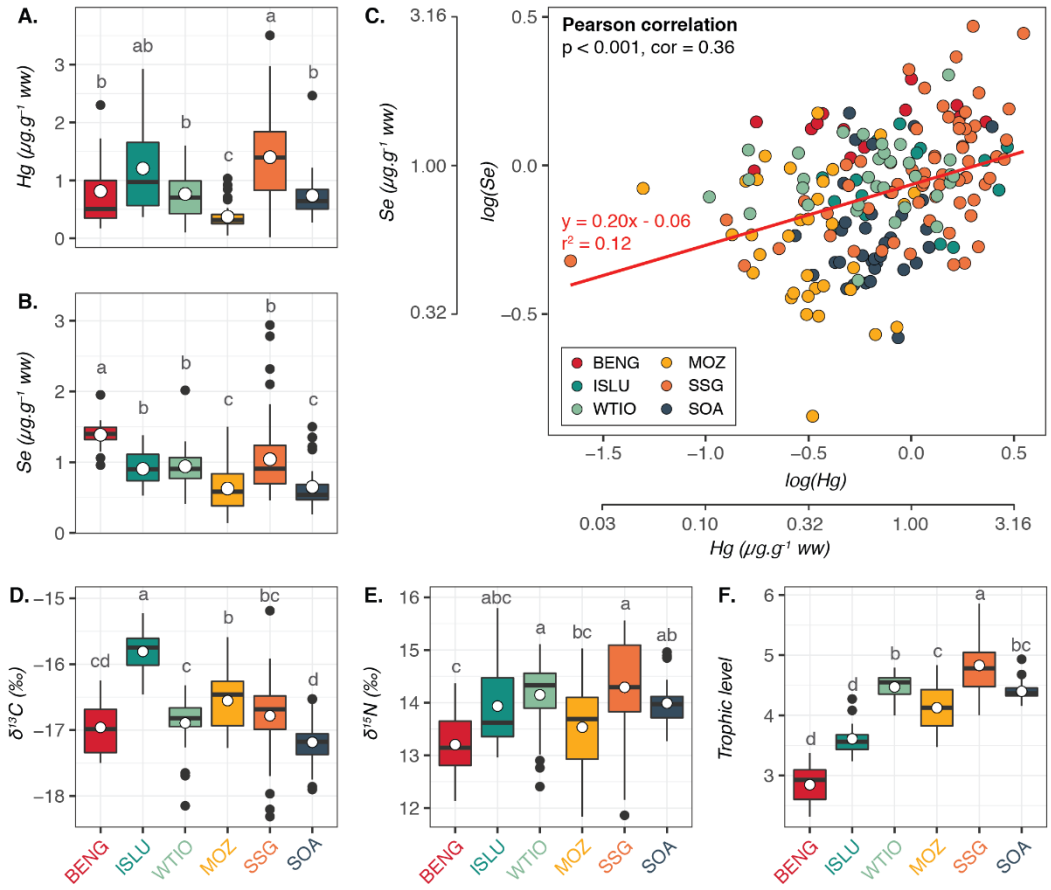

Fig. 2 Mercury (Hg) (A) and selenium (Se) concentrations (µg.g-1 ww) (B), relationship between log-transformed Se and log-transformed Hg concentrations (C), $\delta^{13}C$ (D) and $\delta^{15}N$ values (‰) (E), and trophic level (F) by sampling region. Mean values are indicated in white; a different letter indicates a significant difference between areas (A, B, D, E, F). The linear regression line is indicated in red (C). Mean (± SD) values for each region are presented in Table S2; post-hoc test results are presented in Table S3 (A, B, D, E, F). BENG = Bay of Bengal; ISLU = Indo-Sri Lanka Upwelling; WTIO = Western Tropical Indian Ocean; MOZ = Mozambique Channel; SSG = Southern Subtropical Gyre; SOA = South Africa.

Swordfish from the different Indian Ocean regions significantly differed in lower jaw-fork length (Fig. 3B). Swordfish from the ISLU region were the largest (197 ± 46 cm *vs* 111 ± 16 cm in BENG, Dunn test, $p < 0.001$; 142 ± 35 cm in WTIO, $p < 0.001$; 121 ± 29 cm in MOZ, $p < 0.001$; 151 ± 33 cm in SSG, $p = 0.004$; and 155 ± 35 cm in SOA, $p = 0.009$). Those from the BENG and MOZ regions were also smaller than those from the WTIO, SSG and SOA regions (Dunn test, $p = 0.004$ between BENG and WTIO, $p = 0.010$ between MOZ and WTIO and $p < 0.001$ for the other comparisons).

Swordfish from the SSG region had higher length-standardised Hg concentrations than those from the ISLU, WTIO, MOZ and SOA regions (1.41 ± 0.72 µg.g^{-1} ww *vs* 0.74 ± 0.39 µg.g^{-1} ww in ISLU, 0.79 ± 0.25 µg.g^{-1} ww in WTIO, 0.57 ± 0.22 µg.g^{-1} ww in MOZ, and 0.73 ± 0.41 µg.g^{-1} ww in SOA; Dunn test, $p < 0.001$) (Fig. 3C). Swordfish from the BENG region had intermediate length-standardised Hg concentrations, while also having high concentrations (1.39 ± 1.01 µg.g^{-1} ww). Finally, swordfish from

the MOZ region also had lower length-standardised Hg concentrations than those from the BENG and WTIO regions (Dunn test, $p < 0.001$ with BENG, $p = 0.018$ with WTIO).

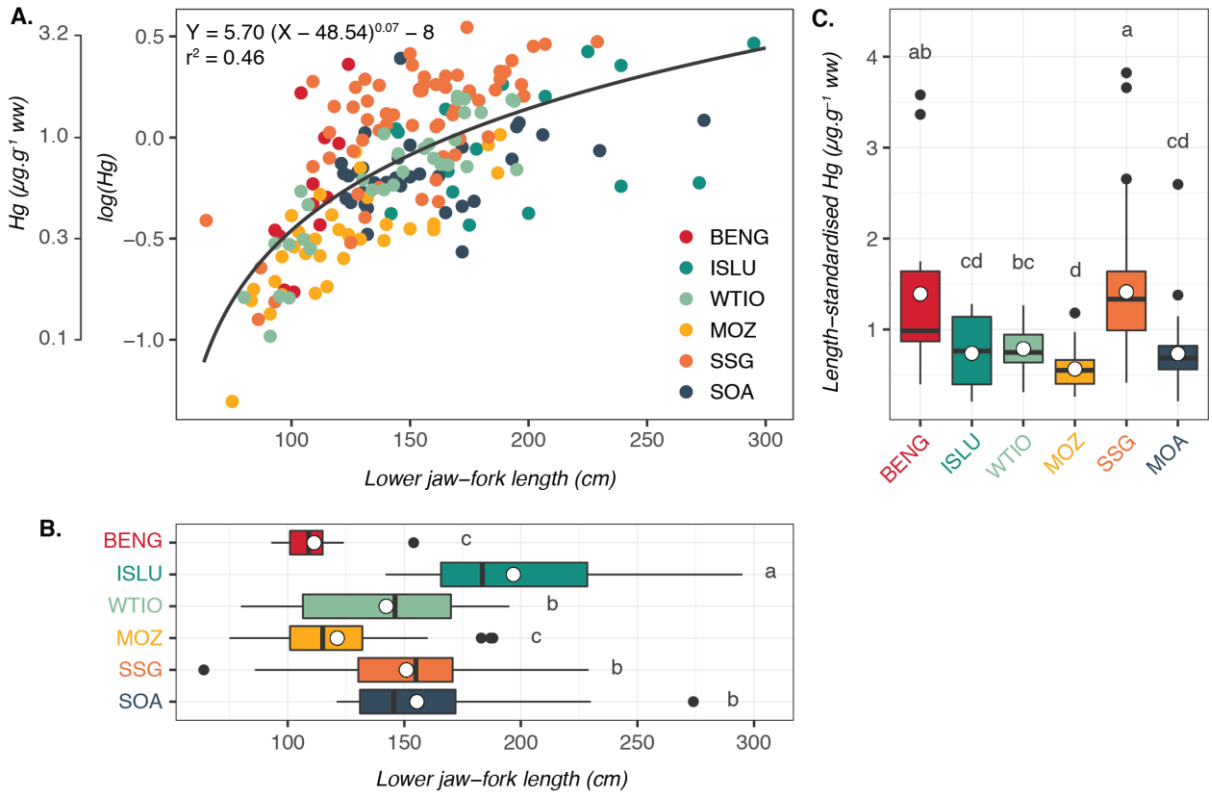

Fig. 3 Power-law relationship between log(Hg) and lower jaw-fork length (A), lower jaw-fork length (cm) (B) and length-standardised Hg concentrations (for a 150 cm fish length, µg.g^{-1} ww) for swordfish of each fishing region. Mean values are indicated in white; a different letter indicates a significant difference between regions (B, C). Mean (± SD) values for each region are presented in Table S2; post-hoc test results are presented in Table S3 (B, C). BENG = Bay of Bengal; ISLU = Indo-Sri Lanka Upwelling; WTIO = Western Tropical Indian Ocean; MOZ = Mozambique Channel; SSG = Southern Subtropical Gyre; SOA = South Africa.

Best GAM models explaining Hg and Se concentrations in swordfish are presented in Table 1. Graphical results (i.e. smoothers) were plotted and are presented in Fig. S2 to S5. For log-transformed Se concentrations, the model including log-transformed Hg concentrations as explanatory variable had a higher total deviance explained and a lower AIC (-137 *vs* -143) than the model only including lower jaw-fork length, $\delta^{13}C$ values, trophic level, longitude, latitude and their interactions terms.

Table 1 Generalised additive model (GAM) results for log-transformed mercury (Hg), log-transformed length-standardised Hg and log-transformed selenium (Se) concentrations.

Trace element	Response variable	Total deviance explained (%)	Explanatory variable used in the best AIC GAM model	*p* value
Hg	log(Hg)	71.7	Lower jaw-fork length	< 0.001
			$\delta^{13}C$	0.031
			Trophic level	0.029
			Latitude	0.005
			Longitude	0.025
			$\delta^{13}C$:Latitude	0.003
			$\delta^{13}C$:Longitude	0.040
			Trophic level:Latitude	0.117
	log(length-standardised Hg)	47.3	$\delta^{13}C$	0.029
			Trophic level	0.018
			Latitude	< 0.001
			Longitude	0.094
			$\delta^{13}C$:Latitude	0.007
			$\delta^{13}C$:Longitude	0.080
			Trophic level:Latitude	< 0.001
Se	log(Se)	43.7	$\delta^{13}C$	0.023
			Trophic level	0.176
			Latitude	0.017
			Longitude	< 0.001
	log(Se) *(with log(Hg) as explanatory variable)*	45.9	$\delta^{13}C$	0.094
			Trophic level	0.036
			Latitude	0.026
			log(Hg)	0.016
			$\delta^{13}C$:Longitude	< 0.001

3.2. Mercury and selenium intakes in human diet

In each sampling region, the molar concentration of Se was higher than the molar concentration of Hg (Fig. 4A). As a consequence, most of sampled swordfish had an MHg:MSe ratio below 1 (Fig. 4B) and an HBVSe above 0 (Fig. 4C). Swordfish from the BENG region had the highest concentrations of theoretically bioavailable Se compared to swordfish from the other regions (1.07 ± 0.29 $\mu g.g^{-1}$ ww *vs* 0.43 ± 0.38 $\mu g.g^{-1}$ ww in ISLU, 0.64 ± 0.30 $\mu g.g^{-1}$ ww in WTIO, 0.48 ± 0.33 $\mu g.g^{-1}$ ww in MOZ, 0.49 ± 0.47 $\mu g.g^{-1}$ ww in SSG and 0.36 ± 0.30 $\mu g.g^{-1}$ ww in SOA; Dunn test, $p = 0.022$ with WTIO, $p < 0.001$ with ISLU, MOZ, SSG and SOA) (Fig. 4E).

Except for the MOZ region, the number of servings necessary to reach PTIof Hg was especially ISLU and SSG regions (lowest number of servings per week ≤ 2 for all age classes) (Table 2). However, after considering the Hg-Se interaction, the contribution of 1 portion of swordfish to RDI of Se was at least of 40% in all regions and for all age classes (Table 2).

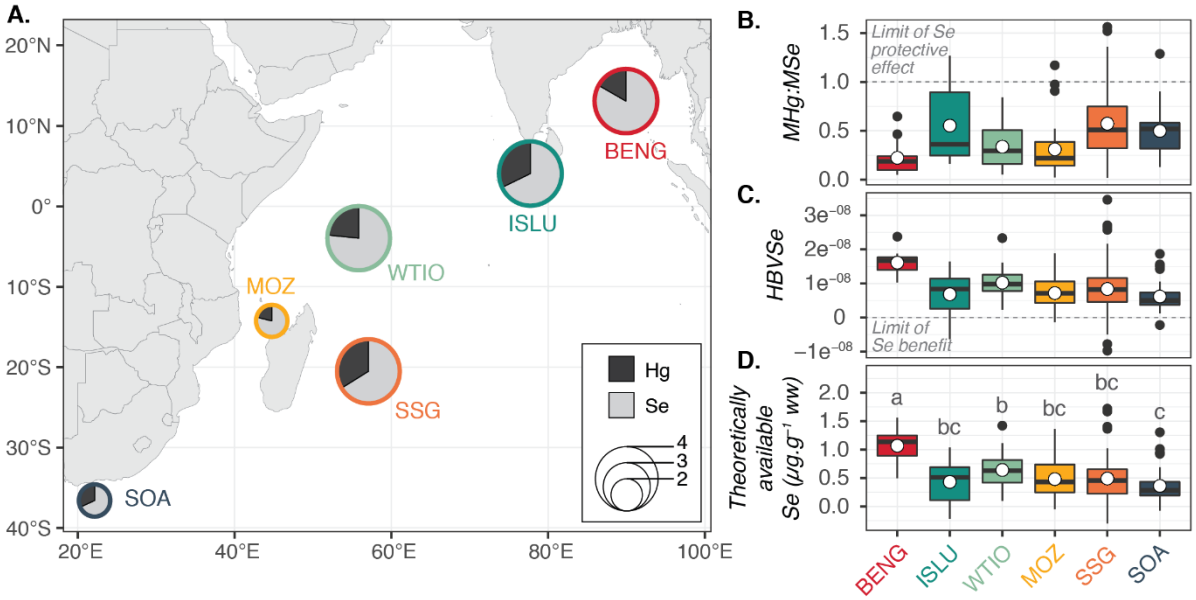

Fig. 4 Molar concentrations (mol.g^{-1} ww) of mercury (MHg) and selenium (MSe) (A), molar ratio of Hg above Se (MHg:MSe) (B), health benefit value of Se (HBV^{Se}) (C) and theoretical concentration of Se after taking into account interaction with Hg (D) in swordfish across the Indian Ocean. Size of circles is proportional to the total molar concentration of Hg and Se (i.e. sum of MHg and MSe concentrations) in each region (A). Mean values are indicated in white (B, C, D) and a different letter indicates a significant difference among sampling regions (D). Post-hoc test results are presented in Table S3 (D). BENG = Bay of Bengal; ISLU = Indo-Sri Lanka Upwelling; WTIO = Western Tropical Indian Ocean; MOZ = Mozambique Channel; SSG = Southern Subtropical Gyre; SOA = South Africa.

Table 2 Number of servings necessary to reach provisional tolerable intakes (PTI) of mercury (Hg)(JECFA 2011) and selenium (Se) (American Food and Nutrition Board of the Institute of Medicine National Academy of Sciences 2019a), and contribution of one serving to Se recommended daily intakes (RDI) set by the American Food and Nutrition Board of the Institute of Medicine National Academy of Sciences (2019b). Data are presented as mean with the associated CI95% between brackets. BENG = Bay of Bengal; ISLU = Indo-Sri Lanka Upwelling; WTIO = Western Tropical Indian Ocean; MOZ = Mozambique Channel; SSG = Southern Subtropical Gyre; SOA = South Africa; C = Children; YA = Young adults; A = Adult women, including pregnant and lactating.

	Hg			Se					Theoretically bioavailable Se				
	Number of servings per week			Contribution to RDI (%)			Number of servings per day		Contribution to RDI (%)			Number of servings per day	
Area	C	YA	A	C	YA	A	C	YA & A	C	YA	A	C	YA & A
BENG	4 (3-5)	5 (3-7)	6 (4-9)	222 (205-239)	252 (227-277)	227 (213-242)	3 (2-3)	3 (3-3)	170 (159-187)	194 (166-222)	175 (159-190)	4 (3-4)	4 (3-5)
ISLU	2 (2-3)	3 (2-3)	4 (2-5)	145 (142-187)	165 (142-187)	148 (136-160)	4 (4-4)	5 (4-5)	69 (51-86)	78 (44-112)	71 (53-88)	8 (6-10)	9 (5-13)
WTIO	4 (3-5)	5 (3-6)	6 (4-8)	104 (94-114)	171 (154-189)	154 (145-164)	4 (4-4)	5 (4-5	102 (97-135)	116 (97-135)	105 (95-115)	7 (6-9)	9 (6-11)
MOZ	7 (6-8)	8 (6-10)	11 (8-14)	100 (90-111)	114 (95-133)	103 (93-113)	7 (6-8)	8 (7-10)	77 (66-87)	87 (67-108)	79 (68-89)	9 (8-10)	10 (8-12)
SSG	4 (2-5)	4 (1-7)	5 (1-9)	189 (166-213)	189 (166-213)	171 (158-183)	4 (4-4)	5 (4-5)	78 (67-89)	89 (68-110)	80 (69-91)	11 (9-12)	12 (8-16)
SOA	3 (3-3)	3 (3-4)	5 (4-5)	118 (99-137)	118 (99-137)	107 (97-117)	6 (6-7)	7 (6-8)	58 (48-67)	66 (47-84)	59 (50-69)	16 (13-19)	18 (13-24)

4. Discussion

The present study is the first to investigate the processes influencing both Hg and Se bioaccumulation in a marine top predator fish, the swordfish, overall the Indian Ocean. The main factor influencing Hg and Se bioaccumulation in swordfish was their regional origin, due to interregional variations in swordfish trophic level and feeding depth (i.e. $\delta^{13}C$). Results also showed signs of co-accumulation of Hg and Se in swordfish muscle tissues. Finally, as both Hg and Se were in high concentrations in all swordfish across the Indian Ocean, we suggest that Se concentrations are high enough to allow protective effect against the Hg present in swordfish edible parts, while still being available in substantial levels for use in human metabolism.

4.1. Factor governing mercury and selenium concentrations in swordfish from the Indian Ocean

Trace element concentrations in marine top predators are well known to vary according to the feeding area of the consumer, either due to regional variations in trace elements' bioavailability or to potential differences in fish trophic ecology among feeding areas (Wang 2002). This was the case for both Hg and Se bioaccumulation in this study, as shown by GAM results in which geographical origin was one of the main factors explaining Hg and Se concentrations.

Latitude was especially important in explaining both length-standardised Hg and Se bioaccumulation, with a decrease from the BENG region in the north-east to the coast of South Africa (SOA region) in the south-west. Such Hg and Se bioaccumulation patterns may be due in part to regional variations in bioavailability of both trace elements. In oceanic waters, these trace elements originate from both natural and anthropogenic sources, like industry and burning of fossil fuel for Hg (Boening 2000), or irrigation of agricultural lands and coal combustion for Se (Schiavon *et al.* 2017). Then, they both enter the food webs through their bioaccumulation by primary producers and are transferred to higher-level consumers through the trophic pathway (Wang 2002; Schiavon *et al.* 2017). In the case of Se, phytoplankton accumulates this element mainly under the inorganic selenite (Se IV) form and it is further incorporated into selenoproteins (Schiavon *et al*. 2017; Ivanenko 2018). These organic compounds are then transferred to higher-level consumers through primary and secondary consumption (Schiavon *et al*. 2017). In the case of Hg, primary producers accumulate both inorganic and organic forms of Hg, but Hg is mainly transferred to higher-level organisms under the MeHg form (Mason *et al.* 1995). The BENG region generally receives high amount of river discharge (Subramanian 1993), which could have led to high Hg and Se input in the waters of this region. In addition, primary production in this region is known to be lower than in other regions of the Indian Ocean in spite of river discharge, due to strong stratification (Dalabehara and Sarma 2021). This could have led to higher Se bioaccumulation in phytoplankton in this region due to high selenite availability, thus high organic Se

compounds production in phytoplankton and thus higher Se bioaccumulation in higher-level organisms. In the case of Hg, MeHg production in subsurface waters (500 m) of the Indian Ocean may have played a large role in the high Hg bioavailability in the BENG region. Modelled MeHg production in this ocean showed a latitudinal gradient, from high production in the BENG region to low production in the MOZ, SSG and SOA regions (Zhang *et al.* 2020). As swordfish usually feed on mesopelagic prey (i.e. depths > 200 m) (Young *et al.* 2006; Potier *et al.* 2007), an interregional difference in MeHg production in mesopelagic waters could have led to different Hg concentrations in swordfish prey (Monteiro *et al.* 1996; Blum *et al.* 2013) and thus to differential Hg bioaccumulation in swordfish tissues.

Although Hg methylation was modelled to be low in the SSG region, length-standardised Hg concentrations were highest in swordfish from this region, suggesting that Hg bioavailability was not the only factor explaining interregional difference in Hg bioaccumulation. Such Hg bioaccumulation pattern could be explained by swordfish trophic ecology, and particularly trophic position. Both $\delta^{15}N$ and trophic level were present in the best AIC model explaining length-standardised Hg concentrations, confirming Hg bioaccumulation potential through food webs (Lavoie *et al.* 2013), and swordfish from the SSG region had higher trophic levels than in all other regions. While an interregional difference in diet composition could explain this, it is more likely that it is the result of a difference in trophic structure at the base of the food web due to nutrient limitation conditions. Indeed, while trophic position is thought to be positively correlated to fish size (Jennings *et al.* 2002), swordfish from this region were not the largest among all regions. In addition, in the SSG region, waters are known to be oligotrophic, with low primary production, which was previously shown to affect food web length (Pethybridge *et al.* 2018) and to increase Hg bioaccumulation in high-trophic level consumers (Chouvelon *et al.* 2018). Here, higher Hg bioaccumulation in oligotrophic conditions could be explained by the domination of N_2 fixation, favouring the presence of diazotrophs like cyanobacteria (Gruber and Sarmiento 1997; Longhurst 1998), as showed in the western Pacific Ocean (Médieu *et al*. 2021). As these organisms are smaller (< 2 µm) than diatom and dinoflagellates (usually 20 to 200 µm), they would favour the presence of mesozooplankton (0.2 to 20 mm) in the food web, causing the presence of an extra step at the bottom of the food chain (Sommer *et al*. 2002). In addition, MeHg proportions in phytoplankton was previously shown to increase with decreasing phytoplankton size, suggesting that diazotrophs could be transfer vectors of Hg to zooplankton and to higher trophic levels (Gosnell and Mason 2015; Lee and Fisher 2016). Thus, by feeding both on a longer food web than in other regions of the Indian Ocean and in oligotrophic waters, swordfish from the SSG region would accumulate higher concentrations of Hg.

Across all sampling regions, swordfish size directly affected their Hg bioaccumulation, with a global increase in Hg with increasing lower jaw-fork length. This was expected, as prey selection, itself influencing trace element bioaccumulation in marine predators (e.g. Metian *et al*. 2013; Chouvelon *et*

al. 2017), varies according to the predator's body size (Jennings *et al*. 2002). This is what led to the theory that the trophic position of a predator is positively correlated with its size (Jennings *et al.* 2002). Size is also used as a proxy of age and, as we have shown previously, Hg both biomagnifies along food chains and bioaccumulates through time in organisms.

Depth played a significant role in both Hg and Se bioaccumulation in swordfish. Indeed, $\delta^{13}C$, which is used to discriminate benthic *vs* pelagic feeding habitats (France 1995), was a significant factor influencing Hg and Se concentrations across all sampling regions. Hg concentration, and especially MeHg availability in oceanic waters, has been positively correlated with depth in previous works (e.g. Choy *et al*. 2009). This was linked mainly with a higher microbial activity, and thus a higher Hg methylation rate in deep waters (Blum et al. 2013). As swordfish are able to dive to depths down to more than 1000 meters (Abascal *et al*. 2010), they would accumulate significantly higher Hg concentrations when feeding on deeper-living prey. In contrast, Se concentrations decreased with increasing $\delta^{13}C$ (Fig. S3), suggesting a relatively higher Se bioaccumulation when feeding closer to the surface. This is consistent with the high Se bioaccumulation potential and subsequent conversion to selenoproteins in phytoplankton (Schiavon *et al*. 2017; Ivanenko 2018). This suggest that prey living closer to the surface would accumulate higher Se concentrations, and would thus transfer higher Se concentrations to swordfish feeding on these prey.

Here, results thus show interregional variations in Hg and Se bioaccumulation in swordfish from the Indian Ocean, due to local conditions in Hg and Se bioavailability and to local trophic structures. Yet, swordfish is a highly migratory species (Nakamura 1985), and studies on the population structure in the Indian Ocean identified one single panmictic population, with no clear subpopulation at the genetic level (Muths *et al*. 2013; Mahé *et al*. 2016). This suggests that swordfish are able to undertake long migrations in the Indian Ocean, even through the strong current systems of this ocean (Schott *et al.* 2009), but hint to a certain level of residency at the scale of their muscle isotopic and trace element turnover rates (i.e. 3 months), as hypothesized by Ménard *et al*. (2007).

4.2. Signs of co-accumulation of mercury and selenium

Due to the antagonist effect between Hg and Se, that is their high binding ability (Raymond and Ralston 2004; Manceau *et al.* 2021), a co-accumulation of these two trace elements can be expected in marine consumers. This bioaccumulation effect is still under debate, as some studies found no significant relationship between both trace elements (e.g. Mikac *et al*. 1985; Chen *et al*. 2001; Kehrig *et al*. 2009), while others found that Se concentrations increased with increasing Hg concentrations in muscle tissues of marine consumers (e.g. Andersen and Depledge 1997; Faganeli *et al*. 2018; Azad *et al*. 2019). However, it is possible that such positive relationship is dependent on Hg concentrations, with

no relationship in species with low Hg concentrations (Azad *et al*. 2019). In this study, log-transformed Se concentrations had a weak but significant positive relationship with log-transformed Hg concentrations, and adding log-transformed Hg concentrations as explanatory variable improved the GAM explaining log-transformed Se concentrations. This suggest a possible co-accumulation of both trace elements in white muscle of swordfish across the Indian Ocean. This would be coherent with previous findings (Azad *et al*. 2019), as swordfish are known to accumulate high concentrations of Hg. Such bioaccumulation process could be the result of both the consumers' physiology and its diet. By binding with Se, Hg would lower Se bioavailability within the consumer's body and, as a result of homeostatic regulation, Se bioaccumulation would increase (Beijer and Jernelov 1978). In addition, fish may receive a part of their dietary Hg as Hg-Se compounds (Khan and Wang 2009), and would thus accumulate both trace elements at the same time. Although we previously showed that Hg and Se bioaccumulation in swordfish from the Indian Ocean could follow inverse or independent trends (e.g. bioaccumulation with depth and with size), implying that co-accumulation is not the main factor influencing both trace element bioaccumulations, correlation and GAM results suggest that the Hg-Se interaction may participate to Hg and Se bioaccumulation in swordfish.

4.3. Swordfish in human diet: mercury risk and selenium benefit

In this study, Hg concentrations were higher than in some previous studies in the Indian Ocean. In the Western Indian Ocean (i.e. WTIO, SSG and MCSA regions) and in the Eastern Indian Ocean (i.e. BENG and ISLU regions), Esposito *et al*. (2018) found Hg concentration ranges of 0.24 – 1.88 $\mu g.g^{-1}$ ww (0.96 ± 0.12 $\mu g.g^{-1}$ ww) and 0.09 – 1.40 $\mu g.g^{-1}$ ww (0.60 ± 0.08 $\mu g.g^{-1}$ ww) respectively (*vs* 0.20 – 6.49 $\mu g.g^{-1}$ ww in WTIO, SSG and MCSA, and 0.04 – 2.92 $\mu g.g^{-1}$ ww in BENG and ISLU in this study). Measured Hg concentrations were also higher in swordfish from the ISLU area than in previous work on swordfish from waters around Sri Lanka (0.3 $\mu g.g^{-1}$ ww Jinadasa *et al*. (2014) *vs* 1.21 ± 0.83 $\mu g.g^{-1}$ ww in this study). On the contrary, Hg concentrations in the SSG area were lower than previous reported concentrations in swordfish from the Reunion Island in Kojadinovic *et al*. (2006), which were of 3.97 ± 2.67 $\mu g.g^{-1}$ ww (*vs* 1.40 ± 0.76 $\mu g.g^{-1}$ ww in this study). Hg and Se concentrations measured in the WTIO area were in the same range as other studies in the same area. Bodin *et al*. (2017) reported Hg and Se concentrations 0.99 ± 0.45 $\mu g.g^{-1}$ ww and 0.76 ± 0.28 $\mu g.g^{-1}$ ww, respectively. Moreover, Hollanda *et al*. (2017) reported 0.16 – 1.80 $\mu g.g^{-1}$ ww (0.63 ± 0.32 $\mu g.g^{-1}$ ww) of Hg and 0.20 – 0.37 $\mu g.g^{-1}$ ww (2.74 ± 1.91 $\mu g.g^{-1}$ ww) of Se in white muscle of swordfish from the Seychelles waters.

Both Hg and Se concentrations were relatively high in swordfish from almost all the Indian Ocean. Indeed, except in the MOZ region, the minimum number of servings allowed before reaching Hg weekly provisional tolerable intake was 4 or below for children, young adults and adults women, and it

was even 2 or below in the ISLU and SSG regions. In the case of Se, one serving of swordfish from all fishing areas was enough to bring more than 90% of daily needs for all age classes. Although Se is essential for human metabolism, it can become toxic if the provided concentrations are too high (Gupta and Gupta 2014), and the minimum number of servings allowed for one day before reaching provisional tolerable intake of Se was low in the BENG region, especially for children (i.e. 2 servings). However, these results do not take into account the interaction potential between Hg and Se, which could considerably lower Hg toxicity risk and risk of excess of Se.

When taking the Hg-Se interaction into account, the exposure risk through swordfish consumption is relatively low, as shown by the Hg:Se molar ratio and HBV_{Se} calculated for all swordfish across the Indian Ocean. As a consequence of the 1:1 molar reaction between Hg and Se, a MHg:MSe ratio < 1 reflects a molar dominance of Se on Hg, and thus is representative of conditions in which Se protects against Hg toxicity (Raymond and Ralston 2004). Similarly, an HBV_{Se}> 0 reflects the amount of physiological Se that is provided after reaction with bioavailable Hg (Ralston *et al*. 2015). Across sampling regions, although the MHg:MSe ratio was above 1 for some swordfish individuals, denoting a dominance of Hg over Se in these individuals, both this ratio median and mean were well below 1. This suggest that, in most of individuals, Se concentrations are high enough to compensate for the Hg risk. Similarly, the HBV_{Se} was above 0 for most of all swordfish individuals in all sampling regions, indicating a Se benefit in case of consumption in human diet. Moreover, after interaction with Hg, concentrations of theoretically bioavailable Se in swordfish from all fishing areas were still high enough to bring at least 40 % of children, young adults and adult women daily needs. This was especially true for swordfish from the BENG region, which was among the regions with the lowest Hg concentrations and which had the highest Se concentrations, and thus the highest theoretically bioavailable Se. Although the minimum number of servings allowed before reaching daily provisional tolerable intake of Se was still of 3 for all age classes in the BENG region, this is equivalent to eating 75 to 225 g of swordfish per day for children, or 300 g for young adults and adults women. These swordfish daily portion sizes are substantial and will likely not be reached, suggesting low risk of Se excess in human diet.

5. Conclusion

This study provides essential baseline information on the occurrence of Hg and Se in the Indian Ocean, at the global ocean scale. By investigating regional patterns of Hg and Se concentrations in muscle of swordfish from six regions of the Indian Ocean, we found that the main factor influencing their bioaccumulation was the geographic origin of swordfish, due to variations in Hg and Se bioavailability and in food web trophic structure. The identification of different regional patterns in Hg and Se concentrations and in stable isotope values despite swordfish being highly-migratory suggests that swordfish may be resident at the scale of their muscle tissue turnover rate. This highlights the

potential of using Hg and Se together with isotopic data (i.e. $\delta^{13}C$ and $\delta^{15}N$ values) for discriminating swordfish metapopulation structures across the Indian Ocean.

Finally, in all regions, Se concentrations in swordfish were high enough to considerably lower Hg risk for human consumers, and to highly contribute to human daily needs regardless of the considered age class, even after interaction with Hg.

Acknowledgements The Institut Universitaire de France (IUF) is acknowledged for its support to Paco Bustamante as a Senior Member. The authors are grateful to Gaël Guillou (plateforme isotopique of LIENSs) for running the stable isotope analyses and to Maud Brault-Favrou and Carine CHurlaud (plateforme Analyses Elémentaires of LIENSs) for her assistance with Hg analyses. Thanks are also due to the CPER (Contrat de Projet Etat-Région) and the FEDER (Fonds Européen de Développement Régional) for funding the AMA and IRMS of LIENSs laboratory.

References

Abascal FJ, Mejuto J, Quintans M, Ramos-Cartelle A (2010) Horizontal and vertical movements of swordfish in the Southeast Pacific. ICES J Mar Sci 67:466–474. doi: 10.1093/icesjms/fsp252

Akaike H (1981) Likelihood of a model and information criteria. J Econom 16:3–14. doi: 10.1016/0304-4076(81)90071-3

American Food and Nutrition Board of the Institute of Medicine National Academy of Sciences (2019a) Dietary Reference Intakes (DRIs): Recommended dietary allowances and adequate intakes, elements. URL: https://ods.od.nih.gov/Health_Information/Dietary_Reference_Intakes.aspx.

American Food and Nutrition Board of the Institute of Medicine National Academy of Sciences (2019b) Dietary Reference Intakes (DRIs): Tolerable upper intake levels, elements. URL: https://www.ncbi.nlm.nih.gov/books/NBK545442/table/appJ_tab9/?report=objectonly.

Andersen JL, Depledge MH (1997) A survey of total mercury and methylmercury in edible fish and invertebrates from Azorean waters. Mar Environ Res 44:331–350. doi: 10.1016/S0141-1136(97)00011-1

Azad AM, Frantzen S, Bank MS, Nilsen BM, Duinker A, Madsen L, Maage A (2019) Effects of geography and species variation on selenium and mercury molar ratios in Northeast Atlantic marine fish communities. Sci Total Environ 652:1482–1496. doi: 10.1016/j.scitotenv.2018.10.405

Beijer K, Jernelov A (1978) Ecological aspects of mercury-selenium interactions in the marine environment. Environ Health Perspect 25:43–45. doi: 10.1289/ehp.782543

Bloom NS (1992) On the chemical form of mercury in edible fish and marine invertebrate tissue. Can J Fish Aquat Sci 49:1010–1017. doi: 10.1139/f92-113

Blum JD, Popp BN, Drazen JC, Anela Choy C, Johnson MW (2013) Methylmercury production below the mixed layer in the North Pacific Ocean. Nat Geosci 6:879–884. doi: 10.1038/ngeo1918

Bodin N, Lesperance D, Albert R, Hollanda S, Michaud P, Degroote M, Churlaud C, Bustamante P (2017) Trace elements in oceanic pelagic communities in the western Indian Ocean. Chemosphere 174:354–362. doi: 10.1016/j.chemosphere.2017.01.099

Boening DW (2000) Ecological effects, transport, and fate of mercury: A general review. Chemosphere 40:1335–1351. doi: 10.1016/S0045-6535(99)00283-0

Bosch AC, O'Neill B, Sigge GO, Kerwath SE, Hoffman LC (2016) Heavy metals in marine fish meat and consumer

health: A review. J Sci Food Agric 96:32–48. doi: 10.1002/jsfa.7360

Carravieri A, Cherel Y, Brault-Favrou M, Churlaud C, Peluhet L, Labadie P, Budzinski H, Chastel O, Bustamante P (2017) From Antarctica to the subtropics: Contrasted geographical concentrations of selenium, mercury, and persistent organic pollutants in skua chicks (Catharacta spp.). Environ Pollut 228:464–473. doi: 10.1016/j.envpol.2017.05.053

Carravieri A, Bustamante P, Labadie P, Budzinski H, Chastel O, Cherel Y (2020) Trace elements and persistent organic pollutants in chicks of 13 seabird species from Antarctica to the subtropics. Environ Int 134:105225. doi: 10.1016/j.envint.2019.105225

Chen YW, Belzile N, Gunn JM (2001) Antagonistic effect of selenium on mercury assimilation by fish populations near Sudbury metal smelters? Limnol Oceanogr 46:1814–1818. doi: 10.4319/lo.2001.46.7.1814

Chouvelon T, Spitz J, Caurant F, Mèndez-Fernandez P, Chappuis A, Laugier F, Le Goff E, Bustamante P (2012) Revisiting the use of δ15N in meso-scale studies of marine food webs by considering spatio-temporal variations in stable isotopic signatures - The case of an open ecosystem: The Bay of Biscay (North-East Atlantic). Prog Oceanogr 101:92–105. doi: 10.1016/j.pocean.2012.01.004

Chouvelon T, Caurant F, Cherel Y, Simon-Bouhet B, Spitz J, Bustamante P (2014) Species-and size-related patterns in stable isotopes and mercury concentrations in fish help refine marine ecosystem indicators and provide evidence for distinct management units for hake in the Northeast Atlantic. ICES J Mar Sci 71:1073–1087. doi: 10.1093/icesjms/fst199

Chouvelon T, Brach-Papa C, Auger D, Bodin N, Bruzac S, Crochet S, Degroote M, Hollanda SJ, Hubert C, Knoery J, Munschy C, Puech A, Rozuel E, Thomas B, West W, Bourjea J, Nikolic N (2017) Chemical contaminants (trace metals, persistent organic pollutants) in albacore tuna from western Indian and south-eastern Atlantic Oceans: Trophic influence and potential as tracers of populations. Sci Total Environ 596–597:481–495. doi: 10.1016/j.scitotenv.2017.04.048

Chouvelon T, Cresson P, Bouchoucha M, Brach-Papa C, Bustamante P, Crochet S, Marco-Miralles F, Thomas B, Knoery J (2018) Oligotrophy as a major driver of mercury bioaccumulation in medium-to high-trophic level consumers: A marine ecosystem-comparative study. Environ Pollut 233:844–854. doi: 10.1016/j.envpol.2017.11.015

Choy CA, Popp BN, Kaneko JJ, Drazen JC (2009) The influence of depth on mercury levels in pelagic fishes and their prey. Proc Natl Acad Sci USA 106:13865–13869. doi: 10.1073/pnas.0900711106

Copaja S V., Pérez CA, Vega-Retter C, Véliz D (2017) Heavy metal content in Chilean fish related to habitat use, tissue type and river of origin. Bull Environ Contam Toxicol 99:695–700. doi: 10.1007/s00128-017-2200-9

Costa MF, Landing WM, Kehrig HA, Barletta M, Holmes CD, Barrocas PRG, Evers DC, Buck DG, Claudia Vasconcellos A, Hacon SS, Moreira JC, Malm O (2012) Mercury in tropical and subtropical coastal environments. Environ Res 119:88–100. doi: 10.1016/j.envres.2012.07.008

Dalabehara HB, Sarma VVSS (2021) Physical forcing controls spatial variability in primary production in the Indian Ocean. Deep Res Part II Top Stud Oceanogr 183:104906. doi: 10.1016/j.dsr2.2020.104906

De Niro M, Epstein S (1978) Influence of diet on the distribution of carbon isotopes in animals. Geochim Cosmochim Acta 42:495–506. doi: 10.1016/0016-7037(78)90199-0

Esposito M, De Roma A, La Nucara R, Picazio G, Gallo P (2018) Total mercury content in commercial swordfish (Xiphias gladius) from different FAO fishing areas. Chemosphere 197:14–19. doi: 10.1016/j.chemosphere.2018.01.015

Faganeli J, Falnoga I, Horvat M, Klun K, Lipej L, Mazej D (2018) Selenium and mercury interactions in apex predators from the gulf of trieste (Northern Adriatic Sea). Nutrients 10:1–11. doi: 10.3390/nu10030278

FAO (2020) Species facts sheet – Xiphias gladius. URL: http://www.fao.org/fishery/species/2503/en.

Ferriss BE, Essington TE (2011) Regional patterns in mercury and selenium concentrations of yellowfin tuna (Thunnus albacares) and bigeye tuna (Thunnus obesus) in the Pacific Ocean. Can J Fish Aquat Sci 68:2046–2056. doi: 10.1139/F2011-120

France RL (1995) Carbon-13 enrichment in benthic compared to planktonic algae: Food web implications. Mar Ecol Prog Ser 124:307–312. doi: 10.3354/meps124307

Gosnell KJ, Mason RP (2015) Mercury and methylmercury incidence and bioaccumulation in plankton from the

central Pacific Ocean. Mar Chem 177:772–780. doi: 10.1016/j.marchem.2015.07.005

Gruber N, Sarmiento JL (1997) Global patterns of marine nitrogen fixation and denitrification. Global Biogeochem Cycles 11:235–266. doi: 10.1029/97GB00077

Gupta UC, Gupta SC (2014) Sources and deficiency diseases of mineral nutrients in human health and nutrition: A review. Pedosphere 24:13–38. doi: 10.1016/S1002-0160(13)60077-6

Hollanda S, Bodin N, Churlaud C, Bustamante P (2017) Mercury and selenium levels in Swordfish (Xiphias gladius) fished in the exclusive economic zone of the Republic of Seychelles. Int J Environ Ecol Eng 11:23–26.

Houssard P, Point D, Tremblay-Boyer L, Allain V, Pethybridge H, Masbou J, Ferriss BE, Baya PA, Lagane C, Menkes CE, Letourneur Y, Lorrain A (2019) A model of mercury distribution in tuna from the western and central pacific ocean: Influence of physiology, ecology and environmental factors. Environ Sci Technol 53:1422–1431. doi: 10.1021/acs.est.8b06058

Ivanenko N V. (2018) The role of microorganisms in transformation of selenium in marine waters. Russ J Mar Biol 44:87–93. doi: 10.1134/S1063074018020049

JECFA (2011) Mercury. URL: https://apps.who.int/food-additives-contaminants-jecfa-database/chemical.aspx?chemID=1806.

Jennings S, Pinnegar JK, Polunin NVC, Warr KJ (2002) Linking size-based and trophic analyses of benthic community structure. Mar Ecol Prog Ser 226:77–85. doi: 10.3354/meps226077

Jinadasa BKKK, Edirisinghe EMRKB, Wickramasinghe I (2014) Total mercury, cadmium and lead levels in main export fish of Sri Lanka. Food Addit Contam Part B Surveill 7:309–314. doi: 10.1080/19393210.2014.938131

Kehrig HDA, Seixas TG, Palermo EA, Baêta AP, Castelo-Branco CW, Malm O, Moreira I (2009) The relationships between mercury and selenium in plankton and fish from a tropical food web. Environ Sci Pollut Res 16:10–24. doi: 10.1007/s11356-008-0038-8

Khan MAK, Wang F (2009) Mercury-selenium compounds and their toxicological significance: Toward a molecular understanding of the mercury-selenium antagonism. Environ Toxicol Chem 28:1567–1577. doi: 10.1897/08-375.1

Kojadinovic J, Potier M, Le Corre M, Cosson RP, Bustamante P (2006) Mercury content in commercial pelagic fish and its risk assessment in the Western Indian Ocean. Sci Total Environ 366:688–700. doi: 10.1016/j.scitotenv.2006.02.006

Kojadinovic J, Potier M, Le Corre M, Cosson RP, Bustamante P (2007) Bioaccumulation of trace elements in pelagic fish from the Western Indian Ocean. Environ Pollut 146:548–566. doi: 10.1016/j.envpol.2006.07.015

Lavoie RA, Jardine TD, Chumchal MM, Kidd KA, Campbell LM (2013) Biomagnification of mercury in aquatic food webs: A worldwide meta-analysis. Environ Sci Technol 47:13385–13394. doi: 10.1021/es403103t

Layman CA, Araujo MS, Boucek R, Hammerschlag-Peyer CM, Harrison E, Jud ZR, Matich P, Rosenblatt AE, Vaudo JJ, Yeager LA, Post DM, Bearhop S (2011) Applying stable isotopes to examine food-web structure: An overview of analytical tools. Biol Rev 87:545–562. doi: 10.1111/j.1469-185X.2011.00208.x

Le Croizier G, Schaal G, Gallon R, Fall M, Le Grand F, Munaron JM, Rouget ML, Machu E, Le Loc'h F, Laë R, De Morais LT (2016) Trophic ecology influence on metal bioaccumulation in marine fish: Inference from stable isotope and fatty acid analyses. Sci Total Environ 573:83–95. doi: 10.1016/j.scitotenv.2016.08.035

Lee CS, Fisher NS (2016) Methylmercury uptake by diverse marine phytoplankton. Limnol Oceanogr 61:1626–1639. doi: 10.1002/lno.10318

Longhurst AR (1998) Chapter 10 - The Indian Ocean. Ecol Geogr Sea 275-. doi: 10.1080/00377996.1953.9957307

Mahé K, Evano H, Mille T, Muths D, Bourjea J (2016) Otolith shape as a valuable tool to evaluate the stock structure of swordfish Xiphias gladius in the Indian Ocean. African J Mar Sci 38:457–464. doi: 10.2989/1814232X.2016.1224205

Manceau A, Azemard S, Hédouin L, Vassileva E, Lecchini D, Fauvelot C, Swarzenski PW (2021) Chemical forms of mercury in blue marlin billfish: Implications for human exposure. Environ Sci Technol Lett 8:405–411. doi: https://doi.org/10.1021/acs.estlett.1c00217

Mason RP, Reinfelder JR, Morel FMM (1995) Bioaccumulation of mercury and methylmercury. Water, Air Soil Pollut 80:915–921.

Médieu A, Point D, Receveur A, Gauthier O, Allain V, Pethybridge H, Menkes CE, Gillikin DP, Revill AT, Somes CJ, Collin J, Lorrain A (2021) Stable mercury concentrations of tropical tuna in the south western Pacific Ocean: An 18-year monitoring study. Chemosphere. doi: 10.1016/j.chemosphere.2020.128024

Ménard F, Lorrain A, Potier M, Marsac F (2007) Isotopic evidence of distinct feeding ecologies and movement patterns in two migratory predators (yellowfin tuna and swordfish) of the western Indian Ocean. Mar Biol 153:141–152. doi: 10.1007/s00227-007-0789-7

Méndez-Fernandez P, Pierce GJ, Bustamante P, Chouvelon T, Ferreira M, González AF, López A, Read FL, Santos MB, Spitz J, Vingada J V., Caurant F (2013) Ecological niche segregation among five toothed whale species off the NW Iberian Peninsula using ecological tracers as multi-approach. Mar Biol 160:2825–2840. doi: 10.1007/s00227-013-2274-9

Mergler D, Anderson HA, Hing Man Chan L, Mahaffey KR, Murray M, Sakamoto M, Stern AH (2007) Methylmercury exposure and health effects in humans: A worldwide concern. AMBIO A J Hum Environ 36:3–11. doi: 10.1579/0044-7447(2007)36

Metian M, Warnau M, Chouvelon T, Pedraza F, Rodriguezy Baena AM, Bustamante P (2013) Trace element bioaccumulation in reef fish from New Caledonia: Influence of trophic groups and risk assessment for consumers. Mar Environ Res 87–88:26–36. doi: 10.1016/j.marenvres.2013.03.001

Mikac N, Picer M, Stegnar P, Tušek-Žnidarić M (1985) Mercury distribution in a polluted marine area, ratio of total mercury, methyl mercury and selenium in sediments, mussels and fish. Water Res 19:1387–1392. doi: 10.1016/0043-1354(85)90305-7

Monteiro LR, Costa V, Furness RW, Santos RS (1996) Mercury concentrations in prey fish indicate enhanced bioaccumulation in mesopelagic environments. Mar Ecol Prog Ser 141:21–25.

Morel FMM, Kraepiel AML, Amyot M (1998) The chemical cycle and bioaccumulation of mercury. Annu Rev Ecol Syst 29:543–566. doi: 10.1146/annurev.ecolsys.29.1.543

Muths D, Le Couls S, Evano H, Grewe P, Bourjea J (2013) Multi-genetic marker approach and spatio-temporal analysis suggest there is a single panmictic population of swordfish Xiphias gladius in the Indian Ocean. PLoS One 8:e63558. doi: 10.1371/journal.pone.0063558

Nakamura I (1985) Vol. 5 Billfishes of the world – An annotated and illustrated catalogue of marlins, sailfishes, spearfishes and swordfishes known to date. FAO Fish Synopsis 5:1–4. doi: 10.1016/S0921-4526(05)00705-2

Ogle DH, Wheeler P, Dinno A (2018) FSA: Fisheries Stock Analysis.

Ordiano-Flores A, Galván-Magaña F, Rosiles-Martínez R (2011) Bioaccumulation of mercury in muscle tissue of yellowfin tuna, Thunnus albacares, of the Eastern Pacific Ocean. Biol Trace Elem Res 144:606–620. doi: 10.1007/s12011-011-9136-4

Payne EJ, Taylor DL (2010) Effects of diet composition and trophic structure on mercury bioaccumulation in temperate flatfishes. Arch Environ Contam Toxicol 58:431–443. doi: 10.1007/s00244-009-9423-7

Pethybridge H, Choy CA, Logan JM, Allain V, Lorrain A, Bodin N, Somes CJ, Young J, Ménard F, Langlais C, Duffy L, Hobday AJ, Kuhnert P, Fry B, Menkes C, Olson RJ (2018) A global meta-analysis of marine predator nitrogen stable isotopes: Relationships between trophic structure and environmental conditions. Glob Ecol Biogeogr 27:1043–1055. doi: 10.1111/geb.12763

Post DM (2002) Using stable isotopes to estimate trophic position: Models, methods, and assumptions. Ecology 83:703–718. doi: 10.2307/3071875

Potier M, Marsac F, Cherel Y, Lucas V, Sabatié R, Maury O, Ménard F (2007) Forage fauna in the diet of three large pelagic fishes (lancetfish, swordfish and yellowfin tuna) in the western equatorial Indian Ocean. Fish Res 83:60–72. doi: 10.1016/j.fishres.2006.08.020

R Core Team (2018) R: A language and environment for statistical computing.

Ralston NVC, Blackwell JL, Raymond LJ (2007) Importance of molar ratios in selenium-dependent protection against methylmercury toxicity. Biol Trace Elem Res 119:255–268. doi: 10.1007/s12011-007-8005-7

Ralston NVC, Ralston CR, Raymond LJ (2015) Selenium Health Benefit Values: Updated criteria for mercury risk assessments. Biol Trace Elem Res 171:262–269. doi: 10.1007/s12011-015-0516-z

Raymond LJ, Ralston NVC (2004) Mercury:selenium interactions and health implications. Seychelles Med Dent J

7:72–77. doi: 10.1016/j.neuro.2020.09.020

Schiavon M, Ertani A, Parrasia S, Vecchia FD (2017) Selenium accumulation and metabolism in algae. Aquat Toxicol 189:1–8. doi: 10.1016/j.aquatox.2017.05.011

Schott FA, Xie S-P, McCreary JP (2009) Indian ocean circulation and climate variability. Rev Geophys 47:1–46. doi: 10.1029/2007RG000245

Somes CJ, Schmittner A, Muglia J, Oschlies A (2017) A three-dimensional model of the marine nitrogen cycle during the last glacial maximum constrained by sedimentary isotopes. Front Mar Sci 4:1–24. doi: 10.3389/fmars.2017.00108

Sommer U, Stibor H, Katechakis A, Sommer F, Hansen T (2002) Pelagic food web configurations at different levels of nutrient richness and their implications for the ratio fish production: Primary production. Hydrobiologia 484:11–20. doi: http://dx.doi.org/10.1023/A:1021340601986

Subramanian V (1993) Sediment load of Indian rivers. Curr Sci 64:928–930.

Syversen T, Kaur P (2012) The toxicology of mercury and its compounds. J Trace Elem Med Biol 26:215–226. doi: 10.1016/j.jtemb.2012.02.004

Velusamy A, Satheesh Kumar P, Ram A, Chinnadurai S (2014) Bioaccumulation of heavy metals in commercially important marine fishes from Mumbai Harbor, India. Mar Pollut Bull 81:218–224. doi: 10.1016/j.marpolbul.2014.01.049

Vieira C, Morais S, Ramos S, Delerue-Matos C, Oliveira MBPP (2011) Mercury, cadmium, lead and arsenic levels in three pelagic fish species from the Atlantic Ocean: Intra- and inter-specific variability and human health risks for consumption. Food Chem Toxicol 49:923–932. doi: 10.1016/j.fct.2010.12.016

Wada E, Hattori A (1976) Natural abundance of 15N in particulate organic matter in the North Pacific Ocean. Geochim Cosmochim Acta 40:249–251. doi: 10.1016/0016-7037(76)90183-6

Wagemann R, Trebacz E, Hunt R, Boila G (1997) Percent methylmercury and organic mercury in tissues of marine mammals and fish using different experimental and calculation methods. Environ Toxicol Chem 16:1859–1866. doi: 10.1897/1551-5028(1997)016<1859:PMAOMI>2.3.CO;2

Wang WX (2002) Interactions of trace metals and different marine food chains. Mar Ecol Prog Ser 243:295–309. doi: 10.3354/meps243295

Weichselbaum E, Coe S, Buttriss J, Stanner S (2013) Fish in the diet: A review. Nutr Bull 38:128–177. doi: 10.1111/nbu.12021

Wood S (2011) Fast stable restricted maximum likelihood and marginal likelihood estimation of semiparametric generalized linear models. J R Stat Soc Ser B 73:3–36. doi: 10.1111/j.1467-9868.2010.00749.x

Young J, Lansdell M, Riddoch S, Revill A (2006) Feeding ecology of broadbill swordfish, Xiphias gladius, off eastern Australia in relation to physical and environmental variables. Bull Mar Sci 79:793–809.

Zhang H, Feng X, Chan HM, Larssen T (2014) New insights into traditional health risk assessments of mercury exposure: Implications of selenium. Environ Sci Technol 48:1206–1212. doi: 10.1021/es4051082

Zhang Y, Soerensen AL, Schartup AT, Sunderland EM (2020) A global model for methylmercury formation and uptake at the base of marine food webs. Global Biogeochem Cycles 34:1–21. doi: 10.1029/2019GB006348

Zuur AF, Ieno EN, Smith GM (2007) Analysing ecological data. Springer, New-York, USA

Supplementary data

Table S1 Mean weight (kg) (Marques-Vidal *et al*. 2008; US-EPA and US-FDA 2019) and portion weights (g) (WorldBank 2017; US-EPA and US-FDA 2019) used to calculate contributions to recommended daily intakes (RDI) and numbers of servings before reaching provisional tolerable intakes (PTI), RDI and PTI for Se (American Food and Nutrition Board of the Institute of Medicine National Academy of Sciences 2019a, 2019b), and PTI given by the Joint FAO/WHO Expert Committee on Food Additives (JECFA 2011) for Hg.

Age class	Age subclass	Mean weight (kg)	Portion weight (g)	Se		Hg[1]
				RDI (µg/day)	PTI (µg/day)	PTI (µg/week)
Children	2-3 years	12	25	20	90	48
	4-8 years	22	50	30	150	88
	9-13 years	36	75	40	280	144
Young Adults	14-19 years	52	100	55	400	208
Adult women	> 19 years	70	100	55	400	280
	> 19 years + pregnant	70	100	60	400	280
	> 19 years + lactating	70	100	70	400	280

[1] Hg PTI given by the JECFA (2011) was of 4 µg/kg body weight/week.

Table S2 Lower jaw-fork length (cm), raw mercury (Hg), length-standardised Hg and selenium (Se) concentrations (µg.g^{-1} ww), $\delta^{13}C$ and $\delta^{15}N$ values (‰), and calculated trophic levels in each sampling region of the Indian Ocean. Data are presented as mean ± SD, with the minimum and maximum values in each region between brackets. BENG = Bay of Bengal; ISLU = Indo-Sri Lanka Upwelling; WTIO = Western Tropical Indian Ocean; MOZ = Mozambique Channel; SSG = Southern Subtropical Gyre; SOA = South Africa.

Region	Lower jaw-fork length (cm)	Hg (µg.g^{-1} ww)	Length-stand. Hg (µg.g^{-1} ww)	Se (µg.g^{-1} ww)	$\delta^{13}C$ (‰)	$\delta^{15}N$ (‰)	Calculated trophic level
BENG	111 ± 16	0.81 ± 0.68	1.39 ± 1.01	1.39 ± 0.25	–17.0 ± 0.4	13.2 ± 0.7	2.9 ± 0.3
	(93 – 154)	(0.17 – 2.30)	(0.40 – 3.58)	(0.96 – 1.95)	(–17.5 – –16.2)	(12.1 – 14.4)	(2.3 – 3.4)
ISLU	197 ± 46	1.21 ± 0.83	0.74 ± 0.39	0.91 ± 0.25	–15.8 ± 0.4	13.9 ± 0.7	3.6 ± 0.3
	(142 – 295)	(0.37 – 2.92)	(0.21 – 1.28)	(0.53 – 1.38)	(–16.5 – –15.2)	(13.0 – 15.8)	(3.2 – 4.3)
WTIO	142 ± 35	0.77 ± 0.46	0.79 ± 0.25	0.94 ± 0.28	–6.7 ± 0.5	14.1 ± 0.7	4.5 ± 0.2
	(80 – 195)	(0.10 – 1.60)	(0.31 – 1.26)	(0.41 – 2.02)	(–18.1 – –16.3)	(12.4 – 15.1)	(4.0 – 4.5)
MOZ	121 ± 29	0.37 ± 0.23	0.57 ± 0.22	0.63 ± 0.31	–16.6 ± 0.4	13.5 ± 0.9	4.1 ± 0.4
	(75 – 188)	(0.05 – 1.03)	(0.26 – 1.18)	(0.14 – 1.50)	(–17.3 – –16.5)	(11.8 – 15.0)	(3.5 – 4.8)
SSG	151 ± 33	1.40 ± 0.76	1.41 ± 0.72	1.04 ± 0.52	–16.8 ± 0.5	14.3 ± 0.9	4.8 ± 0.5
	(64 – 229)	(0.02 – 3.50)	(0.42 – 3.82)	(0.46 – 2.94)	(–18.3 – –15.2)	(11.9 – 15.6)	(4.0 – 5.9)
SOA	155 ± 35	0.74 ± 0.39	0.73 ± 0.41	0.65 ± 0.31	–17.2 ± 0.3	14.0 ± 0.4	4.4 ± 0.1
	(121 – 274)	(0.27 – 2.46)	(0.21 – 2.60)	(0.26 – 1.50)	(–17.9 – –16.5)	(13.3 – 15.0)	(4.1 – 4.9)

Table S3 Post-hoc test results for interregional comparisons of Hg concentrations (A), Se concentrations (B), $\delta^{13}C$ values (C) and $\delta^{15}N$ values (D) measured in the white muscle of sampled swordfish, for interregional comparison of calculated trophic level (E), length-standardised Hg concentrations (G) and theoretically bioavailable Se concentrations (H), and of measured swordfish lower jaw-fork length (F). For each interregional comparison, used post-hoc is indicated in the top left. Significant differences are indicated in bold. BENG = Bay of Bengal; ISLU = Indo-Sri Lanka Upwelling; WTIO = Western Tropical Indian Ocean; MOZ = Mozambique Channel; SSG = Southern Subtropical Gyre; SOA = South Africa.

A.

Hg concentrations					
Dunn test	BENG	ISLU	WTIO	MOZ	SSG
ISLU	0.158				
WTIO	0.913	0.143			
MOZ	**0.037**	**< 0.001**	**0.002**		
SSG	**0.009**	0.399	**0.001**	**< 0.001**	
SOA	0.893	0.155	0.895	**0.001**	**0.001**

B.

Se concentrations					
Dunn test	BENG	ISLU	WTIO	MOZ	SSG
ISLU	**0.007**				
WTIO	**0.005**	0.953			
MOZ	**< 0.001**	**0.006**	**< 0.001**		
SSG	**0.003**	0.908	0.951	**< 0.001**	
SOA	**< 0.001**	**0.006**	**< 0.001**	0.920	**< 0.001**

C.

$\delta^{13}C$ values					
Dunn test	BENG	ISLU	WTIO	MOZ	SSG
ISLU	**< 0.001**				
WTIO	0.595	**< 0.001**			
MOZ	**0.017**	**0.002**	**0.014**		
SSG	0.179	**< 0.001**	0.252	0.090	
SOA	0.175	**< 0.001**	**0.014**	**< 0.001**	**< 0.001**

D.

$\delta^{15}N$ values					
Dunn test	BENG	ISLU	WTIO	MOZ	SSG
ISLU	0.109				
WTIO	**0.002**	0.185			
MOZ	0.255	0.391	**0.009**		
SSG	**< 0.001**	0.068	0.543	**< 0.001**	
SOA	**0.044**	0.773	0.200	0.202	**0.040**

E.

Trophic level					
Dunn test	BENG	ISLU	WTIO	MOZ	SSG
ISLU	0.329				
WTIO	**< 0.001**	**< 0.001**			
MOZ	**0.001**	**0.021**	**0.005**		
SSG	**< 0.001**	**< 0.001**	**0.007**	**< 0.001**	
SOA	**< 0.001**	**< 0.001**	0.322	0.056	**< 0.001**

F.

Lower jaw-fork length					
Dunn test	BENG	ISLU	WTIO	MOZ	SSG
ISLU	**< 0.001**				
WTIO	**0.004**	**< 0.001**			
MOZ	0.333	**< 0.001**	**0.010**		
SSG	**< 0.001**	**0.004**	0.328	**< 0.001**	
SOA	**< 0.001**	**0.009**	0.342	**< 0.001**	0.865

G.

Length-standardised Hg concentrations					
Dunn test	BENG	ISLU	WTIO	MOZ	SSG
ISLU	0.053				
WTIO	0.105	0.536			
MOZ	**< 0.001**	0.179	**0.018**		
SSG	0.441	**< 0.001**	**< 0.001**	**< 0.001**	
SOA	**0.018**	0.898	0.400	0.127	**< 0.001**

H.

Theoretically bioavailable Se concentrations					
Dunn test	BENG	ISLU	WTIO	MOZ	SSG
ISLU	**< 0.001**				
WTIO	**0.022**	0.111			
MOZ	**< 0.001**	0.952	0.087		
SSG	**< 0.001**	0.899	**0.034**	0.947	
SOA	**< 0.001**	0.353	**< 0.001**	0.146	0.135

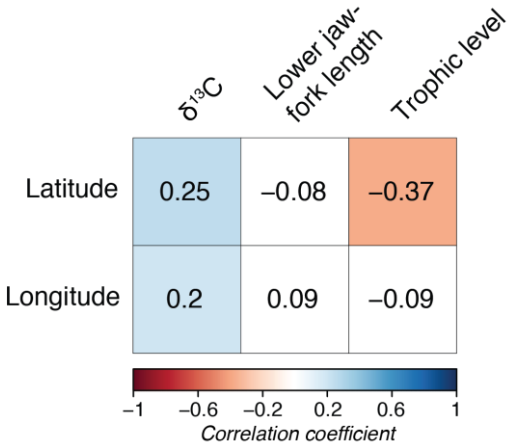

Fig. S1 Correlation (Kendall test) between swordfish sampling coordinates (i.e. latitude and longitude) and $\delta^{13}C$ values measured in swordfish white muscle tissues and swordfish lower jaw-fork length and trophic level. Coloured cells indicate a significant correlation ($p < 0.05$) between two variables, while uncoloured cells indicate a non-significant correlation. Numbers in the cells are the associated correlation coefficients and the cell's colour intensity is proportional to the coefficient.

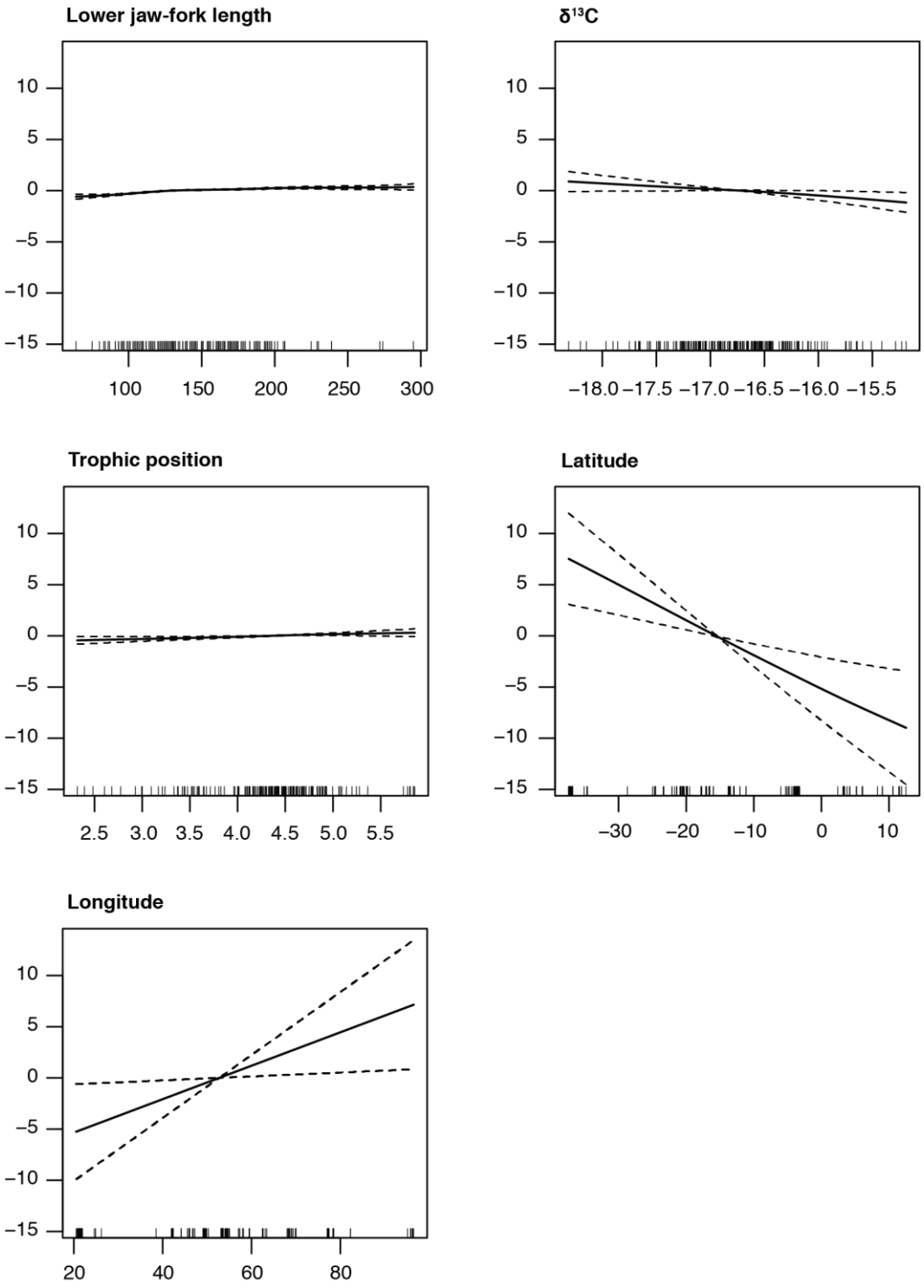

Fig. S2 Graphical results of the generalised additive models (GAM) fitted to log-transformed Hg concentrations in white muscle of swordfish from the Indian Ocean. Smoothers illustrate the partial effect of continuous explanatory variables once the effects of all the other explanatory variables included in the model have been considered. The y-axis shows the contribution of the smoother to the predictor function in the model (in arbitrary units). Dashed lines represent the 95% confidence intervals. Whiskers on the x-axis indicate data presence.

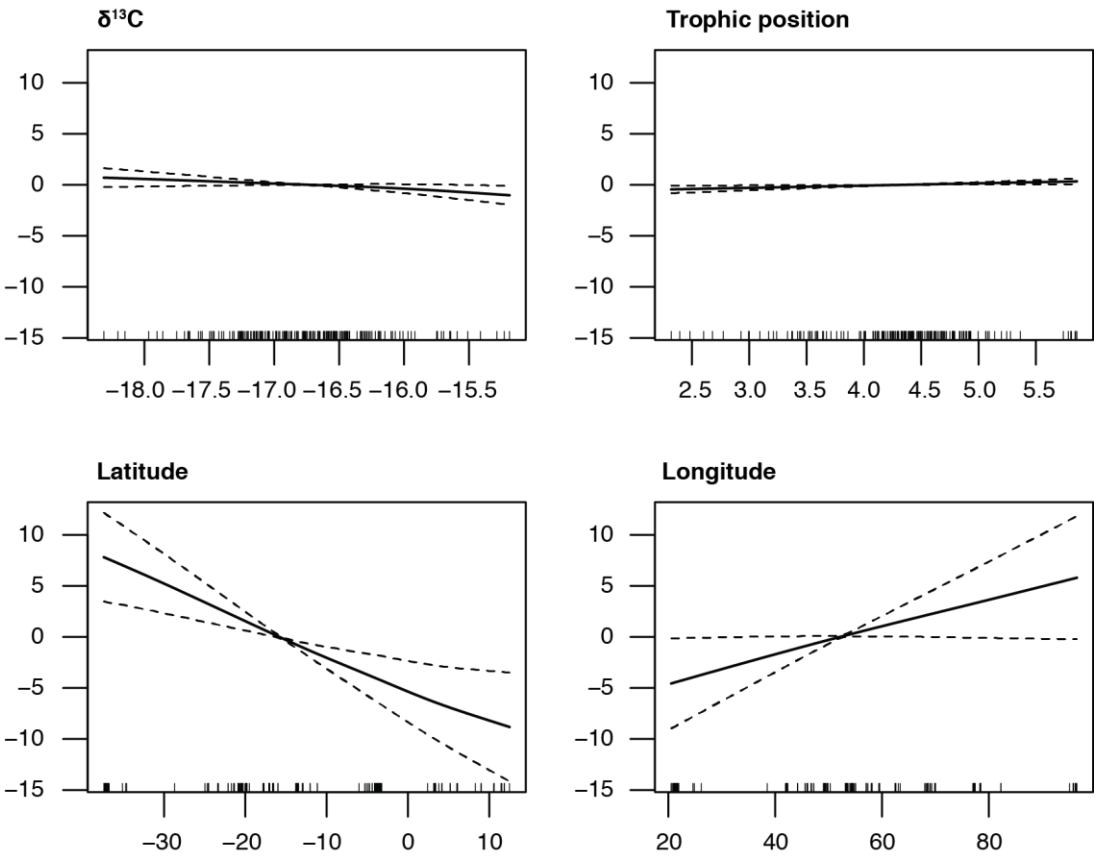

Fig. S3 Graphical results of the generalised additive models (GAM) fitted to log-transformed length-standardised Hg concentrations in white muscle of swordfish from the Indian Ocean. Smoothers illustrate the partial effect of continuous explanatory variables once the effects of all the other explanatory variables included in the model have been considered. The y-axis shows the contribution of the smoother to the predictor function in the model (in arbitrary units). Dashed lines represent the 95% confidence intervals. Whiskers on the x-axis indicate data presence.

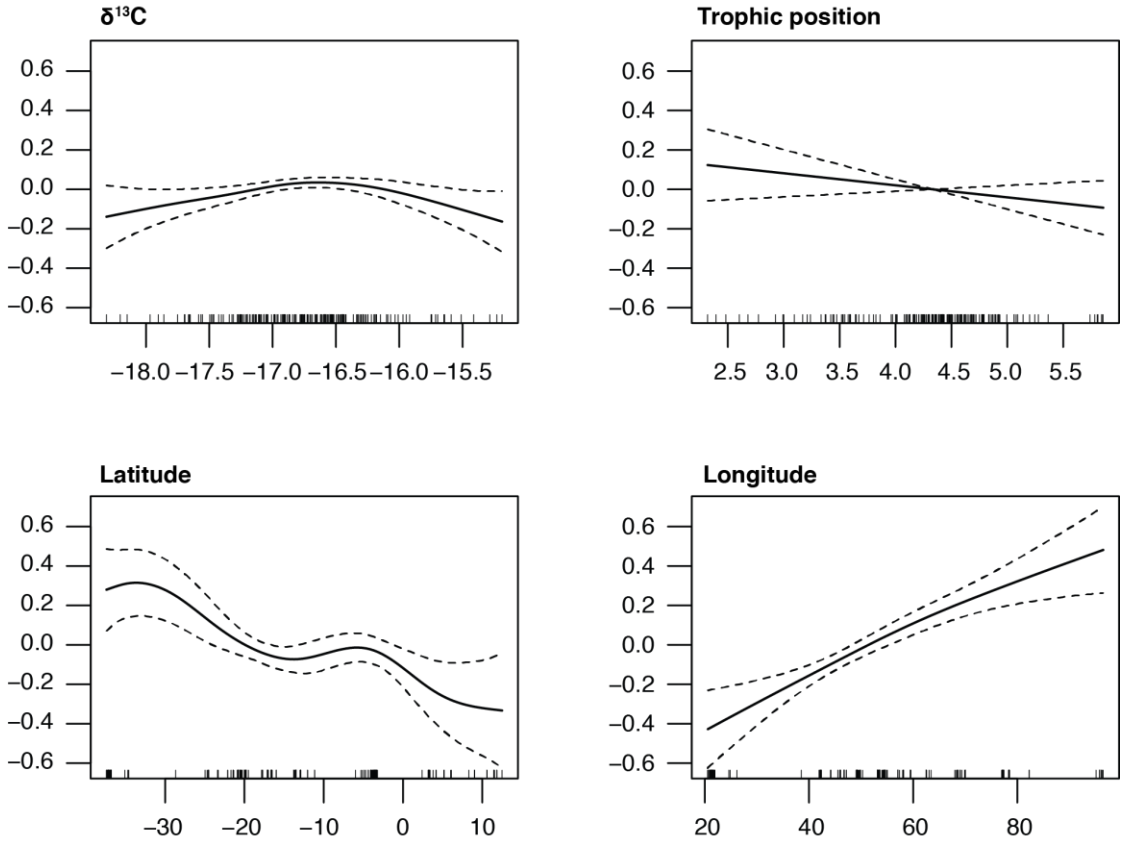

Fig. S4 Graphical results of the generalised additive models (GAM) fitted to log-transformed Se concentrations in white muscle of swordfish from the Indian Ocean. Smoothers illustrate the partial effect of continuous explanatory variables once the effects of all the other explanatory variables included in the model have been considered. The y-axis shows the contribution of the smoother to the predictor function in the model (in arbitrary units). Dashed lines represent the 95% confidence intervals. Whiskers on the x-axis indicate data presence.

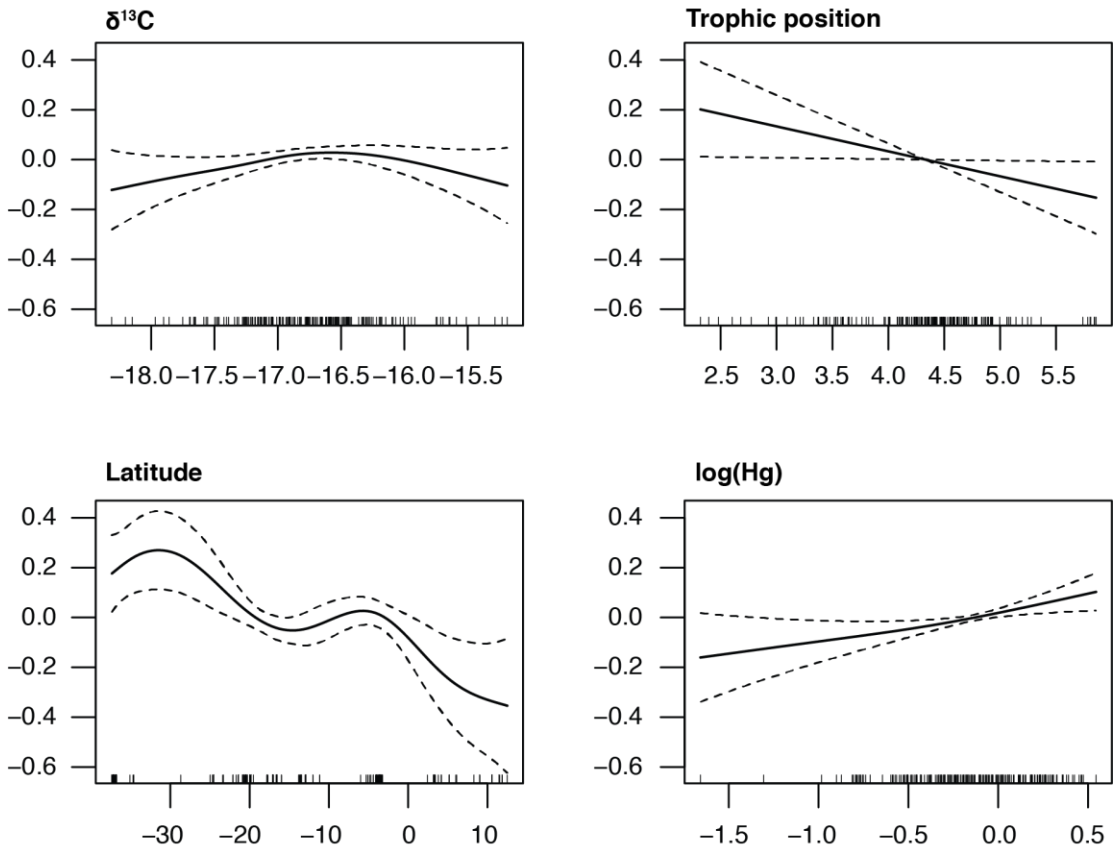

Fig. S5 Graphical results of the generalised additive models (GAM) fitted to log-transformed Se concentrations in white muscle of swordfish from the Indian Ocean, with log-transformed Hg concentrations as explaining variable. Smoothers illustrate the partial effect of continuous explanatory variables once the effects of all the other explanatory variables included in the model have been considered. The y-axis shows the contribution of the smoother to the predictor function in the model (in arbitrary units). Dashed lines represent the 95% confidence intervals. Whiskers on the x-axis indicate data presence.

Text S1

1. Interaction between mercury and selenium

In order to take into account the interaction ability of Hg with Se, the molar ratio of Hg above Se (MHg:MSe) and the Health Benefit Value of Se (HBVSe) were calculated according to the following equations (Ralston *et al*. 2007, 2015):

$$MHg:MSe = (C_{Hg}/M_{Hg}) / (C_{Se}/M_{Se}) \quad \textbf{(Eq.1)}$$

$$HBVSe = [(Mse - MHg)/MSe] \times (MSe + MHg) \quad \textbf{(Eq. 2)}$$

with MHg and MSe being the number of moles of Hg and Se respectively; C_{Hg} and C_{Se} being the concentrations of Hg and Se, respectively; and M_{Hg} and M_{Se} being the molar masses of Hg and Se, respectively (200.59 $g.mol^{-1}$ for Hg and 78.96 $g.mol^{-1}$ for Se).

It is considered that Se and Hg bind in a molar ratio of 1:1 in human tissues (Ralston *etal.* 2007). Thus, the concentration of theoretically bioavailable Se after interaction with Hg was estimated using the following equation:

$$\text{Concentration of theoretically bioavailable Se} = (MSe - MHg) \times M_{Se} \quad \textbf{(Eq. 3)}$$

2. Selenium supply and risk associated with too high intake

In order to assess Se benefit through seafood consumption, measured concentrations were compared to RDI set by the American Food and Nutrition Board of the Institute of Medicine National Academy of Sciences (2019a). Calculations were made for all age subclasses and status given in the guidelines (i.e. 2-3 year old, 4-8 year old, 9-13 year old, 14-18 year old, 19+ year old, pregnant women and lactating women) and were then summarised into the three chosen main age classes (i.e. children, 2-13 year old; young adults, 14-18 year old; and adult women, 19+ year old, including pregnant and lactating women). For this, the percentage of contribution to RDI was calculated for each sampled individual of each species with the following equation:

$$\%RDI = ([Se] \times \text{portion weight}) \times 100 / RDI_{Se} \quad \textbf{(Eq. 4)}$$

with [Se] being the concentrations of Se; portion weight being the weight of the portion for the considered age subclass; and RDI_{Se} being the recommended daily intake for Se. To summarise data into the three age classes, all data related to the corresponding age subclasses were grouped (i.e. 2-3 year old with 4-8 year old and 9-13 year old for children; 14-18 year old for young adults; and women 19+ year old with lactating and pregnant women for adult women). Then, mean value for each age class was calculated, as well as the confidence interval at 95% (CI95%) using the following formula:

$$CI95\% = [mean - (1.96 \times SE); mean + (1.96 \times SE)] \quad \textbf{(Eq. 5)}$$

with SE the standard error.

As Se can be toxic above certain levels, concentrations were also compared to PTI set by the American Food and Nutrition Board of the Institute of Medicine National Academy of Sciences (2019b). Again, calculations

were made for all age subclasses and status given in the guidelines, and were then summarised into the three chosen main age classes. The number of servings necessary before reaching PTI was calculated for each sampled individual of each species with the following equation:

$$\text{Number of servings} = PTI_{Se} / ([Se] * \text{portion weight}) \quad \textbf{(Eq. 6)}$$

with PTI_{Se} being the daily provisional tolerable intake for Se; [Se] being the Se concentrations; and portion weight being the weight of the portion for the considered age subclass. Then, like for %RDI data, all data related to the corresponding age subclasses were grouped and the mean value and CI95% were calculated for each age class.

Number of servings before reaching PTI and %RDI were also calculated for calculated concentrations of theoretically bioavailable Se, using the same method as for raw Se concentrations.

All parameters used in Eq. 4 and 6 are presented in Table S1.

2. Mercury exposure

In order to assess Hg exposure, concentrations were compared to PTI set by the Joint FAO/WHO Expert Committee on Food Additives (JECFA 2011). In order to be consistent with the method used for Se, calculations were again made for all age subclasses and status given in the guidelines (i.e. 2-3 year old, 4-8 year old, 9-13 year old, 14-18 year old, 19+ year old, pregnant women and lactating women) and were then summarised into the three chosen main age classes (i.e. children, 2-13 year old; young adults, 14-18 year old; and adult women, 19+ year old, includes pregnant and lactating women). Again, number of servings before reaching PTI were calculated for each analysed individual of each species using Eq. 6; data related to each age class were grouped together and the CI95% was calculated using Eq. 5. Parameters used in Eq. 6 are presented in Table S1.

Supplementary references

American Food and Nutrition Board of the Institute of Medicine National Academy of Sciences (2019a) Dietary Reference Intakes (DRIs): Recommended dietary allowances and adequate intakes, elements. URL: https://ods.od.nih.gov/Health_Information/Dietary_Reference_Intakes.aspx.

American Food and Nutrition Board of the Institute of Medicine National Academy of Sciences (2019b) Dietary Reference Intakes (DRIs): Tolerable upper intake levels, elements. URL: https://www.ncbi.nlm.nih.gov/books/NBK545442/table/appJ_tab9/?report=objectonly.

JECFA (2011) Mercury. URL: https://apps.who.int/food-additives-contaminants-jecfa-database/chemical.aspx?chemID=1806.

Marques-Vidal P, Madeleine G, Romain S, Gabriel A, Bovet P (2008) Secular trends in height and weight among children and adolescents of the Seychelles, 1956-2006. BMC Public Health 8:1–9. doi: 10.1186/1471-2458-8-166

Ralston NVC, Blackwell JL, Raymond LJ (2007) Importance of molar ratios in selenium-dependent protection against methylmercury toxicity. Biol Trace Elem Res 119:255–268. doi: 10.1007/s12011-007-8005-7

Ralston NVC, Ralston CR, Raymond LJ (2015) Selenium Health Benefit Values: Updated criteria for mercury risk assessments. Biol Trace Elem Res 171:262–269. doi: 10.1007/s12011-015-0516-z

US-EPA, US-FDA (2019) EPA-FDA Fish Advice: Technical Information. URL: https://www.epa.gov/fish-tech/epa-fda-fish-advice-technical-information.

WorldBank (2017) Third South West Indian Ocean Fisheries Governance and Shared Growth Project (SWIOFish3). Washington, DC

Bioaccumulation of trace elements in Seychelles marine food webs

Summary: Food security, that is guarantying food supply and quality while sustainably managing resources, is closely linked to knowing the biology and ecology of consumed species. In a context of global changes that are threatening seafood safety, it is thus necessary to establish baselines on marine ecosystem functioning, as well as nutrient availability and contamination occurrence in seafood. This is all the more important in Small Island Developing States (SIDS), where populations rely on marine resources for their subsistence, and where capture fisheries resources are the main sources of proteins and micronutrients (i.e. essential trace elements) in local populations' diet. In spite of the importance of tropical systems in ensuring food security, they remain largely understudied compared to polar and temperate systems. This thesis thus aims to better understand the functioning of tropical marine systems, and to establish a baseline on micronutrient availability and metal(loid) contamination in a wide diversity of capture fisheries resources from the Seychelles (Western Indian Ocean), a tropical SIDS. By investigating trace element concentration patterns at the inter- and intraspecific levels, it was possible to identify intrinsic and extrinsic factors influencing trace element bioaccumulation in tropical capture fisheries resources. We thus highlighted the importance of considering different scales (individual, species, and ecosystem) to better understand essential trace element availability and non-essential trace element occurrence in seafood.

Keywords: Seafood security, Tropical systems, Small Island Developing States, Indian Ocean, Capture fisheries resources, Trace elements, Bioaccumulation, Trophic ecology

Bioaccumulation des éléments traces dans les chaînes trophiques marines des Seychelles

Résumé : La sécurité alimentaire, qui est la garantie de l'approvisionnement et de la qualité des aliments tout en gérant les ressources de manière durable, est intrinsèquement liée à la connaissance de la biologie et l'écologie des espèces consommées. Dans un contexte de dérèglement climatique menaçant la salubrité des produits de la mer, il est donc nécessaire d'établir un référentiel sur le fonctionnement des systèmes marins, ainsi que sur l'occurrence des nutriments et des contaminants dans les produits de la mer. C'est d'autant plus important pour les Petits Etats Insulaires en Développement (PEID), qui dépendent des ressources marines pour leur subsistance, et où les produits de la pêche sont la première source de protéines et micronutriments (éléments traces essentiels) pour les populations locales. Malgré l'importance des systèmes tropicaux pour la sécurité alimentaire, ces systèmes sont peu étudiés comparés aux systèmes polaires et tempérés. Cette thèse vise à mieux comprendre le fonctionnement des systèmes marins tropicaux, et à établir un référentiel sur l'occurrence des micronutriments et des contaminants métalliques dans les produits de la pêche aux Seychelles (Océan Indien), un PEID tropical. En étudiant les concentrations en éléments traces aux niveaux inter- et intraspécifique, nous avons identifié différents facteurs intrinsèques et extrinsèques influençant la bioaccumulation de ces éléments dans les ressources marines tropicales. Nous avons aussi montré l'importance de considérer différentes échelles (individu, espèce et écosystème) pour mieux comprendre l'occurrence des éléments traces essentiels et non-essentiels dans les produits de la mer.

Mots clés : Sécurité des produits de la mer, Système tropical, Petit Etat Insulaire en Développement, Océan Indien, Produits de la pêche, Eléments traces, Bioaccumulation, Ecologie trophique

Laboratoire LIittoral ENvironnement et Sociétés (LIENSs)
2 rue Olympe de Gouges
17000 La Rochelle

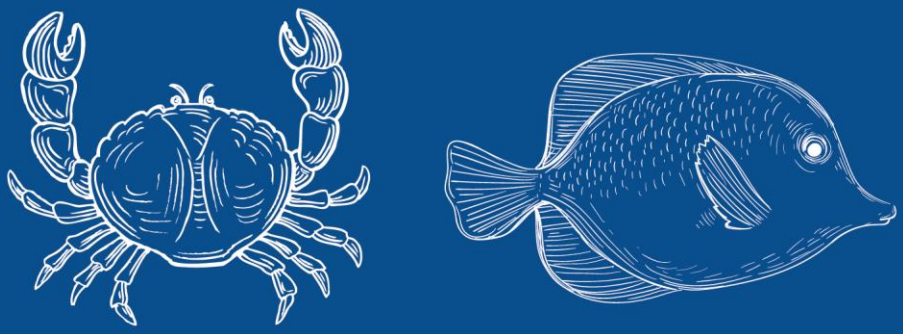

Food security, that is guarantying food supply and quality while sustainably managing resources, is closely linked to knowing the biology and ecology of consumed species. In a context of global changes that are threatening seafood safety, it is thus necessary to establish baselines on marine ecosystem functioning, as well as nutrient availability and contamination occurrence in seafood. This is all the more important in Small Island Developing States (SIDS), where populations rely on marine resources for their subsistence, and where capture fisheries resources are the main sources of proteins and micronutrients (i.e. essential trace elements) in local populations' diet. In spite of the importance of tropical systems in ensuring food security, they remain largely understudied compared to polar and temperate systems.

This thesis thus aims to better understand the functioning of tropical marine systems, and to establish a baseline on micronutrient availability and metal(loid) contamination in a wide diversity of capture fisheries resources from the Seychelles (Western Indian Ocean), a tropical SIDS. By investigating trace element concentration patterns at the inter- and intraspecific levels, it was possible to identify intrinsic and extrinsic factors influencing trace element bioaccumulation in tropical capture fisheries resources. We thus highlighted the importance of considering different scales (individual, species, and ecosystem) to better understand essential trace element availability and non-essential trace element occurrence in seafood.

La Rochelle Université

LIENSs UMR 7266

cnrs

Seychelles Fishing Authority